



ALMA MATER STUDIORUM
UNIVERSITÀ DI BOLOGNA

in cotutela con Université Bourgogne Europe (UBE)

DOTTORATO DI RICERCA IN

TECNOLOGIE INNOVATIVE E USO SOSTENIBILE DELLE RISORSE DI
PESCA E BIOLOGICHE DEL MEDITERRANEO (FISHMED-PHD)

Ciclo 37

Settore Concorsuale: 03/B1 - FONDAMENTI DELLE SCIENZE CHIMICHE E SISTEMI
INORGANICI

Settore Scientifico Disciplinare: CHIM/03 - CHIMICA GENERALE E INORGANICA

ZERO POLLUTION: RECYCLING SEA BY-PRODUCTS OF SHELLFISH
FARMING - SEARCH FOR ANTIBACTERIAL BIOMOLECULES IN THE SHELL
OF BIVALVES OF ECONOMIC INTEREST

Presentata da: Camille Marie Justine Lutet Toti

Coordinatore Dottorato

Mauro Marini

Supervisore

Frédéric Gilles Marin

Co-supervisor

Giuseppe Falini

Stefano Gofferdo

Esame finale anno 2025



**UNIVERSITÉ
BOURGOGNE
EUROPE**



**ÉCOLE DOCTORALE
Environnements - Santé**
Bourgogne | Franche-Comté



**ALMA MATER STUDIORUM
UNIVERSITÀ DI BOLOGNA**



FishMed-PhD

**THESE DE DOCTORAT DE L'ETABLISSEMENT UNIVERSITE BOURGOGNE
EUROPE**

**PREPAREE A Université de Bourgogne Europe – Università di Bologna Alma Mater
Studiorum**

Ecole doctorale n°554

Ecole Doctorale Environnements Santé

Doctorat de Biologie des Organismes

Par

Madame Lutet-Toti Camille

**POLLUTION ZERO : RECYCLAGE DE COPRODUITS DE L'ACTIVITE
CONCHYLICOLE - RECHERCHE DE BIOMOLECULES ANTIBACTERIENNES
DANS LA COQUILLE DE BIVALVES D'INTERET ECONOMIQUE**

Thèse présentée et soutenue à Fano, le 21/03/2025

Composition du Jury:

Pr. Weiss Ingrid	Full Professor, University of Stuttgart	Rapportrice
Dr. Auzoux-Bordenave Stéphanie	Maîtresse de conférences, MNHN	Rapportrice
Dr. Annibaldi Anna	Ass. Professor, Univ. Politecnica delle Marche	Examinatrice
Pr. Penna Antonella	Professor, Univ. degli Studi di Urbino Carlo Bo	Examinatrice
Dr. Fabi Giana	D. R., Consiglio Nazionale delle Ricerche	Examinatrice
Dr. Albéric Marie	C. R. CNRS, Sorbonne Universités	Examinatrice
Dr. Kaandorp Jaap A.	Ass. Professor, Universiteit van Amsterdam	Examinateur
Dr. Marin Frédéric	D. R. CNRS, Université de Bourgogne Europe	Directeur de thèse
Pr. Falini Giuseppe	Full professor, Università di Bologna	Codirecteur de thèse
Pr. Goffredo Stefano	Ass. Professor, Università di Bologna	Codirecteur de thèse

À i mei parenti, à a mo famiglia.

À u mo babbu, chì si n'hè andatu prima ch'èiu cuminciessi stu prugettu,
chì hà sempre cridutu in mè è chì ne saria statu fieru.

À Bastianu, chì hè per mè dinò un veru Duttore.

REMERCIEMENTS – ACKNOWLEDGEMENTS - RICONOSCIMENTI

Avant toute chose, je souhaite remercier le **culot**. Celui qui m'a été nécessaire pour candidater à cette thèse de doctorat, après tant d'essais infructueux, et qui m'a permis de tenir bon face à une administration qui me disait inéligible à l'entrée dans la compétition. Au cours de mes études, j'ai sauté plusieurs fois dans ce vide – le grand bleu ? – Je n'avais rien à perdre et suis très reconnaissante de tout ce que j'y ai gagné, de la position dans laquelle je me retrouve aujourd'hui.

Je suis profondément reconnaissante envers mon directeur de thèse, **Frédéric Marin**, pour son encadrement, sa disponibilité et sa confiance nécessaires à la réalisation d'un projet exploratoire et interdisciplinaire tel que celui-ci. Merci pour ton soutien face aux conditions matériellement et temporellement restrictives de ma thèse, il fut essentiel jusqu'au dernier jour. Tu as su voir en l'écologue marine que j'étais une candidate appropriée pour ce sujet de recherche et m'as convaincue de venir travailler dans les domaines de la microbiologie et de la biominéralisation (moi qui détestais la biologie moléculaire et les bactéries !). Merci de m'avoir formée aux techniques de laboratoire et d'avoir fait de moi la chercheuse interdisciplinaire que je suis aujourd'hui, de m'avoir prouvé qu'il suffit de curiosité et de ~~beaucoup~~ de persévérance. Je tiens également à te remercier pour nos discussions passionnantes, nos débats variés et les missions passées ensemble, nos longs trajets en voiture à travers monts et déluges. Merci d'avoir partagé avec moi ton amour pour la bonne musique, l'écriture et les contes, pour les fous rires des bactéries qui sentent mauvais, du *Paximus* et des *cholocats* (j'en oublie). Avoir un directeur aussi humain a été une réelle chance, et tu n'as cessé de m'impressionner quant au volume astronomique de ta culture générale – Fais attention, tu vas finir par te changer en encyclopédie !

Je souhaite également remercier mes co-directeurs de l'Università di Bologna. Grazie a **Stefano Goffredo** (fondatore di FishMed-PhD e coordinatore al momento del mio inizio) per avermi dato l'opportunità di svolgere questa dottorato presso l'Alma Mater Studiorum – Università di Bologna, la più antica università del mondo occidentale. Ringrazio anche **Giuseppe Falini** per questa opportunità, ma anche per il suo interesse nelle mie ricerche. Ho apprezzato molto visitare il laboratorio di biomineralizzazione a Bologna. Sebbene non abbia avuto l'occasione di svolgere un vero soggiorno di ricerca lì, vi ringrazio entrambi per la vostra partecipazione e per le riletture dei miei lavori di ricerca.

Je tiens à remercier les membres du jury, de mon comité de thèse et mes rapportrices pour avoir suivi et évalué ce travail : **Stéphanie Auzoux-Bordenave, Antoine Serpentine, Ingrid Weiss, Marie Albéric, Anna Annibaldi, Antonella Penna, Giana Fabi, Jaap Kaandorp**, et le coordinateur actuel de FishMed-PhD **Mauro Marini**.

Je remercie l'Ecole Doctorale Environnement Santé de l'Université de Bourgogne Europe pour m'avoir acceptée en cotutelle et pour m'avoir suppléée en aides financières quand je me retrouvais sans solution (~~ou trop maigre~~) de la part de l'Italie. Merci donc aux **Christelle**, ainsi qu'à **Maryia** et **Bibiane** du pôle international pour votre collaboration et votre aide administrativo-financière précieuse. Je remercie la direction du laboratoire Biogéosciences pour m'avoir accueilli, notamment **Thomas Saucède**, et l'équipe SAMBA. Ce travail n'aurait pu aboutir sans mes collègues que je remercie : **Claire** et **Isabelle** pour avoir géré mes missions

alambiquées, **Valeria** dell'UniBo per la gestione dei rimborsi italiani, **Florence** pour la présence le matin et le bureau impeccable au 4^{ème}, **Maria, Jérôme, Adrien, Charlène, Aude, Yannik** et **Anthony** pour votre aide matérielle (consommables et installations incubateurs et machines) ainsi que pour m'avoir secourue quand j'ai failli perdre mon doigt dans un évier (qui eût cru que travailler avec des huîtres et des bactéries pouvait être dangereux !). Un immense merci à **Marie Da Silva Feliciano**, assistante ingénieure qui fut littéralement ma main droite après blessure, a sauvé mes bactéries mourantes et mes manipes, m'a permis de rattraper mon retard et de finir ma thèse dans les temps. Travailler avec toi fut un réel plaisir, nos journées animées par ta bonne humeur et ton caractère bien trempé. Merci d'avoir remis en question les procédures et idées trop fixées et d'avoir si bien participé au design expérimental de ma thèse. Tu as été un véritable binôme dans les recherches exposées dans ce manuscrit.

Je tiens bien sûr à remercier mes collègues doctorants et jeunes chercheurs de Dijon pour ces années de partage au laboratoire et hors de ses murs. Merci pour les verres au Blues, les soirées jeux, les escapades et le ski plaisir. Un merci tout particulier à mon co-bureau et ami **Louis**, pour tes conseils de vie de thèse, l'ambiance incroyable tous les jours, ton gâteau aux pommes, tes rires qui font trembler les murs et le partage de ton esprit critique. Tes remontages de moral et de bretelles ont fondamentalement changé mon expérience de thèse. Merci à **Pierre** d'avoir pris le relais avec un si grand sourire, d'avoir été une force tranquille dans les moments difficiles et de m'avoir supportée sur ma fin de thèse avec **Julien** (tu as raison, les vélos à rétro-pédalage, quel pied) et **Sarah** (banger de thermo-DJ). Merci **Agate** pour ton amitié sincère, ton soutien et ta collaboration qui m'a remis les statistiques à l'heure ! Je remercie également **Alexandrine, Myriam, Batistin, Luc, Jeanne, Robin, Quentin, Léa, Luca, Benazir, Marlisa** (ma lab-partner) et **Esteban** avec toute la clique des internationaux qui a bien voulu de moi malgré mon statut hybride, **Mélissa** ma comparse de fin de rédaction et **Lilla** ma partenaire de lutte féministe (et oui tu es dans cette liste maintenant, hâte de lire ta thèse !).

The international cotutelle implies that I also belong to another PhD student group that became my friends, the unfortunate but brilliant minds of FishMed-PhD, vi ringrazio tutti! **Jenna** e **Marianna** per l'ospitalità, **Filo, Marco, Margherita** e **Yari** (AQUA2024 at København è stata fantastica con voi), **Polina, Carla, Leti**, le due **Fede, Antonio, Alessandro** (caro amico, ci mancherai tanto). Grazie per i bicchieri a Piazza Verdi, i pasti condivisi, l'aiuto reciproco e le passeggiate sulla spiaggia di Fano. Vi voglio bene a tutti!

I have to thank the people from the **Computational Science Lab** of the Universiteit van Amsterdam, for hosting and supporting me, for the friendships in these times of dire need. I wouldn't have been able to go on without you. **Helena, Nik, Victoria** (I'll continue to hang in there), **Joeri, Dhruv, Killian, Martina, Rob** and **Frederike**. A special thanks to **Jaap Kaandorp** who arranged this international collaboration opportunity. **Martina** my roommate from Amstelveen, thank you for making this house bearable, I hope you have only good things ahead of you and Bibi. Dank je wel !

Cette thèse à Dijon fut pour moi l'occasion de réaliser un autre rêve professionnel, malgré la distance de la mer (~~oui Dijon est loin de la mer, je SAIS~~) : passer le certificat d'aptitude à l'hyperbarie pour devenir plongeuse scientifique. Pour cela je remercie chaleureusement **Sébastien Motreuil** et toute la clique de bulleurs du Nautil'uB, **Ben, Géraldine, Chrichri, Maud, Sarah** (ma buddy), **Lisa, Clem, Avi, Théo, Minou Hugo, Anita** et **Damien** mes comparses de Trébeurden.

Je tiens aussi à remercier les ami·es et plus ou moins éloigné·es qui ont accompagné mon évolution dans le monde de la biologie marine, en licence puis en master. Après les épreuves vécues ensemble, vous êtes devenu·es des phares, des îlots en dehors de la tempête : **Anaëlle**, ma Samantha **Caroline, Pierre, Yamara, Baptiste, Coline** et les copains de l'EPHE. From Halifax my derby-wife **Art, Beth-from-Above**, and **Katie** the bat-person (I became math-knight again!). Special thanks to **Chris Harvey-Clark** from Dalhousie University for believing in me, offering me the opportunity to work with sharks and for recommending me. Je veux remercier la communauté du roller derby et plus particulièrement les **Velvet Owls** du Roller Derby Dijon pour ces années en tant que coach, coéquipière, arbitre, capitaine et un passage à la vice-présidence. Merci pour cette confiance jusqu'au bout alors que j'avais le cerveau qui surchauffait ; ces multiples casquettes m'ont appris la gestion de grands projets d'organisation, de groupes, de conflits internes et la diplomatie. **Sala** ma fusion, merci pour les conseils, l'écoute, les rires et les cafés à l'Atheneum, **Killer** ma filleule, **Lily, Anouk** (tu m'as appris tellement en communication), **Badoule, Charline, Gwada, Mulu** et toutes les autres (vous êtes incroyablement nombreuses). Désolée pour celles et ceux que j'ai pu oublier, je vous remercie aussi.

Je remercie bien sûr ma **famille** et mes **parents** qui m'ont offert un éveil intellectuel et une ouverture culturelle incroyable. Merci à ma **mère** d'avoir cru en moi, ti ringraziu è ti saraghju sempre ricunniscente d'avè capitu a mio sete di cunniscenze è d'avè m'aiutatu à spicà u volu. Merci à mon **père** de s'être battu autant que possible pour m'offrir la possibilité de partir faire mes études en mer. Je remercie mes frères et sœurs : **Bastien** pour le partage de la vie de thésard, les petits plats et le soutien alors que tu avais déjà fini ; **Zoé** pour les longues conversations, ton soutien administratif (ça sert une sœur bilingue !) et moral ; **Martin** pour les moments de détente loisirs et les bubble teas. Je remercie ma tante **Florence**, l'autre chercheuse biologiste de la famille, qui était là pour l'écriture du projet de recherche qui m'a permis de candidater et d'être sélectionnée pour cette thèse. Tu étais là au tout début, quand j'ai pris la décision de commencer, et je suis reconnaissante d'avoir pesé le pour et le contre avec toi.

Enfin, un immense merci à **Ségoène**, pour m'avoir soutenue pendant toutes ces années de thèse et m'avoir tant aidée et aimée au quotidien. Merci d'avoir été si patiente avec moi, malgré les gros coups de mou, les horaires démentiels et les difficultés à me lever le matin. Ti tengu cara.

COMMUNICATIONS AND PUBLICATIONS

PUBLICATIONS

2025 **Lutet-Toti, C.**, Da Silva Feliciano, M., Thomas, J., Crosland, A., Develay, C., Debrosse, N., Force, A., Bidault, A., Broussard, C., Falini, G., Goffredo, S., and Marin, F. (2025). Do bivalve shells exhibit antibacterial properties? Screening calcifying organic matrices against two major marine pathogens. *Science of the TOTAL ENvironment (STOTEN)*, submitted.

Lutet-Toti, C., Thomas, J., Falini, G., Goffredo, S., Gabillot, M., and Marin, F. (2025). From ornaments to biotechnologies: The evolution of mollusk shell uses through the ages. *Journal of Ethnobiology*, submitted.

Polacchi, L., **Lutet-Toti, C.**, Basuyaux, O., Guériaux, P., Albéric, M., Pasco, H., Merle, D., Habermeyer, B., Guillard, R., Thoury, M., and Marin, F. (2025). Innovative coupling of non-standard 1D-electrophoresis with luminescence spectral imaging to decipher invisible biochromes in modern and fossil shells. *Methods in Ecology and Evolution*, submitted (third submission).

2024 **Lutet-Toti, C.**, Da Silva Feliciano, M., Debrosse, N., Thomas, J., Plasseraud, L., and Marin, F. (2024). Diverting the Use of Hand-Operated Tablet Press Machines to Bioassays: A Novel Protocol to Test ‘Waste’ Insoluble Shell Matrices. *Methods and Protocols*, 7(2), Article 2.
<https://doi.org/10.3390/mps7020030>

Nahle, S., **Lutet-Toti, C.**, Namikawa, Y., Piet, M.-H., Brion, A., Peyroche, S., Suzuki, M., Marin, F., and Rousseau, M. (2024). Organic Matrices of Calcium Carbonate Biominerals Improve Osteoblastic Mineralization. *Marine Biotechnology*, 26(3), 539–549.
<https://doi.org/10.1007/s10126-024-10316-w>

2023 Andrialovanirina, N., Caillault, É. P., Couette, S., Laffont, R., Poloni, L., **Lutet-Toti, C.**, and Mahé, K. (2023). Asymmetry of Sagittal Otolith Shape Based on Inner Ear Side Tested on Mediterranean Red Mullet (*Mullus barbatus* Linnaeus, 1758): Comparative Analysis of 2D and 3D Otolith Shape Data. *Symmetry*, 15, 1067. <https://doi.org/10.3390/sym150510672023>

ORAL PRESENTATIONS

- 2024** **Lutet-Toti C.**, Da Silva Feliciano M., Bidault A., Thomas J., Falini, G., Goffredo, S., Marin, F. *From profuse waste to antimicrobial peptides: the molluscan shell and its bioactive properties*. **AQUA2024 Circular approach session, WAS-EAS**, 26-30 August 2024, Copenhagen, Denmark.
- 2024** **Lutet-Toti C.**, Goffredo, S., Falini, G., Marin, F. *From profuse waste to antimicrobial peptides: the molluscan shell and its bioactive properties*. **24èmes Journées Françaises de Biologie des Tissus Minéralisés (JFBTM)**, Talence, France.

POSTERS

- 2023** **Lutet-Toti, C.**, Goffredo, S., Falini, G., Marin, F. *Revaloriser les déchets conchylicoles : étude exploratoire de la composition et des propriétés bioactives des matrices coquillières de mollusques*. **23èmes Journées Françaises de Biologie des Tissus Minéralisés (JFBTM)**, 22-24 May 2023, Sète, France. Poster presentation with jury evaluation – **Young Researcher Prize**.
- 2022** **Lutet-Toti, C.**, Goffredo, S., Falini, G., Marin, F. *Repurposing mass-produced mollusk shells: an abundant underrated resource for bactericidal and bioactive biomolecules*, **5th International Conference on Recycling and Waste Management**, 7 November 2022, Paris-Roissy, France.
- Lutet-Toti, C.**, Goffredo, S., Falini, G., Marin., F. *Investigating mollusk shell organic matrices: isolation and characterization of bioactive molecules*. Poster presentation, **Gordon Research Conference on Biomineralization**, 14-19 August 2022, Castelldefels, Spain.
- Lutet-Toti, C.**, Goffredo, S., Falini, G., Marin, F. *Zero pollution: recycling sea by-products of shellfish farming - Search for bactericidal biomolecules in the shell of mollusks of economic interest*. **Forum des Jeunes Chercheurs 2022**, Ecole Doctorale Environnement Santé (ES), Université de Bourgogne Franche Comté, 16-17 June 2022, Dijon, France. **Winning poster** of the conference.

TRAINING COURSES ATTENDED

- Scanning Electron Microscopy and Transmission Electron Microscopy – 6h, APEX UMR703, Dimacell, Micalix
- Confocal and super-resolution microscopy training, applied to imaging bacterial biofilms down to the single cell level – 9h, APEX UMR703, Dimacell, Micalix
- Bioinformatics – 24h, UBE Environment & Health Doctorate School

- Welcome Conference ‘L’avenir de la formation doctorale post-pandémie’ – 1h, UBE Environment & Health Doctorate School
- NEO: lab safety training in CNRS units. Assessment and prevention of the biological chemical, and fire risks – 3h, CNRS
- Scientific integrity and ethics in research “*Intégrité scientifique dans les métiers de la recherche*” – 15h, FUN-MOOC, UBE Environment & Health Doctorate School

- FishMed-PhD teaching week 2022 in Fano headquarters (28/02/2022-04/03/2024)
- FishMed-PhD teaching week 2023 in Fano headquarters (27/02/2023-03/03/2023)
- FishMed-PhD teaching week 2024 in Fano headquarters (26/02/2024-01/03/2024)

- Benvenuti in Italia! Orientarsi con l'italiano – Part 1, 45h, Alma Mater Studiorum - Università di Bologna
- Benvenuti in Italia! Orientarsi con l'italiano – Part 2, 32h, Alma Mater Studiorum - Università di Bologna

- Practical scuba-diving courses for N2 FFESSM (CMAS 2stars) – Nautil’uB FFESSM 25 21 0433
- RIFAP (Reactions and Interventions in case of Diving Accidents): theoretical and practical training for first responders while scuba diving and onboard – 9h, Dijon Plongée, FFESSM
- Certificate of Aptitude for Hyperbaric Activities Class 0B, specialized in scientific research dives – 24h, Centre d’Activités de Plongée de Trébeurden (Oct. 2023 – May2024).

- Teaching Animal Biology and Evolution to first year Bachelor students (lessons, exercices and lab work) – 54h (accounting for 20h of training), UBE UFR Science de la Vie

Total countable duration of the training courses: 179 hours

LIST OF FIGURES

CHAPTER 1

<u>Figure 1.1:</u> Collection of decorative objects made from mollusk shells	33
<u>Figure 1.2:</u> Conch shell trumpets	36
<u>Figure 1.3:</u> Shell money	39
<u>Figure 1.4:</u> Shell molds	42
<u>Figure 1.5:</u> Fishing gears made of mollusk shells and shell products	45
<u>Figure 1.6:</u> Mayan seashell implanted false teeth	48

CHAPTER 2

<u>Figure 2.1:</u> Phylogenetic tree of the molluscan classes	80
<u>Figure 2.2:</u> The physiology of mollusk shell calcification	89
<u>Figure 2.3:</u> Phylogenetic tree of the bivalve orders	91
<u>Figure 2.4:</u> Shells of two specimens of the dog cockle <i>G. glycymeris</i>	92
<u>Figure 2.5:</u> Scanning Electron Microscope images of <i>G. glycymeris</i> shell fragments	94
<u>Figure 2.6:</u> Shell of the Mediterranean mussel <i>M. galloprovincialis</i>	95
<u>Figure 2.7:</u> Scanning Electron Microscopy images of shell fractures of <i>M. galloprovincialis</i>	95
<u>Figure 2.8:</u> Shell of the Pacific cupped oyster <i>M. gigas</i>	97
<u>Figure 2.9:</u> Scanning Electron Microscopy images of slices of the shell of <i>M. gigas</i>	99
<u>Figure 2.10:</u> Pictures of the shell of the great scallop <i>P. maximus</i>	100
<u>Figure 2.11:</u> Scanning Electron Microscopy of slices of the shell of <i>P. maximus</i>	101
<u>Figure 2.12:</u> Shell of the common cockle <i>C. edule</i>	102
<u>Figure 2.13:</u> Scanning Electron Microscopy views of shell fractures of <i>C. edule</i>	103
<u>Figure 2.14:</u> Pictures of the shell of three specimen of the manila clam <i>V. philippinarum</i> ...	104
<u>Figure 2.15:</u> Scanning Electron Microscopy images of the aragonite shell of <i>V. philippinarum</i>	106
<u>Figure 2.16:</u> Pictures of the shell of venus clam <i>V. verrucosa</i>	107
<u>Figure 2.17:</u> Scanning Electron Microscopy images of shell fractures of <i>V. verrucosa</i>	107

CHAPTER 3

<u>Figure 3.1:</u> Phenol red color properties as a colored pH indicator.....	160
<u>Figure 3.2:</u> Electrophoresis gels of all bivalve models	185
<u>Figure 3.3:</u> Positive results of the disk diffusion assay on <i>A. salmonicida</i> and <i>V. harveyi</i> ORM4.....	188
<u>Figure 3.4:</u> boxplots results of the disk diffusion assays for <i>A. Salmonicida</i> and <i>V. harveyi</i> ORM4.....	189
<u>Figure 3.5:</u> Microdilution assays growth curves with <i>A. Salmonicida</i>	192
<u>Figure 3.6:</u> Microdilution assays growth curves with <i>V. harveyi</i> ORM4	193
- - -	
<u>Figure S3.1:</u> growth curves for the positive results of microdilution assays against <i>A.</i> <i>salmonicida</i> under 420 nm wavelength.....	208
<u>Figure S3.2:</u> Growth curves for the negative results of microdilution assays against <i>A.</i> <i>salmonicida</i> under 420 nm and 560 nm wavelengths	210
<u>Figure S3.3:</u> growth curves for the negative results of microdilution assays against <i>V. harveyi</i> ORM4 under 420 nm and 560 nm wavelengths.....	211
<u>Figure S3.4:</u> growth curves for the negative results of microdilution assays against <i>V. harveyi</i> ORM4 under 420 nm and 560 nm wavelengths.....	214

CHAPTER 4

<u>Figure 4.1:</u> Boxplots results of the disk diffusion assays for <i>V. aestuarianus</i>	220
<u>Figure 4.2:</u> Microdilution assays growth curves for <i>V. aestuarianus</i>	225
<u>Figure 4.3:</u> boxplots results of the disk diffusion assays for <i>Vibrio harveyi</i> LMG7890.....	226
<u>Figure 4.4:</u> Microdilution assays growth curves for <i>V. harveyi</i> LMG7890	231
<u>Figure 4.5:</u> boxplots results of the disk diffusion assays for <i>Vibrio mytili</i>	232
<u>Figure 4.6:</u> Microdilution assays growth curves for <i>V. mytili</i>	237
<u>Figure 4.7:</u> boxplots results of the disk diffusion assays for <i>Vibrio tapetis</i> CECT4600.....	238
<u>Figure 4.8:</u> Microdilution assays growth curves for <i>V. tapetis</i> CECT4600	243
<u>Figure 4.9:</u> Growth curves from the phase A of the microdilution assays for <i>A. salmonicida</i>	246
<u>Figure 4.10:</u> Growth curves from the phase A of the microdilution assays for <i>V. aestuarianus</i>	247
<u>Figure 4.11:</u> Growth curves from the phase A of the microdilution assays for <i>V. harveyi</i> ORM4.	248
<u>Figure 4.12:</u> Growth curves from the phase A of the microdilution assays for <i>V. harveyi</i> LMG7890.	249
<u>Figure 4.13:</u> Growth curves from the phase A of the microdilution assays for <i>V. mytili</i>	250
<u>Figure 4.14:</u> Growth curves from the phase A of the microdilution assays for <i>V. tapetis</i> CECT4600.....	251

LIST OF TABLES

<u>Table 1.1:</u> Mass of dry shells produced by seven bivalves of economic interest, in proportion of their live, whole wet body mass	64
<u>Table 2.1:</u> up-to-date inventory of the 373 AMPPs (AntiMicrobial Peptides and Proteins) identified in mollusks soft tissues and secretions.....	112
<u>Table 3.1:</u> Amounts of organic matrix in the shell of the seven tested bivalves.....	157
<u>Table 3.2:</u> Concentrations gradients of the tested ASMs and standard treatments used in the microdilution assay.....	180
<u>Table 3.3:</u> Amounts of the organic matrix extracted in the shell of the seven tested bivalves, in proportion of the powder weight.	183
<u>Table 3.4:</u> Summary of the positive results of the microdilution assay.	191
<u>Table 3.5:</u> Summary of the proteomic results.	195
<u>Table 3.6:</u> Antimicrobial proteins and peptides (AMPPs) identified in the shell extracts of our studied models.....	196
<u>Table 5.1:</u> Summary table of the antibacterial assays for all bacteria and mollusks.....	260

LIST OF ABBREVIATIONS

AIM	Acid Insoluble Matrix
ASM	Acid Soluble Matrix
AM	AntiMicrobial
AMP	AntiMicrobial Peptide
AMPP	AntiMicrobial Peptide and Protein
BLAST	Basic Local Alignment Search Tool
BMP	Bone Morphogenetic Protein
C1qDC	C1q Domain Containing protein
CA	Carbonic Anhydrase
DNA	DesoxyriboNucleic Acid
ECM	ExtraCellular Matrix
ECP	ExoCellular Product
EPS	ExoPolySaccharide
FAD	Fish Aggregating Device
FReP	Fibrinogen-Related domain Protein
GAPDH	GlycerAldehyde 3-Phosphate DeHydrogenase
HAB	Harmful Algal Bloom
IMTA	Integrated Multi-Trophic Aquaculture
kDa	kilo Dalton
LS-AIM	Laemmlli Soluble Acid Insoluble Matrix
LPMO	Lytic Polysaccharide MonoOxygenases
MAPK	Mitogen Activated Protein Kinase
MBC	Minimum Bactericidal Concentration
MIC	Minimum Inhibitory Concentration
MXDM	Multi Xenobiotic Defense Mechanism
NO	Nitric Oxide
OM	Organic Matrix
PGRP	PeptidoGlycan Recognition Protein
PO	PhenolOxidase
PRR	Pattern Recognition Receptor
QS	Quorum Sensing
ROS	Reactive Oxygen Species
T3SS	Type III Secretion System
T4SS	Type IV Secretion System
TLC	Thin Layer Chromatography

TABLE OF CONTENT

RÉSUMÉ ÉTENDU DE LA THÈSE EN FRANÇAIS	1
CHAPTER 1 - INTRODUCTION	21
1.1. Introduction	23
1.2. From Ornaments to Biotechnologies: The Evolution of Mollusk Shell Uses Through the Ages	25
1.2.1. Introduction	25
1.2.2. Aesthetic, Religious and Cultural Uses, Past and Present	27
1.2.2.1. Paleolithic times.....	27
1.2.2.2. Mesolithic Iron Age.....	27
1.2.2.3. Antiquity to Middle Age	29
1.2.2.4. Modern Era.....	29
1.2.2.5. Contemporary Era	30
1.2.3. Derived Shell Products of Pearl Industry: Natural Pearls, Nuclei and Blisters	33
1.2.4. Shells as Religious Symbols and Amulets.....	34
1.2.5. Musical Instruments and Signaling	36
1.2.6. Shell Representations in Art.....	37
1.2.7. Currencies and Wealth	38
1.2.8. Practical Applications, Past and Present.....	40
1.2.8.1. Daily Tools.....	40
1.2.8.2. Shells as Molds.....	41
1.2.8.3. Artistic Tools and Pigments	43
1.2.8.4. Shells in Architecture and Construction	43
1.2.8.5. Shells in Agriculture: Soil Improvers and Food Complement for Poultry.....	44
1.2.8.6. Other Practical Uses.....	45
1.2.9. Traditional Medicinal and Pharmaceutical Uses	46
1.2.10. Recent and Future Applications: Biotechnology, Engineering and Others	49
1.2.10.1. Smart Construction Materials.....	49
1.2.10.2. Depollution	49
1.2.10.3. Biotechnological Research and Production of Bioactive Compounds.....	50
1.2.11. Conclusion.....	51
1.2.12. References	52
1.3. Molluscan Aquaculture: Production Trends, Challenges and Future Developments....	59
1.3.1. Development of Aquaculture and (pre)Historical Trends	59
1.3.2. Contemporary Production Trends	61
1.3.2.1. Shell Products and Pearls.....	61
1.3.2.2. Shellfish and Aquaculture of Edible Mollusks	62
1.3.2.3. Conchyliculture.....	63
1.3.3. Threats and Limitations of Conchyliculture.....	65
1.3.3.1. Diseases	66
1.3.3.2. Food Safety and Human Health Concerns.....	67
1.3.3.3. Climate Change Impacts	67
1.3.3.4. Space Competition	68
1.3.3.5. Impacts on Wild Environments and Communities.....	68
1.3.4. Solutions and their Limits	69
1.3.4.1. Usual Solutions	69
1.3.4.2. Integrated Multi-Trophic Aquaculture (IMTA).....	70

1.3.4.3. <i>Open Ocean Aquaculture</i>	70
1.3.4.4. <i>Innovative Products and Approaches</i>	71
1.4. Concluding Remarks and Thesis Outline	71
1.5. Chapter References	73
CHAPTER 2 - MOLLUSCAN DEFENSES	77
2.1. Introduction: The Molluscan Intrinsic Defense System	79
2.1.1. The Shell as a Primary Defense Mechanism	79
2.1.2. Mucus: The First Line of Chemical Defense	82
2.1.3. Cellular Defenses: The Mobile Immune Response	84
2.1.4. Molecular Defenses: The Chemical Arsenal	85
2.2. The Bivalve Shell	88
2.2.1. Structure and Function	88
2.2.2. Organic Matrix	89
2.2.3. Studied Bivalve Models	91
2.2.3.1. <i>Glycymeris glycymeris: Shell Morphology and Microstructures</i>	92
2.2.3.2. <i>Mytilus galloprovincialis: Shell Morphology and Microstructures</i>	95
2.2.3.3. <i>Magallana gigas: Shell Morphology and Microstructures</i>	97
2.2.3.4. <i>Pecten maximus: Shell Morphology and Microstructures</i>	100
2.2.3.5. <i>Cerastoderma edule: Shell Morphology and Microstructures</i>	102
2.2.3.6. <i>Venerupis philippinarum: Shell Morphology and Microstructures</i>	104
2.2.3.7. <i>Venus verrucosa: Shell Morphology and Microstructures</i>	107
2.3. Antimicrobial Components in Mollusks Soft Tissues: A Review	109
2.4. Chapter References	133
CHAPTER 3 - ANTIBACTERIAL PROPERTIES OF BIVALVE SHELL EXTRACTS ..	151
3.1. Introduction	153
3.2. Antibacterial Screening of Bivalve Shell Extracts: Technical Aspects	153
3.2.1. Resources for Bioactive Substances: Mollusk Models	155
3.2.1.1. <i>Sampling</i>	155
3.2.1.2. <i>Production of Shell Powder</i>	155
3.2.1.3. <i>Organic Matrix Extraction</i>	156
3.2.2. Bacterial Targets	156
3.2.3. Standard Antibacterials	158
3.2.4. Initial Screening: Disk Diffusion Assay	158
3.2.5. Secondary Screening: Microdilution Assay	159
3.3. Diverting the Use of a Hand-Operated Tablet Tress Machine to Bioassays: A Novel Protocol to Test “Waste” Insoluble Shell Matrices	161
3.4. Do Bivalve Shells Exhibit Antibacterial Properties? Screening Calcifying Organic Matrices Against Two Major Marine Pathogens	173
3.4.1. Introduction	173
3.4.2. Materials and Methods	177
3.4.2.1. <i>Mollusk Shell Organic Matrix Extraction</i>	177
3.4.2.2. <i>Gel Electrophoresis</i>	178
3.4.2.3. <i>Bacterial Cultures</i>	178
3.4.2.4. <i>Disk Diffusion Assay</i>	179

3.4.2.5. <i>Microdilution Assay</i>	180
3.4.2.6. <i>Statistical Analysis</i>	182
3.4.2.7. <i>Proteomic Analysis</i>	182
3.4.3. Results	183
3.4.3.1. <i>Shell Organic Matrix Quantification and SDS-PAGE Check</i>	183
3.4.3.2. <i>Disk Diffusion Assay</i>	186
3.4.3.3. <i>Microdilution Assay</i>	190
3.4.3.4. <i>Proteomic Analysis</i>	193
3.4.4. Discussion	197
3.4.5. References	202
3.5. Chapter References	215
CHAPTER 4 - MICELLANEA: UNPUBLISHED DATA AND RESULTS	217
4.1. Negative Results of the Antibacterial Screening	219
4.1.1. <i>Vibrio aestuarianus</i>	220
4.1.2. <i>Vibrio harveyi</i> LMG7890	225
4.1.3. <i>Vibrio mytili</i>	231
4.1.4. <i>Vibrio tapetis</i> CECT4600	237
4.2. Characterization of the Bacterial Strains: Antibiotic Selection and General Growth Analysis	244
4.3. Chapter References	252
CHAPTER 5 - GENERAL DISCUSSION & PERSPECTIVES	253
5.1. Research Activities Carried Out During the Doctorate	255
5.2. Limitations of my Project	256
5.2.1. Time Consuming Preparation and Extraction of the Shell Matrices	256
5.2.2. Non-Standard Marine Bacterial Strains	256
5.2.3. Other Technical Bottlenecks	258
5.2.4. Proteomics on Non-Model Organisms	258
5.3. Antibacterial Screening	259
5.3.1. Comparison of the Results Depending on Bacteria	259
5.3.2. Comparison of the Results Depending on Bivalves	263
5.3.3. Antimicrobial Shellome Exploration by Proteomic Analysis	265
5.3.4. Nature and Mechanism of the Antibacterial Natural Extracts	267
5.4. Perspectives	269
5.4.1. Further Characterizations and Experimentations	269
5.4.2. Applications against Marine Pathogens	272
5.4.2.1. <i>Aquaculture Applications</i>	272
5.4.2.2. <i>Food Safety</i>	273
5.4.3. Applications Targeting Other Microorganisms	273
5.4.3.1. <i>Environmental Applications</i>	273
5.4.3.2. <i>Endolithic Bacteria</i>	274
5.4.3.3. <i>Human Pathogens</i>	274
5.5. Conclusion	275
5.6. Chapter References	277

CHAPTER 6 - ANNEX	281
6.1. Collaboration Paper with Sarah Nahle: Nacre Application in Biomedical Osteoblastic Mineralization.....	283
6.2. Collaboration Paper with Dr. Luca Polacchi: Biochrome Extraction	294
6.2.1. Introduction	295
6.2.2. Materials and Methods	296
6.2.2.1. <i>Materials</i>	296
6.2.2.2. <i>Matrix Extraction</i>	296
6.2.2.3. <i>Analytical Gel Electrophoresis and Acquisition of Spectral Images</i>	297
6.2.2.4. <i>Preparative Gel Electrophoresis</i>	298
6.2.3. Results	299
6.2.3.1. <i>A Non-Standard and Optimized Protocol in Three Steps</i>	299
6.2.3.2. <i>Revealing Biochromes in Gels (Fig. 2A, B)</i>	299
6.2.3.3. <i>In-Gel Identification of Biochromes (Fig. 2C)</i>	300
6.2.3.4. <i>Analysis of Biochrome-Macromolecules Complexes</i>	300
6.2.3.5. <i>Upscaled Purification of Porphyrins</i>	301
6.2.4. Discussion	302
6.2.4.1. <i>Unconventional Features of our Protocol</i>	302
6.2.4.2. <i>Advantages</i>	303
6.2.4.3. <i>Limitations</i>	304
6.2.4.4. <i>Further Developments: Other Objects, Methodologies and Applications</i>	305
6.2.5. References	309
6.3. Certificates.....	312
6.4. Posters.....	314

RÉSUMÉ ÉTENDU DE LA THÈSE EN FRANÇAIS

CHAPITRE I : INTRODUCTION

La recherche présentée dans ce manuscrit est le résultat d'une étude doctorale de trois ans, au cours de laquelle j'ai étudié les propriétés antibactériennes des matrices organiques (MO) de la coquille des bivalves d'intérêt économique. Ce projet s'inscrit dans le cadre du consortium FishMed-PhD piloté par l'Université de Bologne (*Alma Mater Studiorum*, encore appelée UniBo). Il a pour visée à long terme la possibilité de recycler les coquilles de bivalves de consommation courante (huîtres, moules, coques, amande de mer, praire, palourde, etc...) – coproduits de la pêche et de la conchyliculture - en vue de développer une économie vertueuse. Les coquilles vides, après consommation, sont en effet une ressource extrêmement abondante, qui ne sont valorisée à ce jour que par des applications de peu de valeur ajoutée (remblais, bétons, compléments alimentaires pour volaille). Or, ces structures minéralisées résultent d'un processus de biominéralisation, ce qui implique qu'elles contiennent aussi des composés organiques (protéines, polysaccharides), pratiquement pas exploités actuellement. Mon projet a pour but de mettre en évidence certaines propriétés de ces composés organiques coquilliers, et en particulier leur capacité antibactérienne. Notons qu'il s'agit de la toute première tentative de recherche d'agents antibactériens dans les coquilles de bivalves plutôt que dans les tissus mous. La deuxième nouveauté réside dans le fait que le projet cible spécifiquement des pathogènes marins de poissons et de mollusques. Ainsi, à moyen terme, mes recherches peuvent avoir des applications relativement directes dans le domaine de l'aquaculture.

1.1 Introduction

Depuis la naissance de la civilisation au Proche-Orient, les êtres humains ont toujours cherché à s'installer près des côtes. En raison des avantages évidents que procure un accès direct aux mers et aux océans, les peuplements humains sont en effet (pré)historiquement plus concentrés dans les zones côtières, cette tendance se renforçant massivement aujourd'hui avec l'augmentation drastique de la population mondiale. Selon une estimation du Programme des Nations Unies pour l'Environnement (UNEP), environ 40 % de la population mondiale vit à moins de 100 kilomètres de la côte. Ce pourcentage atteint 60 % si l'on considère une zone frangeante de 150 km. Ce phénomène s'illustre de façon remarquable par le fait que parmi les vingt plus grandes villes du monde, treize (Tokyo, Shanghai, Sao Paulo, Mumbai, Osaka, New-York City, Karachi, Buenos Aires, Istanbul, Calcutta, Manille, Lagos, Rio de Janeiro) sont situées sur le littoral. L'augmentation de la densité de population et de l'activité économique

dans les zones côtières génère une intensification des pressions environnementales exercées sur les écosystèmes côtiers. Ce phénomène, qui n'épargne aucune partie du globe, est particulièrement marqué en Europe et dans le bassin méditerranéen, qui déjà soumis à un trafic maritime intense et à une surexploitation de ses ressources aquatiques, voit sa vulnérabilité s'accroître d'année en année.

Outre la favorisation d'exports de produits locaux à longue distance par transport maritime, les environnements côtiers offrent des avantages concrets aux zones densément peuplées en termes de disponibilité alimentaire immédiate. La pêche côtière, la pêche hauturière et les installations aquacoles constituent ainsi les principaux fournisseurs de produits de la mer, notamment de poissons, d'oursins, de crustacés, de mollusques et d'algues. Dans cette liste, les mollusques constituent une source majeure de protéines, de sels minéraux et d'oligo-éléments, dont les bienfaits ont été reconnus très tôt dans l'histoire de l'Humanité. En effet, les premières traces de consommation de mollusques remontent à plus de 100 000 ans (voir Chapitre I). De nos jours, les techniques de conchyliculture et de pêche des mollusques propulsent ces derniers au rang de denrée alimentaire essentielle à l'échelle mondiale. Cette importance est particulièrement marquée en Asie et en Europe où ils constituent une part significative du régime alimentaire et de l'économie maritime. Cependant, leur utilité ne se limite pas à la consommation : depuis la préhistoire, la coquille, organe de protection externe des mollusques, a été recyclée et employée à des fins multiples, allant de l'esthétique au pratique en passant par les us culturels. Ces aspects variés sont explorés plus en détail dans la seconde section du Chapitre I de ma thèse (1.2. « Des ornements aux biotechnologies : L'évolution de l'utilisation des coquillages de mollusques à travers les âges », revue bibliographique soumise à la revue internationale *Journal of Ethnobiology*).

La coquille est un exosquelette biominéralisé et, à ce titre, présente des propriétés physiques et biochimiques particulières dues à sa nature organo-minérale. En effet, la fraction organique, également appelée matrice coquillière, un mélange de macromolécules comprenant des protéines et des sucres, est sécrétée et occluse lors la formation de la coquille. De nombreuses études fondamentales utilisant une approche protéomique ont mis en évidence la complexité moléculaire de cette matrice, qui comprend un large éventail de fonctions peu connues, qui ne sont pas nécessairement associées au processus de biocalcification. En quelques mots, la coquille est devenue une source potentielle de composants intéressants dans plusieurs domaines d'application, notamment dans les biomatériaux, la santé ou l'environnement. La recherche de "molécules utiles dans les coquilles" est d'autant plus pertinente que les tonnages de coquilles vides produits suite à la consommation alimentaire de mollusques sont

considérables : on estime qu'environ 10 millions de tonnes de coquilles provenant d'huîtres, palourdes, coquilles Saint-Jacques et moules sont produites chaque année. Une grande partie de ces déchets reste totalement inexploitée, induisant ainsi d'importantes nuisances environnementales et sociétales (Morris *et al.*, 2019 ; Topić Popović *et al.*, 2023). Dans le présent manuscrit, je revisite l'utilisation des déchets coquilliers, dans la perspective de développer des applications innovantes à forte valeur ajoutée : l'utilisation de substances antimicrobiennes issues de coquilles d'intérêt économique. A cette fin, j'ai extrait et caractérisé les matrices organiques des coquilles de plusieurs espèces de mollusques ; j'ai ainsi mis en place deux types de tests de criblage antibactérien, complétés par une approche d'analyse protéomique. Les résultats de mes travaux peuvent avoir des retombées dans divers domaines, notamment en aquaculture, dans la santé ou dans la protection de l'environnement. Ma recherche s'inscrit dans le cadre du programme pluriannuel FishMed-PhD (*Innovative Technologies and Sustainable Use of Mediterranean Sea Fishery and Biological Resources*) piloté par l'université de Bologne. D'une manière générale, ce programme s'inscrit dans une recherche de mise en place d'une économie circulaire vertueuse, engagée dans le développement de pratiques durables de production alimentaire, de santé et de gestion des déchets.

Avant de présenter certains des résultats expérimentaux que j'ai acquis au cours de ces trois dernières années, je souhaite partager avec le·a lecteur·ice de ce manuscrit une introduction dans laquelle je brosse le tableau des multiples utilisations des coquillages à travers les âges (section 1.2) et passe en revue la production de mollusques et énumère les défis actuels de cette industrie (section 1.3). Enfin, je conclus le premier chapitre en exposant le plan général de la partie pratique de mon travail (section 1.3).

1.2. Des Ornaments Aux Biotechnologies : L'Evolution de l'Utilisation des Coquillages de Mollusques à Travers les Ages

Section calibrée comme un article de revue bibliographique qui est actuellement soumis à une revue internationale (Journal of Ethnobiology) pour publication.

Les mollusques ont toujours représenté une source importante de nourriture pour les populations humaines. Un sous-produit de la consommation de mollusques est la coquille, un squelette externe composé de carbonate de calcium. Plutôt que d'être simplement considérée comme un déchet, la coquille des mollusques a, à de nombreuses reprises au cours des temps, été réutilisée ou recyclée pour des applications diverses et variées. Cette revue énumère les différentes utilisations des coquilles de mollusques au cours des siècles, depuis le paléolithique jusqu'à aujourd'hui. Pour plus de clarté, j'ai regroupé les utilisations en quatre grands thèmes : les utilisations esthétiques, religieuses et culturelles, les utilisations pratiques, les utilisations médicinales et pharmaceutiques traditionnelles et, enfin, les applications récentes et futures. Les coquilles étant des composites organo-minéraux, elles constituent un immense réservoir de macromolécules potentiellement bioactives qu'il convient d'étudier. Le développement d'applications à haute valeur ajoutée basées sur l'exploitation des coquillages représente une perspective fascinante pour les temps à venir, qui s'inscrit dans le cadre général d'une économie circulaire vertueuse, engagée dans la création de secteurs durables de la production alimentaire, de la santé et de la gestion des déchets.

Dans cette revue, brève en comparaison de l'étendue thématique et temporelle du sujet, je tente de couvrir au mieux les multiples utilisations des coquillages à travers le temps et l'espace. Bien que certaines de ces réutilisations soient anciennes ou traditionnelles, elles révèlent des propriétés remarquables mais insoupçonnées des coquillages : pensons simplement à l'exemple étonnant des implants dentaires mayas en nacre de mollusque (section 1.2.3. « Médecine Traditionnelle et Usages Pharmaceutiques »). Aujourd'hui, en 2025, on ne sait toujours pas ce qui a fait le succès de cette opération réalisée il y a 12 ou 13 siècles. Une partie du secret réside probablement dans les composants organiques de la matrice de nacre, qui permettent l'ostéo-intégration d'implants de nacre dans la mâchoire. Un tel exemple nous incite à considérer les coquillages comme d'immenses réservoirs inexplorés de composants bioactifs et à revisiter leur reconversion pour des applications à haute valeur ajoutée.

1.3. Aquaculture des Mollusques : Dynamiques de Production, Défis et Développements Futurs

Dans cette section de ma thèse, je fournis une analyse approfondie de l'évolution historique et des tendances contemporaines de l'aquaculture des mollusques. Je retrace le développement de l'exploitation des mollusques depuis le Paléolithique inférieur jusqu'à nos jours, mettant en lumière les innovations et les pratiques qui ont façonné cette industrie. En effet, la transition du Paléolithique au Néolithique voit l'évolution de la récolte des mollusques vers une activité organisée. Afin de pérenniser cette ressource, les populations articulent les prélèvements autour des cycles de vie des mollusques, développant des pratiques de gestion durable des stocks et allant jusqu'à la création des premières formes d'aquaculture, notamment par l'élevage d'huîtres plates dans la Rome antique. Ces développements historiques ont jeté les bases de l'aquaculture moderne des mollusques.

L'aquaculture des mollusques a connu une croissance significative ces dernières décennies, surpassant pour la première fois la pêche de capture en termes de volume de production en 2022 : atteignant un record de 130,9 millions de tonnes de biomasse, elle représente alors plus de 51% de la production aquatique totale. Les mollusques représentent environ 17-21% de tous les produits aquacoles selon les régions. La conchyliculture, à l'origine de plus de 75% des bivalves sur le marché, atteint une production mondiale annuelle d'environ 18,9 millions de tonnes. Les huîtres creuses et les coquilles Saint-Jacques figurent parmi les espèces marines les plus exploitées. La Chine domine la production mondiale, représentant 85% de la biomasse totale, tandis que l'Europe contribue à hauteur de 5,5%. En Europe, l'Espagne est le plus grand producteur aquacole de mollusques, se concentrant principalement sur la moule méditerranéenne *Mytilus galloprovincialis*. La France, quant à elle, est le principal producteur européen d'huîtres creuses *Magallana gigas*, avec une production annuelle de 78 000 tonnes. Il convient de noter que la génération de sous-produits coquilliers dans la conchyliculture est significative, représentant jusqu'à 75% du poids total de la production dans la plupart des exploitations. Cette proportion varie selon les espèces, allant de 45% pour les moules à 90% pour certaines espèces à coquille épaisses (Table 1.1).

Produisant plus de 14 millions de tonnes de bivalves chaque année dans le monde, la conchyliculture est en passe de devenir le principal producteur de "viande" pour une grande partie de la population humaine. Ce secteur très actif de l'industrie alimentaire génère d'énormes quantités de sous-produits, les coquilles, estimées à environ 10 millions de tonnes par an. Bien que les coquilles de bivalves soient réutilisées dans divers domaines (section 1.2), une large proportion est encore considérée comme un déchet et jetée, générant des nuisances à la fois environnementales et sociales. Les connaissances passées, traditionnelles et contemporaines sur

les propriétés supposées et avérées des coquilles de mollusques suscitent l'intérêt pour ces organes minéralisés prometteurs, qui ne demandent qu'à être réutilisés. En effet, plusieurs études se concentrent déjà sur les propriétés ostéoinductives et cicatrisantes des coquilles de bivalves ; et l'état actuel des problématiques de proliférations de pathogènes soulève des inquiétudes concernant les micro-organismes multirésistants et les maladies émergentes dans les secteurs sensibles que sont la sécurité alimentaire, la conservation des environnements et de la santé humaine en général.

Dans ce contexte, **ma recherche doctorale se concentre sur la recherche de molécules antibactériennes dans une ressource gaspillée très abondante.** J'ai ainsi l'intention de développer une nouvelle approche, innovante et sophistiquée, pour valoriser les coquilles du secteur alimentaire. A cette fin, j'ai extrait et **caractérisé les matrices organiques** de sept bivalves de consommation courante et j'ai réalisé un **criblage antibactérien** contre des **pathogènes marins**, en combinaison avec une approche **protéomique** sur les extraits de coquilles.

La structure de mon manuscrit se déroule comme suit : dans le chapitre suivant, le Chapitre II, je discute des différents systèmes de défense des bivalves, avant de me concentrer sur la description des coquilles des modèles que j'ai étudiés et de leurs microstructures. Ce chapitre se termine par l'établissement d'un inventaire exhaustif et actualisé de tous les peptides et protéines antimicrobiens (AMPP) identifiés dans les tissus mous des mollusques, en établissant un parallèle avec ma recherche doctorale de ces molécules dans les tissus calcifiés de la coquille. Le Chapitre III représente le point central et expérimental de ce manuscrit. J'y présente la mise en place du criblage antibactérien et l'analyse protéomique qui s'ensuit : les espèces modèles utilisées comme sources de molécules potentiellement bioactives, leurs cibles bactériennes et l'adaptation des protocoles de tests sur des micro-organismes marins. Ce chapitre comprend deux articles, l'un portant sur un protocole innovant permettant d'utiliser pour la première fois des composés insolubles de la matrice coquillière, et l'autre soumis pour publication, exposant les résultats positifs du criblage antibactérien. Le Chapitre IV regroupe les miscellanées : les données non publiées (résultats négatifs du criblage) et les phases intermédiaires des expérimentations. Ces données restent au cœur de ma thèse car elles fournissent des informations cruciales sur l'ensemble du criblage antibactérien et sur la culture de bactéries encore peu documentées. Dans le Chapitre V, je développe la discussion générale de ma thèse et je présente une vue d'ensemble des connaissances développées grâce au criblage antibactérien et à l'exploration protéomique des extraits de matrice coquillière. Je discute des limites de mon projet et des perspectives qu'il apporte en termes d'expériences supplémentaires

et de champs d'application potentiels. Enfin, le Chapitre VI est une annexe à mon projet de recherche doctorale. J'y insère deux articles auxquels j'ai collaboré de façon substantielle : l'un publié en 2023, explorant le domaine biomédical à travers les propriétés inductives ostéogéniques de la nacre ; et l'autre sur un nouveau procédé analytique combinant l'imagerie multispectrale et les gels électrophorétiques de pigments de coquilles de gastéropodes existants et fossiles (45 millions d'années).

CHAPITRE II : FOCUS SUR LES MECANISMES DE DEFENSES DES MOLLUSQUES

2.1. Les Mécanismes de Défense Intrinsèques des Mollusques

Pour introduire ce travail de criblage antibactérien au sein de tissus calcifiés des bivalves, il est important d'exposer les mécanismes de défense des mollusques qui sont mis en jeu dans le cadre d'une fonction antibactérienne. Les mollusques constituent l'un des groupes d'animaux les plus diversifiés. Ces organismes à corps mou sont largement répandus dans le monde, ayant colonisé divers écosystèmes - terrestres, marins et d'eau douce - tout en étant confrontés aux menaces de la prédation, de la dessiccation, des attaques de parasites et d'agents pathogènes. Pour survivre, les mollusques ont développé une série de mécanismes de défense adaptés à leurs niches écologiques et aux pressions environnementales locales. Au-delà des stratégies comportementales de survie, leurs défenses intrinsèques comprennent la protection physique par les coquilles, les défenses physico-chimiques par le mucus et les substances antimicrobiennes, et les réponses cellulaires par les hémocytes. Ce chapitre explore ces systèmes de défense intégrés et leurs synergies, avant de se concentrer sur les coquilles des bivalves modèles utilisés au cours de ce doctorat et sur les composants moléculaires identifiés dans les tissus mous des mollusques.

La coquille joue un rôle crucial dans la protection mécanique contre la prédation et les forces d'écrasement, tout en réduisant l'exposition aux parasites et en limitant la dessiccation. Elle sert également de support structurel, permettant aux mollusques de maintenir la forme et l'intégrité de leurs organes internes, et facilite la motilité via l'attachement musculaire (Lowell, 1984; Cortie, 1992; Ponder *et al.*, 2020a). Bien que la présence d'une coquille externe soit caractéristique de nombreux mollusques, ce trait n'est pas systématique au sein du phylum. Les coquilles "vraies" sont observées dans le sous-phylum Conchifera, comprenant cinq classes de mollusques à coquille. Cependant, certains clades ont secondairement internalisé ou même perdu leur coquille au cours de l'évolution. Les coquilles de mollusques sont principalement constituées de carbonate de calcium (95-99% du poids), avec une matrice organique

représentant 1-5%. Cette matrice, composée de diverses biomolécules, joue un rôle de régulation du dépôt minéral lors de la formation de la coquille, mais l'étendue de ses fonctions demeure à ce jour à découvrir (Weiner *et al.*, 1984; Nudelman *et al.*, 2006; Marin, 2020). Chez les conchifères, les coquilles sont généralement constituées de deux polymorphes de carbonate de calcium : l'aragonite ou la calcite. La structure de la coquille est caractérisée par des couches superposées de microstructures définies par des arrangements, des tailles et des directions cristallines spécifiques. Le type et l'organisation des microstructures présentes dans une coquille influencent sa solidité, sa flexibilité et sa durabilité (Marin *et al.*, 2012; Liang *et al.*, 2021).

Les trois mécanismes suivants font partie d'un système de défense chimique et cellulaire intégratif, qui est utile lorsque la protection de la coquille devient insuffisante ou chez les mollusques qui en sont dépourvus. Bien que tous les mécanismes de défense présentés dans ce chapitre interagissent et influencent les autres, le "mucus", les "défenses cellulaires" et les "sécurités moléculaires" sont particulièrement liés par des systèmes d'activations synergiques qui ont lieu dans tous les compartiments du corps de l'animal. Le mucus est une substance viscoélastique complexe, sécrétée par les mucocytes des tissus en contact avec l'environnement extérieur. Composé principalement d'eau et de glycoprotéines, il joue un rôle crucial dans la survie des mollusques, représentant jusqu'à 25% de leur budget énergétique. Il remplit de nombreuses fonctions physiologiques essentielles : il facilite la locomotion, aide à la rétention d'eau chez les espèces terrestres et intertidales, possède des propriétés antifouling et antimicrobiennes, et participe à la cicatrisation et à l'homéostasie. Il sert également de médium pour la migration des hémocytes et l'accumulation d'AMPPs, renforçant ainsi les défenses immunitaires. Sa composition et ses fonctionnalités varient selon les espèces et leurs environnements. Les défenses cellulaires sont assurées par les hémocytes, qui jouent un rôle central dans le système immunitaire inné des mollusques. Ces cellules mobiles, présentes dans l'hémolymphe et les tissus, se divisent en trois catégories selon leur taille et leur granularité. Leurs fonctions principales incluent la reconnaissance de particules étrangères, la signalisation immunitaire, le transport et la sécrétion de substances bioactives (toxines et/ou AMPPs), l'attaque directe des micro-organismes intrus (phagocytose, formation de nodules, encapsulation, mélanisation/biominéralisation) et la régulation de divers processus de réparation tissulaire (coquille, plaies, coagulation sanguine). Les défenses moléculaires des mollusques sont omniprésentes dans tout l'organisme et comprennent des molécules de reconnaissance, des protéines de signalisation et des effecteurs antimicrobiens. Les hémocytes jouent un rôle central en produisant, stockant, transportant et sécrétant ces composés défensifs.

Le système de défenses moléculaires inclut des lectines, des protéines à domaine fibrinogène et C1q, des enzymes lytiques, et la cascade de la phénoloxydase (PO). Les peptides / protéines antimicrobien(ne)s (AMPPs) sont particulièrement efficaces contre un large spectre de pathogènes. Certains mollusques ont développé des défenses moléculaires spécialisées et adaptées à leurs interactions interspécifiques : c'est le cas des venins neurotoxiques chez les gastéropodes ou des pigments permettant de produire de l'encre chez les céphalopodes. L'ensemble de ces mécanismes crée un environnement hostile aux envahisseurs potentiels, illustrant l'adaptation évolutive des mollusques à leurs niches écologiques. Les sections suivantes de ce chapitre approfondissent les aspects des défenses des mollusques qui font l'objet de ma recherche doctorale, à savoir les coquilles des espèces de bivalves étudiées ici et les AMPP présents dans les tissus mous des mollusques.

2.2. Les Bivalves et leurs Coquilles

J'établis dans cette section une description des caractères macroscopiques des coquilles qui ont été utilisées au cours de ma recherche doctorale et une illustration de leurs microstructures via des images de Microscopie Electronique à Balayage (MEB). Les illustrations macroscopiques ont été fournies par Jérôme Thomas (Biogéosciences) tandis que les images MEB ont été acquises par moi-même et par une stagiaire de Master, Marie Aries Lasseron qui a travaillé dans l'équipe Biominéralisation du laboratoire Biogéosciences de février à mai 2024. Pour les microstructures, j'ai vérifié que mes observations étaient en accord avec la littérature antérieure, en particulier Taylor *et al.* (1969, 1973) et Carter (1990). Ma thèse se base sur sept modèles de bivalves d'intérêt économique : quatre ptériomorphes que sont l'amande de mer *Glycymeris glycymeris*, la moule méditerranéenne *Mytilus galloprovincialis*, l'huître creuse du Pacifique *Magallana gigas*, la coquille Saint-Jacques *Pecten maximus*, ainsi que trois euhétérodontes que sont la coque commune *Cerastoderma edule*, la praire *Venus verrucosa* et la palourde japonaise *Venerupis philippinarum*.

2.3. Revue des Composants Antimicrobiens dans les Tissus Mous des Mollusques

Les mollusques sécrètent une variété de composés antimicrobiens comme effecteurs de leur système de défense chimique contre les microorganismes envahissants. Parmi eux, les peptides antimicrobiens (AMPs) sont de petites molécules cationiques à large spectre d'activité, qui peuvent être classés en trois catégories principales basées sur leurs caractéristiques structurelles : les AMPs riches en cystéine (comme les défensines), les AMPs riches en proline,

et les AMPs linéaires à conformation α -hélicale. L'étude des AMPs des mollusques est principalement limitée à leurs tissus mous, avec des disparités importantes dans l'identification des AMPs entre les espèces, en partie dues aux différences dans leur exploitation économique. Je choisis dans ma thèse d'utiliser le terme plus large de peptides et protéines antimicrobiens (AMPPs) pour englober la diversité des molécules impliquées dans le système immunitaire inné des mollusques, y compris les protéines et enzymes qui interagissent fréquemment avec les réseaux d'AMPs. Comme brièvement abordé dans la section 2.1, les AMPPs des mollusques présentent une grande diversité en termes de distribution, de nature et d'expression selon les espèces. Leur expression peut être généralisée dans l'organisme ou spécifique à certains tissus, constitutive ou modulée lors de réponses immunitaires. Les AMPPs remplissent diverses fonctions antimicrobiennes, notamment la destruction directe des pathogènes, l'activité anti-biofilm et des effets bactériostatiques ou fongistatiques. Ils agissent sur différentes cibles cellulaires et moléculaires, comme les membranes microbiennes ou les composants intracellulaires, et peuvent également jouer un rôle dans le déclenchement de l'élimination des pathogènes. Leur efficacité dépend généralement de leur concentration et certains AMPPs peuvent interagir entre eux ou moduler la sensibilité des pathogènes à d'autres AMPPs. Cette diversité fonctionnelle confère aux AMPPs d'origine 'mollusque' un potentiel prometteur dans diverses applications biomédicales : certains ont démontré des propriétés anticancéreuses, antivirales, analgésiques et cicatrisantes. Des activités antibactériennes ont également été observées dans quelques rares cas de coquilles de mollusques (Chen *et al.*, 2016 ; Terada *et al.*, 2017; Ahmad *et al.*, 2018). La présence d'AMPPs dans certains extraits minéralisés motive la recherche de ces composés dans les coquilles de bivalves commerciaux, largement produits et consommés. Dans cette section, je dresse la liste exhaustive des AMPPs de mollusques identifiés à ce jour, en Table 2.1, comportant les espèces sources, les espèces cibles et les éventuels mécanismes antimicrobiens identifiés.

CHAPITRE III : PROPRIETES ANTIBACTERIENNES DES EXTRAITS COQUILLERS

3.1. Introduction

Ce chapitre représente le cœur de la recherche expérimentale qui compose cette thèse, il est axé sur le criblage antibactérien de substances extraites des coquilles de bivalves d'intérêt économique. J'y expose les aspects techniques du protocole de criblage, puis je présente un article publié détaillant le protocole d'extraction de la matrice organique et les méthodes développées pour utiliser la Matrice Insoluble dans l'Acide (Acid-Insoluble Matrix, ou AIM, en anglais). Enfin, les résultats positifs obtenus lors du criblage sont inclus dans un article soumis à une revue internationale, tandis que les résultats négatifs sont présentés dans le Chapitre IV des 'Miscellanées'.

3.2. Criblage Antibactérien

Le criblage antibactérien est un processus systématique visant à identifier et évaluer des agents antibactériens potentiels. Dans le cadre de ma recherche doctorale, ce criblage s'inscrit dans un effort de bioprospection, se concentrant sur la ressource naturelle peu explorée que sont les matrices organiques des coquilles de bivalves (Valgas *et al.*, 2007; Cushnie *et al.*, 2020). Les méthodes de criblage antibactérien sont classées en trois catégories principales : 1) les méthodes de criblage initial (qualitatives ou semi-quantitatives), 2) les méthodes de criblage secondaire (quantitatives), et 3) les méthodes de criblage tertiaire (techniques avancées à haut débit). Chaque méthode offre des avantages spécifiques et présente des limitations en termes de coût, de temps et de ressources nécessaires (Hetru & Bulet, 1997; Balouiri *et al.*, 2016; Cushnie *et al.*, 2020; Massoud *et al.*, 2020). Des exemples tirés de la littérature illustrent l'application de ces méthodes de criblage aux organismes marins, notamment aux mollusques, démontrant le potentiel de ces animaux comme sources de molécules antimicrobiennes, motivant ainsi l'exploration des matrices organiques des coquilles de bivalves comme source potentielle de nouveaux agents antibactériens (Defer *et al.*, 2009; López-Abarrategui *et al.*, 2012).

Les sept modèles bivalves sélectionnés sont, comme décrits précédemment : *G. glycymeris*, *M. galloprovincialis*, *M. gigas*, *P. maximus*, *C. edule*, *V. verrucosa* et *V. philippinarum*. Le processus de nettoyage des coquilles et de production de la poudre qui sert de matériau de base à l'extraction de la matrice organique (OM) est décrit dans cette section. La table 3.1 expose les quantités d'OM extraites pour chaque espèce de bivalve. Les cibles bactériennes sélectionnées sont des pathogènes marins de la famille des Vibrionaceae, un choix

basé sur une revue approfondie de la littérature et des informations écologiques et ethnomédicales : *Aliivibrio salmonicida*, *Vibrio aestuarianus*, *Vibrio harveyi* LMG7890, *Vibrio harveyi* ORM4, *Vibrio mytili* et *Vibrio tapetis* CECT4600. En tant que bactéries marines, ces souches impliquent une adaptation minutieuse des protocoles expérimentaux à leurs conditions de vie, tant en termes de température (certaines étant psychrophiles, c'est-à-dire se développant dans des milieux froids) que d'hygrométrie (Rodrigues & de Carvalho, 2022). La détermination de ces paramètres a nécessité des tests préliminaires exposés dans le Chapitre IV. Deux types de tests sont réalisés pour le criblage antibactérien : un test 'classique' de diffusion sur disques (Bauer *et al.*, 1966), criblage initial permettant notamment de tester les propriétés de l'AIM (Lutet-Toti *et al.*, 2024), et un test de microdilutions sur plaques, criblage secondaire réservé aux Matrices Solubles dans l'Acide (Acid-Soluble Matrix, ASM) pour tenter de caractériser les mécanismes d'action antibactérienne des extraits (Zgoda & Porter, 2001 ; Rudilla *et al.*, 2018; Blazanin, 2024).

3.3. Détourner l'Usage d'une Presse Manuelle de Laboratoire pour des Tests de Bioactivité : Un Protocole Innovant pour Tester les Matrices Insolubles de « Déchets » Coquilliers

Article de protocole publié dans *Methods and Protocols* :

Lutet-Toti, C., Da Silva Feliciano, M., Debrosse, N., Thomas, J., Plasseraud, L., & Marin, F. (2024). Diverting the Use of Hand-Operated Tablet Press Machines to Bioassays: A Novel Protocol to Test 'Waste' Insoluble Shell Matrices. *Methods and Protocols*, 7(2), Article 2. <https://doi.org/10.3390/mps7020030>

Cet article décrit de manière détaillée un nouveau protocole permettant de tester la totalité des matrices coquillières. En effet, lorsque l'on extrait des matrices de coquilles, une fraction importante des extraits est totalement insoluble dans des solvants aqueux, ce qui limite fortement leur utilisation ultérieure pour des tests d'activité antimicrobienne. Dans notre article, nous présentons un protocole qui contourne cet obstacle technique. Après une extraction adaptée des protéines de coquille et la production de deux fractions organiques - l'une soluble, l'autre insoluble - nous utilisons une presse à comprimés manuelle pour générer des comprimés bien calibrés constitués à 100 % d'une matrice de coquille insoluble. Un contrôle FT-IR de la qualité des comprimés montre que la pression utilisée dans la presse n'altère pas les propriétés moléculaires des extraits insolubles. Les comprimés produits peuvent être directement testés dans différents essais biologiques, tels que l'essai de la zone d'inhibition bactéricide en boîte de Pétri. Le détournement de l'utilisation de la presse à comprimés manuelle ouvre de nouvelles

perspectives dans l'analyse des matrices de coquilles insolubles, pour la découverte de nouveaux composants bioactifs.

3.4. Les Coquilles de Bivalves Présentent-Elles des Propriétés Antibactériennes ? Criblage de Matrices Organiques Calcifiantes Contre Deux Pathogènes Marins Majeurs

Section calibrée comme un article de recherche originale, soumis à revue internationale : Science of the TOTal ENvironment (STOTEN).

Chez les mollusques, le processus de biominéralisation de la coquille est régulé par un ensemble de macromolécules, mieux connu sous le nom de matrice organique de la coquille. Les progrès récents des techniques "omiques" à haut débit ont montré que cette matrice est constituée de plusieurs protéines aux fonctions extrêmement diverses. Dans le présent article, nous montrons que certains extraits organiques - solubles ou insolubles - de la coquille de bivalves couramment consommés possèdent des propriétés antibactériennes contre deux pathogènes marins Vibrionaceae, *Aliivibrio salmonicida* et *Vibrio harveyi*, souche ORM4. Cet effet antibactérien est corroboré par l'identification formelle de plusieurs peptides antibactériens par protéomique, dans les différentes fractions de la coquille. Notre étude - la première de ce type - attire l'attention sur les coquilles de bivalves d'intérêt économique en tant que sources précieuses mais sous-estimées de substances antibactériennes, utilisables en aquaculture. Plus généralement, le recyclage des sous-produits de la coquille dans des applications à haute valeur ajoutée contribuera au développement d'une économie circulaire durable.

Les résultats positifs du criblage antibactériens sont exposés dans cette section, ainsi que ceux de l'analyse protéomique, qui a permis d'identifier de nombreux AMPPs au sein des coquilles des bivalves étudiés, il est d'ailleurs notable que la présence d'au moins un type d'AMPP soit détectée dans chaque extrait. Ceux-ci partagent une partie de leur séquence avec des AMPPs d'origines variées, des mammifères aux mollusques en passant par des arthropodes ou des anoures. Ce criblage des extraits par une approche protéomique a permis de détecter des AMPPs déjà identifiés dans d'autres systèmes. Nous n'excluons pas la possibilité que d'autres AMPPs, encore inconnus soient présents dans nos matrices mais non détectés car non-référencés dans les bases de données servant de référence aux interrogations protéomiques.

CHAPITRE IV : MISCELLANEEES

4.1. Résultats Négatifs du Criblage Antibactérien

Dans ce sous-chapitre, je résume les résultats négatifs et les données non publiées du criblage antibactérien susmentionné. Quatre des six pathogènes marins testés n'ont montré aucune sensibilité significative aux extraits : *V. aestuarianus*, *V. harveyi* LMG7890, *V. mytili* et *V. tapetis* CECT4600. Ces résultats négatifs peuvent s'expliquer par diverses raisons, notamment une résistance des souches aux substances antimicrobiennes, l'absence de composés antimicrobiens dans les coquilles testées, ou la nécessité d'une action synergique entre différentes fractions qui sont artificiellement séparées dans les tests de criblages. Les conditions expérimentales, en particulier les concentrations de molécules actives testées, pourraient également être à l'origine de ces résultats négatifs. En effet, nous ne pouvons exclure que les concentrations de nos extraits, utilisées pour nos tests, sont insuffisantes pour observer une quelconque bioactivité.

4.2. Caractérisation des Souches Bactériennes Marines : Sélection des Standards Antibiotiques et Analyse Générale de la Croissance Bactérienne

Cette section décrit les tests préliminaires effectués pour caractériser la dynamique de croissance des souches pathogènes marines utilisées comme cibles du criblage, avant de réaliser le test de microdilution avec les extraits ASM de coquilles. Ces tests préliminaires permettent de déterminer les conditions optimales de croissance de chaque souche, ainsi que les antibiotiques à utiliser comme standards ainsi que leurs gradients de concentrations (tétracycline, azoture de sodium ou agent vibriostatique v0129) en fonction de l'altération graduelle et progressive de la croissance bactérienne observée. Ces cultures ont été menées sur des temps d'incubation permettant d'apprécier l'entièreté de la courbe de croissance des bactéries, c'est-à-dire de leur prolifération à leur mort, en mesurant l'absorbance du milieu liquide. Trois longueurs d'ondes ont alors été mesurées (420 nm, 560 nm et 600nm) afin de sélectionner la plus adéquate au suivi de la dynamique de croissance bactérienne dans le cadre de tests avec des agents colorés. Ces tests ont ainsi permis de déterminer les intervalles de mesure d'absorbance, d'estimer les durées idéales d'incubation et de disqualifier l'agent vibriostatique v0129 en tant que standard antibiotique dans les tests de microdilution en raison de ses propriétés acidifiantes intrinsèques qui interfèrent avec l'indicateur de pH utilisé dans les essais.

CHAPITRE V : DISCUSSION GENERALE

5.1. Récapitulatif des Activités de Recherche Effectuées au Cours du Doctorat

Ces trois ans de recherches doctorales marquent la première exploration des agents antibactériens dans les coquilles des bivalves - plutôt que dans les tissus mous - ciblant spécifiquement des pathogènes marins. Ce projet innovant a impliqué l'extraction des matrices organiques (OM) des coquilles de sept espèces de bivalves, suivie d'une caractérisation biochimique par analyse de gels d'électrophorèse. La composante expérimentale - et donc centrale - de ma thèse est représentée par une étude bioprospective, un criblage antibactérien des extraits coquillers contre six souches bactériennes marines. Ce criblage a consisté en deux tests complémentaires : un test de diffusion sur disque et un test de microdilution en culture liquide. Enfin, une analyse protéomique a été effectuée pour détecter la présence d'AMPPs connus dans les extraits et tenter d'établir des corrélations avec la bioactivité observée.

5.2. Limitations du Projet

Au cours de mon doctorat, et de par sa nature interdisciplinaire et exploratoire, j'ai rencontré plusieurs difficultés qui ont limité certains aspects de mes recherches. La production de poudres décontaminées et l'extraction des matrices organiques se sont révélées être des processus longs et fastidieux, limitant les quantités de matériel biologique disponible pour les tests. La culture de bactéries marines peu caractérisées s'est révélée particulièrement ardue, nécessitant des installations spécifiques pour garantir des conditions de croissance idéales et des adaptations de toutes les techniques et protocoles expérimentaux. Ainsi, les milieux de cultures adaptés aux souches marines, leurs dynamiques de croissances, leurs sensibilités aux substances mais aussi l'aspect intrinsèque de leurs cellules ont imposé des contraintes expérimentales avec lesquelles il a fallu composer pour s'adapter, voir accepter en tant que limite du projet. L'absence de standards établis pour ces pathogènes marins a nécessité de nombreux essais pour optimiser les protocoles expérimentaux et ne permet aujourd'hui pas encore de comparer mes résultats de façon aussi complète que ce qui peut être fait avec des souches dites « classiques » (*E. coli*, *Bacillus spp.* etc...). Le manque de données sur les modèles étudiés a également engendré des limitations dans l'analyse protéomique, notamment par l'omission probable de peptides non renseignés dans les bases de données mais bien présents dans nos extraits. Les quantités d'OM extraite ont également été limitantes dans la nature de l'analyse protéomique effectuée : qualitative (détection ici) plutôt que quantitative (donnant les proportions dans les OM, information intéressante pour déterminer d'éventuelles synergies des AMPPs).

5.3. Compilation de Tous les Résultats du Criblage Antibactérien

Les résultats des deux tests de criblage antibactérien, la diffusion sur disques et la microdilution, sont résumés dans la Table 5.1, qui couvre à la fois les résultats positifs et négatifs des Chapitres III et IV. Je compare dans cette section les résultats en fonction des souches bactériennes et des espèces de bivalves, apportant des hypothèses quant aux différences observées, notamment celle d'un cas entrant dans la théorie de la Reine Rouge : pour survivre, le bivalve hôte développerait des parades contre un pathogène agressif fréquemment rencontré, associant forte virulence et sensibilité dudit pathogène aux extraits coquilliers (Decaestecker & King, 2019).

Les résultats étant complexes et nombreux, je résume ici quelques-uns d'entre eux, qui me semblent les plus représentatifs de ma thèse. En effet, *A. salmonicida* et *V. harveyi* ORM4 présentent le plus de sensibilité aux extraits coquilliers, tandis que les autres souches ne sont affectées que par un ou deux AIM, appartenant à *M. gigas* et *P. maximus*. Ces deux bivalves sont les modèles du criblage démontrant du plus d'effets antibactériens, avec parfois une observation de réponses bactériennes très similaires entre les deux espèces. L'AIM de *C. edule* se démarque en produisant la plus large zone d'inhibition de croissance d'*A. salmonicida*. L'analyse protéomique de cet extrait met en lumière sa composition singulière d'AMPPs au sein des autres bivalves, qui pourrait expliquer cet effet particulier. Autre fait notable, les AIM de *C. edule*, *G. glycymeris* et *V. verrucosa* ont un effet particulier sur *V. harveyi* ORM4, produisant des couronnes blanchâtres frangeant les zones d'inhibition, possiblement dus à des facteurs diffusibles. Ces trois bivalves sont les seuls à montrer une inhibition de la croissance d'ORM4 autour des poudres de coquilles, ce qui suggère la présence de composés antibactériens puissants et/ou en quantité suffisante dans la matrice organique des coquilles « brutes », dont l'effet n'est pas limité par leur occlusion dans les structures carbonatées. En analysant les résultats du second test de criblage (microdilution), on observe que *M. galloprovincialis* est le seul bivalve impactant les deux paramètres de croissance d'*A. salmonicida*.

Les tests de microdilution révèlent que certains extraits ASM altèrent significativement les paramètres de croissance bactérienne (taux de croissance maximal et capacité de charge). Les extraits semblent à première vue bactériostatiques, inhibant la croissance bactérienne et limitant la prolifération en les plaçant dans un état de stase. Cependant, l'hypothèse d'effets bactéricides des extraits coquilliers n'est pas exclue : comme abordé précédemment, les limites expérimentales rencontrées lors de ce criblage peuvent impliquer que la Concentration Bactéricide Minimale (MBC) n'ait pas été atteinte pour certaines substances lors de nos tests.

L'analyse protéomique des extraits a permis d'identifier de nombreux AMPPs au sein des coquilles des bivalves étudiés, il est d'ailleurs notable que la présence d'au moins un type d'AMPP soit détectée dans chaque extrait. Ceux-ci partagent une partie de leur séquence avec des AMPPs d'origines variées, des mammifères aux mollusques en passant par des arthropodes ou des anoures. La détection d'AMPP venant de ces derniers, spécifique à certains extraits, intrigue quant à leur nature et suggère une forme de spécialisation accrue des bivalves aux pathogènes. L'ensemble des résultats de l'analyse protéomique semble révéler de potentielles combinaisons d'AMPPs au sein des extraits, ce qui encourage l'hypothèse de modes d'action synergiques de ces derniers.

5.4. Perspectives

Les résultats obtenus s'inscrivent dans plusieurs perspectives d'applications prometteuses, notamment dans les domaines de l'aquaculture, de la sécurité alimentaire et de la conservation environnementale. La mise en évidence de propriétés antibactériennes contre des pathogènes marins dans les extraits de coquilles de bivalves issus du secteur alimentaire encourage la recherche d'applications dans la lutte contre l'antibiorésistance, dans une meilleure conservation des produits de la mer lors de leur transport, la diminution de l'usage de produits toxiques dans les systèmes d'aquaculture ou dans les antifoulings, et même dans la conservation du patrimoine attaqué par certaines souches. Dans un contexte où les défis environnementaux et sanitaires s'intensifient, il est particulièrement intéressant de chercher des solutions innovantes d'origine naturelle parmi des ressources qui étaient jusque là ignorées, les coquilles de mollusques d'intérêt économique.

5.5. Conclusion

Pour conclure, ma thèse de doctorat se caractérise par une approche interdisciplinaire, couvrant des domaines variés tels que l'histoire de l'art, l'ethnobiologie, la biominéralisation, la biologie moléculaire, la bioinformatique et la microbiologie. Mes recherches expérimentales se sont concentrées sur un criblage antibactérien de coquilles de bivalves d'intérêt économique, appliqué aux pathogènes marins Vibrionaceae, et complété par une exploration protéomique antimicrobienne. Les résultats de mes recherches mettent en évidence une activité antibactérienne de *Magallana gigas* et *Pecten maximus* contre plusieurs de ces pathogènes, ainsi que celle de *Cerastoderma edule* contre *Aliivibrio salmonicida*. Dans le cas de *V. harveyi* ORM4, souche représentant à la fois la bactérie la plus virulente et la plus sensible du criblage,

j'émets l'hypothèse d'une course à l'armement entre bivalves hôtes et pathogènes, suivant la théorie de la Reine Rouge. Ce projet exploratoire apporte de nouvelles perspectives dans l'expérimentation sur les bactéries marines et la bioprospection des ressources naturelles, établissant des normes utiles pour de futures explorations impliquant ces organismes.

CHAPITRE VI : ANNEXE COMPILANT DEUX ARTICLES RESULTANT DE COLLABORATIONS SCIENTIFIQUES

6.1. Collaboration avec Sarah Nahle : Application Biomédicale de la Nacre dans la Minéralisation Ostéoblastique

Article de recherche originale publié dans Marine Biotechnology :

Nahle, S., Lutet-Toti, C., Namikawa, Y. *et al.* Organic Matrices of Calcium Carbonate Biominerals Improve Osteoblastic Mineralization. *Mar Biotechnol* 26, 539–549 (2024). <https://doi.org/10.1007/s10126-024-10316-w>

De nombreux organismes incorporent des solides inorganiques dans leurs tissus afin d'en améliorer les propriétés fonctionnelles et mécaniques. Les tissus minéralisés qui en résultent sont appelés biominéraux. Plusieurs études ont montré que les biominéraux nacrés induisent une minéralisation extracellulaire ostéoblastique. Parmi eux, *Pinctada margaritifera* est bien connue pour la capacité de sa matrice organique à stimuler les cellules osseuses. Dans ce contexte, nous avons voulu étudier les effets des extraits de coquilles de trois autres espèces de *Pinctada* (*Pinctada radiata*, *Pinctada maxima* et *Pinctada fucata*) sur la minéralisation de la matrice extracellulaire ostéoblastique, en utilisant un modèle *in vitro* de cellules précurseurs ostéoblastiques de souris (MC3T3-E1). Pour mieux comprendre la relation *Pinctada*-minéralisation osseuse, nous avons évalué les effets de 4 autres mollusques nacrés qui sont phylogénétiquement éloignés et distincts du genre *Pinctada*. En outre, nous avons testé 12 mollusques non nacrés et un groupe supplémentaire. Des poudres de coquilles biominérales ont été préparées et leur matrice organique a été partiellement extraite à l'aide d'éthanol. Tout d'abord, l'effet de ces poudres et extraits a été évalué sur la viabilité des cellules MC3T3-E1. Nos résultats indiquent que ni la poudre ni la matrice soluble dans l'éthanol (ESM) n'affectent la viabilité cellulaire à de faibles concentrations. Nous avons ensuite évalué la minéralisation ostéoblastique à l'aide de la coloration au rouge d'Alizarine et nous avons constaté que la minéralisation de MC3T3-E1 était principalement induite par les biominéraux nacrés, en particulier ceux qui appartiennent au genre *Pinctada*. Cependant, quelques biominéraux non nacrés ont également été capables de stimuler la minéralisation extracellulaire. Dans l'ensemble,

nos résultats valident la capacité remarquable des extraits de biominéraux CaCO_3 à promouvoir la minéralisation osseuse. Néanmoins, d'autres études *in vitro* et *in vivo* sont nécessaires pour identifier les mécanismes d'action des biominéraux dans l'os.

6.2. Collaboration avec Luca Polacchi : L'Électrophorèse sur Gel Couplée à la Photoluminescence Révèle des Biochromes Complexes dans les Coquillages Modernes et Fossiles

Section calibrée sous forme d'article de recherche originale, soumis à revue internationale : Methods in Ecology and Evolution

L'électrophorèse est couramment utilisée pour visualiser les mélanges de protéines, tels que ceux qui sont occlus dans les biominéraux calcaires. Cependant, elle est inefficace pour détecter les biochromes, une classe importante de composés organiques de faible poids moléculaire communément associés aux exosquelettes calcifiés. Nous décrivons une nouvelle approche basée sur le couplage entre l'électrophorèse et l'imagerie spectrale de luminescence pour révéler les biochromes invisibles, les identifier chimiquement, mettre en évidence leur possible interaction putative avec les macromolécules de la coquille et, enfin, en obtenir de grandes quantités. Notre protocole repose sur trois étapes clés : une extraction douce à partir de poudre de squelette nettoyée (étape 1) ; un fractionnement électrophorétique optimisé immédiatement suivi par l'acquisition directe d'images spectrales sur gel avant la coloration classique du gel (étape 2) ; une purification à grande échelle par électrophorèse préparative couplée à l'imagerie spectrale de luminescence, afin d'obtenir des quantités significatives de biochromes d'intérêt (étape 3). Les étapes 1 à 3 ont été appliquées avec succès à des extraits de coquilles de gastéropodes récents, tandis que les étapes 1 et 2 ont été appliquées à des coquilles fossiles. Notre protocole a permis l'identification directe et non invasive sur gel des molécules de porphyrine, même à l'état de traces. Au-delà des biominéraux de carbonate de calcium, elle ouvre de nouvelles voies pour l'étude d'une large gamme de composites biologiques, minéralisés ou non, qui contiennent des biochromes luminescents. Elle est particulièrement adaptée aux spécimens anciens et aux fossiles, en vue de retracer l'origine et l'évolution des complexes de biochromes dans les archives géologiques.



CHAPTER 1 - INTRODUCTION



1.1. Introduction

Since the emergence of civilization in the Near Eastern region, human beings have always sought to settle near the coast. Because of the evident benefits that accrue from having a direct access to seas and oceans, human settlements have been more concentrated in the coastal zone than elsewhere and this tendency is massively increasing today as the world population is growing. An estimation by the United Nations Environment Programme (UNEP) indicates that about 40% of the world's population lives within 100 kilometers of the coast. This percentage reaches 60% if one considers a zone of 150 kms. Significantly, among the twenty largest cities in the world, thirteen (Tokyo, Shanghai, Sao Paulo, Mumbai, Osaka, New-York City, Karachi, Buenos Aires, Istanbul, Kolkata, Manila, Lagos, Rio de Janeiro) have a coastal location. As population density and economic activity in the coastal zone increases, the environmental pressures on coastal ecosystems become more severe. No region in the world escapes this threat, particularly in Europe and around the Mediterranean basin, an extremely busy Sea becoming increasingly vulnerable each year.

Beside favoring the possibility of long-distance export of local goods via maritime transport, coastal environments offer practical solutions to big-sized human settlements in term of immediate food availability. Coastal fishing, offshore fishing and aquaculture facilities are the main providers of sea food, including fishes, sea urchins, crustaceans, mollusks and algae. In this list, mollusks come as a major source of proteins, mineral salts and oligo-elements, the benefits of which were recognized very early in humankind history. Indeed, the first traces of mollusk consumption date back more than 100.000 years (see section [1.3. Molluscan Aquaculture](#)). Nowadays, because mollusks can be harvested or grown in huge amounts, they represent an indispensable food resource all over the world, especially in Asia and Europe, but food consumption is not the sole way to use them: indeed, since prehistory and antiquity, the external protection organ of mollusks, the shell, has been recycled and utilized for all kinds of purposes, from aesthetical to practical via cultural uses, an aspect that I treat in this chapter, in the next section ([1.2. From Ornaments to Biotechnologies](#)). The shell is a biomineralized exoskeleton and, as such, exhibits peculiar properties due to its organo-mineral nature. Indeed, the organic fraction, also called shell matrix, a mixture of macromolecules comprising proteins and sugars, is secreted and gets occluded during the shell formation. Several fundamental studies have evidenced the molecular complexity of the shell matrix, which comprises a wide range of unsuspected functions, not necessarily associated to the biocalcification process. In few words, the shell has become a potential source of components of interest in several fields

of applications, including biomaterials, health or environment. Searching for “useful molecules in shells” is particularly relevant since the volumes of empty shells following consumption are considerable: one estimates that around 10 million tons of shells coming from consumed oysters, clams, scallops, mussels are produced each year at world scale and a large proportion of this waste materials is totally unexploited (Topić Popović *et al.*, 2023). In addition, these huge concentrations of waste induce environmental and societal nuisances (Morris *et al.*, 2019). In the present manuscript, I revisit the use of waste shells, in the perspective to develop an innovative field of application: the use of antimicrobial substances from shells of economic interest. To this end, I have extracted and characterized several shell matrices and finally set up two types of antibacterial assays, complemented by a proteomics approach. My research can find applications in aquaculture, health and environmental conservation. It takes place in the frame of the pluriannual FishMed-PhD program (Innovative Technologies and Sustainable Use of Mediterranean Sea Fishery and Biological Resources) piloted by the University of Bologna. Generally speaking, this program is part of a search for setting up a virtuous circular economy, committed to generate sustainable sectors of food production, health and waste management.

Before even presenting some of the experimental results I have acquired during these last three years, I want to share with the reader of this manuscript an extended introduction, in which I paint the picture of the multiple uses of shells through the ages (section 1.2) and review the production of mollusks and list the current challenges of this industry (section 1.3). Then, I conclude chapter one by exposing the general plan of the practical part of my work (section 1.3). Note that section 1.2 is calibrated as a review paper that is submitted.

1.2. From Ornaments to Biotechnologies: The Evolution of Mollusk Shell Uses Through the Ages

Submitted in 2025 to Journal of Ethnobiology, SAGE Editions

Lutet-Toti, C.^{1,2}, Thomas J.¹, Falini, G.², Goffredo, S.³, Gabillot, M.⁴, and Marin, F¹.

1 UMR CNRS-uB-EPHE 6282 ‘Biogéosciences’, Université de Bourgogne, Dijon, France.

2 Dipartimento di Chimica “Giacomo Ciamician”, Alma Mater Studiorum Università di Bologna, Bologna, Italy.

3 Dipartimento di Scienze Biologiche Geologiche e Ambientali, Alma Mater Studiorum Università di Bologna, Bologna, Italy.

4 UMR CNRS-UBE 6298 ‘ARTEHIS’, Université de Bourgogne Europe, Dijon, France.

* Correspondence: frederic.marin@u-bourgogne.fr; camille.lutet-toti@u-bourgogne.fr; Tel.: (33) 7 69 50 27 12

Abstract

Mollusks have always represented an important source of food for human beings. A by-product of mollusk consumption is the shell, the mollusk skeleton made of calcium carbonate. Instead of being simply considered as a waste material, the mollusk shell has always been repurposed or recycled for many different applications. This review lists the different uses of mollusk shells over thousands of years, from the Paleolithic times to now. For clarity, we have grouped the uses in ten themes: ornaments and decorative items, derived shell products of pearl industry, religious symbols and amulets, musical instruments and signaling, shell representations in art, currency and wealth, practical applications, shells in medicine, recent and future applications. As shells are organo-mineral composites, they constitute an immense reservoir of potentially bioactive macromolecules that need to be investigated. The development of high added value applications based on the exploitation of shells represents a fascinating prospect for the coming times, which fits into the general frame of a virtuous circular economy, committed to generate sustainable sectors of food production, health and waste management.

Keywords: seashells; mollusks; human applications; recycling

1.2.1. Introduction

“I’m going to throw away my find (a shell, NDA) like one throws away a burnt cigarette. This shell has served me, exciting in turn what I am, what I know, what I don't know... Like Hamlet picking up a skull from the loam, and approaching him to his living face, looks at himself frightfully sows in some way, and as it enters in a meditation without exit, which is limited everywhere by a circle of astonishment, thus, under the human gaze, this little hollow limestone body and spiral calls around you quantity of thoughts, none of which comes to an end” ... This is how the French novelist, poet and philosopher Paul Valéry (1871-1945)

concludes his meditation (“L’Homme et la Coquille et Autres Textes”, *i.e.*, “The Man and The Shell and Other Texts”, 1937) based on the observation of the spiral shell of a gastropod found on the seashore.

The mollusk shell has always exercised a power of fascination over human beings. It is charged with symbols that go well beyond the soft body it encloses and its use as food. It concentrates indeed different properties that made it attractive for repurposing. First of all, shells are aesthetic objects in shape and in color; for some of them - the nautilus, the land snail, the tiger cowrie – the combination of remarkably regular shapes and surprisingly colored patterns makes them classified among the most beautiful objects of Nature. Secondly, they are hard objects, of superior mechanical properties, ‘not easy to break’, the colors of which are stable and stand the test of time; this extended lifespan, far above that of a man, is of major importance when shells are considered as religious symbols or perennial ornaments. Thirdly, shells are made of an abundant raw material, calcium carbonate, which, while compact and solid, is rather easy to work: indeed, it can be pierced, abraded, polished and sculpted; in short, shells can be embellished, manufactured and transformed. At last, shells are not only mineral objects but contain an organic fraction, which, in recent applications, is central in their repurposing. Due to these properties, empty shells have been reused since the prehistoric times, in several manners.

In this context, our interdisciplinary review aims at covering and describing, as exhaustively as possible, all the uses and reuses of mollusk shells by humans, throughout times and geographical space. We have collected data and documentation from several sources, including excavation reports (in archaeology), museum catalogues of art, expedition journals, generalist books and treatises, research papers in sciences, social sciences and humanities, reports of governing institutions or of associations for the environment protection. As the uses of shells are extremely diversified, we grouped them in four themes that are: 1) Aesthetic, religious and cultural uses, past & present; 2) Practical uses, past & present; 3) Traditional medicinal and pharmaceutical uses, past & present; 4) Recent and future applications. For this last part, we will see that the repurposing of shells can be an asset in the context of global warming and environmental changes. We will also emphasize the fact that shell reuse can lead to applications of high added value, in particular in the fields of biomaterials, health and zootechnics.

1.2.2. Aesthetic, Religious and Cultural Uses, Past and Present

1.2.2.1. Paleolithic times

Personal ornaments made from shells have a rich history dating back to the earliest evidence of human symbolic behavior. The oldest records of beads belong to *Tritia gibbosula* gastropods shells from the Middle Paleolithic era in Morocco (Bizmoune cave), more than 142,000 years ago (Sehassseh *et al.*, 2021). To date, these shells are considered as the first evidence of a calcareous material of marine origin to be likely consumed and recycled as ornaments. They were intentionally perforated – minute flint drill stones were found on the site - and used as “beads”, according to the broadest definition, *i.e.* ‘small artifact that is perforated and suitable to be used as adornment’ (Bar-Yosef Mayer, 2015). During the same period (Middle Paleolithic), 50,000 years ago, Iberian Neanderthals of the Cueva de los Aviones deposit used pierced shells of *Acanthocardia*, of *Glycymeris* and of *Spondylus*, decorated with red and black mineral pigments, in what seems to have been body ornaments (Zilhão *et al.*, 2010). The Upper Paleolithic period saw one of the first widespread occurrences of personal ornamentation, with the use of shell beads emerging simultaneously on three continents (Kuhn *et al.*, 2001). This global phenomenon suggests a consistent availability of the shells and a significant leap in human social development. A striking example of shell use in ornamentation comes from the Grimaldi grave, 11 130 year-old (Late Epigravettian), where two children were found in association of thousands of pierced shells of the marine gastropod *Cyclope neritea*. These shells were probably embroidered to garments covering the abdominal region, such as loincloths or tunics (Henry-Gambier *et al.*, 2001; Plankenhorn-Farrell, 2023). In this specific example, shells were associated with funeral rites.

The major symbolic significance of shell ornaments is undoubted in various cultures across time. In South Africa, 46 000 years old beads found in Sibudu Cave show no signs of wear, suggesting a purely symbolic use rather than practical adornment (Vanhaeren *et al.*, 2019).

1.2.2.2. Mesolithic Iron Age

As human societies progressed through the Mesolithic and into the Neolithic period, the use of shell beads became more sophisticated. In Mesolithic Serbia, *Cyclope neritea* beads were added to embroidery, with evidence of prolonged use indicated by wear patterns (Cristiani & Borić, 2012). *Nassa* snails remained particularly popular for creating beads, with archaeological evidence spanning from South Africa to Morocco (Bar-Yosef Mayer, 2015; Vanhaeren *et al.*, 2019). The evolution of beading techniques, including organized processing, fine crafting, and

painting symbols on shells, has been used to trace the development of modern human behavior and symbolism (Henshilwood *et al.*, 2004; Tsoraki *et al.*, 2020). In European Neolithic times, a unique form of shell ornamentation emerged: “Doppelknöpfe”, translated as “double buttons”. These double buttons had a diameter of about half a centimeter and exhibited in their thickness a groove that allowed their simple seamless insertion in holes pierced in skin clothing. Note that this prehistoric feature may be somehow considered as the ancestor of the well-known tradition of “pearlies”, popular in the London working class (with the exception that “pearlies” sew nacre buttons on their jacket). These standardized, pearl-like ornaments were likely used as decorative additions to clothing (Sakalauskaite *et al.*, 2019), likely worn only during special occasions: ceremonies or religious rituals. A tunic could carry dozens to hundreds of these double buttons, aligned or forming geometric motives. The way these ornaments were fabricated was extremely sophisticated: first ribbons of nacre were cut from shells, then they were cut perpendicularly in minute cubes the top of which were polished and rounded by abrasion. Finally, a groove was obtained around the perimeter of the bead by maintaining it on its two flat sides and abrading the tiny cylinder with a thin abrading thread. Interestingly, for a long time, it was thought that the raw material used for making double buttons was coming from marine sources (Mediterranean Sea) and was the subject of long-distance exchanges across Europe. A recent study on three archaeological sites (Danish, German and Romanian) combining proteomics and geochemistry (Sakalauskaite *et al.*, 2019) demonstrated unequivocally that in each case the raw material was the nacre of freshwater Unionoid bivalves, found in the rivers at the vicinity of the three archeological sites. This finding destroyed the hypothesis of long-distance exchanges of raw materials in this specific case (which did not prevent long-distance exchanges of shells in other cases). What is particularly interesting to notice is that while the raw material was common and found locally, the sophisticated fabrication technique was exported throughout Europe. What made “doppelknöpfe” of high price was less the raw material itself than the hours spent to produce each of these remarkable flat pearls.

In the Early Iron Age Kazulu Natal region of South Africa, disk beads made from marine and freshwater mollusk shells were used for necklaces and decorations (Beukes, 2000). The cultural importance of shell ornaments persisted into later periods. In Ukraine’ Saltiv culture, during the late Iron Age, cowries and freshwater mussels were used to make pendants and ornaments. Mostly found in the burials of children and women of childbearing age, these ornaments adorned hair (hairbeads), headwear, clothes, and even bags (Aksionov, 2022).

1.2.2.3. *Antiquity to Middle Age*

Another species frequently used for ornaments in the Mediterranean basin was *Spondylus gaederopus*, the thorny oyster (also called the spiny oyster). The shell of this bivalve combines two advantages: it is extremely thick, compact and solid and exhibits contrasted colors, with an upper valve uniformly dark red, and the lower one, of an immaculate whiteness (Sakalauskaite *et al.*, 2020). Artefacts (rings, buttons, tubes, beads) made from this shell are widespread in Neolithic times in Europe, indicating that they have been traded and exported from the Mediterranean Sea (Adriatic and Aegean Sea) to the North of the continent (Halstead, 1993; Windler, 2019).

The manufacture of shell ornaments continued into later periods, such as the early Mississippian culture on the Georgia coast (800-1200 CE), where whelk and oyster shell beads, pendants, and gorgets were produced using micro-drilling techniques (Pearson & Cook, 2008).

In Egypt, cowrie shells have a particularly long history as popular ornaments showcasing social status: the earliest traces date back to the Epipaleolithic and continue in pre-dynastical tombs, through pharaonic dynasties and to the late iron ages (Golani, 2014).

Pre-Columbian civilizations also used shells for body and architectural ornaments: similarly - but in a completely independent manner - to what happened around the Mediterranean basin, shells of the genus *Spondylus* were also utilized by South American Pacific cultures since the third millennium BC until the 17th century (Lodeiros Seijo *et al.*, 2018). This peculiar example illustrates how remarkably convergent were the aesthetic concerns of populations which never came into contact, on both sides of the Atlantic Ocean. At last, in 16th century Huatulco, Mexico, shell ornamentations, beadings, and decorations were even integrated into common architecture (González, 2002).

1.2.2.4. *Modern Era*

The prestige associated with shell ornaments persisted throughout the 17th century, as an intercontinental trade of shell products flourished. Nacreous shells were heavily (and often unsustainably) traded alongside gold and diamonds among wealthy societies (Buck & Hiroa, 2003; Susanto, 2023). The development of the Dutch East and West India companies quickly established Amsterdam as Europe's primary market for nacreous shells, gathering traveling collectors from around the world. Nautilus shells are a prime example of such precious shell products, which propagation was facilitated by maritime trade: originating from the Indo-Pacific region (in particular, Indonesia), they were highly prized for their rarity and exoticism

(Jalšovec, 2023). In Europe, they found their way into curiosity cabinets, where artisans decorated them through various techniques. These included engraving, painting, and carving intricate representations of flowers, mystical creatures, and scenes in relief on the shell surface. The vivid orange-striped periostracum (outer layer) was often incorporated into designs (wall papers, tapestries). A large majority of these nautilus shells were crafted into decorative containers with precious metal lids and holds (Fig. 1.1, A & B) (Susanto, 2023). The marine origins and intriguing shapes of these decorated shells sparked curiosity: often described as “liminal objects at the intersection of art and nature”, they were inspirations in the quest for naturalistic knowledge. Initially appreciated predominantly for their aesthetic appeal, nautilus shells, and more generally molluscan shells soon became integral to scientific collections and the systematic study of nature (Jalšovec, 2023).

In parallel to the development of these artistic objects which marked the belonging to a noble and wealthy class, the marquetry activity reached its peak between the 17 and the 19 centuries. It consisted in inserting polished pieces of elephant ivory or of mollusk shell – with geometric or more complex shapes - in furniture, mostly of precious exotic wood. This activity, performed in cabinetmaking workshop all over Europe, provided a wide range of furniture, such as dressers, desks, bedside or coffee tables, chests of drawers, sideboards, wardrobes, chests or large boxes. The shell raw material used for marquetry work originated preferentially from few types of nacreous shells, mostly imported from Asia or Oceania: first of all, the abalone gastropod *Haliotis*, highly recognizable by its inserts of greenish reflections, but also the pearl oyster *Pinctada*, which color varies from light grey to dark brown and, at last, the freshwater mussel *Hyriopsis*, which gave white to pinkish nacre inserts.

1.2.2.5. Contemporary Era

The symbolic significance of shells and shell products persisted throughout time and still serve as a connection of communities to cultural heritage and practices (González, 2002). A market for rather aesthetic oriented uses for shells or shell materials has developed from the eighteenth to the twenty-first century, in particular in Europe, Asia and North America. This industry consisted in four types of objects: full shells transformed or not, polished pieces of shells as incrustations in other materials (like wood or metal) to form bigger objects, shells glued together and finally, cut and polished pieces of shell to make buttons. In the first category, one finds all kinds of boxes, in particular, those made of mother-of-pearl: purses, pill boxes, snuff boxes (Fig. 1.1, C-G), rosary boxes or even nacreous fly boxes, very common in the

French noble female society of the 18th century. One has also to mention the specific use of flat rounded valves of the South-East Asian oyster *Placuna placenta*, the particularity of which is their transparency. These shells were and still are used for making composite boxes, coasters or even crystal-clear sound mobiles. This first category comprises also mother-of-pearl cutlery (mostly forks and spoons), extremely popular among the nobility, used more as decorative objects than as kitchen utensils.

The second category encompasses all the marquetry work on furniture, as described in the previous paragraph, an activity that continued in the twentieth century. Beside marquetry, properly speaking, another curiosity, well diffused and popular during the 19th century, consisted in theater binoculars which body was made of nacre plates glued or inserted on a metal frame.

The third category was represented by a wide range of objects, consisting of full shells glued together or glued with other metallic or wooden objects: ashtrays, lampshades, boxes. Enter this category souvenirs of coastal localities, such as boxes made of hundreds of tiny shells glued together, characters made of shells, miniature landscapes made of shell, country or marines scenes sculpted from shells, and so on.... Many of these objects, that are synonym of 'kitsch', were extremely popular along the 20th century and, in a certain way, are still popular, but their wide distribution all over the world poses the problem of resource management.

Finally, the nacre button industry was extremely flourishing all over Europe. In France, the village of Méru (Oise, 40 kms north of Paris) became, at the end of the nineteenth century, the world capital for mother-of-pearl buttons and probably the most important center of production of nacreous objects in Europe. The company counted up to 150 workers ("les tabletiers") in the early fifties. Today, the company comprises 35 employees and still produces nacreous buttons and other ornamental items like boxes and furniture with nacreous inlays.

Here and there in touristic coastal places, shops selling exclusively shell souvenirs are legion (Fig. 1.1, C & D). However, the growing demand of shell goods in the tourism and souvenir industry raises concerns about overexploitation of protected species (Nijman, 2019). As a result, these mollusk shells are under sustained collection pressure, with harvesting of shells both washed up on shore and in the water, often involving poaching. Such practices dysregulate mollusk populations but also the broader beach ecosystems that rely on empty shells.

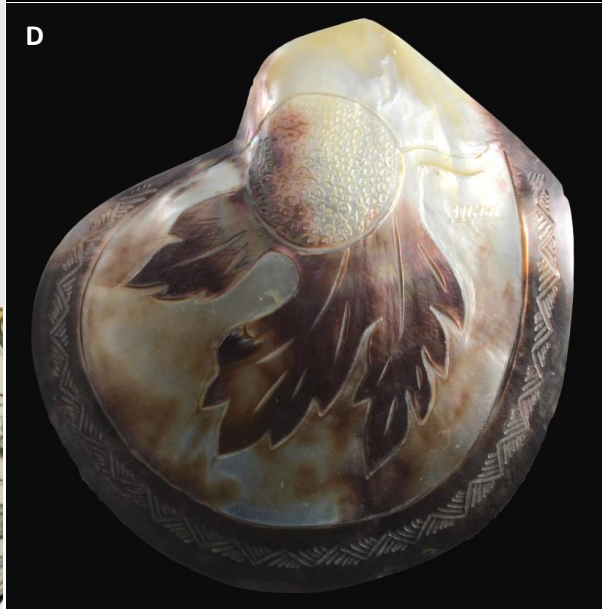


Figure 1.1: Collection of decorative objects made from mollusk shells. A: ‘The Frewen Cup’ by John Plummer of York, polished and engraved, depicting marine life and floral motifs and silver-gilt mounts, *circa.* 1650 (engraved) 1658-1660 (mounts). On display in Victoria and Albert Museum, London, United-Kingdom; B: Naturalistic detail of the reverse side of the ‘Frewen Cup’; C: Souvenir tray from Portugal; D: Souvenir decoration depicting a coconut on a pearl oyster shell, 20th century, Tahiti, France; E: box made of translucent *Placuna* sp. shell plates assembled together with brass rails, 20th century, France; F: Freshwater unionid mussel ladies’ purse with red velvet gussets, 20th century, UK; G: Snail snuffbox, 20th century, France (C-G: F. Marin personal collection; photos C-G by Jérôme Thomas, 2024).

1.2.3. Derived Shell Products of Pearl Industry: Natural Pearls, Nuclei and Blisters

In this review, it was not possible for us not to mention "pearls" as ornamental objects, although, *sensu stricto*, the vast majority of pearls currently on the market are not "pieces of shell" so to speak, but result from a unique biomineralization process, of physiological origin very different from that of the shell: they are cultured pearls, which are made from the grafting of a nucleus accompanied by a graft, in an organ - the gonad - which is not supposed to make shell. In addition, the pearl industry has taken on such economic importance in certain regions of the world (Cook Islands, French Polynesia, China, Japan) that it would deserve in itself an in-depth review and a particular development, which goes well beyond the scope of this review.

However, it is necessary to mention 3 examples of pearl products where the shell is directly involved: the first example is that of fine pearls, also called natural pearls, which can be considered as a derivative of the shell, since they are considered as an accident of secretion of the mantle (Taylor & Strack, 2008). Fine pearls have a long history, dating back to Mesopotamia (Bismaya city), 4500 years BC (Strack, 2008). Fine pearls were continuously exploited during Antiquity, the Middle Ages, Modern Times, the classical period, until the very beginning of the 20th century before being supplanted by cultured pearls, the manufacturing process of which was developed by Kokichi Mikimoto, at the very end of the 19th century. Even today, although confidential, and involving ridiculously low tonnages, there is a market for fine pearls driven by collectors, a market totally independent of that of cultured pearls.

The second product derived from the shell is precisely the nucleus of the cultured pearl: since the development of grafting technology, the nuclei used come traditionally from the Mississippian freshwater mussels of the Unionidae family (*Amblema* sp.). The shells of these mussels exhibit a very thick, white layer of nacre, whose mechanical properties (hardness, gravity, thermal conductivity) make them particularly suitable for the production of nuclei (Taylor & Strack, 2008). In addition, these nuclei can be pierced without bursting. In short, mussel shells are cut in cubes, which are consequently tumbled into a lapping machine to form spherical beads. A last surface etching step with hydrochloric acid allows obtaining a polished

finish (Taylor & Strack, 2008). Different companies commercialize perfectly spherical nuclei of all diameters (from 5 to 13 mm) that can be used by pearl farms in their grafting operations. For three decades, with the worrying decline in Mississippi mussel stocks, interesting alternatives have been found, such as the use of the *Pinctada* pearl oyster nacre for making nuclei, or the development of artificial nuclei made of calcium carbonate-based material ('Bironite').

The third product derived from the shell in the pearl industry is the blister, also called "mabé", a process commonly practiced by every pearl-producing country (Taylor & Strack, 2008). It involves introducing and gluing between the mantle of a recipient pearl oyster and the internal surface of its shell a simple geometric shape in polymer (a half-drop for example) and waiting for the mineralizing activity of the mantle to cover this shape by successive nacre layers. The oyster is then sacrificed, the blister is sawed from the shell and can be then transformed into a pendant or earring. The mabé is a by-product of the pearl industry, certainly much less prestigious than the pearl, but which has the advantage of being less time consuming to produce (6 months are enough, instead of 18 for a pearl). It also allows to maximize the profitability of an "average" recipient oyster (which we know will not produce beautiful pearls), because 2 or 3 mabés per valve can be obtained (*i.e.*, 4 to 6 blisters per specimen). Mabés are relatively cheap but beautiful alternatives to pearls.

1.2.4. Shells as Religious Symbols and Amulets

Seashells are widely believed to have magical properties, ranging from protection to healing. They are often used to safeguard vulnerable members of societies and gifted as amulets to ward off potential health issues or curses, most notably the "evil eye". Their intriguing shapes and shiny, iridescent features have captivated spiritual beliefs worldwide, linking them to natural elements and phenomena like water or the moon (Golani, 2014; Aksionov, 2022). Such connections are quite frequently observed in representations of deities constructed from molluscan shells, where the material is used either as the base element for sculptures or in decorative detailing (Buck & Hiroa, 2003). In this context, the calcified operculum of the *Bolma rugosa* (formerly *Turbo rugosus*) sea snail, known as the "Saint Lucy's eye", is considered both an amulet and a talisman in various coastal communities of the western Mediterranean, proving very popular in Corsican jewelry. Interestingly, similar mythologies surround the Asian *Turbo* snails' "Eye of Shiva" in Hindu culture. Cheaper and more abundant than *Bolma*'s, they are often falsely advertised as such in European souvenirs shops and sustain the majority of global

trades (Cagniard *et al.*, 2024). In addition to the aforementioned protective powers, highly-valued shells were often placed in tombs to accompany the defunct and pay for their passage in the afterlife (Khamis, 2022). As a subgenre of New-Age lithotherapy, modern shamanism promotes wearing nacre beads and pearls for conception, healthy pregnancies, lactation and teething. The roots of these practices can be traced back to historical ethnomedical remedies involving crushed shells, which will be further elaborated upon in another section of this review (González & Vallejo, 2023).

Another famous example of religious symbol in the Catholic church includes the scallop *Pecten jacobaeus* (or *maximus*), the shell of which - when worn on clothes, bags, sticks or as pendants - was used by the pilgrims of Santiago de Compostela as a recognition sign between them and as a safe conduct that was supposed to protect them from banditry and allowed them to ask for alms, and ultimately, as a proof of the completion of the pilgrimage. This symbol was so powerful that during all the Middle-Age, scallop shells were consequently carved as ornament into countless religious buildings (churches, monasteries, abbeys) located on the pilgrimage route.

In churches, fonts, during all the Middle-Age, consisted of cups made of stone. From the Renaissance times, with commercial exchanges with South-East Asia, stone fonts were currently replaced by the lower valves of the giant clam *Tridacna gigas*, the heaviest bivalve known to date. Examples of true *Tridacna* shells used as fonts can be seen in St-Sulpice church in Paris. The fonts of the St-Paul St-Louis church in Paris come from a Caribbean specimen offered by the well-known novelist Victor Hugo, in 1843.

At last, in India and China, from the 13th century to recent, little Buddha figures were frequently inserted and glued inside the shells (between the shell and the mollusk mantle) of the freshwater mussels (*Hyriopsis* and *Cristaria* genera) or of the pearl oyster (*Pinctada* genus), in a similar manner to the production of ‘mabés’ (see section 1.2.3. Derived Shell Products of Pearl Industry). The ‘grafted animals’, so-to-speak, produced over weeks layers of nacre covering the Buddha figures. Animals were sacrificed and shells were then collected. These objects, named Buddhas blister pearls, were and still are used as amulets or talismans in the far east.

1.2.5. Musical Instruments and Signaling

Large gastropods shells have been transformed to produce sound for millennia all over the world. Dating back to Paleolithic societies, they are considered the earliest wind instruments, and second oldest musical instruments after percussions (Montagu, 2018; Fritz *et al.*, 2021). Through reproduction studies, archeologists aim to reconnect each instrument to their past uses and current equivalents, uncovering their frequency-altering properties. Indeed, the helicoidal inner structure of giant conchs opens up opportunities for sound bending, amplification and elongation. Early humans also used paint markings in conch lips and additional finger holes to modulate tones (Kolar *et al.*, 2022).



Figure 1.2: Conch shell trumpets. A: Musical trumpet, Papua New Guinea, 20th century. Displayed in the Royal Ontario Museum, Toronto, Canada (Daderot, 2011); B: *Hora*, Japanese battle horn, late 19th century, conch-shell, German silver, cotton mesh, copper, nickel, zinc and cord (Haa900, 2013); C: 나각 ‘*nagak*’ trumpet used during ceremonies, National Gugak Center, South Korea; D: Trumpet made of conch shell with copper, gilt copper alloy and semi-precious stones, metal pendant with dragon motif, used in the monastic orchestra, Tibet, 18th/19th century. Displayed at the British Museum, London, United-Kingdom (Andreas Praefcke, 2011).

While the simplest altered shells are often referred to as signaling horns for agriculture, long-distance communication, navigation, and war signals (Hiwasaki & Shaw, 2014), more intricately carved ones can be assimilated to oboes, flutes or trumpets and used for musical entertainment (Fig. 1.2, A) (Buck & Hiroa, 2003; Montagu, 2018). These shells have accompanied humans in various cultural aspects, with their craftsmanship, decorations and ergonomic adaptations (such as coated mouthpieces and lanyard attachments) serving as testimonies to our evolution (Moyle, 1990). In this context, the *Hora* described by Fukui (1994) as a “Conch Trumpet”, is a notable example, having played a significant role in Japanese history and culture through its multiple purposes: military maneuvering, religious ceremonies, court ball music (Fig. 1.2, B). The musical use of molluscan shells is not limited to wind instruments; giant mollusks are still used for percussion and string instruments in various coastal or island cultures (Moyle, 1990; Buck & Hiroa, 2003). To conclude on this paragraph, let us point out that many string instruments, like guitars, lutes, violas, mandolins, harps, harpsichords and pianos, from the Baroque era to the present, feature decorative inlays in nacre, which contribute to make these instruments unique and precious. Today, several brands propose mid-range or high-end guitars (classic, folk or electric) with nacre incrustations in their neck and their body. Nacreous guitar picks are also commercialized to give a sharper sound.

1.2.6. Shell Representations in Art

Pictorial and sculptural representations of seashells are prevalent across successive art movements, embodying the magical powers and artifacts associated with founding myths, prophets and saints from various religions. The examples are abundant: let us simply consider the *Birth of Venus*, from Botticelli (1485), with Venus emerging from a valve of a giant scallop, a symbol of fertility, *Oysters* from Edouard Manet (1862) or *Shell* from Salvador Dali (1928). During the golden age of The Netherlands, ornate nautilus shells were meticulously depicted in hyper-realistic still-life paintings, such as that of Willem Claesz-Heda (1594-1680). Sculptures made of shells or sculptures representing a human figure associated to a shell are countless. The use of shells in art would require in itself a full development, far beyond this review: we have chosen indeed to focus on the direct, material uses of the molluscan shells and not their pictorial representation: their intangible symbolism and ensuing portrayals belong to a broad philosophical and art-history investigation.

1.2.7. Currencies and Wealth

Molluscan shells served as currency and precious goods across diverse societies from prehistoric times to the 19th century, illustrating their long-standing economic significance (Fauvelle, 2024). Among these, cowries and *Marginella* shells were the most prevalent, as evidenced by the distribution of archaeological sites across Africa, the Pacific islands, and Asia (Iroko, 1990; Yang, 2011). Either fished or collected from coastal areas, their compact size, simple shapes, durability, and uniformity made them ideal for exchanges and easy to transport. Interestingly, metallic replicas of cowrie shells were also produced, in response to the need for currency regulation as economies expanded. This practice highlights the shells' significance in economic systems and their suitability for standardization (Yang, 2021). In the same context of governance, specific regions favored different gastropod families with easily distinguishable traits and local availability. This is the case of *nzimbu* olive shells, used exclusively in the Kongo kingdom for centuries (Iroko, 1990).

Currency has not always only existed as a collection of singular pieces to be counted. Many cultures developed other methods of registering value, often involving the stringing of shells together. Numerous societies utilized shell disks, pierced and mounted on threads, as a form of money. A prime example is the *diwara* money of Guinea, where the value of shell disk strings was determined by their length (Echterhölter, 2020). Another example is the *tabu* from New-Guinea, consisting of strings of *Nassarius camelus* perforated shells (Thomas, 2007). Similarly, tribes along the Pacific coast of North America exchanged *Dentalium* shells referred to as *haik-wa*. These elongated shells were also strung together, with their value indicated by both each individual shell length and the number that were sewn together (Einzig, 1949; A. M. González, 2002). This approach enabled the development of a nuanced system of valuation based on multiple interacting factors. *Wampum* represents another complex form of currency: this artifact of shell bead embroidery incorporated size, color, and symbolic patterns of the craft to denote value (Fig. 1.3, A & B). In addition to their monetary functions, *wampum* were used as diplomatic tools in treaty-making processes. This use persisted through the European colonization of North America while their exchange as proper currency declined. Today, the majority of their purpose reside as canvas in cultural transmission of techniques, traditions and stories (Einzig, 1949). A similar example is the *tafuliae* from the Solomon Islands, where beads carved of bivalve shells of different biological origins are woven according to geometrical patterns to form armbands or belts. This complex usage highlights the role of shell money as an integrative part of social and political life.



Figure 1.3: Shell money. A: *Wampum* cuff, shell, leather, sinew, Mohawk population, Canada, Great Lakes region, 18th century. Exposed in Musée du Quai Branly, Paris, France (Anonymous, 2013); B: *Wampum* beads made by E. J. Perry (Wampanoag/Eastern Cherokee), the purple ones are quahog and the white ones, whelk (Mary Meredith, 2009); C: *Tabu* shell money harvest. Nathaly, young Melanesian girl collecting Nassariidae snails in the slit of a muddy shoreline; D: Processing *tabu* shell money, hand-drilled shells with plyers onto a string of cane; E: *Tabu* shell money trading, Kokopo market; F: Purchase of ‘*Agogo*’ *tabu* wheels by Japanese representatives as a diplomatic act of apology and reconciliation after World War II (C-F pictures by Claudio Sieber Photography, Papua New-Guinea, Shell Money Project 2018).

Shells were also as accounting to facilitate the exchange of goods, rather than proper currency (Iroko, 1990). As illustrated above with the complex *wampum*, their role extended beyond mere economic transactions: shells, just like gemstones, play a significant part in diplomatic relations. Yang (2021) provides a clear example of this, describing the resolution of a major diplomatic incident in 13th century Tai kingdoms with large bags of cowries as peace offerings. It is noteworthy to highlight that cowrie shells emerged as the first form of globally traded money. They were indeed the first goods to connect all continents, and as such, are often accredited for a part of the development of global commerce (Yang, 2021). However, it is crucial to acknowledge that as any form of money, shells were used in human exploitation: through its widespread use, the cowrie shell even facilitated slavery, supporting and further expanding the human trade.

The decline in shell currencies coincides with the colonial era (Einzig, 1949; Iroko, 1990). Over time, Europeans monetary systems gradually replaced the use of shells as money. This marked a shift in the dynamics of international trades and the end of the long-standing use of one of the world's oldest forms of currency. However, unexpectedly, one notes a persistence of the use – until now - of *tabu* in New-Guinea, among the Tolai tribe, in parallel to the standard metallic currency. This double system led to the creation of the first shell currency exchange office, few years ago (Fig. 1.3, C-F) (Thomas, 2007).

1.2.8. Practical Applications, Past and Present

1.2.8.1. Daily Tools

Shells are particularly suited for use as practical tools thanks to their robustness, durability and shape diversity. Greek archaeological sites dating from the Paleolithic period reveal that smooth venus and clam shells were regularly repurposed after consumption as scrapers and cutting tools for food preparation, leather tanning and woodworking (Darlas, 2007; Colonese *et al.*, 2011). In Hawaii, shells were similarly repurposed for food and herbaceous fiber preparation (Buck & Hiroa, 2003). In Nigeria, shells have been a part of traditional practices for generations and are still utilized nowadays as cutting objects and containers (Kehinde O. *et al.*, 2015). Some of the exploited mollusks, especially large gastropods, were collected post-mortem, suggesting deliberate gathering for tool production. This practice is exemplified by the significant number of whelk shells excavated by Pearson and Cook (2008) on Ossabaw Island, Georgia. Their substantial size, toughness, smooth interior surface and large distribution made them the base material for crafting everyday items in Mississippian 14th

century, including combs, cutters, scrappers, containers, and sewing tools. Not all objects were task-specific: some exhibit traces of wear and rework indicating reuse, repairing and repurposing as early as the Neolithic era in Arabia (Lidour & Cuenca Solana, 2023). Some shells were specifically retouched for crafting, decorating, and engraving purposes, indicating a certain mastering of specialized tool-making and understanding of materials relative toughness (Darlas, 2007; Colonese *et al.*, 2011).

1.2.8.2. Shells as Molds

Among the very peculiar practical uses of shells, let us cite the case of the Mediterranean fan mussel *Pinna nobilis*: during the Iron Age, the South-Eastern Iberia (Siera of Carthagene) was already known as a mining area for the extraction of lead (in the form of galena, *i.e.*, lead sulfide). Lead was melted and poured into molds made of shells of adult specimens of the Mediterranean fan mussel *Pinna nobilis*, the giant nacre (Gosner, 2022). These lead ingots had a fan shape, with one flat surface, suggesting that each mold was constituted of one valve used horizontally during the pouring process (Fig. 1.4, A). The ingots were then transported by boat along the coasts of France and Italy for trading. Their existence was revealed by an underwater archeological search in a sunken boat by the Island of Cabrera, in the South of Majorca, in the early sixties. Some of these ingots (IVth-IIIrd century BC) are preserved in the Museum of Biterrois, Béziers, France.

Interestingly, a similar function (use as cast) was attributed to cuttlebones from *Sepia officinalis* (Ossasepia casting technique) along Normandy coasts (Fig. 1.4, B), during the whole Bronze age (M. Gabillot, *personal communication*), in the region of Bopfingen, Germany during the early Medieval period marked by Allamani predominance (Blumer & Knaut, 1991), and in several other regions. In Central Asia, this technique was used from the IVth century BC to the IVth century AD for creating jewelry, particularly rings, as evidenced by findings in Oxus (Tajikistan) and Tillya-tepe (Afghanistan) (Neva, 2008). The casting process involved cutting the cuttlebone lengthwise, carving calcium carbonate or pressing the object model into it, and finally pouring the hot metal into the mold. As they are mainly made out of porous calcium carbonate and chitin, cuttlebone molds are disposable and burn out after a single use. This technique has been revived today by goldsmith jewelers for casting gold and silver, both for its unique surface patterns and its cost-effective advantage, producing a silver casting in half an hour (Held, 2019).

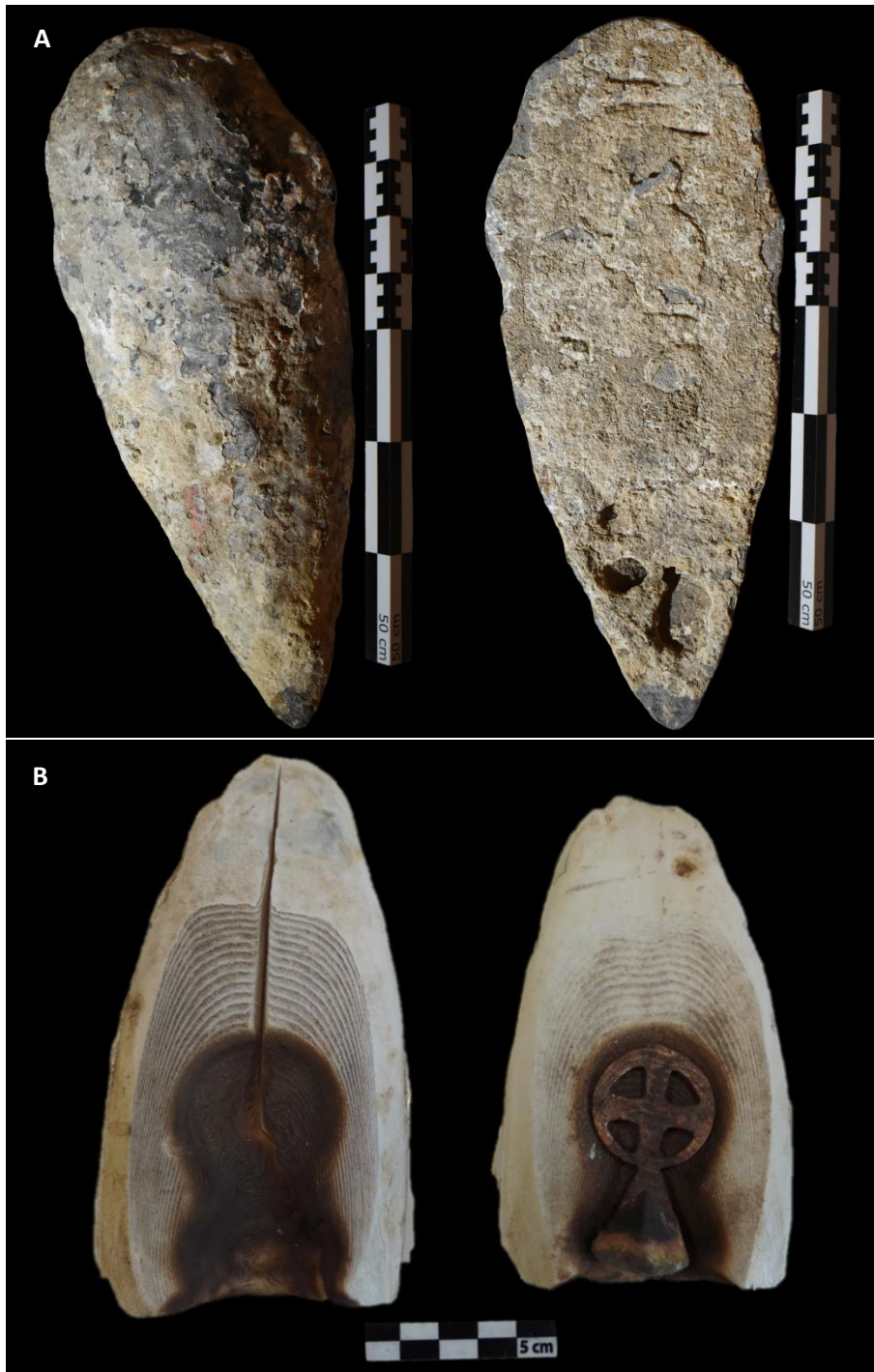


Figure 1.4: Shell molds. A: lead ingot from IV-III century BC (Cabrera Island, Spain), cast from a single shell valve of an adult specimen of *Pinna nobilis* (Musée des Beaux Arts de Béziers, Roxelane Cicekli); B: *Ossasepia* cast with a brooch. Facsimile of a Middle Bronze Age item (around 1500 BC) found in Normandy (collection ArTeHiS, Mareva Gabillot).

1.2.8.3. *Artistic Tools and Pigments*

During the Neolithic period (around 9000 years ago) in southern Anatolian Plateau site of Çatalhöyük, freshwater mussels served as palettes containers to hold and mix pigments for cave paintings (Tsoraki *et al.*, 2020). Ceramics productions also benefited from mollusk shells repurposing. This is the case for the crushed murex shells resulting from dye extraction in ancient Mediterranean workshops: the fragments were burned and mixed into clay as temper to enhance the durability of ceramics and improving their resistance to temperature fluctuations and impacts (Carannante, 2014).

The vibrant colors and shiny surfaces of mollusk shells have been employed in various cultural practices across the globe. In Hawaiian, Micronesian, and Polynesian cultures, smooth, glossy cowries known as *leho* were used to polish *pele* cloths, giving them a shiny finish (Buck & Hiroa, 2003). In Papua New Guinea, a tradition developed of crushing and burning molluscan shells to produce white pigment, essentially creating a form of quicklime (Hill, 2001). Similarly, in Nigeria, crushed shell powder is still used as chalk for writing on boards and as face paint for tribal marks (Kehinde *et al.*, 2015). The use of mollusks for dye production primarily involved the soft tissues, particularly the hypobranchial glands, rather than the shells themselves. The shells were often by-products of these processes, though they found various secondary uses in many cultures (Alberti, 2008).

1.2.8.4. *Shells in Architecture and Construction*

The discovery of shell fragments as integrate parts of architecture and constructions demonstrates the intentional repurposing of shell by-products by ancient societies, with comparable applications across the world. During the Bronze Age, crushed murex shells were often recycled into lime plaster after dye extraction around Aegean purple industries (Brysaert, 2007; Berger *et al.*, 2024). Alberti (2008) and Carannante (2014) note that these crushed shells were either used as-is for filling or calcined in mixtures for construction.

Along the coasts of Brazil, large accumulation of shells, referred to as shell mounds or, more simply *sambaquis*, were built by pre-Columbian tribes, between 8000 and 600 years ago (Okumura & Eggers, 2005; Wagner *et al.*, 2011). Primarily described by the Jesuit Fernão Cardim in 1584, *sambaquis* consisted in large platforms of shells (comprising also other organic remains), of few to several meters high, on which tribes were living. Some of them were also used for sanctuary for dead people.

In addition to maximizing the utility of shell by-products, their reuse as construction materials strengthened the structural integrity of buildings. This is typically the case in pre-Hispanic Mexico, where Pankonien (2008) reports that shells were purposely piled and used in foundations to stabilize high building structures like coastal watchtowers and improve their reflectivity at night. Another frequent application of shells then was the production of shells-and-sand stuccos to isolate walls across cities. Nowadays, excess shells from capture and aquaculture are similarly utilized for solidifying constructions. For instance, crushed scallop shells are used as aggregates to secure paths in Scottish islands, while whole oyster shells are regularly observed in house structures in Florida (USA), China and Spain (Morris *et al.*, 2019). Simpler applications like piles of whole or crushed shells or shells and sand mixtures are frequent in embankments and dikes, improving the solidity and protection power of coastal structures compared to standard concrete. Furthermore, returning shells to marine environments in coastal structures provides additional ecosystem services as substrates to local wild populations and carbon sequestration (Morris *et al.*, 2019; P. Chen *et al.*, 2022).

1.2.8.5. Shells in Agriculture: Soil Improvers and Food Complement for Poultry

Fragments of oyster shells or crushed shells are still currently used for soil amendment. This practice is ancestral, *i.e.*, has been known for centuries, in particular, for improving the quality of poor acidic soils like the ones that develop on granitic substratum (in French Brittany). Such soils require pH increase. The role of calcium carbonate of the oyster shell powder is to buffer the acidic conditions and alkalize the soil (Lee *et al.*, 2008). Soil amendment by shell powder has other beneficial effects, as it brings micro-nutrients, contributes to fix pollutants (heavy metals such as cadmium and lead and poisons as arsenic), modifies the bacterial composition of the soil and, generally, improves its overall quality (Zheng *et al.*, 2023). Although edible oysters represent the main source of soil amendment, mussel shells give similar positive results (Álvarez *et al.*, 2012). Today, there is an active research in this domain of agronomy.

A second utilization of shells in agriculture consist in feeding poultry with food complemented with shell granulates or oyster-shell grit (Henuk & Dingle, 2002; Morris *et al.*, 2019). This traditional practice aiming at increasing the calcium source for improving the quality of eggs and the bone health of poultry is recognized as a good and cheap alternative to sophisticated complements. It is largely encouraged in developing countries. Many food complements for poultry based on shell granulates are nowadays available on the net.

1.2.8.6. Other Practical Uses

Shells played a crucial role in the development of fishing and hunting gear. In 16th century Huatulco, Mexico, shells were crafted into fishing hooks and harpoons heads (A. M. González, 2002). Polynesian and Micronesian communities also assembled and carved shells to create *makau* hooks and fishing lures. They developed sophisticated octopi baits and hook shapes to minimize fish escape that are now deeply intertwined to cultural and spiritual heritages (Fig. 1.5) (Buck & Hiroa, 2003, Thomas, 2007). In Florida and Puerto Rico, pierced shells of the bivalves *Codakia orbicularis* and *Lucina pectinata* identified in archeological sites were used as weights of fishing nets, in pre-Columbian times (Keegan *et al.*, 2009). These examples highlight the importance of shells in subsistence activities across different societies.



Figure 1.5: Fishing gears made of mollusk shells and shell products. A: Tahitian lure for octopus hunting, cowries, sticks, plant fibre, mother-of-pearl, l. 44 cm, Tahiti and the Society Islands, Hanover 1854, exposed in the National Museum of Australia, Canberra, Australia; B: Tahitian lure for octopus hunting, cowries, sticks, plant fibre, mother-of-pearl, l. 33 cm, 6.5 cm (fish-hook), Tahiti and the Society Islands, Inv. Oz 391, exposed in the National Museum of Australia, Canberra, Australia. C: Mother of pearl fish hook. Collected from the Society Islands during Cook's voyages to the Pacific, 1768-1780. Exposed at the Australian Museum, Darlinghurst, Australia (AM, Photography Dept - Paul Ovenden, 2009); D: Bone fish hook backed by mother of pearl and with a barbed tortoise shell hook bound by fibre. Probably collected from Tonga during Cook's second and third voyages to the Pacific 1773-1780. Exposed at the Australian Museum, Darlinghurst, Australia (AM, Photography Dept - Paul Ovenden, 2009).

Early productions of shell tools are crucial in understanding human cognitive and cultural development, also providing information about population movements and connections (Lidour & Cuenca Solana, 2023). Indeed, some species were found in places and communities outside their range of distribution, or where specific crafting techniques were not mastered yet. In her book documenting economic and cultural structuration of modern Mexican society, González (2002) describes the market of processed molluscan shells spreading across regions. Households were respectfully specialized in collecting, cleaning, crafting, packaging and distributing the shells. Uncovered far from the sea and in mountains, they highlight the trades with inland communities, particularly Pueblo and Teotihuacan. These exchanges, combined with the previously discussed roles as currency, demonstrate the impact that molluscan shells had on societies by structuring the economy.

1.2.9. Traditional Medicinal and Pharmaceutical Uses

Medicinal and pharmaceutical uses of molluscan shells have been documented in traditional ethnomedicines worldwide, demonstrating their versatility in both historical and modern medical practices across different therapeutic areas. The influence of spiritual beliefs on the popularity of molluscan derived materials in medicine is non-negligible, but the long-term existence and documented empirical observations suggests that some remedies may be actually effective.

Calcium carbonate itself, as the predominant component of molluscan shells, plays a significant part in the effects of these treatments. Its documented bioactivity corroborates the healing preparations and recommendations in various cultures. In medieval Jewish communities of Cairo, crushed pearl powder was sold as a cardiac tonic to cure palpitations (Lev, 2007; Lev & Amar, 2008). In Nigeria, shell-derived materials were incorporated into healing concoctions and measles treatments (Kehinde *et al.*, 2015). Cowrie shells (*Cypraea moneta*) have found numerous applications in Seddha and Ayurvedic medicine, including calcium supplementation for both humans and animals (Immanuel *et al.*, 2012; Krishna & Singh, 2012). The pH buffering properties of calcium carbonate have been exploited in antacid formulations. Cuttlebone preparations, for instance, exhibit high antacid capacity, offering a natural alternative for treating conditions like heartburn, dyspepsia (Immanuel *et al.*, 2012; Ansari, 2019; J. A. González & Vallejo, 2023). The absorbent nature of shell-derived powders has also been utilized in anti-diarrheal treatments. Today, sachets of finely ground nacre powder are commercialized in the modern Chinese pharmacopoeia. The abrasiveness of shell pastes

makes them particularly effective for scrubbing in exfoliation, depilation and dental hygiene: ashes of burned shells from mussels and oysters were used in the Greek world and early Byzantium for oral care (Voultsiadou, 2010). In contemporary Spanish ethnomedicine, dried powdered cuttlebone is still used for this purpose (González *et al.*, 2016).

Beyond the bioactivity strictly attributed to calcium carbonate, shell remedies seem to display properties that could be attributed to its other component, the organic matrix. Nacre, for instance, has been shown to improve collagen production by stimulating fibroblast activity and proliferation (Almeida *et al.*, 2000). This property has led to various dermatological applications, from cosmetic products to more sophisticated drugs treating skin conditions. In coastal areas of Spain, shell preparations dissolved in lemon juice or vinegar are used to reduce sunspots, acne, and freckles (González & Vallejo, 2023). Terrestrial snail shells and ashes of burned Muricidae shells were used for skin diseases in medieval Eastern Mediterranean and ancient Greco-Roman communities (Lev & Amar, 2008; Ahmad *et al.*, 2018). Cuttlebone and nacre powder extracts have demonstrated wound healing properties by promoting cell proliferation and stimulating fibroblasts (González & Vallejo, 2023). In digestive health, snail shells and ashes of burned Muricidae shells were used to heal stomach wounds or as purgatives in medieval Eastern Mediterranean and ancient Greco-Roman communities (Lev & Amar, 2008; Ahmad *et al.*, 2018). However, in traditional Unani medicine, some shell preparations were considered hard on the stomach and counter-indicated in respiratory diseases (Ansari, 2019), while they were rather indicated for kidney functions acting as diuretics and aids in kidney stone removal.

One of the most fascinating examples of the use of shell are Maya dental implants, studied by Bobbio (1972). In the lower mandible of an individual who lived between the 7th and 8th century AD, three nacre implants, cut into tooth shape, were identified in replacement of three missing incisors. Surprisingly, these implants were not inserted *post-mortem* but during life: they represent the most ancient evidence of alloplastic implants performed on humans so far. Strikingly, these implants were fully tolerated by the body and perfectly osteo-integrated, without any trace of rejection or infection (Fig. 1.6). This suggests that the nacre matrix may contain bioactive factors, such as BMPs (Bone Morphogenetic Proteins) or other factors that contribute to activate human osteoblasts to produce bone tissues to fix the dental implants (Westbroek & Marin, 1998). It is also possible that potential antimicrobial factors contained in nacre implants precluded the infection of the lower jaw.



Figure 1.6: Mayan seashell implanted false teeth, Peabody Museum of Archaeology and Ethnology, Harvard University, Cambridge, USA (E. Marin, 2023).

Gynecological applications of shell-derived materials include using ground cuttlebone as a suppository or pad to stop bleeding during pregnancy in ancient Greece and early Byzantine civilizations (Voultsiadou, 2010). Marine gastropod opercula were prescribed in medieval Cairo Jewish communities to regulate menstrual cycles and treat uterine diseases (Lev & Amar, 2008).

Interestingly, nacre powder and its water-soluble components have shown anticonvulsant and sedative-hypnotic activities, suggesting potential applications in neurological treatments. In ophthalmology, pulverized ashes of *Mytilus galloprovincialis* (the edible mussel) and cuttlebone shells have been used to treat eye infections and dryness in both veterinary and human medicine (Voultsiadou, 2010; González *et al.*, 2016).

The immune-modulating properties of shell materials have also been explored. Burned shells of Muricidae and Ranellidae were used in ancient Greco-Roman and early Byzantine communities for their anti-inflammatory and immune-enhancing effects (Voultsiadou, 2010; Ahmad *et al.*, 2018). These preparations were also used to treat arthritis (Lev & Amar, 2008). Similarly, powdered cuttlebones and bivalve shells have been traditionally used as anti-gout treatments and alexipharmics in the Hispanic peninsula (J. A. González & Vallejo, 2023).

While many of the aforementioned cosmetological, medical and veterinary applications seem plausible or are supported by scientific or medical consensus, others are based solely on potentially biased empirical observations and spiritual beliefs. Further clinical studies are necessary to validate these claims and elucidate the underlying mechanisms of action (Benkendorff *et al.*, 2015; Summer *et al.*, 2020). Such research could uncover new therapeutic applications for shell-derived materials and contribute to the development of novel pharmaceutical products.

1.2.10. Recent and Future Applications: Biotechnology, Engineering and Others

1.2.10.1. Smart Construction Materials

One of the main branches of emerging mollusk shell recycling today is the production of “smart” concrete, in continuity with the repurposing practices in (pre)History. When used as cementitious binder, powdered shells enhance concrete properties in drainage, elasticity and resistance to high-pressure and heat shocks (Bamigboye *et al.*, 2021; P. Chen *et al.*, 2022; Shetty *et al.*, 2023). The variety of applications (high seismic risk localities, urbanization in extreme-heat environments, increase of extreme climatic events like cyclones, high flooding risk roads) for these concretes requires a high specialization of processing protocols to determine the adapted thermal preparation, sieving, and mixing proportions. With proper treatment, these concretes can surpass the performance of traditional concrete (Mo *et al.*, 2018; Y. Zhang *et al.*, 2020; Ahmed *et al.*, 2024). Another advantage of using mollusk shell waste in construction is that it acts as an alternative binder to sand: it reduces the reliance of concrete industries on natural sand, thus decreasing anthropogenic pressure on coastal regions (Mo *et al.*, 2018; Shetty *et al.*, 2023).

These mixes have also demonstrated better thermal insulation by limiting heat leakage (P. Zhang *et al.*, 2019; Supar *et al.*, 2021). Recently, painting companies like Cool Roof France released paints containing oyster shell powder, with the goal to increase the albedo - the reflective power - of building roofs, thereby reducing the need for air cooling systems. Further research and development are required to set-up sustainable maintenance of these innovative paints (Agence Qualité Construction, 2024).

Seashell fragments can also be found in interior design applications for soundproofing. As key elements of composite panels, their microstructures and layers function as diffuser-absorbers for acoustic dissipation. They are used to soundproof workspaces and musical theaters, with the potential to broader applications in urban design, such as reducing sound pollution around transportation and industrial infrastructures (Setyowati *et al.*, 2019).

1.2.10.2. Depollution

Mollusk shells powders, particularly those rich in calcite and aragonite, are capable of absorbing several polluting substances, such as heavy metals, oils or excessive nutrients. For instance, calcitic oyster pastes are very efficient in lead retention, while aragonitic clams show better capacities with cadmium. One explanation of their efficiency in binding heavy metal cations is the presence of negatively charged macromolecules contained in the shell matrix.

These macromolecules, while bound to the mineral grains, are able to actively sequester cations in standard pH conditions. Consequently, shell supplemented amendments are developed to reduce potential soil contaminations in agricultural settings (Zeng *et al.*, 2022). These properties are also applicable to liquid environments, notably for water depollution, as powder treatments, innovative polymers or sponge-like textures that trap, kill or flocculate harmful substances (Tudor *et al.*, 2006; Weerasooriyagedra & Kumar, 2018; Triunfo *et al.*, 2022; Basile *et al.*, 2024). Additionally, when crushed at varying grain sizes, mollusk shells make good filtration mediums for powerful biofilters that are easy to implement on a large scale while not requiring high-energy processing (Morris *et al.*, 2019; Summa *et al.*, 2022).

1.2.10.3. Biotechnological Research and Production of Bioactive Compounds

Following the leads of ethnomedicine and empirical observations of biochemical properties of shell products, a significant attention has been put towards biotechnological research and extraction of bioactive compounds from mollusk shells. This research often incorporates biomimetic approaches, drawing inspiration from the properties of natural structures like byssal threads and adhesive plaques, while also exploring the bioactive organic matrix of the shells (Venier *et al.*, 2019). A growing push for an integrated, large-scale approach to reuse and revalorize these abundant by-products has emerged, with both industrial and academic researchers exploring several methods of bioconversion (Morris *et al.*, 2019; Naik & Hayes, 2019). Such attempts are mainly made in two fields of applications: biotechnological development and biomedical innovation.

Although not as effective as eggshells, snail shells can be used as catalysts for biodiesel production (Viriyapempikul *et al.*, 2010). The development of advanced functional biomaterials is a strong lead among biotechnological applications. Mollusk derived calcium carbonates can sustain good covalent functionalization, granting them tailoring properties for a broad range of specific uses, such as detection systems, catalysis, electrical conduction or even in biomedicine as localized drug delivery systems (Magnabosco *et al.*, 2021; Triunfo *et al.*, 2022).

Expanding on biomedical applications, recent studies on shell powders demonstrate the participation of some microstructures – namely, mother-of-pearl - in bone mineralization improvement by stimulating osteoblast activity (Flausse *et al.*, 2013; Brion *et al.*, 2015; Nahle *et al.*, 2024). This remarkable property was observed for the first time more than thirty-three years ago, first *in vitro* (Silve *et al.*, 1992) and later, *in vivo* (Atlan *et al.*, 1997). The osteoinductive and osteogenic effect of nacre was explained by the presence, in the nacre

matrix, of signaling molecules – such as BMPs (Bone Morphogenetic Proteins) but not exclusively – involved in the transduction pathway for activating osteoblasts, *i.e.*, bone-forming cells, in the synthesis of bone collagen and of the complete cortege of proteins required for bone mineral deposition. Interestingly, from an evolutionary viewpoint, the effect of nacre matrix on bone cells strongly suggests that the signaling pathway for mineralizing either calcium phosphate (vertebrate bone) or calcium carbonate (mollusk shell) is common to both phyla. Let us remind that mollusks and vertebrates lineages diverged somewhere in the Proterozoic times, more than 600 million years ago (Westbroek & Marin, 1998). The pioneering works on nacre effects on bone mineralization were followed by a large number of *in vivo* and *in vitro* studies summarized in (Zhang *et al.*, 2017). Interestingly, the nacre matrix, in particular its lipidic fraction, was also found to exert a beneficial and restorative effect on the skin (Rousseau *et al.*, 2006).

Other shell innovations fit in the frame of human biomineralization research: the shells of multiple mollusks (marine and terrestrial) have been successfully used to synthesize hydroxyapatite and other natural bioceramics, which can be then utilized as highly biocompatible osteoinductive grafts (Kel *et al.*, 2012; Fernández-Penas *et al.*, 2023). Likewise, the properties of the calcifying organic matrix are gradually being uncovered and assessed, revealing fibroblast stimulation and anti-inflammatory effects (Almeida *et al.*, 2000; Immanuel *et al.*, 2012; Z.-C. Chen *et al.*, 2016). These recent advances come as preliminary validations of some ethnomedicine applications described earlier in this review: some mollusk shells can indeed promote wound healing and modulate immune responses in humans.

At last, we should mention that shells, whatever their geographical or taxonomical origins, are likely to contain bacteria-killing substances. Our recent findings (Lutet-Toti *et al.*, 2024; Lutet-Toti *et al.*, 2025, *submitted to STOTEN*) suggest indeed that different cocktails of antimicrobial peptides and proteins (AMPPs) are present in the mineralizing matrix of the shell of different bivalves of economic interest. This discovery can find applications in the fields of aquaculture and health.

1.2.11. Conclusion

In this short review, we have tried to cover as best as possible the multiple uses of shells through time and space. Although some of these repurposing practices are ancient or traditional, they reveal remarkable but unsuspected properties of shells: let us simply think of the astonishing example of Maya dental implants made of mollusk nacre. Today, in 2024, we still

do not know what made this operation, performed 12 or 13 centuries ago, so successful. A part of the secret lies probably in the organic components of the nacre matrix. Such an example should encourage us to consider shells as huge and unexplored reservoirs of bioactive components and to revisit their repurposing for applications of high added value.

Acknowledgements

We thank Claudio Sieber Photography for his collaboration and consent to illustrate our work with pictures from ‘Shell Money Project’ (2018) (Fig. 1.3, C-F); and Ms. Roxelane Cicekli (Curator at the Museum of Béziers) for her contribution in providing photos of *Pinna nobilis* molds (Fig. 1.4, A).

Authors Contributions

C.L.T.: conception of the study, literature searching, data extraction, original draft writing, review, editing, funding. G.F. and S.G.: project advising and funding. J. T. and M. G.: contribution to figures and advises on some shell uses. F.M.: conception of the study, project administration including funding acquisition and supervision, original draft writing, review, and editing. All authors have read and agreed to the published version of the manuscript.

Statements and Declarations

Ethical considerations

Not applicable.

Consent to participate

Not applicable.

Consent for publication

Claudio Sieber gave consent for the publication of his photographs from ‘Shell Money Project’ (2018), under the license CC4.0.

Declaration of conflicting interest

The authors declared no potential conflicts of interest with respect to the research, authorship, and/or publication of this article.

Funding statement

CLT is the recipient of a PhD fellowship under joint-supervision between Université de Bourgogne (uB) and Università di Bologna Alma Mater Studiorum (UniBo). The research leading to these results has been conceived under the International PhD Program “Innovative Technologies and Sustainable Use of Mediterranean Sea Fishery and Biological Resources” (www.FishMed-PhD.org). This study represents partial fulfilment of the requirements for the Ph.D. thesis of CLT at the FishMed PhD Program (University of Bologna, Italy). In addition, CLT was supported by a one-off grant from AFFDU (Association des Femmes Françaises Diplômées de l’Université) in 2022 and an award from the Société Française de Biologie des Tissus Minéralisés (SFBTM) and from the Fondation Arthritis, in May 2023. Other supports to FM include the following: (1) the MAELSTROM project (les MATricEs coquiLLières bacTéRicides au secOurs des géoMatériaux) from TELLUS-INTERRVIE program (CNRS, 2022); (2) the PRELUDE project (Peptides antimicrobiens des coquilles de mollusques d’intérêt Economique) financed by Observatoire des Sciences de l’Univers (OSU) Theta, Besançon, in 2023; (3) the MAELSTROM-bis project, financed by the TELLUS-INTERRVIE program from CNRS, in 2024.

1.2.12. References

- Agence Qualité Construction. (2024). Toitures - «Cool roofing»: Une technique séduisante à manier avec précaution. *Revue “Qualité Construction,”* 202, 10.
- Ahmad, T. B., Liu, L., Kotiw, M., and Benkendorff, K. (2018). Review of anti-inflammatory, immune-modulatory and wound healing properties of molluscs. *Journal of Ethnopharmacology*, 210, 156–178. <https://doi.org/10.1016/j.jep.2017.08.008>

- Ahmed, S. M., Chávez-Delgado, M., and Avudaiappan, S. (2024). Experimental investigations on sustainable mortar containing recycled seashell powder as cement partial replacement. *Engineering Research Express*, 6(2), 025101. <https://doi.org/10.1088/2631-8695/ad3717>
- Aksionov, V. (2022). Shells as a Costume Element of the Turkic-Ugric Population of the Saltiv Culture (Based on Materials from the Krasna Hirka Biritual Burial Ground). *Arheologia*, Article 1. <https://doi.org/10.15407/arheologia2022.01.101>
- Alberti, M. E. (2008). Murex Shells as Raw Material: The Purple-Dye Industry and Its By-products : Interpreting the Archaeological Record. *Kaskal : Rivista Di Storia, Ambiente e Culture Del Vicino Oriente Antico. Volume 5, 2008*, 1000–1018. <https://doi.org/10.1400/118340>
- Almeida, M. J., Milet, C., Peduzzi, J., Pereira, L., Haigle, J., Barthélemy, M., and Lopez, E. (2000). Effect of water-soluble matrix fraction extracted from the nacre of *Pinctada maxima* on the alkaline phosphatase activity of cultured fibroblasts. *Journal of Experimental Zoology*, 288(4), 327–334. [https://doi.org/10.1002/1097-010X\(20001215\)288:4<327::AID-JEZ5>3.0.CO;2-#](https://doi.org/10.1002/1097-010X(20001215)288:4<327::AID-JEZ5>3.0.CO;2-#)
- Álvarez, E., Fernández-sanjurjo, M. J., Seco, N., and Núñez, A. (2012). Use of Mussel Shells as a Soil Amendment: Effects on Bulk and Rhizosphere Soil and Pasture Production. *Pedosphere*, 22(2), 152–164. [https://doi.org/10.1016/S1002-0160\(12\)60002-2](https://doi.org/10.1016/S1002-0160(12)60002-2)
- Ansari, S. (2019). Cuttlefish bone/ *sepia officinalis* (kafe dariya): Recovery of long forgotten Unani drug. *CELLMED*, 9(4), 7.1-7.4. <https://doi.org/10.5667/tang.2019.0022>
- Atlan, G., Balmain, N., Berland, S., Vidal, B., and Lopez, É. (1997). Reconstruction of human maxillary defects with nacre powder: Histological evidence for bone regeneration. *C. R. Acad. Sci. Paris*, 320(3), 253–258. [https://doi.org/10.1016/S0764-4469\(97\)86933-8](https://doi.org/10.1016/S0764-4469(97)86933-8)
- Bamigboye, G., Enabulele, D., Odetoyan, A. O., Kareem, M. A., Nworgu, A., and Bassey, D. (2021). Mechanical and durability assessment of concrete containing seashells: A review. *Cogent Engineering*, 8(1), 1883830. <https://doi.org/10.1080/23311916.2021.1883830>
- Bar-Yosef Mayer, D. E. (2015). *Nassarius* shells: Preferred beads of the Palaeolithic. *Quaternary International*, 390, 79–84. <https://doi.org/10.1016/j.quaint.2015.05.042>
- Basile, M. L., Triunfo, C., Gärtner, S., Fermani, S., Laurenzi, D., Maoloni, G., Mazzon, M., Marzadori, C., Adamiano, A., Iafisco, M., Montroni, D., Gómez Morales, J., Cölfen, H., and Falini, G. (2024). Stearate-Coated Biogenic Calcium Carbonate from Waste Seashells: A Sustainable Plastic Filler. *ACS Omega*, 9(10), 11232–11242. <https://doi.org/10.1021/acsomega.3c06186>
- Benkendorff, K., Rudd, D., Nongmaithe, B. D., Liu, L., Young, F., Edwards, V., Avila, C., and Abbott, C. A. (2015). Are the Traditional Medical Uses of Muricidae Molluscs Substantiated by Their Pharmacological Properties and Bioactive Compounds? *Marine Drugs*, 13(8), Article 8. <https://doi.org/10.3390/md13085237>
- Berger, L., Forstenpointner, G., Frühauf, P., and Kanz, F. (2024). More than just a color: Archaeological, analytical, and procedural aspects of Late Bronze Age purple-dye production at Cape Kolonna, Aegina. *PloS One*, 19(6), e0304340. <https://doi.org/10.1371/journal.pone.0304340>
- Beukes, C. F. (2000). KwaGandaganda: An archaeozoological case study of the exploitation of animal resources during the early Iron Age in KwaZulu-Natal. *Anthropology Master's Thesis, University of South Africa: UNISA Institutional Repository*, 389p. <https://uir.unisa.ac.za/handle/10500/18087>
- Blumer, R.-D., and Knaut, M. (1991). Zum Edelmetallguß in Ossa-Sepia-Formen im Frühmittelalter. *Fundberichte aus Baden-Württemberg*, 16, 545–553. <https://doi.org/10.11588/fbbw.1991.0.41982>
- Bobbio, A. (1972). The first endosseous alloplastic implant in the history of man. *Bulletin of the History of Dentistry*, 20(1), 1–6.
- Brion, A., Zhang, G., Dossot, M., Moby, V., Dumas, D., Hupont, S., Piet, M. H., Bianchi, A., Mainard, D., Galois, L., Gillet, P., and Rousseau, M. (2015). Nacre extract restores the mineralization capacity of subchondral osteoarthritis osteoblasts. *Journal of Structural Biology*, 192(3), 500–509. <https://doi.org/10.1016/j.jsb.2015.10.012>
- Brysbaert, A. (2007). Murex uses in plaster features in the Aegean and Eastern Mediterranean bronze age. *Mediterranean Archaeology and Archaeometry*, 7(2), Article 2.
- Buck, P. H., and Hiroa, T. R. (2003). Arts And Crafts Of Hawaii. *Native Hawaiian Culture and Arts Program, Bishop Museum*, 606p.
- Cagniard, T., Gauthier, J.-P., and Fereire, J. (2024). L'œil de Sainte-Lucie (The eye of Saint-Lucia). *GEMMES, La Revue de l'Association Gemmologie & Francophonie*, 3, 28–44. <https://doi.org/10.63000/wq5XXR9f68>
- Carannante, A. (2014). Archaeomalacology and Purple-Dye. State of the Art and New Prospects of Research. In: *Moluscos y púrpura en contextos arqueológicos atlántico-mediterráneos—Nuevos datos y reflexiones en clave de proceso histórico* (Cantillo, J. J., Bernal, D., and Ramos, J., eds.). *Universidad de Cádiz, Servicio de Publicaciones*, pp. 273–282.

- Chen, P., Sun, J., Ma, L., Chen, Y., and Xia, J. (2022). Effects of shell sand content on soil physical properties and salt ions under simulated rainfall leaching. *Geoderma*, 406, 115520. <https://doi.org/10.1016/j.geoderma.2021.115520>
- Chen, Z.-C., Wu, S.-Y. S., Su, W.-Y., Lin, Y.-C., Lee, Y.-H., Wu, W.-H., Chen, C.-H., and Wen, Z.-H. (2016). Anti-inflammatory and burn injury wound healing properties of the shell of *Haliotis diversicolor*. *BMC Complementary and Alternative Medicine*, 16(1), 487. <https://doi.org/10.1186/s12906-016-1473-6>
- Colonese, A. C., Mannino, M. A., Bar-Yosef Mayer, D. E., Fa, D. A., Finlayson, J. C., Lubell, D., and Stiner, M. C. (2011). Marine mollusc exploitation in Mediterranean prehistory: An overview. *Quaternary International*, 239(1), 86–103. <https://doi.org/10.1016/j.quaint.2010.09.001>
- Cristiani, E., and Borić, D. (2012). 8500-year-old Late Mesolithic garment embroidery from Vlasac (Serbia): Technological, use-wear and residue analyses. *Journal of Archaeological Science*, 39(11), 3450–3469. <https://doi.org/10.1016/j.jas.2012.05.016>
- Darlas, A. (2007). Le Moustérien de Grèce à la lumière des récentes recherches. *L'Anthropologie*, 111(3), 346–366. <https://doi.org/10.1016/j.anthro.2007.04.001>
- Echterhöfner, A. (2020). Shells and Order: Questionnaires on Indigenous Law in German New Guinea. *Journal for the History of Knowledge*, 1(1), Article 1. <https://doi.org/10.5334/jhk.21>
- Einzig, P. (1949). Primitive Money in Its Ethnological, Historical and Economic Aspects. *Canadian Journal of Economics and Political Science / Revue Canadienne de Economiques et Science Politique*, 15(2). <https://doi.org/10.2307/137742>
- Fauvelle, M. (2024). Shell Money: A Comparative Study. *Cambridge University Press and Assessment*. <https://doi.org/10.1017/9781009263344>
- Fernández-Penas, R., Verdugo-Escamilla, C., Triunfo, C., Gärtner, S., D'Urso, A., Oltolina, F., Follenzi, A., Maoloni, G., Cölfen, H., Falini, G., and Gómez-Morales, J. (2023). A sustainable one-pot method to transform seashell waste calcium carbonate to osteoinductive hydroxyapatite micro-nanoparticles. *Journal of Materials Chemistry B*, 11(32), 7766–7777. <https://doi.org/10.1039/D3TB00856H>
- Flausse, A., Henrionnet, C., Dossot, M., Dumas, D., Hupont, S., Pinzano, A., Mainard, D., Galois, L., Magdalou, J., Lopez, E., Gillet, P., and Rousseau, M. (2013). Osteogenic differentiation of human bone marrow mesenchymal stem cells in hydrogel containing nacre powder. *Journal of Biomedical Materials Research Part A*, 101(11), 3211–3218. <https://doi.org/10.1002/jbm.a.34629>
- Fritz, C., Tosello, G., Fleury, G., Kasarhérou, E., Walter, Ph., Duranthon, F., Gaillard, P., and Tardieu, J. (2021). First record of the sound produced by the oldest Upper Paleolithic seashell horn. *Science Advances*, 7(7), eabe9510. <https://doi.org/10.1126/sciadv.abe9510>
- Fukui, H. (1994). The Hora (Conch Trumpet) of Japan. *The Galpin Society Journal*, 47, 47–62. <https://doi.org/10.2307/842662>
- Golani, A. (2014). Cowrie shells and their imitations as ornamental amulets in Egypt and the Near East. *Polish Archaeology in the Mediterranean*, 2(XXIII), 71–83.
- González, A. M. (2002). The Edge of Enchantment: Sovereignty and Ceremony in Huatulco, Mexico. *National Museum of the Amer Indian, Smithsonian*, 192p.
- González, J. A., Amich, F., Postigo-Mota, S., and Vallejo, J. R. (2016). Therapeutic and prophylactic uses of invertebrates in contemporary Spanish ethnoveterinary medicine. *Journal of Ethnobiology and Ethnomedicine*, 12(1), 36. <https://doi.org/10.1186/s13002-016-0111-1>
- González, J. A., and Vallejo, J. R. (2023). The Use of Shells of Marine Molluscs in Spanish Ethnomedicine: A Historical Approach and Present and Future Perspectives. *Pharmaceuticals*, 16(10), Article 10. <https://doi.org/10.3390/ph16101503>
- Gosner, L. R. (2022). Coastal Resource Integration and Reuse in Iron Age South-Eastern Iberia: The Lead Ingots Cast from *Pinna nobilis* Shells. *European Journal of Archaeology*, 25(4), 504–522. <https://doi.org/10.1017/eea.2022.24>
- Halstead, P. (1993). Spondylus shell ornaments from late Neolithic Dimini, Greece: Specialized manufacture or unequal accumulation? *Antiquity*, 67(256), 603–609. <https://doi.org/10.1017/S0003598X00045816>
- Held, M. (2019). Cuttlefish Bone Casting: Theory of Mold Making, Design Possibilities, Practical Casting Technique and Analysis. *The Santa Fe Symposium*, p253–270.
- Henry-Gambier, D., Courty, M. A., Crubézy, E., Kervazo, B., Tisnérat-Laborde, N., and Valladas, H. (2001). La Sépulture des enfants de Grimaldi (Baoussé-Roussé, Italie) — Anthropologie et paléontologie funéraire des populations de la fin du Paléolithique supérieur. *Documents préhistoriques*, 14 pp.177. <https://hal.science/hal-02987856>
- Henshilwood, C., d'Errico, F., Vanhaeren, M., van Niekerk, K., and Jacobs, Z. (2004). Middle Stone Age Shell Beads from South Africa. *Science*, 304(5669), 404–404. <https://doi.org/10.1126/science.1095905>
- Henuk, Y. L., and Dingle, J. G. (2002). Practical and economic advantages of choice feeding systems for laying poultry. *World's Poultry Science Journal*, 58(2), 199–208. <https://doi.org/10.1079/WPS20020018>

- Hill, R. (2001). Traditional paint from Papua New Guinea: Context, materials and techniques, and their implications for conservation. *The Conservator*, 25(1), 49–61. <https://doi.org/10.1080/01410096.2001.9995164>
- Hiwasaki, L., and Shaw, R. (2014). Local and indigenous knowledge for community resilience: Hydro-meteorological disaster risk reduction and climate change adaptation in coastal and small island communities. *UNESCO*, 60p. <https://www.apn-gcr.org/publication/local-and-indigenous-knowledge-for-community-resilience-hydro-meteorological-disaster-risk-reduction-and-climate-change-adaptation-in-coastal-and-small-island-communities/>
- Immanuel, G., Thaddaeus, B. J., Usha, M., Ramasubburayan, R., Prakash, S., and Palavesam, A. (2012). Antipyretic, wound healing and antimicrobial activity of processed shell of the marine mollusc *Cypraea moneta*. *Asian Pacific Journal of Tropical Biomedicine*, 2(3, Supplement), S1643–S1646. [https://doi.org/10.1016/S2221-1691\(12\)60469-9](https://doi.org/10.1016/S2221-1691(12)60469-9)
- Iroko, A. F. (1990). Mollusc money. *UNESCO Courier*, 43(1), 20–26.
- Jalšovec, P. (2023). The nautilus shell as a liminal object between naturalia and artificialia in seventeenth-century Amsterdam. Master Thesis, *Faculty of Humanities, Utrecht University*, 123 p. <https://studenttheses.uu.nl/handle/20.500.12932/44783>
- Keegan, L., Keegan, W., Carlson, L., and Altes, C. (2009). Shell Net Weights from Florida and Puerto Rico. *Proceedings of the XXIII Congress of the International Association for Caribbean Archaeology*.
- Kehinde O., A., Mariam Y., A., Adebimpe O., O., and Blessing A., A. (2015). Traditional utilization and biochemical composition of six mollusc shells in Nigeria. *Revista de Biología Tropical*, 63(2), 459–464.
- Kel, D., Gökçe, H., Bilgiç, D., Ağaoğulları, D., Duman, I., Öveçoğlu, M. L., Kayali, E. S., Kiyici, I. A., Agathopoulos, S., and Oktar, F. N. (2012). Production of Natural Bioceramic from Land Snails. *Key Engineering Materials*, 493–494, 287–292. *Bioceramics* 23. <https://doi.org/10.4028/www.scientific.net/KEM.493-494.287>
- Khamis, Z. (2022). Seashells and snails in Egypt during prehistoric times. *Egyptian Journal of Archaeological and Restoration Studies*, 12(2), 233–247. <https://doi.org/10.21608/ejars.2022.276170>
- Kolar, M. A., Fritz, C., and Tosello, G. (2022). Acoustics in Music Archaeology: Re-Sounding the Marsoulas Conch and Its Cave. *Acoustics Today*, 18(2), 52–61. <https://doi.org/10.1121/AT.2022.18.2.52>
- Krishna, K. M., and Singh, K. K. (2012). A critical review on Ayurvedic drug Kapardika (*Cypraea moneta*, Linn.). *International Research Journal of Pharmacy (IRJP)*, 3(10), Article 10.
- Kuhn, S. L., Stiner, M. C., Reese, D. S., and Güleş, E. (2001). Ornaments of the earliest Upper Paleolithic: New insights from the Levant. *Proceedings of the National Academy of Sciences of the United States of America*, 98(13), 7641–7646. <https://doi.org/10.1073/pnas.121590798>
- Lee, C. H., Lee, D. K., Ali, M. A., and Kim, P. J. (2008). Effects of oyster shell on soil chemical and biological properties and cabbage productivity as a liming materials. *Waste Management*, 28(12), 2702–2708. <https://doi.org/10.1016/j.wasman.2007.12.005>
- Lev, E. (2007). Drugs held and sold by pharmacists of the Jewish community of medieval (11–14th centuries) Cairo according to lists of *materia medica* found at the Taylor–Schechter Genizah collection, Cambridge. *Journal of Ethnopharmacology*, 110(2), 275–293. <https://doi.org/10.1016/j.jep.2006.09.044>
- Lev, E., and Amar, Z. (2008). *Practical Materia medica of the medieval eastern mediterranean according to the Cairo Genizah*. 7, 1–629.
- Lidour, K., and Cuenca Solana, D. (2023). Shell Tools and Use-Wear Analysis: A Reference Collection for Prehistoric Arabia. *Journal of Archaeological Method and Theory*. <https://doi.org/10.1007/s10816-023-09622-9>
- Lodeiros Seijo, C., Santana Cabrera, J. A., Jaramillo Arango, A., Soria, R. G., and Marcos, J. (2018). Short history of spondylus in the south american pacific: A symbol that returns at present. *Interiencia*, 43(12), 871–877. <https://ri.conicet.gov.ar/handle/11336/104040>
- Lutet-Toti, C., Da Silva Feliciano, M., Thomas, J., Crosland, A., Develay, C., Debrosse, N., Force, A., Bidault, A., Broussard, C., Falini, G., Goffredo, S., and Marin, F. (2025). Do bivalve shells exhibit antibacterial properties? Screening calcifying organic matrices against two major marine pathogens. *Science of the TOTAL ENvironment (STOTEN)*, submitted.
- Lutet-Toti, C., Da Silva Feliciano, M., Debrosse, N., Thomas, J., Plasseraud, L., and Marin, F. (2024). Diverting the Use of Hand-Operated Tablet Press Machines to Bioassays: A Novel Protocol to Test ‘Waste’ Insoluble Shell Matrices. *Methods and Protocols*, 7(2), Article 2. <https://doi.org/10.3390/mps7020030>
- Magnabosco, G., Giuri, D., Di Bisceglie, A. P., Scarpino, F., Fermani, S., Tomasini, C., and Falini, G. (2021). New Material Perspective for Waste Seashells by Covalent Functionalization. *ACS Sustainable Chemistry and Engineering*, 9(18), 6203–6208. <https://doi.org/10.1021/acssuschemeng.1c01306>
- Marin, E. (2023). History of dental biomaterials: Biocompatibility, durability and still open challenges. *Heritage Science*, 11(1), 207. <https://doi.org/10.1186/s40494-023-01046-8>

- Mo, K. H., Alengaram, U. J., Jumaat, M. Z., Lee, S. C., Goh, W. I., and Yuen, C. W. (2018). Recycling of seashell waste in concrete: A review. *Construction and Building Materials*, 162, 751–764. <https://doi.org/10.1016/j.conbuildmat.2017.12.009>
- Montagu, J. (2018). The Conch horn—Shell trumpets of the World from Prehistory to Today. *Hataf Segol. Publications*, 214p.
- Morris, J. P., Bäckeljau, T., and Chapelle, G. (2019). Shells from aquaculture: A valuable biomaterial, not a nuisance waste product. *Reviews in Aquaculture*, 11(1), 42–57. <https://doi.org/10.1111/raq.12225>
- Moyle, R. (1990). Polynesian Sound-producing Instruments. *Shire Ethnography*, 72p.
- Nahle, S., Lutet-Toti, C., Namikawa, Y., Piet, M.-H., Brion, A., Peyroche, S., Suzuki, M., Marin, F., and Rousseau, M. (2024). Organic Matrices of Calcium Carbonate Biominerals Improve Osteoblastic Mineralization. *Marine Biotechnology*, 26(3), 539–549. <https://doi.org/10.1007/s10126-024-10316-w>
- Naik, A. S., and Hayes, M. (2019). Bioprocessing of mussel by-products for value added ingredients. *Trends in Food Science and Technology*, 92, 111–121. <https://doi.org/10.1016/j.tifs.2019.08.013>
- Neva, E. (2008). Technical Aspects in Ancient time (4BC-4 AD). In: Jewelry of Central Asia. *Transoxiana*. https://www.transoxiana.com.ar/13/neva-jewelry_central_asia.php
- Nijman, V. (2019). Souvenirs, Shells, and the Illegal Wildlife Trade. *Journal of Ethnobiology*, 39(2), 282–296. <https://doi.org/10.2993/0278-0771-39.2.282>
- Okumura, M. M. M., and Eggers, S. (2005). The people of Jabuticabeira II: Reconstruction of the way of life in a Brazilian shellmound. *Homo: Internationale Zeitschrift Fur Die Vergleichende Forschung Am Menschen*, 55(3), 263–281. <https://doi.org/10.1016/j.jchb.2004.10.001>
- Pankonien, D. (2008). She Sells Seashells: Women and Mollusks in Huatulco, Oaxaca, Mexico. *Archaeological Papers of the American Anthropological Association*, 18(1), 102–114. <https://doi.org/10.1111/j.1551-8248.2008.00008.x>
- Pearson, C. E., and Cook, F. C. (2008). Excavations at the “Bead Maker’s Midden,” Ossabaw Island, Georgia: An Examination of Mississippi Period Craft Specialization on the Georgia Coast. *Ossabaw Island Project, the Digital Archeological Record* (tDAR id: 366083). <https://doi.org/10.6067/XCV80C4TKK>
- Plankenhorn-Farrell, L. (2023). Early Childhood Graves 20,000 to 9,000 Years Ago and Their Cultural Implications. *Master’s Thesis, University of Colorado at Denver*.
- Rousseau, M., Bédouet, L., Lati, E., Gasser, P., Le Ny, K., and Lopez, E. (2006). Restoration of stratum corneum with nacre lipids. *Comparative Biochemistry and Physiology Part B: Biochemistry and Molecular Biology*, 145(1), 1–9. <https://doi.org/10.1016/j.cbpb.2006.06.012>
- Sakalauskaite, J., Andersen, S. H., Biagi, P., Borrello, M. A., Cocquerez, T., Colonese, A. C., Bello, F. D., Girod, A., Heumüller, M., Koon, H., Mandili, G., Medana, C., Penkman, K. E., Plasseraud, L., Schlichtherle, H., Taylor, S., Tokarski, C., Thomas, J., Wilson, J., Marin, F., Demarchi, B. (2019). Palaeoshellomics’ reveals the use of freshwater mother-of-pearl in prehistory. *eLife*, 8. https://www.academia.edu/39225000/Palaeoshellomics_reveals_the_use_of_freshwater_mother_of_pearl_in_prehistory
- Sakalauskaite, J., Plasseraud, L., Thomas, J., Albéric, M., Thoury, M., Perrin, J., Jamme, F., Broussard, C., Demarchi, B., and Marin, F. (2020). The shell matrix of the european thorny oyster, *Spondylus gaederopus*: Microstructural and molecular characterization. *Journal of Structural Biology*, 211(1), 107497. <https://doi.org/10.1016/j.jsb.2020.107497>
- Sehasseh, E. M., Fernandez, P., Kuhn, S., Stiner, M., Mentzer, S., Colarossi, D., Clark, A., Lanoe, F., Pailes, M., Hoffmann, D., Benson, A., Rhodes, E., Benmansour, M., Laissaoui, A., Ziani, I., Vidal-Matutano, P., Morales, J., Djellal, Y., Longet, B., Hublin, J.-J., Mouhiddine, M., Rafi, F. Z., Worthey, K. B., Sanchez-Morales, I., Ghayati, N., Bouzouggar, A. (2021). Early Middle Stone Age personal ornaments from Bizmoune Cave, Essaouira, Morocco. *Science Advances*, 7(39), eabi8620. <https://doi.org/10.1126/sciadv.abi8620>
- Setyowati, E., Hardiman, G., Purwanto, and Budihardjo, M. A. (2019). On the Role of Acoustical Improvement and Surface Morphology of Seashell Composite Panel for Interior Applications in Buildings. *Buildings*, 9(3), Article 3. <https://doi.org/10.3390/buildings9030071>
- Shetty, P. P., Rao, A. U., Pai, B. H. V., and Kamath, M. V. (2023). Performance of High-Strength Concrete with the Effects of Seashell Powder as Binder Replacement and Waste Glass Powder as Fine Aggregate. *Journal of Composites Science*, 7(3), Article 3. <https://doi.org/10.3390/jcs7030092>
- Silve, C., Lopez, E., Vidal, B., Smith, D. C., Camprasse, S., Camprasse, G., and Couly, G. (1992). Nacre initiates biomineralization by human osteoblasts maintained *In vitro*. *Calcified Tissue International*, 51(5), 363–369. <https://doi.org/10.1007/BF00316881>
- Strack, E. (2008). Introduction, Chapter 1. In: The Pearl Oyster (P. C. Southgate & J. S. Lucas, eds.), Elsevier, Oxford, UK: pp 1-35.

- Summa, D., Lanzoni, M., Castaldelli, G., Fano, E. A., and Tamburini, E. (2022). Trends and Opportunities of Bivalve Shells' Waste Valorization in a Prospect of Circular Blue Bioeconomy. *Resources*, 11(5), Article 5. <https://doi.org/10.3390/resources11050048>
- Summer, K., Browne, J., Liu, L., and Benkendorff, K. (2020). Molluscan Compounds Provide Drug Leads for the Treatment and Prevention of Respiratory Disease. *Marine Drugs*, 18(11), Article 11. <https://doi.org/10.3390/md18110570>
- Supar, K., Rani, F. A. A., Mazlan, N. L., and Musa, M. K. (2021). Partial Replacement of Fine Aggregate Using Waste Materials in Concrete as Roof Tile: A Review. *IOP Conference Series: Materials Science and Engineering*, 1200(1), 012008. <https://doi.org/10.1088/1757-899X/1200/1/012008>
- Susanto, M. (2023). The Travelling Nautilus: Spaces of Circulation from the Indian Ocean to Britain. In: *Ichthyology in Context (1500-1880)*. Brill, *Intersections* Vol. 87, pp. 495–522. https://doi.org/10.1163/9789004681187_018
- Taylor, J., and Strack, E. (2008). Pearl production, Chapter 8. In: *The Pearl Oyster* (P. C. Southgate & J. S. Lucas, eds.), Elsevier, Oxford, UK: pp 273–302.
- Thomas, I. (2007). Coquillages : De la parure aux arts décoratifs. *Citadelles & Mazenod*, 255p.
- Topić Popović, N., Lorencin, V., Strunjak-Perović, I., and Čož-Rakovac, R. (2023). Shell Waste Management and Utilization: Mitigating Organic Pollution and Enhancing Sustainability. *Applied Sciences*, 13(1), Article 1. <https://doi.org/10.3390/app13010623>
- Triunfo, C., Gärtner, S., Marchini, C., Fermani, S., Maoloni, G., Goffredo, S., Gomez Morales, J., Cölfen, H., and Falini, G. (2022). Recovering and Exploiting Aragonite and Calcite Single Crystals with Biologically Controlled Shapes from Mussel Shells. *ACS Omega*, 7(48), 43992–43999. <https://doi.org/10.1021/acsomega.2c05386>
- Tsoraki, C., Lingle, A., Schotsmans, E., Veropoulidou, R., Tibbetts, B., Vasic, M., and Bennison-Chapman, L. E. (2020). Pigment Use at Neolithic Çatalhöyük. *Near Eastern Archaeology*. <https://doi.org/10.1086/710215>
- Tudor, H. E. A., Gryte, C. C., and Harris, C. C. (2006). Seashells: Detoxifying Agents for Metal-Contaminated Waters. *Water, Air, and Soil Pollution*, 173(1–4), 209–242. <https://doi.org/10.1007/s11270-005-9060-3>
- Vanhaeren, M., Wadley, L., and d'Errico, F. (2019). Variability in Middle Stone Age symbolic traditions: The marine shell beads from Sibudu Cave, South Africa. *Journal of Archaeological Science: Reports*, 27, 101893. <https://doi.org/10.1016/j.jasrep.2019.101893>
- Venier, P., Gerdol, M., Domeneghetti, S., Sharma, N., Pallavicini, A., and Rosani, U. (2019). Biotechnologies from Marine Bivalves. In: *Goods and Services of Marine Bivalves* (A. C. Smaal, J. G. Ferreira, J. Grant, J. K. Petersen, and Ø. Strand, eds.). Springer International Publishing, pp. 95–112. https://doi.org/10.1007/978-3-319-96776-9_6
- Viriya-empikul, N., Krasae, P., Puttasawat, B., Yoosuk, B., Chollacoop, N., and Faungnawakij, K. (2010). Waste shells of mollusk and egg as biodiesel production catalysts. *Bioresour Technol*, 101(10), 3765–3767. <https://doi.org/10.1016/j.biortech.2009.12.079>
- Voultsiadou, E. (2010). Therapeutic properties and uses of marine invertebrates in the ancient Greek world and early Byzantium. *Journal of Ethnopharmacology*, 130(2), 237–247. <https://doi.org/10.1016/j.jep.2010.04.041>
- Wagner, G., Hilbert, K., Bandeira, D., Tenório, M. C., and Okumura, M. M. (2011). *Sambaquis* (shell mounds) of the Brazilian coast. *Quaternary International*, 239(1), 51–60. <https://doi.org/10.1016/j.quaint.2011.03.009>
- Weerasooriyagedra, M. S., and Kumar, S. A. (2018). A review of utilization of Mollusca shell for the removal of contaminants in industrial waste water. *Int. Jour. of Scientific and Research Publications*, 8(1), 6.
- Westbroek, P., and Marin, F. (1998). A marriage of bone and nacre. *Nature*, 392(6679), 861–862. <https://doi.org/10.1038/31798>
- Windler, A. (2019). The Use of *Spondylus gaederopus* during the Neolithic of Europe. *Journal of Open Archaeology Data*, 7, 7. <https://doi.org/10.5334/joad.59>
- Yang, B. (2021). Once As Money: Cowrie Shells that Made Our World. *Detours: Social Science Education Research Journal*, 2(1), Article 1.
- Yang, B. (2011). The Rise and Fall of Cowrie Shells: The Asian Story. *Journal of World History*, 22(1), 1–25.
- Zeng, T., Guo, J., Li, Y., and Wang, G. (2022). Oyster shell amendment reduces cadmium and lead availability and uptake by rice in contaminated paddy soil. *Environmental Science and Pollution Research*, 29(29), 44582–44596. <https://doi.org/10.1007/s11356-022-18727-9>
- Zhang, G., Brion, A., Willemin, A.-S., Piet, M.-H., Moby, V., Bianchi, A., Mainard, D., Galois, L., Gillet, P., and Rousseau, M. (2017). Nacre, a natural, multi-use, and timely biomaterial for bone graft substitution. *Journal of Biomedical Materials Research Part A*, 105(2), 662–671. <https://doi.org/10.1002/jbm.a.35939>
- Zhang, P., Tang, J., Tang, Q., Zhang, M., Shen, L., Tian, W., Zhang, Y., and Sun, Z. (2019). Shell powder as a novel bio-filler for thermal insulation coatings. *Chinese Journal of Chemical Engineering*, 27(2), 452–458. <https://doi.org/10.1016/j.cjche.2018.02.006>

- Zhang, Y., Chen, D., Liang, Y., Qu, K., Lu, K., Chen, S., and Kong, M. (2020). Study on engineering properties of foam concrete containing waste seashell. *Construction and Building Materials*, 260, 119896. <https://doi.org/10.1016/j.conbuildmat.2020.119896>
- Zheng, Y., Yu, C., Xiao, Y., Ye, T., and Wang, S. (2023). The impact of utilizing oyster shell soil conditioner on the growth of tomato plants and the composition of inter-root soil bacterial communities in an acidic soil environment. *Frontiers in Microbiology*, 14, 1276656. <https://doi.org/10.3389/fmicb.2023.1276656>
- Zilhão, J., Angelucci, D. E., Badal-García, E., d’Errico, F., Daniel, F., Dayet, L., Douka, K., Higham, T. F. G., Martínez-Sánchez, M. J., Montes-Bernárdez, R., Murcia-Mascarós, S., Pérez-Sirvent, C., Roldán-García, C., Vanhaeren, M., Villaverde, V., Wood, R., and Zapata, J. (2010). Symbolic use of marine shells and mineral pigments by Iberian Neandertals. *Proceedings of the National Academy of Sciences*, 107(3), 1023–1028. <https://doi.org/10.1073/pnas.0914088107>

1.3. Molluscan Aquaculture: Production Trends, Challenges and Future Developments

1.3.1. Development of Aquaculture and (pre)Historical Trends

The consumption of shellfish meat by humans is thought to have started during the lower Paleolithic. The oldest archaeological site that exhibits consumed shell remains is that of Pinnacle Point site (cave PP13B), located on the Southern coast of South Africa, dated to 164,000 years (Marean, 2010). The menu was then constituted mostly of brown mussels. The next earliest archaeological site containing consumed seashells was found on the coast of Red Sea in Eritrea and is dated to 125,000 years ago. Neandertals, about 110,000 years ago, were cooking shellfish in caves in coastal Italy. As often, the consumption of sea shells was probably a fortuitous but opportunistic discovery, which brought a supplementary source of proteins (Colonese *et al.*, 2011). This became then a common practice, which meant an adaptation to coastal environments and a likely change in daily activities, with an increase of the shell gathering activity. This augmentation can be attested by the regular and global observation of shell mounds, *concheiros*, or “middens”: quite common in coastal regions, they consist of large deposits of shells emptied after meat consumption, whether marine or freshwater (Bailey, 1975; Rabett *et al.*, 2011; Wijsman *et al.*, 2019; Rick, 2024). The stratification of shell middens and the dating of layers show that this consumption was neither likely intensive nor exclusive in most sites, but rather persistent through long periods of time. The durability of seashells compared to other food waste, also tends to an over-estimation of their representation in the archaeological record. This potential bias must be taken into consideration when researching the composition of past diets and evolution of food related behaviors and subsistence strategies (Hausmann *et al.*, 2019).

During the transition from the Paleolithic to the Neolithic period, the harvesting of mollusks evolved alongside the development of agriculture. Initially, foraged mollusks served as temporary food substitutes during times of scarcity (Colonese *et al.*, 2011). However, through sedentarization, mollusks became a consistent part of the diet: for instance, gastropod harvesting persisted in northeastern Moroccan communities while cultivated crops provided stable food stocks (Hutterer *et al.*, 2014; Yanes *et al.*, 2018). The collection of mollusks was species selective, all year-round, with seasonal variation of volumes, over centuries. In some of these communities, terrestrial snails were gathered and even kept alive before planned consumption, while systematic perforations suggest active processing for food (Hutterer *et al.*, 2014). These early domestication practices imply long-term resources management skills and

an understanding of molluscan life cycles, marking the switch from plain harvesting to nascent forms of (aqua)culture (Yanes *et al.*, 2018).

The purple dye industry in the Mediterranean region, which flourished from the Late Bronze Age through the Byzantine period, represents one of the earliest large-scale exploitations of mollusks for their derived products (here, dye). The first non-domestic, large-scale workshops emerged in Minoan Crete, eventually spreading along the entire Mediterranean coast. This industry primarily utilized Muricidae gastropods for producing dyes used in ceramics, textiles, and wall paintings (Carannante, 2014; Iacovou & Mylona, 2019; Berger *et al.*, 2024). The process involved collecting live animals using baited baskets and exclusively using them for dye production, with no alimentary use. Multiple species of Muricidae were employed, each producing varying shades of purple. The extraction process involved deliberately crushing the shell to access the hypobranchial gland (Alberti, 2008), resulting in the animal's death, with the shells becoming significant by-products of the industry. The dye production was labor-intensive, requiring large quantities of animals to extract sufficient amounts of ink. Some of these purple dyes were reserved for royalty, palaces, and priests, indicating their high value and the industrialized nature of their production (Iacovou & Mylona, 2019; Berger *et al.*, 2024). In Huatulco, Mexico, a more sustainable approach to dye extraction developed, particularly with the *caracol púrpura* (Pankonien, 2008): initiated around 500 BCE, the production of purple *tixinda* is a women-led artisanship that continues to thrive today. They invented specific methods for hand-shellfishing in intertidal zones and for low-impact, non-lethal dye extraction, allowing long-term management of the gastropods. Additionally, harvesting sites were - and are still – periodically selected, preventing overexploitation and ensuring sufficient time for gastropods to produce enough ink. By allowing the resource populations to remain viable and stable to this day, the dye exploitation of *caracol púrpura* can be regarded as sustainable aquaculture. Adaptive harvesting strategies were not limited to dye extraction, but were also applied to mollusks consumed for food: for example, Mississippian cultures developed extensive knowledge on mollusks biology and behavior, adapting their methods to nocturnal harvesting and even following migrations (Pearson & Cook, 2008).

The beginning of proper molluscan aquaculture can be dated back to ancient Rome (around 200 BCE), when the reproductive selection and rearing of flat oysters spread through Italian coasts. Mussel culture developed strongly in France 13th century with the introduction of *bouchots* which are artificial substrates made of ropes and put in the intertidal zones to

increase and localize juvenile recruitment. By the 19th century, France was already yearly producing 20 000 tons of flat oysters (Wijsman *et al.*, 2019).

1.3.2. Contemporary Production Trends

1.3.2.1. Shell Products and Pearls

As illustrated in the first half of this introductory chapter (Lutet-toti *et al.*, 2025, *submitted to Journal of Ethnobiology*), molluscan shells are vastly exploited for their ornamental qualities. With over 2700 tons produced in 2022, pearl culture and shell goods production are significant sectors of the broader mollusk aquaculture industry (Martinez *et al.*, 2018; Smaal *et al.*, 2018). Various mollusks, including some oysters, scallops, some freshwater mussels and gastropods like abalones and conchs, produce pearls as a defense mechanism. Indeed, the secretion of a pearl is triggered when foreign objects enter the extra-pallial space, potentially harming the soft-tissues or transmitting pathogens. Concentric layers of minerals eventually encapsulate the intruding object, forming a smooth pearl, *i.e.*, a natural pearl, over time (Shen *et al.*, 2020). These natural pearls are only exceptionally ‘nacreous’, *i.e.* made of mother-of-pearl. For example, the queen conch shells (*Lobatus (ex-Strombus) gigas*) produces natural pink pearls made of aragonite, but with a fully crossed-lamellar microstructure. Other natural pearls can be prismatic calcitic, like the very rare brown-to-red pearls of the Mediterranean fan mussel, *Pinna nobilis*.

As truly nacreous pearls were recognized to be the most beautiful, the most valuable and stable in time, considerable efforts were made to produce them at large scale, in particular in Japan, at the end of the 19th / beginning of the 20th century. Naigai (2013) reports the development of pearl culture in Japan in this period during which numerous attempts were made to develop a reproducible protocol to induce pearl formation in the Akoya oyster, *Pinctada fucata*. Several methods were successively developed, including the “Meiji method”, and the “wrapping method” and the “piece method”, aimed at enhancing the productivity, quality of pearls and survival rates of the mollusks. Since these early developments, the pearl industry has grown into a global enterprise spanning over 30 countries and the process of pearl formation has been standardized: pearl oysters are grafted with a spherical nucleus and a minute piece of mantle tissue of a donor oyster, the ‘graft’; the grafting process is a quasi-surgical operation, performed in the gonad; after 18 months (in French Polynesia), a single pearl – protected inside the pearl sack that emanates from the development of the graft - can be collected. Then, a second nucleus can be inserted into the pearl sack, for generating a second pearl 18 months later. China has emerged as the world’s largest producer, with an annual production of 3 540 tons,

representing 98% of the global output. However, it is worth noticing that more than 99% of this Chinese production consists of pearls of the freshwater triangle shell mussel, *Sinohyriopsis* (ex-*Hyriopsis*) *cumingii*. In the marine pearls sector, Japan leads with an annual production of 23 tons, followed by China with 18 tons and French Polynesia with 12,9 tons, which is exclusively exploiting *Pinctada margaritifera* oysters (Zhu *et al.*, 2019). Other relatively important players in the production of marine pearls are Australia, Indonesia, Philippines, Myanmar, Papua New Guinea, India, Cook Islands, Mexico. While pearls represent the flagship product of pearl industry, a derived product – of lesser value – consist in inserting and glueing an object between the inner surface of the pearl oyster and the mantle tissue. This object, usually a semi-sphere, or a semi drop, is progressively covered by nacre deposits. After six months in the lagoon, the oyster is collected and the ‘blister pearl’, also called ‘*mabé*’ or ‘semi-pearl’ is cut from the shell and can be commercialized. One oyster can produce at the same time 4 to 8 *mabés* (2 to 4 per valve). Usually, *mabé*-producing oysters are specimens of lesser quality for grafting, or old specimens that have already been grafted once or twice. Contrarily to pearls, *mabés* are truly shell products.

It is important to note that pearl culture and shell product industries, while significant aspects of molluscan aquaculture, primarily focus on commercializing their biomineralized products rather than discarding them. Consequently, this review will not delve further into these topics, as it is primarily centered on the by-product shells derived from molluscan exploitation for food consumption.

1.3.2.2. Shellfish and Aquaculture of Edible Mollusks

In the 1990s, fisheries and aquaculture accounted for approximately 80% and 20% of global aquatic production by mass, respectively. By the early 2020s, both sectors had greatly increased their outputs, effectively doubling total production and attaining 223.2 million tons (FAO, 2024). However, the distribution between the two sectors has significantly shifted, with aquaculture’s share escalating to nearly 51% of total production. According to the latest FAO’s State of the World Fisheries Report (2024), 2022 marked a milestone as aquaculture production volumes surpassed those of capture fisheries for the first time, reaching a record of 130.9 million tons of biomass.

According to Wijsman *et al.* (2019), bivalves account for 14% of all marine production worldwide. In these 14%, only 11% coming from wild capture fisheries, while the remaining 89% comes from aquaculture. In Europe, this proportion rises up to 25%, with the United

Kingdom leading in wild catches, followed by Denmark (primarily for mussels), France (essentially scallops), and Italy (specializing in venus clams) (Tičina *et al.*, 2020). The FAO's State of World Fisheries and Aquaculture report (2024) highlights that wild-captures are mainly specialized in certain molluscan species, particularly squids, scallops, and cephalopods, which collectively amounted to 6,150 thousand tons in 2022.

In New Zealand, in order to protect natural bivalve resources, wild capture and harvesting have been discouraged. Laws and subventions facilitate the establishment of nurseries populated through natural recruitment or hatchery reproduction (Ministry of Primary Industries, 2013; Wijsman *et al.*, 2019).

1.3.2.3. Conchyliculture

At world scale, the total mollusk aquaculture production accounts for approximately 18,911,320 tons annually (FAO, 2024). Mollusks represent around 17% of all aquaculture products in the Americas, 20% in Europe, and 21% in Asia. Although some species are still harvested in the wild, more than 75% of bivalve production is sourced from conchyliculture (Wijsman *et al.*, 2019; Hough, 2022; FAO, 2024). China dominates the global market, producing 85% of its total biomass, while Europe accounts for 5.5%, yielding over 800,000 tons annually. On their part, Oceania and Africa contribute roughly 1% of the global production, with the majority primarily coming from New Zealand, which produces 94 000 tons of blue mussels (*Mytilus edulis*) annually (Wijsman *et al.*, 2019).

With over 6 million tons produced annually worldwide almost entirely through conchyliculture, cupped oysters (*Magallana gigas*) represent the second-largest group of exploited marine animals in weigh, fisheries and aquaculture combined. China is the primary producer, providing 87% of the global output in 2021, followed by Korea (5%), Japan (2%), the USA (2%) and Europe (2%) (EUMOFA, 2024). Scallops also rank among the top ten marine animal species produced, exceeding 4 million tons annually. Despite locally developed wild-captures cited above, scallops are predominantly exploited through aquaculture facilities (FAO, 2024). In the Mediterranean Sea, conchyliculture mainly involves the mussel *Mytilus galloprovincialis* and the warty venus *Venerupis philippinarum*, with limited or experimental culture of Pacific cupped oysters *Magallana gigas*. This can be explained by the fact that the two main actors of this industry, France and Spain, locate their facilities on their Atlantic coasts where the space pressure is less intense. Indeed, the densely populated coasts of the Mediterranean Sea leave little space available for conchyliculture, leading to a finfish-oriented

distribution of aquaculture industries among Mediterranean countries (Tičina *et al.*, 2020; Carvalho & Guillen, 2021; United Nations Environment Programme, 2021).

In Europe, Spain is the largest producer of mollusks through aquaculture in weight, contributing to approximately 50% of the total production. Its conchyliculture primarily focuses on the Mediterranean mussel *Mytilus galloprovincialis*, which constitutes 83% of its production and a third of total European exports in weight. France represents Europe's leading producer of cupped oysters *Magallana gigas* with an annual output of 78,000 tons accounting for 76% of production. While the majority of the produced oysters is destined to its domestic market, France still leads European countries in global exports with 18% of global revenues (Hough, 2022; FAO, 2024). Conversely to the specialized conchyliculture organization of Spain, France has a more balanced strategy, cultivating a variety of bivalves: Pacific oysters *Magallana gigas* account for 46.6%, blue mussels *Mytilus edulis* for 37.9%, and Mediterranean mussels *Mytilus galloprovincialis* for 8.8% (Wijsman *et al.*, 2019).

As bivalves are shell-bearing mollusks primarily harvested for their soft tissues, the generation of shell byproducts in conchyliculture represents a significant aspect of the industry. Indeed, shells account for a substantial portion of the total bivalve biomass, with approximately 10 million tons of shells produced annually in aquaculture systems, representing up to 75% of the total output weight in most operations (Morris *et al.*, 2019; Summa *et al.*, 2022). The proportion of shell mass varies among species due to differences in shell thickness and structure, as illustrated in the Table 1.1 below. For bivalves with very thin shells - like mussels - this proportion drops to around 45%, while some make up 90% of the animal's weight (Japanese scallop *Mizuhopecten yessoensis*) (Summa *et al.*, 2022).

Table 1.1: Mass of dry shells produced by seven bivalves of economic interest, in proportion of their live, whole wet body mass (with soft tissues). These values were calculated on live animals collected, emptied, cleaned and dried, that were acquired from local seafood markets (Dijon, France). Note that these seven species of bivalves represent the experimental models used in the following chapters of my doctoral thesis.

Mollusk species	<i>Glycymeris glycymeris</i>	<i>Mytilus galloprovincialis</i>	<i>Magallana gigas</i>	<i>Pecten maximus</i>	<i>Cerastoderma edule</i>	<i>Venus verrucosa</i>	<i>Venerupis philippinarum</i>
Mean mass of the whole wet body (g)	55.03	7.42	67.22	142	6.99	43.01	19.44
Mean mass of the emptied dry shell (g)	40.26	3.42	44.24	94	4.46	29.23	11.05
% mass of the shell / whole wet body	73%	47%	66%	66%	64%	68%	57%

As previously briefly introduced while discussing the history of aquaculture, various methods have been specifically developed in consideration of each species needs for optimal production rates in conchyliculture. Mussels are reared using suspended substrates like rafts and *bouchots* or bottom-sheltered bed systems. Oysters are gathered in cages or netted bags either on the bottom floor or suspended in the water column to benefit from the tumbling of the waves. Clams and cockles are typically cultivated directly in sandy or muddy substrates, while scallops may be grown using suspended nets or on the seabed (EUMOFA, 2024; Palomares & Pauly, 2024).

Conchyliculture is often encouraged as a form of meat production, as it is highly efficient in land use compared to terrestrial animal production. Studies have shown that bivalve aquaculture can produce up to 28,000 kg of protein per hectare per year, which is significantly higher than terrestrial livestock systems: for example, annual beef production typically yields only about 9.5 kg of protein per hectare. Moreover, bivalve aquaculture generates significantly lower greenhouse gas emissions, producing about 11 tons per ton of edible protein compared to 340 tons for beef. This is further enhanced by the filter feeding type of the large majority of bivalves, which greatly reduces the need for energetic input in aquaculture systems. Consequently, conchyliculture is often referred to as "unfed aquaculture" (Willer & Aldridge, 2020; Azra *et al.*, 2021; Verdegem *et al.*, 2023).

1.3.3. Threats and Limitations of Conchyliculture

Evaluating aquaculture carrying capacity is essential for a sustainable management of bivalve production. This concept encompasses four main dimensions: physical capacity (the total area allocated to rearing), production capacity (the maximum sustainable yield of cultured bivalves), ecological capacity (the density above which ecological impacts appear), and social capacity (the level of development acceptable to local communities). Depending on the implantation site, limitations can occur in any or multiple of these dimensions, coming as obstacles in the production rates and sustainability of conchyliculture installations (Smaal & van Duren, 2019). For instance, a significant challenge in land-based closed systems of mollusk aquaculture is water filtration, recycling, and depollution to limit environmental impact and reduce resource consumption (Verdegem *et al.*, 2023).

Another challenge is the waste management of shell byproducts, which constitute a substantial portion of conchyliculture production. While some shells are repurposed for various applications described in section 1.1. From Ornaments to Biotechnologies, the majority is

discarded either at sea (when space is available), or on land. The disposal of shell waste is costly and problematic. For instance, in the UK, it costs around 80£ per ton to dispose of shells in landfills, which can lead to illegal dumping in uncontrolled piles. Additionally, in some countries, landfills may not even be a viable option for disposal, forcing producers and consumers to resort to less regulated methods. This terrestrial accumulation causes issues beyond mere space occupation, including soil pollution, disease spread, and attraction of wild animals due to decomposing organic matter. These factors raise health and safety concerns, necessitating the implementation of organized shell waste management strategies (Morris *et al.*, 2019; Summa *et al.*, 2022). While waste management represents one of the challenges facing conchyliculture, the following sections will explore other critical threats and challenges currently facing conchyliculture.

1.3.3.1. Diseases

Bivalves are predominantly filter feeders, making them good candidates for rearing as minimal impact animals. However, this feeding strategy also makes them highly sensitive to environmental stressors such as climate, physicochemical changes, and microbial pathogens (Ponder *et al.*, 2020; Verdegem *et al.*, 2023). This vulnerability has been demonstrated throughout History, with significant impacts that even participated in shaping today's shellfish production landscape. For instance, during the 1950s, Portugal experienced mass mortalities of bivalves related to protozoan parasitism that led to drastic population declines. Similarly, the French oyster industry faced a crisis in the 1970s when local populations were wiped out after successive infections, necessitating their replacement with exotic species from Canada. This introduction, while intended to revive the industry, subsequently led to disease outbreaks in other species due to exotic parasitic infections (Wijsman *et al.*, 2019).

Bivalves are susceptible to a diverse range of microorganisms, including herpesvirus, gill necrosis virus, *Roseovarius* (affecting juvenile oysters), *Vibrio* species, *Nocardia* bacteria, *Perkinsus* spp. (attacking the mantle epithelium), *Marteilia* (Travers *et al.*, 2015; Kunselman *et al.*, 2024). Their proliferation and transmission, facilitated by global maritime trade, can severely impact aquaculture production at a large scale. For instance, since 2008, repetitive herpesvirus outbreaks caused a persistent drop in global oyster and scallop production yield rates (Wijsman *et al.*, 2019). *Vibrio* bacteria represent another global threat: while some strains induce cold-water vibriosis, physiologically limited geographically, others are adapted to warmer waters and can be observed around multiple continents (Kashulin *et al.*, 2017; Triga *et*

al., 2023). In France, Manila clams were subjected to the “brown ring disease” by *V. tapetis* outbreaks. This infection induced high mortality rates, with alteration of the tissues, and progressing colored markings on the shell (Paillard, 2004).

Abiotic environmental factors can also be at the origin of bivalve diseases like abnormal developments of the bivalve shell. Antifouling chemicals have been shown to exert dramatic effects on shell growth: during the 80s, the use of Tributyltin spread on ship hulls and port beams caused severe losses for nearby bivalve exploitations. Bivalves exposed to this chemical often exhibited shell deformities (with the formation of ‘chambers’ in shell thickness), abnormal growth patterns, and finally, a decreased thickness and heightened brittleness (Dyrynda, 1992; Lacoste & Gaertner-Mazouni, 2015).

1.3.3.2. Food Safety and Human Health Concerns

When consuming infected bivalves, interspecific pathogen transmission is sometimes possible towards humans. This is the case for microorganisms such as *Vibrio spp.*, norovirus, and hepatitis A virus, which can cause severe (sometime life-threatening) conditions in humans. In cases when pathogens are effectively barred from entering the body, unsuspecting consumers could still be ingesting harmful amounts of microbial toxins. For example, brevetoxins and saxitoxins provoke neurological illnesses in humans, ranging from chronic pain to paralysis (affections better known to the general public as the grouped paralytic shellfish poisoning). These toxins accumulated in mollusk tissues are produced by cyanobacteria, particularly dinoflagellates like *Alexandrium catenella* or *Karenia spp.*, which thrive in rising sea temperatures (Arnich *et al.*, 2021).

1.3.3.3. Climate Change Impacts

The spread of bivalve microbial diseases is exacerbated by climate change and anthropogenic activities. As warming temperatures favor the proliferation of some cyanobacteria and microalgae species, Harmful Algal Blooms (HABs) lead to declines in conchyliculture production and substantial economic losses. HABs are indeed capable of directly killing bivalves by producing toxins, inducing hypoxic/anoxic water conditions, or even clogging their gills and digestive tracks. For instance, France incurred \$2 million in losses for *Mytilus edulis* in 2019 due to market closures and suspensions after chronic exposures to HABs (PICES Scientific Reports, 2020).

Climate change also impacts mollusks defenses mechanisms and resistance to pathogens: under heatwaves, their defenses mechanisms are more rapidly overwhelmed which increases mortality and reduces reproductive success in surviving individuals. Weakened pathogen resistances almost always result in secondary infections: pathogenic *Vibrio* bacteria have been observed to opportunistically contaminate oysters infected by the cyanobacteria *A. catenella* (Abi-Khalil *et al.*, 2016).

The combination of both higher sea water temperatures and low pH (hypercapnia) has significantly negative impacts on overall bivalve fitness and physicochemical resilience. Mussel for example show a sharp decline in byssus strength, valve opening time, shell growth and thickness under hypercapnia and extreme water temperature events (Fitzer *et al.*, 2014; Martinez *et al.*, 2018; Cubillo *et al.*, 2021; Lassoued *et al.*, 2021). This tendency is even more often observed among populations that are not used to experiencing great temperature gradients throughout the year (Lattos *et al.*, 2023; Azizan *et al.*, 2024). In itself, ocean acidification mainly impacts larval development, notably in shell formation. The adults show indeed better resilience to low pH thanks to their periostracum (the organic outer layer of the shell) and behavioral adaptations (Hendriks *et al.*, 2010; Auzoux-Bordenave *et al.*, 2019).

1.3.3.4. Space Competition

The space used for mollusk rearing can come into competition with wild habitats and other anthropic coastal uses, such as maritime transport, environmental conservation, construction, and recreational activities. This space competition is even more visible in densely populated areas. For example, Europe's bivalve production has declined by 100,000 tons over 20 years due to reduction of available cultivable marine zones: the vast majority of this decrease was observed in the Netherlands, which is currently expanding its territory on previously submerged areas (Wijsman *et al.*, 2019).

1.3.3.5. Impacts on Wild Environments and Communities

Bivalve aquaculture, while far less polluting than other types of meat production, can still negatively impact the surrounding wild ecosystems. As bivalves possess high fecundity with dispersive qualities, the reared populations are often at high risk of genetic drift and inbreeding depression. When in open-systems, the circulation of their offsprings might greatly challenge the genetic diversity of wild populations (Hollenbeck & Johnston, 2018; Zenger *et al.*, 2019).

Although the impact of cultivating allochthonous mollusks on wild autochthonous mollusks is still poorly understood and studied, one can presume that a constant input of allochthonous larvae bring imbalance the native ecosystems by creating invasive populations (Tičina *et al.*, 2020).

By introducing changes in nutrients availability dynamics, conchyliculture locally impacts planktonic communities, but long-term significant modifications have not been documented yet. The beneficial or detrimental nature of these impacts depend on the trophic charge of the sites, seasonal changes and pre-installation situation (anthropized or wild pristine areas) (Ministry of Primary Industries, 2013). Digestive waste from mollusks can modify sediment composition and create mudbeds, impacting benthic communities (Tičina *et al.*, 2020; Smaal *et al.*, 2021). The installation of bivalve culture sites creates artificial habitats and reefs that modify tridimensional complexity of the area, modifying water circulation. Like the previous alterations brought by conchyliculture, this can have both positive and negative impacts depending on the pre-existing environment and volume of the artificial habitat. Often considered as Fish Aggregating Devices (FADs), they can provide new habitats to struggling native species. However, their installation has to be well thought-over, as they could have adverse effects by promoting invasive species recruitment (tunicates in New-Zealand, Ministry of Primary Industries, 2013) or experience excessive nutrient discharge that can lead to nitrophilic algae growth and alter fish feeding behavior.

1.3.4. Solutions and their Limits

1.3.4.1. Usual Solutions

The sanitary quality of shellfish products is closely monitored worldwide, with France being particularly rigorous in its surveillance. Aquaculture, due to its liquid environment, increases the transmission of parasites and pathogens. While antibiotics are traditionally used in bath treatments as prophylactic, therapeutics, metaphylactics and growth promoters, this same environment can foster the rise and spread of antibiotic resistance, which can persist long-term in the water and be transmitted to untreated populations. This spread has been observed beyond aquaculture systems, leaking into the natural environment (Miranda *et al.*, 2013; Ali *et al.*, 2014; Hossain *et al.*, 2022).

Sustainable alternatives to antibiotics include probiotics, phage therapy, and ultrafiltration of water in closed systems. Like in terrestrial agriculture, selective breeding and genomic selection are performed - among oysters notably – in order to increase growth rates

and resistance to pathogens (Hollenbeck & Johnston, 2018; Zenger *et al.*, 2019). However, as mentioned earlier, these methods have cost limitations, are solely applicable to closed systems, and/or might sustain ecological impacts on wild microbial communities (Kunselman *et al.*, 2024). A method to increase volumes while ensuring high genetic mixing has been developed, where the larvae or juveniles of wild bivalves are collected in the water column to input rearing installations. This method, called “seed” or “spat” collection, can be regarded as quite sustainable as it has virtually no impact on the wild adult population volumes. The advantages of this solution have to be somehow nuanced, as the health and quality of seeds may more often than not be unfit for exploitation (Smaal *et al.*, 2021).

1.3.4.2. Integrated Multi-Trophic Aquaculture (IMTA)

The development of the marine polyculture branch of conchyliculture mainly comes as a sustainable effort to reduce fish farming impacts (Carballeira Braña *et al.*, 2021). While effectively reducing these negative impacts, Integrated Multi-Trophic Aquaculture (IMTA) also improves mollusk production but requires more space and complex maintenance than marine aquaculture. It faces challenges in installations and struggles to develop in areas with limited space like Europe (Hughes & Black, 2016; Yu *et al.*, 2017).

IMTA is improving mollusk production in length, growth rate and weigh, as the filter feeding bivalves act as allochthonous nutrient feeders, reducing aquaculture-originated eutrophication of wild environments (Sarà *et al.*, 2009). Structural organization designs have to be adapted to the species involved so that they share positive interactions rather hinder each other’s development (Yu *et al.*, 2017). Outside of Mediterranean Sea, IMTA exploitations are often coupled with multi activity platforms offshore, such as wind energy plants (van den Burg *et al.*, 2017). More studies and development of these integrative systems are needed to assess and evaluate the environmental benefits compared to economical costs (Yu *et al.*, 2017; Giangrande *et al.*, 2021; Nederlof *et al.*, 2022).

1.3.4.3. Open Ocean Aquaculture

Transitioning from inshore to offshore aquaculture is often seen as a solution to space competition, particularly in the Mediterranean Sea. There, the creation of artificial substrate and habitats in previously purely pelagic environments can be linked to carbon sequestration and reef restoration, but open ocean aquaculture systems face challenges in poor nutrient availability and low economic viability (Giangrande *et al.*, 2021).

1.3.4.4. Innovative Products and Approaches

Sustainable solutions are developed to reduce the impacts and prevalence of microbial pathogens in mollusk aquaculture. They currently include research on water ultrafiltration, probiotics, and phage therapy. While ultrafiltration through sand filters has shown promising results against some *Vibrio* species, it is a lengthy and costly process, applicable only to closed systems. Depuration, a similar method, also faces these limitations (Zhang *et al.*, 2018; Kunselman *et al.*, 2024).

While certain fish diseases are prevented by vaccines, their development is not achievable in mollusks because of their lack of acquired immune system. However, it is possible to induce immunization through “immune priming” (see Chapter [2.1.4. Molecular defenses](#)) and form proto vaccines treatments (Delisle *et al.*, 2023; Tammas *et al.*, 2024).

The use of probiotics from sponge associated fungi secreting enzymes has shown anti-*vibrio* capacities and comes as an interesting solution in vibrioses combatting drugs (Syaifudien Bahry *et al.*, 2021). It is however important to consider the consequences of probiotics and phage therapy in open environments, they may have unintended ecological impacts on wild microbial communities (Ringø, 2020; Kunselman *et al.*, 2024).

Medication administration through feeding, and new antibiotic use strategies are being explored, but face challenges such as the rise of antibiotic resistance. The filter-feeding strategy of bivalves also complexifies the distribution of drugs: they often have to be suspended into the water and thus have to exert limited effects on non-target organisms or be used in closed-systems (Lulijwa *et al.*, 2020; Pepi & Focardi, 2021; Bondad-Reantaso *et al.*, 2023).

1.4. Concluding Remarks and Thesis Outline

Producing over 14 million tons of bivalve each year globally, conchyculture is on the rise as the major meat producer for a significant portion of the human population. This very active sector of food industry generates huge amounts of by-products, the shells, that are estimated around 10 million tons annually. While bivalve shells are repurposed in various fields, as described above (section 1.2), a large majority is still considered as waste and discarded, posing a risk of becoming environmental and social nuisances. Past, traditional and contemporary knowledge on mollusk shells assumed and proved properties sparks the interest on these mineralized organs packed with potential, that are just waiting to be repurposed. Indeed, several studies already focus on the osteoinductive and wound healing properties of

bivalve shells; and the current state of pathogen landscapes raises concerns regarding multidrug-resistant microorganisms and emerging diseases around the sensitive sectors of food security, environmental conservation and human health. In this frame, my doctoral research focuses on the search for antibacterial molecules in a very abundant wasted resource. I thereby intend to develop a new, innovative, sophisticated way to valorize shells. To this end, I extracted and characterize the organic matrices of seven bivalves from the common consumption and performed antibacterial screening against marine pathogens, in combination with a proteomic approach on the shell extracts.

The structure of my manuscript unfolds as follows: in the next chapter, Chapter 2, I discuss the general system of bivalve defenses, before focusing on the description of the shells and shells microstructure of my studied models. This chapter ends with the establishment of an exhaustive up-to-date inventory of all the identified AntiMicrobial Peptides and Proteins (AMPP) in mollusk soft tissues, drawing a parallel with my search for these molecules in the hard tissue of the shell.

Chapter 3 represents the main course of this manuscript. There, I present the set-up of the antibacterial screening and following proteomic analysis: the studied model sources of putative bioactive molecules, the bacterial targets, and the required adaptation for marine microorganisms. This chapter encompasses two papers, one published on the innovative protocol allowing the first-time use of insoluble compounds of the shell's matrix; and one submitted, exposing the positive results of the screening.

Chapter 4 regroups the miscellanea: the non-published data (negative results of the screening) and the intermediate phases of experimentations. These data remain in the core of my doctoral dissertation because they provide crucial information on the overall antibacterial screening and the growth of poorly documented bacteria under several conditions.

In Chapter 5, I build the general discussion of my thesis, and produce an overview of the knowledge developed with this antibacterial screening and proteomic exploration. I discuss the limits of my projects and the perspectives it brings in terms of further experiments and potential application fields.

Finally, the annex is available in Chapter 6. There, I insert two papers on which I collaborated: one published in 2023, exploring the biomedical field through the osteogenic inductive properties of nacre; and one on a novel analytical process combining multispectral imaging and electrophoretic gels of shell pigments of extant and fossil gastropods (45 million-year-old). In these two papers, my contribution was substantial.

1.5. Chapter References

- Abi-Khalil, C., Lopez-Joven, C., Abadie, E., Savar, V., Amzil, Z., Laabir, M., and Rolland, J.-L. (2016). Exposure to the Paralytic Shellfish Toxin Producer *Alexandrium catenella* Increases the Susceptibility of the Oyster *Crassostrea gigas* to Pathogenic Vibrios. *Toxins*, 8(1), Article 1. <https://doi.org/10.3390/toxins8010024>
- Alberti, M. E. (2008). Murex Shells as Raw Material: The Purple-Dye Industry and Its By-products : Interpreting the Archaeological Record. *Kaskal : Rivista Di Storia, Ambiente e Culture Del Vicino Oriente Antico. Volume 5, 2008*, 1000–1018. <https://doi.org/10.1400/118340>
- Ali, M., Rahman, M., Hossain, M. B., and Rahman, Md. Z. (2014). Aquaculture Drugs Used for Fish and Shellfish Health Management in the Southwestern Bangladesh. *Asian Journal of Biological Sciences*, 7, 25–32. <https://doi.org/10.3923/ajbs.2014.225.232>
- Arnich, N., Abadie, E., Amzil, Z., Dechraoui Bottein, M.-Y., Comte, K., Chaix, E., Delcourt, N., Hort, V., Mattei, C., Molgó, J., and Le Garrec, R. (2021). Guidance Level for Brevetoxins in French Shellfish. *Marine Drugs*, 19(9), Article 9. <https://doi.org/10.3390/md19090520>
- Auzoux-Bordenave, S., Wessel, N., Badou, A., Martin, S., M'Zoudi, S., Avignon, S., Roussel, S., Huchette, S., and Dubois, P. (2019). Ocean acidification impacts growth and shell mineralization in juvenile abalone (*Haliotis tuberculata*). *Marine Biology*, 167(1), 11. <https://doi.org/10.1007/s00227-019-3623-0>
- Azizan, A., Venter, L., Zhang, J., Young, T., Ericson, J. A., Delorme, N. J., Ragg, N. L. C., and Alfaro, A. C. (2024). Interactive effects of elevated temperature and *Photobacterium swingsii* infection on the survival and immune response of marine mussels (*Perna canaliculus*): A summer mortality scenario. *Marine Environmental Research*, 196, 106392. <https://doi.org/10.1016/j.marenvres.2024.106392>
- Azra, M. N., Okomoda, V. T., Tabatabaei, M., Hassan, M., and Ikhwanuddin, M. (2021). The Contributions of Shellfish Aquaculture to Global Food Security: Assessing Its Characteristics From a Future Food Perspective. *Frontiers in Marine Science*, 8. <https://www.frontiersin.org/articles/10.3389/fmars.2021.654897>
- Bailey, G. N. (1975). The role of molluscs in coastal economies: The results of midden analysis in Australia. *Journal of Archaeological Science*, 2(1), 45–62. [https://doi.org/10.1016/0305-4403\(75\)90045-X](https://doi.org/10.1016/0305-4403(75)90045-X)
- Berger, L., Forstenpointner, G., Frühauf, P., and Kanz, F. (2024). More than just a color: Archaeological, analytical, and procedural aspects of Late Bronze Age purple-dye production at Cape Kolonna, Aegina. *PloS One*, 19(6), e0304340. <https://doi.org/10.1371/journal.pone.0304340>
- Bondad-Reantaso, M. G., MacKinnon, B., Karunasagar, I., Fridman, S., Alday-Sanz, V., Brun, E., Le Groumellec, M., Li, A., Surachetpong, W., Karunasagar, I., Hao, B., Dall'Occo, A., Urbani, R., and Caputo, A. (2023). Review of alternatives to antibiotic use in aquaculture. *Reviews in Aquaculture*, 15(4), 1421–1451. <https://doi.org/10.1111/raq.12786>
- Carannante, A. (2014). *Archaeomalacology and Purple-Dye. State of the Art and New Prospects of Research*. (pp. 273–282).
- Carballeira Braña, C. B., Cerbule, K., Senff, P., and Stolz, I. K. (2021). Towards Environmental Sustainability in Marine Finfish Aquaculture. *Frontiers in Marine Science*, 8. <https://doi.org/10.3389/fmars.2021.666662>
- Carvalho, N., and Guillen, J. (2021). Aquaculture in the Mediterranean. In: IEMed. Mediterranean Yearbook 2021: Vol. Strategic Sectors | Economy and Territory. *European Commission*, p. 6. https://www.iemed.org/wp-content/uploads/2021/11/Aquaculture-in-Mediterranean_MedYearbook2021.pdf
- Colonese, A. C., Mannino, M. A., Bar-Yosef Mayer, D. E., Fa, D. A., Finlayson, J. C., Lubell, D., and Stiner, M. C. (2011). Marine mollusc exploitation in Mediterranean prehistory: An overview. *Quaternary International*, 239(1), 86–103. <https://doi.org/10.1016/j.quaint.2010.09.001>
- Cubillo, A. M., Ferreira, J. G., Lencart-Silva, J., Taylor, N. G. H., Kennerley, A., Guilder, J., Kay, S., and Kamermans, P. (2021). Direct effects of climate change on productivity of European aquaculture. *Aquaculture International*, 29(4), 1561–1590. <https://doi.org/10.1007/s10499-021-00694-6>
- Delisle, L., Rolton, A., and Vignier, J. (2023). Inactivated ostreid herpesvirus-1 induces an innate immune response in the Pacific oyster, *Crassostrea gigas*, hemocytes. *Frontiers in Immunology*, 14. <https://doi.org/10.3389/fimmu.2023.1161145>
- Dyrynda, E. A. (1992). Incidence of abnormal shell thickening in the Pacific oyster *Crassostrea gigas* in Poole Harbour (UK), subsequent to the 1987 TBT restrictions. *Marine Pollution Bulletin*, 24(3), 156–163. [https://doi.org/10.1016/0025-326X\(92\)90244-Z](https://doi.org/10.1016/0025-326X(92)90244-Z)
- EUMOFA. (2024). The EU market overview. *European Market Observatory for Fisheries and Aquaculture Products (EUMOFA)*, *European Commission*. <https://eumofa.eu/>
- FAO. (2024). The State of World Fisheries and Aquaculture 2024 (SOFIA) - Blue Transformation in action. *Food and Agriculture Org. (FAO) of the United Nations*, Rome, Italy, 264 p. <https://doi.org/10.4060/cd0683en>
- Fitzer, S. C., Phoenix, V. R., Cusack, M., and Kamenos, N. A. (2014). Ocean acidification impacts mussel control on biomineralisation. *Scientific Reports*, 4(1), 6218. <https://doi.org/10.1038/srep06218>

- Giangrande, A., Gravina, M. F., Rossi, S., Longo, C., and Pierri, C. (2021). Aquaculture and Restoration: Perspectives from Mediterranean Sea Experiences. *Water*, 13(7), Article 7. <https://doi.org/10.3390/w13070991>
- Hausmann, N., Meredith-Williams, M., Douka, K., Inglis, R. H., and Bailey, G. (2019). Quantifying spatial variability in shell midden formation in the Farasan Islands, Saudi Arabia. *PLOS ONE*, 14(6), e0217596. <https://doi.org/10.1371/journal.pone.0217596>
- Hendriks, I. E., Duarte, C. M., and Álvarez, M. (2010). Vulnerability of marine biodiversity to ocean acidification: A meta-analysis. *Estuarine, Coastal and Shelf Science*, 86(2), 157–164. <https://doi.org/10.1016/j.ecss.2009.11.022>
- Hollenbeck, C. M., and Johnston, I. A. (2018). Genomic Tools and Selective Breeding in Molluscs. *Frontiers in Genetics*, 9, 253. <https://doi.org/10.3389/fgene.2018.00253>
- Hossain, A., Habibullah-Al-Mamun, Md., Nagano, I., Masunaga, S., Kitazawa, D., and Matsuda, H. (2022). Antibiotics, antibiotic-resistant bacteria, and resistance genes in aquaculture: Risks, current concern, and future thinking. *Environmental Science and Pollution Research*, 29(8), 11054–11075. <https://doi.org/10.1007/s11356-021-17825-4>
- Hough, C. (2022). *Regional review on status and trends in aquaculture development in Europe – 2020* (FAO). Food and Agriculture Org. (FAO) of the United Nations, Rome, Italy, Circular No. 1232/1, 114p. <https://doi.org/10.4060/cb7809en>
- Hughes, A. D., and Black, K. D. (2016). Going beyond the search for solutions: Understanding trade-offs in European integrated multi-trophic aquaculture development. *Aquaculture Environment Interactions*, 8, 191–199. <https://doi.org/10.3354/aei00174>
- Hutterer, R., Linstädter, J., Eiwanger, J., and Mikdad, A. (2014). Human manipulation of terrestrial gastropods in Neolithic culture groups of NE Morocco. *Quaternary International*, 320, 83–91. <https://doi.org/10.1016/j.quaint.2013.12.006>
- Iacovou, M., and Mylona, D. (2019). Purple dye production under royal management: Evidence from the Cypro-Classical citadel of Ancient Paphos. *Cahiers Du Centre d'Études Chypriotes*, 49, Article 49. <https://doi.org/10.4000/cchyp.586>
- Kashulin, A., Seredkina, N., and Sørum, H. (2017). Cold-water vibriosis. The current status of knowledge. *Journal of Fish Diseases*, 40(1), 119–126. <https://doi.org/10.1111/jfd.12465>
- Kunselman, E., Wiggin, K., Diner, R. E., Gilbert, J. A., and Allard, S. M. (2024). Microbial threats and sustainable solutions for molluscan aquaculture. *Sustainable Microbiology*, 1(1), qvae002. <https://doi.org/10.1093/sumbio/qvae002>
- Lacoste, E., and Gaertner-Mazouni, N. (2015). Biofouling impact on production and ecosystem functioning: A review for bivalve aquaculture. *Reviews in Aquaculture*, 7(3), 187–196. <https://doi.org/10.1111/raq.12063>
- Lassoued, J., Padín, X. A., Comeau, L. A., Bejaoui, N., Pérez, F. F., and Babarro, J. M. F. (2021). The Mediterranean mussel *Mytilus galloprovincialis*: Responses to climate change scenarios as a function of the original habitat. *Conservation Physiology*, 9(1), coaa114. <https://doi.org/10.1093/conphys/coaa114>
- Lattos, A., Papadopoulos, D. K., Feidantsis, K., Giantsis, I. A., Georgoulis, I., Karagiannis, D., and Michaelidis, B. (2023). Antioxidant Defense of *Mytilus galloprovincialis* Mussels Induced by Marine Heatwaves in Correlation with *Marteilia Pathogen Presence*. *Fishes*, 8(8), Article 8. <https://doi.org/10.3390/fishes8080408>
- Lulijwa, R., Rupia, E. J., and Alfaro, A. C. (2020). Antibiotic use in aquaculture, policies and regulation, health and environmental risks: A review of the top 15 major producers. *Reviews in Aquaculture*, 12(2), 640–663. <https://doi.org/10.1111/raq.12344>
- Lutet-toti, C., Thomas, J., Falini, G., Goffredo, S., Gabillot, M., and Marin, F. (2025). From ornaments to biotechnologies: The evolution of mollusk shell uses through the ages. *Journal of Ethnobiology*, submitted.
- MPI. (2013). Overview of ecological effects of aquaculture - Growing and Protecting New-Zealand. *Ministry of Primary Industries (MPI)*, 81p.
- Marean, C. W. (2010). Pinnacle Point Cave 13B (Western Cape Province, South Africa) in context: The Cape Floral kingdom, shellfish, and modern human origins. *Journal of Human Evolution*, 59(3–4), 425–443. <https://doi.org/10.1016/j.jhevol.2010.07.011>
- Martinez, M., Mangano, M. C., Maricchiolo, G., Genovese, L., Mazzola, A., and Sarà, G. (2018). Measuring the effects of temperature rise on Mediterranean shellfish aquaculture. *Ecological Indicators*, 88, 71–78. <https://doi.org/10.1016/j.ecolind.2018.01.002>
- Miranda, C. D., Rojas, R., Garrido, M., Geisse, J., and González, G. (2013). Role of shellfish hatchery as a reservoir of antimicrobial resistant bacteria. *Marine Pollution Bulletin*, 74(1), 334–343. <https://doi.org/10.1016/j.marpolbul.2013.06.032>
- Morris, J. P., Backeljau, T., and Chapelle, G. (2019). Shells from aquaculture: A valuable biomaterial, not a nuisance waste product. *Reviews in Aquaculture*, 11(1), 42–57. <https://doi.org/10.1111/raq.12225>

- Nagai, K. (2013). A History of the Cultured Pearl Industry. *Zoological Science*, 30(10), 783–793. <https://doi.org/10.2108/zsj.30.783>
- Nederlof, M. A. J., Verdegem, M. C. J., Smaal, A. C., and Jansen, H. M. (2022). Nutrient retention efficiencies in integrated multi-trophic aquaculture. *Reviews in Aquaculture*, 14(3), 1194–1212. <https://doi.org/10.1111/raq.12645>
- Paillard, C. (2004). A short-review of brown ring disease, a vibriosis affecting clams, *Ruditapes philippinarum* and *Ruditapes decussatus*. *Aquatic Living Resources*, 17(4), Article 4. <https://doi.org/10.1051/alr:2004053>
- Palomares, M. L. D., and Pauly, D. (2024, August). *Magallana gigas* (Thunberg, 1793), giant cupped oyster. SeaLifeBase. <https://www.sealifebase.ca/summary/Magallana-gigas.html>
- Pankonien, D. (2008). She Sells Seashells: Women and Mollusks in Huatulco, Oaxaca, Mexico. *Archaeological Papers of the American Anthropological Association*, 18(1), 102–114. <https://doi.org/10.1111/j.1551-8248.2008.00008.x>
- Pearson, C. E., and Cook, F. C. (2008). Excavations at the “Bead Maker’s Midden,” Ossabaw Island, Georgia: An Examination of Mississippi Period Craft Specialization on the Georgia Coast. *Ossabaw Island Project, the Digital Archeological Record* (tDAR id: 366083). <https://doi.org/10.6067/XCV80C4TKK>
- Pepi, M., and Focardi, S. (2021). Antibiotic-Resistant Bacteria in Aquaculture and Climate Change: A Challenge for Health in the Mediterranean Area. *International Journal of Environmental Research and Public Health*, 18(11), 5723. <https://doi.org/10.3390/ijerph18115723>
- PICES Scientific Reports. (2020). GlobalHAB: Evaluating, Reducing and Mitigating the Cost of Harmful Algal Blooms: A Compendium of Case Studies. *North Pacific Marine Science Organization (PICES)*, Vera L. Trainer (eds.) Vol. 59, 112p. <https://meetings.pices.int/publications/scientific-reports>
- Ponder, W. F., Lindberg, D. R., and Ponder, J. M. (2020). Biology and Evolution of the Mollusca, Volume 1. *CRC Press, Taylor and Francis Group*, 924p.
- Rabett, R., Appleby, J., Blyth, A., Farr, L., Gallou, A., Griffiths, T., Hawkes, J., Marcus, D., Marlow, L., Morley, M., Tân, N. C., Son, N. V., Penkman, K., Reynolds, T., Stimpson, C., and Szabó, K. (2011). Inland shell midden site-formation: Investigation into a late Pleistocene to early Holocene midden from Trảng An, Northern Vietnam. *Quaternary International*, 239(1), 153–169. <https://doi.org/10.1016/j.quaint.2010.01.025>
- Rick, T. C. (2024). Shell Midden Archaeology: Current Trends and Future Directions. *Journal of Archaeological Research*, 32(3), 309–366. <https://doi.org/10.1007/s10814-023-09189-9>
- Ringø, E. (2020). Probiotics in shellfish aquaculture. *Aquaculture and Fisheries*, 5(1), 1–27. <https://doi.org/10.1016/j.aaf.2019.12.001>
- Sarà, G., Zenone, A., and Tomasello, A. (2009). Growth of *Mytilus galloprovincialis* (mollusca, bivalvia) close to fish farms: A case of integrated multi-trophic aquaculture within the Tyrrhenian Sea. *Hydrobiologia*, 636(1), 129–136. <https://doi.org/10.1007/s10750-009-9942-2>
- Shen, W., Hu, Y., He, Z., Xu, S., Xu, X., Zhang, G., and Ren, G. (2020). Histological and Comparative Transcriptome Analyses Provide Insights Into the Immune Response in Pearl Sac Formation of *Hyriopsis cumingii*. *Frontiers in Marine Science*, 7. <https://doi.org/10.3389/fmars.2020.00256>
- Smaal, A. C., Craeymeersch, J. A., and van Stralen, M. R. (2021). The impact of mussel seed fishery on the dynamics of wild subtidal mussel beds in the western Wadden Sea, The Netherlands. *Journal of Sea Research*, 167, 101978. <https://doi.org/10.1016/j.seares.2020.101978>
- Smaal, A. C., Ferreira, J. G., Grant, J., Petersen, J. K., and Strand, Ø. (2018). Goods and Services of Marine Bivalves. *Springer International Publishing*, 591 p.
- Smaal, A. C., and van Duren, L. A. (2019). Bivalve Aquaculture Carrying Capacity: Concepts and Assessment Tools. In: A. C. Smaal, J. G. Ferreira, J. Grant, J. K. Petersen, and Ø. Strand (Eds.), *Goods and Services of Marine Bivalves* (pp. 451–483). *Springer International Publishing*. https://doi.org/10.1007/978-3-319-96776-9_23
- Summa, D., Lanzoni, M., Castaldelli, G., Fano, E. A., and Tamburini, E. (2022). Trends and Opportunities of Bivalve Shells’ Waste Valorization in a Prospect of Circular Blue Bioeconomy. *Resources*, 11(5), Article 5. <https://doi.org/10.3390/resources11050048>
- Syaifudien Bahry, M., Radjasa, O. K., and Trianto, A. (2021). Potential of marine sponge-derived fungi in the aquaculture system. *Biodiversitas Journal of Biological Diversity*, 22, 2883–2892. <https://doi.org/10.13057/biodiv/d220740>
- Tammas, I., Bitchava, K., and Gelasakis, A. I. (2024). Transforming Aquaculture through Vaccination: A Review on Recent Developments and Milestones. *Vaccines*, 12(7), Article 7. <https://doi.org/10.3390/vaccines12070732>
- Tičina, V., Katavić, I., and Grubišić, L. (2020). Marine Aquaculture Impacts on Marine Biota in Oligotrophic Environments of the Mediterranean Sea – A Review. *Frontiers in Marine Science*, 7. <https://www.frontiersin.org/articles/10.3389/fmars.2020.00217>

- Travers, M.-A., Boettcher Miller, K., Roque, A., and Friedman, C. S. (2015). Bacterial diseases in marine bivalves. *Journal of Invertebrate Pathology*, 131, 11–31. <https://doi.org/10.1016/j.jip.2015.07.010>
- Triga, A., Smyrli, M., and Katharios, P. (2023). Pathogenic and Opportunistic *Vibrio* spp. Associated with Vibriosis Incidences in the Greek Aquaculture: The Role of *Vibrio harveyi* as the Principal Cause of Vibriosis. *Microorganisms*, 11(5), Article 5. <https://doi.org/10.3390/microorganisms11051197>
- United Nations Environment Programme. (2021). State of the Environment and Development in the Mediterranean (SoED) 2020. *United Nations*, 340. <https://doi.org/10.18356/9789280737967>
- van den Burg, S. W. K., Kamermans, P., Blanch, M., Pletsas, D., Poelman, M., Soma, K., and Dalton, G. (2017). Business case for mussel aquaculture in offshore wind farms in the North Sea. *Marine Policy*, 85, 1–7. <https://doi.org/10.1016/j.marpol.2017.08.007>
- Verdegem, M., Buschmann, A. H., Latt, U. W., Dalsgaard, A. J. T., and Lovatelli, A. (2023). The contribution of aquaculture systems to global aquaculture production. *Journal of the World Aquaculture Society*, 54(2), 206–250. <https://doi.org/10.1111/jwas.12963>
- Wijsman, J. W. M., Troost, K., Fang, J., and Roncarati, A. (2019). Global Production of Marine Bivalves. Trends and Challenges. In: A. C. Smaal, J. G. Ferreira, J. Grant, J. K. Petersen, and Ø. Strand (Eds.), Goods and Services of Marine Bivalves (pp. 7–26). *Springer International Publishing*. https://doi.org/10.1007/978-3-319-96776-9_2
- Willer, D. F., and Aldridge, D. C. (2020). Sustainable bivalve farming can deliver food security in the tropics. *Nature Food*, 1(7), 384–388. <https://doi.org/10.1038/s43016-020-0116-8>
- Yanes, Y., Hutterer, R., and Linstädter, J. (2018). On the transition from hunting-gathering to food production in NE Morocco as inferred from archeological *Phorcus turbinatus* shells. *The Holocene*, 28(8), 1301–1312. <https://doi.org/10.1177/0959683618771474>
- Yu, L. Q. J., Mu, Y., Zhao, Z., Lam, V. W. Y., and Sumaila, U. R. (2017). Economic challenges to the generalization of integrated multi-trophic aquaculture: An empirical comparative study on kelp monoculture and kelp-mollusk polyculture in Weihai, China. *Aquaculture*, 471, 130–139. <https://doi.org/10.1016/j.aquaculture.2017.01.015>
- Zenger, K. R., Khatkar, M. S., Jones, D. B., Khalilisamani, N., Jerry, D. R., and Raadsma, H. W. (2019). Genomic Selection in Aquaculture: Application, Limitations and Opportunities With Special Reference to Marine Shrimp and Pearl Oysters. *Frontiers in Genetics*, 9. <https://doi.org/10.3389/fgene.2018.00693>
- Zhang, H., Yang, Z., Zhou, Y., Bao, H., Wang, R., Li, T., Pang, M., Sun, L., and Zhou, X. (2018). Application of a phage in decontaminating *Vibrio parahaemolyticus* in oysters. *International Journal of Food Microbiology*, 275, 24–31. <https://doi.org/10.1016/j.ijfoodmicro.2018.03.027>
- Zhu, C., Southgate, P. C., and Li, T. (2019). Production of Pearls. In: A. C. Smaal, J. G. Ferreira, J. Grant, J. K. Petersen, and Ø. Strand (Eds.), Goods and Services of Marine Bivalves (pp. 73–93). *Springer International Publishing*. https://doi.org/10.1007/978-3-319-96776-9_5



CHAPTER 2 - MOLLUSCAN DEFENSES



2.1. Introduction: The Molluscan Intrinsic Defense System

Mollusks represent one of the most diversified groups of animals. These soft bodied organisms are widely distributed globally, thriving in various ecosystems - terrestrial, marine, and freshwater – while facing threats from predation, desiccation, parasites, and pathogens. To survive, mollusks have developed a range of defense mechanisms adapted to their ecological niches and environmental pressure. Beyond behavioral survival strategies, intrinsic defenses include physical protection from shells, chemical defenses through mucus and antimicrobial substances, and cellular responses via hemocytes. This chapter explores these integrated defense systems and their synergies, before focusing on the shells of bivalve models used during this doctorate and molecular components identified in mollusk soft tissues.

2.1.1. The Shell as a Primary Defense Mechanism

When present, the shell serves as the first line of defense for mollusks against environmental threats. Creating a controlled environment for the vulnerable soft body (Marin *et al.*, 2012), the shell provides mechanical protection against predation and crushing forces, reduces parasite exposure, and limits desiccation by minimizing the evaporative surface area (Lowell, 1984; Cortie, 1992; Ponder *et al.*, 2020a). This rigid construction also serves as a structural support, enabling mollusks to maintain shape and integrity of internal organs, as well as facilitating motility via muscle attachment or even as proper moving appendices and buoyancy aids (Cortie, 1992).

Although mollusks are mostly known for their external shell, this character is not systematic amongst members of this phylum: the *Aplacophora* superclass for instance, consists of shell-less wormlike mollusks, while their close relatives, the *Polyplacophora* - one of the most notable examples being the chitons - develop shell-like overlapping plates and spicules that partially cover their body. “True” shells as one usually intends when talking about seashells are observed in the *Conchifera* subphylum, which comprises five classes of “shelly” mollusks: the *Bivalvia*, *Gastropoda*, *Scaphopoda*, *Cephalopoda*, and *Monoplacophora* (Fig. 2.1). Even in these classes, note that some clades have secondarily internalized their shell or even lost it by evolution: among gastropods, this is the case for sea hares (*Aplysia*), land slugs or sea slugs (nudibranchs); among cephalopods, one finds cuttlefish (internal cuttlebone), squids (internal organic skeleton) or octopus (no skeleton). However, these examples are exceptions and one estimates that more than 95% of conchiferan mollusks possess an external shell. Molluscan shells are primarily made of calcium carbonate (CaCO_3), which accounts for 95 to 99% of their

weight. The remaining 1 to 5% consists of an organic matrix, a cocktail of biomolecules that includes proteins and peptides, polysaccharides, glycoproteins, lipids, pigments and diverse metabolites (Marin *et al.*, 2012). This matrix is supposed to regulate the mineral deposition during shell formation but its precise role is still being discussed (Weiner *et al.*, 1984; Nudelman *et al.*, 2006; Marin, 2020). In *Conchifera*, shells are typically made of two polymorphs of calcium carbonate: aragonite or calcite, with some taxa displaying both forms of crystallization. The shell structure is characterized by superimposed layers of microstructures which are defined by specific crystalline arrangements, sizes and directions. The type and organization of microstructures found in a shell affect its toughness, flexibility and durability (Marin *et al.*, 2012; Liang *et al.*, 2021). A few examples are: aragonitic nacre (or mother-of-pearl), foliated calcite, crossed-lamellar aragonite, prismatic calcite. Million years of evolution have allowed these microstructures to acquire peculiar physical properties, in relation to protective function: to give an example, aragonitic nacre possesses a fracture toughness about thousand times higher than that of a geological abiotic aragonite (Jackson *et al.*, 1988). These microstructures will be discussed further in the following part of this chapter (see 2.2. The bivalve shell), where I introduce the shells of the bivalve models used during my doctorate.

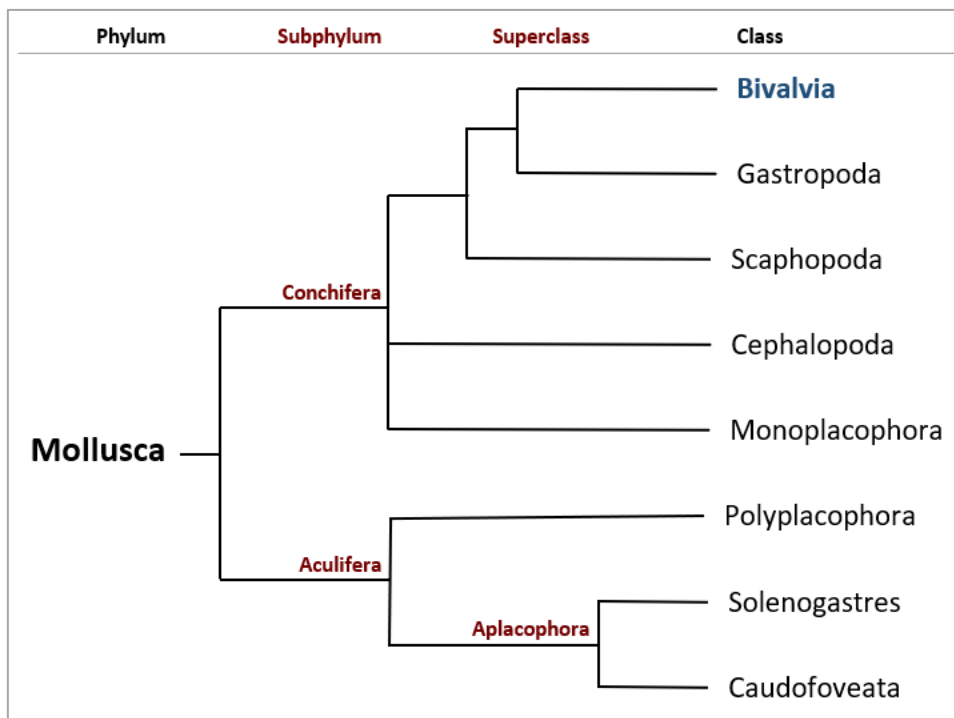


Figure 2.1: Phylogenetic tree of the molluscan classes, elaborated after the classifications of Ponder and Lindberg (2020b), Bieler (2014), and the latest accepted entries of the WoRMS and MolluscaBase (Ahyong *et al.*, 2024; MolluscaBase eds., 2024). The Subphyla and a discriminating superclass are represented in burgundy red. In blue, I put the emphasis on the Bivalvia class, which encompasses the models studied in this thesis.

As mollusks colonized a vast diversity of environments, marine, freshwater or terrestrial, they evolved shells with a high variability in shapes, organization, composition, development strategies, thickness and density (Irie & Iwasa, 2005; Lowenstam *et al.*, 1989; Ponder *et al.*, 2020a). Multiple adaptations have been documented on shell thickness and microstructural composition depending on predator presence and on their appendices: for example, specific valve curvatures and sizes can put crab claws into failure (Blundon & Kennedy, 1982; Leonard *et al.*, 1999; Brönmark *et al.*, 2011). Another interesting adaptation to stressors is the mitigation of physicochemical pressure by the development of rounder, more globular shapes of shells as inducible defense under elevated pCO₂ conditions (*i.e.* low pH waters) (Stallings *et al.*, 2021). This plasticity in shell morphology in response to environmental cues can even be found within species, in cases where the pressure is particularly strong (Stanley, 1970; Leonard *et al.*, 1999; Bourdeau & Johansson, 2012). While a thick, robust shell might appear as the perfect foolproof defense mechanism against both predation and physicochemical threats, its formation is costly for the organism and it can be quite limiting in terms of movements that are much needed to achieve proper fitness (foraging, mate research, reproduction...). Furthermore, some predators have developed specific organs and strategies to overcome shells, underlining the tradeoff nature of shell adaptations, between mechanical strength and behavioral defenses (*i.e.* compromising between escape or defensive aggression, see sections 2.1.2. Mucus and 2.1.4. Molecular defenses) (Rundle & Brönmark, 2001; Johnson, 2020).

Although acellular, mollusk shells are neither inert exoskeletons, nor ‘dead’ secretory products: they can slightly remodel by superficial internal dissolution, during hypoxia or anaerobiosis phases. Furthermore, repair and regeneration processes ensure continued protection even in case of breakage or fragilization. The damaged sites can be visible under SEM, where localized increases of microstructure volumes and layers indicate efforts and “bursts” in rapid mineralization (Watabe, 1983; Fleury *et al.*, 2008; Crane *et al.*, 2021). As shells also sustain damage from microbial attacks, a similar increase of mineralization can be observed under these stressors, supported by heightened hemocyte recruitment (Trinkler *et al.*, 2011). This last response shares nature with other biomineralization-involving mechanisms that will be discussed later in this chapter (see 2.1.3. Cellular defenses).

The following three mechanisms are part of an integrated chemical and cellular defense system, that is efficient when the shell fails to protect mollusks or when they lack one. While all defense mechanisms introduced in this chapter interact and impact the others, the “mucus”,

“cellular defenses”, and “molecular securities” are particularly connected through synergetic activations occurring across every compartment of the molluscan body.

2.1.2. Mucus: The First Line of Chemical Defense

The molluscan mucus is a viscoelastic substance secreted by mucocytes in the tissues that are in contact with the exterior environment (*i.e.* mantle epithelium, gills, foot and digestive system) and, in bivalves, accumulated in the pallial and extrapallial space. It is composed of 90 to 99.7% of water and 0.3 to 10% of glycoproteins (mainly mucins), lipids, proteoglycans, enzymes, and various other bioactive compounds (Davies & Hawkins, 1998; Allam & Raftos, 2015; Pales Espinosa *et al.*, 2016). The metabolic cost of mucus production can exceed 25% of a mollusk's energy budget, indicating its crucial role in survival: mucosal functions are indeed involved in almost all physiological processes and acts as both a physical and chemical barrier for mollusks (Davies *et al.*, 1990; Davies & Hawkins, 1998; Ponder *et al.*, 2020a).

The adhesive and lubricant properties of mucus are essential to molluscan locomotion, allowing them to glide adhere to various surfaces, but also to digestion by facilitation food bolus transit in the esophagus. In terrestrial and intertidal mollusks, mucus plays a vital role in water retention: as they lack a waterproof tegument, they are particularly vulnerable to dehydration and the hydrated gel nature of the mucus acts as moisture control (Gliński & Jarosz, 1997; Davies & Hawkins, 1998; Iwamoto *et al.*, 2014).

Another key function of mucus lies in its antifouling and entrapping properties, which along with beating cilia, immobilizes microorganisms and rids the body and its close surroundings of potential pathogens (Franzenburg *et al.*, 2013; Cerullo *et al.*, 2023). Its composition is modulated by secretions of various bioactive molecules and compounds to create a hostile environment for microorganisms: a number of potent antimicrobial factors can be observed in the mucus, such as lysozymes, lectins, antimicrobial peptides or other antimicrobial enzymes and proteins; the mucin fraction often demonstrating superior antibacterial efficacy (Gliński & Jarosz, 1997; Allam & Raftos, 2015; Pales Espinosa *et al.*, 2016). Some species of gastropods even secrete a mucus charged in metal ions (*e.g.*, copper, iron, manganese, zinc), which showed high toxicity against Gram positive and negative bacteria (Pitt *et al.*, 2015; Greistorfer *et al.*, 2017).

Mucus also plays a role in maintaining bodily and cellular integrity in mollusks. It provides a setting for extracellular matrix assembly and the stimulation of fibroblast proliferation, which are critical processes in wound healing and hemostasis (Gliński & Jarosz,

1997). Furthermore, the mucus exhibits detoxifying properties through the presence of antioxidants like Glutathione-S-Transferase (GST) and Superoxide Dismutase (SOD), which offer protection against free radical damage (Pitt *et al.*, 2015).

As indicated by its composition, the mucus is part of a synergetic defensive effort for mollusks: it serves as a medium for hemocytes migration (cellular defense mechanism), facilitating their movements, pathogen recognition (Gliński & Jarosz, 1997; Davies & Hawkins, 1998; Allam & Raftos, 2015) and phagocytic activity by entrapping and concentrating exogenous particles (Pales Espinosa *et al.*, 2016). This medium function is further appreciated in the accumulation of enzymes and other molecular defenses at the interface with the environment, seconded by the delivery of antimicrobial peptides to infection sites (Franzenburg *et al.*, 2013, Allam & Pales Espinosa, 2016). The creation of a controlled microenvironment, with high concentrations of antimicrobial compounds further enhances their effectiveness and co-activations against pathogens (Allam & Raftos, 2015).

The composition and functionality of mucus is highly variable among and even within mollusk species depending on ecological niches and individual living conditions. The hydration and secretion ratios of certain enzymatic and proteinaceous compounds can be adapted to modify the physicochemical and mechanical properties, creating mucus specialized in specific physiological functions. This is exemplified by the terrestrial gastropod *Cornu aspersum*, which produces three types of mucus: an adhesive one for the pedal surface, a lubricating one for foot and shell movements, and finally an antimicrobial one covering the mantle (Campion, 1961; Cerullo *et al.*, 2023). Some species' mucus (*e.g.*, *Phyllidia varicosa*) contains volatile compounds that can be toxic to predators (Cimino *et al.*, 1985; Dutertre *et al.*, 2014). Other specialized functions include the dehydrated mucus ropes for suspension, mucus trails for interindividual signaling, and mucus sacks for food capture and reproduction (Chase *et al.*, 1978; Davies & Hawkins, 1998). These mucus types will not be further discussed here, as they do not fall into the defense mechanism category.

The mucus is a versatile and complex substance essential to the integrative combined defense mechanism of mollusks. Its broad range of physicochemical and bioactive properties discussed above make it a subject of interest in current research: the mucus could have promising applications in biomedicine and materials science as solutions in skincare, drug delivery, tissue engineering, and composite materials (Pitt *et al.*, 2015).

2.1.3. Cellular Defenses: The Mobile Immune Response

Aside from mucocytes (the secretory “goblet” cells producing the mucus), the cellular defenses of mollusks are carried by hemocytes, which represent the main cellular component of their innate immune system. Hemocytes are particularly mobile cells that circulate in the hemolymph and infiltrate tissues, and can also be found in the pallial and extra pallial cavities (Destoumieux-Garzón *et al.*, 2020). According to Grinchenko and Kumeiko, (2022) they can be divided in three categories depending on their sizes and the presence/quantity of granules in their nuclei: 1) small hyalinocytes (small agranulocytes); 2) hyalinocytes (simple agranulocytes); and 3) granulocytes. Hemocytes specialization is associated to their morphology, and their main functions include: cellular immune response, synthesis and secretion of humoral factors, transport of substances and regulation of various tissue processes such as repairs, mineralization and growth (Gliński & Jarosz, 1997; Al-Khalaifah, 2022).

The first defensive mechanism of hemocytes is the production of Pattern Recognition Receptors (PRRs) to enable the recognition of exogenous particles. Their attachment to other cells triggers the production of signaling compounds by the hemocytes on site, stimulating the recruitment of other hemocytes and starting the immune response. Some recent advances in mollusk immunity research reveal that PRRs might undergo bacterial species-specific triggers through pathogen-associated molecular patterns attachment and be linked to a form of “priming” immunity, where the individuals display stronger immune responses after secondary infections, but they do not appear to depend on the virulence of the strains (Rubio *et al.*, 2019; Al-Khalaifah, 2022).

In a second step, when granulocytes have reached and come into contact with the foreign particle, the later are usually eliminated via phagocytosis. When the size or abundance of the invaders are too much for a single hemocyte, they gather in large numbers and engage in nodule formation or encapsulation (Destoumieux-Garzón *et al.*, 2020; Al-Khalaifah, 2022; Grinchenko & Kumeiko, 2022). In some cases, specific hemocytes secrete phenoloxydase enzymes to start an additional process of melanization, introducing toxic molecules into the closed environment of the capsule and further creating a physical barrier between the pathogen and the host. This process is often followed by biomineralization of the capsule, before elimination (Allam & Raftos, 2015).

Aside from direct attacks on the exogenous organisms and particles, hemocytes build “passive” – with the nuance that their secretion can be heightened after pathogen challenge - defense systems: they synthesize, transport and secrete the toxic compounds that create inhospitable environments for other organisms (in internal compartments as well as in the

mucus, see section [2.1.2. Mucus](#)). These compounds include highly reactive oxygen species (ROS), nitric oxide (NO), antimicrobial peptides and proteins (AMPPs) and hydrolytic enzymes (Canesi & Pruzzo, 2016). Additionally, infected hemocytes can perform ETosis: they sacrifice themselves to release a combination of DNA-backbone structures forming extracellular traps that are adorned with histones and granulocyte antimicrobial proteins, thus immobilizing and killing the pathogens and triggering a foolproof phagocytosis (Guimarães-Costa *et al.*, 2012).

As mentioned earlier, hemocytes have multiple locations and action sites, namely around the epithelium and the extrapallial cavity, where they interact with the mucus by secreting some of its key components, namely antimicrobial molecules. Hemocytes are also engaged in shell repair, wound healing and blood clotting (Ivanina *et al.*, 2017). In addition, although largely understudied, their role in shell formation in mollusks has been mentioned several times (Mount *et al.*, 2004; Song *et al.*, 2019), suggesting that the shell biomineral deposition is not solely a process regulated by the mantle epithelium.

2.1.4. [Molecular Defenses: The Chemical Arsenal](#)

Although mollusks do not possess antibodies, such as the ones identified in vertebrate systems that are part of the acquired immunity, they have evolved a sophisticated array of molecular defense mechanisms that constitute the backbone of their immune system and inner protections. Although they might often be presented as humoral defenses, these factors are not confined to a single compartment but are ubiquitous throughout the whole mollusk body, present in intracellular and extracellular spaces, every tissue, and secreted into the mucus by epithelial cells and mucocytes in the pallial cavity and extrapallial space (Pales Espinosa *et al.*, 2016).

A key component of this system is the production and storage of a range of specialized defensive molecules within the hemocytes granules in the form of inactive precursors (propeptides and pre-propeptides). These cells, circulating in the hemolymph and residing in connective tissues, carry and release their contents in infected sites upon immunological triggers (see hemocytes recruitment in [2.1.3. Cellular Defenses](#)), inducing quick and localized increase in concentrations of defensive factors (Gliński & Jarosz, 1997; Gerdol *et al.*, 2015).

The molecular defenses of mollusks can be classified according to their functional activities and their involvement in the successive stages of the immune response. The initiation of the process is carried out by recognition molecules such as PRRs and proteoglycan

recognizing proteins (PGRPs) These are supported by more versatile proteins like lectins, fibrinogen-related domain proteins (FReP) and C1q domain-containing proteins (C1qDC), which also participate in chemotaxis and direct elimination of pathogens (Adema, 2015; Gerdol *et al.*, 2015). Extracellular signaling is facilitated by cytokines and cytokine-like proteins, which have powerful immunomodulatory effects even at low concentrations. The effector molecules, responsible for directly killing and destroying pathogens, include various lytic factors such as bactericidal and permeability-increasing proteins, the phenoloxidase cascade (PO), enzymes like lysozyme and protease along with microbial protease inhibitors. The PO cascade, for instance, leads to melanization both intracellularly and extracellularly, affecting extracellular matrix arrangement and shell mineralization, as seen in *Venerupis philippinarum* shells during *Vibrio tapetis* infection causing "brown ring disease" (Borrego *et al.*, 1996; Gliński & Jarosz, 1997; Paillard, 2004). Additionally, as mentioned above, FReP, C1qDC, opsonin and agglutinins (lectin being the main representative for this category) also contribute to pathogen destruction (Gliński & Jarosz, 1997; Canesi & Pruzzo, 2016; Grinchenko & Kumeiko, 2022).

Last but not least, antimicrobial peptides (AMPs) make up for some of the most effective effectors of the immune response: these small cationic macromolecules exhibit a broad-spectrum antimicrobial activity through widely diversified mechanisms (Allam & Raftos, 2015; Bachère *et al.*, 2015). Their variety and specific features are discussed later in this chapter (see section 2.3. Antimicrobial Components in Mollusks Soft Tissues), as I list the identified AMPs and proteins (AMPPs) extracted from mollusk soft tissues (Table 2.1). Finally, the transportation of dead or incapacitated intruders is carried out by transport cells (see section 2.1.3. Cellular Defenses) but also at a molecular scale by transmembrane pumps that rid the intracellular spaces and humoral compartments from exogenous particles: the Multixenobiotic Defense Mechanism (MXDM) is a generalist system that can deal with various xenobiotics, limiting the accumulation of waste, toxins and microorganisms in bivalve cells (Pain & Parant, 2003).

As previously mentioned in the context of cellular and mucosal defenses (see sections 2.1.2 and 2.1.3), mollusks maintain an inhospitable environment for potential invaders through various molecular factors. Among these, Reactive Oxygen Species (ROS) and Nitric Oxide (NO) produced by granulocytes are commonly produced in mollusks (Canesi & Pruzzo, 2016).

Some mollusk groups have evolved highly specialized defensive molecules adapted to their ecological niches and interspecific relationships, generated and stored in specialized appendices and glands. For instance, certain gastropods produce powerful neurotoxic venoms to either kill preys or predators by injection with their harpoon-like proboscis (Dutertre *et al.*,

2014), while cephalopods secrete ink for escape (stored in ink sacs) and pigments for camouflage (Derby, 2007).

The intrinsic defense mechanisms of mollusks form an intricate, interconnected system operating across multiple levels that work synergistically. Under the protection of the shell - when it is present - performing the “heavy duty” and providing a controlled environment, the mucus facilitates hemocyte movement and concentrates antimicrobial compounds, while constantly cleaning epithelial tissues in contact with the environment. Hemocytes produce and transport molecular defenses, while molecular factors enhance cellular responses. This integrated system allows mollusks to respond effectively to a wide range of environmental challenges and external threats. The following sections of this chapter will delve deeper into the aspects of mollusk defenses that are involved in my doctoral research, *i.e.* specific bivalve shells and the AMPPs found in soft mollusk tissues.

2.2. The Bivalve Shell

2.2.1. Structure and Function

Bivalves are characterized by their distinctive two-valved shells. While serving the general protective functions discussed earlier (see [2.1.1. The Shell](#)), bivalve shells exhibit some features that are also observed in other shell-bearing mollusk classes. These shells are typically composed of two to four superimposed layers: the most external one, called the periostracum is not mineralized and remains fully organic. Usually carrying a large part of shell pigments, polysaccharides and proteins, it impermeabilizes and provides protection to the underlying calcified layers against erosion and pH variations (Lowenstam *et al.*, 1989; Ponder *et al.*, 2020a).

The inner layers of bivalve shells are mineralized, with aragonite and calcite representing the predominant polymorphs in the class. The organization of microstructures is species specific, each contributing to the overall mechanical properties of the shell. As mentioned earlier (see [2.1.1. The Shell](#)), variations can occur among species at population levels depending on environmental stressors (both biotic and abiotic) (Marin *et al.*, 2012; Checa *et al.*, 2018). The emergence of common shell microstructures is a complex topic that spans over millions of years, challenging the retracing of bivalve shell evolution. Their distribution among taxa has been used in classification attempts, but their relationships are still discussed. The most ancient ones are the prismatic structures, dated around 540 million years ago at the Lower Cambrian period. The apparition of nacreous structure (also called mother-of-pearl) would be slightly younger, with early identifications around 480 million years ago, during the early Ordovician period. Crossed-lamellar and foliated structures are thought to have evolved later around the 443 million years ago, becoming more prevalent in later geological periods (Taylor *et al.*, 1969; Carter (ed.), 1990; Ponder *et al.*, 2020a). Typical examples of bivalve microstructures are presented in the later section, where I describe the organization and characteristics of the shells of the mollusk models used of this thesis.

Shell formation occurs through biomineralization by the mantle tissue, which secretes CaCO₃ minerals and the organic matrix (OM) into the extrapallial space (Fig. 2.2) (Addadi *et al.*, 2006; Marin *et al.*, 2008). This is a continuous process that begins during larval development and continues throughout the whole bivalve life. In early stages (trochophore larva), an initial organic layer serving as a template for mineral deposition is secreted by the shell gland. This organic layer will be the future periostracum. After larva settlement and metamorphosis, the mantle takes over as the shell secreting tissue, with specialized regions

secreting different microstructures, resulting in the complex and layered architecture observed in adult bivalve shells (Kniprath, 1981; Checa, 2000; Ponder *et al.*, 2020a). For instance, the outer mantle folds typically secrete the periostracum, while the middle and inner are responsible for the prismatic and nacreous layers, respectively. In the case of nacro-prismatic bivalves. Below, illustrated by Figure 2.2 is the example of *Arca*, a bivalve exhibiting a fibrous prismatic layer and, internally, a crossed-lamellar one.

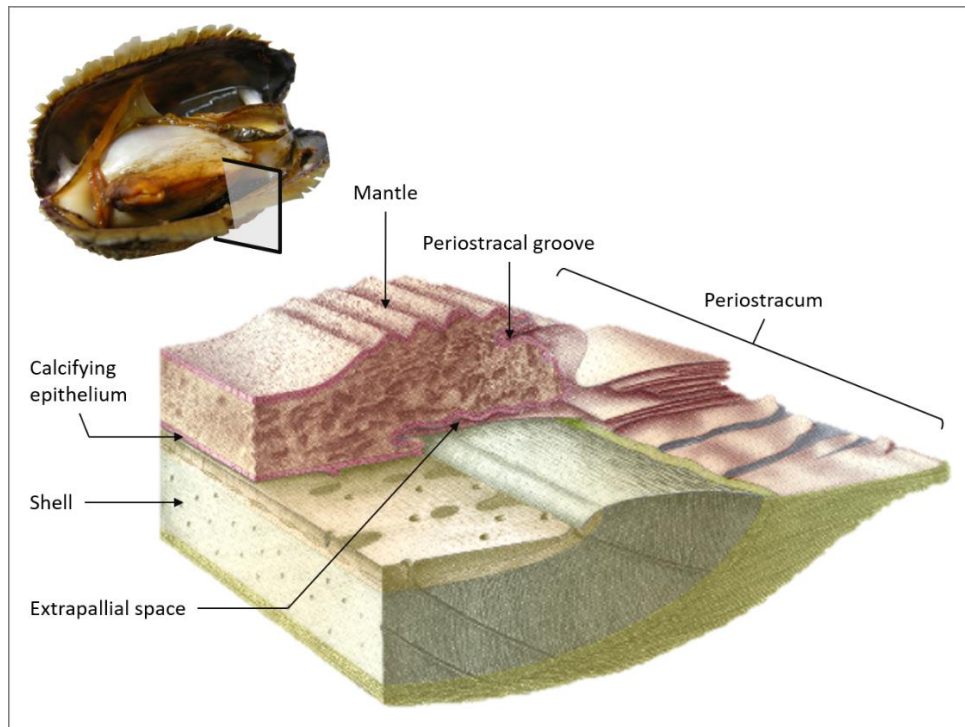


Figure 2.2: The physiology of mollusk shell calcification with the example of *Arca sp.* Figure adapted from (Marin *et al.*, 2012) and redrawn from (Waller, 1980).

2.2.2. Organic Matrix

As briefly mentioned above (see [2.1.1. The Shell](#)) the shell contains a complex cocktail of organic molecules that are an integral part of the shell. These molecules define the “shell matrix”. They are an amalgamate of proteins, glycoproteins, peptides, polysaccharides (among which chitin), lipids, pigments and metabolites. The most known part of the matrix are proteins, polysaccharides are less investigated. Lipids, pigments and metabolites are largely understudied. The shell matrix has been studied for almost 170 years (Frémy, 1855), but the first modern biochemical characterizations are from the fifties and the ‘omics’ approach, allowing to characterize all proteinaceous constituents of a shell matrix (the so-called “shellome”), was implemented only 15 years ago (Marin, 2020).

For a long time, until the use of proteomics, the mainstream idea was that the shell proteins were mostly devoted to their interaction with calcium ions in solution, or with calcium carbonate surfaces (either crystalline nuclei or amorphous nanometric grains). First sketched in the eighties, a molecular model of nacre was proposed in the early 2000 (Levi-Kalisman *et al.*, 2001). This model targets the interaction of three major components: chitin (an insoluble “sugar” polymer of N-acetylglucosamine), forming a 3D flexible framework, hydrophobic (silk-fibroin-like) proteins forming a gel containing the third ingredient, acidic polyanionic (*i.e.*, aspartic acid-rich) proteins which are the mineral nucleators and, at the same time, can inhibit crystal growth. This ternary model relies on the most abundant constituents of shell matrices.

With the intrusion of proteomics in biomineralization research, the perspective changed: hundreds of proteins were identified in just few years (Marin *et al.*, 2013; Marin, 2020). Many of them are minor, in term of quantity, in the shell matrix. However, it is interesting to note that, from biological model to model, some constant features can be listed about molecular functions and functional domains. The shell matrix always comprises a set of enzymes, such as carbonic anhydrase (CA), tyrosinase, proteases, peroxidase, cyclophilin. It also comprises some proteins with an ExtraCellular Matrix signature (ECM), such as laminin, decorin, EGF-like, vWFA, in addition to proteins involved in interacting with sugars (lectins, chitin-binding, peritrophin A). Other key-players are proteins involved in protease inhibitor functions (serpin, Kunitz-like, Kazal-type domains), proteins interacting with divalent cations (ependymin, Ca-binding proteins with EF hands) and a large array of proteins that exhibit low-complexity domains. In this last category one finds Asp/Glu-rich proteins, Asn/Gln-rich proteins, Ser/Thr-rich proteins, Arg/Lys-rich proteins, Cys/Met-rich proteins (Marin, 2020).

Except the acidic proteins, the functions of most of these proteins exhibiting low-complexity domains are completely unknown. Interestingly, what proteomics revealed rather unexpectedly was that the shell matrix contains also histones. Histones are nuclear proteins, strongly associated to DNA. They are positively charged proteins, rich in arginine and lysine, which interact with the negatively charged phosphate groups of DNA. They were first suspected to be cellular contaminants of the shell matrix. However, their persistence in many matrices invites us to reconsider their putative functions. The idea that these histone or histone-like proteins could serve as antimicrobial factors in the shell matrix has emerged in the last few years (Marin, 2020; Oudot *et al.*, 2020). It then becomes logical to explore this possibility.

2.2.3. Studied Bivalve Models

The presentation that follows comprises a description of the macroscopic characters of the shells that were used during my doctoral research and an illustration of their microstructures via Scanning Electron Microscopy (SEM) pictures. Macroscopic illustrations were provided by Jérôme Thomas (Biogéosciences) while SEM pictures were acquired by me and by a Master trainee, Marie Aries Lasseron who worked in the Biomineralization team of Biogéosciences lab from February to May 2024. For the microstructures, we checked that our findings were in agreement with earlier literature, in particular Taylor *et al.* (1969, 1973) and Carter (1990). Our models are presented according to the classical phylogeny of Bivalvia, namely pteriomorphid bivalves first (*G. glycymeris*, *M. galloprovincialis*, *M. gigas*, *P. maximus*), then euheterodont ones (*C. edule*, *V. philippinarum*, *V. verrucosa*) (Figure 2.3).

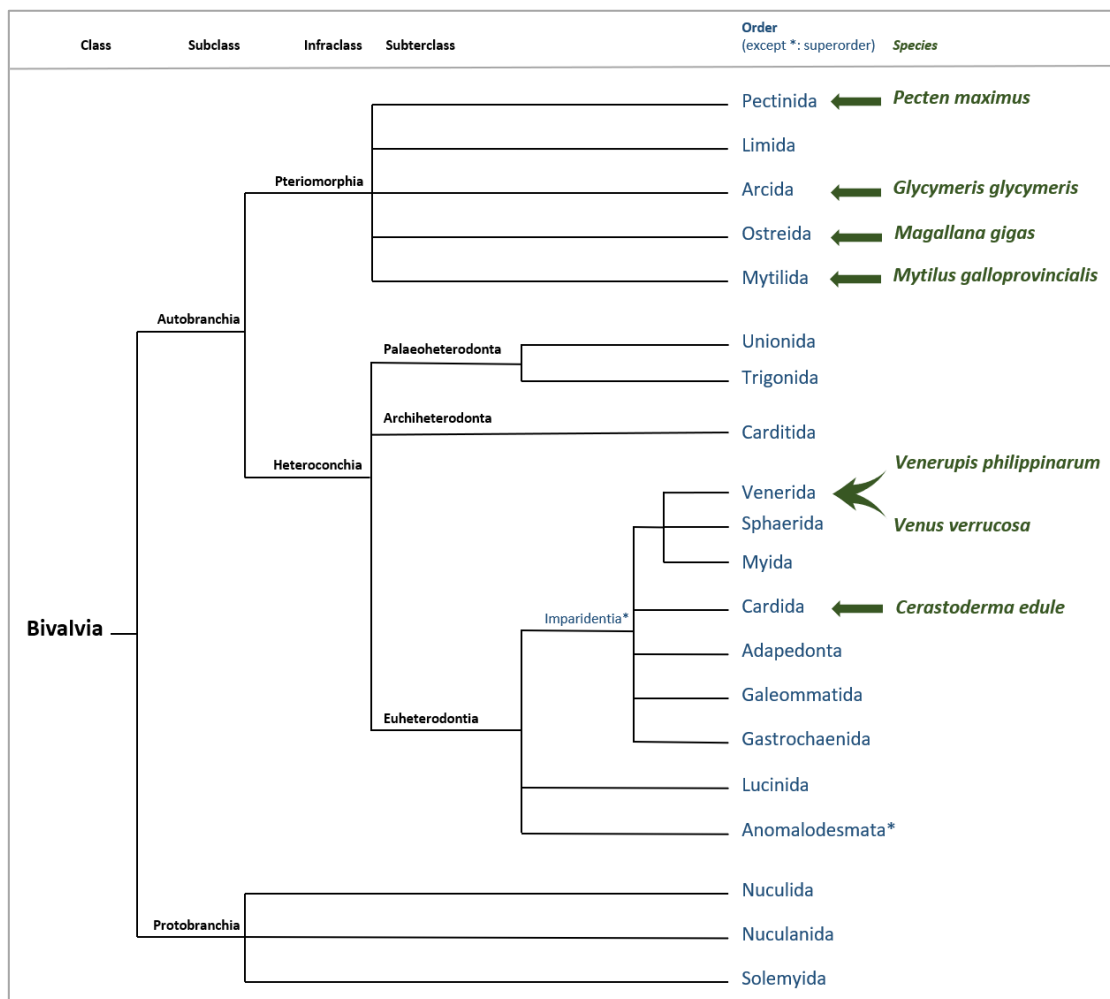


Figure 2.3: Phylogenetic tree of the bivalve orders (in blue) showing the relationship of our model species (in green). This tree was elaborated after the classifications of Ponder and Lindberg (2020b), Bieler (2014) and the latest accepted entries of the WoRMS and MolluscaBase (Ahyong *et al.*, 2024; MolluscaBase eds., 2024).

2.2.3.1. *Glycymeris glycymeris*: Shell Morphology and Microstructures

The shell of the dog cockle *Glycymeris glycymeris* (Linné *et al.*, 1758; Mendes da Costa *et al.*, 1778) is circular, convex, thick and solid. It is fully aragonitic, equivalved and exhibits a taxodont hinge, characterized by several teeth organized in chevron. The outer surface is smooth and shows apparent growth lines. The periostracum is vividly white, orange and brown colored with zig-zag patterns, displaying high intra-specific variability (Fig. 2.4). Similarly to other *Glycymeris* species, the periostracum can be “hairy”, in particular along the outer shell border. The internal shell surface exhibits a simple pallial line (integripalliate) and two brownish adductor muscle scars of similar size (isomyarian). Ribs are visible in the outer shell border (Huber, 2010; Nolf & Swinnen, 2013).

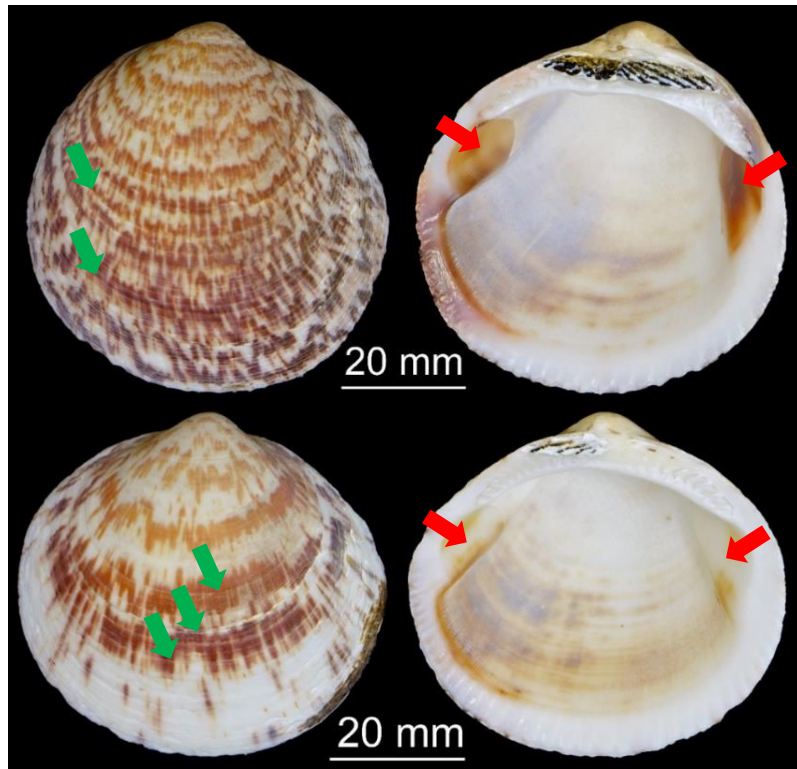
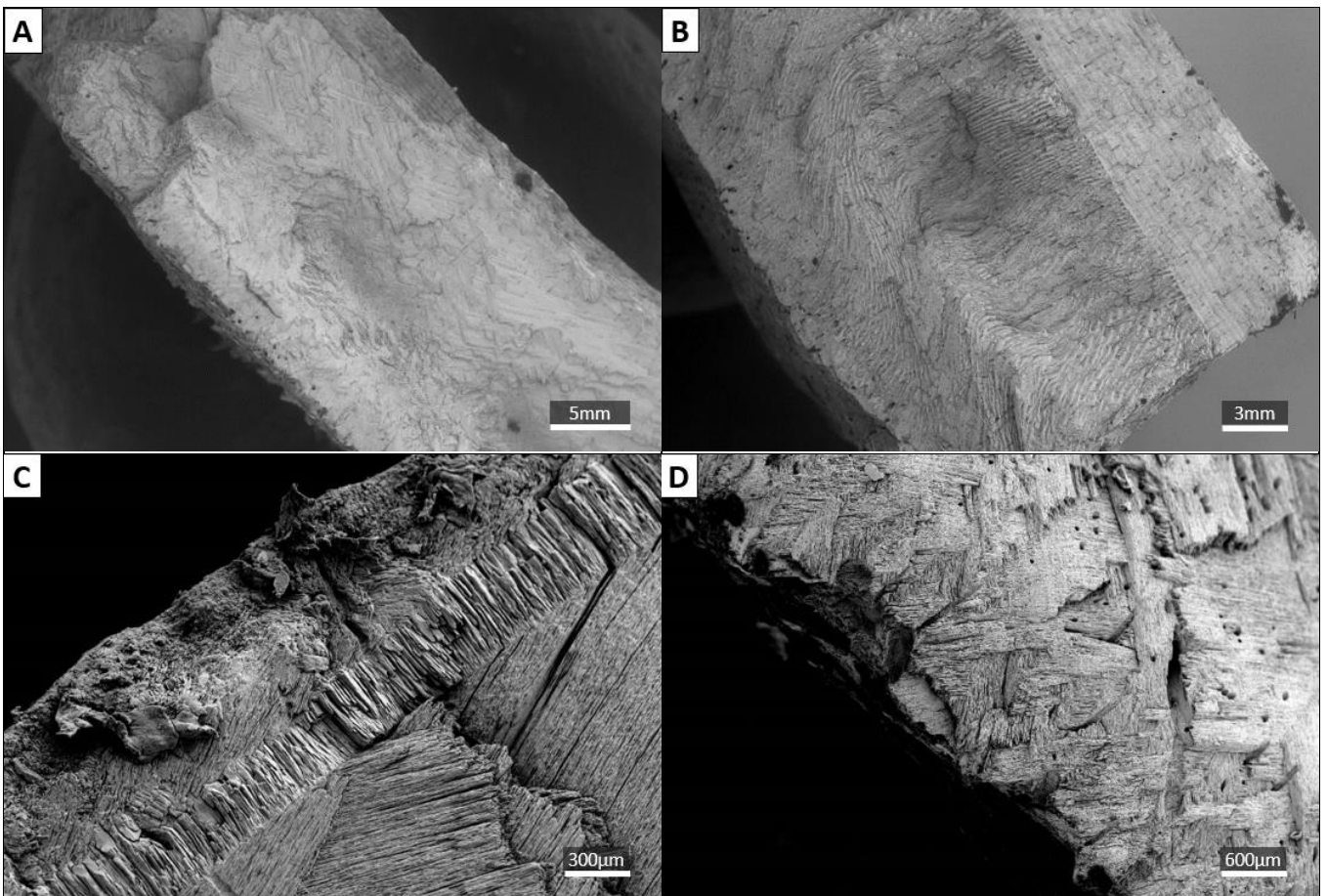


Figure 2.4: Shells of two specimens of the dog cockle *G. glycymeris*, showing both inside and outside views. Red arrows: myostraca; Green arrows: concentric growth lines.

The first mineralized outer layer consists of a crossed-lamellar structure (Fig. 2.5, A-C). The structuration of the aragonite crystals gradually transitions to a middle layer made of “simple” straighter crossed lamellae. This gradual change makes this layer not easily distinguishable from the previously described outer layer. The inner layer of the shell is again made of crossed-lamellar aragonite, but this time orthogonally oriented from the outer layer

(“brick”-looking feature, Fig. 2.4, B), providing higher pressure resistance. Growth bands are observable through the presence of fibrous prism features in the inner layer along the general shell curvature (Fig. 2.5, H). The periostracum exhibits pili on the shell border (Fig. 2.5, I-J). The whole shell is perforated by secondary microtubules that are formed from the interior of the shell to the exterior surface (Fig. 2.5, H green arrows). These regular perforations are thought to increase the shell’s resistance to crushing, acting as “crack arrestors” and preventing further propagation through the whole shell. Biological functions are also suggested, as they could play a role in the sensory system of the dog-cockle, during the biomineralization process, or in the attachment of the mantle of its shell. As in other species of bivalves, the *myostracal* layer contains prismatic calcite for muscle attachments (Carter (ed.), 1990; Böhm *et al.*, 2016; Crippa *et al.*, 2020b, 2020a).



(See verso for the remaining pannels and legend)

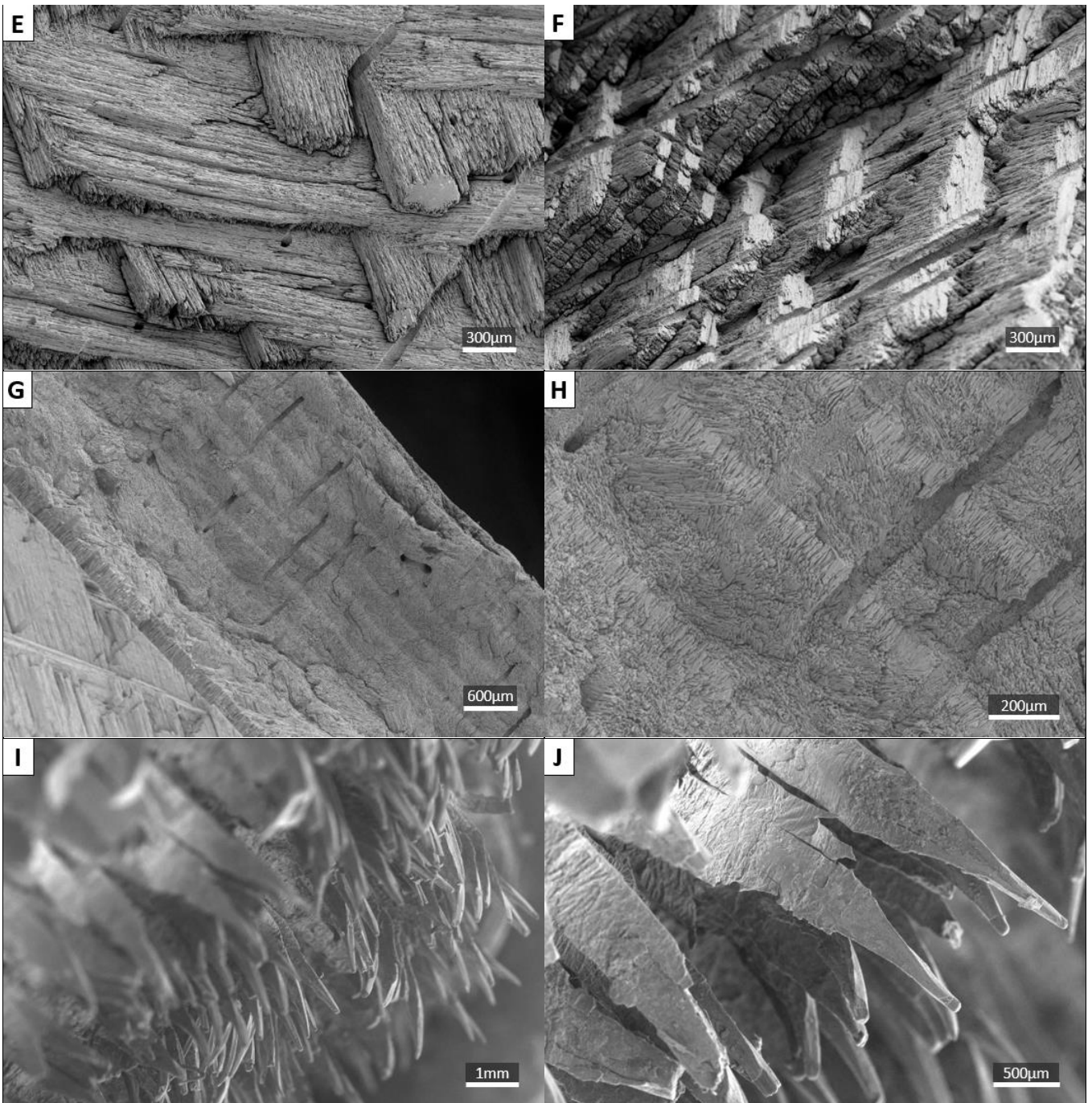


Figure 2.5: Scanning Electron Microscope images of *G. glycymeris* shell fragments. A-B: whole-thickness view of a fractured shell; C: fibrous prism growth band encased in the crossed-lamellar microstructure; D- F: crossed-lamellar layer; G-H: inner crossed-lamellar layer with alternations of fibrous prismatic structures; I: whole view of a shell fragment with the hairy periostracum; J: detailed view of the pili.

2.2.3.2. *Mytilus galloprovincialis*: Shell Morphology and Microstructures

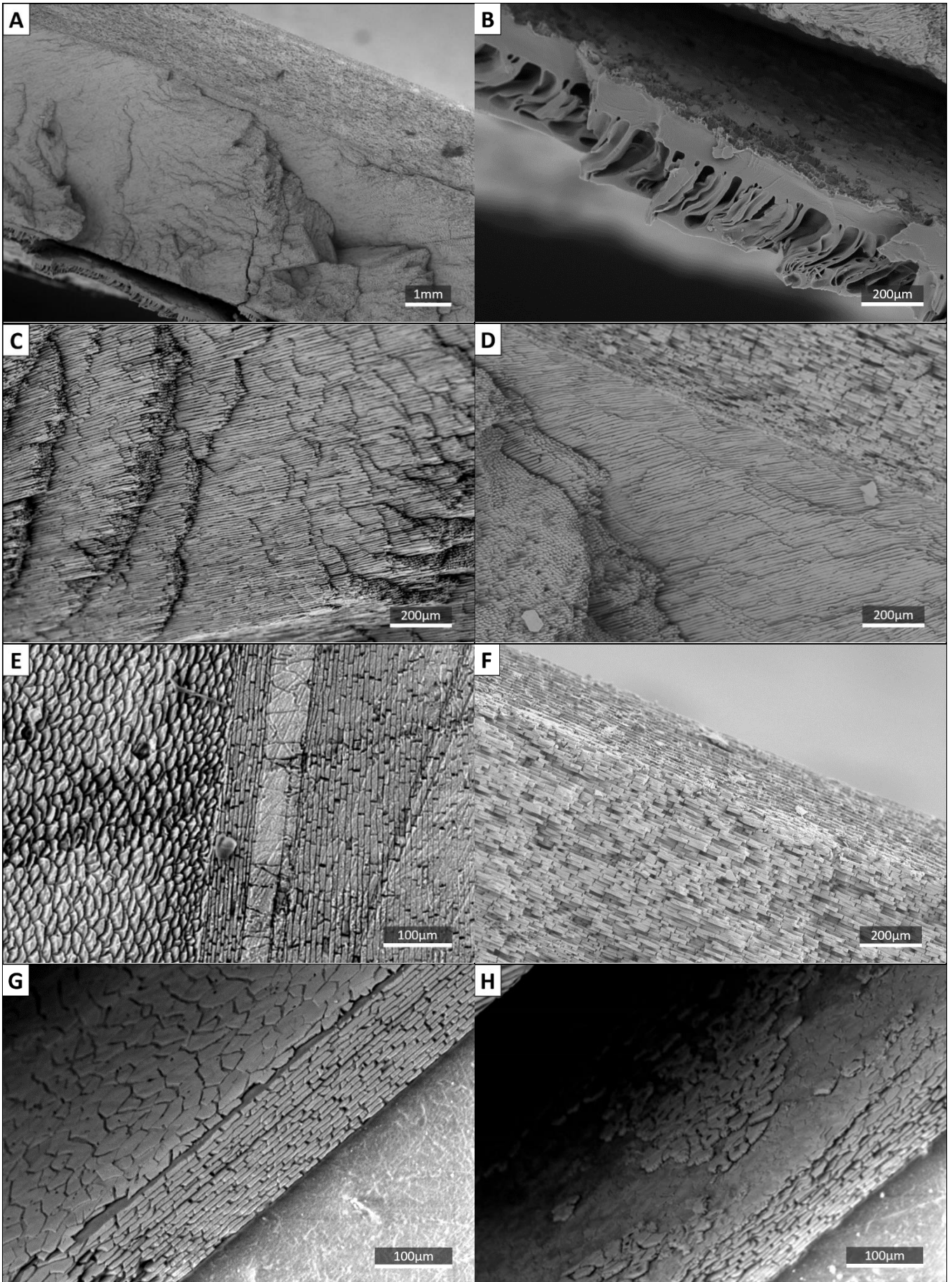
The Mediterranean mussel, *Mytilus galloprovincialis* (Lamarck, 1819) form equivalve, thin shells reaching up to 15cm. The organic periostracum is dark-brown colored, thick when compared to the whole shell thickness. It is often intact, or if not, eroded only at the umbo region. Its surface is entirely covered by regular microtopographic folds, preventing parasitic attachments and biofouling (Fig. 2.7, B). Growth lines are highly visible, concentric in the umbo region and commarginal on the rest of the shell (Fig. 2.6). The inner surface displays bright iridescent blue layers, hinting towards the presence of nacre. The hinge is thin and the teeth are hardly visible (dysondont) while the ligament is well developed. The posterior adductor muscle print is visible close to the border of the shell. The pallial line is simple. The myostracum for abductor muscle insertion is not always visible (Scardino *et al.*, 2003; Oliver *et al.*, 2016).



Figure 2.6: Shell of the Mediterranean mussel *M. galloprovincialis*, showing both valves with inside and outside views.

The mineral shell of *M. galloprovincialis* is composed of two layers of different crystalline forms of CaCO_3 (Fig. 2.7, A). The outer layer is made of dense calcitic prisms, unidirectionally inclined following the general shell curvature (Fig. 2.7, C-D). These prisms are extremely thin (1-2 μm in diameter). The inner layer of the shell is aragonitic, with layers of flat nacre tablets assembled together in the typical ‘brick wall’ structure. The tablet’s thickness is about 1 μm or less (Fig. 2.7, F-H). The transition zone between the prismatic and nacreous layers is abrupt and shows the highly oblique orientations of their microstructures (Fig. 2.7, D-E) (Taylor *et al.*, 1969; Carter (ed.), 1990; Gao *et al.*, 2015).

Figure 2.7: Scanning Electron Microscopy images of shell fractures of *M. galloprovincialis*. A: whole shell showing all the layers, including the periostracum; B: close-up of the organic periostracum showcasing microtopographic folds; C: calcitic prismatic layer; D-E: transition zones between the calcitic prisms and aragonitic nacre layers; F: aragonitic flat nacre tablets; G-H: aragonitic nacre with ongoing biomineralization and formation of tablets (Lasseron, 2024).



2.2.3.3. *Magallana gigas*: Shell Morphology and Microstructures

The Pacific cupped oyster *Magallana gigas* presents a large inequivalve shell with an upper (left) flat valve and a lower (right) deeply concave one. Both valves are irregular and generally elongated, oval to curved and are covered by an irregularly purple-pigmented periostracum. The valves are colored from light grey to brown or dark purple, with an alternance of whiter bands radiating from the umbo. The outer sculpture of the shell is marked by successions of concentric laminae following growth periods, with irregular curvatures and borders creating undulations and folds (Fig. 2.8). When closed, the valves are hermetically sealed in spite of their irregularity. The interior of the valves is smooth and contains only one large and heavily colored adductor muscle scar (monomyarian); the pallial line is simple. The hinge is well developed and of dysodont type, characterized by regressed teeth (Taylor *et al.*, 1969; Thunberg, 1793; Salvi & Mariottini, 2017).



Figure 2.8: Shell of the Pacific cupped oyster *M. gigas*, showing both valves with outside (top) and inside (bottom) views. Left: lower valve; Right: upper valve. Red arrows: aragonitic adductor myostracum; Green arrows: calcitic chalky deposits.

The mineral shell of *M. gigas* is entirely made of calcite, with the exception of the aragonitic myostracal layer (particularly visible in the adductor myostracum, Fig. 2.8, red arrow). The outer layer is a thin, prismatic calcite (Fig. 2.9, A, G-H), with a smooth gradual transition into the thick inner layer of foliated calcite (Fig. 2.9, H). This foliated calcite is made of thin compact micrometric laminations, without lateral separations like in nacre microstructures. The thickness of the shell is not homogenous, since one observes an alternation of dense foliae and disjointed sheets of “chalky” lenticular (*i.e.*, discontinuous) deposits (Fig. 2.9, B). The chalky layers are in fact porous foliae with anarchic directions, milk-white looking and brittle under pressure and torsion (Fig. 2.9, C-F). They can be observed in any part of the shell, with high variability in thickness and numbers, but it is interesting to note that they are mostly present in the deep curve of the lower valve, or around the hinge and the umbo. The chalky layers are mainly attributed to rapid growth and bursts in biomineralization rates during the oyster shell development (either as stress-responses or in a broader fitness strategy), and can also be associated with crushing resistance via break dissipation. Finally, they are also considered as compensation layers for a sessile genus that grows attached on a rocky, irregular substrate (Gray, 1833; Checa *et al.*, 2018; Banker & Sumner, 2020).

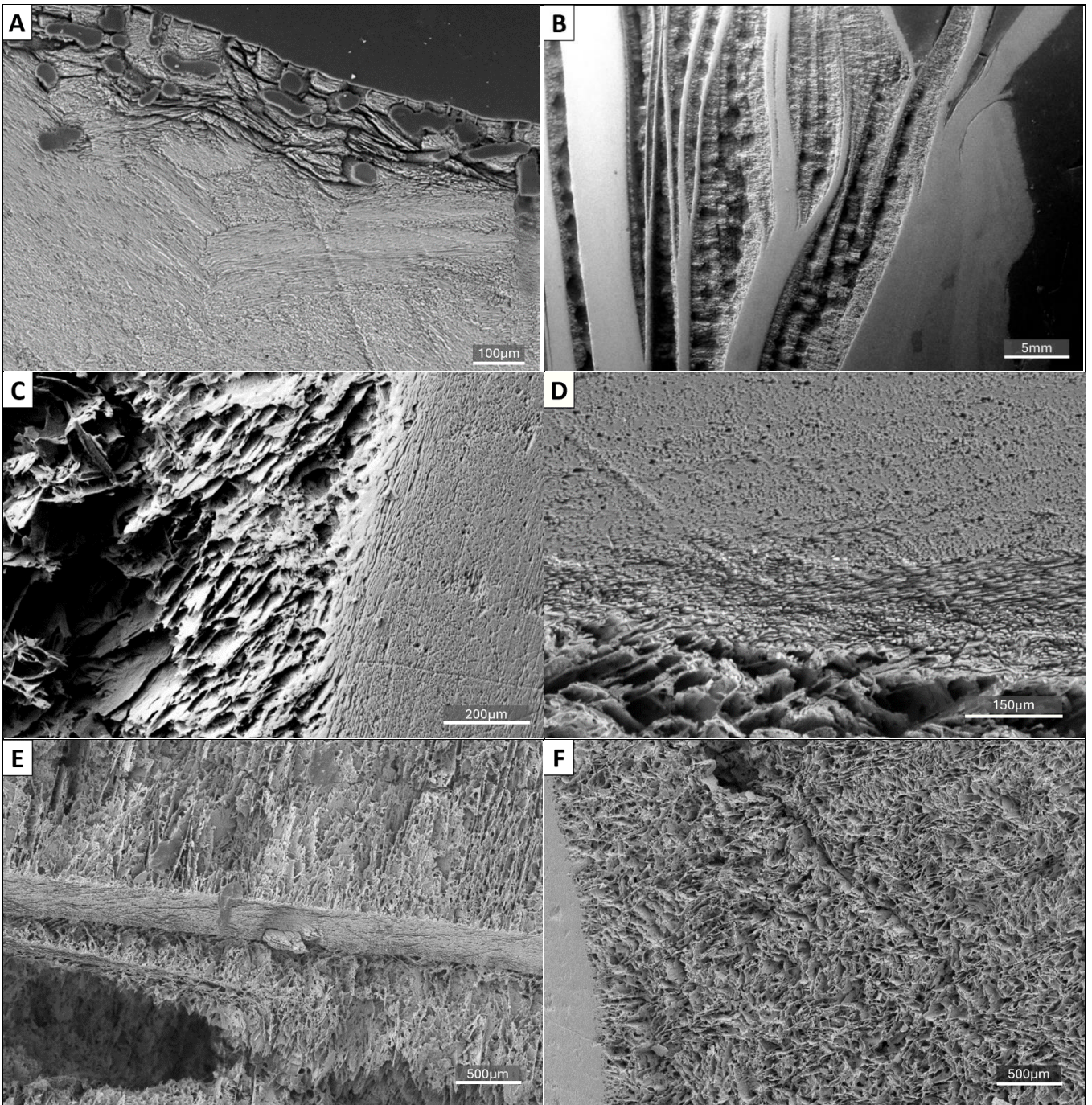


Figure 2.9: Scanning Electron Microscopy images of the shell of *M. gigas*, polished and briefly etched with 1% (wt/vol) EDTA for better contrast. A: view of the outer parts of the shell, with prismatic and foliated calcite layers, the grey spots are resin invasion in the hollow chambers of the outer shell; B: alternance of layers of foliated calcite and chalky lenses; C-E: transition zones between the foliated calcite and the chalky lenses, with apparent sheets of calcite. F: close-up of a section of a chalky lens. The thin elements forming the reticulate pattern of the chalky layer appear as extensions of the laminae of the foliated layer.

2.2.3.4. *Pecten maximus*: Shell Morphology and Microstructures

The shell of the great scallop *Pecten maximus* (Linné *et al.*, 1758) is robust and can reach lengths of 15cm. It is inequivalve, with a concave lower valve and a flat upper valve. The organic periostracum is thin but strongly pigmented with brown-red colors. This pigmentation is comparably observable in the mineral underlying layers of the shell, with creamy whites on the inner surface. The sculpture is very pronounced, with 14 to 17 deep broad radiating ribs, themselves striated by radial grooves. On the upper valve, these broad ribs are tabulated. Concentric growth lines are observable with marked discolorations on significant life-history events (Fig. 2.10). The hinge is flocked with symmetric ears, strengthening the shell for swimming behaviors (Mendes da Costa *et al.*, 1778; Dijkstra, 1999; Oliver *et al.*, 2016).

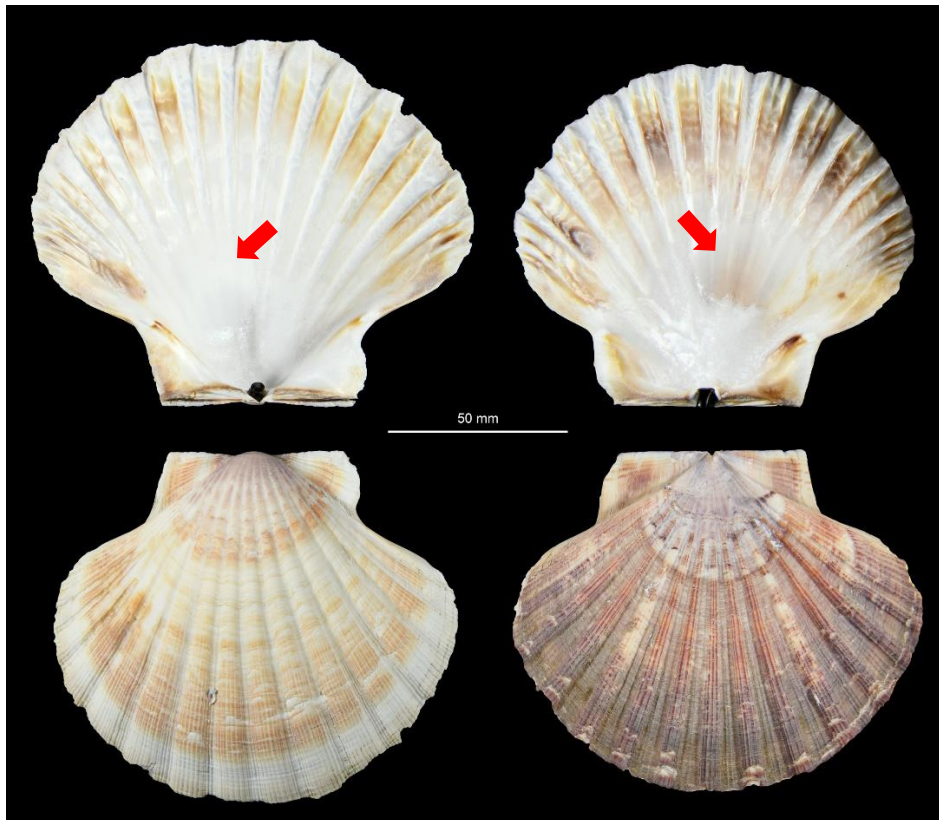


Figure 2.10: Pictures of the shell of the great scallop *P. maximus*, showing both valves with inside (top) and outside (bottom) views. Left: lower valve; Right: upper valve. Red arrow: aragonitic adductor myostracum.

Like in the mussels, the giant scallop's mineralized shell is composed of two layers. The outer layer is thin, prismatic calcite, with prisms perpendicular to the outer shell surface (Fig. 2.11, A), while the thicker inner layer is made of calcitic foliae, further sub-layered with diverging orientations (Fig. 2.11, B-F) The myostraca are locally layered with prismatic aragonite (Taylor *et al.*, 1969; Larvor *et al.*, 1996).

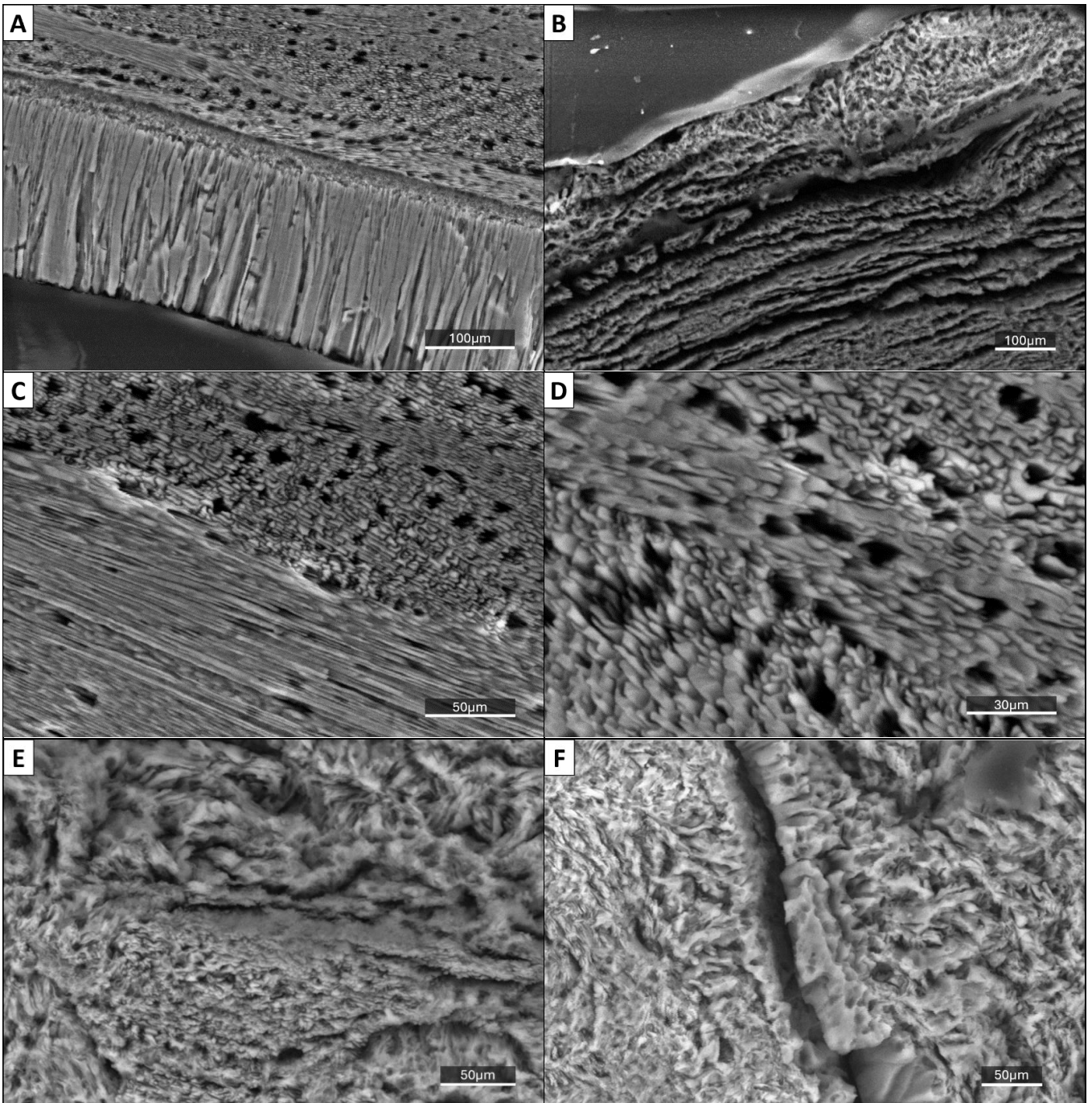


Figure 2.11: Scanning Electron Microscopy of slices of the shell of *P. maximus*, polished then briefly treated with 1% (wt/vol) EDTA for better contrast. A: outer calcitic prismatic layer; B: layers of foliated calcite; C-D: foliated calcitic inner layer with diverging orientations of the foliae; E-F: details of the calcitic foliated inner layer (Lasseron, 2024).

2.2.3.5. *Cerastoderma edule*: Shell Morphology and Microstructures

The common cockle *Cerastoderma edule* (Linné *et al.*, 1758) is protected by a small globular equivalved shell reaching a mean maximum length of 4 cm (most of the specimens have a shell diameter around 2 to 3 cm). The hinge is of heterodont type. The outer layer covering the whole shell is the organic periostracum, lightly pigmented with cream and brown colors. The shell is sculpted with very apparent radial ribs (between 22 and 28), over which shallow concentric growth rings create a reticular pattern. The interior surface of the shell is mainly white and marked by a brown or purple pigmentation of the abductor muscle. The pallial line without sinus (integripalliate) is well marked. Two adductor muscles prints (dimyarian) of similar size (isomyarian) are visible (Fig. 2.12) (Boyden, 1973; Oliver *et al.*, 2016; Maia *et al.*, 2021).



Figure 2.12: Shell of the common cockle *C. edule*, showing both valves with outside (top) and inside (bottom) views.

The shell mineral microstructure of the common cockle is entirely aragonitic, with two layers: the peripheral crossed-lamellar layer (Fig. 2.13, A-E) and the inner homogeneous complex crossed-lamellar layer (Fig. 2.13, E-F) (Boyden, 1973; Brock & Christiansen, 1989). The concentric growth bands previously described on the sculpture of the shell can be observed as bands in the peripheral crossed-lamellar layer (Fig. 2.13, C-E). These bands are used in sclerochronological methods to age specimens and calculate the seasonal growth rates. The ribs

are also visible in the inner-structure of the shells, creating manifest folds of the outermost layers (Fig. 2.13, C-D) (Richardson *et al.*, 1980; Jelesias & Navarro, 1990; Füllenbach *et al.*, 2017; Milano *et al.*, 2017).

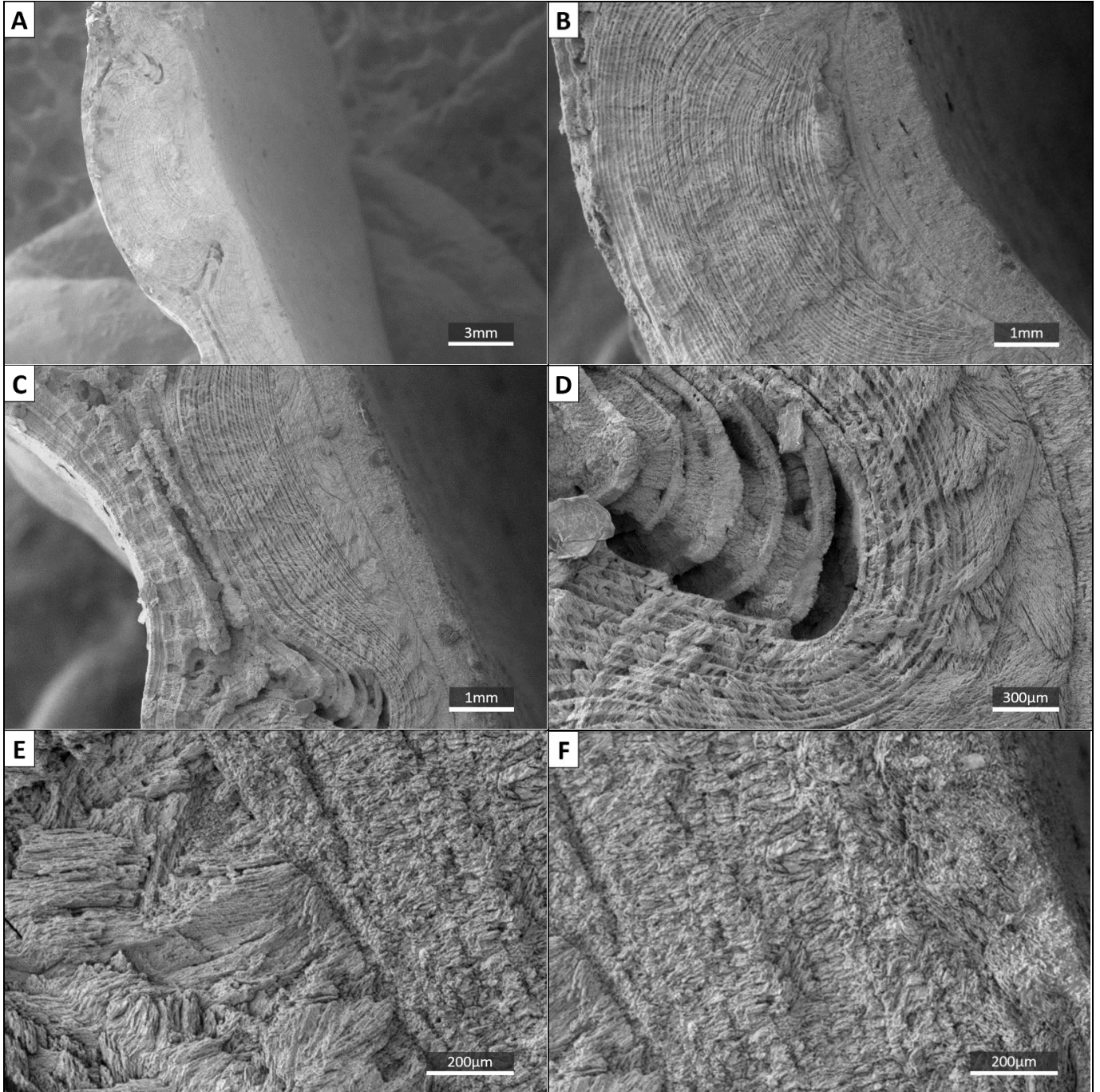


Figure 2.13: Scanning Electron Microscopy views of shell fractures of *C. edule*. A: transversal fracture of the shell, centered around a radiating rib; B: full thickness view of the shell in transversal view; C: focus on a ridge (two folds) in-between two ribs, transversal view; D: close-up view (transversal) of the same zone; note the superimposition of laminae (growth bands) and crossed-lamellar structures; E: transition zone in between the outer crossed-lamellar (left) and inner complex crossed-lamellar (right), red dotted-line; F: complex crossed-lamellar layer. Red arrows: growth bands from mineralization increments; Green arrows: inner complex crossed-lamellar aragonitic layer.

2.2.3.6. *Venerupis philippinarum*: Shell Morphology and Microstructures

The Manila clam *Venerupis philippinarum* (Adams & Reeve, 1850) exhibits an equivalve shell, which presents reticulated outer sculptures with radial ribs. The organic periostracum is highly variable in color, although predominantly cream-colored or gray, with streaks - almost symbol looking - forming patterns of brown, purple or yellow. The inner surface of the shell shows purple, yellow and brown pigmentations of the periphery and the myostraca (Fig. 2.14). The hinge is of heterodont type and two adductor muscle scars are observed (dimyarian). The pallial line exhibits a sinus (sinupalliate) (Mikkelsen *et al.*, 2006; Oliver *et al.*, 2016).

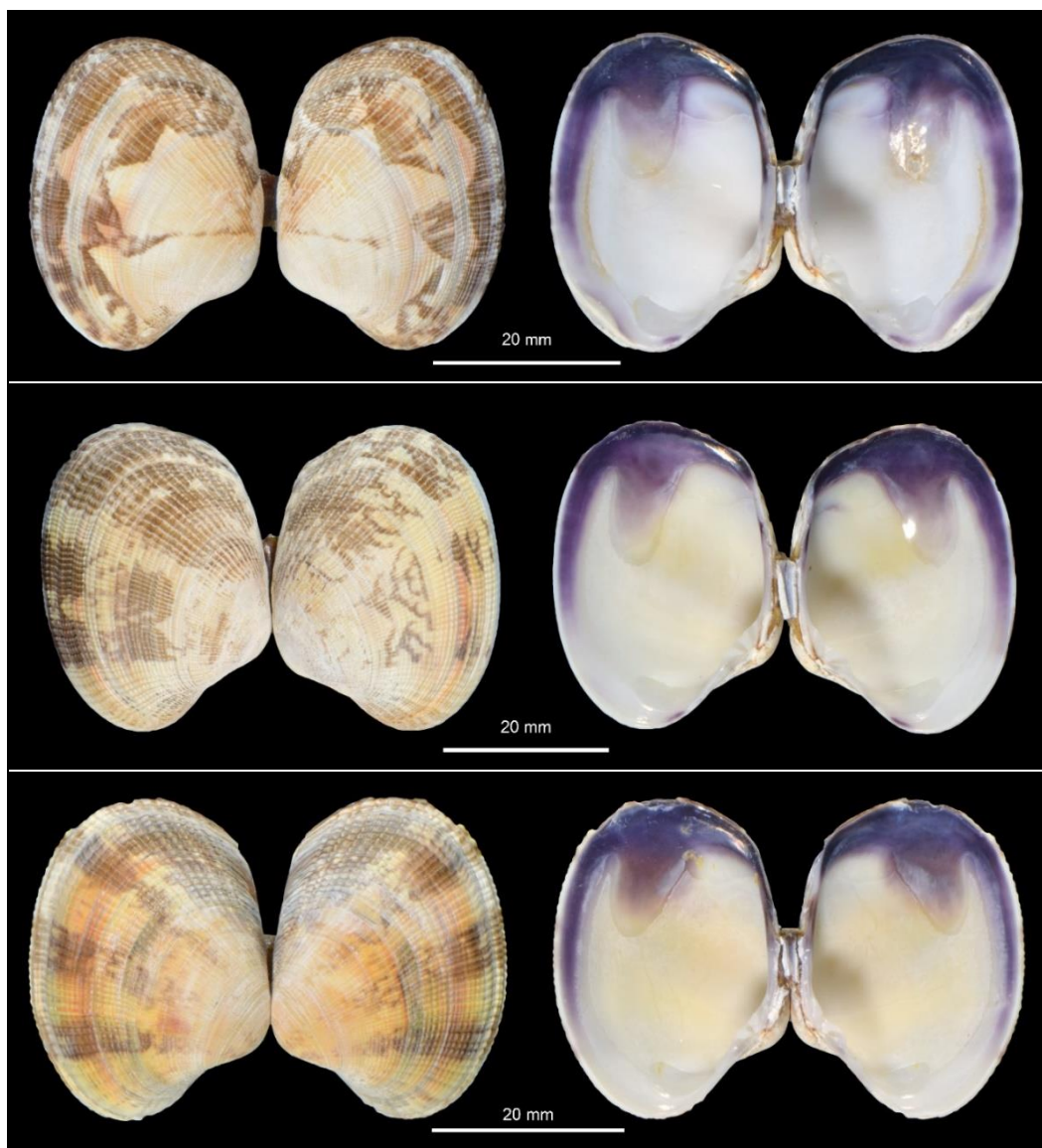
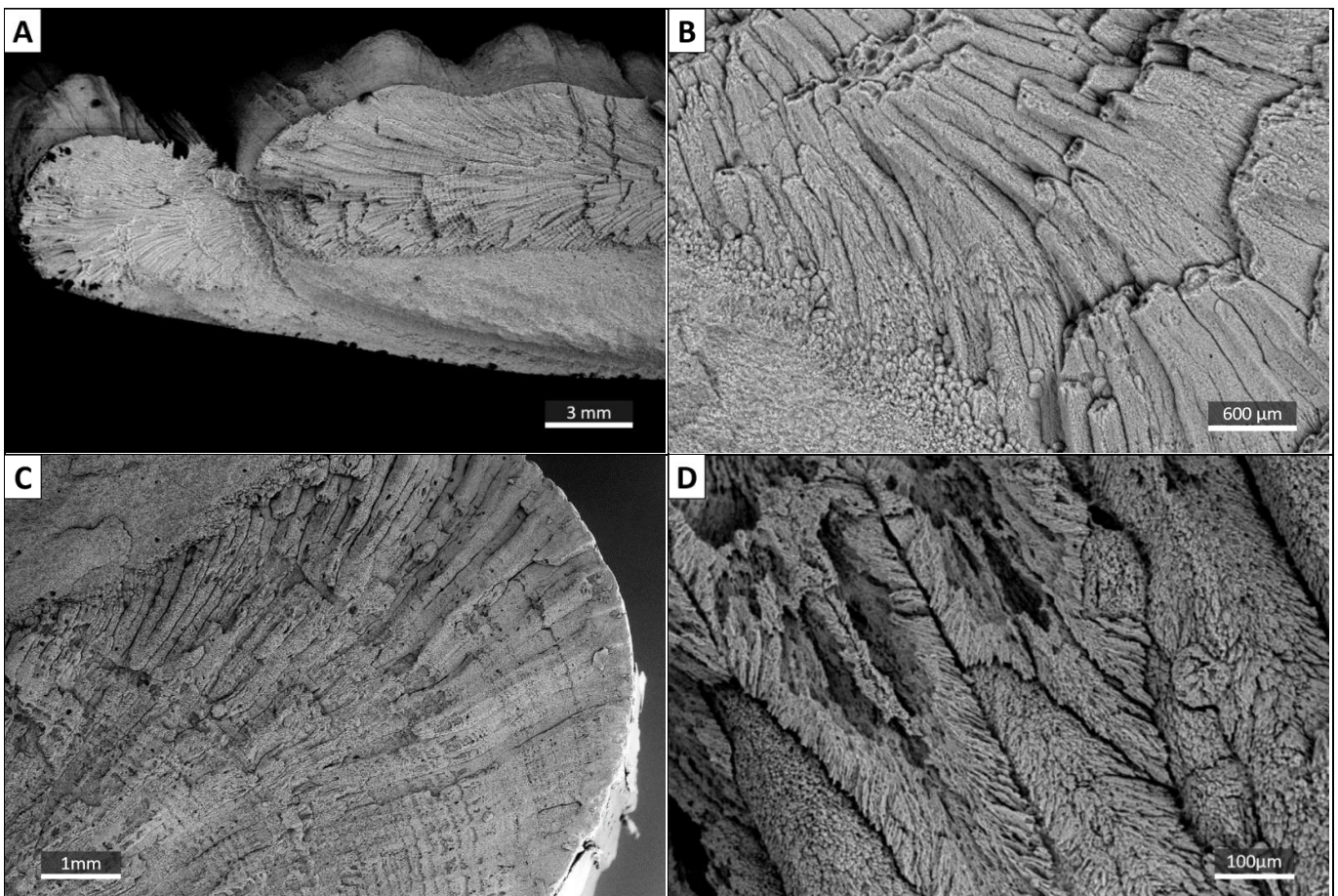


Figure 2.14: Pictures of the shell of three specimen of the manila clam *V. philippinarum*, showing both valves with inside and outside views. Note the variation of colors in the inner surface of the valves.

V. philippinarum shells are fully aragonitic and composed of 2 to 3 mineralized layers. The outer layer is a composite prismatic structure with diverging directions (Fig. 2.15, A-C). The composite-prisms are made of a collection of curved prismatic biominerals (Fig. Ch2.14, D) which, after etching with EDTA, exhibit individually thin crystallites arranged in a “Christmas tree” porous pattern. This complex prismatic layer is sometimes subdivided by authors into two layers, with a middle layer made of the biggest, less dense columnar crystals (Fig. 2.15, E-F). The inner layer is made of a complex crossed-lamellar structure, often marked by bands of unidirectional lamellae following the curvature of the shell. Frequently, this layer, characterized by chevron patterns (Fig. 2.15, I-J), transforms into a granular layer in the most inner part of the shell (Fig. 2.15, I-J) (Mikkelsen *et al.*, 2006; Oliver *et al.*, 2016; Mu *et al.*, 2018).



(See verso for the remaining pannels and legend)

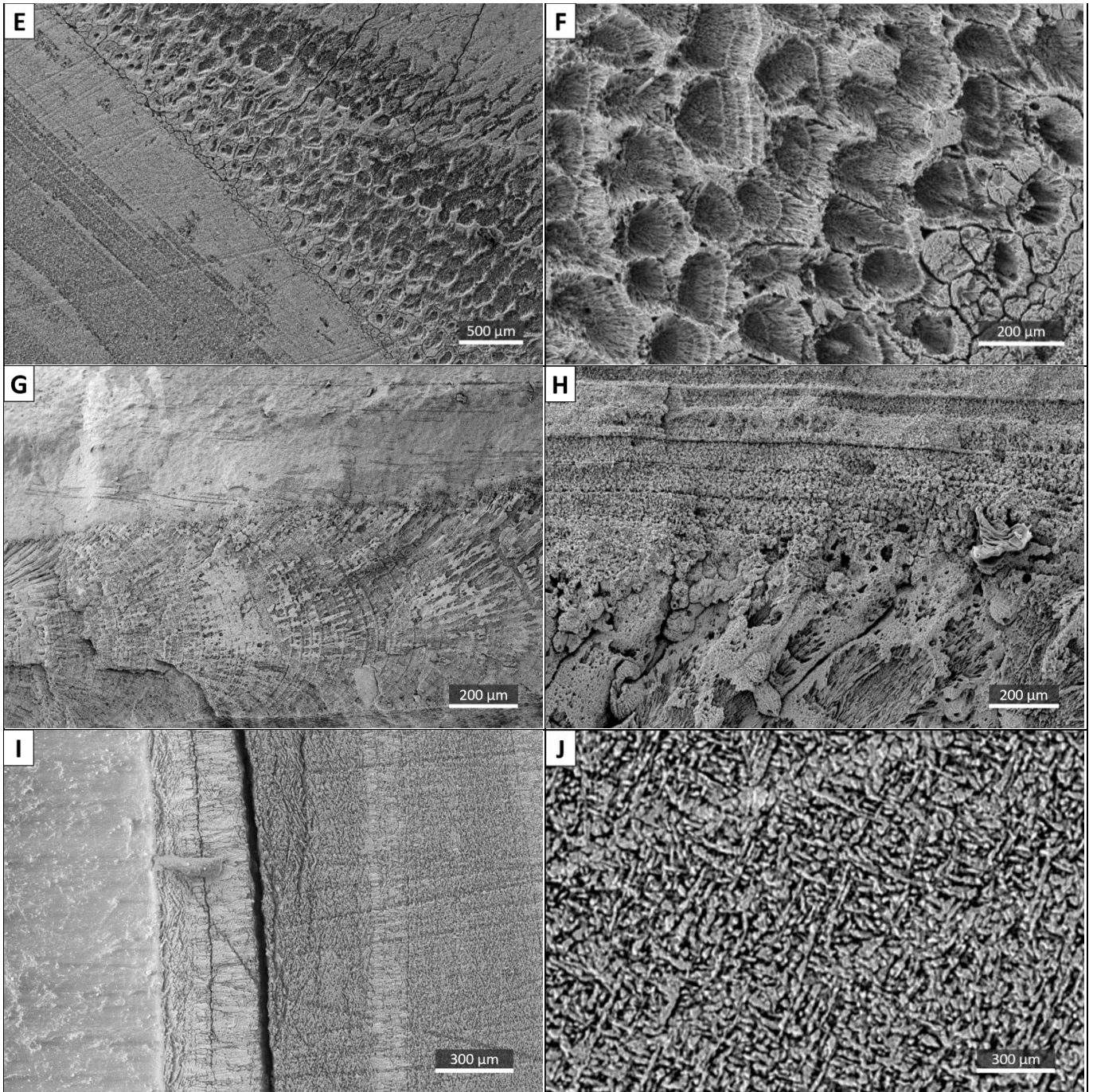


Figure 2.15: Scanning Electron Microscopy images of the aragonite shell of *V. philippinarum*. A: General view of the broken slice of the shell, with the border and the ribs visible; B: close-up of the transition zone between the composite prismatic layer and the crossed-lamellar layer; C: composite prismatic layer; D: detail of the composite prisms; E: transversal section view of the transition zone between the composite prismatic layer and crossed-lamellar layer; F: transversal section view of the composite prisms; G: general view of the transition between the complex prismatic and crossed-lamellar layers; H-I: crossed-lamellar layer with bands of orientation alternations; J: detail of the crossed-lamellar layer.

2.2.3.7. *Venus verrucosa*: Shell Morphology and Microstructures

The warty venus *Venus verrucosa* (Linné *et al.*, 1758) forms a thick, robust, equivalve shell reaching up to 7.6 cm in length. The external surface is marked by deep concentric curved lamellae, that could be simply described as “gutters”. Fine radial lines are intersecting these lamellae, often sculpting frills profusions (or warts). The organic periostracum is thin and matte, lightly colored with cream or orange tones. The interior surface of the shell is almost uniformly white and porcelaneous at its border (Fig. 2.16). The pallial line exhibits a sinus (sinupalliate) and two adductor muscle scars of similar size are observed (dimyarian, isomyarian). The hinge is heterodont and the ligament is well developed (Glover & Taylor, 2010; Oliver *et al.*, 2016; Uvanović *et al.*, 2021; Peharda *et al.*, 2023).

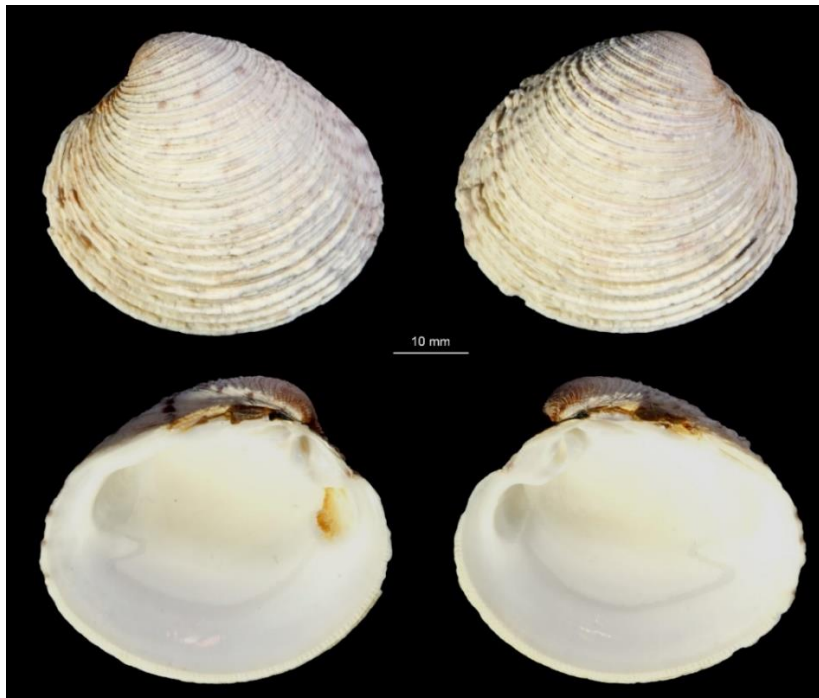
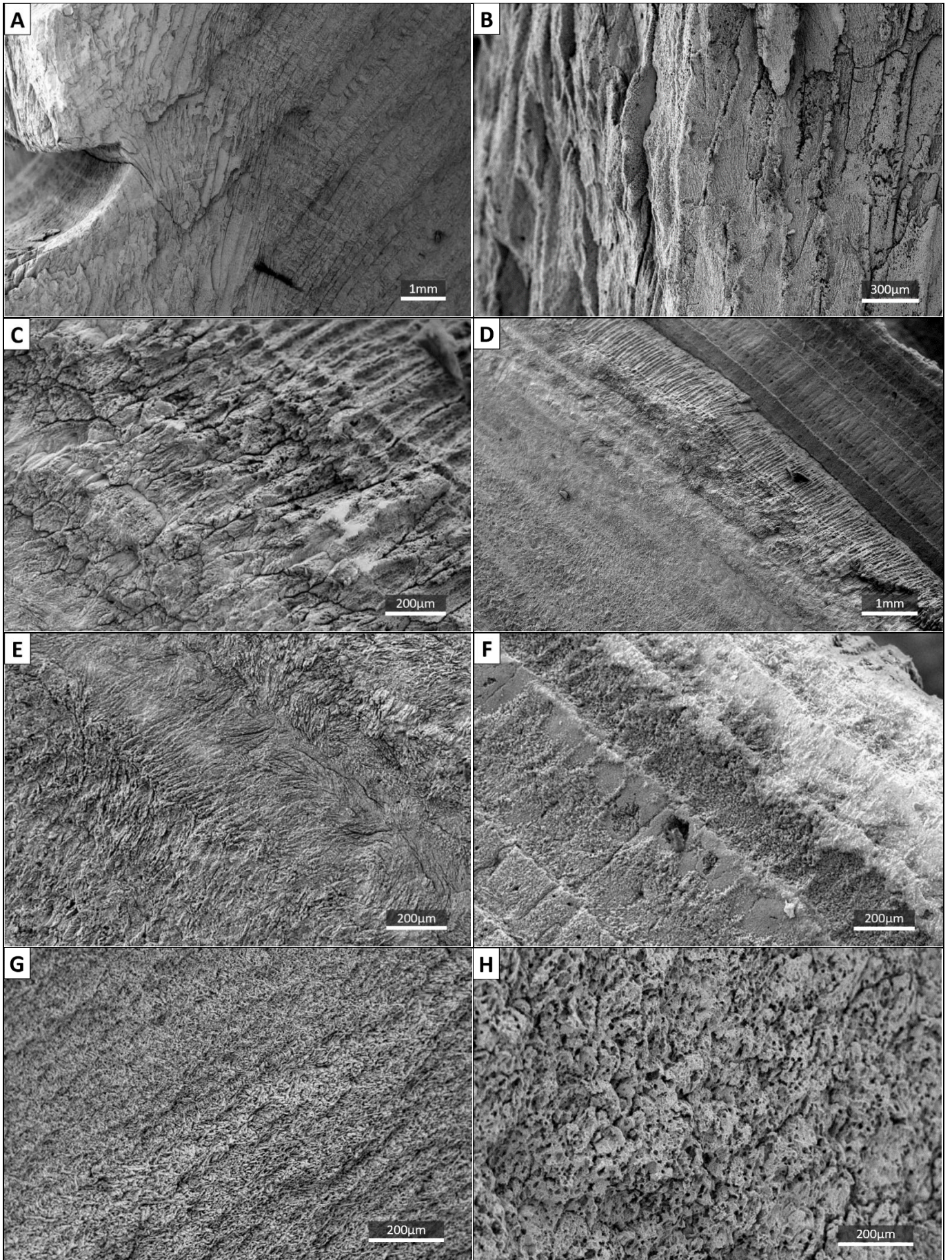


Figure 2.16: Pictures of the shell of venus clam *V. verrucosa*, showing both valves with inside and outside views.

The mineralized shell of the warty venus presents 3 types of aragonitic microstructures. The outer layer is made of composite prisms (Fig. 2.17, A-C), while the middle layer consists of crossed-lamellar superimposed layers (Fig. 2.17, D-G). The inner layer shows homogeneous aragonite, with gradual transition with the lamellae of the middle layer (Fig. 2.17, G) (Popov, 1986; Morton *et al.*, 2011).

Figure 2.17: (verso) Scanning Electron Microscopy images of shell fractures of *Venus verrucosa*. A-D: composite prismatic outer layer. C: detailed view of the tips of some composite prisms. E-H: Crossed-lamellar microstructure, organized in layers. This microstructure exhibits a gradual transition to homogeneous one (G).



2.3. Antimicrobial Components in Mollusks Soft Tissues: A Review

Mollusks secrete a diverse array of antimicrobial components as effectors of their chemical defense system against intruding microorganisms (as discussed in section [2.1.4. Molecular defenses](#)). Among them, antimicrobial peptides (AMPs) are small, cationic molecules that exhibit broad-spectrum antimicrobial activity against bacteria, viruses, fungi and protists. AMPs can be categorized based on their structural characteristics (Venier *et al.*, 2019; Grinchenko & Kumeiko, 2022):

1) Cysteine-rich AMPs include defensins, large defensins, defensin-like proteins, macins, mytilins, and mytimycins. The disulfide bonds between their cysteine residues provide high structural stability, making them resistant to thermic and chemical stress and pathogenic responses. These AMPs exert strong antimicrobial properties through interactions with negatively charged components of the microbial membrane and its subsequent permeabilization, inducing cell death. Some defensins have shown immunomodulatory effects, working in a joint effort with other AMPs and defense molecules (Gueguen *et al.*, 2006; Gerdol *et al.*, 2012).

2) Proline-rich AMPs, like Cg Prp, are also quite stable and often form extended flexible conformations, which is uncommon in other AMPs. This structure enables them to penetrate pathogenic cells without disrupting the membrane, effectively acting on intracellular targets and limiting the possibility for microorganisms to develop paradises. These AMPs tend to show high specificity and usually function in synergy with defensins (Schmitt *et al.*, 2010).

3) The third category comprises linear AMPs, with α -helical conformations, which are especially effective in interacting with membranes, whether for pathogen elimination, transport, agglutination or signaling. Examples include myticalins and modiocalsins, which regulate naturally occurring microorganisms in bivalve gills on top of their participation in the innate immune system (Allam & Raftos, 2015; Grinchenko & Kumeiko, 2022).

The study of molluscan AMPs is still almost exclusively limited to their soft tissues. Differences in exploitation (see Chapter [1.2. Production](#)) leads to discrepancies in DNA and transcriptomic sequencing among mollusk species, further increasing the imbalance in AMP identification. This phenomenon is particularly visible in Table 2.1, where I compile the most comprehensive and up-to-date list of antimicrobial peptides and proteins (AMPs) identified and tested in mollusk soft tissues. For instance, the bivalves *Magallana gigas*, *Crassostrea virginica*, *Mytilus galloprovincialis* and *Venerupis philippinarum* are overrepresented compared to other species and classes. One can also note that only three classes of mollusks are

represented: Bivalvia, Gastropoda and a few taxa from Cephalopoda. Here, I have chosen to focus on AMPPs rather than simply AMPs because of the high proportion of proteins and enzymes in the innate immune systems of mollusks, frequently engaged in AMPs networks, such as histones, lectins or even lysozymes. Some of these proteins are even considered as carriers for – putatively cleavable - AMP sequences, blurring the limits between these compounds in mollusks. The term AMPP therefore appears as the appropriate designation within the context of my thesis.

As illustrated in Table 2.1, the distribution, nature and expression of AMPPs vary among mollusk classes and species. These molecules may be present across the whole body or specific to certain tissues and compartments, constitutively expressed or subjected to modulations following pathogen challenge, though not invariably resulting in upregulation: downregulation has also been observed in certain instances (*M. gigas* Gg-IgPrp, Gonzalez *et al.*, 2007; Gueguen *et al.*, 2009; Schmitt *et al.*, 2012). Notably, AMPPs can be expressed in response to opportunistic pathogens or during secondary infections, suggesting previously unsuspected potential "immune priming" capacities in mollusks (*A. broughtonii* SbCTL, D. Wang *et al.*, 2022). The diversity of AMPPs functions is appreciable: some serve dual roles as recognition factors and effectors, while others exhibit more specialized functions. Their antimicrobial activities can be grouped under the following categories:

1) Effectively killing or destroying the pathogen. Some AMPPs encompass bactericidal, fungicidal, or virucidal properties, often achieved through cell or membrane lysis and viral plaque reduction (*H. discus hannai* HDH-LGBP-A1, Nam *et al.*, 2016; *O. minor* Octominin, Nikapitiya *et al.*, 2020; Dias *et al.*, 2023).

2) Antibiofilm activity by disrupting intercellular communication, disaggregation or preventing cellular adhesion (*O. vulgaris* OctoPaternopin, Maselli *et al.*, 2020, *P. poeyana* Pom-1, González García *et al.*, 2020).

3) Bacteriostatic or fungistatic effects by inhibiting microbial growth, replication or reproduction (*C. gigas* cgUbiquitin, Seo, Lee, Go, *et al.*, 2013; *C. californicus* Cm-p5, López-Abarrategui *et al.*, 2015; *M. galloprovincialis* Mytilec-1, Hasan *et al.*, 2016).

AMPPs can act against various cellular and molecular targets like microbial membranes, where they induce permeabilization, deformation, disintegration or clog transportation ports (*Conus* snails venom, Z. Liu *et al.*, 2009; Kwon *et al.*, 2016; *S. kobeensis* chitosan, Shanmugam *et al.*, 2016). They can also act on intracellular targets by degrading DNA and RNA or halting transcription processes (*B. corneum* KelletinA, Silvestri *et al.*, 1995; Orlando *et al.*, 1996). Furthermore, AMPPs indirectly contribute to pathogen elimination by triggering the production of toxic compounds via cellular defenses (see section 2.1.3. Cellular defenses) or by forming extracellular nanonets to trap pathogens (*M. gigas* Cg-BigDef1, Loth *et al.*, 2019; *V. philippinarum* RRpdef1 α , C. Lv *et al.*, 2020; *A. purpuratus* ApBD1, Stambuk *et al.*, 2021). The efficacy of these peptides is often concentration-dependent, with some exhibiting antimicrobial activity at remarkably low minimum inhibitory concentrations (MICs) (*C. ximenes* Conopeptide X11.1, Figueroa-Montiel *et al.*, 2018). Some AMPPs are capable of interacting with others and to modulate antibiotic sensitivity of pathogens (*O. hiatula* peptide extracts, Gasu *et al.*, 2018).

In addition to their antimicrobial properties, mollusk-derived AMPPs have shown potential in other biomedical applications. For example, lectins from mollusks have demonstrated anticancer properties by inducing apoptosis in tumor cells (Chernikov *et al.*, 2017; Hasan *et al.*, 2015), leading to the development of artificial lectins like Mitsuba, which is under testing for antitumoral treatments (Terada *et al.*, 2017). AMPPs from marine snails and slugs hemocyanin have been identified as promising sources of antiviral peptides, especially against human viruses (Dang *et al.*, 2015). Additionally, some gastropod-derived compounds have shown potential in pain management, such as the analgesic ziconotide derived from cone snail venom (Ahmad *et al.*, 2018). Antiseptic properties coupled with hemocyte chemotaxis capacities of certain AMPPs like myticin C make them also good candidates in wound healing treatments (Rey-Campos *et al.*, 2020).

Interestingly, a few rare examples of mollusk shells demonstrating antibacterial activities have been documented. For instance, Cypraeidae shell powder has shown efficacy against *Micrococcus* and has antipyretic properties (Immanuel *et al.*, 2012). Similarly, chitosan derived from *Sepia officinalis* cuttlebone exhibits activity against both Gram-positive and Gram-negative bacteria, as well as fungi, and has antitumor properties (Hajji *et al.*, 2015; Shanmugam *et al.*, 2016). The use of *Shi Jue Ming*, a powder made of *Haliotis diversicolor* shells, in Chinese traditional medicine as cataplasms and ingestible suspensions also proved effective in wound healing and stimulation of phagocytosis (Z. C. Chen *et al.*, 2016).

The multifunctionality of AMPPs in mollusks highlights the complexity and adaptability of their innate immune system. Understanding these components not only provides insights into mollusk immunity but also opens perspectives for potential applications in medicine and biotechnology. Their presence in a few of the mineralized extracts further motivates the search for AMPPs in the shells of commercial bivalves that are massively produced and consumed.

Table 2.1: up-to-date inventory of the 373 AMPPs (AntiMicrobial Peptides and Proteins) identified in mollusks soft tissues and secretions. The table summarizes their targets, mechanisms and expressions depending on the availability of experimental data in the original studies. The information displayed in grey represent hypothesis or putative characteristics proposed by original authors based on sequence similarities between AMPPs. The target or challenging bacteria from Vibrionaceae family are colored in blue, as they regroup the microorganisms screened in this thesis. Note that some AMPPs presented here are exceptions, in that they are extracted from the cuttlefish bone, an internal shell. AMPPs are sorted by mollusk classes (Bivalvia, Gastropoda, Cephalopoda). Within each class, the alphabetical order of the mollusk names is the sorting system.

Mollusk class	Mollusk species	Peptide/protein name	Target organism	Mechanism and expression	Reference	
BIVALVIA	<i>Adamussium colbecki</i>	Ac-Big Defensin	-	-	(Gerdol <i>et al.</i> , 2020)	
		Big defensin 2	-	<i>de novo</i> assembled from transcriptome	(Moro <i>et al.</i> , 2019)	
		Big defensin 3	-			
	<i>Alasmidonta varicosa</i>	Av-Big Defensin	-	-	(Shallom <i>et al.</i> , 2010)	
	<i>Amblema plicata</i>	Apl-Big Defensin	-	-	(Gerdol <i>et al.</i> , 2020)	
	<i>Anadara (Scapharca) broughtonii</i>	Sb-BDef1	-	-	Constitutively expressed in all tissues Up-regulated in hemocytes and hepatopancreas after <i>V. anguillarum</i> challenge	(M. Li <i>et al.</i> , 2012)
		Sb-BDef2	-	-	Chromosomal assemblage	(Bai <i>et al.</i> , 2019)
		Sb-BDef3	-	-		
		SbCTL (C-type lectin)	OsHV-1 and secondary <i>Vibrio</i> infection	Pathogen recognition and binding, key role in immune priming Constitutive expression in all tissues	(D. Wang <i>et al.</i> , 2022)	
		SbFer (ferritin)	Gram+ bacteria	Cell wall interaction or ROS production Expressed in all tissues, up-regulated after <i>V. anguillarum</i> challenge	(Zheng <i>et al.</i> , 2016)	
	<i>Argopecten irradians</i>	Big Defensin (AiBD)	Gram± bacteria Fungi <i>V. anguillarum</i>	Bacterial growth inhibition Strong fungicide	(Zhao <i>et al.</i> , 2007)	
		AiThymosin-β	<i>Micrococcus sp.</i> <i>V. splendidus</i>	Immunomodulation	(M. Wang <i>et al.</i> , 2019)	
	<i>Argopecten purpuratus</i>	Ap	Gram+ bacteria Fungi	-	(Arenas <i>et al.</i> , 2009)	

	Big defensin ApBD1	Gram± bacteria	Entrapping bacteria via peptide nanonets formation	(Stambuk <i>et al.</i> , 2021)
<i>Bathymodiolus azoricus</i>	Ba-Big Defensin	-	<i>de novo</i> assembled	(Detree <i>et al.</i> , 2016)
<i>Brachidontes variabilis</i>	Whole body crude extract	<i>P. aeruginosa</i> <i>K. pneumoniae</i>	-	(Sake <i>et al.</i> , 2020)
<i>Gigantidas (Bathymodiolus) platifrons</i>	Big defensin	-	-	(Wong <i>et al.</i> , 2015; Sun <i>et al.</i> , 2017)
	Gp-Big Defensin	-	<i>de novo</i> assembled	
	Macin	-	Bacteria aggregation	
<i>Calyptogena marissinica</i>	Cm-Big Defensin	-	-	(Gerdol <i>et al.</i> , 2020)
<i>Cardites antiquatus</i>	Can-Big Defensin 1	-	<i>de novo</i> assembled	(V. L. González <i>et al.</i> , 2015)
	Can-Big Defensin 2	-		
<i>Chamelea gallina</i>	Cga-Big Defensin	-	<i>de novo</i> assembled	(Milan <i>et al.</i> , 2019)
<i>Chlamys farreri</i>	CfThymosin-β	<i>Micrococcus sp.</i>	Immunomodulation	(M. Wang <i>et al.</i> , 2019)
<i>Corbicula fluminea</i>	Pcar-Big Defensin	-	<i>de novo</i> assembled	(H. Chen <i>et al.</i> , 2013)
	Cf-ncBigDef	-	-	
<i>Crassostrea corteziensis</i>	Cc-Big Defensin	-	<i>de novo</i> assembled	(CIBNor, 2014)
<i>Magallana (Crassostrea) angulata</i>	Ma-Big Defensin 1 & 3	-	<i>de novo</i> assembled	(Z. Zeng <i>et al.</i> , 2019, Gerdol <i>et al.</i> , 2020)
<i>Magallana (Crassostrea) gigas</i>	Cg-Def	Gram+ bacteria	Bactericidal activity by membrane disruption and inhibition of vital cellular processes	(Gueguen <i>et al.</i> , 2006)

Cg-Defh1	Gram± bacteria <i>V. splendidus</i>	Constitutively expressed	(Gonzalez <i>et al.</i> , 2007;
Cg-Defh2	<i>V. aestuarianus</i> <i>V. anguillarum</i>	Synergy with other defensins	Schmitt <i>et al.</i> , 2012)
Cg-IgPrp	Gram+ bacteria	Down-regulated during infection Synergy with other defensins	(Gonzalez <i>et al.</i> , 2007; Gueguen <i>et al.</i> , 2009; Schmitt <i>et al.</i> , 2012)
Cg-IgPrp P/Q	Gram+ bacteria	Synergy with other defensins	(Gonzalez <i>et al.</i> , 2007; Schmitt <i>et al.</i> , 2012)
CgCLec-4	Gram± bacteria <i>V. anguillarum</i> Fungi	Bacteria agglutination and binding to other AMPs Growth suppression	
CgCLec-5	Gram- bacteria <i>E. coli</i> <i>V. anguillarum</i>	Bacteria recognition, agglutination and binding to other AMPs Growth suppression Hemocytes quasi-specific expression	(Jia <i>et al.</i> , 2016)
cgMolluscidin-1	Broad range of Gram± bacteria <i>V. parahaemolyticus</i>	Constitutively expressed, up-regulated in <i>Vibrio sp.</i> infections	(Seo, M.J. Lee, Nam, <i>et al.</i> , 2013)
Cgpep33	Gram± bacteria Fungi	-	(Z. Liu <i>et al.</i> , 2008)
cgThymosin-β	Gram± bacteria <i>C. albicans</i>	-	(Nam <i>et al.</i> , 2015)
cgUbiquitin	Broad spectrum of Gram± bacteria <i>S. iniae</i> <i>V. parahaemolyticus</i>	Bacteriostasis	(Seo, M.J. Lee, Go, <i>et al.</i> , 2013)
Lysozyme	Gram+ bacteria	Specific forms for defensive functions Stressors-dependent regulation	(Matsumoto <i>et al.</i> , 2006; Itoh <i>et al.</i> , 2010)

	Big-defensin / Cg-BigDef1	Broad range of Gram± bacteria Drug resistant <i>S. aureus</i>	Bactericidal by hydrophobic nanonets entrapping, strongly upregulated following <i>Vibrio</i> infection C-terminal region structure similar to vertebrate β-defensins	(Rosa <i>et al.</i> , 2011; Loth <i>et al.</i> , 2019)
	Cg-BigDef2	-	Strongly upregulated following <i>Vibrio</i> infection C-terminal region structure similar to vertebrate β-defensins	(Rosa <i>et al.</i> , 2011; X.
	Cg-BigDef3	-	Constitutively expressed, non-regulated C-terminal region structure similar to vertebrate β-defensins	Wang <i>et al.</i> , 2019; Gerdol <i>et al.</i> , 2020)
	Cg-BigDef 4-6 & 8-10	-	C-terminal region structure similar to vertebrate β-defensins	
	Cg-BigDef7 / Ma-Big Defensin 2	-	Highly expressed in the digestive gland	(G. Zhang <i>et al.</i> , 2012)
	NAD(P)H oxidase	Hemolymph microbes <i>V. parahaemolyticus</i>	Recognition and signaling for elimination of hemocyte-binding bacteria	(Sun <i>et al.</i> , 2020)
	Two hexapeptides	HIV-1	Protease inhibition	(T.G. Lee & Maruyama, 1998)
	AVP	Herpes viruses	Strong antiviral activity	(M. Zeng <i>et al.</i> , 2008)
	Peptide extract	OsHV-1	Viral replication inhibition	(Olicard <i>et al.</i> , 2005)
<i>Magallana</i> (<i>Crassostrea</i>) <i>hongkongensis</i>	URP20	Gram± bacteria Foodborne pathogens Fungi	Aggregation and membrane permeabilization Up-regulated expression after <i>V.</i> <i>parahaemolyticus</i> challenge	(Mao <i>et al.</i> , 2021)
	Ch-Big Defensin 1 & 2	-	-	(Gerdol <i>et al.</i> , 2020)

<i>Magallana nippona</i>	Mn-Big Defensin 1 & 2	-	-	(Gerdol <i>et al.</i> , 2020)
<i>Crassostrea virginica</i>	American Oyster Defensin (AOD)	Gram± bacteria	-	(Seo <i>et al.</i> , 2005)
	Cv-BigDef 1/3 - 12	-	<i>de novo</i> assembled	(Milbury & Gaffney, 2005; Jenny <i>et al.</i> , 2011; Gómez-Chiarri <i>et al.</i> , 2015; Gerdol <i>et al.</i> , 2020)
	Lysozyme 1	Gram± bacteria <i>V. vulnificus</i>	Bacterial wall disruption by hydrolyzation	(Q.-G. Xue <i>et al.</i> , 2004)
	Lysozyme 2	Gram± bacteria <i>V. vulnificus</i>	Bacterial wall disruption by hydrolyzation	
	Lysozyme 3	Gram± bacteria	Bacterial wall disruption by hydrolyzation Bacterial growth inhibition	(Q. Xue <i>et al.</i> , 2010)
	Cvsi-1	Protozoan parasite <i>P. marinus</i>	Serine protease inhibitor Thermostable	(Q.-G. Xue <i>et al.</i> , 2006)
	Paolin-1	Bacteria	-	(C. P. Li <i>et al.</i> , 1965)
	Paolin-2	Viruses	-	(C. P. Li <i>et al.</i> , 1962; Prescott <i>et al.</i> , 1966)
<i>Crenomytilus grayanus</i>	CGL (lectin)	HIV	Viral particle agglutination	(Luk'yanov <i>et al.</i> , 2007; Jakób <i>et al.</i> , 2015)
<i>Dreissena polymorpha</i>	Zebra mussel defensin Dpd	<i>Morganella</i> sp., <i>P. shigelloides</i> , <i>E. tarda</i> , <i>E. coli</i> , <i>S. aureus aureus</i>	Collected in the foot Upregulated by hemocytes during byssogenesis	(Xu & Faisal, 2010)
	Dp-Big Defensin 1 & 2	-	<i>de novo</i> assembled	(Gerdol <i>et al.</i> , 2020)

<i>Dreissena rostriformis</i>	Dr-BigDef 1-3			
	Dr-ncBigDef 1-8 (non-conventional sequence)	-		<i>de novo</i> assembled (Calcino <i>et al.</i> , 2019)
<i>Eucrassatella cumingii</i>	Ec-Big Defensin	-		<i>de novo</i> assembled (V. L. González <i>et al.</i> , 2015)
<i>Eurhomalea rufa</i>	Er-Big Defensin 1 & 2	-	-	(Gerdol <i>et al.</i> , 2020)
<i>Galatea paradoxa</i>	Peptide extract	Gram± bacteria	-	(Borquaye <i>et al.</i> , 2015, 2016)
<i>Lamychaena hians</i>	Lh-Big Defensin	-		<i>de novo</i> assembled (V. L. González <i>et al.</i> , 2015)
<i>Latona faba</i>	Shell extracts	Human & fish pathogens <i>S. paratyphi</i> , <i>Shigella sp.</i> , <i>B. cereus</i> , <i>V. harveyi</i> and <i>V. parahaemolyticus</i>	-	(Giftson & Patterson, 2014)
<i>Leaunio lienosus lienosus</i>	Lli-Big Defensin 1 & 2	-		<i>de novo</i> assembled (R. Wang <i>et al.</i> , 2012)
<i>Lobatus (Strombus) gigas</i>	Paolin-1	<i>Strep. Pyogenes</i> <i>S. aureus</i>	-	(C. P. Li <i>et al.</i> , 1962, 1965)
	Paolin-2	Viruses	-	(C. P. Li <i>et al.</i> , 1965)
<i>Mercenaria mercenaria</i>	Paolin-1	<i>Strep. Pyogenes</i> <i>S. aureus</i>	-	(C. P. Li <i>et al.</i> , 1962, 1965)
	Paolin-2	Adenovirus Herpesvirus Polyoma virus Influenza virus	-	(C. P. Li <i>et al.</i> , 1965)
<i>Meretrix lusoria</i>	Ml-Big Defensin	-	-	(Y. S. Lee <i>et al.</i> , 2015)
<i>Meretrix meretix</i>	Mm-Big Defensin 1 & 2	-		<i>de novo</i> assembled (Gerdol <i>et al.</i> , 2020)

<i>Mimachlamys crassicostata</i> (<i>Chlamys nobilis</i>)	CnBD (big defensin)	<i>V. parahaemolyticus</i>	Up-regulated after challenge of <i>V. parahaemolyticus</i> . High similarity with <i>A. irradians</i> ' big defensin	(J. Yang <i>et al.</i> , 2013)
<i>Mimachlamys varia</i>	Mv-Big Defensin	-	-	(Gerdol <i>et al.</i> , 2020)
<i>Mizuhopecten yessoensis</i>	My-BigDef	-	-	(W. Liu <i>et al.</i> , 2009)
<i>Modiolus modiolus</i>	Modiolin	Marine bacteria <i>A. Salmonicida</i> <i>V. anguillarum</i> <i>V. ordalii</i> <i>V. viscosus</i> <i>V. wodanis</i>	Strong antibacterial activity Putative bacteriostasis Putative bactericidal activity	(Tunkijjanukij & Olafsen, 1998 ; Leoni <i>et al.</i> , 2017; Rao <i>et al.</i> , 2020)
<i>Modiolus kurilensis</i>	Modiocalin	-	High variability	(Leoni <i>et al.</i> , 2017)
<i>Modiolus philippinarum</i>	Modiocalin-1	-	High variability	(Leoni <i>et al.</i> , 2017; Sun <i>et al.</i> , 2017)
	Modiocalin-4	-	High variability	
<i>Mya arenaria</i>	Ma-Big Defensin 1 & 2	-	Up-regulated in fast growth individuals	(Wilson <i>et al.</i> , 2016)
<i>Mytilus californianus</i>	Mca-Big Defensin 1 & 2	-	Adhesive properties, <i>de novo</i> assembled from foot glands transcriptomes	(Gracey <i>et al.</i> , 2008; DeMartini <i>et al.</i> , 2017)
<i>Mytilus chilensis</i>	Defensin	-	Constitutively expressed	(Núñez-Acuña <i>et al.</i> , 2012)
	Mchi-Big Defensin	-	-	
	Mytilin B	-	Environmental pathogenic charge dependent expression	
<i>Mytilus coruscus</i>	Mytichitin-A	Gram+ bacteria	Tissue type and infection dependent expression	(Oh <i>et al.</i> , 2018; H. Liu <i>et al.</i> , 2019)
	Mytichitin-1			
	Mytichitin-CB	Fungi	Cell wall hydrolysis	(Qin <i>et al.</i> , 2014; H. Liu <i>et al.</i> , 2019)

	Myticusin-1	Gram± bacteria Fungi	Cell morphological alterations	(Liao <i>et al.</i> , 2013)
	Myticusin-alpha	Gram± bacteria	Membrane disruption linked to charge and hydrophobicity	(Pane <i>et al.</i> , 2017)
	RMchi-N	-	-	(H. Liu <i>et al.</i> , 2019)
	RMchi-F	-	-	(H. Liu <i>et al.</i> , 2019)
<i>Mytilus edulis</i>	Mytilus defensin (mytilin) A	Marine Gram- bacteria Filamentous fungi <i>L. braziliensis</i>	Constitutive expression in haemolymph Membrane destabilization	(Charlet <i>et al.</i> , 1996; Löfgren <i>et al.</i> , 2008)
	Mytimycin Mytilmycin	Marine Gram- bacteria Filamentous fungi	Constitutive expression in haemolymph Membrane destabilization	(Charlet <i>et al.</i> , 1996)
	Mytilus defensin (mytilin) B	Marine Gram- bacteria Filamentous fungi	Constitutive expression in haemolymph Membrane destabilization	(Charlet <i>et al.</i> , 1996)
	Mfp-5 (foot protein derived peptide)	<i>S. aureus</i> <i>S. epidermidis</i>	Important antifouling activity	(Gauna <i>et al.</i> , 2022)
	Me-Big Defensin 1-3	-	-	(Philipp <i>et al.</i> , 2012, Gerdol <i>et al.</i> , 2020)
<i>Mytilus galloprovincialis</i>	Mytilin B antimicrobial peptide MGD2b	Various bacteria <i>Marine Vibrio</i>	Signaling peptide, over-expression under environmental physical stressors Pathogen-induced expression reduction	(Mitta, Hubert, <i>et al.</i> , 2000)
	MGD-1 (defensin)	Gram± bacteria <i>V. alginolyticus</i> <i>V. P1 (likely tapetis)</i> <i>V. splendidus</i>	Strong antibacterial activity	(Hubert <i>et al.</i> , 1996)
	MGD-1 fragment	Gram+ bacteria Protozoa Viruses, HIV-1 Fungi	β-hairpin loop-3 binding targets	(Mitta, Vandenbulcke, <i>et al.</i> , 1999; Y.-S. Yang <i>et al.</i> , 2000; Romestand <i>et al.</i> , 2003; Roch <i>et al.</i> , 2004)

MGDefensin-2	Gram+ bacteria <i>M. luteus</i> Marine fungi	Bacterial challenge dependent expression and release by hemocytes	(Mitta, Vandenbulcke, <i>et al.</i> , 1999)
MgBD-1 a-c (Big Defensin)			
MgBD-2 a-h			
MgBD-3 a-g	Broad range of Gram ± bacteria	Bacterial membrane binding and disruption	(Gerdol <i>et al.</i> , 2012; 2020)
MgBD-4 a/b			
MgBD-5 a-g			
MgBD-6			
MgBD-7 a-e			
MgEP	<i>E. coli</i> <i>V. cholerae</i>	Opsonin activity	(Canesi <i>et al.</i> , 2016)
Myticin-A	Gram+ bacteria	Bacteriolysis	(Mitta, Hubert, <i>et al.</i> , 1999)
Myticin-B	Gram± bacteria <i>V. splendidus</i> <i>V. anguillarum</i> Fungi White Spot Synd. Virus	Bacteriolysis Antiviral activity	(Mitta, Hubert, <i>et al.</i> , 1999; Roch <i>et al.</i> , 2008)
Myticin C	Gram+ bacteria <i>Vibrio</i> strains Herpesvirus	Membrane disruption Inhibition of viral particles replication	(Pallavicini <i>et al.</i> , 2008; Novoa <i>et al.</i> , 2016)
Mytimacin-1	Gram± bacteria	Constitutive expression across all tissues, none in hemocytes	(Gerdol <i>et al.</i> , 2012; 2020)
Mytimacin-2	Gram± bacteria	Expression specific to foot and gills	
Mytimacin-3	Gram± bacteria	Constitutive expression in low levels, specific to the mantle	

	Mytimacin-4	Gram± bacteria <i>V. anguillarum</i> <i>V. parahaemolyticus</i>	Expression inducible upon <i>Vibrio</i> challenge in posterior adductor muscle	(Gerdol <i>et al.</i> , 2015; J. Lv <i>et al.</i> , 2019)
	Mytimacin-5 (partial)	-	-	(Gerdol <i>et al.</i> , 2012)
	Mytilin C	Gram± bacteria <i>V. splendidus</i> Fungi Protozoan parasite	Rapid specialized bactericidal activity	(Mitta, Vandenbulcke, <i>et al.</i> , 2000)
	Mytilin D	Gram± bacteria Fungi	Specialized bactericidal activity	
	Myticalin A5	Gram± bacteria	Bacterial protein synthesis inhibition	
	Myticalin A8			
	Myticalin C9	Gram± bacteria	High interindividual sequence variability and tissue-specific expression	(Leoni <i>et al.</i> , 2017)
	Myticalin D2			
	Myticalin B1			
	Myticalin C6	Gram± bacteria	Moderate antibacterial activity	
	Truncated myticin C	-	High variability in pathogen recognition function	(Vera <i>et al.</i> , 2011)
	MytiLec-1 (mytilectin)	Gram± bacteria	Bacteriostasis by agglutination	(Hasan <i>et al.</i> , 2016)
<i>Nodipecten subnodosus</i>	Ns-Big defensin	-	-	(Gerdol <i>et al.</i> , 2020)
<i>Pecten maximus</i>	Big Defensin	-	-	(Kenny <i>et al.</i> , 2020)
	Pm-BigDef	-	-	(Pauletto <i>et al.</i> , 2013)
<i>Perna canaliculus</i>	Pc-Big Defensin	-	-	(Gerdol <i>et al.</i> , 2020)
	Mytilin 1	-	Neutral charge, potentially lower binding affinity with negatively charged bacterial cell membranes	(Greco <i>et al.</i> , 2020)

	Glycosaminoglycan-like moieties from whole body extract	<i>S. aureus</i> (also methicillin-resistant strains) <i>E. faecalis</i>	Fucose chondroitin sulphated-like polysaccharide	(Aldairi <i>et al.</i> , 2022)
<i>Perna viridis</i>	AMP	ESKAPE pathogens	-	(Poyil <i>et al.</i> , 2020)
	Pvir mytilin 1-7			
	Pernalin A	-	-	(Greco <i>et al.</i> , 2020)
	Pernalin B (predicted)			
	Pv-Big Defensin 1 & 2	-	<i>de novo</i> assembled	(Leung <i>et al.</i> , 2014)
Pv-def	<i>V. parahaemolyticus</i> Potentially other targets	Highly expressed in hepatopancreas, potential induction following <i>V. parahaemolyticus</i> challenge Closest to arthropod defensins	(Y. Wang <i>et al.</i> , 2018)	
<i>Pinctada fucata martensii</i>	PmAMP-1	<i>E. coli</i>	Cell wall disintegration starting at the extremities Constitutively expressed in all tissues Increased expression after bacterial challenge	(He <i>et al.</i> , 2019)
<i>Pinctada (Margaritifera) margaritifera</i>	Mmar-Big Defensin 1	-	-	(Bertucci <i>et al.</i> , 2017;
	Mmar-Big Defensin 2	-	<i>de novo</i> assembled	Gerdol <i>et al.</i> , 2020)
<i>Pinctada radiata</i>	Whole body crude extract	<i>E. coli</i> , <i>P. aeruginosa</i> , <i>S. aureus</i>	-	(Sake <i>et al.</i> , 2020)
<i>Placopecten magellanicus</i>	Pmag-Big Defensin	-	<i>de novo</i> assembled	(Pairett & Serb, 2013)
<i>Pteria penguin</i>	Pp-Big Defensin	-	-	(Gerdol <i>et al.</i> , 2020)
<i>Sinohyriopsis cumingii</i>	Hc-BD (big defensin)	Gram± bacteria	Infection-regulated expression	(G.-L. Wang <i>et al.</i> , 2014)

<i>Sinohyriopsis schlegelii</i>	Hs-defn (defensin)	-	Up-regulated expression after bacterial challenge	(Peng <i>et al.</i> , 2012)
<i>Ruditapes decussatus</i>	Rd-Big Defensin 1	-	<i>de novo</i> assembled	(De Sousa <i>et al.</i> , 2014)
	Rd-Big Defensin 2	-	-	(Yan <i>et al.</i> , 2019)
<i>Saccostrea sp.</i>	S-Big Defensin 1 & 2	-	-	(McDougall, 2018)
<i>Saccostrea glomerata</i>	Sg-BigDef 1-13	-	-	(Powell <i>et al.</i> , 2018)
<i>Tegillarca granosa</i>	TgBD (big defensin)	Gram+ bacteria <i>V. parahaemolyticus</i>	Bactericidal activity by putative nanonets production Expression in all tissues, dependent on bacterial challenge	(Ri <i>et al.</i> , 2022)
<i>Trichomya hirsuta</i>	Th-Big Defensin	-	<i>de novo</i> assembled	(Saarman <i>et al.</i> , 2017)
<i>Venerupis (Ruditapes) philippinarum</i>	MCdef (defensin)	Gram± bacteria <i>V. logei</i> <i>A. salmonicida</i>	<i>V. tapetis</i> infection-induced expression	(Adhya <i>et al.</i> , 2012)
	VpBD (big defensin)	Gram± bacteria	Growth inhibition	(Zhao <i>et al.</i> , 2010; Yan <i>et al.</i> , 2019)
	Rp-ncBigDef 1-5 (non-conventional)	<i>V. anguillarum</i>	Stress and infection-induced expression	
	RPD-1 / Rp-BigDef1 (big defensin)	Gram± bacteria <i>V. anguillarum</i> <i>V. parahaemolyticus</i>	-	(Wei <i>et al.</i> , 2003; Yan <i>et al.</i> , 2019)
	Rp-BigDef 2-8	-	-	(Yan <i>et al.</i> , 2019)
	Rpdef3 (defensin)	Gram± bacteria <i>V. anguillarum</i> <i>V. harveyi</i> <i>V. parahaemolyticus</i> <i>V. splendidus</i>	Nanonet production and membrane permeabilization	(Q. Wang <i>et al.</i> , 2015 ; Han <i>et al.</i> , 2021)

	VpDef (defensin)	Gram± bacteria <i>V. anguillarum</i>	Highest activity against Gram+ bacteria Membrane lesions inducing Constitutively expressed in hemocytes	(Zhang <i>et al.</i> , 2015)
	rVpDef	Gram± bacteria	Growth inhibition Resistance to protease and pH and thermal shocks	(Meng <i>et al.</i> , 2018)
	RRpdef1α	Gram± bacteria	Bacterial membrane permeabilization Opsonin action: promotion of phagocytosis and chemotaxis from hemocytes	(C. Lv <i>et al.</i> , 2020)
	Rp-hdmc (hydramacin)	-	Up-regulated expression in gill and hemocytes after <i>V. tapetis</i> challenge	(Y. Lee <i>et al.</i> , 2014)
	<i>Venustaconcha ellipsiformis</i>	Ve-Big Defensin 1 & 2	-	Hybrid <i>de novo</i> assembly (Renaut <i>et al.</i> , 2108)
GASTROPODA	<i>Aplysia californica</i>	Escapin	Gram± bacteria Yeasts Fungi <i>V. harveyi</i>	Bacteriostasis (hydrogen peroxide production) Bactericide (lysine dependent mechanisms) (H. Yang <i>et al.</i> , 2005)
	<i>Aplysia kurodai</i>	Aplysianin-A	Gram± bacteria <i>V. anguillarum</i>	Growth inhibition (Takamatsu <i>et al.</i> , 1995)
	<i>Buccinum corneum</i>	Kelletinin A	Viruses	Antiviral activity Antimitosis Viral DNA, RNA and transcription inhibition (Orlando <i>et al.</i> , 1991; Silvestri <i>et al.</i> , 1995; Orlando <i>et al.</i> , 1996)
	<i>Californiconus californicus</i>	Conotoxin O1_cal29b	<i>Mycobacterium tuberculosis</i>	Growth inhibition Neurotoxic venom (Bernáldez-Sarabia <i>et al.</i> , 2019)

<i>Cenchritis muricatus</i>	Cm-p1	Yeasts Filamentous fungi	Fungistasis	(López-Abarrategui, Alba, Silva, <i>et al.</i> , 2012; López-Abarrategui <i>et al.</i> , 2015)
	Cm-p2	Not tested, sharing 70% identity with Cm-p1		(López-Abarrategui, Alba, Silva, <i>et al.</i> , 2012)
	Cm-p3 & Cm-p4	Fungi	Fungistasis	(López-Abarrategui <i>et al.</i> , 2015)
	Cm-p5	<i>C. albicans</i> Broad range of fungi	Strong fungistasis by cell adhesion	
	Putative antimicrobial protein 1	<i>E. coli</i> <i>S. aureus</i>	Strong growth inhibition	(López-Abarrategui, Alba, Lima, <i>et al.</i> , 2012)
	Putative AMP 2			
<i>Conasprella ximenes</i>	Conopeptide X11.1	<i>Mycobacterium tuberculosis</i>	Concentration dependent growth inhibition, low MIC Neurotoxic venom	(Figueroa-Montiel <i>et al.</i> , 2018)
<i>Conus achatinus</i>	Body tissue	Gram± bacteria, human pathogens	-	(Chandramathi & Thilaga, 2018)
<i>Conus betulinus</i>	Acipensin-6 1-3	Fungi	-	(R. Li <i>et al.</i> , 2022)
	cbTbeta	Gram- bacteria Fungi	-	
	CcAMP1-CB	Fungi	-	
	Histone H4	Gram- bacteria Fungi	-	
	Ubiquicidin 31-38	Fungi	-	
	TCP-1	Gram+ bacteria Fungi	-	
	YFGAP-CB	Gram+ bacteria	-	

<i>Conus magus</i>	ω -conotoxin MVIIA, Ziconotide	Gram \pm bacteria Fungi Mammalian Cells	Lipid bilayer	(Hemu & Tam, 2006)
<i>Conus mustelinus</i>	Conolysin-Mt1	Eukaryotic cells Gram + bacteria	High cytolytic activity (permeabilization)	(Biggs <i>et al.</i> , 2007)
	Conolysin-Mt2	Eukaryotic cells Gram + bacteria	Cytolytic activity	
<i>Conus purpurascens</i>	Conopeptide κ -PVIIA	No specificity	Membrane channels occlusion Highly stable peptide	(Kwon <i>et al.</i> , 2016)
<i>Crepidula atrasolea</i>	Cat-Big Defensin	-	<i>de novo</i> assembled	(Henry <i>et al.</i> , 2017)
<i>Dolabella auricularia</i>	Dolabellin B2	Fungi Gram+ bacteria <i>V. vulnificus</i>	Fungicide action and fungistasis Bacterial cytotoxicity	(Iijima <i>et al.</i> , 2003)
<i>Elysia grandifolia</i>	Kahalalide R	<i>M. tuberculosis</i>	Antimycobacterial activity	(Ashour <i>et al.</i> , 2006)
<i>Elysia rufescens</i>	Kahalalide A	<i>M. tuberculosis</i>	Antimycobacterial activity	(Bourel-Bonnet <i>et al.</i> , 2005)
<i>Euchelus asper</i>	EA-Extract	<i>C. albicans</i>	Immunomodulation of phagocytosis	(Ponkshe & Indap, 2002)
<i>Euselenops luniceps</i>	Whole body tissue extract	<i>P. aeruginosa</i> , <i>P. mirabilis</i> , <i>S. Aureus</i> , <i>K. oxytoca</i> , <i>V. parahaemoliticus</i> Fungus <i>Rhizopus sp.</i>	-	(Ramya <i>et al.</i> , 2018)
<i>Filopaludina (Bellamya) bengalensis</i>	Bb-AMP4	<i>Staphylococcus epidermidis</i>	Bacterial membrane permeabilization	(Gauri <i>et al.</i> , 2011)

<i>Haliotis discus</i>	hdMolluscidin	Broad range of gram± bacteria <i>C. albicans</i>	Constitutively expressed Membrane permeabilization	(Seo <i>et al.</i> , 2016)
<i>Haliotis discus hannai</i>	HDH-LGBP-A1 HDH-LGBP-A2	Gram± bacteria <i>Yeast</i>	Membrane lysis	(Nam <i>et al.</i> , 2016)
<i>Haliotis diversicolor</i>	Mytimacin-6 (HD-mtmc 6)	-	Up-regulated expression by <i>V. harveyi</i> challenge	(Xie <i>et al.</i> , 2021)
	Hdiv-Big Defensin	-	<i>de novo</i> assembled and BLAST search from total body extracts	(Jiang <i>et al.</i> , 2011)
<i>Haliotis laevigata</i>	Hemolymph and digestive gland peptide extracts	<i>H. simplex</i> HSV-1	Antiviral activity	(Dang <i>et al.</i> , 2011)
<i>Haliotis rufescens</i>	Paolin-1	<i>Strep. Pyogenes</i> <i>S. aureus</i>	-	(C. P. Li <i>et al.</i> , 1962, 1965)
	Paolin-2	Viruses	-	(C. P. Li <i>et al.</i> , 1965)
<i>Haliotis tuberculata</i>	Haliotisin peptide 3-4-5	Gram± bacteria	Haemocyanin region Microbial cell wall disruption	(Zhuang <i>et al.</i> , 2015)
	Synthetic haliotisin	Human pathogenic viruses	Binding competition with viral particles	(Krepstakies <i>et al.</i> , 2012)
	Htub-Big Defensin	-	<i>de novo</i> assembled	(Harvney <i>et al.</i> , 2016)
<i>Helix lucorum</i>	HHH (hemocyanin peptide)	HSV type 1	Viral replication inhibition	(Dolashka <i>et al.</i> , 2010)
<i>Laevistrombus turturella</i>	GSS meat extract AMP	<i>S. aureus</i> <i>E. coli</i>	Membrane disruption Intracellular interference of growth Pathogen inhibition by disruption of protein translation	(Viruly <i>et al.</i> , 2023)

<i>Limacus flavus</i>	Cystatin c-b	Bacteria, viruses Fungi	Protease inhibitor	
	Defensin Defensin-like	Bacteria, virus Fungi	-	
	Thaumatococin-like	Fungi	Membrane permeabilization, enzyme and protein degradation, apoptosis	(Z. Li <i>et al.</i> , 2020)
	Peritrophin-1 Peritrophin-44 like	Bacteria	Membrane binding and growth inhibition	
<i>Lissachatina fulica</i>	Mytimacin-AF	Gram± bacteria <i>C. albicans</i>	-	(Zhong <i>et al.</i> , 2013)
<i>Littorina littorea</i>	Peptide extract	Gram± bacteria	-	(Borquaye <i>et al.</i> , 2016)
	Littorein	Firmicutes Gracilicutes Viruses	Bactericidal activity Antiviral activity	(Defer <i>et al.</i> , 2009)
<i>Lottia gigantea</i>	Lg-Big Defensin	-	<i>de novo</i> assembled	(Simakov <i>et al.</i> , 2013)
<i>Lymnaea stagnalis</i>	AMP	Drug resistant <i>S. epidermidis</i>	Bactericide by membrane disruption	(Gauri <i>et al.</i> , 2016; Seppälä <i>et al.</i> , 2021)
<i>Nerita versicolor</i>	Nvp-1	Gram- bacteria <i>P. aeruginosa</i> Fungi	Strong anti-biofilm activity	
	Nvp-2	Gram- bacteria <i>P. aeruginosa</i> <i>C. albicans</i>	Anti-biofilm activity	(Rodriguez <i>et al.</i> , 2023)
	Nvp-3	Gram- bacteria <i>P. aeruginosa</i> <i>C. albicans</i>	Small MIC for antibacterial activity Anti-biofilm activity	

<i>Olivancillaria hiatula</i>	Peptide extract	Broad range of Gram± bacteria	Bacteriostasis Strain-specific bactericidal activity Antibiotic sensitivity modulation	(Gasu <i>et al.</i> , 2018)
<i>Patella rustica</i>	Crude peptide extract	Gram± bacteria Fungi	-	(Borquaye <i>et al.</i> , 2015)
<i>Pomacea canaliculata</i>	Pca-Big Defensin	-	-	(C. Liu <i>et al.</i> , 2018)
<i>Pomacea poeyana</i>	Pom-1	Gram± bacteria Zika virus, Candida fungi	Biofilm inhibition	(González García <i>et al.</i> , 2020; Raber <i>et al.</i> , 2021)
	Pom-2	Gram- bacteria Candida fungi	Putative bacterial membrane disruption	
<i>Potamopyrgus antipodarum</i>	Pa-Big Defensin	-	Involved in response to trematode <i>Microphallus</i> infection	(Bankers <i>et al.</i> , 2017)
<i>Rapana venosa</i>	RvH1 (hemocyanin peptides)	HSV type 1 EBV	Viral replication suppression	(Dolashka <i>et al.</i> , 2010; Nesterova <i>et al.</i> , 2011)
	RvH2	HSV type 1 EBV Drug-resistant Herpesviruses	Viral replication inhibition and suppression	(Genova-Kalou <i>et al.</i> , 2008; Dolashka <i>et al.</i> , 2010; Nesterova <i>et al.</i> , 2011)
	Peptide 2	Gram± bacteria	Bacterial surface binding and membrane disruption	(Dolashka <i>et al.</i> , 2011)
	Peptide 4-9			
<i>Tugalina gigas</i>	Tugalistatin	Viruses	Protease inhibition	(Yoshino <i>et al.</i> , 1993)
<i>Volegalea cochlidium</i>	HP-Extract	<i>C. albicans</i>	Immunomodulation of phagocytosis	(Ponkshe & Indap, 2002; Arumugasamy & Cyril, 2017)

CEPHALOPODA	Architeuthis dux	Adux-Big Defensin	-	<i>de novo</i> assembled	(Da Fonseca <i>et al.</i> , 2020)
	Dosidicus gigas	DGExtract ommochrome (skin pigment)	Food spoilage bacteria <i>Lactic acid bacteria</i> <i>Enterobacteriaceae spp.</i> Fungi	Growth inhibition by induction of membrane imbalance	(Esparza-Espinoza <i>et al.</i> , 2021)
	Nautilus pompilius	NpHM4	Gram - bacteria <i>V. alginolyticus</i>	Bactericidal activity by membrane permeabilization	(Yuan <i>et al.</i> , 2022)
	Octopus indicus	AMP	ESKAPE pathogens	-	(Poyil <i>et al.</i> , 2020)
	Octopus (Callistoctopus) minor	Octominin	Gram+ bacteria <i>S. parauberis</i> Viruses Fungi <i>C. albicans</i>	Biofilm inhibition and eradication Cell wall deformation and permeabilization Antibiotic resistance inhibition by DNA-binding Viral plaque reduction Increase of ROS production in target cell Immunomodulatory cells activation	(Nikapitiya <i>et al.</i> , 2020; Thulshan Jayathilaka <i>et al.</i> , 2021; Thulshan Jayathilaka, Nikapitiya, <i>et al.</i> , 2022 ; Dias <i>et al.</i> , 2023)
		Octominin-CNPs	<i>A. baumannii</i> <i>C. albicans</i>	Morphological alterations Membrane permeabilization Biofilm inhibition and eradication	(Thulshan Jayathilaka, Nikapitiya, <i>et al.</i> , 2022)
		Octominin 2	Drug-resistant <i>Candida</i> fungi	Increase of ROS production in target cell Virulence genes suppression <i>In nucleo</i> target DNA - RNA degradation Biofilm inhibition and eradication	(Jayasinghe <i>et al.</i> , 2023)
		Octopromycin	Multidrug-resistant <i>A. baumannii</i>	Strong biofilm inhibition and eradication	(Rajapaksha <i>et al.</i> , 2021)
		Octoprohibitin	Multidrug-resistant	Bactericidal activity by DNA-binding	(Thulshan Jayathilaka, Rajapaksha, <i>et al.</i> , 2022)
		Octoprohibitin-CNPS	<i>A. baumannii</i>	Biofilm inhibition and eradication	

	<i>Octopus ocellatus</i>	OoLyz	Gram± bacteria	Bacteriolysis by cell wall degradation Bacterial challenge induced expression	(H. Li <i>et al.</i> , 2019)
	<i>Octopus sinensis</i>	Os-Big Defensin	-	<i>de novo</i> assembled and BLAST analysis	(Albertin <i>et al.</i> , 2015)
	<i>Octopus vulgaris</i>	OctoPartenopin	Gram± bacteria	Antibiofilm by cell disaggregation Expressed in suckers' tissues, putative role in egg protection	(Maselli <i>et al.</i> , 2020)
		OVExtract ommochrome (skin pigment)	Food spoilage bacteria <i>Lactic acid bacteria</i> <i>Enterobacteriaceae spp.</i> Fungi	Growth inhibition by induction of membrane imbalance	(Esparza-Espinoza <i>et al.</i> , 2021)
	<i>Pterygioteuthis hoylei</i>	Pho-Big Defensin	-	<i>de novo</i> assembled from transcriptome	(Francis <i>et al.</i> , 2017)
	<i>Sepia kobeensis</i>	Cuttlebone chitosan	Gram± bacteria <i>V. alginolyticus</i> <i>V. cholerae</i> <i>V. parahaemolyticus</i> <i>V. vulnificus</i>	Putative membrane disruption and blocking cell wall transports	(Shanmugam <i>et al.</i> , 2016)
	<i>Sepia officinalis</i>	Cuttlebone chitosan	Gram± bacteria Fungi	Putative inhibition of metabolism or membrane disruption	(Hajji <i>et al.</i> , 2015)
	<i>Uroteuthis (Photololigo) duvaucelii</i>	Peptide extracts	Gram± bacteria	-	(Musthafa <i>et al.</i> , 2015)
POLY - PLACOPHORA	<i>Chiton magnificus</i>	Col-Big Defensin	-	<i>de novo</i> assembled	(Riesgo <i>et al.</i> , 2012)

2.4. Chapter References

- Adams, A., and Reeve, L. (1850). The Zoology of the Voyage of HMS Samarang, under the command of Captain Sir Edward Belcher, C.B., F.R.A.S., F.G.S., during the years 1843-1846. Mollusca. *Reeve and Benham*, London, *Smithsonian Libraries and Archives*.
- Addadi, L., Joester, D., Nudelman, F., and Weiner, S. (2006). Mollusk Shell Formation: A Source of New Concepts for Understanding Biomineralization Processes. *Chemistry – A European Journal*, 12(4), 980–987. <https://doi.org/10.1002/chem.200500980>
- Adema, C. M. (2015). Fibrinogen-Related Proteins (FREPs) in Mollusks. In: E. Hsu and L. Du Pasquier (Eds.), Pathogen-Host Interactions: Antigenic Variation v. Somatic Adaptations (pp. 111–129). *Springer International Publishing*. https://doi.org/10.1007/978-3-319-20819-0_5
- Adhya, M., Jeung, H.-D., Kang, H.-S., Choi, K.-S., Lee, D. S., and Cho, M. (2012). Cloning and localization of MCdef, a defensin from Manila clams (*Ruditapes philippinarum*). *Comp. Biochemistry and Physiology Part B: Biochemistry and Molecular Biology*, 161(1), 25–31. <https://doi.org/10.1016/j.cbpb.2011.09.003>
- Ahmad, T. B., Liu, L., Kotiw, M., and Benkendorff, K. (2018). Review of anti-inflammatory, immune-modulatory and wound healing properties of molluscs. *Journal of Ethnopharmacology*, 210, 156–178. <https://doi.org/10.1016/j.jep.2017.08.008>
- Ahyong, S., Boyko, C. B., Bernot, J., Brandão, S. N., Daly, M., De Grave, S., de Voogd, N. J., Gofas, S., Hernandez, F., Hughes, L., Neubauer, T. A., Paulay, G., van der Meij, S., Boydens, B., Decock, W., Dekeyser, S., Goharimanesh, M., Vandepitte, L., Vanhoorne, B., ... Zullini, A. (2024). World Register of Marine Species (WoRMS) [Dataset]. *WoRMS Editorial Board*. Available from <https://www.marinespecies.org> at VLIZ. doi:10.14284/170
- Al-Khalaifah, H. (2022). Cellular and humoral immune response between snail hosts and their parasites. *Frontiers in Immunology*, 13. <https://doi.org/10.3389/fimmu.2022.981314>
- Albertin, C. B., Simakov, O., Mitros, T., Wang, Z. Y., Pungor, J. R., Edsinger-Gonzales, E., Brenner, S., Ragsdale, C. W., and Rokhsar, D. S. (2015). The octopus genome and the evolution of cephalopod neural and morphological novelties. *Nature*, 524(7564), 220–224. <https://doi.org/10.1038/nature14668>
- Aldairi, A. F., Al-Ahmadi, R. A., Al-Hazmi, A., Alsafi, R. T., Bagasi, A., Basfar, G. T., Alsaid, H. M., Alghamdi, A. A., Mujalli, A., Atwah, B., and Ashgar, S. S. (2022). GAG-like Moiety Derived from Marine Mollusks with Antibacterial Activities. *Journal of Research in Medical and Dental Science*, 10(8), 10–15.
- Allam, B., and Raftos, D. (2015). Immune responses to infectious diseases in bivalves. *Journal of Invertebrate Pathology*, 131, 121–136. <https://doi.org/10.1016/j.jip.2015.05.005>
- Arenas, G., Guzmán, F., Cárdenas, C., Mercado, L., and Marshall, S. H. (2009). A novel antifungal peptide designed from the primary structure of a natural antimicrobial peptide purified from *Argopecten purpuratus* hemocytes. *Peptides*, 30(8), 1405–1411. <https://doi.org/10.1016/j.peptides.2009.05.019>
- Arumugasamy, K., and Cyril, R., (2017). Cytotoxicity, antibacterial and antioxidant activities of the tissue extracts of marine gastropod *Hemifusus pugilinus* 792 (Born, 1778). *J Chem Pharmaceut Res.* 9(10): 267- 274.
- Ashour, M., Edrada, R., Ebel, R., Wray, V., Wätjen, W., Padmakumar, K., Müller, W. E. G., Lin, W. H., and Proksch, P. (2006). Kahalalide Derivatives from the Indian Sacoglossan Mollusk *Elysia grandifolia*. *Journal of Natural Products*, 69(11), 1547–1553. <https://doi.org/10.1021/np060172v>
- Bachère, E., Rosa, R. D., Schmitt, P., Poirier, A. C., Merou, N., Charrière, G. M., and Destoumieux-Garzón, D. (2015). The new insights into the oyster antimicrobial defense: Cellular, molecular and genetic view. *Fish and Shellfish Immunology*, 46(1), 50–64. <https://doi.org/10.1016/j.fsi.2015.02.040>
- Bai, C.-M., Xin, L.-S., Rosani, U., Wu, B., Wang, Q.-C., Duan, X.-K., Liu, Z.-H., and Wang, C.-M. (2019). Chromosomal-level assembly of the blood clam, *Scapharca (Anadara) broughtonii*, using long sequence reads and Hi-C. *GigaScience*, 8(7), giz067. <https://doi.org/10.1093/gigascience/giz067>
- Banker, R. M. W., and Sumner, D. Y. (2020). Structure and distribution of chalky deposits in the Pacific oyster using x-ray computed tomography (CT). *Scientific Reports*, 10(1), 12118. <https://doi.org/10.1038/s41598-020-68726-4>
- Bankers, L., Fields, P., McElroy, K. E., Boore, J. L., Logsdon Jr., J. M., and Neiman, M. (2017). Genomic evidence for population-specific responses to co-evolving parasites in a New Zealand freshwater snail. *Molecular Ecology*, 26(14), 3663–3675. <https://doi.org/10.1111/mec.14146>
- Bernaldez-Sarabia, J., Figueroa-Montiel, A., Dueñas, S., Cervantes-Luévano, K., Beltrán, J. A., Ortiz, E., Jiménez, S., Possani, L. D., Paniagua-Solís, J. F., Gonzalez-Canudas, J., and Licea-Navarro, A. (2019). The Diversified O-Superfamily in *Californiconus californicus* Presents a Conotoxin with Antimycobacterial Activity. *Toxins*, 11(2), Article 2. <https://doi.org/10.3390/toxins11020128>
- Bertucci, A., Pierron, F., Thébault, J., Klopp, C., Bellec, J., Gonzalez, P., and Baudrimont, M. (2017). Transcriptomic responses of the endangered freshwater mussel *Margaritifera margaritifera* to trace metal

- contamination in the Dronne River, France. *Environmental Science and Pollution Research*, 24(35), 27145–27159. <https://doi.org/10.1007/s11356-017-0294-6>
- Bieler, R., Mikkelsen, P. M., Collins, T. M., Glover, E. A., González, V. L., Graf, D. L., Harper, E. M., Healy, J., Kawauchi, G. Y., Sharma, P. P., Staubach, S., Strong, E. E., Taylor, J. D., Tëmkin, I., Zardus, J. D., Clark, S., Guzmán, A., McIntyre, E., Sharp, P., and Giribet, G. (2014). Investigating the Bivalve Tree of Life – an exemplar-based approach combining molecular and novel morphological characters. *Invertebrate Systematics*, 28(1), 32–115. <https://doi.org/10.1071/IS13010>
- Biggs, J. S., Rosenfeld, Y., Shai, Y., and Olivera, B. M. (2007). Conolysin-Mt: A Conus Peptide That Disrupts Cellular Membranes. *Biochemistry*, 46(44), 12586–12593. <https://doi.org/10.1021/bi700775p>
- Blundon, J. A., and Kennedy, V. S. (1982). Mechanical and behavioral aspects of blue crab, *Callinectes sapidus* (Rathbun), predation on Chesapeake Bay bivalves. *Journal of Experimental Marine Biology and Ecology*, 65(1), 47–65. [https://doi.org/10.1016/0022-0981\(82\)90175-7](https://doi.org/10.1016/0022-0981(82)90175-7)
- Böhm, C. F., Demmert, B., Harris, J., Fey, T., Marin, F., and Wolf, S. E. (2016). Structural commonalities and deviations in the hierarchical organization of crossed-lamellar shells: A case study on the shell of the bivalve *Glycymeris glycymeris*. *Journal of Materials Research*, 31(5), 536–546. <https://doi.org/10.1557/jmr.2016.46>
- Borquaye, L. S., Darko, G., Ocansey, E., and Ankomah, E. (2015). Antimicrobial and antioxidant properties of the crude peptide extracts of *Galatea paradoxa* and *Patella rustica*. *SpringerPlus*, 4, 500. <https://doi.org/10.1186/s40064-015-1266-2>
- Borquaye, L. S., Darko, G., Oklu, N., Anson-Yevu, C., and Ababio, A. (2016). Antimicrobial and antioxidant activities of ethyl acetate and methanol extracts of *Littorina littorea* and *Galatea paradoxa*. *Cogent Chemistry*, 2(1), 1161865. <https://doi.org/10.1080/23312009.2016.1161865>
- Borrego, J. J., Castro, D., Luque, A., Paillard, C., Maes, P., Garcia, M. T., and Ventosa, A. (1996). *Vibrio tapetis* sp. Nov., the Causative Agent of the Brown Ring Disease Affecting Cultured Clams. *International Journal of Systematic and Evolutionary Microbiology*, 46(2), 480–484. <https://doi.org/10.1099/00207713-46-2-480>
- Bourdeau, P., and Johansson, F. (2012). Predator-induced morphological defences as by-products of prey behaviour: A review and prospectus. *Oikos*, 121, 1175–1190. <https://doi.org/10.2307/23261003>
- Bourel-Bonnet, L., Rao, K. V., Hamann, M. T., and Ganesan, A. (2005). Solid-Phase Total Synthesis of Kahalalide A and Related Analogues. *Journal of Medicinal Chemistry*, 48(5), 1330–1335. <https://doi.org/10.1021/jm049841x>
- Boyden, C. R. (1973). Observations on the shell morphology of two species of cockle *Cerastoderma edule* and *C. glaucum*. *Zoological Journal of the Linnean Society*, 52(4), 269–292. <https://doi.org/10.1111/j.1096-3642.1973.tb01885.x>
- Brock, V., and Christiansen, G. (1989). Evolution of *Cardium* (*Cerastoderma*) *edule*, *C. lamarcki* and *C. glaucum*: Studies of DNA-variation. *Marine Biology*, 102(4), 505–511. <https://doi.org/10.1007/BF00438352>
- Brönmark, C., Lakowitz, T., and Hollander, J. (2011). Predator-Induced Morphological Plasticity Across Local Populations of a Freshwater Snail. *PLOS ONE*, 6(7), e21773. <https://doi.org/10.1371/journal.pone.0021773>
- CIBNor. (2014). Transcriptome of *Crassostrea corteziensis* infected by *Perkinsus marinus* from northwestern Mexico. *Centro de Investigaciones Biológicas del Noroeste (CIBNor)*. Transcriptome or Gene Expression PRJNA237222. <https://www.ncbi.nlm.nih.gov/bioproject/PRJNA237222/>
- Calcino, A. D., de Oliveira, A. L., Simakov, O., Schwaha, T., Zieger, E., Wollesen, T., and Wanninger, A. (2019). The quagga mussel genome and the evolution of freshwater tolerance. *DNA Research*, 26(5), 411–422. <https://doi.org/10.1093/dnares/dsz019>
- Campion, M. (1961). The Structure and Function of the Cutaneous Glands in *Helix aspersa*. *Journal of Cell Science*, s3-102(58), 195–216. <https://doi.org/10.1242/jcs.s3-102.58.195>
- Canesi, L., Grande, C., Pezzati, E., Balbi, T., Vezzulli, L., and Pruzzo, C. (2016). Killing of *Vibrio cholerae* and *Escherichia coli* Strains Carrying D-mannose-sensitive Ligands by *Mytilus* Hemocytes is Promoted by a Multifunctional Hemolymph Serum Protein. *Microbial Ecology*, 72(4), 759–762. <https://doi.org/10.1007/s00248-016-0757-1>
- Canesi, L., and Pruzzo, C. (2016). Specificity of Innate Immunity in Bivalves: A Lesson From Bacteria. In: L. Ballarin and M. Cammarata (Eds.), *Lessons in Immunity* (pp. 79–91). *Academic Press*. <https://doi.org/10.1016/B978-0-12-803252-7.00006-0>
- Carter (ed.), J. G. (1990). Skeletal Biomineralization: Patterns, Processes and Evolutionary Trends. *American Geophysical Union*, Vol. 1, vii-I-832 pp.; Vol. 2 (Atlas and index) v+101 p. <https://link.springer.com/book/9781489953933>
- Cerullo, A. R., McDermott, M. B., Pepi, L. E., Liu, Z.-L., Barry, D., Zhang, S., Yang, X., Chen, X., Azadi, P., Holford, M., and Braunschweig, A. B. (2023). Comparative mucomic analysis of three functionally distinct *Cornu aspersum* Secretions. *Nature Communications*, 14, 5361. <https://doi.org/10.1038/s41467-023-41094-z>

- Chandramathi, V., and Thilaga, R. D. (2018). Identification of bioactive compounds and antibacterial activity of marine gastropod *Conus achatinus* Gmelin, 1791. *International Journal of Advanced Research*, 6(8), 941–948. <https://doi.org/10.21474/IJAR01/7598>
- Charlet, M., Chernysh, S., Philippe, H., Hetru, C., Hoffmann, J. A., and Bulet, P. (1996). Innate immunity. Isolation of several cysteine-rich antimicrobial peptides from the blood of a mollusc, *Mytilus edulis*. *The Journal of Biological Chemistry*, 271(36), 21808–21813. <https://doi.org/10.1074/jbc.271.36.21808>
- Chase, R., Pryer, K., Baker, R., and Madison, D. (1978). Responses to conspecific chemical stimuli in the terrestrial snail *Achatina fulica* (Pulmonata: Sigmurethra). *Behavioral Biology*, 22(3), 302–315. [https://doi.org/10.1016/S0091-6773\(78\)92366-0](https://doi.org/10.1016/S0091-6773(78)92366-0)
- Checa, A. (2000). A new model for periostracum and shell formation in Unionidae (Bivalvia, Mollusca). *Tissue and Cell*, 32(5), 405–416. <https://doi.org/10.1054/tice.2000.0129>
- Checa, A., Harper, E. M., and González-Segura, A. (2018). Structure and crystallography of foliated and chalk shell microstructures of the oyster *Magallana*: The same materials grown under different conditions. *Scientific Reports*, 8(1), 7507. <https://doi.org/10.1038/s41598-018-25923-6>
- Chen, Z.-C., Wu, S.-Y. S., Su, W.-Y., Lin, Y.-C., Lee, Y.-H., Wu, W.-H., Chen, C.-H., and Wen, Z.-H. (2016). Anti-inflammatory and burn injury wound healing properties of the shell of *Haliotis diversicolor*. *BMC Complementary and Alternative Medicine*, 16(1), 487. <https://doi.org/10.1186/s12906-016-1473-6>
- Chen, H., Zha, J., Liang, X., Bu, J., Wang, M., and Wang, Z. (2013). Sequencing and *de novo* Assembly of the Asian Clam (*Corbicula fluminea*) Transcriptome Using the Illumina GAIIx Method. *PLOS ONE*, 8(11), e79516. <https://doi.org/10.1371/journal.pone.0079516>
- Chernikov, O., Kuzmich, A., Chikalovets, I., Molchanova, V., and Hua, K.-F. (2017). Lectin CGL from the sea mussel *Crenomytilus grayanus* induces Burkitt's lymphoma cells death via interaction with surface glycan. *International Journal of Biological Macromolecules*, 104, 508–514. <https://doi.org/10.1016/j.ijbiomac.2017.06.074>
- Cimino, G., De Rosa, S., De Stefano, S., Morrone, R., and Sodano, G. (1985). The chemical defense of nudibranch molluscs: Structure, biosynthetic origin and defensive properties of terpenoids from the dorid nudibranch *Dendrodoris grandiflora*. *Tetrahedron*, 41(6), pages 1093–1100. [https://doi.org/10.1016/S0040-4020\(01\)96477-4](https://doi.org/10.1016/S0040-4020(01)96477-4)
- Cortie, M. (1992). The form, function, and synthesis of the molluscan shell. In: *Spiral Symmetry* (pp. 369–387). *World Scientific*. https://doi.org/10.1142/9789814343084_0019
- Crane, R. L., Diaz Reyes, J. L., and Denny, M. W. (2021). Bivalves rapidly repair shells damaged by fatigue and bolster strength. *Journal of Experimental Biology*, 224(19), jeb242681. <https://doi.org/10.1242/jeb.242681>
- Crippa, G., Griesshaber, E., Checa, A. G., Harper, E. M., Simonet Roda, M., and Schmahl, W. W. (2020a). Orientation patterns of aragonitic crossed-lamellar, fibrous prismatic and myostracal microstructures of modern *Glycymeris* shells. *Journal of Structural Biology*, 212(3), 107653. <https://doi.org/10.1016/j.jsb.2020.107653>
- Crippa, G., Griesshaber, E., Checa, A. G., Harper, E. M., Simonet Roda, M., and Schmahl, W. W. (2020b). SEM, EBSD, laser confocal microscopy and FE-SEM data from modern *Glycymeris* shell layers. *Data in Brief*, 33, 106547. <https://doi.org/10.1016/j.dib.2020.106547>
- Da Fonseca, R. R., Couto, A., Machado, A. M., Brejova, B., Albertin, C. B., Silva, F., Gardner, P., Baril, T., Hayward, A., Campos, A., Ribeiro, Â. M., Barrio-Hernandez, I., Hoving, H.-J., Tafur-Jimenez, R., Chu, C., Frazão, B., Petersen, B., Peñaloza, F., Musacchia, F., ... Gilbert, M. T. P. (2020). A draft genome sequence of the elusive giant squid, *Architeuthis dux*. *GigaScience*, 9(1), giz152. <https://doi.org/10.1093/gigascience/giz152>
- Dang, V. T., Benkendorff, K., Green, T., and Speck, P. (2015). Marine Snails and Slugs: A Great Place To Look for Antiviral Drugs. *Journal of Virology*, 89(16), 8114–8118. <https://doi.org/10.1128/jvi.00287-15>
- Dang, V. T., Benkendorff, K., and Speck, P. (2011). *In vitro* antiviral activity against herpes simplex virus in the abalone *Haliotis laevigata*. *Journal of General Virology*, 92(3), 627–637. <https://doi.org/10.1099/vir.0.025247-0>
- Davies, M. S., and Hawkins, S. J. (1998). Mucus from Marine Molluscs. In: J. H. S. Blaxter, A. J. Southward, and P. A. Tyler (Eds.), *Advances in Marine Biology* (Vol. 34, pp. 1–71). *Academic Press*. [https://doi.org/10.1016/S0065-2881\(08\)60210-2](https://doi.org/10.1016/S0065-2881(08)60210-2)
- Davies, M. S., Hawkins, S. J., and Jones, H. D. (1990). Mucus production and physiological energetics in *Patella vulgata* L. *Journal of Molluscan Studies*, 56(4), 499–503. <https://doi.org/10.1093/mollus/56.4.499>
- De Sousa, J. T., Milan, M., Bargelloni, L., Pualetto, M., Matias, D., Joaquim, S., Matias, A. M., Quillien, V., Leitão, A., and Huvet, A. (2014). A Microarray-Based Analysis of Gametogenesis in Two Portuguese Populations of the European Clam *Ruditapes decussatus*. *PLOS ONE*, 9(3), e92202. <https://doi.org/10.1371/journal.pone.0092202>

- Defer, D., Bourgougnon, N., and Fleury, Y. (2009). Detection and partial characterisation of an antimicrobial peptide (littorein) from the marine gastropod *Littorina littorea*. *International Journal of Antimicrobial Agents*, 34(2), 188–190. <https://doi.org/10.1016/j.ijantimicag.2009.02.016>
- DeMartini, D. G., Errico, J. M., Sjoestroem, S., Fenster, A., and Waite, J. H. (2017). A cohort of new adhesive proteins identified from transcriptomic analysis of mussel foot glands. *Journal of The Royal Society Interface*, 14(131), 20170151. <https://doi.org/10.1098/rsif.2017.0151>
- Derby, C. D. (2007). Escape by inking and secreting: Marine molluscs avoid predators through a rich array of chemicals and mechanisms. *The Biological Bulletin*, 213(3), 274–289. <https://doi.org/10.2307/25066645>
- Destoumieux-Garzón, D., Canesi, L., Oyanedel, D., Travers, M.-A., Charrière, G., Pruzzo, C., Vezzulli, L., Oyanedel, D., Travers, M.-A., Charrière, G., Pruzzo, C., and Vezzulli, L. (2020). *Vibrio*-bivalve interactions in health and disease. *Environmental Microbiology*, 22(10), 4323–4341. <https://doi.org/10.1111/1462-2920.15055>
- Detree, C., Chabenat, A., Lallier, F. H., Satoh, N., Shoguchi, E., Tanguy, A., and Mary, J. (2016). Multiple I-Type Lysozymes in the Hydrothermal Vent Mussel *Bathymodiolus azoricus* and Their Role in Symbiotic Plasticity. *PLOS ONE*, 11(2), e0148988. <https://doi.org/10.1371/journal.pone.0148988>
- Dias, M. K. H. M., Jayathilaka, E. H. T. T., Edirisinghe, S. L., Lim, J.-W., Nikapitiya, C., Kang, S. Y., Whang, I., and De Zoysa, M. (2023). *In-vitro* immunomodulatory responses and antiviral activities of antimicrobial peptide octominin against fish pathogenic viruses. *Fish and Shellfish Immunology*, 142, 109129. <https://doi.org/10.1016/j.fsi.2023.109129>
- Dijkstra, H. H. (1999). Type specimens of Pectinidae (Mollusca: Bivalvia) described by Linnaeus (1758–1771). *Zoological Journal of the Linnean Society*, 125, 383–443.
- Dolashka, P., Moshtanska, V., Borisova, V., Dolashki, A., Stevanovic, S., Dimanov, T., and Voelter, W. (2011). Antimicrobial proline-rich peptides from the hemolymph of marine snail *Rapana venosa*. *Peptides*, 32(7), 1477–1483. <https://doi.org/10.1016/j.peptides.2011.05.001>
- Dolashka, P., Velkova, L., Shishkov, S., Kostova, K., Dolashki, A., Dimitrov, I., Atanasov, B., Devreese, B., Voelter, W., and Van Beeumen, J. (2010). Glycan structures and antiviral effect of the structural subunit RvH2 of *Rapana* hemocyanin. *Carbohydrate Research*, 345(16), 2361–2367. <https://doi.org/10.1016/j.carres.2010.08.005>
- Dutertre, S., Jin, A.-H., Vetter, I., Hamilton, B., Sunagar, K., Lavergne, V., Dutertre, V., Fry, B. G., Antunes, A., Venter, D. J., Alewood, P. F., and Lewis, R. J. (2014). Evolution of separate predation- and defence-evoked venoms in carnivorous cone snails. *Nature Communications*, 5(1), 3521. <https://doi.org/10.1038/ncomms4521>
- Esparza-Espinoza, D. M., Plascencia-Jatomea, M., López-Saiz, C. M., Parra-Vergara, N. V., Carbonell-Barrachina, A. A., Cárdenas-López, J., and Ezquerro-Brauer, J. M. (2021). Improving the shelf life of chicken burgers using *Octopus vulgaris* and *Dosidicus gigas* skin pigment extracts. *Food Science and Technology*, 42, e18221. <https://doi.org/10.1590/fst.18221>
- Figueroa-Montiel, A., Bernáldez, J., Jiménez, S., Ueberhide, B., González, L. J., and Licea-Navarro, A. (2018). Antimycobacterial Activity: A New Pharmacological Target for Conotoxins Found in the First Reported Conotoxin from *Conasprella ximenes*. *Toxins*, 10(2), Article 2. <https://doi.org/10.3390/toxins10020051>
- Fleury, C., Marin, F., Marie, B., Luquet, G., Thomas, J., Josse, C., Serpentin, A., and Lebel, J. M. (2008). Shell repair process in the green ormer *Haliotis tuberculata*: A histological and microstructural study. *Tissue and Cell*, 40(3), 207–218. <https://doi.org/10.1016/j.tice.2007.12.002>
- Francis, W. R., Christianson, L. M., and Haddock, S. H. D. (2017). Symplectin evolved from multiple duplications in bioluminescent squid. *PeerJ*, 5, e3633. <https://doi.org/10.7717/peerj.3633>
- Franzenburg, S., Fraune, S., Altrock, P. M., Künzel, S., Baines, J. F., Traulsen, A., and Bosch, T. C. G. (2013). Bacterial colonization of Hydra hatchlings follows a robust temporal pattern. *The ISME Journal*, 7(4), 781–790. <https://doi.org/10.1038/ismej.2012.156>
- Frémy, M. E. (1855). Recherches chimiques sur les os. *Ann Chim Phys*, 43, 47–107.
- Füllenbach, C. S., Schöne, B. R., Shirai, K., Takahata, N., Ishida, A., and Sano, Y. (2017). Minute co-variations of Sr/Ca ratios and microstructures in the aragonitic shell of *Cerastoderma edule* (Bivalvia) – Are geochemical variations at the ultra-scale masking potential environmental signals? *Geochimica et Cosmochimica Acta*, 205, 256–271. <https://doi.org/10.1016/j.gca.2017.02.019>
- Gao, P., Liao, Z., Wang, X., Bao, L., Fan, M., Li, X., Wu, C., and Xia, S. (2015). Layer-by-Layer Proteomic Analysis of *Mytilus galloprovincialis* Shell. *PLoS ONE*, 10(7), e0133913. <https://doi.org/10.1371/journal.pone.0133913>
- Gasu, E. N., Ahor, H. S., and Borquaye, L. S. (2018). Peptide Extract from *Olivancillaria hiatula* Exhibits Broad-Spectrum Antibacterial Activity. *BioMed Research International*, 2018, 6010572. <https://doi.org/10.1155/2018/6010572>

- Gauna, A., Mercado, L., and Guzmán, F. (2022). Antimicrobial characterization of a titanium coating derived from mussel-glue and *Bothrops asper* snake venom for the prevention of implant-associated infections caused by *Staphylococcus*. *Electronic Journal of Biotechnology*, 56, 31–38. <https://doi.org/10.1016/j.ejbt.2022.02.001>
- Gauri, S. S., Bera, C. K., Bhattacharyya, R., and Mandal, S. M. (2016). Identification of an antimicrobial peptide from large freshwater snail (*Lymnaea stagnalis*): Activity against antibiotics resistant *Staphylococcus epidermidis*. *International Journal of Experimental Research and Review*, 2, 5–9. <https://doi.org/10.52756/ijerr.2016.v2.002>
- Gauri, S. S., Mandal, S. M., Pati, B. R., and Dey, S. (2011). Purification and structural characterization of a novel antibacterial peptide from *Bellamya bengalensis*: Activity against ampicillin and chloramphenicol resistant *Staphylococcus epidermidis*. *Peptides*, 32(4), 691–696. <https://doi.org/10.1016/j.peptides.2011.01.014>
- Genova-Kalou, P., Dundarova, D., Idakieva, K., Mohmmmed, A., Dundarov, S., and Argirova, R. (2008). Anti-Herpes Effect of Hemocyanin Derived from the Mollusk *Rapana thomasiana*. *Zeitschrift Für Naturforschung C*, 63(5–6), 429–434. <https://doi.org/10.1515/znc-2008-5-619>
- Gerdol M, Schmitt P, Venier P, Rocha G, Rosa RD and Destoumieux-Garzón D (2020). Functional insights from the evolutionary diversification of big defensins. *Front. Immunol.* 11:758. doi: 10.3389/fimmu.2020.00758
- Gerdol, M., Puillandre, N., Moro, G. D., Guarnaccia, C., Lucafò, M., Benincasa, M., Zlatev, V., Manfrin, C., Torboli, V., Giulianini, P. G., Sava, G., Venier, P., and Pallavicini, A. (2015). Identification and Characterization of a Novel Family of Cysteine-Rich Peptides (MgCRP-I) from *Mytilus galloprovincialis*. *Genome Biology and Evolution*, 7(8), 2203–2219. <https://doi.org/10.1093/gbe/evv133>
- Gerdol, M., De Moro, G., Manfrin, C., Venier, P., and Pallavicini, A. (2012). Big defensins and mytimacins, new AMP families of the Mediterranean mussel *Mytilus galloprovincialis*. *Developmental and Comparative Immunology*, 36(2), 390–399. <https://doi.org/10.1016/j.dci.2011.08.003>
- Giftson, H., Patterson, J., and Devadason, S. (2014). Antibacterial Activity of the Shell Extracts of Marine Mollusc *Donax faba* against Pathogens. *International Journal of Microbiological Research*, 2(5), 140–143. <https://doi.org/10.5829/idosi.ijmr.2014.5.2.85216>
- Gliński, Z., and Jarosz, J. (1997). Molluscan immune defenses. *Archivum Immunologiae et Therapiae Experimentalis*, 45(2–3), 149–155.
- Glover, E., and Taylor, J. (2010). Needles and pins: Acicular crystalline periostracal calcification in venerid bivalves (*Bivalvia*: Veneridae). *Journal of Molluscan Studies*, 76, 157–179. <https://doi.org/10.1093/mollus/eyp054>
- Gómez-Chiarri, M., Warren, W. C., Guo, X., and Proestou, D. (2015). Developing tools for the study of molluscan immunity: The sequencing of the genome of the eastern oyster, *Crassostrea virginica*. *Fish and Shellfish Immunology*, 46(1), 2–4. <https://doi.org/10.1016/j.fsi.2015.05.004>
- González, V. L., Andrade, S. C. S., Bieler, R., Collins, T. M., Dunn, C. W., Mikkelsen, P. M., Taylor, J. D., and Giribet, G. (2015). A phylogenetic backbone for Bivalvia: An RNA-seq approach. *Proceedings of the Royal Society B: Biological Sciences*, 282(1801), 20142332. <https://doi.org/10.1098/rspb.2014.2332>
- González García, M., Rodríguez, A., Alba, A., Vázquez, A. A., Morales Vicente, F. E., Pérez-Erviti, J., Spellerberg, B., Stenger, S., Grieshaber, M., Conzelmann, C., Münch, J., Raber, H., Kubiczek, D., Rosenau, F., Wiese, S., Ständker, L., and Otero-González, A. (2020). New Antibacterial Peptides from the Freshwater Mollusk *Pomacea poeyana* (Pilsbry, 1927). *Biomolecules*, 10(11), Article 11. <https://doi.org/10.3390/biom10111473>
- Gonzalez, M., Gueguen, Y., Desserre, G., de Lorgeril, J., Romestand, B., and Bachère, E. (2007). Molecular characterization of two isoforms of defensin from hemocytes of the oyster *Crassostrea gigas*. *Developmental and Comparative Immunology*, 31(4), 332–339. <https://doi.org/10.1016/j.dci.2006.07.006>
- Gracey, A., Grimwood, J., Schmutz, J., and Myers, R. M. (2008). *Expressed sequence tags from Mytilus californianus*. [mRNA sequence] *Stanford Univ. School of Medicine, NCBI Nucleotide Database*. <http://www.ncbi.nlm.nih.gov/nuccore/GE761911.1>
- Gray, J. E. (1833). Some Observations on the Economy of Molluscous Animals, and on the Structure of Their Shells. *Philosophical Transactions of the Royal Society of London*, 123, 771–819.
- Greco, S., Gerdol, M., Edomi, P., and Pallavicini, A. (2020). Molecular Diversity of Mytilin-Like Defense Peptides in Mytilidae (Mollusca, Bivalvia). *Antibiotics*, 9(1), Article 1. <https://doi.org/10.3390/antibiotics9010037>
- Greistorfer, S., Klepal, W., Cyran, N., Gugumuck, A., Rudoll, L., Suppan, J., and von Byern, J. (2017). Snail mucus – glandular origin and composition in *Helix pomatia*. *Zoology*, 122, 126–138. <https://doi.org/10.1016/j.zool.2017.05.001>
- Grinchenko, A. V., and Kumeiko, V. V. (2022). Bivalves Humoral Immunity: Key Molecules and Their Functions. *Russian Journal of Marine Biology*, 48(6), 399–417. <https://doi.org/10.1134/S1063074022060062>
- Gueguen, Y., Herpin, A., Aumelas, A., Garnier, J., Fievet, J., Escoubas, J.-M., Bulet, P., Gonzalez, M., Lelong, C., Favrel, P., and Bachère, E. (2006). Characterization of a Defensin from the Oyster *Crassostrea gigas*:

- Recombinant production, folding, solution structure, antimicrobial activities and gene expression. *Journal of Biological Chemistry*, 281(1), 313–323. <https://doi.org/10.1074/jbc.M510850200>
- Gueguen, Y., Romestand, B., Fievet, J., Schmitt, P., Delphine, D., Vandenbulcke, F., Bulet, P., and Bachère, E. (2009). Oyster hemocytes express a proline-rich peptide displaying synergistic antimicrobial activity with a defensin. *Molecular Immunology*, 46(4), 516–522. <https://doi.org/10.1016/j.molimm.2008.07.021>
- Guimarães-Costa, A. B., Nascimento, M. T. C., Wardini, A. B., Pinto-da-Silva, L. H., and Saraiva, E. M. (2012). ETosis: A Microbicidal Mechanism beyond Cell Death. *Journal of Parasitology Research*, 2012, 929743. <https://doi.org/10.1155/2012/929743>
- Hajji, S., Younes, I., Rinaudo, M., Jellouli, K., and Nasri, M. (2015). Characterization and *in vitro* Evaluation of Cytotoxicity, Antimicrobial and Antioxidant Activities of Chitosans Extracted from Three Different Marine Sources. *Applied Biochemistry and Biotechnology*, 177(1), 18–35. <https://doi.org/10.1007/s12010-015-1724-x>
- Han, Y., Hu, G., Chen, Y., Chen, L., Yu, D., Zhang, Q., and Yang, D. (2021). Antimicrobial Defensin and DNA Traps in Manila Clam *Ruditapes philippinarum*: Implications for Their Roles in Immune Responses. *Frontiers in Marine Science*, 8. <https://doi.org/10.3389/fmars.2021.690879>
- Harney, E., Dubief, B., Boudry, P., Basuyaux, O., Schilhabel, M. B., Huchette, S., Paillard, C., and Nunes, F. L. D. (2016). *De novo* assembly and annotation of the European abalone *Haliotis tuberculata* transcriptome. *Marine Genomics*, 28, 11–16. <https://doi.org/10.1016/j.margen.2016.03.002>
- Hasan, I., Gerdol, M., Fujii, Y., Rajia, S., Koide, Y., Yamamoto, D., Kawsar, S. M. A., and Ozeki, Y. (2016). cDNA and Gene Structure of MytiLec-1, A Bacteriostatic R-Type Lectin from the Mediterranean Mussel (*Mytilus galloprovincialis*). *Marine Drugs*, 14(5), Article 5. <https://doi.org/10.3390/md14050092>
- Hasan, I., Sugawara, S., Fujii, Y., Koide, Y., Terada, D., Iimura, N., Fujiwara, T., Takahashi, K. G., Kojima, N., Rajia, S., Kawsar, S. M. A., Kanaly, R. A., Uchiyama, H., Hosono, M., Ogawa, Y., Fujita, H., Hamako, J., Matsui, T., and Ozeki, Y. (2015). MytiLec, a Mussel R-Type Lectin, Interacts with Surface Glycan Gb3 on Burkitt's Lymphoma Cells to Trigger Apoptosis through Multiple Pathways. *Marine Drugs*, 13(12), Article 12. <https://doi.org/10.3390/md13127071>
- He, J., Liang, H., Zhu, J., and Fang, X. (2019). Separation, identification and gene expression analysis of PmAMP-1 from *Pinctada fucata martensii*. *Fish and Shellfish Immunology*, 92, 728–735. <https://doi.org/10.1016/j.fsi.2019.07.002>
- Hemu, X., and Tam, J. P. (2017). Macrocyclic Antimicrobial Peptides Engineered from ω -Conotoxin. *Current Pharmaceutical Design*, 23(14), 2131–2138. <https://doi.org/10.2174/1381612822666161027120518>
- Henry, J. Q., Lesoway, M. P., Perry, K. J., Osborne, C. C., Shankland, M., and Lyons, D. C. (2017). Beyond the sea: *Crepidula atrasolea* as a spiralian model system. *The International Journal of Developmental Biology*, 61(8–9), Article 8–9. <https://doi.org/10.1387/ijdb.170110jh>
- Huber, M. (2010). Compendium of bivalves. A full-color guide to 3,300 of the World's Marine Bivalves. A status on Bivalvia after 250 years of research. In: Huber, M. (2010). Compendium of bivalves. A full-color guide to 3,300 of the World's Marine Bivalves. A status on Bivalvia after 250 years of research. *Hackenheim D: ConchBooks*. <https://www.zora.uzh.ch/id/eprint/35871/>
- Hubert, F., Noël, T., and Roch, P. (1996). A Member of the Arthropod Defensin Family from Edible Mediterranean Mussels (*Mytilus galloprovincialis*). *European Journal of Biochemistry*, 240(1), 302–306. <https://doi.org/10.1111/j.1432-1033.1996.0302h.x>
- Iijima, R., Kisugi, J., and Yamazaki, M. (2003). A novel antimicrobial peptide from the sea hare *Dolabella auricularia*. *Developmental and Comparative Immunology*, 27(4), 305–311. [https://doi.org/10.1016/S0145-305X\(02\)00105-2](https://doi.org/10.1016/S0145-305X(02)00105-2)
- Immanuel, G., Thaddaeus, B. J., Usha, M., Ramasubburayan, R., Prakash, S., and Palavesam, A. (2012). Antipyretic, wound healing and antimicrobial activity of processed shell of the marine mollusc *Cypraea moneta*. *Asian Pacific Journal of Tropical Biomedicine*, 2(3, Supplement), S1643–S1646. [https://doi.org/10.1016/S2221-1691\(12\)60469-9](https://doi.org/10.1016/S2221-1691(12)60469-9)
- Irie, T., and Iwasa, Y. (2005). Optimal Growth Pattern of Defensive Organs: The Diversity of Shell Growth among Mollusks. *The American Naturalist*, 165(2), 238–249. <https://doi.org/10.1086/427157>
- Itoh, N., Okada, Y., Takahashi, K. G., and Osada, M. (2010). Presence and characterization of multiple mantle lysozymes in the Pacific oyster, *Crassostrea gigas*. *Fish and Shellfish Immunology*, 29(1), 126–135. <https://doi.org/10.1016/j.fsi.2010.02.027>
- Ivanina, A. V., Falfushynska, H. I., Beniash, E., Piontkivska, H., and Sokolova, I. M. (2017). Biomineralization-related specialization of hemocytes and mantle tissues of the Pacific oyster *Crassostrea gigas*. *The Journal of Experimental Biology*, 220(Pt 18), 3209–3221. <https://doi.org/10.1242/jeb.160861>
- Iwamoto, M., Ueyama, D., and Kobayashi, R. (2014). The advantage of mucus for adhesive locomotion in gastropods. *Journal of Theoretical Biology*, 353, 133–141. <https://doi.org/10.1016/j.jtbi.2014.02.024>

- Jackson, A. P., Vincent, J. F. V., Turner, R. M., and Alexander, R. M. (1988). The mechanical design of nacre. *Proceedings of the Royal Society of London. Series B. Biological Sciences*, 234(1277), 415–440. <https://doi.org/10.1098/rspb.1988.0056>
- Jakób, M., Lubkowski, J., O’Keefe, B. R., and Wlodawer, A. (2015). Structure of a lectin from the sea mussel *Crenomytilus grayanus* (CGL). *Acta Crystallographica. Section F, Structural Biology Communications*, 71(Pt 11), 1429–1436. <https://doi.org/10.1107/S2053230X15019858>
- Jayasinghe, J. N. C., Whang, I., and De Zoysa, M. (2023). Antifungal Efficacy of Antimicrobial Peptide Octominin II against *Candida albicans*. *International Journal of Molecular Sciences*, 24(18), Article 18. <https://doi.org/10.3390/ijms241814053>
- Jelesias, J. I. P., and Navarro, R. (1990). Shell growth of the cockle *Cerastoderma edule* in the Mundaca estuary (North Spain). *Journal of Molluscan Studies*, 56(2), 10. <https://doi.org/10.1093/mollus/56.2.229>
- Jenny, M. J., Warr, G. W., Gross, P. S., Almeida, J. S., Chen, Y., McKillen, D. J., Wu, S., and Chapman, R. W. (2011). Hepatopancreas *Crassostrea virginica* cDNA, mRNA sequence (51567664); cDNA, mRNA Sequence CV088315.1). *NCBI Nucleotide Database*. <http://www.ncbi.nlm.nih.gov/nuccore/CV088315.1>
- Jia, Z., Zhang, H., Jiang, S., Wang, M., Wang, L., and Song, L. (2016). Comparative study of two single CRD C-type lectins, CgCLec-4 and CgCLec-5, from pacific oyster *Crassostrea gigas*. *Fish and Shellfish Immunology*, 59, 220–232. <https://doi.org/10.1016/j.fsi.2016.10.030>
- Jiang, J.-Z., Zhang, W., Guo, Z.-X., Cai, C.-C., Su, Y.-L., Wang, R.-X., and Wang, J.-Y. (2011). Functional annotation of an expressed sequence tag library from *Haliotis diversicolor* and analysis of its plant-like sequences. *Marine Genomics*, 4(3), 189–196. <https://doi.org/10.1016/j.margen.2011.05.001>
- Johnson, E. H. (2020). Experimental tests of bivalve shell shape reveal potential tradeoffs between mechanical and behavioral defenses. *Scientific Reports*, 10(1), 19425. <https://doi.org/10.1038/s41598-020-76358-x>
- Kenny, N. J., McCarthy, S. A., Dudchenko, O., James, K., Betteridge, E., Corton, C., Dolucan, J., Mead, D., Oliver, K., Omer, A. D., Pelan, S., Ryan, Y., Sims, Y., Skelton, J., Smith, M., Torrance, J., Weisz, D., Wipat, A., Aiden, E. L., ... Williams, S. T. (2020). The gene-rich genome of the scallop *Pecten maximus*. *GigaScience*, 9(5), g1aa037. <https://doi.org/10.1093/gigascience/g1aa037>
- Kniprath, E. (1981). Ontogeny of the Molluscan Shell Field: A Review. *Zoologica Scripta*, 10(1), 61–79. <https://doi.org/10.1111/j.1463-6409.1981.tb00485.x>
- Krepstakies, M., Lucifora, J., Nagel, C.-H., Zeisel, M. B., Holstermann, B., Hohenberg, H., Kowalski, I., Gutsmann, T., Baumert, T. F., Brandenburg, K., Hauber, J., and Protzer, U. (2012). A New Class of Synthetic Peptide Inhibitors Blocks Attachment and Entry of Human Pathogenic Viruses. *The Journal of Infectious Diseases*, 205(11), 1654–1664. <https://doi.org/10.1093/infdis/jis273>
- Kwon, S., Bosmans, F., Kaas, Q., Cheneval, O., Conibear, A. C., Rosengren, K. J., Wang, C. K., Schroeder, C. I., and Craik, D. J. (2016). Efficient enzymatic cyclization of an inhibitory cystine knot-containing peptide. *Biotechnology and Bioengineering*, 113(10), 2202–2212. <https://doi.org/10.1002/bit.25993>
- Lamarck, J.-B.-P.-A. de M. de. (1819). Histoire naturelle des animaux sans vertèbres ... Précédée d’une introduction offrant la détermination des caractères essentiels de l’animal, sa distinction du végétal et des autres corps naturels, enfin, l’exposition des principes fondamentaux de la zoologie. *Verdière*, Vol. 6 : pt.1-2 (1819-1822), pp. 1–598. <https://doi.org/10.5962/bhl.title.12712>
- Larvor, H., Cuif, J. P., Devauchelle, N., Dauphin, Denis, A., Gautret, P., and Marin, F. (1996). Development of a brown internal coloration in the scallop shell (*Pecten maximus*): Study of microstructural characteristics and analyses of crystal organic matrices. *Bulletin de l’Institut Océanographique, Monaco*, 14(4), 171–182.
- Lee, T.-G., and Maruyama, S. (1998). Isolation of HIV-1 Protease-Inhibiting Peptides from Thermolysin Hydrolysate of Oyster Proteins. *Biochemical and Biophysical Research Communications*, 253(3), 604–608. <https://doi.org/10.1006/bbrc.1998.9824>
- Lee, Y., Kasthuri, S. R., Lee, S., Whang, I., Oh, C., Kang, D.-H., Shin, G.-W., Lee, J., and Zoysa, M. D. (2014). First molluscan antimicrobial peptide hydramacin in Manila clam: Molecular characterization and expression analysis. *Journal of Coastal Life Medicine*, 2(6), 447–452. <https://doi.org/10.12980/JCLM.2.201414J6>
- Lee, Y. S., Jeong, J. E., Hwang, H. J., Kang, S. W., and Lee, J. S. (2015). *Meretrix lusoria* whole body cDNA library (754314217) [mRNA sequence]. *Inje Univ. Col. of Medicine, Dpt. of Parasitology, NCBI Nucleotide Database*. <http://www.ncbi.nlm.nih.gov/nuccore/FY999568.1>
- Leonard, G. H., Bertness, M. D., and Yund, P. O. (1999). Crab Predation, Waterborne Cues, and Inducible Defenses in the Blue Mussel, *Mytilus edulis*. *Ecology*, 80(1), 1–14. <https://doi.org/10.2307/176976>
- Leoni, G., De Poli, A., Mardirossian, M., Gambato, S., Florian, F., Venier, P., Wilson, D. N., Tossi, A., Pallavicini, A., and Gerdol, M. (2017). Myticalins: A Novel Multigenic Family of Linear, Cationic Antimicrobial Peptides from Marine Mussels (*Mytilus* spp.). *Marine Drugs*, 15(8), Article 8. <https://doi.org/10.3390/md15080261>

- Leung, P. T., Ip, J. C., Mak, S. S., Qiu, J. W., Lam, P. K., Wong, C. K., Chan, L. L., and Leung, K. M. (2014). De novo transcriptome analysis of *Perna viridis* highlights tissue-specific patterns for environmental studies. *BMC Genomics*, 15(1), 804. <https://doi.org/10.1186/1471-2164-15-804>
- Levi-Kalisman, Y., Falini, G., Addadi, L., and Weiner, S. (2001). Structure of the Nacreous Organic Matrix of a Bivalve Mollusk Shell Examined in the Hydrated State Using Cryo-TEM. *Journal of Structural Biology*, 135(1), 8–17. <https://doi.org/10.1006/jsbi.2001.4372>
- Li, C. P., Prescott, B., Eddy, B., Caldes, G., Green, W. R., Martino, E. C., and Young, A. M. (1965). Antiviral Activity of Paolins from Clams. *Annals of the New York Academy of Sciences*, 130(1), 374–382. <https://doi.org/10.1111/j.1749-6632.1965.tb12571.x>
- Li, C. P., Prescott, B., Jahnes, W. G., and Martino, E. C. (1962). Antimicrobial Agents from Mollusks. *Transactions of the New York Academy of Sciences*, 24(5 Series II), 504–509. <https://doi.org/10.1111/j.2164-0947.1962.tb01427.x>
- Li, H., Wei, X., Yang, J., Zhang, R., Zhang, Q., and Yang, J. (2019). The bacteriolytic mechanism of an invertebrate-type lysozyme from mollusk *Octopus ocellatus*. *Fish and Shellfish Immunology*, 93, 232–239. <https://doi.org/10.1016/j.fsi.2019.07.060>
- Li, M., Zhu, L., Zhou, C., Sun, S., Fan, Y., and Zhuang, Z. (2012). Molecular characterization and expression of a novel big defensin (*Sb-BDef1*) from ark shell, *Scapharca broughtonii*. *Fish and Shellfish Immunology*, 33(5), 1167–1173. <https://doi.org/10.1016/j.fsi.2012.09.008>
- Li, R., Huang, Y., Peng, C., Gao, Z., Liu, J., Yin, X., Gao, B., Ovchinnikova, T. V., Qiu, L., Bian, C., and Shi, Q. (2022). High-throughput prediction and characterization of antimicrobial peptides from multi-omics datasets of Chinese tubular cone snail (*Conus betulinus*). *Frontiers in Marine Science*, 9. <https://doi.org/10.3389/fmars.2022.1092731>
- Li, Z., Yuan, Y., Meng, M., Li, S., Deng, B., and Wang, Y. (2020). The transcriptome analysis of the whole-body of the gastropod mollusk *Limax flavus* and screening of putative antimicrobial peptide and protein genes. *Genomics*, 112(6), 3991–3999. <https://doi.org/10.1016/j.ygeno.2020.06.046>
- Liang, S. M., Ji, H. M., and Li, X. W. (2021). A high-strength and high-toughness nacreous structure in a deep-sea *Nautilus* shell: Critical role of platelet geometry and organic matrix. *Journal of Materials Science and Technology*, 88, 189–202. <https://doi.org/10.1016/j.jmst.2021.01.082>
- Liao, Z., Wang, X., Liu, H., Fan, M., Sun, J., and Shen, W. (2013). Molecular characterization of a novel antimicrobial peptide from *Mytilus coruscus*. *Fish and Shellfish Immunology*, 34(2), 610–616. <https://doi.org/10.1016/j.fsi.2012.11.030>
- Linné, C. von, Linné, C. von, and Salvius, L. (1758). *Caroli Linnaei...Systema naturae per regna tria naturae: secundum classes, ordines, genera, species, cum characteribus, differentiis, synonymis. Impensis Direct. Laurentii Salvii*, Vol. v.1 pp. 1–847. <https://doi.org/10.5962/bhl.title.542>
- Liu, C., Zhang, Y., Ren, Y., Wang, H., Li, S., Jiang, F., Yin, L., Qiao, X., Zhang, G., Qian, W., Liu, B., and Fan, W. (2018). The genome of the golden apple snail *Pomacea canaliculata* provides insight into stress tolerance and invasive adaptation. *GigaScience*, 7(9), giy101. <https://doi.org/10.1093/gigascience/giy101>
- Liu, H., Fan, M., Liu, H., Qi, P., and Zhi, L. (2019). Production and Function of Different Regions from Mytichitin-1 of *Mytilus coruscus*. *Fish and Shellfish Immunology*, 84, 1018–1029. <https://doi.org/10.1016/j.fsi.2018.10.081>
- Liu, W., Li, W., He, C., Gao, X., Li, Y., Bao, X., Sun, F., Fu, L., Geng, H., Liu, Y., Liu, X., Wang, J., and Zhu, D. (2009). Analysis of Expressed Sequence Tags from mantle and kidney of Japanese scallop (*Mizuhopecten yessoensis*). [cDNA Library, mRNA Sequence GH736001.1] *Liaoning Ocean and Fisheries Science Research Inst., NCBI Nucleotide Database*. <http://www.ncbi.nlm.nih.gov/nuccore/GH736001.1>
- Liu, Z., Dong, S., Xu, J., Zeng, M., Song, H., and Zhao, Y. (2008). Production of cysteine-rich antimicrobial peptide by digestion of oyster (*Crassostrea gigas*) with alcalase and bromelin. *Food Control*, 19(3), 231–235. <https://doi.org/10.1016/j.foodcont.2007.03.004>
- Löfgren, S. E., Miletti, L. C., Steindel, M., Bachère, E., and Barracco, M. A. (2008). Trypanocidal and leishmanicidal activities of different antimicrobial peptides (AMPs) isolated from aquatic animals. *Experimental Parasitology*, 118(2), 197–202. <https://doi.org/10.1016/j.exppara.2007.07.011>
- López-Abarrategui, C., Alba, A., Lima, L. A., Maria-Neto, S., Vasconcelos, I. M., Oliveira, J. T. A., Dias, S. C., Otero-Gonzalez, A. J., and Franco, O. L. (2012). Screening of Antimicrobials from Caribbean Sea Animals and Isolation of Bactericidal Proteins from the Littoral Mollusk *Cenchrithis muricatus*. *Current Microbiology*, 64(5), 501–505. <https://doi.org/10.1007/s00284-012-0096-5>
- López-Abarrategui, C., Alba, A., Silva, O. N., Reyes-Acosta, O., Vasconcelos, I. M., Oliveira, J. T. A., Migliolo, L., Costa, M. P., Costa, C. R., Silva, M. R. R., Garay, H. E., Dias, S. C., Franco, O. L., and Otero-González, A. J. (2012). Functional characterization of a synthetic hydrophilic antifungal peptide derived from the marine snail *Cenchrithis muricatus*. *Biochimie*, 94(4), 968–974. <https://doi.org/10.1016/j.biochi.2011.12.016>

- López-Abarrategui, C., McBeth, C., Mandal, S. M., Sun, Z. J., Heffron, G., Alba-Menéndez, A., Migliolo, L., Reyes-Acosta, O., García-Villarino, M., Nolasco, D. O., Falcão, R., Cherobim, M. D., Dias, S. C., Brandt, W., Wessjohann, L., Starnbach, M., Franco, O. L., and Otero-González, A. J. (2015). Cm-p5: An antifungal hydrophilic peptide derived from the coastal mollusk *Cenchritis muricatus* (Gastropoda: Littorinidae). *The FASEB Journal*, 29(8), 3315–3325. <https://doi.org/10.1096/fj.14-269860>
- Loth, K., Vergnes, A., Barreto, C., Voisin, S. N., Meudal, H., Da Silva, J., Bressan, A., Belmadi, N., Bachère, E., Aucagne, V., Cazevielle, C., Marchandin, H., Rosa, R. D., Bulet, P., Touqui, L., Delmas, A. F., and Destoumieux-Garçon, D. (2019). The Ancestral N-Terminal Domain of Big Defensins Drives Bacterially Triggered Assembly into Antimicrobial Nanonets. *mBio*, 10(5), 10.1128/mbio.01821-19. <https://doi.org/10.1128/mbio.01821-19>
- Lowell, R. B. (1984). Desiccation of intertidal limpets: Effects of shell size, fit to substratum, and shape. *Journal of Experimental Marine Biology and Ecology*, 77(3), 197–207. [https://doi.org/10.1016/0022-0981\(84\)90120-5](https://doi.org/10.1016/0022-0981(84)90120-5)
- Lowenstam, H. A., Weiner, S., Lowenstam, H. A., and Weiner, S. (1989). On Biomineralization. *Oxford University Press*, 336p.
- Luk'yanov, P. A., Chernikov, O. V., Kobelev, S. S., Chikalovets, I. V., Molchanova, V. I., and Li, W. (2007). Carbohydrate-binding proteins of marine invertebrates. *Russian Journal of Bioorganic Chemistry*, 33(1), 161–169. <https://doi.org/10.1134/S1068162007010190>
- Lv, C., Han, Y., Yang, D., Zhao, J., Wang, C., and Mu, C. (2020). Antibacterial activities and mechanisms of action of a defensin from manila clam *Ruditapes philippinarum*. *Fish and Shellfish Immunology*, 103, 266–276. <https://doi.org/10.1016/j.fsi.2020.05.025>
- Lv, J., Zhao, J., Yang, D., Wu, H., and Cong, M. (2019). Tissue distribution and functional characterization of mytimacin-4 in *Mytilus galloprovincialis*. *Journal of Invertebrate Pathology*, 166, 107215. <https://doi.org/10.1016/j.jip.2019.107215>
- Maia, F., Barroso, C. M., and Gaspar, M. B. (2021). Biology of the common cockle *Cerastoderma edule* (Linnaeus, 1758) in Ria de Aveiro (NW Portugal): Implications for fisheries management. *Journal of Sea Research*, 171, 102024. <https://doi.org/10.1016/j.seares.2021.102024>
- Mao, F., Bao, Y., Wong, N.-K., Huang, M., Liu, K., Zhang, X., Yang, Z., Yi, W., Shu, X., Xiang, Z., Yu, Z., and Zhang, Y. (2021). Large-Scale Plasma Peptidomic Profiling Reveals a Novel, Nontoxic, *Crassostrea hongkongensis*-Derived Antimicrobial Peptide against Foodborne Pathogens. *Marine Drugs*, 19(8), Article 8. <https://doi.org/10.3390/md19080420>
- Marin, F. (2020). Mollusc shellomes: Past, present and future. *Journal of Structural Biology*, 212(1), 107583. <https://doi.org/10.1016/j.jsb.2020.107583>
- Marin, F., Le Roy, N., and Marie, B. (2012). The formation and mineralization of mollusk shell. *Frontiers in Bioscience (Scholar Edition)*, 4, 1099–1125.
- Marin, F., Luquet, G., Marie, B., and Medakovic, D. (2008). Molluscan Shell Proteins: Primary Structure, Origin, and Evolution. *Curr. Top. Dev. Biol.*, 80, 209–276. [https://doi.org/10.1016/S0070-2153\(07\)80006-8](https://doi.org/10.1016/S0070-2153(07)80006-8)
- Marin, F., Marie, B., Hamada, S., Ramos-Silva, P., Le Roy, N., Guichard, N., Wolf, S., Montagnani, C., Joubert, C., Piquemal, D., Saulnier, D., and Gueguen, Y. (2013). “Shellome”: Proteins Involved in Mollusc Shell Biomineralization —Diversity, Functions. In *Recent Advances in Pearl Research* (pp. 149–166).
- Maselli, V., Galdiero, E., Salzano, A. M., Scaloni, A., Maione, A., Falanga, A., Naviglio, D., Guida, M., Di Cosmo, A., and Galdiero, S. (2020). OctoPartenopin: Identification and Preliminary Characterization of a Novel Antimicrobial Peptide from the Suckers of *Octopus vulgaris*. *Marine Drugs*, 18(8), Article 8. <https://doi.org/10.3390/md18080380>
- Matsumoto, T., Nakamura, A. M., and Takahashi, K. G. (2006). Cloning of cDNAs and hybridization analysis of lysozymes from two oyster species, *Crassostrea gigas* and *Ostrea edulis*. *Comparative Biochemistry and Physiology Part B: Biochemistry and Molecular Biology*, 145(3), 325–330. <https://doi.org/10.1016/j.cbpb.2006.08.003>
- McDougall, C. (2018). Comparative *de novo* transcriptome analysis of the Australian black-lip and Sydney rock oysters reveals expansion of repetitive elements in *Saccostrea* genomes. *PLOS ONE*, 13(10), e0206417. <https://doi.org/10.1371/journal.pone.0206417>
- Mendes da Costa, E., Mendes da Costa, E., Elmsley, P., Millan, J., Robson, J., and White, B. (1778). *Historia naturalis testaceorum Britanniae, or, The British conchology: Containing the descriptions and other particulars of natural history of the shells of Great Britain and Ireland: illustrated with figures, in English and in French.* Printed for the author, and sold by Millan, B. White, Elmsley, and Robson, 322p. <https://doi.org/10.5962/bhl.title.13179>
- Meng, D.-M., Lv, Y.-J., Zhao, J.-F., Liu, Q.-Y., Shi, L.-Y., Wang, J.-P., Yang, Y.-H., and Fan, Z.-C. (2018). Efficient production of a recombinant *Venerupis philippinarum* defensin (VpDef) in *Pichia pastoris* and characterization of its antibacterial activity and stability. *Protein Expression and Purification*, 147, 78–84. <https://doi.org/10.1016/j.pep.2018.03.001>

- Mikkelsen, P. M., Bieler, R., Kappner, I., and Rawlings, T. A. (2006). Phylogeny of Veneroidea (Mollusca: Bivalvia) based on morphology and molecules. *Zoological Journal of the Linnean Society*, 148(3), 439–521. <https://doi.org/10.1111/j.1096-3642.2006.00262.x>
- Milan, M., Smits, M., Dalla Rovere, G., Iori, S., Zampieri, A., Carraro, L., Martino, C., Papetti, C., Ianni, A., Ferri, N., Iannaccone, M., Patarnello, T., Brunetta, R., Ciofi, C., Grotta, L., Arcangeli, G., Bargelloni, L., Cardazzo, B., and Martino, G. (2019). Host-microbiota interactions shed light on mortality events in the striped venus clam *Chamelea gallina*. *Molecular Ecology*, 28(19), 4486–4499. <https://doi.org/10.1111/mec.15227>
- Milano, S., Schöne, B. R., and Witbaard, R. (2017). Changes of shell microstructural characteristics of *Cerastoderma edule* (Bivalvia)—A novel proxy for water temperature. *Palaeogeography, Palaeoclimatology, Palaeoecology*, 465, 395–406. <https://doi.org/10.1016/j.palaeo.2015.09.051>
- Milbury, C. A., and Gaffney, P. M. (2005). Complete Mitochondrial DNA Sequence of the Eastern Oyster *Crassostrea virginica*. *Marine Biotechnology*, 7(6), 697–712. <https://doi.org/10.1007/s10126-005-0004-0>
- Mitta, G., Hubert, F., Dyrzynda, E. A., Boudry, P., and Roch, P. (2000). Mytilin B and MGD2, two antimicrobial peptides of marine mussels: Gene structure and expression analysis. *Developmental and Comparative Immunology*, 24(4), 381–393. [https://doi.org/10.1016/S0145-305X\(99\)00084-1](https://doi.org/10.1016/S0145-305X(99)00084-1)
- Mitta, G., Hubert, F., Noël, T., and Roch, P. (1999). Myticin, a novel cysteine-rich antimicrobial peptide isolated from haemocytes and plasma of the mussel *Mytilus galloprovincialis*. *European Journal of Biochemistry*, 265(1), 71–78. <https://doi.org/10.1046/j.1432-1327.1999.00654.x>
- Mitta, G., Vandenbulcke, F., Hubert, F., and Roch, P. (1999). Mussel defensins are synthesised and processed in granulocytes then released into the plasma after bacterial challenge. *Journal of Cell Science*, 112(23), 4233–4242. <https://doi.org/10.1242/jcs.112.23.4233>
- Mitta, G., Vandenbulcke, F., Hubert, F., Salzet, M., and Roch, P. (2000). Involvement of Mytilins in Mussel Antimicrobial Defense *. *Journal of Biological Chemistry*, 275(17), 12954–12962. <https://doi.org/10.1074/jbc.275.17.12954>
- MolluscaBase eds. (2024). *MolluscaBase*. [Dataset]. <https://doi.org/doi:10.14284/448>
- Moro, G., Buonocore, F., Barucca, M., Spazzali, F., Canapa, A., Pallavicini, A., Scapigliati, G., and Gerdol, M. (2019). The first transcriptomic resource for the Antarctic scallop *Adamussium colbecki*. *Marine Genomics*, 44, 61–64. <https://doi.org/10.1016/j.margen.2018.09.007>
- Morton, B., Peharda, M., and Petrić, M. (2011). Functional morphology of *Roccellaria dubia* (Bivalvia: Gastrochaenidae) with new interpretations of crypt formation and adventitious tube construction, and a discussion of evolution within the family. *Biological Journal of the Linnean Society*, 104(4), 786–804. <https://doi.org/10.1111/j.1095-8312.2011.01763.x>
- Mount, A. S., Wheeler, A. P., Paradkar, R. P., and Snider, D. (2004). Hemocyte-Mediated Shell Mineralization in the Eastern Oyster. *Science*, 304(5668), 297–300. <https://doi.org/10.1126/science.1090506>
- Mu, G., Duan, F., Zhang, G., Li, X., Ding, X., and Zhang, L. (2018). Microstructure and mechanical property of *Ruditapes philippinarum* shell. *Journal of the Mechanical Behavior of Biomedical Materials*, 85, 209–217. <https://doi.org/10.1016/j.jmbbm.2018.06.012>
- Musthafa, M., Narayanan, S., Karuppiah, P., and Raja, S. (2015). Bioactive peptides from *Loligo duvauceli* (Indian marine squid) orbigny against multi drug resistant clinical pathogens. *South Indian Journal of Biological Sciences*, 2015, 24–29. <https://doi.org/10.22205/sijbs/2015/v1/i1/100438>
- Nam, B.-H., Moon, J. Y., Park, E. H., Kong, H. J., Kim, Y.-O., Kim, D.-G., Kim, W.-J., An, C. M., and Seo, J.-K. (2016). Antimicrobial and Antitumor Activities of Novel Peptides Derived from the Lipopolysaccharide- and β -1,3-Glucan Binding Protein of the Pacific Abalone *Haliotis discus hannai*. *Marine Drugs*, 14(12), Article 12. <https://doi.org/10.3390/md14120227>
- Nam, B.-H., Seo, J.-K., Lee, M. J., Kim, Y.-O., Kim, D.-G., An, C. M., and Park, N. G. (2015). Functional analysis of Pacific oyster (*Crassostrea gigas*) β -thymosin: Focus on antimicrobial activity. *Fish and Shellfish Immunology*, 45(1), 167–174. <https://doi.org/10.1016/j.fsi.2015.03.035>
- Nesterova, N. V., Zagorodnya, S. D., Moshanska, V., Dolashka, P., Baranova, G. V., Golovan, A. V., and Kurova, A. O. (2011). Antiviral Activity of Hemocyanin Isolated from Marine Snail *Rapana venosa*. *Antiviral Research*, 90(2), A38. <https://doi.org/10.1016/j.antiviral.2011.03.052>
- Nikapitiya, C., Dananjaya, S. H. S., Chandrarathna, H. P. S. U., De Zoysa, M., and Whang, I. (2020). Octominin: A Novel Synthetic Anticandidal Peptide Derived from Defense Protein of *Octopus minor*. *Marine Drugs*, 18(1), Article 1. <https://doi.org/10.3390/md18010056>
- Nolf, F., and Swinnen, F. (2013). The Glycymerididae (Mollusca: Bivalvia) of the NE Atlantic and the Mediterranean Sea. *Neptunea*, 12(3), 35.
- Novoa, B., Romero, A., Álvarez, Á. L., Moreira, R., Pereiro, P., Costa, M. M., Dios, S., Estepa, A., Parra, F., and Figueras, A. (2016). Antiviral Activity of Myticin C Peptide from Mussel: An Ancient Defense against Herpesviruses. *Journal of Virology*, 90(17), 7692–7702. <https://doi.org/10.1128/jvi.00591-16>

- Nudelman, F., Gotliv, B. A., Addadi, L., and Weiner, S. (2006). Mollusk shell formation: Mapping the distribution of organic matrix components underlying a single aragonitic tablet in nacre. *Journal of Structural Biology*, 153(2), 176–187. <https://doi.org/10.1016/j.jsb.2005.09.009>
- Núñez-Acuña, G., Tapia, F. J., Haye, P. A., and Gallardo-Escárate, C. (2012). Gene expression analysis in *Mytilus chilensis* populations reveals local patterns associated with ocean environmental conditions. *Journal of Experimental Marine Biology and Ecology*, 420–421, 56–64. <https://doi.org/10.1016/j.jembe.2012.03.024>
- Oh, R., Lee, M. J., Kim, Y.-O., Nam, B.-H., Kong, H. J., Kim, J.-W., Park, J. Y., Seo, J.-K., and Kim, D.-G. (2018). Purification and characterization of an antimicrobial peptide mytichitin-chitin binding domain from the hard-shelled mussel, *Mytilus coruscus*. *Fish and Shellfish Immunology*, 83, 425–435. <https://doi.org/10.1016/j.fsi.2018.09.009>
- Olicard, C., Didier, Y., Marty, C., Bourgougnon, N., and Renault, T. (2005). *In vitro* research of anti-HSV-1 activity in different extracts from Pacific oysters *Crassostrea gigas*. *Diseases of Aquatic Organisms*, 67(1–2), 141–147. <https://doi.org/10.3354/dao067141>
- Oliver, P. G., Holmes, A. M., Killeen, I. J., and Turner, J. A. (2016). Marine Bivalve Shells of the British Isles. *Amgueddfa Cymru - National Museum Wales*. <http://naturalhistory.museumwales.ac.uk/britishbivalves>
- Orlando, P., Strazzullo, G., Carretta, F., De Falco, M., and Grippo, P. (1996). Inhibition mechanisms of HIV-1, Mo-MuLV and AMV reverse transcriptases by Kelletin A from *Buccinum corneum*. *Experientia*, 52(8), 812–817. <https://doi.org/10.1007/BF01923995>
- Orlando, P., Carretta, F., Grippo, P., Cimino, G., De Stefano, S., and Strazzullo, G. (1991). Kelletin I and kelletin A from the marine mollusc *Buccinum corneum* are inhibitors of eukaryotic DNA polymerase α . *Experientia*, 47(1), 64–66. <https://doi.org/10.1007/BF02041254>
- Oudot, M., Neige, P., Shir, I. B., Schmidt, A., Strugnell, J. M., Plasseraud, L., Broussard, C., Hoffmann, R., Lukeneder, A., and Marin, F. (2020). The shell matrix and microstructure of the Ram’s Horn squid: Molecular and structural characterization. *Journal of Structural Biology*, 211(1), 107507. <https://doi.org/10.1016/j.jsb.2020.107507>
- Paillard, C. (2004). A short-review of brown ring disease, a vibriosis affecting clams, *Ruditapes philippinarum* and *Ruditapes decussatus*. *Aquatic Living Resources*, 17(4), Article 4. <https://doi.org/10.1051/alr:2004053>
- Pain, S., and Parant, M. (2003). Le mécanisme de défense multixénobiotique (MDMX) chez les bivalves. *Comptes Rendus. Biologies*, 326(7), 659–672. [https://doi.org/10.1016/S1631-0691\(03\)00156-2](https://doi.org/10.1016/S1631-0691(03)00156-2)
- Pairett, A. N., and Serb, J. M. (2013). *de novo* Assembly and Characterization of Two Transcriptomes Reveal Multiple Light-Mediated Functions in the Scallop Eye (Bivalvia: Pectinidae). *PLOS ONE*, 8(7), e69852. <https://doi.org/10.1371/journal.pone.0069852>
- Pales Espinosa, E., Koller, A., and Allam, B. (2016). Proteomic characterization of mucosal secretions in the eastern oyster, *Crassostrea virginica*. *Journal of Proteomics*, 132. <https://doi.org/10.1016/j.jprot.2015.11.018>
- Pallavicini, A., del Mar Costa, M., Gestal, C., Dreos, R., Figueras, A., Venier, P., and Novoa, B. (2008). High sequence variability of myticin transcripts in hemocytes of immune-stimulated mussels suggests ancient host–pathogen interactions. *Developmental and Comparative Immunology*, 32(3), 213–226. <https://doi.org/10.1016/j.dci.2007.05.008>
- Pane, K., Durante, L., Crescenzi, O., Cafaro, V., Pizzo, E., Varcamonti, M., Zanfardino, A., Izzo, V., Di Donato, A., and Notomista, E. (2017). Antimicrobial potency of cationic antimicrobial peptides can be predicted from their amino acid composition: Application to the detection of “cryptic” antimicrobial peptides. *Journal of Theoretical Biology*, 419, 254–265. <https://doi.org/10.1016/j.jtbi.2017.02.012>
- Pauletto, M., Milan, M., Bargelloni, L., and Babbucci, M. (2013). A first deep sequencing on *Pecten maximus* hemocytes: A genomic resource to address farming production. [Transcribed RNA] Dpt. of Comparative Biomedicine and Food Science, Univ. of Padova, NCBI Nucleotide Database. <http://www.ncbi.nlm.nih.gov/nuccore/GA0X01020488.1>
- Peharda, M., Uvanović, H., Castrillejo, M., Ezgeta-Balić, D., and Vrgoč, N. (2023). (Re-)Examining age and growth increments of the clam *Venus verrucosa*. *Fisheries Research*, 267, 106812. <https://doi.org/10.1016/j.fishres.2023.106812>
- Peng, K., Wang, J., Sheng, J., Zeng, L., and Hong, Y. (2012). Molecular characterization and immune analysis of a defensin from freshwater pearl mussel, *Hyriopsis schlegelii*. *Aquaculture*, 334–337, 45–50. <https://doi.org/10.1016/j.aquaculture.2011.12.039>
- Philipp, E. E. R., Kraemer, L., Melzner, F., Poustka, A. J., Thieme, S., Findeisen, U., Schreiber, S., and Rosenstiel, P. (2012). Massively Parallel RNA Sequencing Identifies a Complex Immune Gene Repertoire in the lophotrochozoan *Mytilus edulis*. *PLOS ONE*, 7(3), e33091. <https://doi.org/10.1371/journal.pone.0033091>
- Pitt, S. J., Graham, M. A., Dedi, C. G., Taylor-Harris, P. M., and Gunn, A. (2015). Antimicrobial properties of mucus from the brown garden snail *Helix aspersa*. *British Journal of Biomedical Science*, 72(4). <https://doi.org/10.1080/09674845.2015.11665749>

- Ponder, W. F., Lindberg, D. R., and Ponder, J. M. (2020a). *Biology and Evolution of the Mollusca*, Volume 1. CRC Press, Taylor and Francis Group.
- Ponder, W. F., Lindberg, D. R., and Ponder, J. M. (2020b). *Biology and Evolution of the Mollusca*, Volume 2. CRC Press, Taylor and Francis Group.
- Ponkshe, C. A., and Indap, M. M. (2002). *in vivo* and *in vitro* evaluation for immunomodulatory activity of three marine animal extracts with reference to phagocytosis. *Indian Journal of Experimental Biology*, 40(12), 1399–1402.
- Popov, S. V. (1986). Composite prismatic structure in bivalve shell. *Acta Palaeontologica Polonica*, 31(1–2). <http://agro.icm.edu.pl/agro/element/bwmeta1.element.agro-32dc5e85-53aa-432a-a464-a05f64875aff>
- Powell, D., Subramanian, S., Suwansa-ard, S., Zhao, M., O'Connor, W., Raftos, D., and Elizur, A. (2018). The genome of the oyster *Saccostrea* offers insight into the environmental resilience of bivalves. *DNA Research*, 25(6), 655–665. <https://doi.org/10.1093/dnares/dsy032>
- Poyil, M., Bari, N., SanjayPrasad, S., and Alfaki, M. A. (2020). Extraction of Antimicrobial Peptides (AMPs) from *Portunus sanguinolentus* Herbst, *Perna viridis* Linneaus and *Octopus indicus* Orbigny: Identifying the best Solvent for AMP Recovery and Determining its Anti-ESKAPE Activity. *Journal of Research in Medical and Dental Science*, Vol. 9(1), 20–26p. [https://www.semanticscholar.org/paper/Extraction-of-Antimicrobial-Peptides-\(AMPs\)-from-Poyil-Bari/e794a0f100268e8e12346496503e50a303e95f85](https://www.semanticscholar.org/paper/Extraction-of-Antimicrobial-Peptides-(AMPs)-from-Poyil-Bari/e794a0f100268e8e12346496503e50a303e95f85)
- Prescott, B., Li, C. P., Caldes, G., and Martino, E. C. (1966). Chemical Studies of Paolin II, an Antiviral Substance from Oysters. *Proceedings of the Society for Experimental Biology and Medicine*, 123(2), 460–464. <https://doi.org/10.3181/00379727-123-31514>
- Qin, C., Huang, W., Zhou, S., Wang, X., Liu, H., Fan, M., Wang, R., Gao, P., and Liao, Z. (2014). Characterization of a novel antimicrobial peptide with chiting-biding domain from *Mytilus coruscus*. *Fish and Shellfish Immunology*, 41(2), 362–370. <https://doi.org/10.1016/j.fsi.2014.09.019>
- Raber, H. F., Sejfijaj, J., Kissmann, A.-K., Wittgens, A., Gonzalez-Garcia, M., Alba, A., Vázquez, A. A., Morales Vicente, F. E., Erviti, J. P., Kubiczek, D., Otero-González, A., Rodríguez, A., Ständker, L., and Rosenau, F. (2021). Antimicrobial Peptides Pom-1 and Pom-2 from *Pomacea poeyana* Are Active against *Candida auris*, *C. parapsilosis* and *C. albicans* Biofilms. *Pathogens*, 10(4), Article 4. <https://doi.org/10.3390/pathogens10040496>
- Rajapaksha, D. C., Jayathilaka, E. H. T. T., Edirisinghe, S. L., Nikapitiya, C., Lee, J., Whang, I., and De Zoysa, M. (2021). Octopromycin: Antibacterial and antibiofilm functions of a novel peptide derived from *Octopus minor* against multidrug-resistant *Acinetobacter baumannii*. *Fish and Shellfish Immunology*, 117, 82–94. <https://doi.org/10.1016/j.fsi.2021.07.019>
- Ramya, S., Ravichandran, S., and Kannan, M. (2018). Antimicrobial potential of crude extracts from Sea slug, *Euselenops luniceps* (Cuvier, 1817). *Drug Discovery*, 12, 49–53.
- Rao, G. P., Mohan, B. S., and Siddaiah, V. (2020). First Stereoselective Total Synthesis of Modiolin. *Russian Journal of Organic Chemistry*, 56(11), 2028–2031. <https://doi.org/10.1134/S1070428020110184>
- Renaut, S., Guerra, D., Hoeh, W. R., Stewart, D. T., Bogan, A. E., Ghiselli, F., Milani, L., Passamonti, M., and Breton, S. (2018). Genome Survey of the Freshwater Mussel *Venustaconcha ellipsiformis* (Bivalvia: Unionida) Using a Hybrid De Novo Assembly Approach. *Genome Biology and Evolution*, 10(7), 1637–1646. <https://doi.org/10.1093/gbe/evy117>
- Rey-Campos, M., Moreira, R., Romero, A., Medina-Gali, R. M., Novoa, B., Gasset, M., and Figueras, A. (2020). Transcriptomic Analysis Reveals the Wound Healing Activity of Mussel Myticin C. *Biomolecules*, 10(1), 133. <https://doi.org/10.3390/biom10010133>
- Ri, S., Zha, S., Kim, T., Ju, K., Zhou, W., Shi, W., Wu, M., Kim, C., Bao, Y., Sun, C., and Liu, G. (2022). Identification, characterization, and antimicrobial activity of a novel big defensin discovered in a commercial bivalve mollusc, *Tegillarca granosa*. *Fish and Shellfish Immunology*, 124, 174–181. <https://doi.org/10.1016/j.fsi.2022.04.003>
- Richardson, C. A., Crisp, D. J., Runham, N. W., and Gruffydd, L. D. (1980). The use of tidal growth bands in the shell of *Cerastoderma edule* to measure seasonal growth rates under cool temperate and sub-arctic conditions. *Journal of the Marine Biological Association of the United Kingdom*, 60(4), 977–989. <https://doi.org/10.1017/S002531540004203X>
- Riesgo, A., Andrade, S. C. S., Sharma, P. P., Novo, M., Pérez-Porro, A. R., Vahtera, V., González, V. L., Kawauchi, G. Y., and Giribet, G. (2012). Comparative description of ten transcriptomes of newly sequenced invertebrates and efficiency estimation of genomic sampling in non-model taxa. *Frontiers in Zoology*, 9(1), 33. <https://doi.org/10.1186/1742-9994-9-33>
- Roch, P., Beschin, A., and Bernard, E. (2004). Antiprotozoan and Antiviral Activities of Non-cytotoxic Truncated and Variant Analogues of Mussel Defensin. *Evidence-Based Complementary and Alternative Medicine*, 1(2), 167–174. <https://doi.org/10.1093/ecam/neh033>

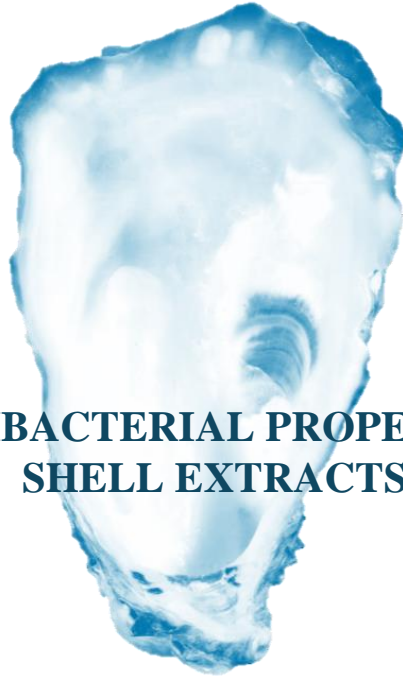
- Roch, P., Yang, Y., Toubiana, M., and Aumelas, A. (2008). NMR structure of mussel mytilin, and antiviral–antibacterial activities of derived synthetic peptides. *Developmental and Comparative Immunology*, 32(3), 227–238. <https://doi.org/10.1016/j.dci.2007.05.006>
- Rodriguez, A., Martell-Huguet, E. M., González-García, M., Alpízar-Pedraza, D., Alba, A., Vazquez, A. A., Grieshober, M., Spellerberg, B., Stenger, S., Münch, J., Kissmann, A.-K., Rosenau, F., Wessjohann, L. A., Wiese, S., Ständker, L., and Otero-Gonzalez, A. J. (2023). Identification and Characterization of Three New Antimicrobial Peptides from the Marine Mollusk *Nerita versicolor* (Gmelin, 1791). *International Journal of Molecular Sciences*, 24(4), 3852. <https://doi.org/10.3390/ijms24043852>
- Romestand, B., Molina, F., Richard, V., Roch, P., and Granier, and Claude. (2003). Key role of the loop connecting the two beta strands of mussel defensin in its antimicrobial activity. *European Journal of Biochemistry*, 270(13), 2805–2813. <https://doi.org/10.1046/j.1432-1033.2003.03657.x>
- Rosa, R. D., Santini, A., Fievet, J., Bulet, P., Destoumieux-Garzón, D., and Bachère, E. (2011). Big defensins, a diverse family of antimicrobial peptides that follows different patterns of expression in hemocytes of the oyster *Crassostrea gigas*. *PLoS One*, 6(9), e25594. <https://doi.org/10.1371/journal.pone.0025594>
- Rubio, T., Oyanedel, D., Labreuche, Y., Toulza, E., Luo, X., Bruto, M., Chaparro, C., Torres, M., de Lorgeril, J., Haffner, P., Vidal-Dupiol, J., Lagorce, A., Petton, B., Mitta, G., Jacq, A., Le Roux, F., Charrière, G. M., and Destoumieux-Garzón, D. (2019). Species-specific mechanisms of cytotoxicity toward immune cells determine the successful outcome of *Vibrio* infections. *Proceedings of the National Academy of Sciences of the United States of America*, 116(28), 14238–14247. <https://doi.org/10.1073/pnas.1905747116>
- Rundle, S. D., and Brönmark, C. (2001). Inter- and intraspecific trait compensation of defence mechanisms in freshwater snails. *Proceedings of the Royal Society of London. Series B: Biological Sciences*, 268(1475), 1463–1468. <https://doi.org/10.1098/rspb.2001.1682>
- Saarman, N. P., Kober, K. M., Simison, W. B., and Pogson, G. H. (2017). Sequence-Based Analysis of Thermal Adaptation and Protein Energy Landscapes in an Invasive Blue Mussel (*Mytilus galloprovincialis*). *Genome Biology and Evolution*, 9(10), 2739–2751. <https://doi.org/10.1093/gbe/evx190>
- Sake, F., Nasser, O., and Sabha, A. (2020). Antimicrobial Activity of Some Crude Marine Mollusca Extracts Against Some Human Pathogenic Bacteria. *International Journal of Agriculture and Environmental Science, Volume 7*. <https://doi.org/10.14445/23942568/IJAES-V7I1P102>
- Salvi, D., and Mariottini, P. (2017). Molecular taxonomy in 2D: A novel ITS2 rRNA sequence-structure approach guides the description of the oysters' subfamily Saccostreinae and the genus *Magallana* (Bivalvia: Ostreidae). *Zoological Journal of the Linnean Society*, 179(2), 263–276. <https://doi.org/10.1111/zoj.12455>
- Scardino, A., De Nys, R., Ison, O., O'Connor, W., and Steinberg, P. (2003). Microtopography and antifouling properties of the shell surface of the bivalve molluscs *Mytilus galloprovincialis* and *Pinctada imbricata*. *Biofouling*, 19(sup1), 221–230. <https://doi.org/10.1080/0892701021000057882>
- Schmitt, P., Gueguen, Y., Desmarais, E., Bachère, E., and de Lorgeril, J. (2010). Molecular diversity of antimicrobial effectors in the oyster *Crassostrea gigas*. *BMC Evolutionary Biology*, 10(1), 23. <https://doi.org/10.1186/1471-2148-10-23>
- Schmitt, P., Lorgeril, J. de, Gueguen, Y., Destoumieux-Garzón, D., and Bachère, E. (2012). Expression, tissue localization and synergy of antimicrobial peptides and proteins in the immune response of the oyster *Crassostrea gigas*. *Developmental and Comparative Immunology*, 37(3), 363–370. <https://doi.org/10.1016/j.dci.2012.01.004>
- Seo, J.-K., Crawford, J. M., Stone, K. L., and Noga, E. J. (2005). Purification of a novel arthropod defensin from the American oyster, *Crassostrea virginica*. *Biochemical and Biophysical Research Communications*, 338(4), 1998–2004. <https://doi.org/10.1016/j.bbrc.2005.11.013>
- Seo, J.-K., Go, H.-J., Kim, C.-H., Nam, B.-H., and Park, N. G. (2016). Antimicrobial peptide, hdMolluscidin, purified from the gill of the abalone, *Haliotis discus*. *Fish and Shellfish Immunology*, 52, 289–297. <https://doi.org/10.1016/j.fsi.2016.03.150>
- Seo, J.-K., Lee, M. J., Go, H.-J., Kim, G. D., Jeong, H. D., Nam, B.-H., and Park, N. G. (2013). Purification and antimicrobial function of ubiquitin isolated from the gill of Pacific oyster, *Crassostrea gigas*. *Molecular Immunology*, 53(1), 88–98. <https://doi.org/10.1016/j.molimm.2012.07.003>
- Seo, J.-K., Lee, M. J., Nam, B.-H., and Park, N. G. (2013). cgMolluscidin, a novel dibasic residue repeat rich antimicrobial peptide, purified from the gill of the Pacific oyster, *Crassostrea gigas*. *Fish and Shellfish Immunology*, 35(2), 480–488. <https://doi.org/10.1016/j.fsi.2013.05.010>
- Seppälä, O., Walser, J.-C., Cereghetti, T., Seppälä, K., Salo, T., and Adema, C. M. (2021). Transcriptome profiling of *Lymnaea stagnalis* (Gastropoda) for ecoimmunological research. *BMC Genomics*, 22(1), 144. <https://doi.org/10.1186/s12864-021-07428-1>
- Shallom, J. M., Johnson, R. L., Eackles, M. S., Lubinski, B. A., Springmann, M. J., Wicklow, B., Lellis, W. A., Printz, J. E., Hallerman, E. M., and King, T. L. (2010). Development of expressed sequence tags, type I microsatellite loci, and single nucleotide polymorphisms for three unionid genomes: *Alasmidonta*

- heterodon*, *Alasmidonta varicosa* and *Elliptio complanata* (315935070) [mRNA sequence]. *NCBI Nucleotide Database*. <http://www.ncbi.nlm.nih.gov/nucleotide/HP641713.1>
- Shanmugam, A., Kathiresan, K., and Nayak, L. (2016). Preparation, characterization and antibacterial activity of chitosan and phosphorylated chitosan from cuttlebone of *Sepia kobeensis* (Hoyle, 1885). *Biotechnology Reports*, 9, 25–30. <https://doi.org/10.1016/j.btre.2015.10.007>
- Simakov, O., Marletaz, F., Cho, S.-J., Edsinger-Gonzales, E., Havlak, P., Hellsten, U., Kuo, D.-H., Larsson, T., Lv, J., Arendt, D., Savage, R., Osoegawa, K., de Jong, P., Grimwood, J., Chapman, J. A., Shapiro, H., Aerts, A., Otiillar, R. P., Terry, A. Y., ... Rokhsar, D. S. (2013). Insights into bilaterian evolution from three spiralian genomes. *Nature*, 493(7433), 526–531. <https://doi.org/10.1038/nature11696>
- Silvestri, I., Albonici, L., Ciotti, M., Lombardi, M. P., Sinibaldi, P., Manzari, V., Orlando, P., Carretta, F., Strazzullo, G., and Grippo, P. (1995). Antimitotic and antiviral activities of Kelletin A in HTLV-1 infected MT2 cells. *Experientia*, 51(11), 1076–1080. <https://doi.org/10.1007/BF01946920>
- Song, X., Liu, Z., Wang, L., and Song, L. (2019). Recent Advances of Shell Matrix Proteins and Cellular Orchestration in Marine Molluscan Shell Biomineralization. *Frontiers in Marine Science*, 6, 41. <https://doi.org/10.3389/fmars.2019.00041>
- Stallings, C. D., Freytes-Ortiz, I. M., Plafcan, M. M., and Langdon, C. (2021). Inducible defenses in an estuarine bivalve do not alter predator handling times and are not affected by climate change. *Marine Ecology Progress Series*, 679, 73–84. <https://doi.org/10.3354/meps13901>
- Stambuk, F., Ojeda, C., Machado Matos, G., Rosa, R. D., Mercado, L., and Schmitt, P. (2021). Big defensin from the scallop *Argopecten purpuratus* ApBD1 is an antimicrobial peptide which entraps bacteria through nanonets formation. *Fish and Shellfish Immunology*, 119, 456–461. <https://doi.org/10.1016/j.fsi.2021.10.037>
- Stanley, S. M. (1970). Relation of Shell Form to Life Habits of the Bivalvia (Mollusca). In: S. M. Stanley (Ed.), Relation of Shell Form to Life Habits of the Bivalvia (Mollusca). *Geological Society of America*. <https://doi.org/10.1130/MEM125-pl>
- Sun, J., Wang, L., Yang, W., Wang, L., Fu, Q., and Song, L. (2020). IgIT-Mediated Signaling Inhibits the Antimicrobial Immune Response in Oyster Hemocytes. *The Journal of Immunology*, 205(9), 2402–2413. <https://doi.org/10.4049/jimmunol.2000294>
- Sun, J., Zhang, Y., Xu, T., Zhang, Y., Mu, H., Zhang, Y., Lan, Y., Fields, C. J., Hui, J. H. L., Zhang, W., Li, R., Nong, W., Cheung, F. K. M., Qiu, J.-W., and Qian, P.-Y. (2017). Adaptation to deep-sea chemosynthetic environments as revealed by mussel genomes. *Nature Ecology and Evolution*, 1(5), 1–7. <https://doi.org/10.1038/s41559-017-0121>
- Takamatsu, N., Shiba, T., Muramoto, K., and Kamiya, H. (1995). Molecular cloning of the defense factor in the albumen gland of the sea hare *Aplysia kurodai*. *FEBS Letters*, 377(3), 373–376. [https://doi.org/10.1016/0014-5793\(95\)01375-X](https://doi.org/10.1016/0014-5793(95)01375-X)
- Taylor, J. D., Taylor, J. D., and Kennedy, W. J. (1973). The shell structure and mineralogy of the Bivalvia. II. Lucinacea-Clavagellacea conclusions. *Bulletin of the British Museum (Natural History) Zoology*, 22, 253–294. <https://doi.org/10.5962/p.314199>
- Taylor, J. D., Taylor, J. D., Kennedy, W. J., and Hall, A. (1969). The Shell Structure and Mineralogy of the Bivalvia. Introduction. Nuculacea—Trigonacea. *Bulletin of the British Museum (Natural History) Zoology. Supplement, Supplement 3*, 1–125. <https://doi.org/10.5962/p.312694>
- Terada, D., Voet, A. R. D., Noguchi, H., Kamata, K., Ohki, M., Addy, C., Fujii, Y., Yamamoto, D., Ozeki, Y., Tame, J. R. H., and Zhang, K. Y. J. (2017). Computational design of a symmetrical β -trefoil lectin with cancer cell binding activity. *Scientific Reports*, 7(1), 5943. <https://doi.org/10.1038/s41598-017-06332-7>
- Thulshan Jayathilaka, E. H. T., Liyanage, T. D., Rajapaksha, D. C., Dananjaya, S. H. S., Nikapitiya, C., Whang, I., and De Zoysa, M. (2021). Octominin: An antibacterial and anti-biofilm peptide for controlling the multidrug resistance and pathogenic *Streptococcus parauberis*. *Fish and Shellfish Immunology*, 110, 23–34. <https://doi.org/10.1016/j.fsi.2020.12.017>
- Thulshan Jayathilaka, E. H. T., Nikapitiya, C., De Zoysa, M., and Whang, I. (2022). Antimicrobial Peptide Octominin-Encapsulated Chitosan Nanoparticles Enhanced Antifungal and Antibacterial Activities. *International Journal of Molecular Sciences*, 23(24), Article 24. <https://doi.org/10.3390/ijms232415882>
- Thulshan Jayathilaka, E. H. T., Rajapaksha, D. C., Nikapitiya, C., Lee, J., De Zoysa, M., and Whang, I. (2022). Novel Antimicrobial Peptide “Octoprohibitin” against Multidrug Resistant *Acinetobacter baumannii*. *Pharmaceuticals*, 15(8), Article 8. <https://doi.org/10.3390/ph15080928>
- Thunberg, C. P. (1793). Tekning och Beskrifning på en stor Ostronsort ifrån Japan. *Kongliga Vetenskaps Academiens Nya Handlingar*, Vol. 14. <https://www.biodiversitylibrary.org/item/180096>
- Trinkler, N., Guichard, N., Labonne, M., Plasseraud, L., Paillard, C., and Marin, F. (2011). Variability of shell repair in the Manila clam *Ruditapes philippinarum* affected by the Brown Ring Disease: A microstructural and biochemical study. *Journal of Invertebrate Pathology*, 106(3), 407–417. <https://doi.org/10.1016/j.jip.2010.12.011>

- Tunkijjanukij, S., and Olafsen, J. A. (1998). Sialic acid-binding lectin with antibacterial activity from the horse mussel: Further characterization and immunolocalization. *Developmental and Comparative Immunology*, 22(2), 139–150. [https://doi.org/10.1016/S0145-305X\(98\)00017-2](https://doi.org/10.1016/S0145-305X(98)00017-2)
- Uvanović, H., Schöne, B. R., Markulin, K., Janeković, I., and Peharda, M. (2021). Venerid bivalve *Venus verrucosa* as a high-resolution archive of seawater temperature in the Mediterranean Sea. *Palaeogeography, Palaeoclimatology, Palaeoecology*, 561, 110057. <https://doi.org/10.1016/j.palaeo.2020.110057>
- Venier, P., Gerdol, M., Domeneghetti, S., Sharma, N., Pallavicini, A., and Rosani, U. (2019). Biotechnologies from Marine Bivalves. In: A. C. Smaal, J. G. Ferreira, J. Grant, J. K. Petersen, and Ø. Strand (Eds.), *Goods and Services of Marine Bivalves*. Springer International Publishing, pp. 95–112. https://doi.org/10.1007/978-3-319-96776-9_6
- Vera, M., Martínez, P., Poisa-Beiro, L., Figueras, A., and Novoa, B. (2011). Genomic Organization, Molecular Diversification, and Evolution of Antimicrobial Peptide Myticin-C Genes in the Mussel (*Mytilus galloprovincialis*). *PLOS ONE*, 6(8), e24041. <https://doi.org/10.1371/journal.pone.0024041>
- Viruly, L., Suhartono, M. T., Nurilmala, M., Saraswati, S., and Andarwulan, N. (2023). Identification and characterization of antimicrobial peptide (AMP) candidate from Gonggong Sea Snail (*Leavistrombus turturella*) extract. *Journal of Food Science and Technology*, 60(1), 44–52. <https://doi.org/10.1007/s13197-022-05585-z>
- Waller, T. R. (1980). Scanning electron microscopy of shell and mantle in the order Arcoidea (Mollusca: Bivalvia). *Smithsonian Libraries*. <http://repository.si.edu/xmlui/handle/10088/5283>
- Wang, D., Huang, B., Yu, J., Bai, C., Li, C., Wang, C., Xin, L., and Zhou, H. (2022). Characterization of a Novel C-type Lectin against OsHV-1 infection in *Scapharca broughtonii*. *Invertebrate Survival Journal*, 42–52. <https://doi.org/10.25431/1824-307X/isj.v19i1.42-52>
- Wang, G.-L., Xia, X.-L., Li, X.-L., Dong, S.-J., and Li, J.-L. (2014). Molecular characterization and expression patterns of the big defensin gene in freshwater mussel (*Hyriopsis cumingii*). *Genetics and Molecular Research: GMR*, 13(1), 704–715. <https://doi.org/10.4238/2014.January.29.1>
- Wang, M., Wang, B., Liu, M., Jiang, K., and Wang, L. (2019). Comparative study of β -thymosin in two scallop species *Argopecten irradians* and *Chlamys farreri*. *Fish and Shellfish Immunology*, 86, 516–524. <https://doi.org/10.1016/j.fsi.2018.11.050>
- Wang, Q., Zhang, L., Yang, D., Yu, Q., Li, F., Cong, M., Ji, C., Wu, H., and Zhao, J. (2015). Molecular diversity and evolution of defensins in the manila clam *Ruditapes philippinarum*. *Fish and Shellfish Immunology*, 47(1), 302–312. <https://doi.org/10.1016/j.fsi.2015.09.008>
- Wang, R., Li, C., Stoeckel, J., Moyer, G., Liu, Z., and Peatman, E. (2012). Rapid development of molecular resources for a freshwater mussel, *Villosa lienosa* (Bivalvia:Unionidae), using an RNA-seq-based approach. *Freshwater Science*, 31(3), 695–708. <https://doi.org/10.1899/11-149.1>
- Wang, X., Xu, W., Wei, L., Zhu, C., He, C., Song, H., Cai, Z., Yu, W., Jiang, Q., Li, L., Wang, K., and Feng, C. (2019). Nanopore Sequencing and De Novo Assembly of a Black-Shelled Pacific Oyster (*Crassostrea gigas*) Genome. *Frontiers in Genetics*, 10. <https://doi.org/10.3389/fgene.2019.01211>
- Wang, Y., Zeng, Z., Zhang, X., Shi, Q., Wang, C., Hu, Z., and Li, H. (2018). Identification and characterization of a novel defensin from Asian green mussel *Perna viridis*. *Fish and Shellfish Immunology*, 74, 242–249. <https://doi.org/10.1016/j.fsi.2017.12.029>
- Watabe, N. (1983). Shell Repair. In A. S. M. Saleuddin and K. M. Wilbur (Eds.), *The Mollusca* (pp. 289–316). Academic Press. <https://doi.org/10.1016/B978-0-12-751404-8.50015-3>
- Wei, Y.-X., Guo, D.-S., Li, R.-G., Chen, H.-W., and Chen, P.-X. (2003). Purification of a big defensin from *Ruditapes philippinensis* and its antibacterial activity. *Sheng Wu Hua Xue Yu Sheng Wu Wu Li Xue Bao Acta Biochimica et Biophysica Sinica*, 35(12). <https://pubmed.ncbi.nlm.nih.gov/14673509/>
- Weiner, S., Traub, W., Miller, A., Phillips, D. C., and Williams, R. J. P. (1984). Macromolecules in mollusc shells and their functions in biomineralization. *Philosophical Transactions of the Royal Society of London. B, Biological Sciences*, 304(1121), 425–434. <https://doi.org/10.1098/rstb.1984.0036>
- Wilson, J. J., Grendler, J., Dunlap-Smith, A., Beal, B. F., and Page, S. T. (2016). Analysis of Gene Expression in an Inbred Line of Soft-Shell Clams (*Mya arenaria*) Displaying Growth Heterosis: Regulation of Structural Genes and the NOD2 Pathway. *International Journal of Genomics*, 2016(1), 6720947. <https://doi.org/10.1155/2016/6720947>
- Wong, Y. H., Sun, J., He, L. S., Chen, L. G., Qiu, J.-W., and Qian, P.-Y. (2015). High-throughput transcriptome sequencing of the cold seep mussel *Bathymodiolus platifrons*. *Scientific Reports*, 5, 16597. <https://doi.org/10.1038/srep16597>
- Xie, Z., Yao, T., Ye, L., and Wang, J. (2021). Molecular characterization and expression analysis of an antimicrobial peptide, mytimacin-6, in the small abalone, *Haliotis diversicolor*. *Israeli Journal of Aquaculture - Bamidgeh*, 73, 1–11. <https://doi.org/10.46989/001c.25815>

- Xu, W., and Faisal, M. (2010). Defensin of the zebra mussel (*Dreissena polymorpha*): Molecular structure, *in vitro* expression, antimicrobial activity, and potential functions. *Molecular Immunology*, 47(11), 2138–2147. <https://doi.org/10.1016/j.molimm.2010.01.025>
- Xue, Q., Hellberg, M. E., Schey, K. L., Itoh, N., Eytan, R. I., Cooper, R. K., and La Peyre, J. F. (2010). A new lysozyme from the eastern oyster, *Crassostrea virginica*, and a possible evolutionary pathway for i-type lysozymes in bivalves from host defense to digestion. *BMC Evolutionary Biology*, 10(1), 213. <https://doi.org/10.1186/1471-2148-10-213>
- Xue, Q.-G., Schey, K. L., Volety, A. K., Chu, F.-L. E., and La Peyre, J. F. (2004). Purification and characterization of lysozyme from plasma of the eastern oyster (*Crassostrea virginica*). *Comparative Biochemistry and Physiology Part B: Biochemistry and Molecular Biology*, 139(1), 11–25. <https://doi.org/10.1016/j.cbpc.2004.05.011>
- Xue, Q.-G., Waldrop, G. L., Schey, K. L., Itoh, N., Ogawa, M., Cooper, R. K., Losso, J. N., and La Peyre, J. F. (2006). A novel slow-tight binding serine protease inhibitor from eastern oyster (*Crassostrea virginica*) plasma inhibits perkinsin, the major extracellular protease of the oyster protozoan parasite *Perkinsus marinus*. *Comparative Biochemistry and Physiology Part B: Biochemistry and Molecular Biology*, 145(1), 16–26. <https://doi.org/10.1016/j.cbpb.2006.05.010>
- Yan, X., Nie, H., Huo, Z., Ding, J., Li, Z., Yan, L., Jiang, L., Mu, Z., Wang, H., Meng, X., Chen, P., Zhou, M., Rbbani, Md. G., Liu, G., and Li, D. (2019). Clam Genome Sequence Clarifies the Molecular Basis of Its Benthic Adaptation and Extraordinary Shell Color Diversity. *iScience*, 19, 1225–1237. <https://doi.org/10.1016/j.isci.2019.08.049>
- Yang, H., Johnson, P. M., Ko, K.-C., Kamio, M., Germann, M. W., Derby, C. D., and Tai, P. C. (2005). Cloning, characterization and expression of escapin, a broadly antimicrobial FAD-containing l-amino acid oxidase from ink of the sea hare *Aplysia californica*. *Journal of Experimental Biology*, 208(18), 3609–3622. <https://doi.org/10.1242/jeb.01795>
- Yang, J., Luo, J., Zheng, H., Lu, Y., and Zhang, H. (2016). Cloning of a big defensin gene and its response to *Vibrio parahaemolyticus* challenge in the noble scallop *Chlamys nobilis* (Bivalve: Pectinidae). *Fish and Shellfish Immunology*, 56, 445–449. <https://doi.org/10.1016/j.fsi.2016.07.030>
- Yang, Y.-S., Mitta, G., Chavanieu, A., Calas, B., Sanchez, J. F., Roch, P., and Aumelas, A. (2000). Solution Structure and Activity of the Synthetic Four-Disulfide Bond Mediterranean Mussel Defensin (MGD-1). *Biochemistry*, 39(47), 14436–14447. <https://doi.org/10.1021/bi0011835>
- Yoshino, Y., Muramoto, K., Goto, R., and Kamiya, H. (1993). Isolation and Characterization of a Protease Inhibitor from the Marine Gastropod *Tugali gigas*. *Nippon Suisan Gakkaishi*, 59(11), 1923–1928. <https://doi.org/10.2331/suisan.59.1923>
- Yuan, C., Zheng, X., Liu, K., Yuan, W., Zhang, Y., Mao, F., and Bao, Y. (2022). Functional Characterization, Antimicrobial Effects, and Potential Antibacterial Mechanisms of NpHM4, a Derived Peptide of *Nautilus pompilius* Hemocyanin. *Marine Drugs*, 20(7), 459. <https://doi.org/10.3390/md20070459>
- Zeng, M., Cui, W., Zhao, Y., Liu, Z., Dong, S., and Guo, Y. (2008). Antiviral active peptide from oyster. *Chinese Journal of Oceanology and Limnology*, 26(3), 307–312. <https://doi.org/10.1007/s00343-008-0307-x>
- Zeng, Z., Tan, Q., Huang, Z., Shi, B., and Ke, C. (2019). Differential Gene expression related to morphological variation in the adductor muscle tissues of diploid and triploid fujian oysters, *Crassostrea angulata*. *Aquaculture Research*, 50(12), 3567–3578. <https://doi.org/10.1111/are.14312>
- Zhang, G., Fang, X., Guo, X., Li, L., Luo, R., Xu, F., Yang, P., Zhang, L., Wang, X., Qi, H., Xiong, Z., Que, H., Xie, Y., Holland, P. W. H., Paps, J., Zhu, Y., Wu, F., Chen, Y., Wang, J., ... Wang, J. (2012). The oyster genome reveals stress adaptation and complexity of shell formation. *Nature*, 490(7418), 49–54. <https://doi.org/10.1038/nature11413>
- Zhang, L., Yang, D., Wang, Q., Yuan, Z., Wu, H., Pei, D., Cong, M., Li, F., Ji, C., and Zhao, J. (2015). A defensin from clam *Venerupis philippinarum*: Molecular characterization, localization, antibacterial activity, and mechanism of action. *Developmental and Comparative Immunology*, 51(1), 29–38. <https://doi.org/10.1016/j.dci.2015.02.009>
- Zhao, J., Li, C., Chen, A., Li, L., Su, X., and Li, T. (2010). Molecular Characterization of a Novel Big Defensin from Clam *Venerupis philippinarum*. *PLOS ONE*, 5(10), e13480. <https://doi.org/10.1371/journal.pone.0013480>
- Zhao, J., Song, L., Li, C., Ni, D., Wu, L., Zhu, L., Wang, H., and Xu, W. (2007). Molecular cloning, expression of a big defensin gene from bay scallop *Argopecten irradians* and the antimicrobial activity of its recombinant protein. *Molecular Immunology*, 44(4), 360–368. <https://doi.org/10.1016/j.molimm.2006.02.025>
- Zheng, L., Liu, Z., Wu, B., Dong, Y., Zhou, L., Tian, J., Sun, X., and Yang, A. (2016). Ferritin has an important immune function in the ark shell *Scapharca broughtonii*. *Developmental and Comparative Immunology*, 59, 15–24. <https://doi.org/10.1016/j.dci.2015.12.010>

- Zhong, J., Wang, W., Yang, X., Yan, X., and Liu, R. (2013). A novel cysteine-rich antimicrobial peptide from the mucus of the snail of *Achatina fulica*. *Peptides*, 39, 1–5. <https://doi.org/10.1016/j.peptides.2012.09.001>
- Zhuang, J., Coates, C. J., Zhu, H., Zhu, P., Wu, Z., and Xie, L. (2015). Identification of candidate antimicrobial peptides derived from abalone hemocyanin. *Developmental and Comparative Immunology*, 49(1), 96–102. <https://doi.org/10.1016/j.dci.2014.11.008>



**CHAPTER 3 - ANTIBACTERIAL PROPERTIES OF BIVALVE
SHELL EXTRACTS**

3.1. Introduction

In this chapter, I present the applied focus of this doctoral thesis, the antibacterial screening of substances extracted from the shells of bivalves of economic interest. At first, in section 3.2, I introduce the technical aspects of screening design and protocol adaptations to unusual targets: marine bacteria. Then, in section 3.3, follows a paper where I present the organic matrix extraction protocol and the methods I developed with my lab in order to use the Acid Insoluble Matrix (AIM) in bioassays for the first time, in a paper that was published this year (Lutet-Toti *et al.*, 2024). Finally, I present in section 3.4 the core part of my doctoral research, the “pearl on the crown”, the positive results obtained in the context of this screening. These are included in a submitted paper (Lutet-Toti *et al.*, 2025, *submitted to STOTEN*), while the negative results of the screening (complementary but which could not be integrated into the paper) are presented in Chapter 4. Miscellanea.

3.2. Antibacterial Screening of Bivalve Shell Extracts: Technical Aspects

Antibacterial screening is defined as the systematic process aimed at identifying and evaluating potential antibacterial agents from diverse sources against various bacterial targets. In the context of my doctoral research, this screening is part of a bioprospecting effort, focusing on natural sources that have been little to not explored in the current literature to develop new drugs (Valgas *et al.*, 2007; Cushnie *et al.*, 2020). Specifically, I am investigating the antibacterial potential of bivalve shell organic matrices, which composition in bioactive molecules and their characteristics have not been elucidated yet. The bacterial targets I selected for this screening also come as unusual elements: after thorough examination of the existing literature and the review of ecological and ethnomedical information regarding the interactions between bivalves and bacteria (see section 1.2.3. Traditional Medicinal and Pharmaceutical Uses and 1.3.3. Threats and Limitations of Conchyliculture), the targeting choice fell on marine pathogens of the Vibrionaceae family.

Several antibacterial screening methods can be used to assess antibacterial activity, each providing different types of data regarding the bacterial response. These have to be adapted to the specific sources of tested products and targets (Cushnie *et al.*, 2020). They are typically categorized into three main types:

1) Initial screening methods are primarily qualitative (or semi-quantitative) techniques used for rapid detection of antibacterial activity. They include agar diffusion assays (such as disk diffusion and well diffusion) and Thin Layer Chromatography (TLC) - bioautography. These methods are low cost, quick and simple to develop, resource-conservative, suitable for screening large numbers of samples and provide basic indication of antibacterial potency (Balouiri *et al.*, 2016). Disk diffusion assays were the main method used during the “golden age” of antibiotic exploration and it still represents the most accepted and performed protocols in antimicrobial testing globally, particularly in laboratories with limited funding (Hetru & Bulet, 1997; Cushnie *et al.*, 2020; Massoud *et al.*, 2020).

2) Secondary screening methods are quantitative techniques mainly used to determine the Minimum Inhibitory Concentration (MIC) and characterize the mode of action of the tested substances on their targets. They include broth dilution (macro- in culture tubes and micro- in microplates wells), agar dilution and Etest (antimicrobial gradient on diffusible paper applied to agar plates). These methods are usually more expensive than the initial screening, time-consuming and require lab adaptations and skills to perform accurately (Valgas *et al.*, 2007; Balouiri *et al.*, 2016). Microdilution assays are adapted to small quantities of natural products and can, in certain settings, determine whether a substance is bactericidal or bacteriostatic and its putative Minimum Bactericidal Concentration (MBC) (Cushnie *et al.*, 2020; Massoud *et al.*, 2020).

3) Tertiary screening methods are advanced high-throughput techniques that are used to further investigate the mechanism of action of antibacterial agents and their specific effects on bacterial cells (membrane defects, disordered expression of proteins...). They include flow cytometry, ATP-bioluminescence assays, time-kill kinetics and various molecular and genetic approaches. These methods can precisely determine the presence of combined effects (synergistic or antagonistic interaction) between fractions, the nature of antibacterial mechanisms (differentiation between viable, dead or injured bacteria) and bring robustness to the analysis by their automation (Balouiri *et al.*, 2016). However, they often come as very costly and resource consuming: they have to be designed carefully and therefore require the previous initial and secondary screenings.

Examples from the literature illustrate the application of these screening methods to marine organisms. Defer *et al.* (2009) investigated the antibacterial and antiviral activities of acidic extracts from the whole soft bodies of five marine mollusks – among them two bivalves

that are my models here, *Cerastoderma edule* and *Venerupis philippinarum*. They employed well diffusion assays for initial screening, followed by microdilution assays and detected antimicrobial activity against common Gram-negative and Gram-positive mesophilic bacterial species and herpesvirus. In another study, López-Abarrategui *et al.* (2012) used a microdilution method to assess the antibacterial activity of *Cenchritis muricatus* (a littorinid gastropod) crude soft-body extracts against *Escherichia coli* and *Staphylococcus aureus*. After the detection of near total growth inhibitions, the involved antibacterial proteins were isolated and characterized, uncovering new antimicrobial domains. These discoveries demonstrate the potential of mollusks as sources for antimicrobial molecules and substances. They further motivate, along with the aforementioned observed or reported bioactive properties of shells, the exploration of bivalve shells organic matrices as such.

3.2.1. Resources for Bioactive Substances: Mollusk Models

3.2.1.1. Sampling

Several shells of seven bivalve species of economic interest were collected from live animals in local seafood markets and supermarkets around Dijon (Burgundy, France). The sampled species include four pteriomorphs: the dog cockle *Glycymeris glycymeris*, the Mediterranean mussel *Mytilus galloprovincialis*, the Pacific cupped oyster *Magallana gigas*, and the great scallop *Pecten maximus*; and three heteroconchs: the common cockle *Cerastoderma edule*, the warty venus *Venus verrucosa* and the manila clam *Venerupis philippinarum*.

3.2.1.2. Production of Shell Powder

Each specimen was carefully cleaned with a knife to remove soft tissues, tissues, including adductor muscles. The shell and shell valves were thoroughly cleaned, hand scrubbed with soap and water, and soaked in a 10% (vol/vol) sodium hypochlorite solution overnight. Some sample needed multiple cleaning cycles and mechanically agitated baths over a few days and nights in order to get rid of any remaining organic matter. After fully drying the shells at 37°C, the periostracum (organic outer layer of the shell), hinge ligament (organic tissue) and any epibionts (*e.g.* barnacles or mud blister worms) were removed with scalpels and Dremel drills. The cleaned dried shells, clear of any organic tissue, were crushed with a jaw crusher, producing small pieces of 1 cm maximum. Subsequently, a mechanical agate bowl and mortar (Pulverisette 2 grinder, Fritsch, Fig. 1B) was used to grind the coarse shell powder into fine

powder. Multiple cycles of grinding and sieving were required to bring the powder grains to a diameter below 200µm.

3.2.1.3. Organic Matrix Extraction

The decontaminated regular whole shell powder that was produced earlier served as the raw material for the extraction of the organic matrix: the powders were gently decalcified at 4°C in cold dilute acetic acid, following the extraction protocol described in the two following papers (Lutet-Toti *et al.*, 2024; 2025, *submitted to STOTEN*). In brief, for each of the seven species, Acid Soluble Matrix (ASM) and Acid Insoluble Matrix (AIM) were produced. The ASM was further fractionated according to molecular weight via ultrafiltration, with successive cutoffs of 10 kDa and 1 kDa, resulting in the production of two fractions: ASM>10 kDa and 1<ASM<10 kDa. An additional intermediate cutoff of 3kDa was used for two species (*M. galloprovincialis* and *V. philippinarum*), which showed high viscosity of the total ASM, resulting in three ASM fractions: ASM>10 kDa; 3<ASM<10 kDa; 1<ASM<3 kDa. All obtained ASM fractions were then thoroughly dialyzed against Milli-Q water, and all matrix extracts (ASM and AIM) were freeze-dried and weighed in a precision balance. The quantities of all extracted matrix fractions for each bivalve model are documented bellow in Table 3.1, where I also show the percentage of whole matrices in the shells and the ratio of insoluble over total matrix.

3.2.2. Bacterial Targets

Six strains de marine bacteria of the Vibrionaceae family were selected: *Aliivibrio salmonicida*, *Vibrio aestuarianus*, *Vibrio harveyi* LMG7890, *Vibrio harveyi* ORM4, *Vibrio mytili* and *Vibrio tapetis* CECT4600. These strains were chosen as ideal candidates for assessing the antibacterial potential of bivalve models due to their well-documented interactions with the later, their diversity in host-distribution, virulence, pathogenic mechanisms (when reported) and defense against the host. This diverse panel is key in differentiating specific antibacterial modes of action of the bivalve shell extracts against microorganisms.

As marine bacteria, these strains come with peculiar optimal growth conditions that can come as limiting in efficient culture and require adaptation of the experimentations: they grow on marine agar (only 15% agar, around 3% NaCl composition, low nutrient availability), in high hygrometry environments and are sometimes described as psychrophilic (*A. salmonicida* grows at 12°C for example, while *V. harveyi* thrives at 28°C). Finding “the right

accommodation” thus requires preliminary testing of cultures in different configurations (Rodrigues & de Carvalho, 2022). The specific parameters of bacterial culture are described for each strain in the following paper in section 3.4 (Lutet-Toti *et al.*, 2025, *submitted to STOTEN*) and in Chapter 4. Miscellanea.

Table 3.1: Amounts of organic matrix in the shell of the seven tested bivalves.

Mollusk species	Mineralogy & shell microstructures	Matrix fraction	Mean matrix quantity (mg) per gram of shell powder	% matrix in shell powder	% AIM / total matrix
<i>Glycymeris glycymeris</i> Dog cockle	 ARAGONITIC OL: crossed-lamellar ML: straight crossed-lamellar IL: orthogonal crossed-lamellar	AIM	0.5746	0.0840%	68.41%
		ASM>10 kDa	0.0480		
		1<ASM<10 kDa	0.2173		
<i>Mytilus galloprovincialis</i> Mediterranean mussel	 CALCITIC & ARAGONITIC OL: prismatic calcite IL: flat nacre aragonite	AIM	6.7466	0.7428%	90.82%
		ASM>10 kDa	0.2339		
		3<ASM<10 kDa	0.3292		
		1<ASM<3 kDa	0.1187		
<i>Magallana gigas</i> Pacific oyster	 CALCITIC OL: prismatic IL: foliated + chalky lenses	AIM	4.3491	0.5667%	76.74%
		ASM>10 kDa	1.1353		
		1<ASM<10 kDa	0.1827		
<i>Pecten maximus</i> Giant scallop	 CALCITIC OL: prismatic IL: foliated + chalky lenses	AIM	3.5918	0.5253%	68.37%
		ASM>10 kDa	1.3426		
		1<ASM<10 kDa	0.3188		
<i>Cerastoderma edule</i> Common cockle	 ARAGONITIC OL: crossed-lamellar IL: complex crossed-lamellar	AIM	0.5125	0.0785%	65.25%
		ASM>10 kDa	0.0975		
		1<ASM<10 kDa	0.1755		
<i>Venerupis philippinarum</i> Manila clam	 ARAGONITIC OL: composite prismatic IL: crossed-lamellar becoming homogeneous	AIM	1.1839	0.1519%	77.96%
		ASM>10 kDa	0.2222		
		3<ASM<10 kDa	0.0850		
		1<ASM<3 kDa	0.0274		
<i>Venus verrucosa</i> Warty venus	 ARAGONITIC OL: composite prismatic ML: crossed-lamellar IL: homogeneous	AIM	1.1104	0.2011%	55.23%
		ASM>10 kDa	0.7224		
		1<ASM<10 kDa	0.1776		

3.2.3. Standard Antibacterials

To establish positive controls for the following screening assays, antibiotics were selected according to literature on Vibrionaceae, specifically targeting each strain when possible. The selected antibiotics include ampicillin, tetracycline, metabolic inhibitor sodium azide and vibriostatic agent 0/129 (2,4-diamino-6,7-diisopropylpteridine phosphate), which will be referred to as v0129 from this point forward for improved readability (Johnson & Shunk, 1936; Tison & Seidler, 1983; Pujalte *et al.*, 1993; Borrego *et al.*, 1996; Urbanczyk *et al.*, 2007).

3.2.4. Initial Screening: Disk Diffusion Assay

For this antibacterial screening, two methods were selected and tailored to fit the models and targets described earlier. The initial screening was performed using a disk diffusion assay on agar plates to detect antibacterial activity (Bauer *et al.*, 1966). This method is perfectly adapted for a rapid screening of a lot of combinations of fractions and bacterial strains, remains cost-effective and is not overly consuming the extracted fractions that are, as observable in Table 3.1, a minor part of the shell and thus represent a precious limiting resource. This assay enabled a systematic screening adapted to psychrophilic bacteria: it only requires the use of the spread plate technique – *i.e.*, applying bacteria once the agar is solidified at room temperature – whereas other methods like the well diffusion assay require the bacteria to be mixed to agar, remaining above 40°C during the pouring process. It is also the only method allowing the use of the AIM, which insolubility usually precludes its employ in any bioassay: using a manual lab press, I was able to develop a technique to produce AIM tablets similar to diffusible disks used for soluble compounds, thus incorporating these extracts to a standardized broad antibacterial screening by disk diffusion (Lutet-Toti *et al.*, 2024).

In total, 23 organic matrix fractions were tested, along with whole shell powder tablets and positive (v0129) and negative controls (pure CaCO₃ and ultra-pure water). ASM disks were saturated with a standard quantity of 20µg, following working values observed in literature on antimicrobial screening from invertebrate crude extracts (Hetru & Bulet, 1997). As my research focuses on unusual targets, no standard values against which to compare results are edited by the Clinical and Laboratory Standard Institute (CLSI) or the European Union Reference Laboratory for Alternatives to Animal Testing (EUCAST). The results that follow are thus not interpreted as either “resistant” or “sensitive” compared to existing drugs, but rather as biological observations of bacterial growth inhibition, following the guidelines of operating

“without breakpoints” (EUCAST, 2024). The whole protocol is accurately described in details in the section 3.4 of this manuscript (Lutet-Toti *et al.*, 2025, *submitted to STOTEN*).

3.2.5. Secondary Screening: Microdilution Assay

Similarly to the initial screening, the limited quantities of tested resources guided the selection of the secondary screening towards microdilution assays (Zgoda & Porter, 2001). This approach aimed to validate initial screening results, to understand the dynamic interactions between shell extracts and bacteria (*i.e.*, MIC determination and discrimination between bactericidal and bacteriostatic mechanisms), and detect activity that may have been previously overlooked due to insufficient ASM in disks or poor diffusion of the ASM on agar (Rudilla *et al.*, 2018; Cushnie *et al.*, 2020). This assay was only performed on soluble extracts (ASM), as the AIM could not be solubilized in biocompatible solvents. In a first step, a preliminary round of microdilutions was performed for each strain to establish the gradient of the antibiotic standard and compare the effects of three antibiotics: sodium azide, tetracycline and v0129. This preliminary procedure was also required to determine the regularity of absorbance measurements and total incubation time (see section 4.2. Characterization of the Bacterial Strains).

In a second step, for each target and model species, increasing concentrations of the fractionated extracts were added to liquid cultures and then incubated in optimal conditions. Optical densities were measured using a spectrophotometer at regular intervals, producing curves used as proxies for bacterial metabolism and growth phases analysis. These growth curves were compared to those produced by the selected antibiotic standard, and key growth parameters (maximum growth rate – during the exponential growth phase – and carrying capacity) were extracted and statistically analyzed (Rudilla *et al.*, 2018; Blazanin, 2024).

A key adaptation was the addition of red phenol as a colored pH indicator to the cloudy-yellow marine broth. This allowed precise monitoring of slight metabolic changes, especially important given the limited literature in these bacteria’s growth phases and metabolism. Indeed, the target bacteria are fermentative and their carbohydrate metabolism acidifies their environment during active growth; when they are not active anymore, this acidification slows down and stops. Eventually, when all resources have been consumed, bacteria start to die and experience bacterial cell lysis, releasing their basic components and thus, increasing the pH of the medium to higher values than before bacterial proliferation (Leifson, 1963). Color changes were monitored by spectrophotometry, measuring the absorbance at both peak values: 420 nm

for the acidic yellow, and 560 nm for the basic fuchsia. The pH gradient (A) and absorbance spectra (B) of red phenol are presented in Figure 3.1. Note that the peak value for 560 nm is high and narrow, while the one for 420 nm is significantly lower and wider (Held, 2022; Weiskirchen *et al.*, 2023). This hints towards potential influence from the yellow broth at 420 nm and better accuracy at 560 nm. Notably, the absorbance at 600 nm (or neighboring values) was not measured: although it was (and still is) standard procedure in a lot of studies (Hetru & Bulet, 1997; Boyle *et al.*, 2015; Li *et al.*, 2016), this wavelength is associated to bacterial membrane density and does not differentiate between viable active bacteria from injured, dead or fragmented cells (Rudilla *et al.*, 2018; Mira *et al.*, 2022). Again, the detailed protocol is described in the section 3.4 of this manuscript (Lutet-Toti *et al.*, 2025, *submitted to STOTEN*).

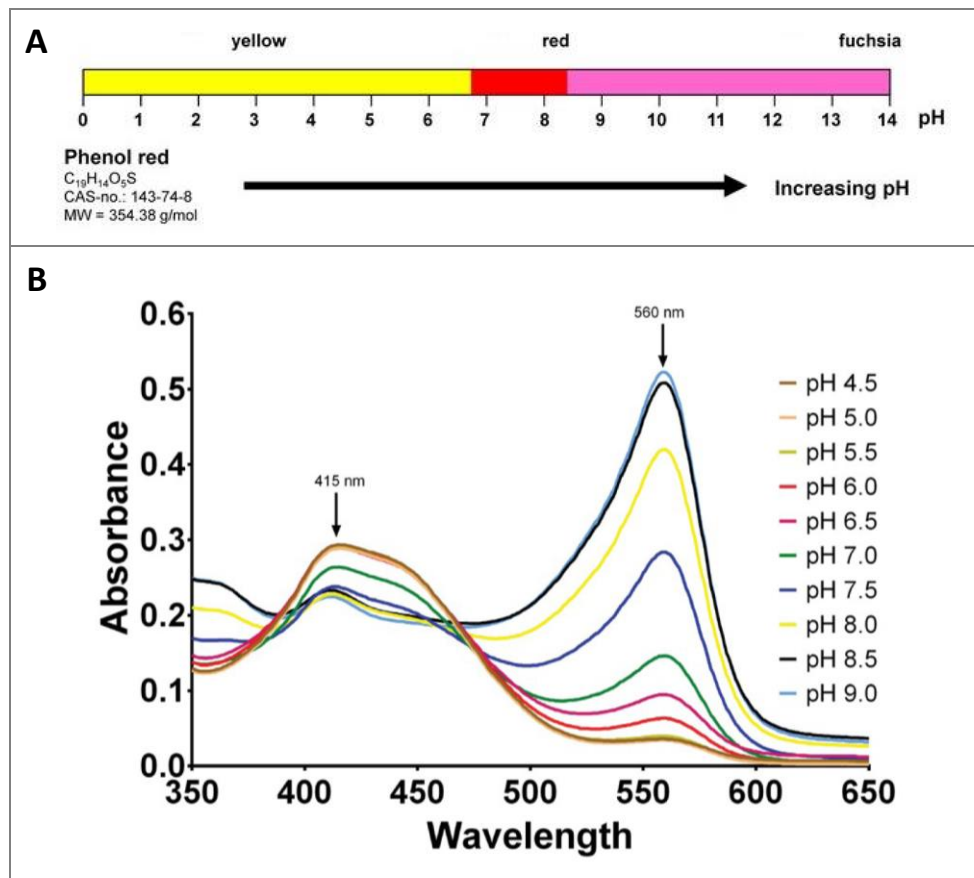


Figure 3.1 Phenol red color properties as a colored pH indicator. A: Color gradient depending on pH scale (Weiskirchen *et al.*, 2023); B) Absorbance spectra of red phenol in yellow cell culture medium (Held, 2022).

3.3. Diverting the Use of a Hand-Operated Tablet Tress Machine to Bioassays: A Novel Protocol to Test “Waste” Insoluble Shell Matrices



*methods
and protocols*



Protocol

Diverting the Use of Hand-Operated Tablet Press Machines to Bioassays: A Novel Protocol to Test ‘Waste’ Insoluble Shell Matrices

Camille Lutet-Toti, Marie Da Silva Feliciano, Nelly Debrosse, Jérôme Thomas, Laurent Plasseraud and Frédéric Marin



<https://doi.org/10.3390/mps7020030>



Protocol

Diverting the Use of Hand-Operated Tablet Press Machines to Bioassays: A Novel Protocol to Test ‘Waste’ Insoluble Shell Matrices

Camille Lutet-Toti ^{1,2,*} , Marie Da Silva Feliciano ¹, Nelly Debrosse ¹, Jérôme Thomas ¹ , Laurent Plasseraud ³ and Frédéric Marin ^{1,*}

¹ UMR CNRS-uB-EPHE 6282 ‘Biogéosciences’, Université de Bourgogne, 21000 Dijon, France

² Dipartimento di Chimica ‘Giacomo Ciamician’, Alma Mater Studiorum Università di Bologna, 40126 Bologna, Italy

³ Institut de Chimie Moléculaire de l’Université de Bourgogne, ICMUB UMR CNRS-uB 6302, 21000 Dijon, France; laurent.plasseraud@u-bourgogne.fr

* Correspondence: camille.lutet-toti@u-bourgogne.fr (C.L.-T.); frederic.marin@u-bourgogne.fr (F.M.); Tel.: +33-7-69-50-27-12 (F.M.)

Abstract: To mineralize their shells, molluscs secrete a complex cocktail of proteins—collectively defined as the calcifying shell matrix—that remains occluded in the exoskeleton. Nowadays, protein extracts from shells are recognized as a potential source of bioactive substances, among which signalling molecules, bactericides or protease inhibitors offer the most tangible perspectives in applied sciences, health, and aquaculture. However, one technical obstacle in testing the activity of shell extracts lies in their high insolubility. In this paper, we present a protocol that circumvents this impediment. After an adapted shell protein extraction and the production of two organic fractions—one soluble, one insoluble—we employ a hand-operated tablet press machine to generate well-calibrated tablets composed of 100% insoluble shell matrix. FT-IR monitoring of the quality of the tablets shows that the pressure used in the press machine does not impair the molecular properties of the insoluble extracts. The produced tablets can be directly tested in different biological assays, such as the bactericidal inhibition zone assay in Petri dish, as illustrated here. Diverting the use of the hand-operated tablet press opens new perspectives in the analysis of insoluble shell matrices, for discovering novel bioactive components.

Keywords: shell extract; recycling; bioactive factors; insoluble matrix; hand-operated tablet press machine



Citation: Lutet-Toti, C.; Da Silva

Feliciano, M.; Debrosse, N.; Thomas, J.; Plasseraud, L.; Marin, F. Diverting the Use of Hand-Operated Tablet

Press Machines to Bioassays: A Novel Protocol to Test ‘Waste’ Insoluble Shell Matrices. *Methods Protoc.* **2024**, *7*, 30.

<https://doi.org/10.3390/mps7020030>

Academic Editor: Léon Reubsaet

Received: 22 February 2024

Revised: 21 March 2024

Accepted: 26 March 2024

Published: 1 April 2024



Copyright: © 2024 by the authors. Licensee MDPI, Basel, Switzerland.

This article is an open access article distributed under the terms and conditions of the Creative Commons Attribution (CC BY) license (<https://creativecommons.org/licenses/by/4.0/>).

1. Introduction

In Europe, the consumption of shellfish of economic interest, such as oysters, mussels, clams, scallops, or cockles generates huge amounts of waste in the form of empty shells [1]. The partial recycling of this mass-produced by-product consists mostly in applications of low-added value: constituents of concretes [2], dietary supplement for poultry [3], amendment of acidic or heavy metal-contaminated soils [4], and depollution of industrial waters [5]. Yet, shells are not only 100% mineral objects. They are biocomposite materials consisting of the superimposition of two to three calcified layers exhibiting different microstructures, each of them containing about 0.1 to 2% organics, collectively defined as the shell matrix [6]: indeed, when they mineralize their shells, molluscs—through their specialized organ, the mantle—secrete a complex cocktail of proteins and saccharides that interact with the inorganic mineral precursors—calcium and bicarbonate—and remain occluded in the mineral phase [6]. This shell matrix is usually retrieved by dissolving the mineral phase. Over decades, thousands of fundamental studies have biochemically characterized the shell matrix, in particular the protein moieties. While early works from the seventies/eighties evidenced the pivotal role of shell proteins in regulating mineral

deposition [7,8], only recently was it discovered that this mixture may display numerous additional molecular and cellular key functions in connection with biomineralization [9].

Indeed, recent high-throughput screening, combining transcriptomics on mollusc mantle and proteomics on shell extracts, has shown that the shell matrix is composed of tens—not to say hundreds—of proteins that can be classified in several families [9–11]. While many proteins, in particular those with low-complexity domains (LCDs) are orphans of functions, others exhibit amino acid sequences that bring them close to bioactive factors of interest, such as bactericides, signalling molecules or protease inhibitors [12,13]. Today, shell proteins, and more generally shell macromolecules, are considered as a potential reservoir of useful substances, not only in biomaterials domain, but also in health research, aquaculture, and zootechnics [9,14].

One major drawback of shell protein extracts is that many of them are totally insoluble, and therefore not easily—not to say, not at all—testable for their biological properties. To give a striking example, the organic matrix of nacre—the most iconic and studied mollusc shell microstructure so far—represents between 1 and 2% of nacre weight, but 90% of this matrix is insoluble [15] in standard aqueous decalcifying solutions (acids, or EDTA), and consequently, this fraction is ignored for further analysis of its *in vitro* bioactivity. In other words, only 10% of nacre matrix, corresponding to the most soluble moieties, is currently used for testing its effects in the presence of cells [16,17].

In this paper, we present a protocol that circumvents this drawback. We have developed a mild shell matrix extraction that identifies two fractions: an acetic acid-soluble one and an acetic acid-insoluble one. While the soluble fraction can be further subdivided into smaller fractions according to different ultrafiltration cutoffs, the insoluble fraction, after lyophilization, can be transformed in tablets, owing to a hand-operated tablet press machine, and the resulting tablets can be tested *in vitro*, in Petri dishes, for their effects in the presence of cells, here, a marine pathogenic vibrio strain. FT-IR monitoring shows that the pressure used for making tablets does not affect the chemical functions of the insoluble matrix. We suppose that our protocol is extremely useful for testing in bulk all shell matrix components—and not only soluble ones—in order to discover novel biological properties of interest in aquaculture and health.

2. Materials and Methods

2.1. Material Samples

The four species selected for the study are all commercially available; they live along the coasts of Western Europe. As bivalves, they are not subject to the European Directive 2010/63/UE relating to the protection of animals used for scientific purposes. The shells were collected from fresh living animals in a local supermarket in Quetigny, Burgundy, France. They include the Pacific edible oyster (*Magallana gigas*, formerly *Crassostrea gigas*), the warty venus (*Venus verrucosa*), the Manila clam (*Venerupis philippinarum*), and the common cockle (*Cerastoderma edule*).

Shells were carefully sorted visually and specimens with no shell defects, and no epibionts were chosen. The selected shells were opened with a knife and the soft tissues were scrupulously removed. In particular, the junctions between pallial muscles and shells were carefully scrubbed, as well as the outer shell surfaces. The leathery hinges were removed with a knife and the shells were incubated at room temperature in an aqueous solution of sodium hypochlorite (0.26% active chlorine, 10 times dilution) for two days, on a laboratory rotary shaker, with at least four changes in solution. Shells were then extensively rinsed with tap water and dried. Dried shells were mechanically cleaned: in particular, the hinges were cut from the shells with a diamond saw (Dremel rotary saw). In addition, all remains of epibionts and periostracum (if still present) were removed by abrasion with a dental drill. Shells were cleaned again with dilute sodium hypochlorite (0.26% active chlorine) for hours then thoroughly rinsed with double distilled water and dried at 40 °C. Shells were coarsely crushed in a mechanical jaw-crusher (BB200 model, Retsch, Eragny, Luxemburg), and fragments were further milled with an agate mortar grinder (Pulverisette

2 model, Fritsch, Idar-Oberstein, Germany) and the resulting powder was sieved to 200 μm . The powders were stored in dry containers for further use.

2.2. Shell Matrix Extraction

For each species, the powder (25 g) was resuspended in double-distilled water (DDW, around 20 mL) in a glass beaker and decalcified overnight by addition of 200 μL of 10% (vol/vol) glacial acetic acid, every 5 s, to reach a final volume of 1 L. The solution was constantly stirred with a magnetic glass bar. The resulting clear solution was centrifuged at $3893 \times g$ for 20 min. The pellet, containing the acid-insoluble matrix (AIM), was collected and resuspended in DDW before being centrifuged (10 min, $3893 \times g$). Five cycles of resuspension–centrifugation were performed to ensure the removal of all remaining salts, acetic acid, and soluble matrix. One drop of the 5th supernatant was put on pH indicator paper to check that the solution was around neutrality. All the intermediate supernatants were added to the initial supernatant. The collected AIM was then lyophilised in a freeze-dryer (Telstar Cryodos, Terrassa, Spain) after a preliminary quick-freeze in liquid nitrogen.

The supernatant, defined as the acid-soluble matrix (ASM), was further filtered on a 5 μm membrane mounted on a Nalgene filtration device connected to a pump (Millipore France, Molsheim). The ASM was then ultrafiltered in an ultrafiltration stirred cell (Millipore, model 8400, 400 mL) against a membrane of 10 kiloDalton (kDa) cutoff. Both retentate (>10 kDa) and filtrate (<10 kDa) were collected, and the filtrate was ultrafiltered again on a 1 kDa cutoff membrane. The new retentate (>1 kDa and <10 kDa) was collected. In one case (*Venerupis philippinarum*), since the 10 kDa filtrate was too viscous, i.e., generating a low flow rate, an intermediate ultrafiltration cutoff of 3 kDa was added. All soluble fractions (>1 kDa) were dialyzed against ultra-pure water, with a minimum of 5 water changes (over two days), in a ready-to-use dialysis bag (SpectraP/Por 6 dialysis membrane, pre-wetted RC tubing) of 1 kDa cutoff.

All soluble matrices including fractions of ASM >10 kDa, of $1 < \text{ASM} < 10$ kDa, and, for *V. philippinarum*, of $1 < \text{ASM} < 3$ kDa and $3 < \text{ASM} < 10$ kDa, were freeze-dried similarly to the AIMS. After complete lyophilisation, all fractions (AIMs and ASMs) were weighed on a precision balance (Quintix35-1S model, precision 0.01 mg, Sartorius, Göttingen, Germany) for their quantification.

2.3. Hand-Operated Tablet Press for AIMS

The freeze-dried AIM was transformed into pellets with a hand-operated tablet press (HP-mini, LC-Instru, Lisses, France) by using a 5 mm diameter piston mould set (Maassen Spektroskopie, Möglingen, Germany). Briefly, chips of freeze-dried AIM were manually disaggregated with a clean spatula and subsequently homogenized in an agate mortar before being introduced into the piston mould set. A pressure of one ton was applied to produce tablets of 2 to 5 mg, which were weighed on the same precision balance (as for lyophilisates) then stored individually, in dry conditions, in 24-well polystyrene flat bottom microplates (Nunc, Roskilde, Denmark) before use.

2.4. Fourier Transform Infra-Red Spectroscopy of AIMS

FT-IR spectroscopy was performed to monitor whether the applied pressure (1 ton) did not denature the extracts nor modify their chemical functions. To this end, for each species, FT-IR spectra were acquired on AIM samples that were not submitted to pelletisation and on tablet-formed AIMS. An FT-IR Bruker Alpha spectrometer was used (ICMUB, Dijon, France): this apparatus was equipped with an Attenuated Total Reflectance (ATR) ALPHA-P device comprising a mono-reflection diamond crystal. Spectra were recorded in a $4000\text{--}375$ cm^{-1} wavenumber range, with 24 scans at a spectral resolution of 4 cm^{-1} . The qualitative assignment of absorption bands was performed by comparison with previous spectra descriptions, achieved by our group or available in the literature [12,18]. We made an ultimate check on the potential effect of a high pressure on the FTIR spectra by making tablets with a hand-operated tablet press at high pressure (9 tons, 5 min, Atlas press, Specac,

Orpington, UK) in the presence of potassium bromide (0.5% AIM in KBr) and few spectra were acquired in transmittance mode.

2.5. Antibacterial Assay

The produced AIM pellets were unconventionally used in disk diffusion assays, also called radial diffusion assay, adapted from the Kirby–Bauer Test [19] aiming at screening a large set of substances for their putative antibacterial properties. The test was performed on standard Petri dishes (94 mm diameter, Greiner Bio-One, Courtaboeuf, France). Before use, the pellets were sterilised under UV lights for 20 min on each side. *Aliivibrio salmonicida* (CIP103166T, Centre de Ressources Biologiques de l'Institut Pasteur, Paris, France), a marine fish pathogen, was grown in a liquid culture (marine broth 2216 DIFCO), lightly stirred for 11 days at 12 °C. Once in log phase, the culture suspension (600 µL) was spread using the “spread plate method” on marine agar (marine agar 2216 DIFCO). After absorption of the bacterial suspension by the medium, the sterile AIM pellets were evenly distributed on top of the agar. As a positive control, 7 mm diameter disks containing the Vibrio static agent O.129 (2,4-Diamino-6,7-diisopropylpteridine, ref. 53872, lot 64478673, 500 µg per disk, Bio-Rad, Hercules, CA, USA) were added to the test. The plates were allowed to incubate upside-down for 9 days at 12 °C. Inhibitions zones were observed around the pellets and their diameters were measured. Macrophotos were obtained with a Digital Nikon D750 Camera (Nikon, Tokyo, Japan), equipped with AF-S VR Micro-Nikkor 105 mm f/2.8 G IF-ED or AF-P DX Nikkor 18–55 mm f/3.5–5.6 G VR objectives. The test was reproduced in triplicate.

3. Results

3.1. Shell Matrix Extraction

The flow chart of Figure 1 indicates the succession of steps that allow the obtaining of different organic fractions, depending, firstly, on their solubility (soluble vs. insoluble), and secondly—only for the soluble fraction—on their molecular weights when ultrafiltered on filters of different cutoffs (high-molecular-weight soluble fraction vs. low-molecular-weight soluble fraction). Two soluble fractions were obtained for *C. edule*, *M. gigas* and *V. verrucosa*, and three for *V. philippinarum*.

The quantification of the extracted shell matrices, obtained by weighing of the lyophilisates, is indicated in Table 1. The obtained matrix percentages vary between 0.08% (*M. gigas*) and 0.55% (*M. gigas*) of the total shell powder. In other words, this represents 0.8 mg to 5.5 mg of matrix per gram of shell powder, respectively. Interestingly, the percentage of AIM compared with the total matrix (AIM + all ASM fractions) varies from 55% (*V. verrucosa*) to almost 78% (*V. philippinarum*). In all four examples, this represents the preponderant part of the total shell matrix.

Table 1. Amounts of organic matrix in the shell of the four tested bivalves.

Mollusc Species	Mineralogy and Shell Microstructure *	Matrix Fraction	Mean Matrix Quantity (mg) per Gram of Shell Powder	% Matrix in Shell Powder	% AIM/Total Matrix
<i>Magallana gigas</i> Pacific oyster	 CALCITIC OL: prismatic IL: foliated + chalky lenses	AIM	4.35	0.57%	76.74%
		ASM > 10 kDa	1.14		
		1 < ASM < 10 kDa	0.18		
<i>Cerastoderma edule</i> Common cockle	 ARAGONITIC OL: crossed-lamellar IL: complex crossed-lamellar	AIM	0.51	0.08%	65.25%
		ASM > 10 kDa	0.10		
		1 < ASM < 10 kDa	0.18		

Table 1. Cont.

Mollusc Species	Mineralogy and Shell Microstructure *	Matrix Fraction	Mean Matrix Quantity (mg) per Gram of Shell Powder	% Matrix in Shell Powder	% AIM/Total Matrix
<i>Venerupis philippinarum</i> Manila clam 	ARAGONITIC OL: composite prismatic IL: crossed-lamellar becoming homogeneous	AIM	1.18	0.15%	77.96%
		ASM > 10 kDa	0.22		
		3 < ASM < 10 kDa	0.09		
		1 < ASM < 3 kDa	0.03		
<i>Venus verrucosa</i> Warty venus 	ARAGONITIC OL: composite prismatic ML: crossed-lamellar IL: homogeneous	AIM	1.11	0.20%	55.23%
		ASM > 10 kDa	0.72		
		1 < ASM < 10 kDa	0.18		

* The mineralogy and shell microstructures are indicated in the second column. Abbreviations: OL: outer layer; ML: middle layer; IL: internal layer; AIM: acetic acid-insoluble matrix; ASM: acetic acid-soluble matrix.

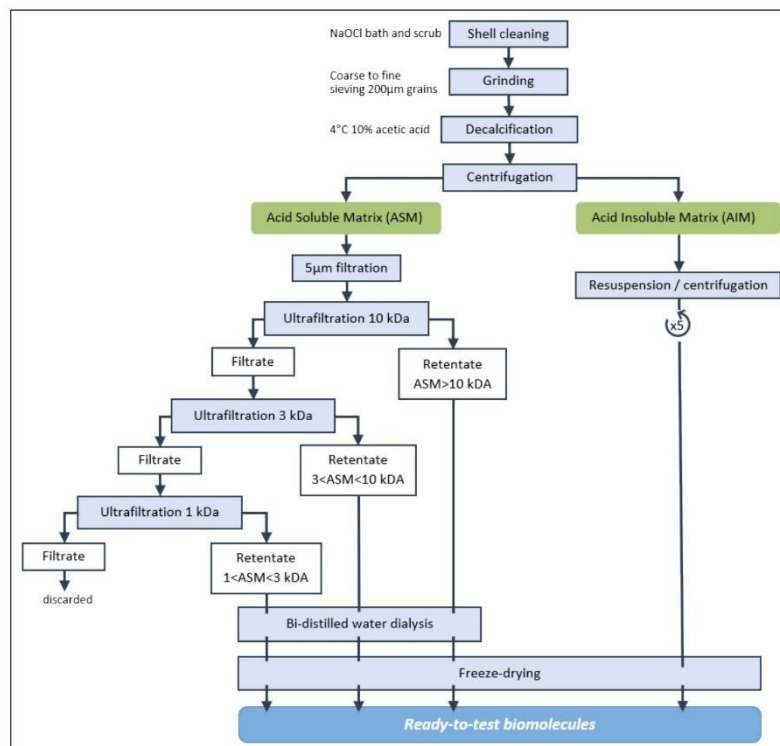


Figure 1. Flow chart of the extraction steps of shell matrices (acetic acid-soluble and insoluble). The ASM was passed in successive ultrafiltration filters of decreasing cutoff. The different ASMs and the AIM were *in fine* freeze-dried.

3.2. Hand-Operated Tablet Press for Insoluble Matrix

As shown in Figure 2, the use of a hand-operated tablet press machine generated tablets of AIM, of weights between 3.2 and 4.6 mg. The tablets were homogeneous, compact, and did not disaggregate. They could be handled easily with forceps and could be sterilized on each side by UV-light. Depending on the species considered, and taking into account

the loss when manipulating the AIM lyophilisates, 100 g of initial shell powder allowed us to make between 13 (*C. edule*) and 123 (*M. gigas*) tablets.



Figure 2. Pelletisation process. (A) Hand-operated tablet press machine, showing a force of 1 ton put onto the AIM to make a tablet (PH-mini, LC-Instru). (B) Freeze-dried AIM extracted from *Cerastoderma edule*, next to the pellet mould set. (C) Freshly produced AIM pellet of *C. edule*.

3.3. Fourier Transform Infrared Spectroscopy

Figure 3 illustrates the results obtained from AIM fractions of the four species. The four tested species exhibit an overall similarity of their IR spectral signature; i.e., most of the absorption bands are shared by all samples. The main differences are found in the 1700–400 cm^{-1} domain, where the relative amplitudes of the absorption bands can be rather dissimilar from species to species. Among the shared absorption bands, one finds the characteristic bands of proteins: the broad one between 3290 and 3260 cm^{-1} corresponding to amide A stretching ($\nu\text{N-H}$), the amide I band ($\nu\text{C=O}$ stretching) between 1632 and 1648 cm^{-1} , the amide II bands ($\nu\text{C-N}$ stretching) between 1534 and 1514 cm^{-1} , and the amide III band ($\nu\text{C-N}$ stretching, δNH bending) around 1226/1233 cm^{-1} . In the latter case, we cannot discount that it combines to the $\nu\text{S=O}$ vibration, frequently assigned to the presence of sulphate groups. The shoulders visible around 3500 cm^{-1} , and more or less pronounced depending on the sample (in particular *Magallana* and *Venus*), suggest the presence of νOH absorptions. In addition to infrared bands of peptide linkage, all spectra present also $\nu\text{C-O}$ broad absorption bands specific to carbohydrates, between 1000 and 1080 cm^{-1} and the band around 2920–2930 cm^{-1} , characteristic of ($\nu\text{C-H}$) stretching vibrations. Other absorption bands of interest observed in all samples are located in the [1445–1390 cm^{-1}] zone, which make a doublet in *Cerastoderma*, *Venerupis*, and *Venus*. One of these absorption bands is often attributed to carboxylate groups [$\nu_{\text{sym}}(\text{COO}^-)$] [12].

Interestingly, when comparing the FT-IR spectra obtained from AIM samples not submitted to pelletisation to those after pelletisation, we observe that they are entirely superimposable, for each of the four species. This clearly suggests that the hand-operated tablet press treatment does not affect the chemical structure of the insoluble extracts.

As an ultimate check, we verified if a nine-times-higher pressure (9 tons, 5 min) than the one used for making our AIM tablets had an effect on the IR spectral properties of the extract. The control tablets, made with KBr and AIM, were read in transmittance mode. No modification of the spectra was recorded but was not shown here.

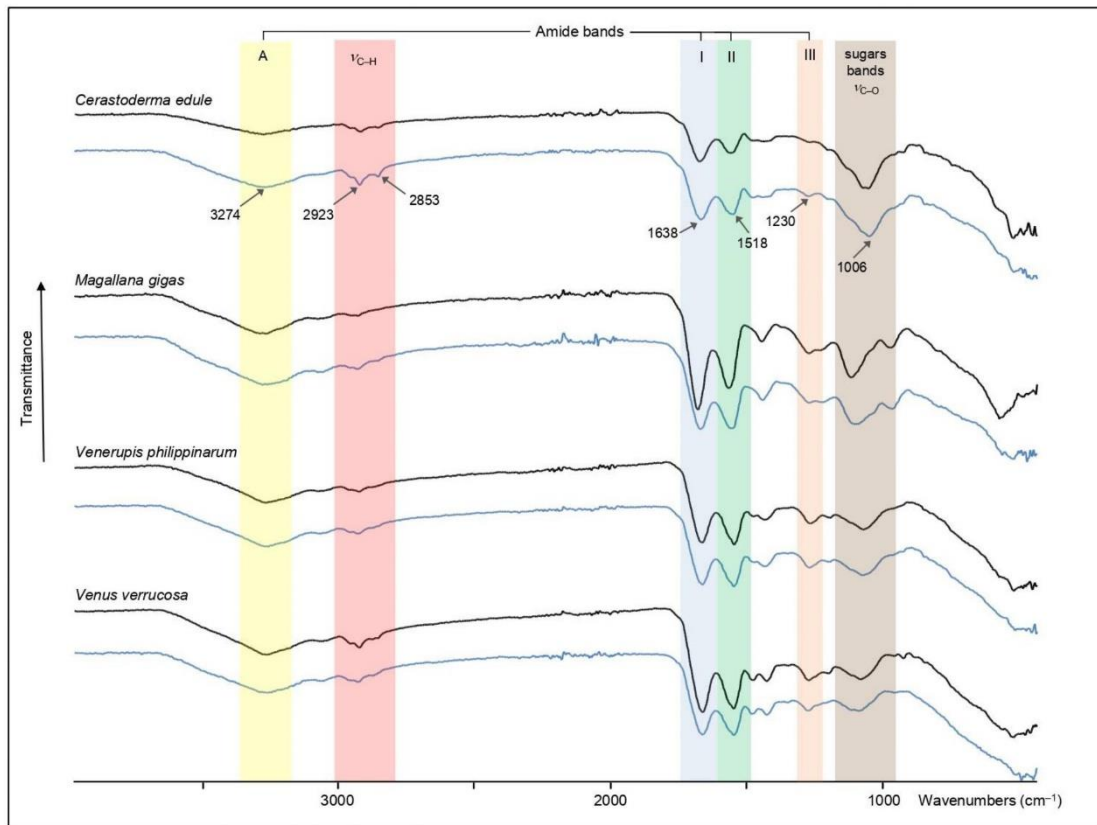


Figure 3. FT-IR spectra of the AIMs of the four tested bivalve shell matrices. The AIMs were monitored in two conditions: before (black curve) and after (blue curve) pelletisation. Note that the pelletisation process did not modify the IR signature of the spectra. A, I, II and III correspond to the different amide absorption bands of proteins.

3.4. Antibacterial Assay on AIMs

Figure 4 shows the effect of the four AIM tablets on the growth of *Aliivibrio salmonicida*. The *Cerastoderma edule* tablet (Figure 4A), as well as the *Magallana gigas* tablet (Figure 4B), exerts an inhibitory effect, since this bacterial strain does not grow in contact to the tablet; in other words, a clear growth inhibition zone is visible. The effect is stronger with *C. edule* AIM, and moderate for *M. gigas*. On the contrary, *Venerupis philippinarum* (Figure 4C) and *Venus verrucosa* (Figure 4D) do not exhibit any inhibitory effect. The control with *Vibrio* static agent O.129 shows a large inhibition zone. The test, performed in triplicate, gave consistent and reproducible results.

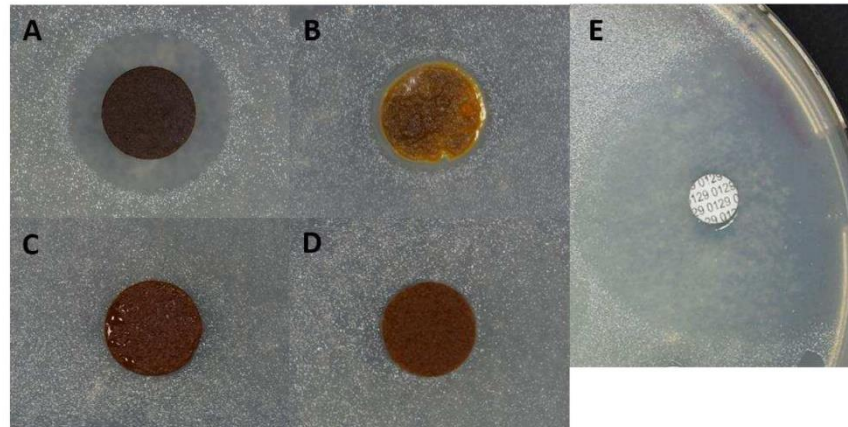


Figure 4. Antibacterial assays of AIM tablets on *Aliivibrio salmonicida* cultures grown on marine agar. (A) *Cerastoderma edule* AIM; (B) *Magallana gigas* AIM; (C) *Venerupis philippinarum* AIM; (D) *Venus verrucosa* AIM. (E) positive control with vibrio static agent O.129 (Bio-Rad). While (C,D) give negative signals, (A,B) induce inhibition zones, and show bactericidal ability against *A. salmonicida*. The positive control shows a large inhibition zone.

4. Discussion

In this paper we present a novel manner of utilizing insoluble matrices extracted from diverse mollusc shells of economic interest. From a theoretical viewpoint, our protocol, based on the complete decalcification of shell powder, allows the extraction of all the organics contained in shells, whatever they are (proteins, polysaccharides) and whatever their state in water or in dilute acid (soluble vs. insoluble). Interestingly, by using different ultrafiltration cutoffs, most of the acetic acid-soluble organic fractions (ASMs) are collected with a minimal loss and can be further analysed. The exception is the fraction inferior to 1 kDa, corresponding to very short peptides (fewer than ten amino acid residues on average) that pass through the 1 kDa ultrafiltration membrane: there is no easy way to concentrate this fraction and separate it from the free inorganic ions resulting from the decalcification, including calcium, carbonate, bicarbonate, and acetate. However, previous research suggests that the fraction below 1 kDa is extremely minor in comparison to the other soluble ones of a molecular mass above 1 kDa [20].

The main focus of this work is the acetic acid-insoluble fraction (AIM) and its subsequent use. Because of its high insolubility, the AIM is neither characterized biochemically in detail nor utilized in biological assays: most of the literature dealing with the bioactivity of shell extracts concerns only soluble fractions [16,17,21,22]. The peculiar insolubility property of AIM is known since the very first chemical analysis performed on shells (the ‘conchioline’ of Frémy) [23] and has been underlined many times [24]. Strong chaotropic solvents like guanidinium chloride, sodium dodecyl sulphate, or urea may help to solubilise the AIM, but its solubilisation is very partial; i.e., an important insoluble residue still remains after the treatment. Furthermore, these denaturing solvents should be proscribed when one wants to test the biological activity of the extracts.

From a cellular and molecular viewpoint, although poorly documented, it is admitted that the partial insolubilisation of the matrix occurs just after the secretion of water-soluble precursors in the space between the mantle and the shell mineralization front [25]. These soluble precursors are putatively cross-linked/polymerized/sclerotized. Among the different molecular mechanisms involved, one may cite an oxidative process called ‘quinone-tanning’, which occurs on the DOPA-containing proteins [26]. Another mechanism involves the secretion of silk-fibroin-like proteins [27], forming, together with chitin, a gel that hardens by expelling water molecules and by making intermolecular cross-linking,

to form chitin–protein complexes [24]. The end product, the AIM, is strong, flexible, and hydrophobic and is often organized in sheaths around crystallites. The presence of the sheaths, together with the ordered spatial organization of crystallites, precludes the propagation of cracks in the mineralized layer and contributes to reinforce the mechanical properties of the whole shell.

It is striking to observe that, in molluscs, the amount of shell matrix varies a lot, together with the ratio between soluble and insoluble fractions. For one given mollusc, these variations seem to depend on two parameters: its phylogenetic position in the mollusc tree and its shell microstructures. For example, most pteriomorphid bivalves are known to have shells with a higher organic matrix content (0.5% to more than 1%), while those of all caenogastropods are very poor in organics (between 0.1 and 0.01%) [28]. It is also known that shell microstructures [29] like calcitic prisms or nacre (both present in the edible mussel, or in the pearl oyster) contain a high proportion of matrix (usually more than 1% of the shell weight) and that this matrix is predominantly insoluble [15]. At the opposite end, other types of microstructures, such as some crossed-lamellar ones, are usually far less rich and exhibit mostly soluble components [28]. The four bivalves of commercial interest treated here represent one pteriomorphid (*M. gigas*) and three heterodonts (*C. edule*, *V. philippinarum*, *V. verrucosa*). We noticed a relatively high amount of organic matrix for the first one (0.55%, i.e., 5.5 mg of matrix per gram of shell powder), a species that exhibits a calcitic shell mostly composed of foliated and chalky microstructures, with a thin outer prismatic layer [29]. The amount of organics extracted from this species lies in the range indicated above [30].

The three heterodont bivalves (*V. verrucosa*, *V. philippinarum*, *C. edule*) exhibit lower amounts of organics (0.2% to less than 0.08%, meaning 2 to 0.8 mg of organics per gram of shell powder). These three specimens are entirely aragonitic and are composed of different combinations of composite prismatic, crossed-lamellar, complex crossed-lamellar, and homogeneous microstructures (Table 1). The amounts of organics extracted from these three species are congruent with earlier findings on heterodont bivalves [30]. Interestingly, we found out that, for the four species, the acetic acid-insoluble matrix (AIM) represents 55 to almost 78% of the total shell matrix, that is to say, quantitatively, the most important part of the matrix. In itself, this finding fully justifies focusing on this shell extract which is rarely—not to say never—utilized in bioactivity assays. In addition to this fact, proteomic investigations conducted by us [9,12,15] have shown that mollusc shell AIMs contain a complex cocktail of different proteins (up to few hundreds). Usually, for a given species, the AIM protein content partly overlaps with that of the corresponding ASM [31]. However, we also observed that AIMs contain usually more proteins than ASMs (F.M., in preparation). This constitutes another argument to find a manner to exploit in an optimized way the diversity of the protein content of shell AIMs.

To this end, we have diverted the use of a hand-operated tablet press machine to generate calibrated AIM tablets. This represents undoubtedly the best and easiest way to test shell AIMs in biological assays. Hand-operated tablet press machines are used normally for generating potassium bromide (KBr) tablets in standard FT-IR spectroscopy in transmittance mode, or for making drug tablets in pharmaceutical studies. At first sight, generating a high pressure (1 ton or more) for making tablets that can be easily manipulated with tweezers does not affect the AIM chemical properties, as its spectral IR signatures, checked and validated by FT-IR before and after pelletisation, did not show any variation and were fully superimposable. Our attempt to test the efficiency of the insoluble extracts in a hardly modified Kirby–Bauer test was successful, since two of the tested AIM tablets, that of *Cerastoderma edule* (the common cockle) and of *Magallana gigas* (the edible oyster), exhibited bactericidal capacity against the marine strain *Aliivibrio salmonicida*, a pathogenic agent responsible for cold-water vibriosis in salmon. In consequence, our paper has demonstrated two points: (1) the feasibility of using shell AIM tablets in biological assays; (2) the capability of shell AIMs to induce different responses in biological assays. This clearly indicates that our ‘tablet’ approach is adapted to the screening of a large array of

shell waste products from the shellfish industry, heliculture, and pearl farming, in the perspective of discovering novel useful molecules of natural origin.

In conclusion, this paper emphasizes the utilisation of insoluble shell matrices, which are usually discarded in most applications so far. We are convinced that transforming ‘useless’ shell AIMS in tablets opens new possibilities for developing adapted bioactivity assays, such as the bactericidal assay illustrated here. Besides their relative abundance in many shells, AIM extracts are easier to produce than ASMs, since they require only the dissolution of the mineral phase, centrifugation, and thorough rinsing before freeze-drying. This line of research is one part of a general long-term strategy that follows the rules of green (sustainable) chemistry and aims at recycling and adding value to quantitatively abundant waste sea products, emptied shells from commonly consumed molluscs. In addition, our complete protocol, from the extraction to the production of tablets, employs standard, cheap, and highly accessible chemicals (sodium hypochlorite, acetic acid) and simple inexpensive processes (centrifugation, ultrafiltration).

Author Contributions: C.L.-T.: conception of the study, experimental work, data analysis, original draft writing, conception of figures, funding. M.D.S.F.: assistance in experimental work. N.D.: assistance in experimental work. J.T.: assistance in experimental work. L.P.: FTIR analysis, original draft writing. F.M.: conception of the study, project administration including funding acquisition and supervision, data analysis, original draft writing, review, and editing. All authors have read and agreed to the published version of the manuscript.

Funding: CLT is the recipient of a PhD fellowship under joint-supervision between Université de Bourgogne (uB) and Università di Bologna Alma Mater Studiorum (UniBo). The research leading to these results has been conceived under the International PhD Program “Innovative Technologies and Sustainable Use of Mediterranean Sea Fishery and Biological Resources” (www.FishMed-PhD.org). This study represents partial fulfilment of the requirements for the Ph.D. thesis of CLT at the FishMed PhD Program (University of Bologna, Italy). In addition, CLT was supported by a one-off grant from AFFDU (Association des Femmes Françaises Diplômées de l’Université) in 2022 and an award from the Société Française de Biologie des Tissus Minéralisés (SFBTM) and from the Fondation Arthritis, in May 2023. Other supports to FM include the following: (1) the MAELSTROM project (les MATricEs coquILlières bacTéRicides au secOurs des géoMatériaux) from TELLUS-INTERRVIE program (CNRS, 2022); (2) the PRELUDE project (Peptides antimicrobiens dEs coquILles de mollUSques D’intérêt Economique) financed by Observatoire des Sciences de l’Univers (OSU) Theta, Besançon, in 2023; (3) the MAELSTROM-bis project, financed by the TELLUS-INTERRVIE program from CNRS, in 2024.

Conflicts of Interest: The authors declare no conflict of interest.

References

- Summa, D.; Lanzoni, M.; Castaldelli, G.; Fano, E.A.; Tamburini, E. Trends and opportunities of bivalve shells’ waste valorization in a prospect of circular blue bioeconomy. *Resources* **2022**, *11*, 48. [[CrossRef](#)]
- Bourdot, A.; Martin-Cavaillé, C.; Vacher, M.; Honorio, T.; Sebaibi, N.; Bennacer, R. Microstructure and durability properties of concretes based on oyster shell co-products. In Proceedings of the 75th RILEM Annual Week 2021, Merida, Mexico, 29 August–3 September 2021; Volume 40, pp. 65–73.
- Alm, M.; Tauson, R.; Wall, H. Mussel shells as an environment enrichment and calcium source for floor-housed laying hens. *J. Appl. Poult. Res.* **2017**, *26*, 159–167. [[CrossRef](#)]
- Zeng, T.; Guo, J.; Li, Y.; Wang, G. Oyster shell amendment reduces cadmium and lead availability and uptake by rice in contaminated paddy soil. *Environ. Sci. Pollut. Res.* **2022**, *29*, 44582–44596. [[CrossRef](#)]
- Weerasooriyagedra, M.S.; Kumar, S.A. A review of utilization of Mollusca shell for the removal of contaminants in industrial waste water. *Int. J. Sci. Res. Public* **2018**, *8*, 282–287.
- Suzuki, M.; Nagasawa, H. Mollusk shell structures and their formation mechanism. *Can. J. Zool.* **2013**, *91*, 349–366. [[CrossRef](#)]
- Weiner, S.; Hood, L. Soluble proteins of the organic matrix of mollusc shells: A potential template for shell formation. *Science* **1975**, *190*, 987–989. [[CrossRef](#)] [[PubMed](#)]
- Wheeler, A.P.; George, J.W.; Evans, C.A. Control of calcium carbonate nucleation and crystal growth by soluble matrix of oyster shell. *Science* **1981**, *212*, 1397–1398. [[CrossRef](#)]
- Marin, F. Mollusk shellomes: Past, present and future. *J. Struct. Biol.* **2020**, *212*, 107583. [[CrossRef](#)]
- Sleight, V.A.; Marie, B.; Jackson, D.J.; Dyrzynda, E.A.; Marie, A.; Clark, M.S. An Antarctic molluscan biomineralisation tool-kit. *Sci. Rep.* **2016**, *6*, 36978. [[CrossRef](#)]

11. Herlitzte, I.; Marie, B.; Marin, F.; Jackson, D.J. Molecular modularity and asymmetry of the molluscan mantle revealed by a gene expression atlas. *Gigascience* **2018**, *7*, giy056. [[CrossRef](#)]
12. Oudot, M.; Neige, P.; Ben Shir, I.; Schmidt, A.; Strugnelli, J.M.; Plasseraud, L.; Broussard, C.; Hoffmann, R.; Lukeneder, A.; Marin, F. The shell matrix and microstructure of the Ram's horn squid: Molecular and structural characterization. *J. Struct. Biol.* **2020**, *211*, 107507. [[CrossRef](#)] [[PubMed](#)]
13. Shimizu, K.; Negishi, L.; Ito, T.; Touma, S.; Matsumoto, T.; Awaji, M.; Kurumizaka, H.; Yoshitake, K.; Kinoshita, S.; Asakawa, S.; et al. Evolution of nacre- and prisms-related shell matrix proteins in the pen shell, *Atrina pectinata*. *Comp. Biochem. Physiol. D—Genom. Proteom.* **2022**, *44*, 101025. [[CrossRef](#)] [[PubMed](#)]
14. Magnabosco, G.; Giuri, D.; Di Bisceglie, A.P.; Scarpino, F.; Fermari, S.; Tomasini, C.; Falini, G. New Material perspective for waste seashells by covalent functionalization. *ACS Sustain. Chem. Eng.* **2021**, *9*, 6203–6208. [[CrossRef](#)]
15. Marin, F.; Marie, B.; Benhamada, S.; Silva, P.; Le Roy, N.; Guichard, N.; Wolf, S.; Montagnani, C.; Joubert, C.; Piquemal, D.; et al. 'Shellome': Proteins involved in mollusk shell biomineralization-diversity, functions. In *Recent Advances in Pearl Research: Proceedings of the International Symposium on Pearl Research 2011*; Watabe, S., Maeyama, K., Nagasawa, H., Eds.; Terrapub: Tokyo, Japan, 2013; pp. 149–166.
16. Mouriès, L.P.; Almeida, M.-J.; Milet, C.; Berland, S.; Lopez, E. Bioactivity of nacre water-soluble organic matrix from the bivalve mollusk *Pinctada maxima* in three mammalian cell types: Fibroblasts, bone marrow stromal cells and osteoblasts. *Comp. Biochem. Physiol. B—Biochem. Mol. Biol.* **2002**, *132*, 217–229. [[CrossRef](#)] [[PubMed](#)]
17. Rousseau, M.; Bouzalguet, H.; Biagianni, J.; Duplat, D.; Milet, C.; Lopez, E.; Bédouet, L. Low molecular weight molecules of oyster nacre induce mineralization of the MC3T3-E1 cells. *J. Biomed. Mater. Res. Part A* **2008**, *85A*, 487–497. [[CrossRef](#)] [[PubMed](#)]
18. Barth, A. Infrared spectroscopy of proteins. *Biochim. Biophys. Acta* **2007**, *1767*, 1073–1101. [[CrossRef](#)] [[PubMed](#)]
19. Bauer, A.W.; Kirby, W.M.M.; Sherris, J.C.; Turck, M. Antibiotic susceptibility testing by a standardized single disk method. *Am. J. Clin. Pathol.* **1966**, *45*, 493–496. [[CrossRef](#)]
20. Bédouet, L.; Rusconi, F.; Rousseau, M.; Duplat, D.; Marie, A.; Dubost, L.; Le Ny, K.; Berland, S.; Péduzzi, J.; Lopez, E. Identification of low molecular weight molecules as new components of the nacre organic matrix. *Comp. Biochem. Physiol. B Biochem. Mol. Biol.* **2006**, *144*, 532–543. [[CrossRef](#)]
21. Sud, D.; Doumenc, D.; Lopez, E.; Milet, C. Role of water-soluble matrix fraction, extracted from the nacre of *Pinctada maxima*, in the regulation of cell activity in abalone mantle cell culture (*Haliotis tuberculata*). *Tissue Cell* **2001**, *33*, 154–160. [[CrossRef](#)]
22. Milet, C.; Berland, S.; Lamghari, M.; Mouriès, L.; Jolly, C.; Borzeix, S.; Doumenc, D.; Lopez, E. Conservation of signal molecules involved in biomineralization control in calcifying matrices of bone and shell. *Comptes-Rendus Palevol* **2004**, *3*, 493–501. [[CrossRef](#)]
23. Frémy, M.E. Recherches chimiques sur les os. *Ann. Chim. Phys.* **1855**, *43*, 47–107.
24. Grégoire, C. Structure of the molluscan shell. In *Chemical Zoology, Vol. VII: Mollusca*; Florin, M., Scheer, B.T., Eds.; Academic Press: New York, NY, USA, 1972; pp. 45–102.
25. Wilbur, K.M.; Saleuddin, A.S.M. Shell formation. In *The Mollusca, Vol. 4 Physiology, Part 1*; Saleuddin, A.S.M., Wilbur, K.M., Eds.; Academic Press: New York, NY, USA, 1983; pp. 235–287.
26. Almeida, M.; Machado, J.; Coelho, M.V.; da Silva, P.S.; Coimbra, J. L-3,4-dihydroxyphenylalanine (L-DOPA) secreted by oyster (*Crassostrea gigas*) mantle cells: Functional aspects. *Comp. Biochem. Physiol. B Biochem. Mol. Biol.* **1998**, *120*, 709–713. [[CrossRef](#)]
27. Levi-Kalisman, Y.; Falini, G.; Addadi, L.; Weiner, S. Structure of the nacreous organic matrix of a bivalve mollusk shell examined in the hydrated state using Cryo-TEM. *J. Struct. Biol.* **2001**, *135*, 8–17. [[CrossRef](#)] [[PubMed](#)]
28. Weiner, S.; Traub, W.; Lowenstam, H.A. Organic matrix in calcified exoskeletons. In *Biomineralization and Biological Metal Accumulation—Biological and Geological Perspectives*; Westbroek, P., de Jong, E.W., Eds.; D. Reidel Publishing Company: Dordrecht, Holland, 1983; pp. 205–224.
29. Carter, J.G. (Ed.) *Skeletal Biomineralization: Patterns, Processes and Evolutionary Trends*; Van Nostrand Reinhold: New York, NY, USA, 1990; Volume 1, 832p.
30. Hare, P.E.; Abelson, P.H. Amino acid composition of some calcified proteins. *Carnegie Inst. Wash. Yearb.* **1965**, *64*, 223–232.
31. Marie, B.; Marin, F.; Marie, A.; Bédouet, L.; Dubost, L.; Alcaraz, G.; Milet, C.; Luquet, G. Evolution of nacre: Biochemistry and 'shellomics' of the shell organic matrix of the cephalopod *Nautilus macromphalus*. *ChemBioChem* **2009**, *10*, 1495–1510. [[CrossRef](#)]

Disclaimer/Publisher's Note: The statements, opinions and data contained in all publications are solely those of the individual author(s) and contributor(s) and not of MDPI and/or the editor(s). MDPI and/or the editor(s) disclaim responsibility for any injury to people or property resulting from any ideas, methods, instructions or products referred to in the content.

3.4. Do Bivalve Shells Exhibit Antibacterial Properties? Screening Calcifying Organic Matrices Against Two Major Marine Pathogens

Submitted in 2025 to Science of the TOTAL ENvironment (STOTEN), Elsevier Editions

Lutet-Toti, C.^{1,2}, Da Silva Feliciano, M.¹, Thomas, J.¹, Crosland A.¹, Develay, C.¹, Debrosse, N.¹, Force, A.¹, Bidault, A.⁵, Broussard C.⁶, Falini, G.², Goffredo, S.^{3,4}, and Marin, F.¹.

1 UMR CNRS-UBE-EPHE 6282 ‘Biogéosciences’, Université Bourgogne Europe, Dijon, France

2 Dipartimento di Chimica “Giacomo Ciamician”, Alma Mater Studiorum Università di Bologna, Bologna, Italy

3 Marine Science Group, Department of Biological, Geological and Environmental Sciences, University of Bologna, Via F. Selmi 3, I-40126, Bologna, Italy

4 Fano Marine Center, The Inter-Institute Center for Research on Marine Biodiversity, Resources and Biotechnologies, Viale Adriatico 1/N, 61032 Fano, Italy

5 Univ Brest, CNRS, IRD, Ifremer, LEMAR, Plouzané, France

6 Proteom’IC platform 3P5, Cochin Institute, Université de Paris-Descartes, Paris, France

* Correspondence: frederic.marin@u-bourgogne.fr; camille.lutet-toti@u-bourgogne.fr

Abstract

In mollusks, the shell biomineralization process is regulated by an array of macromolecules, better known as the shell organic matrix. Recent advancements in high throughput ‘omics’ techniques have shown that this matrix consists of a large number of proteins with extremely diverse functions. In the present paper, we report for the first time that some organic extracts – either soluble or insoluble - from the shell of commonly consumed bivalves possess antibacterial properties against two marine pathogens Vibrionaceae, *Aliivibrio salmonicida* and *Vibrio harveyi*, strain ORM4. This antibacterial effect is corroborated by the formal identification of several antibacterial peptides by proteomics, in the different shell fractions. Our study – the first of its kind - draws attention to shells of bivalves of economic interest as valuable but underestimated sources of antibacterial substances, usable in aquaculture. More generally, recycling shell byproducts in high added value applications will contribute to the development of a sustainable circular economy.

Keywords: antibacterial; mollusk shell; organic matrix; vibriosis

3.4.1. Introduction

Vibrioses, *i.e.* infections caused by bacteria of the Vibrionaceae family, represent major economic and ecological issues in aquaculture worldwide. These diseases affect fish, mollusks and decapod crustaceans at all life stages, resulting in production depletion and high mortality rates in both reared and wild environments (Thompson *et al.*, 2004; Travers *et al.*, 2015; de

Souza Valente and Wan, 2021; Hegde *et al.*, 2023). The economic impact of vibriosis outbreaks on the industry has been escalating, with estimated loss reaching more than 6\$ billion in 2020, which is twice as much as 20 years ago (Burge *et al.*, 2014; Sanches-Fernandes *et al.*, 2022). The reasons of this dramatic increase have probably to be searched in a more intense exploitation of seafood (with a higher concentration of specimens per square unit) but also in the global warming of seawater which weakens organism's immune system and stimulate growth of pathogens (Ferchichi *et al.*, 2021; Thompson *et al.*, 2024).

Among these pathogens, *Vibrio harveyi* infects finfish and invertebrates in warm waters in Asia, Europe and South America, where frequent outbreaks are reported (Triga *et al.*, 2023). Like all members of the Vibrionaceae family, this fermentative bacterium is Gram-negative, rod-shaped and highly motile thanks to its numerous polar flagella (Johnson & Shunk, 1936; Zhang *et al.*, 2020). In fish, *V. harveyi* vibriosis leads to vasculitis, eye lesions and blindness, necrotizing gastro-enteritis, muscle necrosis, skin ulcers and tail rot disease (Rico *et al.*, 2008; Zhang *et al.*, 2020). This pathogen is also associated with multiple syndromes affecting different life stages of crustaceans, like necrotic sepsis, hepatic lesions, luminous vibriosis, *bolitas nigricans*, *i.e.*, occlusive lesions in the gastrointestinal tract, with drastic alterations of feeding and predator avoidance behaviors as early as the larval stage (de Souza Valente & Wan, 2021). High densities of *V. harveyi* were also found in mollusk hatcheries and natural beds, where all stages of life of bivalves and gastropods can be affected. This bacterium is indeed the causative agent of the famous “white foot syndrome” of the abalone *Haliotis tuberculata*, which fatally prevents the mollusk to adhere to surfaces (Austin & Zhang, 2006; Travers *et al.*, 2015; Zhang *et al.*, 2020). The strain tested in this paper, *V. harveyi* ORM4, was isolated in Normandy (France) in the 90s, when a severe outbreak of “white foot syndrome” decimated close to 90% of the cultivated abalone population (Nicolas *et al.*, 2002). *V. harveyi* ORM4 represents a very serious microbial threat for abalone, a mollusk of high economic value (Cook, 2014), as it effectively suppresses its immunity by reducing hemocyte activity. This infection has a very high mortality rate and fast incidence, killing up to 80% of its hosts after incubations of 3 to 5 days (Cardinaud *et al.*, 2015; Morot *et al.*, 2021). This strain is described as a “true” environmental strain of the *V. harveyi* specie, exerting typical virulence, biology and behavior, making it particularly fitting for microbial and epidemiological studies regarding the pathogen (Austin & Zhang, 2006).

The second pathogen studied here, *Aliivibrio salmonicida*, is closely related to *Vibrio* species and represents the agent causing cold water vibriosis in Norwegian salmon, trouts and

cods (not to be confused with *Aeromonas salmonicida*). Like *V. harveyi*, it is Gram-negative, rod-shaped with multiple polar flagella but thrives in marine water and has a long survival out of the host. *A. salmonicida* has been observed in aquaculture for a long time and is highly associated with fish farming (Egidius *et al.*, 1986). Fish skin and gills are the major routes for infection, the transmission being possible via direct contact between fish or through infected water. *A. salmonicida* displays extremely rapid proliferation rates with usually high densities upon invasion of the organism, becoming detectable within a few minutes in the bloodstream (Austin, 2006; Bjelland *et al.*, 2012; Kashulin *et al.*, 2017). Cold water vibriosis is a growing threat in fish aquaculture, as the pathogen develops resistance to treatments and vaccines: the disease has indeed resurfaced after the previously successful vaccination of Atlantic salmon in the North of Europe (Kashulin & Sørum, 2014; Kashulin *et al.*, 2017).

Multiple attempts have been made in developing solutions to mitigate vibriosis effects on aquaculture. In fish, vaccination is technically possible and has been implemented through immersion or injection, but it comes with drawbacks (Colquhoun *et al.*, 2002; Håstein *et al.*, 2005; Sun *et al.*, 2014; Huang *et al.*, 2019; Tammas *et al.*, 2024). Indeed, is time-consuming and costly to treat every animal, and some vaccines have even been observed to have adverse effects on fish size and growth rates. As discussed above with cold water vibriosis, the provided protection also usually declines over time as Vibrionaceae mutate to thwart their hosts immune responses and thus build resistance against immunity-related treatments (Kashulin *et al.*, 2017; Sanches-Fernandes *et al.*, 2022). Other forms of therapy have been developed for a broader use among vertebrates and invertebrates, including antibiotic treatments, immuno-stimulation through immersion or oral medication (Duff, 1942; Baleta and Gómez-Chiarri, 2016) and supplemented feeds (Talpur & Ikhwanuddin, 2012; Talpur *et al.*, 2013; Talpur, 2014).

Antibiotics are extensively used as prophylaxes in aquaculture, with more than half of the world's facilities using combinations of at least three different molecules (Ina-Salwany *et al.*, 2019; Schar *et al.*, 2020). This practice has led to a rapid increase in antibiotic resistance among pathogens in aquaculture, including Vibrionaceae (Davies & Davies, 2010; Jiang *et al.*, 2013; Kashulin *et al.*, 2017; Schar *et al.*, 2021; Caputo *et al.*, 2023). Beyond the risks for production rates, the escalating global antibiotic resistance raises concerns about food security and diseases associated with seafood consumption. Contaminated food can indeed be filled with toxins leading to paralysis or numerous neurological illnesses, and the microorganisms they carry might also be pathogenic to humans. Some cases of transmission of antibiotic resistance to quinolones in human pathogens were reported as well (Laabir *et al.*, 2011; Ina-Salwany *et*

al., 2019; Arnich *et al.*, 2021). Antibiotic resistance also impacts natural environments and ecosystems: persistent resistance genes were indeed detected in coastal soils (Griffin *et al.*, 2019).

To address these issues, new antimicrobial products are tested and developed in an effort to reduce antibiotic use. Various alternatives are being explored, including the use of nanoparticles baths, probiotics or bacteriophages (Oliveira *et al.*, 2012; Sanches-Fernandes *et al.*, 2022; Bondad-Reantaso *et al.*, 2023; Kah Sem *et al.*, 2023). However, these solutions do not come without consequences, as they can impact wild microbial communities and drastically modify their ecological balance. The use of natural substances, endemic to the environments, then appears as a more sustainable substitute to polluting chemicals: studies using mussel hemolymph (Canesi *et al.*, 2016) and antimicrobial peptides (AMPs) collected from marine animals (Cole *et al.*, 1997) have shown encouraging results against *Vibrio*.

Conchyliculture aquaculture is a very active sector of aquaculture, with more than 18 million tons of mollusks produced each year in the world (FAO, 2024). Although this industry is often described as a sustainable alternative to wild fisheries, it generates significant amounts of by-products, such as emptied shells. Shells are mostly made of calcium carbonate, either aragonite or calcite, and contain in addition a minor fraction of organics, from 0.1 to 1 or 2 wt-% (Marin *et al.*, 2012). Some efforts are made to recycle shells, but mostly based on their mineralogical properties. Consequently, the end products are of low added value: construction materials (shell ‘concrete’, embankments made of shells), powder for soil amendment or calcium supplement for poultry feed (Lutet-Toti *et al.*, 2025, *Submitted to Journal of Ethnobiology*; Zhan *et al.*, 2021). So far, the organic fraction of mollusk shells has never been utilized in large-scale applications. However, it is an integral part of the shell, since it is secreted by the mollusk mantle outer epithelium, simultaneously to the inorganic ionic precursors (calcium, bicarbonate), to form the shell. The organic fraction, also called shell matrix, regulates the mineral deposition and controls the shape of the crystalline units that compose the different shell layers (Weiner and Hood, 1975; Addadi *et al.*, 2006; Marin *et al.*, 2008). It remains then occluded in the calcified structure, once formed. Classical molecular models of shell biomineralization attribute a preponderant role to acidic proteins (aspartic acid-rich), because of their capacity to bind calcium ions, to interact with the mineral surfaces of calcium carbonate *nuclei*, and to inhibit the growth of these *nuclei* (Weiner and Hood, 1975; Marin and Luquet, 2007). However, during the last decade, high-throughput techniques, *i.e.* transcriptomics and proteomics, have shown that the shell matrix contains many other proteins, (Marin, 2020), some

of which are unexpectedly basic, *i.e.* enriched in arginine or lysine (Oudot *et al.*, 2020b). Such molecular property is often associated with antimicrobial peptides (Zasloff, 2002). Antimicrobial peptides, referred to as AMPs, are among the most effective molecules in innate immune systems of several non-vertebrate metazoans. These substances are promising, as their antibacterial mechanism precludes the development of almost any form of resistance; among the molecular processes most often involved, bacterial membrane-binding, immediately followed by membrane destabilization and permeabilization constitute a mechanism against which the bacteria cannot develop a parade (Zasloff, 2002; Yeaman and Yount, 2003; Kosikowska and Lesner, 2016). To date, the identification of AMPs in mollusks has been restricted to soft tissues (Sathyan *et al.*, 2012; Leoni *et al.*, 2017; Maselli *et al.*, 2020; Oh *et al.*, 2020), but their putative presence in shells may explain *pro parte* certain natural observations: at first, in spite of living in an aqueous environment favorable to microbial contaminations, mollusk shells are not very prone – at least on their internal face – to the development of bacterial biofilms. Secondly, in traditional medicine, poultices made of shell powder were frequently applied on wounds and injuries to heal them and avoid their infection (González and Vallejo, 2023).

In the present paper, we intend to demonstrate *in vitro* the antimicrobial properties of shell organic matrices from seven species of commonly consumed bivalves in Europe against two marine pathogens described above, *Vibrio harveyi* ORM4 and *Aliivibrio salmonicida*. To this end, organic matrices were extracted from whole cleaned shell powders, fractionated and checked on electrophoretic gels before being tested for their capacity to exert an antimicrobial effect on these two strains. Two screening methods were performed: a) a classical disk diffusion assay, to detect antimicrobial activity in both soluble and insoluble fractions; b) a microdilution assay of the soluble extracts, to check for putative minimum inhibitory concentrations (MIC) and characterize the antibacterial mechanisms in action. Finally, in addition, all the extracts were analyzed by proteomics to check the occurrence of antimicrobial peptides or proteins (AMPPs) previously identified in metazoan or mollusk datasets.

3.4.2. Materials and Methods

3.4.2.1. Mollusk Shell Organic Matrix Extraction

Numerous shells of seven species of commercially available bivalves were collected from live animals in supermarkets around Dijon (Burgundy, France). As bivalves possess a diffuse nervous system, they are not subject to the European Directive 2010/63/UE relating to the protection of animals used for scientific purposes. The collected species include the dog

cockle *Glycymeris glycymeris*, the Mediterranean mussel *Mytilus galloprovincialis*, the Pacific cupped oyster *Magallana gigas*, the great scallop *Pecten maximus*; the common cockle *Cerastoderma edule*, the warty venus *Venus verrucosa* and the manila clam *Venerupis philippinarum*. The first four belong to the Pteriomorpha infraclass, and the last three to the Heteroconchia (Bieler *et al.*, 2014).

For each mollusk species, cleaned fine shells powders with a granulometry below 200 μm were produced. The organic shell matrices were extracted at 4 °C by gentle powder dissolution with cold dilute acetic acid, following the protocol explained in detail in our previous publication (Lutet-Toti *et al.*, 2024). For each of the seven species, Acid Insoluble Matrix (AIM) and Acid Soluble Matrix (ASM) were obtained. The ASM was further fractionated by ultrafiltration in two batches, by using two successive cutoffs: 10 and 1 kDa. This resulted in the production of an ASM >10 kDa and of 1 $<$ ASM <10 kDa. Due to high viscosity of the extracts, in two cases (*Venerupis philippinarum* and *Mytilus galloprovincialis*), we had to intercalate a supplementary ultrafiltration at 3 kDa, resulting in three soluble matrices: ASM >10 kDa; 3 $<$ ASM <10 kDa; 1 $<$ ASM <3 kDa. After ultrafiltration, all fractions were thoroughly dialyzed against Milli-Q grade water comprising at least six water changes, then freeze-dried. The resulting pellets were weighed on a precision balance. They were ready for further biochemical analysis and antibacterial assays.

3.4.2.2. Gel Electrophoresis

All extracted fractions were checked on a mono-dimensional analytical electrophoresis system in denaturing conditions (SDS-PAGE) on a mini-Protean III cell (Bio-Rad, Hercules, CA, USA). In brief, 12% acrylamide gels were hand cast, while shell extracts were heat denatured in Laemmli sample buffer: 5 minutes for all ASMs, 10 minutes for AIMs. In this latter case, only a part of the AIMs was dissolved and is referred to as LS-AIM (Laemmli Soluble fraction of the AIM), in the following gel descriptions. Extracts were cooled down on ice and quickly centrifuged before being applied on top of the gel and run at 120 V for about 90 minutes. After running, gels were de-cast and stained with silver nitrate, according to a procedure derived from Morrissey (1981).

3.4.2.3. Bacterial Cultures

Aliivibrio salmonicida (strain CIP103166T) were ordered from Pasteur Institute Collections, Paris, France. They were activated from dry stocks following guidelines of the

Centre de Ressources Biologiques of this institute, then cultured in lightly stirred marine broth (Difco marine broth 2216, Thermo Fisher Scientific, France) for 11 days at 12 °C. *Vibrio harveyi* ORM4 strains were provided by LEMAR Lab, Université de Bretagne Occidentale, France. They were grown in liquid culture using the same marine broth, lightly stirred for 24 hours at 28 °C. Once in log phase (DO = [0.6:1.0]), the suspensions were ready to be used for antibacterial assays.

3.4.2.4. Disk Diffusion Assay

Bioactivity detection of the extracts was conducted on agar Petri dishes following the classical disk diffusion method (Bauer *et al.*, 1966) using cellulose antibiotics disks (6 mm diameter, Ahlstrom, Helsinki, Finland) or hand-made tablets (see below).

Disks and tablets preparation. Disks were prepared as follows. The ASM lyophilisates were re-dissolved in ultrapure water at a final concentration of 1 µg/µL and homogenized by pipetting up and down just before use. Soluble extracts (20 µg, 20 µL) were simply absorbed into cellulose disks. Negative controls with ultrapure water were prepared similarly. Sterile commercial v0129 disks (ref. 53872, lot 64478673, Bio-Rad, Hercules, CA, USA) containing 500µg of vibriostatic agent (2,4- diamino-6,7-di-isopropyl-pteridine phosphate) were used as positive controls. AIM extracts, shell powders and pure calcium carbonate (Sigma-Aldrich, ref. 239216-00G) were transformed into 5 mm tablets, by using a lab hand-press machine (HP-mini, LC-Instru, Lisses, France), following a protocol we recently published (Lutet-Toti *et al.*, 2024). Tablets of 3 to 5 mg AIM were produced, which could be manipulated with tweezers. All disks and tablets were sterilized under UV light on each side for 20 minutes, except the sterile disks containing the bacteriostatic agent, not stable under UV.

Disk diffusion method. 600 µL bacterial suspensions were evenly spread on fresh marine agar plates (Difco marine agar 2216, Thermo Fisher Scientific, France) using the “spread-plate method” in standard Petri dishes (94 mm diameter, Greiner Bio-One, Courtabœuf, France). After absorption of the suspension by the agar medium, sterilized disks and tablets were disposed and spaced evenly on the plates. Each Petri dish received 7 or 8 disks or tablets, comprising: one disk with ultrapure water (negative control), one tablet of pure calcium carbonate (second negative control), one tablet of shell powder, one tablet of AIM, one disk containing ASM>10 kDa, one disk with 1<ASM<10 kDa and finally, one v0129 disk (positive control). In the case of *Venerupis philippinarum* and *Mytilus galloprovincialis*, three ASM disks were used instead of two: ASM>10 kDa, 3<ASM<10 kDa and 1<ASM<3 kDa. he

plates were incubated upside-down, following microbial collections guidelines for each strain: *A. salmonicida* at 12 °C for 9 days, *V. harveyi* at 28 °C for 48 hours. After incubation time, macrophotos were obtained under direct light, in front of a dark background and on a transparent surface to ensure inhibition zone visibility with a Digital Nikon D750 Camera (Nikon, Tokyo, Japan), equipped with AF-S VR Micro-Nikkor 105 mm f/2.8 G IF-ED or AF-P DX Nikkor 18–55 mm f/3.5–5.6 G VR objectives. When present, the inhibition zone diameters were read and measured following EUCAST guidelines on testing bacterial sensitivity to natural products without breakpoints (EUCAST, 2024). Sterile conditions were maintained during the whole preparation, inoculation and treatment procedures. The assays were reproduced in triplicate. When the experiment failed (contamination or invalid controls), additional plates were produced and treated again to ensure the number of replicates.

Antibiogram assessment. Additional plates were produced in triplicates for antibiogram testing on inoculated cellulose disks for potential diffusion differences with pre-made disks and select the suitable positive control for each strain. Tested antibacterials products were for *A. salmonicida*: ampicillin 10µg, sodium azide 0.20 µg, v0129 10 µg, v0129 150 µg, v0129 500 µg; for *V. harveyi*: sodium azide 0.20 µg, tetracycline 0.20 µg, v0129 150 µg and v0129 500 µg.

3.4.2.5. Microdilution Assay

Microdilution assays were performed on liquid cultures, using the alteration of bacterial metabolism as proxy for antibacterial activity. Standard 96 wells flat bottom sterile microplates (Greiner, Bio-One, ref. 655161GBIO) with their cover were used after 20 minutes of UV sterilization. As the fermentative metabolism of both bacteria lowers the pH of the medium under natural growth condition, red phenol (pKa = 6.8) was added to the marine broth as a pH indicator, with a final concentration of 20 mg/L. Only the ASM fractions could be tested with this assay, along with solutions of antibiotics as standards. The decreasing concentrations of treatments were obtained via six serial dilutions with a quotient of 3 (Table 3.2).

Table 3.2: Concentrations gradients of the tested ASMs and standard treatments used in the microdilution assay.

	C1	C2	C3	C4	C5	C6
ASM extracts	100 µg/mL	33.33 µg/mL	11.11 µg/mL	3.70 µg/mL	1.3 µg/mL	0.41 µg/mL
Tetracycline standard	10.00 µg/mL	3.33 µg/mL	1.11 µg/mL	0.37 µg/mL	0.13 µg/mL	0.04 µg/mL
Sodium azide standard	2.00 mg/mL	0.66 mg/mL	0.22 mg/mL	74.07 µg/mL	24.69 µg/mL	8.23 µg/mL

For each gradient, negative controls were made with the replacement of the treatment by 0.9% (wt/vol) NaCl in water. Positive controls were made using maximum concentrations of treatments (S1 and C1) in absence of bacterial suspension. Blanks were made for each treatment to subtract absorbance bias due to the slightly yellow marine broth. A general blank containing solely marine broth and bacteria was performed to monitor correct bacterial growth under ideal conditions for each plate. Every well was filled to a final volume of 200 μ L. All treatments and conditions were performed in triplicate. Sterile conditions were maintained during the whole preparation, inoculation and treatment procedures.

The plates were incubated under conditions for ideal growth determined during previous testing for each strain: *A. salmonicida* plates were incubated, with a gentle stirring, at 12°C for 72 hours. *V. harveyi* plates were incubated at 28°C for 4 hours, lightly stirred. Absorbances were read using Spectramax ID3 spectrophotometer (Molecular Devices, San José, CA, USA) at two wavelengths for detection of finer metabolic changes: 420 nm to detect yellow (low pH) and 560 nm to detect red/fuchsia (high pH) (Held, 2022). For the following analysis (including statistical treatment), we selected the 560 nm wavelength data: the 420 nm wavelength curves did not indeed reflect with accuracy the progressive color changes induced by bacterial metabolism. At 560 nm, the natural growth curve (under optimal conditions) exhibits an inverted profile compared to a typical curve describing the bacterial density. In other terms, one can observe, after a more or less reduced lag phase, a decrease in absorbance, which testifies the acidification of the medium by active bacteria (transition from red to yellow). Then, after an optimum (lowest absorbance point at 560 nm), an increase of the absorbance comes from the decrease of bacterial metabolism and the start of the death phase, marked by cellular lysis (transition from yellow to fuchsia). At the end of the incubation, the absorbance is higher than the initial one, highlighting the release of basic metabolites. The absorbance at 600 nm was not used as it induces major bias due to non-differentiation of live and dead bacteria (Gelman *et al.*, 2021). The absorbance was measured every 8 hours for *A. salmonicida*, every 30 minutes for *V. harveyi*.

3.4.2.6. Statistical Analysis

Disk diffusion assay. The means and standard deviations for inhibition zones diameters were compared among treatments. Shapiro-Wilk's tests were performed to determine homoscedasticity. Due to non-normal distributions, non-parametric tests were performed: Kruskal-Wallis tests were followed by Dunn's post-hoc comparisons of diameter sizes. Holm-Bonferroni correction was applied to reduce type I errors while maintaining statistical power in the case of a study with groups displaying expected zero variances (*i.e.* negative control groups).

Microdilution assay. The mean absorbance of the triplicates was used, and a background subtraction using blanks was performed for each well to create growth curves for each condition (Theophel *et al.*, 2014). Blazannin's `gplyr` package (2024) was used to extract key growth parameters to analyze antibacterial activity: lag phase duration, maximum growth rate (growth rate during the exponential growth phase), maximum density (estimation of the carrying capacity, *i.e.*, the maximal amount of viable bacteria in a population). The maximum growth rate was pondered by population size to reduce potential bias while comparing different wells, adding maximum per capita growth rate to the list. Growth parameters were then statistically compared between conditions and concentrations. Shapiro-Wilk tests were performed for normality checking of the variances. One-way ANOVAs were performed for group comparisons, followed by Tukey's HSD test post-hoc for pairwise comparisons.

The overall analysis necessitated R software (R Core Team, 2023). Tidyverse was used for data manipulation and visualization (Wickham *et al.*, 2019), statistical analysis was performed with the packages `rstatix` and `FSA` (Kassambara, 2023; Ogle *et al.*, 2023).

3.4.2.7. Proteomic Analysis

Proteomic analyses were conducted at the Proteom'IC 3P5 platform of Institut Cochin. Aliquots of all ASM and AIM matrices (23 samples) were in-gel digested with trypsin, as previously described (Immel *et al.*, 2016). Mass spectrometry analyses were performed using an Ultimate 3000 Rapid Separation Liquid Chromatographic (RSLC) system (ThermoFisher Scientific) online with a timsTOF Pro mass spectrometer (Bruker Daltonics). Briefly, peptides were dissolved in 6 μL of 10% ACN-0.1% FA. One microliter of peptides was then loaded and washed on a C_{18} reverse phase pre-column (5 μm particle size, 100 \AA pore size, 300 μm i.d., 5mm length). The loading buffer contained 98% H_2O , 2% ACN and 0.1% TFA. Peptides were then separated on a C_{18} reverse phase resin (1.7 μm particle size, 120 \AA pore size, 75 μm i.d.,

25 cm length, IonOpticks) with a 1-hour gradient from 99% A (100% H₂O and 0.1% FA) to 40% B (80% ACN, 0.085% FA and 20% H₂O).

The mass spectrometer acquired data throughout the elution process and operated in DDA PASEF mode with a total cycle time of 1.88 s, with Timed Ion Mobility Spectrometry (TIMS) enabled. Ion accumulation and ramp time in the dual TIMS analyzer were set to 166 ms each and the ion mobility range was set from $1/K0 = 0.6 \text{ Vs cm}^{-2}$ to 1.6 Vs cm^{-2} . Precursor ions for MS/MS analysis were isolated in positive polarity with PASEF in the 100-1.700 m/z range by synchronizing quadrupole switching events with the precursor elution profile from the TIMS device.

Database searches were carried out using Mascot version 2.5 (MatrixScience, London, UK) by providing two sets of data: the first one compiles 3172 non redundant antimicrobial peptides or proteins (AMPPs) of metazoan source taken from the DRAMP (Data Repository of AntiMicrobial Peptides) database (<http://dramp.cpu-bioinfor.org/>), referred to in Ramazi *et al.* (2022). The second dataset, compiled by us from several bibliographical sources, focuses on AMPPs of mollusk origin. It comprises 329 entries and represents so far, the most exhaustive list of AMPP sequences in this phylum (Table S1). For each dataset, we considered as significant the peptides/proteins identifications supported by at least two supporting peptide sequences.

3.4.3. Results

3.4.3.1. Shell Organic Matrix Quantification and SDS-PAGE Check

Table 3.3 shows the percentage of whole shell matrices for each of the seven models used in this study (line 2), and the ratio between insoluble matrix to total matrix (line 3). The percentage of shell matrix varies between 0.078 for *C. edule* to 0.74 % for *M. galloprovincialis*, while the ratio of AIM to whole matrix varies from 55% for *V. verrucosa* to almost 91% for *M. galloprovincialis*.

Table 3.3: Amounts of the organic matrix extracted in the shell of the seven tested bivalves, in proportion of the powder weight. The ratios of the AIM / total matrix are also given here.

Mollusk species	<i>Glycymeris glycymeris</i>	<i>Mytilus galloprovincialis</i>	<i>Magallana gigas</i>	<i>Pecten maximus</i>	<i>Cerastoderma edule</i>	<i>Venus verrucosa</i>	<i>Venerupis philippinarum</i>
% matrix in shell powder	0.0840%	0.7428%	0.5667%	0.5253%	0.0785%	0.2011%	0.1519%
% AIM / total matrix	68.41%	90.82%	76.74%	68.37%	65.25%	55.23%	77.96%

All extracted fractions were analyzed by one-dimensional gel electrophoresis in denaturing conditions (SDS-PAGE) and stained with silver nitrate, as shown by Figure 3.2. Lanes A corresponds to ASM fraction above 10 kDa and lanes B, to ASM fraction between 1 and 10 kDa. In the case of *Mytilus* (Figure 3.2, E) and of *Venerupis* (Figure 3.2, G), lanes C correspond to ASM fraction between 3 and 10 kDa, and lanes D, to ASM fraction between 1 and 3 kDa. Note that LS-AIM stands for Laemmli-soluble extracts of acetic acid insoluble fraction.

All lanes are characterized by smearing “polydisperse” materials, a feature commonly found in shell organic matrices. Three ASM above 10 kDa (lanes A) exhibit only few discrete bands (like that of *G. glycymeris*, *M. galloprovincialis*, *V. verrucosa*); three other extracts, including that of *M. gigas*, *P. maximus* and *C. edule* exhibit almost no band but a very diffuse smear. Exceptionally, the ASM>10 kDa of *V. philippinarum* presents a set of 7 clear and discrete bands, two of them, at 27 and about 60 kDa being exceptionally prominent. It has to be noted that all ASM>10 kDa fractions tend all to stain poorly with silver, a fact usually attributed to negatively charged proteins. The low molecular weight soluble fractions of lanes B, C and D exhibit almost no band, with the exception of *Glycymeris* and *Venerupis*, for which the faint bands observed correspond to the one of the high molecular weight ASM. As the first cutoff used for the ultrafiltration (10 kDa) is lower than the weight limit of the migration front (slightly below 15 kDa, see lanes STD), it is consequently logical not to observed much organic molecules, either discrete or smearing, in these lanes: indeed, proteins/peptides of low molecular weights are expected to be concentrated in the migration front. In all cases, the Laemmli-soluble fractions of the AIM (lanes LS-AIM) stain more intensely than the soluble ones. They show both discrete bands and smears. In some extracts, like the ones of *Glycymeris*, *Pecten* and *Venerupis*, the bands are numerous, thin and diffuse: about 15 bands can be counted, ranging from 15 to more than 100 kDa. Interestingly, one notes that LS-AIM profiles are not superimposable but are all different.

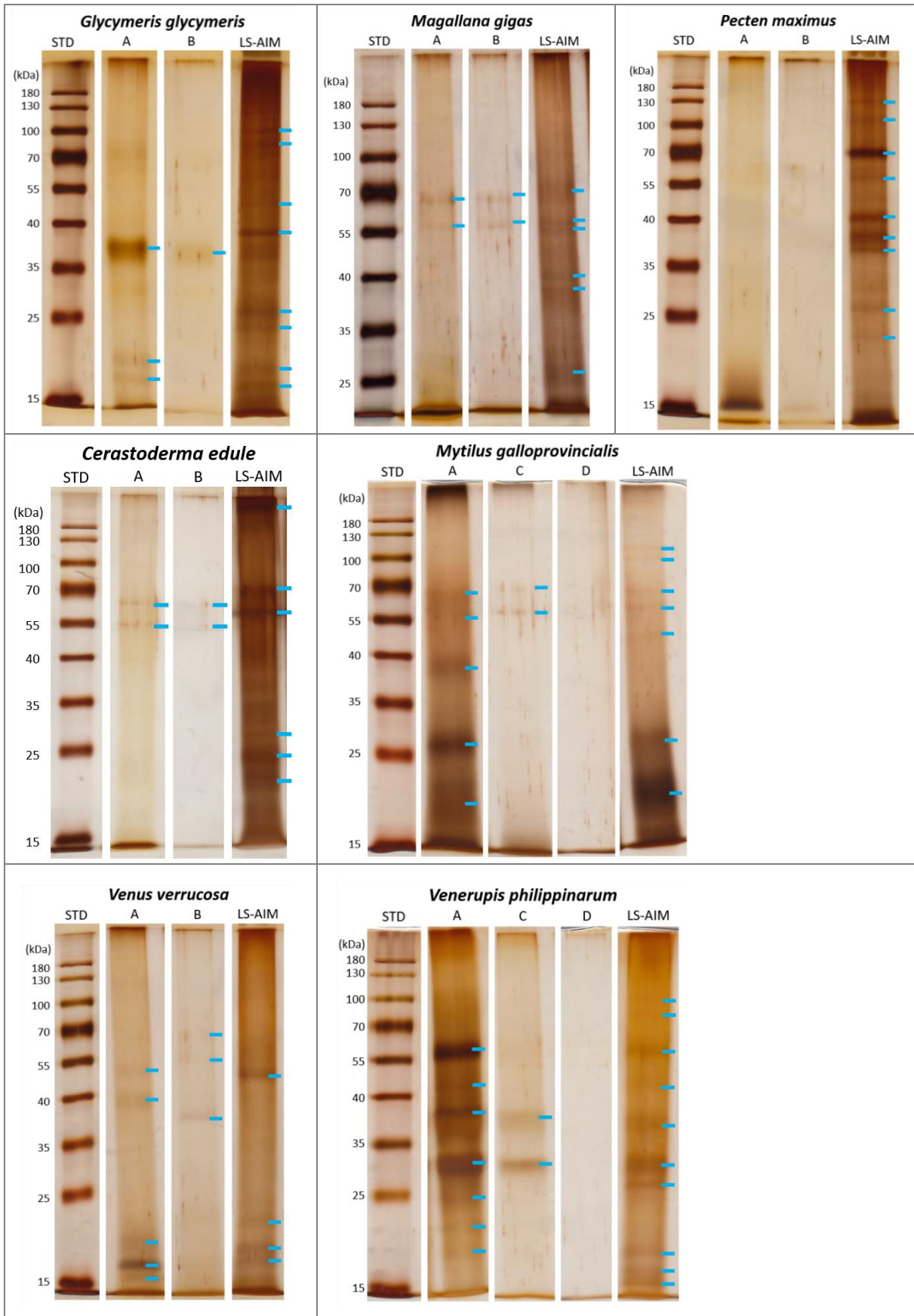


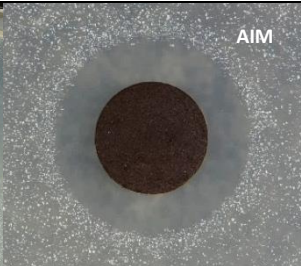
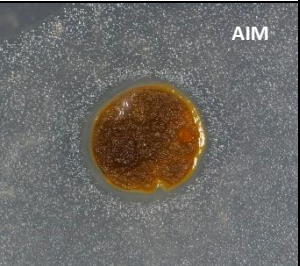
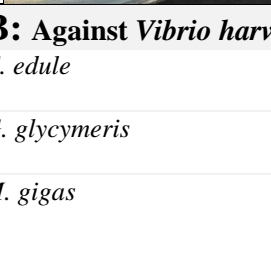
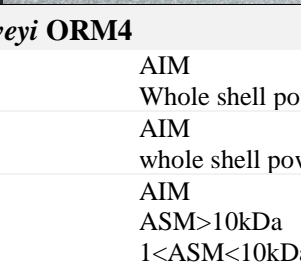
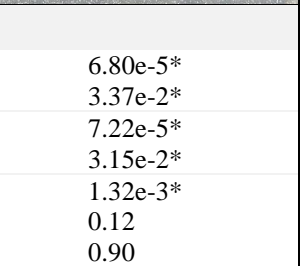
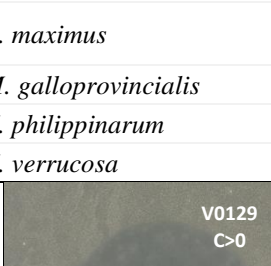
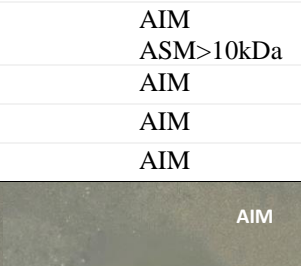
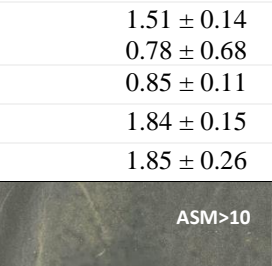
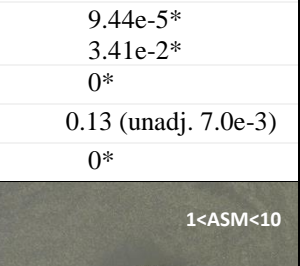
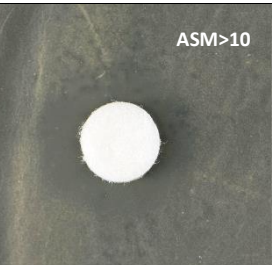
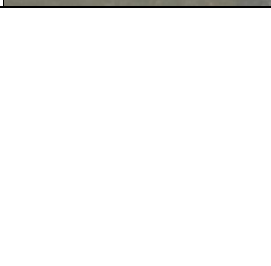
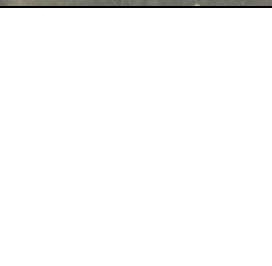
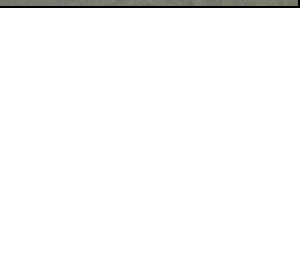
Figure 3.2: Electrophoresis gels of all bivalve models. STD: standard molecular weight markers; A: ASM>10kDa; B: 1<ASM<10kDa; C: 3<ASM<10kDa; D: 1<ASM<3kDa. Blue dashes: marks for discrete bands of interest.

3.4.3.2. Disk Diffusion Assay

The results of the disk diffusion assay are summarized in Figure 3.3: the upper panel (Figure 3.3A) represents the positive responses obtained with *A. salmonicida* plated bacteria, while the lower one (Figure 3.3, B), to positive results obtained with *Vibrio harveyi* ORM4. Only three AIMs extracts showed clear inhibition zones with *A. salmonicida*. These are respectively *C. edule* (0.95 ± 0.10 cm, Dunn's test adjusted p-value=0.01*), which gives the larger inhibition zone, followed by *M. gigas* (0.74 ± 0.03 cm, Dunn's test adjusted p-value=0.048*) and *Pecten maximus* (0.70 ± 0.08 , Dunn's test adjusted p-value=0.13; Dunn's test p-value=0.01*) (Fig. 3.3, A). As a comparison, the AIM of *G. glycymeris* did not induce any inhibition zone. We did not record any inhibition zone, whatever the ASM (above or below 10 kDa) tested. Positive and negative controls were valid. Large inhibition zones around the positive control v0129 (500 µg) were recorded, with a global mean diameter of 2.73 ± 0.84 cm. With identical quantity of active principle, the standard deviation of pre-made commercial v0129 disks (2.82 ± 0.84 cm) was greater than that of inoculated ones (1.94 ± 0.07 cm) prepared for antibiogram assays. On antibiogram plates, the inhibition zone diameter was positively correlated with the quantity of v0129. Other antibacterial products (ampicillin and sodium azide) did not show clear inhibition of bacterial growth.

The lower panel (Figure 3.3, B) shows results obtained with *V. harveyi* ORM4. Inhibition zones were detected around all seven AIM tablets (results column 2), with some marked differences: AIMs of *M. gigas*, *P. maximus*, *V. philippinarum* and *V. verrucosa* give particularly large inhibition zones, varying from 1.44 (*M. gigas*) to 1.85 cm (*V. verrucosa*) - which diameters are similar to that of the positive control v0129. The inhibition zones of *G. glycymeris*, *C. edule* and *M. galloprovincialis* are moderate, ranging from 1.26 (*G. glycymeris*) to 0.85 cm (*M. galloprovincialis*) of diameter around the tablet. Four AIM tablets (*C. edule*, *G. glycymeris*, *M. galloprovincialis* and *V. verrucosa*) exhibit a whitish crown of diffusible compounds close to the edge of the inhibition zone. Interestingly, contrarily to the test with *A. salmonicida*, three soluble (ASM) extracts gave a clear inhibition zone: the two matrices (ASM>10 kDa ;1<ASM<10 kDa) of the cupped oyster *M. gigas* and the ASM>10 kDa of *P. maximus*. None of the other ASMs produced inhibition zone. 2 shell powder tablets, that of *G. glycymeris* and of *C. edule*, also gave a slight inhibition zone. Positive and negative controls were valid. The positive controls performed with v0129 (500µg) showed large inhibition zones with a global mean diameter of 1.76 ± 0.13 cm (column 1, Figure 3.3, B). As for *A. salmonicida*, the inhibition zone was dose-dependent and increased with the quantity of v0129. Antibiogram

plates showed inhibition zones around all antibacterial products, with high variability around sodium azide (0.95 ± 1.34 cm) and a maximum for tetracycline (1.82 ± 0.20 cm).

Mollusk species	Extract	Inhibition zone diameter (cm)	Adjusted p-value	
A: Against <i>Aliivibrio salmonicida</i>				
<i>C. edule</i>	AIM	0.95 ± 0.10	0.01*	
<i>M. gigas</i>	AIM	0.74 ± 0.03	$4.8e-2^*$	
<i>P. maximus</i>	AIM	0.70 ± 0.08	0.13 (unadj. 0.01)	
<i>C. edule</i>				
				
<i>P. maximus</i>				
				
B: Against <i>Vibrio harveyi</i> ORM4				
<i>C. edule</i>	AIM	1.24 ± 0.09	$6.80e-5^*$	
	Whole shell powder	0.62 ± 0.54	$3.37e-2^*$	
<i>G. glycymeris</i>	AIM	1.26 ± 0.03	$7.22e-5^*$	
	whole shell powder	0.64 ± 0.55	$3.15e-2^*$	
<i>M. gigas</i>	AIM	1.44 ± 0.10	$1.32e-3^*$	
	ASM>10kDa	0.76 ± 0.66	0.12	
	1<ASM<10kDa	0.30 ± 0.53	0.90	
<i>P. maximus</i>	AIM	1.51 ± 0.14	$9.44e-5^*$	
	ASM>10kDa	0.78 ± 0.68	$3.41e-2^*$	
<i>M. galloprovincialis</i>	AIM	0.85 ± 0.11	0*	
<i>V. philippinarum</i>	AIM	1.84 ± 0.15	0.13 (unadj. $7.0e-3$)	
<i>V. verrucosa</i>	AIM	1.85 ± 0.26	0*	
<i>M. gigas</i>				
				
				

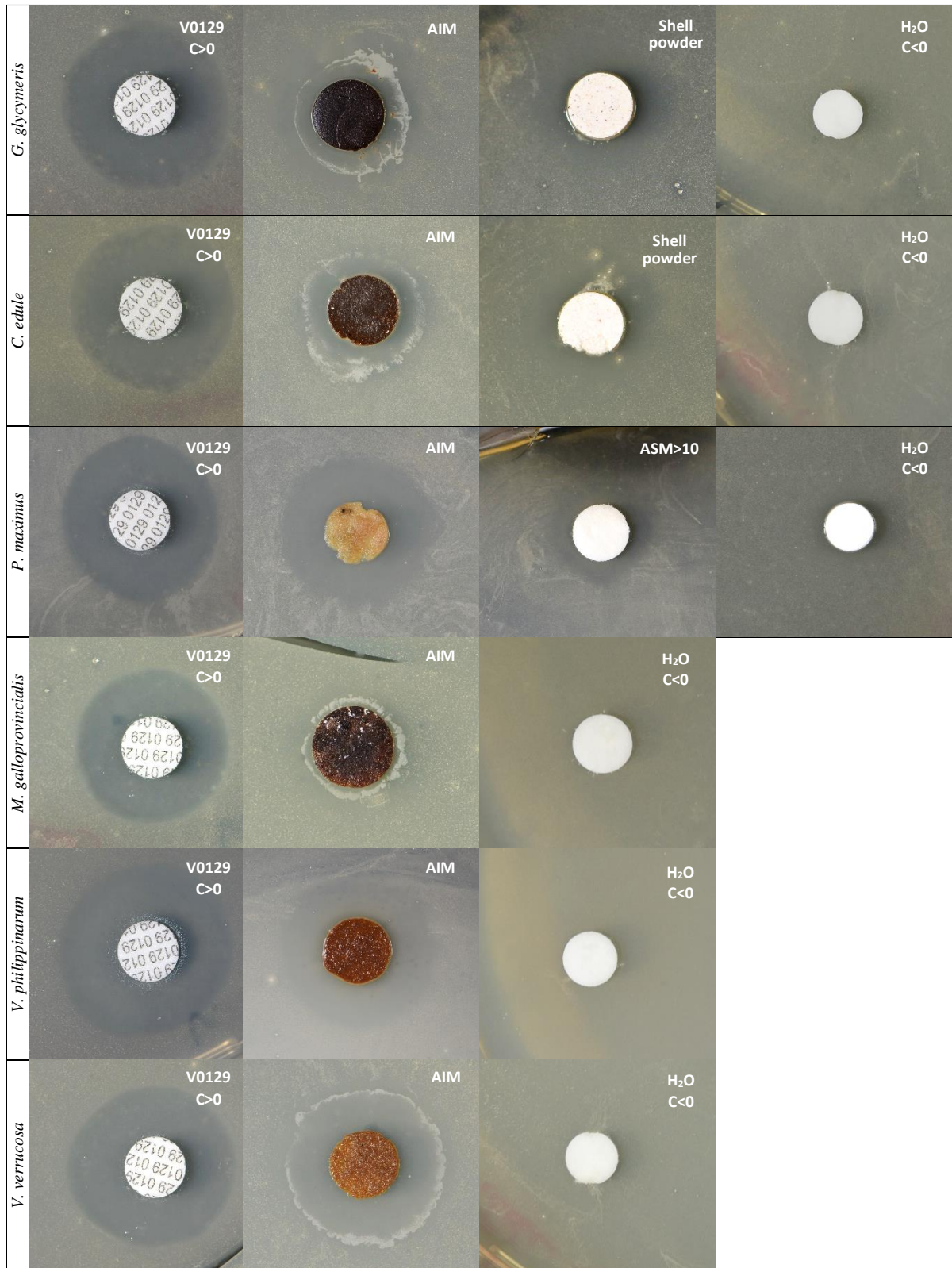


Figure 3.3: positive results of the disk diffusion assay on *A. salmonicida* (top panel, A) and *V. harveyi* ORM4 (lower panel, B).

A summary of the disk diffusion assay is also shown with the boxplot of Figure 3.4, which compiles all data obtained from disk diffusion assay. The eight graphs of the left panel describe results with *A. salmonicida* (7 mollusk models, plus antibiogram). The AIMs of *C. edule*, *M. gigas* and *P. maximus* gave significant positive results but all the other tested matrices did not show any effect on the inhibition of *A. salmonicida* growth. The eight graphs of the right panel describe results obtained with *V. harveyi* ORM4, with all 7 AIM extracts having a significant inhibitory effect, the two soluble matrices from *M. gigas*, the soluble matrix above 10 kDa from *P. maximus* and finally, the shell powders of *G. glycymeris* and *C. edule*.

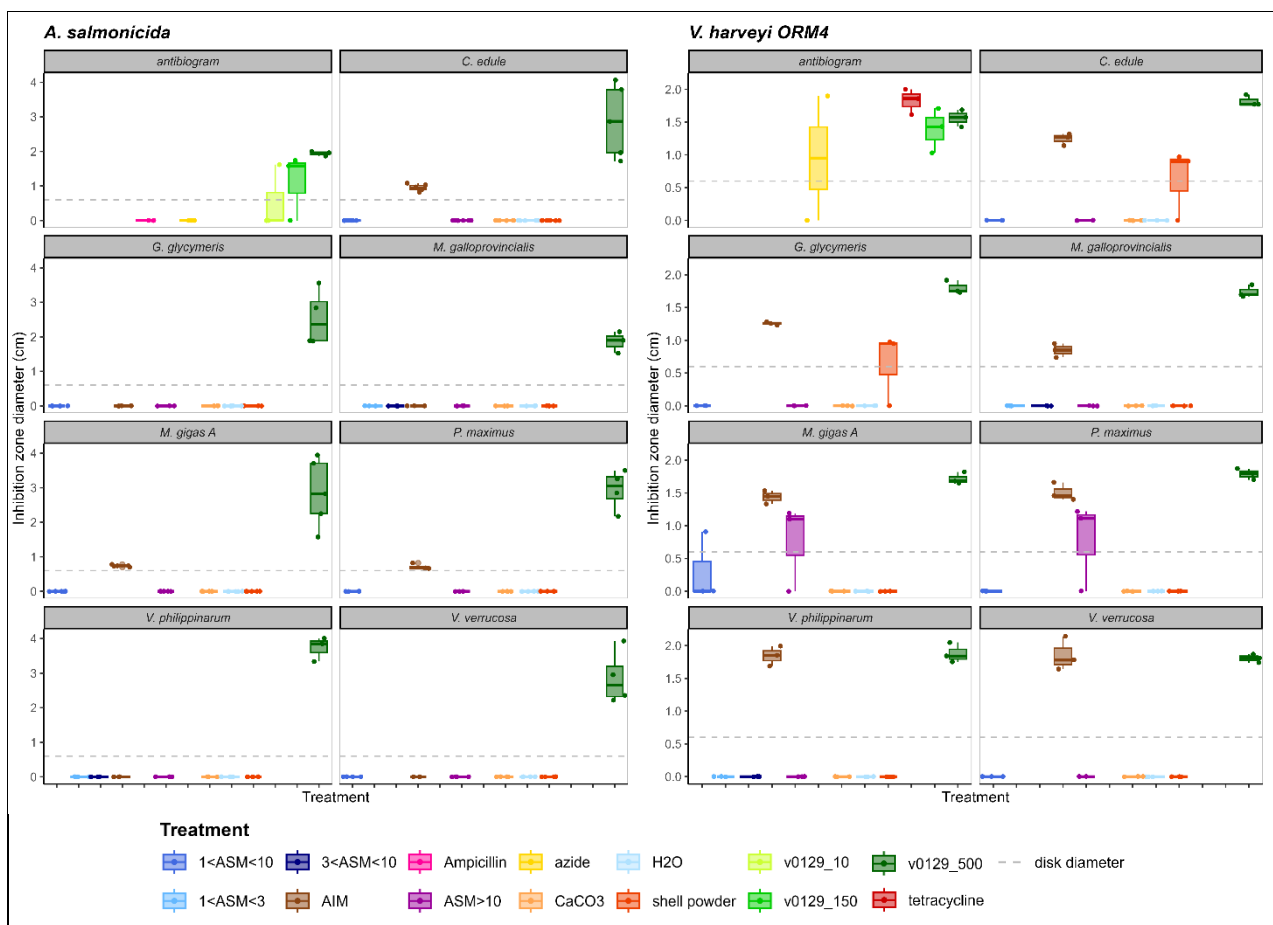


Figure 3.4: boxplots results of the disk diffusion assays for *A. Salmonicida* (left) and *V. harveyi* ORM4 (right). The dotted line represents the disk and tablet diameter, and consequently, the threshold above which the inhibition is significant.

3.4.3.3. Microdilution Assay

Figures 3.5 and 3.6 display the results obtained with the two bacterial strains, recorded at wavelength of 560 nm. Corresponding curves obtained at 420 nm are available in the supplementary data Figures S1 and S3.

Figure 3.5 summarizes the positive results, *i.e.*, results indicating an inhibitory effect of the extract, obtained with ASM fractions, when tested against *A. salmonicida*. In addition, we also include a negative result (that obtained with *G. glycymeris*) for comparison (Figure 3.5, D). The upper curves of Figure 3.5, A, B, C, D correspond to the antibacterial standards performed with sodium azide, at different concentrations. The curves exhibit a characteristic profile for bacterial cultures: at low concentrations (8.2 to 74.1 $\mu\text{g/mL}$, green and light blue), the curves keep a sigmoid shape (with a descending slope before ascending and an inflexion point between 40 and 50 hours), indicating low but dose-dependent inhibitory effect, clearly distinct from the yellow curve (negative control). One aspect of this difference is the delayed time to reach the carrying capacity. At higher concentrations of sodium azide (0.22 to 2 mg/mL), the curves abruptly flatten and come close to that of the positive control (flat line in black): this reflects a dramatic inhibition of the maximum growth rate and of the carrying capacity itself.

The soluble extracts induce two types of responses: 1) the ASM >10 kDa of *M. gigas* induces a dose-dependent alteration of the maximal growth rate (during the exponential phase, Figure 3.5, A, red arrow) without any delay in the time to reach the carrying capacity; the dose-dependent effect is also observed in the second part of the curve, corresponding to the bacterial death phase. In a lesser extent, we also observe a dose-dependent reduction of the carrying capacity induced by the low molecular weight ASM of *P. maximus* (Figure 3.5, B, red arrow); 2) a non-dose-dependent alteration is visible with the ASM of *P. maximus* (Figure 3.5, B, central panel) and *M. galloprovincialis*. However, the curves with these two species are slightly different: in the case of *M. galloprovincialis*, the growth rate is reduced regardless of the concentration of ASMs (both ASM >10 kDa, 3 < ASM < 10 kDa), in comparison to the negative control. In the case of *P. maximus*, while most of the curves (from 0.41 $\mu\text{g/mL}$ to 33.3 $\mu\text{g/mL}$) exhibit a reduction of the carrying capacity and maximum growth rate, the maximal ASM concentration (100 $\mu\text{g/mL}$, dark blue curve) displays a slightly different growth behavior, in the [16; 32 hours] time interval. For the other curves, *i.e.*, *M. galloprovincialis* (1 < ASM < 3 kDa), the two ASMs of *G. glycymeris*, we did not observe any alteration of the growth. The other negative results obtained with *A. salmonicida* are listed in the supplementary Figure S3.2.

Figure 3.6 illustrates the positive results obtained with the second strain, *V. harveyi* ORM4. In that case, only two mollusks, *M. gigas* and *P. maximus*, produced an effect. Similarly to Figure 3.5, the two upper graphs correspond to the results with the positive standard control, tetracycline. One observes a dose-dependent effect, inducing a decreased growth rate and carrying capacity. Non-dose-dependent alterations of the maximum growth rates are observed for the two ASMs of *M. gigas* and the ASM>10 kDa of *P. maximus*. The low molecular weight fraction of *P. maximus* does not show any alteration of the bacterial growth. We note that for all ASMs, the negative controls are displayed with a steeper, distinct, increase in pH (bacterial death phase, starting after 3 hours). The other negative results obtained with *V. harveyi* ORM4 are listed in the supplementary Figure S3.4.

All the previously discussed positive results acquired with the microdilution assay are summarized in Table 3.4. Key growth parameters are exposed, including: the proposed minimum inhibitory concentration (MIC), the inhibition percentages, and their significance, according to the ANOVAs & Tukey's HSD tests. Note that in three cases, the maximum *per capita* (pc) growth rates are indicated, in order to reduce population size bias. The inhibitions percentages vary between 15 (for *P. maximus*) and 56% (for *M. gigas*), while the MIC are distributed in two values: either 0.41 µg/mL (the minimal concentration that we used) or 100 µg/mL (the maximal one).

Table 3.4: Summary of the positive results of the microdilution assay. * mark the significative results.

Mollusk species	Extract	MIC (µg/mL)	Growth parameter	Inhibition	Adjusted p-value
Against Aliivibrio salmonicida					
<i>M. gigas</i>	ASM>10 kDa	0.41	max pc growth rate	56.10%	0.01 *
<i>M. galloprovincialis</i>	ASM>10 kDa	0.41	max growth rate	44.10%	1.43e-3 *
	3<ASM<10 kDa	0.41	carrying capacity	15.17%	0.04 *
<i>P. maximus</i>	ASM>10 kDa	0.41	max growth rate	17.68%	0.84
			carrying capacity	24.81%	1.66e-3 *
	1<ASM<10 kDa	-	max growth rate	14.95%	6.49e-4 *
			carrying capacity	55.2%	3.28e-7*
Against Vibrio harveyi					
<i>M. gigas</i>	ASM>10 kDa	100	max pc growth rate	38.05%	3.69e-3 *
	1<ASM<10 kDa			70.89%	0.69
<i>P. maximus</i>	ASM>10 kDa	100	max pc growth rate	27.16%	3.53e-4 *
	1<ASM<10 kDa			36.51%	0.99

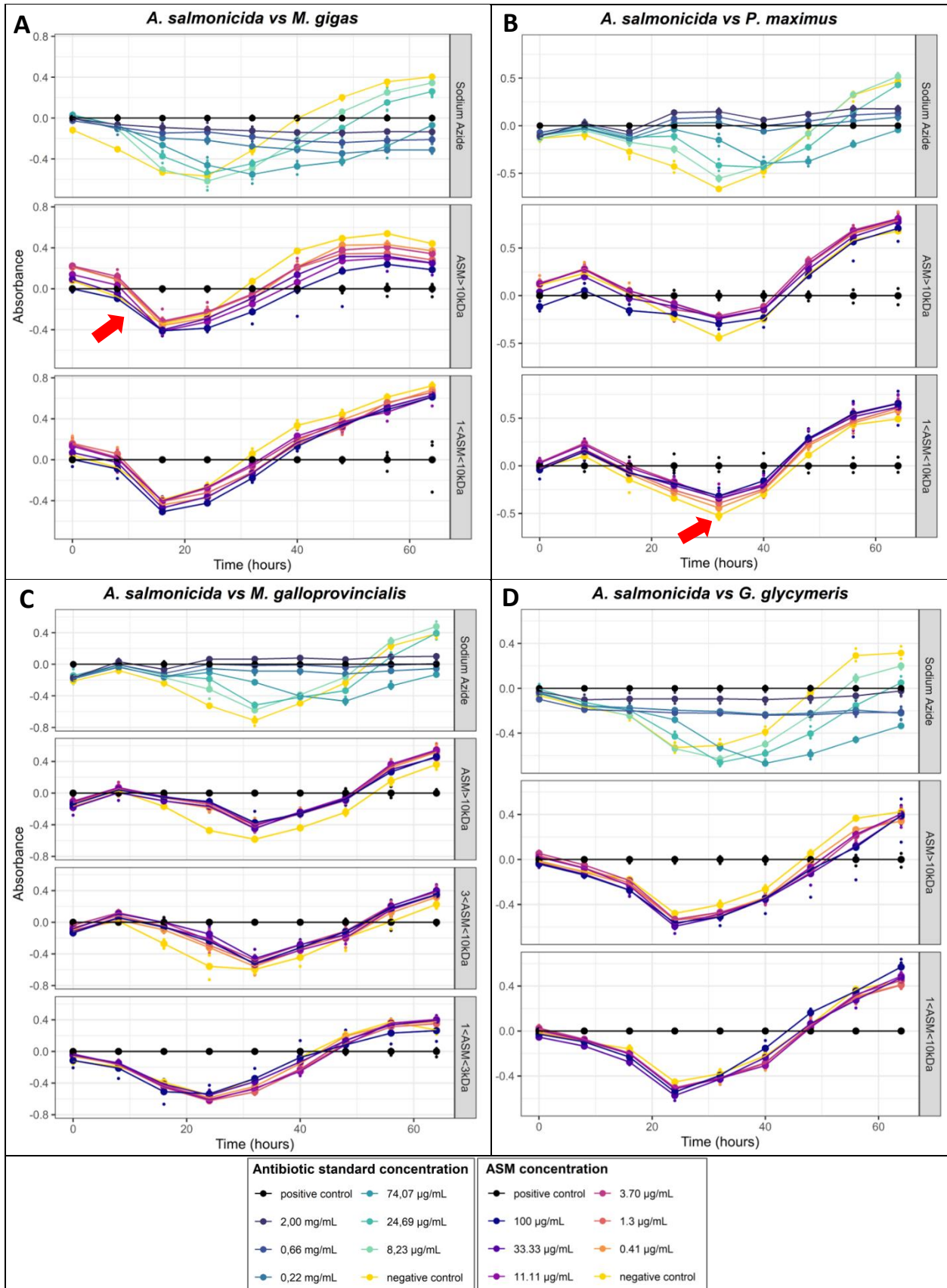


Figure 3.5: Microdilution assays growth curves with *A. Salmonicida*. The upper graphs of each panel correspond to positive controls with sodium azide. Test with ASMs extracts from *M. gigas* (A), *P. maximus* (B), *M. galloprovincialis* (C) and *G. glycymeris* (D).

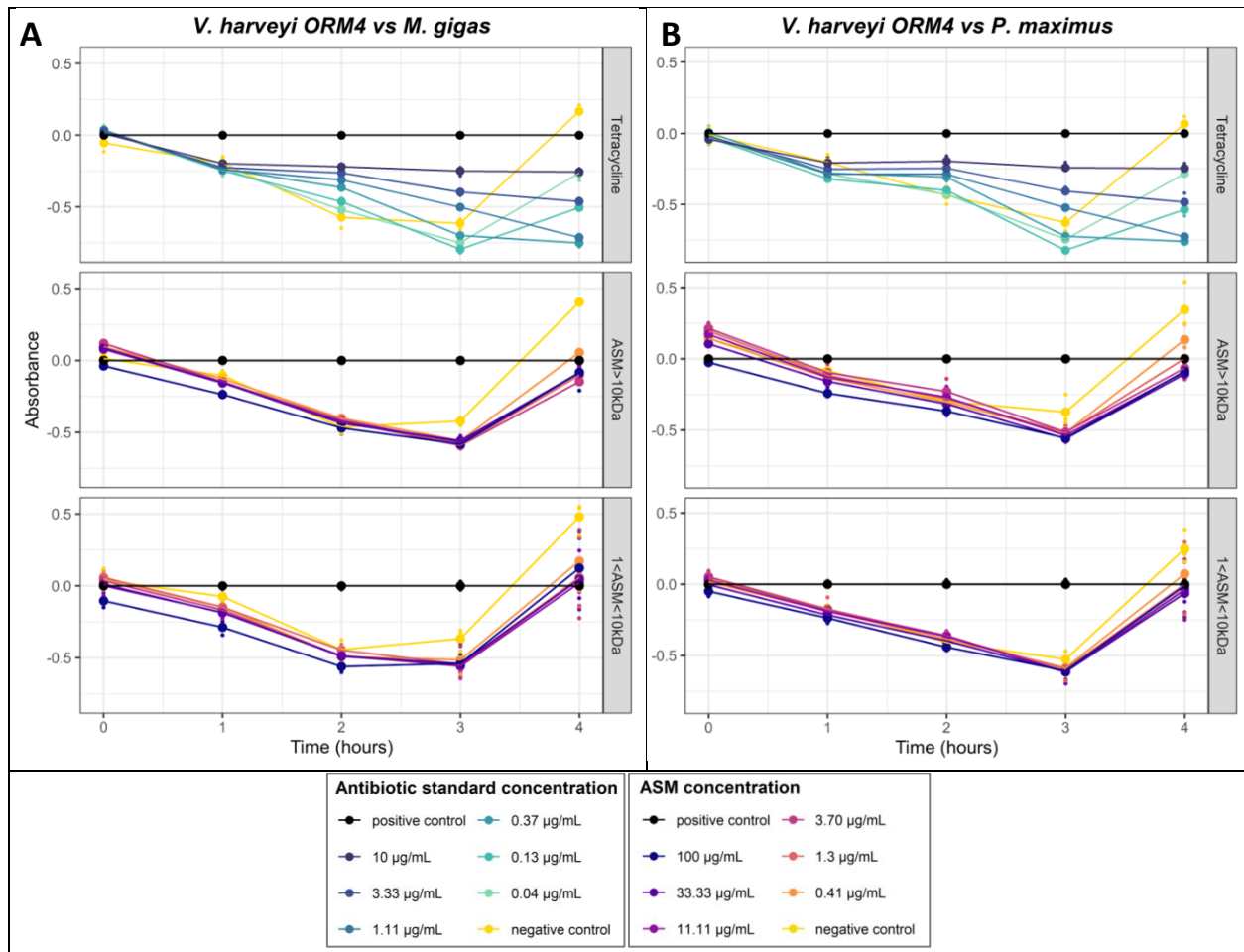


Figure 3.6: Microdilution assays growth curves with *V. harveyi* ORM4. The upper graphs of each panel correspond to positive controls with tetracycline. Test with ASMs extracts from *M. gigas* (A) and *P. maximus* (B).

3.4.3.4. Proteomic Analysis

The proteomic results are summarized in Tables 3.5 and 3.6: Table 3.5 lists the number of AMPP (antimicrobial peptides or proteins) families identified per extract as well as the total number of supporting peptides for each AMPP family. Table 3.6 provides a detailed view of the identified antimicrobial peptides/proteins in each extract, sorted according to biological source (color coded), with the corresponding number of supporting peptides. We remind that these tables consider only hits supported by at least two peptides.

Table 3.5 emphasizes a relative disparity of the number of identified AMPP families depending on the bivalve model: the lowest count was obtained with *V. philippinarum* (12 hits), and the highest, with *M. galloprovincialis* (34), the other models giving intermediate numbers of hits, 13 (*G. glycymeris*), 16 (*C. edule*), 19 (*V. verrucosa*), 21 (*M. gigas*) and 23 (*P. maximus*). Interestingly, one notices that most of the hits are identified in soluble extracts (ASMs), in particular among the low molecular weight fractions of five models. This is especially evident

for the 1<ASM<3 kDa fractions of *M. galloprovincialis* and *V. philippinarum*. In this latter case, it is remarkable that most of the hits - 10 out of 12 - are identified in this fraction, while no hit was found in the AIM. *M. gigas* and *P. maximus* show slightly different AMPP signatures, with a highest number of hits in the ASM>10 kDa fraction. We observe a relative variability of the number of supporting peptides (right column) ranging from 2 (ASM>10 kDa of *V. philippinarum*) to 77 (1<ASM<10 kDa of *V. verrucosa*). In total, 17 extracts are covered by more than 13 supporting peptides.

Table 3.6 complements Table 3.5, by detailing the AMPP families identified in the analysis. Some AMPP are well represented in the different shell extracts: this is the case for molluscan histone 4 (H4), cgUbiquitin, histones 2B (H2B), histone 3 (H3) and lysozyme; they are all represented in at least 10 extracts. H4 (of molluscan source) is particularly well-represented since it occurs in 19 extracts out of 23. 13 AMPPs are represented only in one extract: Pm-AMP-1, maculatin, maximin, ocellatin-6, ctenidin-1, Apl_AvBD-2, acipensin-6, mammalian H4, mSAA3, calcitermin, HMGN, psoriasin and Enterocin L50. Note that 6 of them occur solely in the shell extracts of *M. galloprovincialis*. Among the seven others, we note the occurrence of enterocin L50, which is the single AMPP present in the AIM of *G. glycymeris*, but also the only one of prokaryotic origin; similarly, maculatin and maximin, are only present in the AIM of *M. gigas*. For five species, five AMPPs occur across all fractions: molluscan H4 (*M. galloprovincialis*, *M. gigas*, *P. maximus*, *V. verrucosa*), cgUbiquitin (*P. maximus*), BHP (*M. galloprovincialis*), H2B (*M. gigas*, *P. maximus*), lysozyme (*C. edule*). Some AMPPs, present more than once, are also discriminant between fractions. As an example, H2B, while occurring in most ASMs, is only present in two AIMS: those of *M. gigas* and of *P. maximus*; another example is armadillidin H, occurring only in the soluble low molecular weight fraction of *G. glycymeris* and *M. galloprovincialis*. When reading the table vertically (from the ‘shell fraction viewpoint’), one notices peculiar combinations of AMPPs: in particular, the AIM of *C. edule* encompasses buforin, H3 and lysozyme, three AMPPs rather associated to soluble fractions in the other models. The implications of AMPP distribution in the different fractions are debated in the discussion below.

Table 3.5: Summary of the proteomic results.

Mollusk species	Extract	Identified AMPP families	Supporting peptides
<i>G. glycymeris</i>	AIM	1	6
	ASM>10 kDa	6	41
	1<ASM<10 kDa	6	35
<i>M. galloprovincialis</i>	AIM	3	13
	ASM>10 kDa	8	42
	3<ASM<10 kDa	10	30
	1<ASM<3 kDa	13	50
<i>M. gigas</i>	AIM	6	19
	ASM>10 kDa	9	41
	1<ASM<10 kDa	6	30
<i>P. maximus</i>	AIM	6	15
	ASM>10 kDa	10	36
	1<ASM<10 kDa	7	28
<i>C. edule</i>	AIM	4	6
	ASM>10 kDa	5	23
	1<ASM<10 kDa	7	39
<i>V. verrucosa</i>	AIM	1	4
	ASM>10 kDa	6	58
	1<ASM<10 kDa	12	77
<i>V. philippinarum</i>	AIM	0	0
	ASM>10 kDa	1	2
	3<ASM<10 kDa	1	5
	1<ASM<3 kDa	10	42

Table 3.6: Antimicrobial proteins and peptides (AMPPs) identified in the shell extracts of our studied models. The numbers at the intersection between columns and lines are the numbers of supporting peptides for each AMPP hit.

AMPP hits		Samples (specie, fraction)																							
		<i>G. glycymeris</i>			<i>M. galloprovincialis</i>				<i>M. gigas</i>			<i>P. maximus</i>			<i>C. edule</i>			<i>V. verrucosa</i>			<i>V. philippinarum</i>				
		AIM	ASM>10 kDa	1<ASM<10 kDa	AIM	ASM>10 kDa	3<ASM<10 kDa	1<ASM<3 kDa	AIM	ASM>10 kDa	1<ASM<10 kDa	AIM	ASM>10 kDa	1<ASM<10 kDa	AIM	ASM>10 kDa	1<ASM<10 kDa	AIM	ASM>10 kDa	1<ASM<10 kDa	AIM	ASM>10 kDa	3<ASM<10 kDa	1<ASM<10 kDa	
Mollusca	H4		13	11	5	4	5	6	8	8	9	5	7	8		6	8	4	8	13		2	5	8	
	cgUbiquitin (oyster)		2			2	2	3	2		2	2	3	3			2		3	3				2	
	PmAMP-1 (<i>P. fucata</i>)							4																	
Anura	Brevinin-1						2						3	2											
	Buforin								2		2				2	2			4						
	Gaegurin RN5									4			2							2				3	
	Maculatin								2																
	Maximin								2																
	Ocellatin-6				6																				
Arthropoda	Armadillidin H			2				3																2	
	Ctenidin-1					4																			
	H2A (shrimp)		2	4			3			6			3	4		5				5				4	
Aves	Apl_AvBD-2						2																		
Teleostei	H1 (Atlantic salmon)											2		2	2				35						
	Acipensin-6																				4				
Mammalia	BHP				2	2	2	3													2				
	HRNR1132 (hornerin)							3		2				2										2	
	H2B		14	10			2	6	3	8	9	2	7	7		7	14		6	27				12	
	H3		7	6				2		4	5		4	2	2		6				7			4	
	H4						4																		
	mSAA3 (mouse)											2													
Homo sapiens sapiens	Calcitermin																				4				
	Dermcidin-1							2		3															
	Filaggrin-2 peptide					3		3					2												
	GAPDH			2				3		3			3				2							3	
	HMGN																				2				
	KAMP-19		3			7	4	5				2									6				
	Lysozyme					7	4	7			3		2		2	6	2		2	2				2	
	Psoriasisin					13																			
	Enterocin L50 (Human microbiote)	6																							

3.4.4. Discussion

In the present paper, we have explored the potential antibacterial properties of shell matrices from a range of mollusks of economic interest. To this end, we extracted the whole shell organic matrix of seven model bivalves, which includes both soluble and insoluble fractions. We further fractionated the soluble fraction, according to two cutoffs, one at 10 kDa, the other one at 1 kDa. Only for two models (*M. galloprovincialis*, *V. philippinarum*), an additional cutoff was required, due to the high viscosity, *i.e.*, the richness in organics, of the ASM below 10 kDa. Then, after complete removal of salts by dialysis, followed by lyophilization, we checked the quality of our extracts on gel, then tested them for their ability to inhibit the growth of two selected marine bacterial pathogens. In disk diffusion assays, we showed that some extracts, in particular some insoluble ones, were capable of inhibiting bacterial growth. In microdilution assay performed only with soluble extracts, we observed that some of them had the ability to alter the growth of tested bacteria, mainly by slowing their growth rate and by reducing their carrying capacity. However, at the concentrations tested, we did not find a soluble extract able to fully inhibit bacterial growth. Qualitative proteomics investigations on all shell extracts emphasized that they all contain – without exception - a set of peptides/proteins (from one for *G. glycymeris* AIM to thirteen for $1 < \text{ASM} < 3$ kDa of *M. galloprovincialis*) that are known to exhibit antibacterial properties.

In our approach and strategy, we made some assumptions and took certain technical decisions, listed hereafter: 1) first of all, we selected seven bivalve species that are among the most consumed ones in Europe, in particular in France. Their consumption generates an important tonnage of emptied shells byproducts that may be a valuable source of bioactive molecules; 2) secondly, we adapted our standard extraction protocol, to be able to test the totality of shell organic components, whatever their solubility (Lutet-Toti *et al.*, 2024). In particular, one of the novelties of our protocol is the first-time use of the AIM (acetic acid insoluble matrix) transformed into tablets. This *a priori* choice proves to be successful since all AIMS give positive results, at different degrees, against *V. harveyi* ORM4 and three of them, against *A. salmonicida*, in zone inhibition assay; 3) thirdly, for dealing with the soluble matrix, we used two cutoffs, for fractionating a high molecular weight moiety from a low molecular weight one. The selection of these two cutoffs is not arbitrary but based on our personal experience. The first cutoff allows collecting rapidly a large proportion of shell matrix proteins (Oudot *et al.*, 2020). However, it is not sufficient if one wants to collect almost all (99%) shell macromolecules. Given that most antibacterial substances are peptides and not proteins -

implying that their molecular weight is below 5 kDa – the use of a second cutoff (1 kDa) was necessary in the perspective to collect most of all low molecular weight molecules. In our ultrafiltration system, and from a theoretical viewpoint, only very short peptides (< 1 kDa) may pass through the membrane, *i.e.*, may be lost. However, we have shown that they represent a negligible fraction of the shell organics: attempts by one of us to extract free pigments from shells have shown that these molecules (predominantly porphyrins and carotenoids) of molecular weight below 1 kDa are also retained by the 1kDa cutoff ultrafiltration membrane (Polacchi *et al.*, *submitted*); 4) at last, we selected for our tests two marine bacterial strains that are common pathogens inducing vibriosis. They cover a broad range of water temperatures (warm waters for *V. harveyi* ORM4, cold waters for *A. salmonicida*) and target a large range of marine organisms, from mollusks to teleost fishes. Consequently, the outcome of our research has direct implications in aquaculture.

When setting up our tests, we faced some technical difficulties and limitations, involving the bacterial strains used, the antibacterial tests developed and the proteomics approach. About the first issue, growing marine bacteria was time-consuming and more challenging than growing standard strains (Rodrigues & de Carvalho, 2022). In particular, *A. salmonicida*'s *in vitro* growth rate is low, with an optimal culture temperature of 12°C, difficult to maintain in standard incubators. In addition, our two strains require solid marine agar and liquid broth media that are both turbid: in Petri dishes, this makes the reading and measuring of the inhibition zone diameters more difficult than with a standard NZY agar; in liquid cultures, the spectrophotometric reading of the yellowish background has to include different blank measurements.

The second set of limitations concerns the two standard assays used (paper disks/tablets and microplate/dilution assay) *versus* the soluble matrix extracts. By definition, soluble shell matrices contain a complex amalgamate of proteins (Marin, 2020) and potential antibacterial substances may be 'diluted' by other non-reactive proteins. Consequently, we cannot exclude that even at high quantity of matrix tested on a disk (typically 20 µg), the quantity of antibacterial substance was low and produced reduced or no effect. Another constraint appeared with the dilution assay test on microplate using phenol red: increasing the concentration of the ASM above 100 µg/mL in the starting solution (C1, see Table 3.2) was simply not possible, since the soluble matrix, known to contain an abundance of polyanionic proteins (Aspartic acid-rich) lowered the pH of the solution and induced the red-to-yellow color transition spontaneously, even before any addition of bacteria. One way to circumvent this bottleneck

would be to ‘concentrate’ cationic molecules of the different soluble shell matrix fractions, by performing a post-dialysis preparative ion-exchange chromatography on an anionic resin. This operation would separate putative antimicrobial peptides (belonging to the cationic fraction) from the polyanionic macromolecules. However, it would introduce an extra step in the analytical process, beyond the scope of this initial screening.

The third type of limitations relies on the proteomic investigations: firstly, the analysis we performed is qualitative and not quantitative: it gives us indications on the presence/absence of a given antimicrobial peptide, but not on its concentration in the mixture. In our analytical system, even traces of peptides can be detected. In addition, because we used as reference a standard antimicrobial database assembled from known AMPPs of diverse sources, including insects, toads, fishes, mammals and few mollusks, we only obtained results on the presence/absence of these known AMPPs. In other words, we may have missed novel and/or undiscovered important AMPPs, not identified by MASCOT software. If they exist, these AMPPs will require a deepened characterization, by, for example, performing 2D gels and doing proteomics on 2D spots, but such a detailed study lays far beyond the scope of our screening. At last, we focused our investigations on the proteinaceous moieties of the shell fractions. However, it is known for a long time that shell matrices also contain pigments, oligo- and polysaccharides, which may exert antimicrobial activity. Antimicrobial activity of saccharide moieties of mollusk origin has been reported (Hajji *et al.*, 2015; Shanmugam *et al.*, 2016) as has that of pigment (Esparza-Espinoza *et al.*, 2021) but the involvement of mollusk shell saccharides and pigments in antimicrobial activity remains to be documented.

In spite of these limitations, we were able to identify a true antimicrobial activity from some shell extracts. Three AIMS inhibited the growth of *A. salmonicida*, among which that of *C. edule* gives the most remarkable results. Against *V. harveyi* ORM4, all AIMS showed inhibition zones of varying diameters among which four tablets (*M. gigas*, *P. maximus*, *V. philippinarum*, *V. verrucosa*) induce an effect comparable to that of the positive control. These positive results imply the presence of diffusible factors in AIMS, which, at first sight, may appear counterintuitive, given the overall insolubility of these extracts. However, as previously shown here (Figure 3.2, see LS-AIM lanes) and elsewhere (Mouchi *et al.*, 2016), AIMS also contain molecules that are not tightly bound to the insoluble organic scaffold and can be further solubilized. We propose that the AMPPs responsible for the inhibition zones here have to be found among these diffusible factors, the identity of which remains to be verified. In particular, the whitish crown of diffusible compounds close to the edge of the inhibition zone in four AIM

tablets warrants further investigation. Correlating disk diffusion results on AIM tablets to proteomic data does not provide an immediately explicit link to their antibacterial properties. However, in some cases, the occurrence or combinations of some AMPPs in these extracts suggest their involvement in the antibacterial properties: for example, *C. edule* AIM contains an unusual set of AMPPs including buforin, H3 and lysozyme, that might explain its remarkable ability to inhibit the growth of *A. salmonicida*. Coincidentally, extracts from the soft tissues of *C. edule* have been found to exert a broad antimicrobial activity against both terrestrial and marine Gram+ and Gram- bacteria (Defer *et al.*, 2009). The combination of AMPPs in *C. edule* is not found in the two other positive AIMS, that of *M. gigas* and of *P. maximus*, which exhibit a much weaker inhibitory effect on *A. salmonicida*. For these two models, we suggest that the occurrence of cgUbiquitin and H2B may be at the origin of their inhibiting capacity, low for *A. salmonicida*, high for *V. harveyi*, against both pathogens. The AIM of *M. galloprovincialis* exerts no inhibitory activity against *A. salmonicida*, and very reduced – compared to the other AIMS – against *V. harveyi*. This singularity might be correlated to its peculiar AMPP composition.

The soluble extracts exhibited a more nuanced response in the two *in vitro* tests: first, some results on ASM show more variability than others and are consequently less robust as indicated by p-values of Figure 2B and Table 3. Secondly, in the disk assay, only three extracts (the two ASMs of *M. gigas*, the ASM>10 kDa of *P. maximus*) gave a positive response, corroborated with an alteration of the growth of *V. harveyi* in the microdilution assay. Two of them (the ASMs above 10 kDa) induced an alteration of the growth of *A. salmonicida*, together with three other ASM extracts (1<ASM<10 kDa of *P. maximus*; the ASM>10 kDa and 3<ASM<10 kDa of *M. galloprovincialis*). The alterations can take different forms: a reduction of maximal growth rate during the exponential phase, a reduction of carrying capacity, a mix of both phenomena, and finally, a delay in reaching the carrying capacity (due either to a lengthening of the lag phase or a non-linear growth rate). So far, with the current range of ASMs concentration used, it is difficult to determine whether these alterations are due to bactericidal or bacteriostatic effects. When one integrates the ASM responses to their proteomics signatures, we obtain a blurred signal: there is no obvious AMPP or combination of AMPPs that may explain the peculiar antibacterial activity of some ASMs.

We identified by proteomics several types of AMPPs, among which lysozyme, ubiquitin, and above all, a set of histones, *i.e.*, nuclear proteins, such as H1, H2A, H2B, H3 and H4. The occurrence of such proteins in shells may seem odd. However, previous studies

reported the presence of histones in biocalcified tissues such as the eggshell (Réhault-Godbert *et al.*, 2011) or the Ram's horn squid shell (Oudot *et al.*, 2020). From a mechanistic viewpoint, we think that histones or histone-derived peptides may be secreted as components of the calcifying matrix, which are then occluded in the shell during mineral deposition. In general, the calcifying shell matrix in mollusks contains not only the macromolecules required for interacting with calcium ions or calcium carbonate nuclei, but also a large set of proteins that insure the stability and protection of the system (Oudot *et al.*, 2020). By their presence in the shell, AMPPs are a part of this defense line.

This exploratory screening has revealed some antibacterial properties of the shells of seven commercial bivalves. The insoluble extracts show the most striking results against two marine pathogens, *A. salmonicida* and *V. harveyi* ORM4, making them promising candidates as antibacterial drugs. Our experimental results may feed potential applications in aquaculture: the extraction and purification of AIMs from shells are relatively easy and do not require harmful eco-unfriendly chemicals. Thus, in spite of a relatively low proportion of AIM in the shell of the tested bivalves (less than 1%), upscaling the extraction process is realistic and adaptable to multiple formulations, like mixing of the extract with food granulates. This of course will need further development and optimization, but to give an example, between 4 and 5 kgs of AIM can be extracted from one ton of *M. gigas* shell, which makes the process still profitable.

Antibacterial effects are more nuanced with ASMs. However, two species stand out, the Pacific oyster *Magallana gigas* and the great scallop *Pecten maximus*, for which all the organic extracts show some antibacterial activity. For these two models, a formal quantification and testing one per one of the AMPPs constitutes the next analytical step. At last, one should keep in mind that cleaned shell powders may be potentially used too, before any extraction: as illustrated in our study, the powders of the common (*C. edule*) and dog (*G. glycymeris*) cockles exhibit an antibacterial activity. This finding corroborates the use of shell powders in ethnomedicines (González, J. A., & Vallejo 2023) and provides a putative easy and cost-effective alternative to more sophisticatedly produced extracts. The mollusk shell constitutes a promising source of bioactive molecules and its repurposing in aquaculture may contribute to the development of a virtuous circular economy.

Authors contribution

C.L.T.: conception of the study, experimental work, data analysis, original draft writing, review, editing, conception of figures, funding. M.D.S.F.: assistance in experimental conception and in experimental work. J.T., N.D., and A.F.: assistance in experimental work. C.D.: assistance in experimental conception. A.C.: assistance in data analysis. A.B.: assistance in conception of the study, bacterial strains acquisition. C.B.: proteomic analysis and data analysis. G.F. and S.G.: funding and corrections to the original draft. F.M.: conception of PhD project, conception of the study, project administration including funding acquisition and supervision, data analysis, original draft writing, review, and editing. All authors have read and agreed to the published version of the manuscript.

Acknowledgement

We thank Christine Paillard from UBO LEMAR lab for providing us with *Vibrio harveyi* stains, and Pasteur Institute Collections for *Aliivibrio salmonicida* strains. The JASCO company is acknowledged for providing the manual press used for AIM tablet production.

Funding

CLT is the recipient of a PhD fellowship under joint-supervision between Université de Bourgogne (uB) and Alma Mater Studiorum - Università di Bologna (UniBo). The research leading to these results has been conceived under the International PhD Program “Innovative Technologies and Sustainable Use of Mediterranean Sea Fishery and Biological Resources” (www.FishMed-PhD.org). This study represents partial fulfilment of the requirements for the Ph.D. thesis of CLT at the FishMed PhD Program (University of Bologna, Italy). In addition, CLT was supported by a one-off grant from AFFDU (Association des Femmes Françaises Diplômées de l’Université) in 2022 and an award from the Société Française de Biologie des Tissus Minéralisés (SFBTM) and from the Fondation Arthritis, in May 2023. Other supports to FM include the following: (1) the MAELSTROM project (les MATricEs coquiLLières bacTÉricides au secOurs des géoMatériaux) from TELLUS-INTERRVIE program (CNRS, 2022); (2) the PRELUDE project (Peptides antimicrobiens des coquilles de mollusques d’intérêt Economique) financed by Observatoire des Sciences de l’Univers (OSU) Theta, Besançon, in 2023; (3) the MAELSTROM-bis project, financed by the TELLUS-INTERRVIE program from CNRS, in 2024.

3.4.5. References

- Addadi, L., Joester, D., Nudelman, F., and Weiner, S. (2006). Mollusk Shell Formation: A Source of New Concepts for Understanding Biomineralization Processes. *Chemistry – A European Journal*, 12(4), 980–987. <https://doi.org/10.1002/chem.200500980>
- Arnich, N., Abadie, E., Amzil, Z., Dechraoui Bottein, M.-Y., Comte, K., Chaix, E., Delcourt, N., Hort, V., Mattei, C., Molgó, J., and Le Garrec, R. (2021). Guidance Level for Brevetoxins in French Shellfish. *Marine Drugs*, 19(9), Article 9. <https://doi.org/10.3390/md19090520>
- Austin, B. (2006). *Vibrio salmonicida*. In: The Biology of Vibrios (pp. 281–284). John Wiley and Sons, Ltd. <https://doi.org/10.1128/9781555815714.ch20>
- Austin, B., and Zhang, X.-H. (2006). *Vibrio harveyi*: A significant pathogen of marine vertebrates and invertebrates. *Letters in Applied Microbiology*, 43(2), 119–124. <https://doi.org/10.1111/j.1472-765X.2006.01989.x>
- Baletta, F. N., and Gómez-Chiarri, M. (2016). Effect of *Sargassum oligocystum* Hot-Water Extract on Innate Immune Response and Survival of Summer Flounder *Paralichthys dentatus* to *Vibrio harveyi* Challenge. *Israeli Journal of Aquaculture - Bamidgeh*, 68. <https://doi.org/10.46989/001c.20811>
- Balouiri, M., Sadiki, M., and Ibensouda, S. K. (2016). Methods for *in vitro* evaluating antimicrobial activity: A review. *Journal of Pharmaceutical Analysis*, 6(2), 71–79. <https://doi.org/10.1016/j.jpha.2015.11.005>
- Bauer, A. W., Kirby, W. M., Sherris, J. C., and Turck, M. (1966). Antibiotic susceptibility testing by a standardized single disk method. *American Journal of Clinical Pathology*, 45(4), 493–496.
- Bieler, R., Mikkelsen, P. M., Collins, T. M., Glover, E. A., González, V. L., Graf, D. L., Harper, E. M., Healy, J., Kawauchi, G. Y., Sharma, P. P., Staubach, S., Strong, E. E., Taylor, J. D., Tëmkin, I., Zardus, J. D., Clark, S., Guzmán, A., McIntyre, E., Sharp, P., and Giribet, G. (2014). Investigating the Bivalve Tree of Life – an exemplar-based approach combining molecular and novel morphological characters. *Invertebrate Systematics*, 28(1), 32–115. <https://doi.org/10.1071/IS13010>

- Bjelland, A. M., Johansen, R., Brudal, E., Hansen, H., Winther-Larsen, H. C., and Sørum, H. (2012). *Vibrio salmonicida* pathogenesis analyzed by experimental challenge of Atlantic salmon (*Salmo salar*). *Microbial Pathogenesis*, 52(1), 77–84. <https://doi.org/10.1016/j.micpath.2011.10.007>
- Blazanin, M. (2024). gcplyr: An R package for microbial growth curve data analysis. *BMC Bioinformatics*, 25(1), 232. <https://doi.org/10.1186/s12859-024-05817-3>
- Bondad-Reantaso, M. G., MacKinnon, B., Karunasagar, I., Fridman, S., Alday-Sanz, V., Brun, E., Le Groumellec, M., Li, A., Surachetpong, W., Karunasagar, I., Hao, B., Dall’Occo, A., Urbani, R., and Caputo, A. (2023). Review of alternatives to antibiotic use in aquaculture. *Reviews in Aquaculture*, 15(4), 1421–1451. <https://doi.org/10.1111/raq.12786>
- Borrego, J. J., Castro, D., Luque, A., Paillard, C., Maes, P., Garcia, M. T., and Ventosa, A. (1996). *Vibrio tapetis* sp. Nov., the Causative Agent of the Brown Ring Disease Affecting Cultured Clams. *International Journal of Systematic and Evolutionary Microbiology*, 46(2), 480–484. <https://doi.org/10.1099/00207713-46-2-480>
- Boyle, K. E., Monaco, H., Ditmarsch, D. van, Deforet, M., and Xavier, J. B. (2015). Integration of Metabolic and Quorum Sensing Signals Governing the Decision to Cooperate in a Bacterial Social Trait. *PLOS Computational Biology*, 11(6), e1004279. <https://doi.org/10.1371/journal.pcbi.1004279>
- Burge, C. A., Eakin, C. M., Friedman, C. S., Froelich, B., Hershberger, P. K., Hofmann, E. E., Petes, L. E., Prager, K. C., Weil, E., Willis, B. L., Ford, S. E., and Harvell, C. D. (2014). Climate Change Influences on Marine Infectious Diseases: Implications for Management and Society. *Annual Review of Marine Science*, 6(Volume 6, 2014), 249–277. <https://doi.org/10.1146/annurev-marine-010213-135029>
- Canesi, L., Grande, C., Pezzati, E., Balbi, T., Vezzulli, L., and Pruzzo, C. (2016). Killing of *Vibrio cholerae* and *Escherichia coli* Strains Carrying D-mannose-sensitive Ligands by *Mytilus* Hemocytes is Promoted by a Multifunctional Hemolymph Serum Protein. *Microbial Ecology*, 72(4), 759–762. <https://doi.org/10.1007/s00248-016-0757-1>
- Caputo, A., Bondad-Reantaso, M. G., Karunasagar, I., Hao, B., Gaunt, P., Verner-Jeffreys, D., Fridman, S., and Dorado-Garcia, A. (2023). Antimicrobial resistance in aquaculture: A global analysis of literature and national action plans. *Reviews in Aquaculture*, 15(2), 568–578. <https://doi.org/10.1111/raq.12741>
- Cardinaud, M., Dheilily, N. M., Huchette, S., Moraga, D., and Paillard, C. (2015). The early stages of the immune response of the European abalone *Haliotis tuberculata* to a *Vibrio harveyi* infection. *Developmental and Comparative Immunology*, 51(2), 287–297. <https://doi.org/10.1016/j.dci.2015.02.019>
- Cole, A. M., Weis, P., and Diamond, G. (1997). Isolation and characterization of pleurocidin, an antimicrobial peptide in the skin secretions of winter flounder. *The Journal of Biological Chemistry*, 272(18), 12008–12013. <https://doi.org/10.1074/jbc.272.18.12008>
- Colquhoun, D. J., Alvheim, K., Dommarsnes, K., Syvertsen, C., and Sørum, H. (2002). Relevance of incubation temperature for *Vibrio salmonicida* vaccine production. *Journal of Applied Microbiology*, 92(6), 1087–1096. <https://doi.org/10.1046/j.1365-2672.2002.01643.x>
- Cushnie, T. P. T., Cushnie, B., Echeverría, J., Fowsantear, W., Thammawat, S., Dodgson, J. L. A., Law, S., and Clow, S. M. (2020). Bioprospecting for Antibacterial Drugs: A Multidisciplinary Perspective on Natural Product Source Material, Bioassay Selection and Avoidable Pitfalls. *Pharmaceutical Research*, 37(7), 125. <https://doi.org/10.1007/s11095-020-02849-1>
- Davies, J., and Davies, D. (2010). Origins and Evolution of Antibiotic Resistance. *Microbiology and Molecular Biology Reviews: MMBR*, 74(3), 417–433. <https://doi.org/10.1128/MMBR.00016-10>
- de Souza Valente, C., and Wan, A. H. L. (2021). *Vibrio* and major commercially important vibriosis diseases in decapod crustaceans. *Journal of Invertebrate Pathology*, 181, 107527. <https://doi.org/10.1016/j.jip.2020.107527>
- Defer, D., Bourgognon, N., and Fleury, Y. (2009). Screening for antibacterial and antiviral activities in three bivalve and two gastropod marine molluscs. *Aquaculture*, 293(1), 1–7. <https://doi.org/10.1016/j.aquaculture.2009.03.047>
- Duff, D. C. B. (1942). The Oral Immunization of Trout Against Bacterium *salmonicida*. *The Journal of Immunology*, 44(1), 87–94. <https://doi.org/10.4049/jimmunol.44.1.87>
- Egidius, E., Wiik, R., Andersen, K., Hoff, K. A., and Hjeltnes, B. (1986). *Vibrio salmonicida* sp. Nov., a New Fish Pathogen. *International Journal of Systematic and Evolutionary Microbiology*, 36(4), 518–520. <https://doi.org/10.1099/00207713-36-4-518>
- Esparza-Espinoza, D. M., Plascencia-Jatomea, M., López-Saiz, C. M., Parra-Vergara, N. V., Carbonell-Barrachina, A. A., Cárdenas-López, J., and Ezquerro-Brauer, J. M. (2021). Improving the shelf life of chicken burgers using *Octopus vulgaris* and *Dosidicus gigas* skin pigment extracts. *Food Science and Technology*, 42, e18221. <https://doi.org/10.1590/fst.18221>
- EUCAST. (2024). EUCAST guidance on: When there are no Breakpoints in breakpoint tables? *European Society of Clinical Microbiology and Infectious Diseases - European Committee on Antimicrobial Susceptibility Testing*. <https://www.eucast.org/eucastguidancedocuments>

- FAO (2024). The State of World Fisheries and Aquaculture 2024—Blue Transformation in action. *Food and Agriculture Organization of the United Nations*, 264 p. <https://doi.org/10.4060/cd0683en>
- Ferchichi, H., St-Hilaire, A., Ouarda, T. B. M. J., and Lévesque, B. (2021). Impact of the future coastal water temperature scenarios on the risk of potential growth of pathogenic *Vibrio* marine bacteria. *Estuarine, Coastal and Shelf Science*, 250, 107094. <https://doi.org/10.1016/j.ecss.2020.107094>
- Gelman, D., Yerushalmy, O., Alkalay-Oren, S., Rakov, C., Ben-Porat, S., Khalifa, L., Adler, K., Abdalrhman, M., Copenhagen-Glazer, S., Aslam, S., Schooley, R. T., Nir-Paz, R., and Hazan, R. (2021). Clinical Phage Microbiology: A suggested framework and recommendations for the *in-vitro* matching steps of phage therapy. *The Lancet Microbe*, 2(10), e555–e563. [https://doi.org/10.1016/S2666-5247\(21\)00127-0](https://doi.org/10.1016/S2666-5247(21)00127-0)
- González, J. A., and Vallejo, J. R. (2023). The Use of Shells of Marine Molluscs in Spanish Ethnomedicine: A Historical Approach and Present and Future Perspectives. *Pharmaceuticals*, 16(10), Article 10. <https://doi.org/10.3390/ph16101503>
- Griffin, D. W., Benzel, W. M., Fisher, S. C., Focazio, M. J., Iwanowicz, L. R., Loftin, K. A., Reilly, T. J., and Jones, D. K. (2019). The presence of antibiotic resistance genes in coastal soil and sediment samples from the eastern seaboard of the USA. *Environmental Monitoring and Assessment*, 191(Suppl 2), 300. <https://doi.org/10.1007/s10661-019-7426-z>
- Hajji, S., Younes, I., Rinaudo, M., Jellouli, K., and Nasri, M. (2015). Characterization and *In vitro* Evaluation of Cytotoxicity, Antimicrobial and Antioxidant Activities of Chitosans Extracted from Three Different Marine Sources. *Applied Biochemistry and Biotechnology*, 177(1), 18–35. <https://doi.org/10.1007/s12010-015-1724-x>
- Håstein, T., Gudding, R., and Evensen, O. (2005). Bacterial vaccines for fish—An update of the current situation worldwide. *Developments in Biologicals*, 121, 55–74.
- Hegde, A., Kabra, S., Basawa, R. M., Khile, D. A., Abbu, R. U. F., Thomas, N. A., Manickam, N. B., and Raval, R. (2023). Bacterial diseases in marine fish species: Current trends and future prospects in disease management. *World Journal of Microbiology and Biotechnology*, 39(11), 317. <https://doi.org/10.1007/s11274-023-03755-5>
- Held, P. (2022). Using Phenol Red to Assess pH in Tissue Culture Media. Application Notes - Cancer Biology. *Agilent Technologies Inc*, 9p.
- Hetru, C., and Bulet, P. (1997). Strategies for the isolation and characterization of antimicrobial peptides of invertebrates. *Methods in Molecular Biology (Clifton, N.J.)*, 78, 35–49. <https://doi.org/10.1385/0-89603-408-9:35>
- Huang, P., Cai, J., Yu, D., Tang, J., Lu, Y., Wu, Z., Huang, Y., and Jian, J. (2019). An IL-6 gene in humphead snapper (*Lutjanus sanguineus*): Identification, expression analysis and its adjuvant effects on *Vibrio harveyi* OmpW DNA vaccine. *Fish and Shellfish Immunology*, 95, 546–555. <https://doi.org/10.1016/j.fsi.2019.11.013>
- Immel, F., Broussard, C., Catherinet, B., Plasseraud, L., Alcaraz, G., Bundeleva, I., and Marin, F. (2016). The Shell of the Invasive Bivalve Species *Dreissena polymorpha*: Biochemical, Elemental and Textural Investigations. *PLOS ONE*, 11(5), e0154264. <https://doi.org/10.1371/journal.pone.0154264>
- Ina-Salwany, M. Y., Al-saari, N., Mohamad, A., Mursidi, F.-A., Mohd-Aris, A., Amal, M. N. A., Kasai, H., Mino, S., Sawabe, T., and Zamri-Saad, M. (2019). Vibriosis in Fish: A Review on Disease Development and Prevention. *Journal of Aquatic Animal Health*, 31(1), 3–22. <https://doi.org/10.1002/aah.10045>
- Jiang, Q., Shi, L., Ke, C., You, W., and Zhao, J. (2013). Identification and characterization of *Vibrio harveyi* associated with diseased abalone *Haliotis diversicolor*. *Diseases of Aquatic Organisms*, 103(2), 133–139. <https://doi.org/10.3354/dao02572>
- Johnson, F. H., and Shunk, I. V. (1936). An Interesting New Species of Luminous Bacteria. *Journal of Bacteriology*, 31(6), 585–593.
- Kah Sem, N. A. D., Abd Gani, S., Chong, C. M., Natrah, I., and Shamsi, S. (2023). Management and Mitigation of Vibriosis in Aquaculture: Nanoparticles as Promising Alternatives. *International Journal of Molecular Sciences*, 24(16), Article 16. <https://doi.org/10.3390/ijms241612542>
- Kashulin, A., Seredkina, N., and Sørum, H. (2017). Cold-water vibriosis. The current status of knowledge. *Journal of Fish Diseases*, 40(1), 119–126. <https://doi.org/10.1111/jfd.12465>
- Kashulin, A., and Sørum, H. (2014). A novel *in vivo* model for rapid evaluation of *Aliivibrio salmonicida* infectivity in Atlantic salmon. *Aquaculture*, 420–421, 112–118. <https://doi.org/10.1016/j.aquaculture.2013.10.025>
- Kassambara, A. (2023). rstatix: Pipe-Friendly Framework for Basic Statistical Tests. *CRAN.R-project*. <https://CRAN.R-project.org/package=rstatix>
- Kosikowska, P., and Lesner, A. (2016). Antimicrobial peptides (AMPs) as drug candidates: A patent review (2003–2015). *Expert Opinion on Therapeutic Patents*, 26(6), 689–702. <https://doi.org/10.1080/13543776.2016.1176149>

- Laabir, M., Jauzein, C., Genovesi, B., Masseret, E., Grzebyk, D., Cecchi, P., Vaquer, A., Perrin, Y., and Collos, Y. (2011). Influence of temperature, salinity and irradiance on the growth and cell yield of the harmful red tide dinoflagellate *Alexandrium catenella* colonizing Mediterranean waters. *Journal of Plankton Research*, 33(10), 1550–1563. <https://doi.org/10.1093/plankt/fbr050>
- Leifson, E. (1963). Determination of carbohydrate metabolism of marine bacteria. *Journal of Bacteriology*, 85(5), 1183–1184. <https://doi.org/10.1128/jb.85.5.1183-1184.1963>
- Leoni, G., De Poli, A., Mardirossian, M., Gambato, S., Florian, F., Venier, P., Wilson, D. N., Tossi, A., Pallavicini, A., and Gerdol, M. (2017). Myticalins: A Novel Multigenic Family of Linear, Cationic Antimicrobial Peptides from Marine Mussels (*Mytilus* spp.). *Marine Drugs*, 15(8), Article 8. <https://doi.org/10.3390/md15080261>
- Li, B., Qiu, Y., Shi, H., and Yin, H. (2016). The importance of lag time extension in determining bacterial resistance to antibiotics. *Analyst*, 141(10), 3059–3067. <https://doi.org/10.1039/C5AN02649K>
- López-Abarrategui, C., Alba, A., Lima, L. A., Maria-Neto, S., Vasconcelos, I. M., Oliveira, J. T. A., Dias, S. C., Otero-Gonzalez, A. J., and Franco, O. L. (2012). Screening of Antimicrobials from Caribbean Sea Animals and Isolation of Bactericidal Proteins from the Littoral Mollusk *Cenchritis muricatus*. *Current Microbiology*, 64(5), 501–505. <https://doi.org/10.1007/s00284-012-0096-5>
- Lutet-Toti, C., Da Silva Feliciano, M., Debrosse, N., Thomas, J., Plasseraud, L., and Marin, F. (2024). Diverting the Use of Hand-Operated Tablet Press Machines to Bioassays: A Novel Protocol to Test ‘Waste’ Insoluble Shell Matrices. *Methods and Protocols*, 7(2), Article 2. <https://doi.org/10.3390/mps7020030>
- Lutet-Toti, C., Da Silva Feliciano, M., Thomas, J., Crosland, A., Develay, C., Debrosse, N., Force, A., Bidault, A., Broussard, C., Falini, G., Goffredo, S., and Marin, F. (2025). Do bivalve shells exhibit antibacterial properties? Screening calcifying organic matrices against two major marine pathogens. *Science of the TOTAL ENvironment (STOTEN)*, submitted.
- Marin, F. (2020). Mollusc shellomes: Past, present and future. *Journal of Structural Biology*, 212(1), 107583. <https://doi.org/10.1016/j.jsb.2020.107583>
- Marin, F., and Luquet, G. (2007). Unusually Acidic Proteins in Biomineralization. In *Handbook of Biomineralization* (pp. 273–290). John Wiley and Sons, Ltd. <https://doi.org/10.1002/9783527619443.ch16>
- Marin, F., Luquet, G., Marie, B., and Medakovic, D. (2008). Molluscan Shell Proteins: Primary Structure, Origin, and Evolution. In: *Current Topics in Developmental Biology* (Vol. 80, pp. 209–276). Academic Press. [https://doi.org/10.1016/S0070-2153\(07\)80006-8](https://doi.org/10.1016/S0070-2153(07)80006-8)
- Maselli, V., Galdiero, E., Salzano, A. M., Scaloni, A., Maione, A., Falanga, A., Naviglio, D., Guida, M., Di Cosmo, A., and Galdiero, S. (2020). OctoPartenopin: Identification and Preliminary Characterization of a Novel Antimicrobial Peptide from the Suckers of *Octopus vulgaris*. *Marine Drugs*, 18(8), Article 8. <https://doi.org/10.3390/md18080380>
- Massoud, R., Saffari, H., Massoud, A., and Moteian, M. (2020). Screening methods for assessment of antibacterial activity in nature. Conference Paper, *4th Int. Conf. on Applied Research in Science and Engineering*, 11p.
- Mira, P., Yeh, P., and Hall, B. G. (2022). Estimating microbial population data from optical density. *PLOS ONE*, 17(10), e0276040. <https://doi.org/10.1371/journal.pone.0276040>
- Morot, A., El Fekih, S., Bidault, A., Le Ferrand, A., Jouault, A., Kavousi, J., Bazire, A., Pichereau, V., Dufour, A., Paillard, C., and Delavat, F. (2021). Virulence of *Vibrio harveyi* ORM4 towards the European abalone *Haliotis tuberculata* involves both quorum sensing and a type III secretion system. *Environmental Microbiology*, 23(9), 5273–5288. <https://doi.org/10.1111/1462-2920.15592>
- Morrissey, J. H. (1981). Silver stain for proteins in polyacrylamide gels: A modified procedure with enhanced uniform sensitivity. *Analytical Biochemistry*, 117(2), 307–310. [https://doi.org/10.1016/0003-2697\(81\)90783-1](https://doi.org/10.1016/0003-2697(81)90783-1)
- Mouchi, V., Lartaud, F., Guichard, N., Immel, F., de Rafélis, M., Broussard, C., Crowley, Q. G., and Marin, F. (2016). Chalky versus foliated: A discriminant immunogold labelling of shell microstructures in the edible oyster *Crassostrea gigas*. *Marine Biology*, 163(12), 256. <https://doi.org/10.1007/s00227-016-3040-6>
- Nicolas, J. L., Basuyaux, O., Mazurié, J., and Thébault, A. (2002). *Vibrio carchariae*, a pathogen of the abalone *Haliotis tuberculata*. *Diseases of Aquatic Organisms*, 50(1), 35–43. <https://doi.org/10.3354/dao050035>
- Ogle, D. H., Doll, J. C., Wheeler, A. P., and Dinno, A., (2023). FSA: Simple Fisheries Stock Assessment Methods (Version 0.9.5). *CRAN.R-project*. <https://cran.r-project.org/web/packages/FSA/index.html>
- Oh, R., Lee, M. J., Kim, Y.-O., Nam, B.-H., Kong, H. J., Kim, J.-W., Park, J.-Y., Seo, J.-K., and Kim, D.-G. (2020). Myticusin-beta, antimicrobial peptide from the marine bivalve, *Mytilus coruscus*. *Fish and Shellfish Immunology*, 99, 342–352. <https://doi.org/10.1016/j.fsi.2020.02.020>
- Oliveira, J., Castilho, F., Cunha, A., and Pereira, M. J. (2012). Bacteriophage therapy as a bacterial control strategy in aquaculture. *Aquaculture International*, 20(5), 879–910. <https://doi.org/10.1007/s10499-012-9515-7>
- Oudot, M., Neige, P., Shir, I. B., Schmidt, A., Strugnell, J. M., Plasseraud, L., Broussard, C., Hoffmann, R., Lukeneder, A., and Marin, F. (2020). The shell matrix and microstructure of the Ram’s Horn squid:

- Molecular and structural characterization. *Journal of Structural Biology*, 211(1), 107507. <https://doi.org/10.1016/j.jsb.2020.107507>
- Oudot, M., Shir, I. B., Schmidt, A., Plasseraud, L., Broussard, C., Neige, P., and Marin, F. (2020). A Nature's Curiosity: The Argonaut "Shell" and Its Organic Content. *Crystals*, 10(9), Article 9. <https://doi.org/10.3390/cryst10090839>
- Polacchi, L., Lutet-Toti, C., Basuyaux, O., Guériaux, P., Albéric, M., Pasco, H., Merle, D., Habermeyer, B., Guilard, R., Thoury, M., and Marin, F. (2025). Innovative coupling of non-standard 1D-electrophoresis with luminescence spectral imaging to decipher invisible biochromes in modern and fossil shells. *Methods in Ecology and Evolution*, submitted.
- Pujalte, M.-J., Ortigosa, M., Urdaci, M.-C., Garay, E., and Grimont, P. A. D. (1993). *Vibrio mytili* sp. Nov., from Mussels. *International Journal of Systematic and Evolutionary Microbiology*, 43(2), 358–362. <https://doi.org/10.1099/00207713-43-2-358>
- Core Team. (2023). R: A Language and Environment for Statistical Computing. *R Foundation for Statistical Computing*. <https://www.R-project.org/>
- Ramazi, S., Mohammadi, N., Allahverdi, A., Khalili, E., and Abdolmaleki, P. (2022). A review on antimicrobial peptide databases and the computational tools. *Databases* vol. 2022: art baac011, 1-17.
- Réhault-Godbert, S., Hervé-Grépinet, V., Gautron, J., Cabau, C., Nys, Y., and Hincke, M. (2011). Molecules involved in chemical defence of the chicken egg. In: Y. Nys, M. Bain, and F. Van Immerseel (Eds.), *Improving the Safety and Quality of Eggs and Egg Products* (pp. 183–208). Woodhead Publishing. <https://doi.org/10.1533/9780857093912.2.183>
- Rodrigues, C. J. C., and de Carvalho, C. C. C. R. (2022). Cultivating marine bacteria under laboratory conditions: Overcoming the "unculturable" dogma. *Frontiers in Bioengineering and Biotechnology*, 10. <https://www.frontiersin.org/articles/10.3389/fbioe.2022.964589>
- Rudilla, H., Merlos, A., Sans-Serramitjana, E., Fusté, E., Sierra, J. M., Zalacaín, A., Vinuesa, T., and Viñas, M. (2018). New and old tools to evaluate new antimicrobial peptides. *AIMS Microbiology*, 4(3), 522–540. <https://doi.org/10.3934/microbiol.2018.3.522>
- Sanches-Fernandes, G. M. M., Sá-Correia, I., and Costa, R. (2022). Vibriosis Outbreaks in Aquaculture: Addressing Environmental and Public Health Concerns and Preventive Therapies Using Gilthead Seabream Farming as a Model System. *Frontiers in Microbiology*, 13, 904815. <https://doi.org/10.3389/fmicb.2022.904815>
- Sathyan, N., Philip, R., Chaithanya, E. R., and Anil Kumar, P. R. (2012). Identification and Molecular Characterization of Molluskin, a Histone-H2A-Derived Antimicrobial Peptide from Molluscs. *ISRN Molecular Biology*, 2012, 219656. <https://doi.org/10.5402/2012/219656>
- Schar, D., Klein, E. Y., Laxminarayan, R., Gilbert, M., and Van Boeckel, T. P. (2020). Global trends in antimicrobial use in aquaculture. *Scientific Reports*, 10(1), 21878. <https://doi.org/10.1038/s41598-020-78849-3>
- Schar, D., Zhao, C., Wang, Y., Larsson, D. G. J., Gilbert, M., and Van Boeckel, T. P. (2021). Twenty-year trends in antimicrobial resistance from aquaculture and fisheries in Asia. *Nature Communications*, 12(1), 5384. <https://doi.org/10.1038/s41467-021-25655-8>
- Shanmugam, A., Kathiresan, K., and Nayak, L. (2016). Preparation, characterization and antibacterial activity of chitosan and phosphorylated chitosan from cuttlebone of *Sepia kobeensis* (Hoyle, 1885). *Biotechnology Reports*, 9, 25–30. <https://doi.org/10.1016/j.btre.2015.10.007>
- Sun, B., Dang, W., Sun, L., and Hu, Y. (2014). *Vibrio harveyi* Hsp70: Immunogenicity and application in the development of an experimental vaccine against *V. harveyi* and *Streptococcus iniae*. *Aquaculture*, 418–419, 144–147. <https://doi.org/10.1016/j.aquaculture.2013.10.018>
- Talpur, A. D. (2014). *Mentha piperita* (Peppermint) as feed additive enhanced growth performance, survival, immune response and disease resistance of Asian seabass, *Lates calcarifer* (Bloch) against *Vibrio harveyi* infection. *Aquaculture*, 420–421, 71–78. <https://doi.org/10.1016/j.aquaculture.2013.10.039>
- Talpur, A. D., and Ikhwanuddin, M. (2012). Dietary effects of garlic (*Allium sativum*) on haemato-immunological parameters, survival, growth, and disease resistance against *Vibrio harveyi* infection in Asian sea bass, *Lates calcarifer* (Bloch). *Aquaculture*, 364–365, 6–12. <https://doi.org/10.1016/j.aquaculture.2012.07.035>
- Talpur, A. D., Ikhwanuddin, M., and Ambok Bolong, A.-M. (2013). Nutritional effects of ginger (*Zingiber officinale* Roscoe) on immune response of Asian sea bass, *Lates calcarifer* (Bloch) and disease resistance against *Vibrio harveyi*. *Aquaculture*, 400–401, 46–52. <https://doi.org/10.1016/j.aquaculture.2013.02.043>
- Tammas, I., Bitchava, K., and Gelasakis, A. I. (2024). Transforming Aquaculture through Vaccination: A Review on Recent Developments and Milestones. *Vaccines*, 12(7), Article 7. <https://doi.org/10.3390/vaccines12070732>
- Theophel, K., Schacht, V. J., Schlüter, M., Schnell, S., Stingu, C.-S., Schaumann, R., and Bunge, M. (2014). The importance of growth kinetic analysis in determining bacterial susceptibility against antibiotics and silver nanoparticles. *Frontiers in Microbiology*, 5, 544. <https://doi.org/10.3389/fmicb.2014.00544>

- Thompson, C. C., Wasielesky, W., Landuci, F., Lima, M. S., Bacha, L., Perazzolo, L., Lourenço-Marques, C., Soares, F., Pousão-Ferreira, P., Hanson, L., Gomez-Gil, B., Thompson, M., Varasteh, T., Silva, T. A., Swings, J., Zhang, X.-H., de Souza, W., and Thompson, F. L. (2024). Understanding the role of microbes in health and disease of farmed aquatic organisms. *Marine Life Science and Technology*. <https://doi.org/10.1007/s42995-024-00248-8>
- Thompson, F. L., Iida, T., and Swings, J. (2004). Biodiversity of vibrios. *Microbiology and Molecular Biology Reviews: MMBR*, 68(3), 403–431. <https://doi.org/10.1128/MMBR.68.3.403-431.2004>
- Tison, D. L., and Seidler, R. J. (1983). *Vibrio aestuarianus*: A New Species from Estuarine Waters and Shellfish†. *International Journal of Systematic and Evolutionary Microbiology*, 33(4), 699–702. <https://doi.org/10.1099/00207713-33-4-699>
- Travers, M.-A., Boettcher Miller, K., Roque, A., and Friedman, C. S. (2015). Bacterial diseases in marine bivalves. *Journal of Invertebrate Pathology*, 131, 11–31. <https://doi.org/10.1016/j.jip.2015.07.010>
- Triga, A., Smyrli, M., and Katharios, P. (2023). Pathogenic and Opportunistic *Vibrio* spp. Associated with Vibriosis Incidences in the Greek Aquaculture: The Role of *Vibrio harveyi* as the Principal Cause of Vibriosis. *Microorganisms*, 11(5), Article 5. <https://doi.org/10.3390/microorganisms11051197>
- Urbanczyk, H., Ast, J. C., Higgins, M. J., Carson, J., and Dunlap, P. V. (2007). Reclassification of *Vibrio fischeri*, *Vibrio logei*, *Vibrio salmonicida* and *Vibrio wodanis* as *Aliivibrio fischeri* gen. Nov., comb. Nov., *Aliivibrio logei* comb. Nov., *Aliivibrio salmonicida* comb. Nov. And *Aliivibrio wodanis* comb. Nov. *International Journal of Systematic and Evolutionary Microbiology*, 57(12), 2823–2829. <https://doi.org/10.1099/ijs.0.65081-0>
- Valgas, C., Souza, S. M. de, Smânia, E. F. A., and Smânia Jr., A. (2007). Screening methods to determine antibacterial activity of natural products. *Brazilian Journal of Microbiology*, 38, 369–380. <https://doi.org/10.1590/S1517-83822007000200034>
- Weiner, S., and Hood, L. (1975). Soluble Protein of the Organic Matrix of Mollusk Shells: A Potential Template for Shell Formation. *Science*, 190(4218), 987–989. <https://doi.org/10.1126/science.1188379>
- Weiskirchen, S., Schröder, S., Buhl, M., and Weiskirchen, R. (2023). A Beginner’s Guide to Cell Culture: Practical Advice for Preventing Needless Problems. *Cells*, 12, 682. <https://doi.org/10.3390/cells12050682>
- Wickham, H., Averick, M., Bryan, J., Chang, W., McGowan, L. D., François, R., Grolemund, G., Hayes, A., Henry, L., Hester, J., Kuhn, M., Pedersen, T. L., Miller, E., Bache, S. M., Müller, K., Ooms, J., Robinson, D., Seidel, D. P., Spinu, V., ... Yutani, H. (2019). Welcome to the tidyverse. *Journal of Open Source Software*, 4(43), 1686. <https://doi.org/10.21105/joss.01686>
- Yeaman, M. R., and Yount, N. Y. (2003). Mechanisms of Antimicrobial Peptide Action and Resistance. *Pharmacological Reviews*, 55(1), 27–55. <https://doi.org/10.1124/pr.55.1.2>
- Zasloff, M. (2002). Antimicrobial peptides of multicellular organisms. *Nature*, 415(6870), 389–395. <https://doi.org/10.1038/415389a>
- Zgoda, J. R., and Porter, J. R. (2001). A Convenient Microdilution Method for Screening Natural Products Against Bacteria and Fungi. *Pharmaceutical Biology*, 39(3), 221–225. <https://doi.org/10.1076/phbi.39.3.221.5934>
- Zhan, J., Lu, J., and Wang, D. (2021). Review of shell waste reutilization to promote sustainable shellfish aquaculture. *Reviews in Aquaculture*, 14. <https://doi.org/10.1111/raq.12610>
- Zhang, X.-H., He, X., and Austin, B. (2020). *Vibrio harveyi*: A serious pathogen of fish and invertebrates in mariculture. *Marine Life Science and Technology*, 2(3), 231–245. <https://doi.org/10.1007/s42995-020-00037-z>

SUPPLEMENTARY DATA

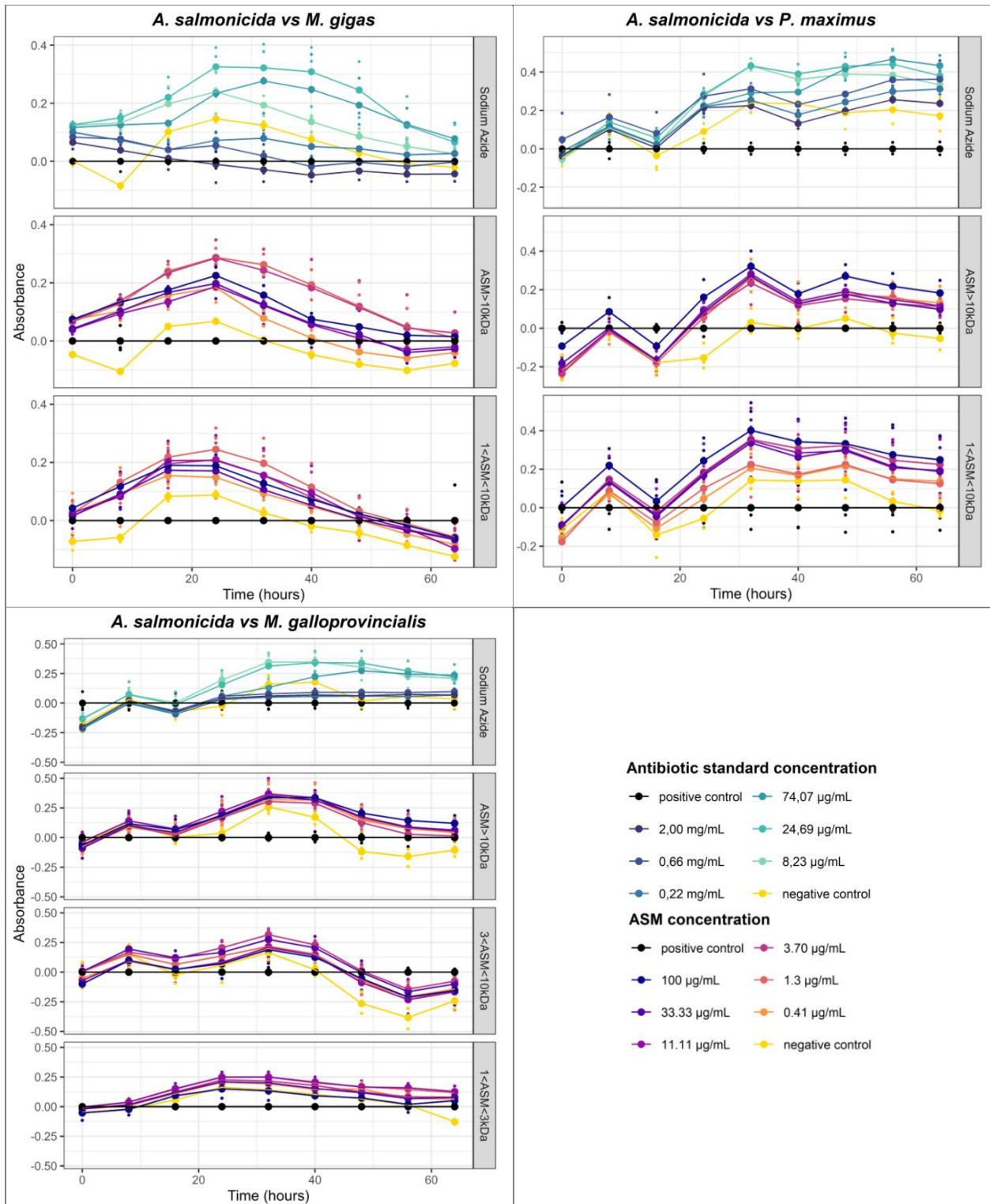
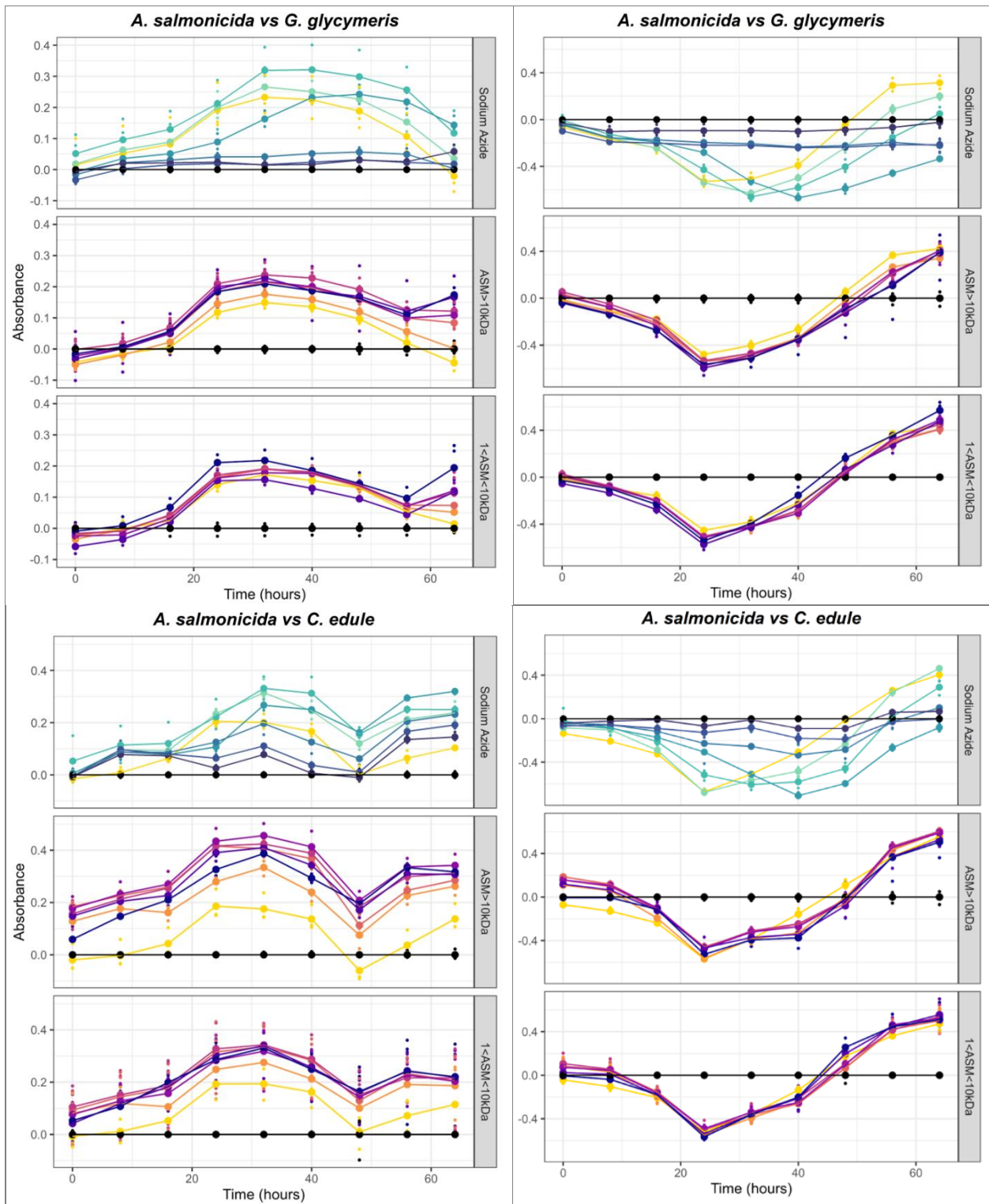


Figure S 3.1: growth curves for the positive results of microdilution assays against *A. salmonicida* under 420 nm wavelength.



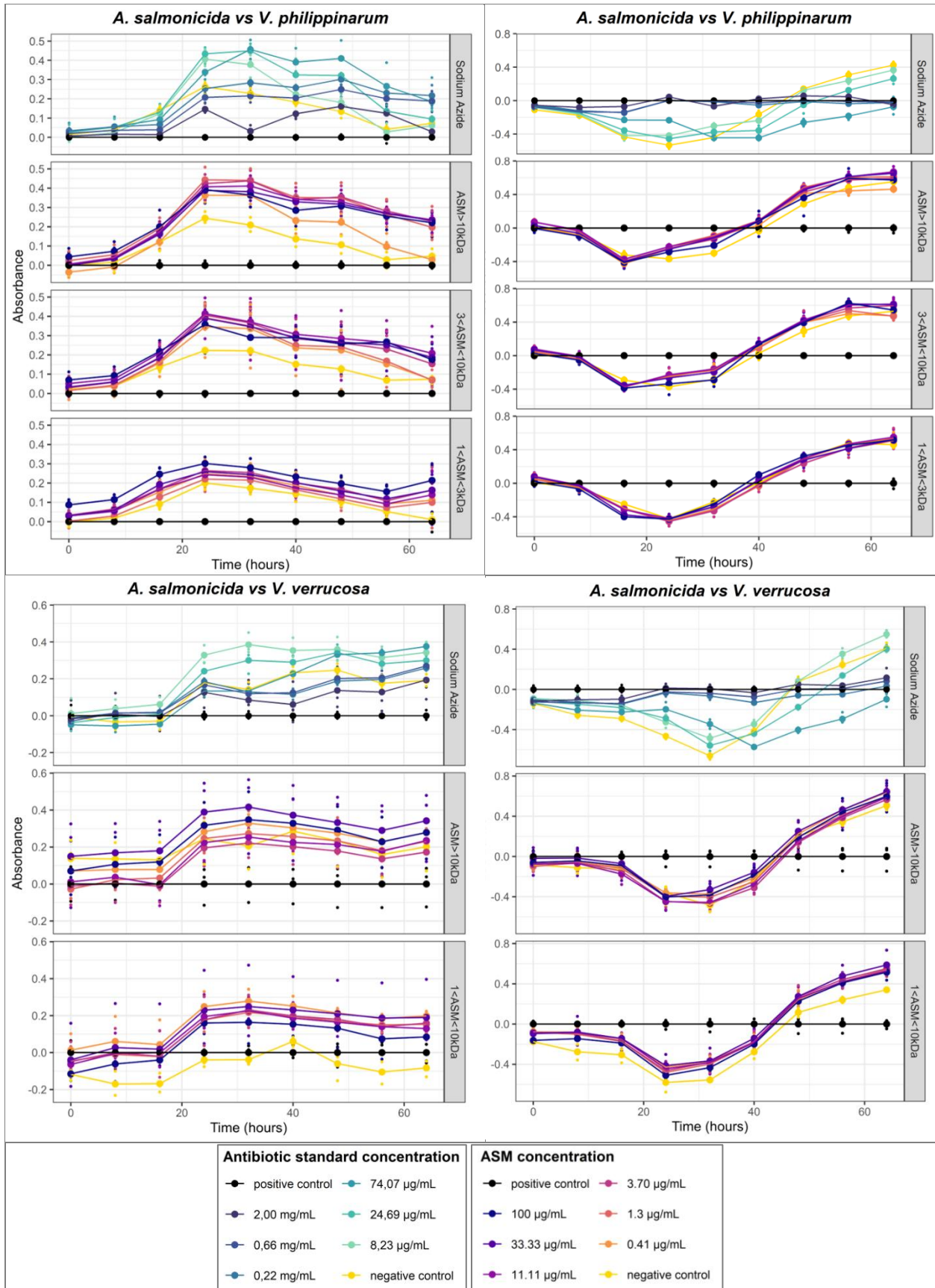


Figure S 3.2: Growth curves for the negative results of microdilution assays against *A. salmonicida* under 420 nm and 560 nm wavelengths.

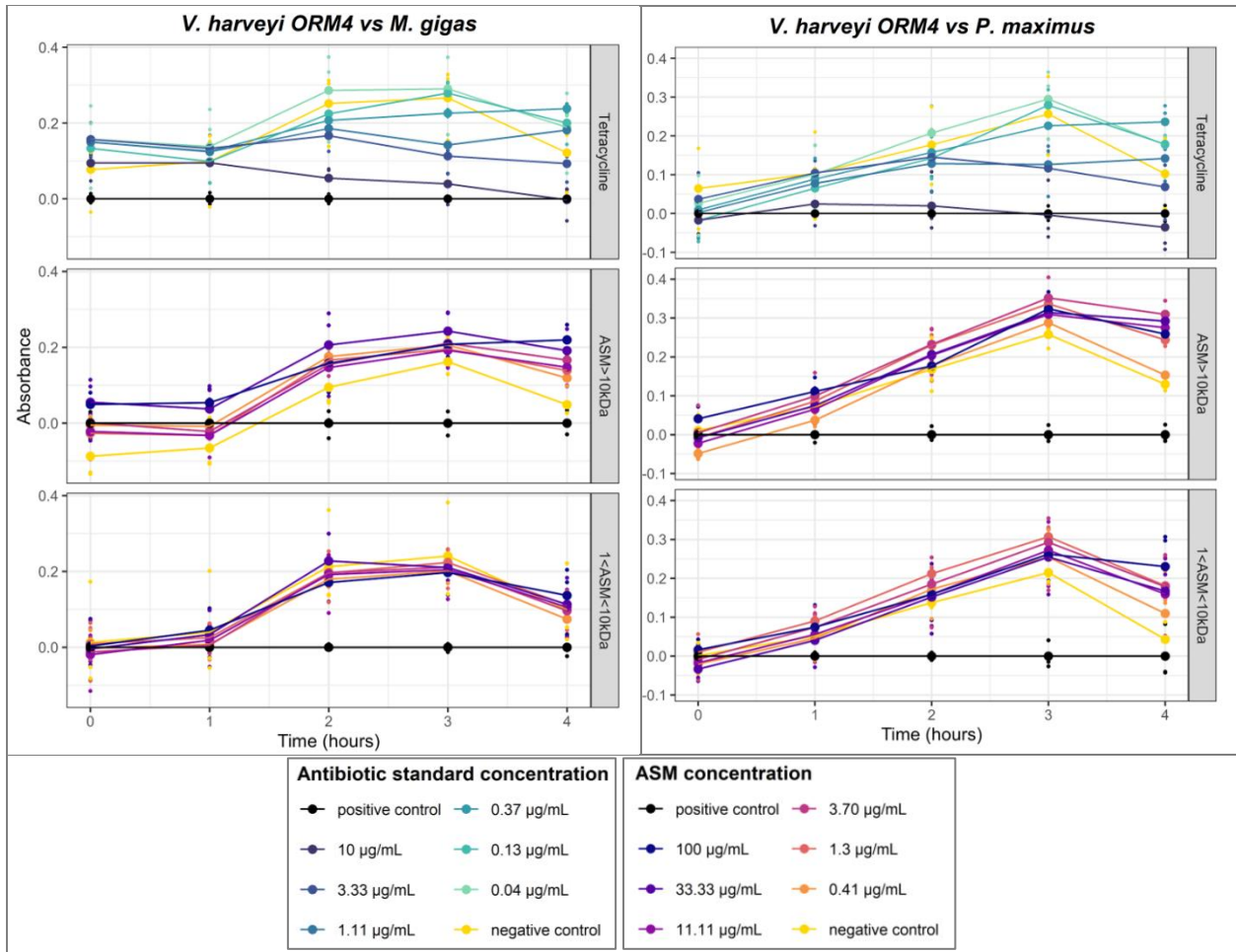
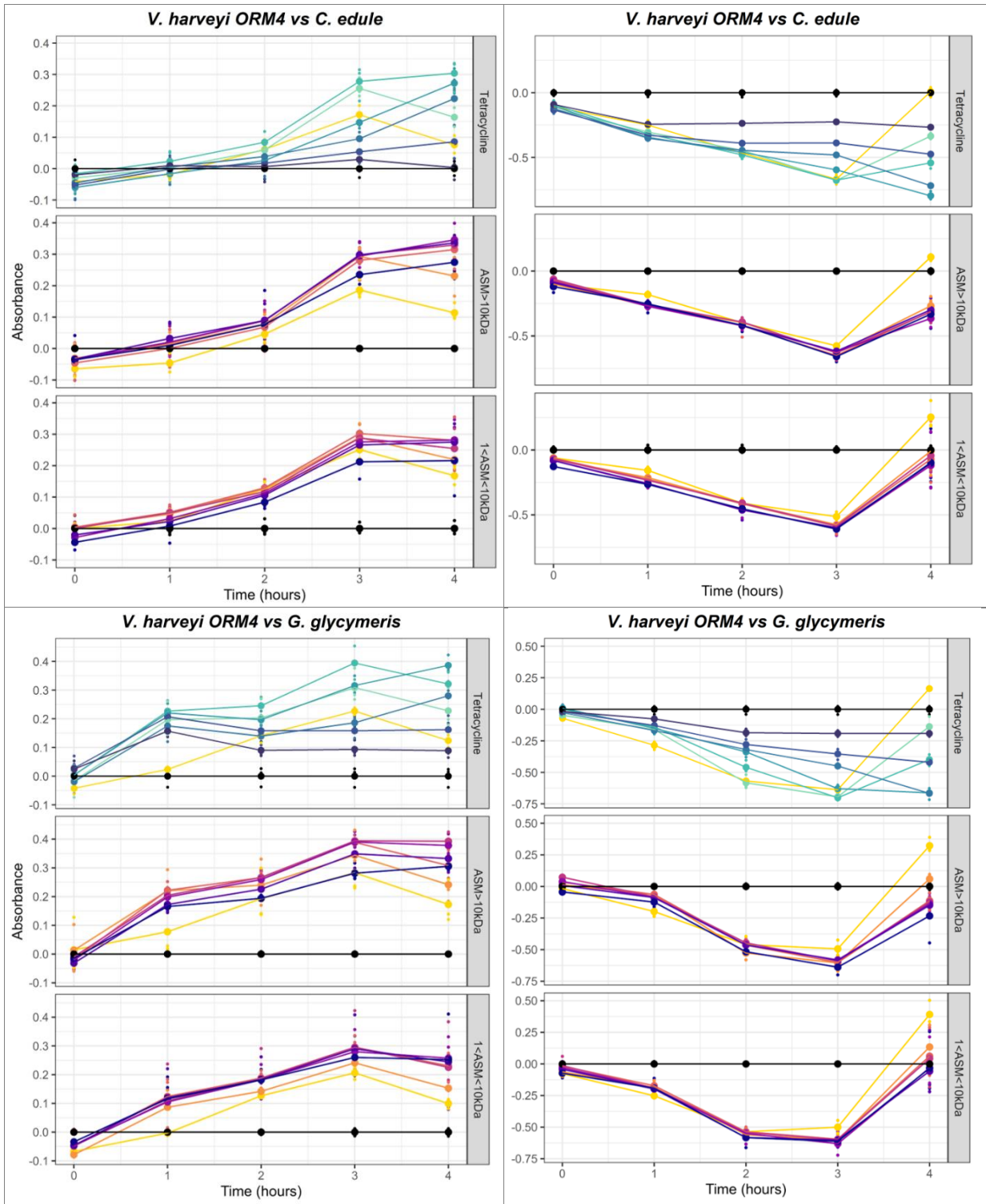
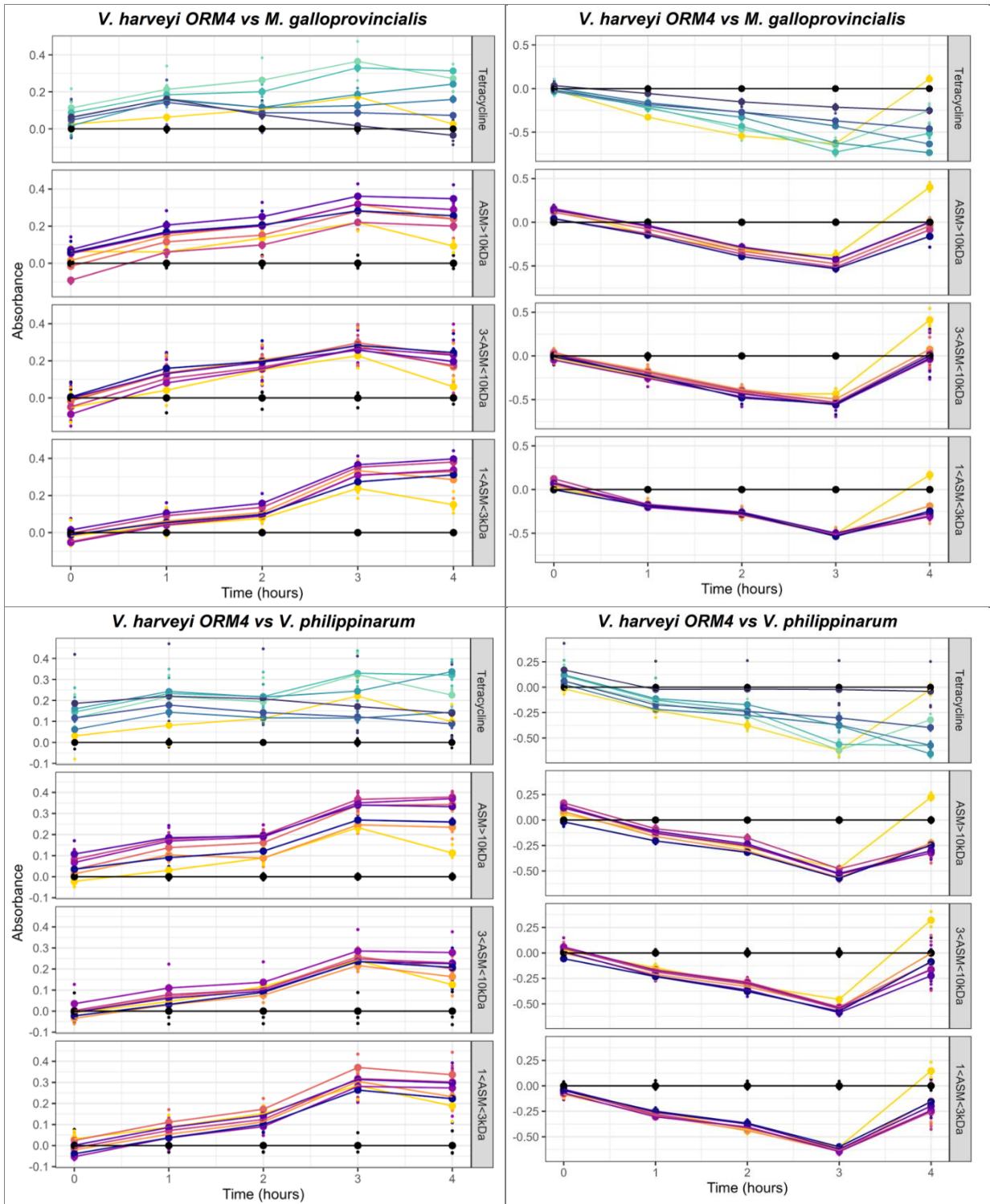


Figure S 3.3: growth curves for the negative results of microdilution assays against *V. harveyi* ORM4 under 420 nm and 560 nm wavelengths.





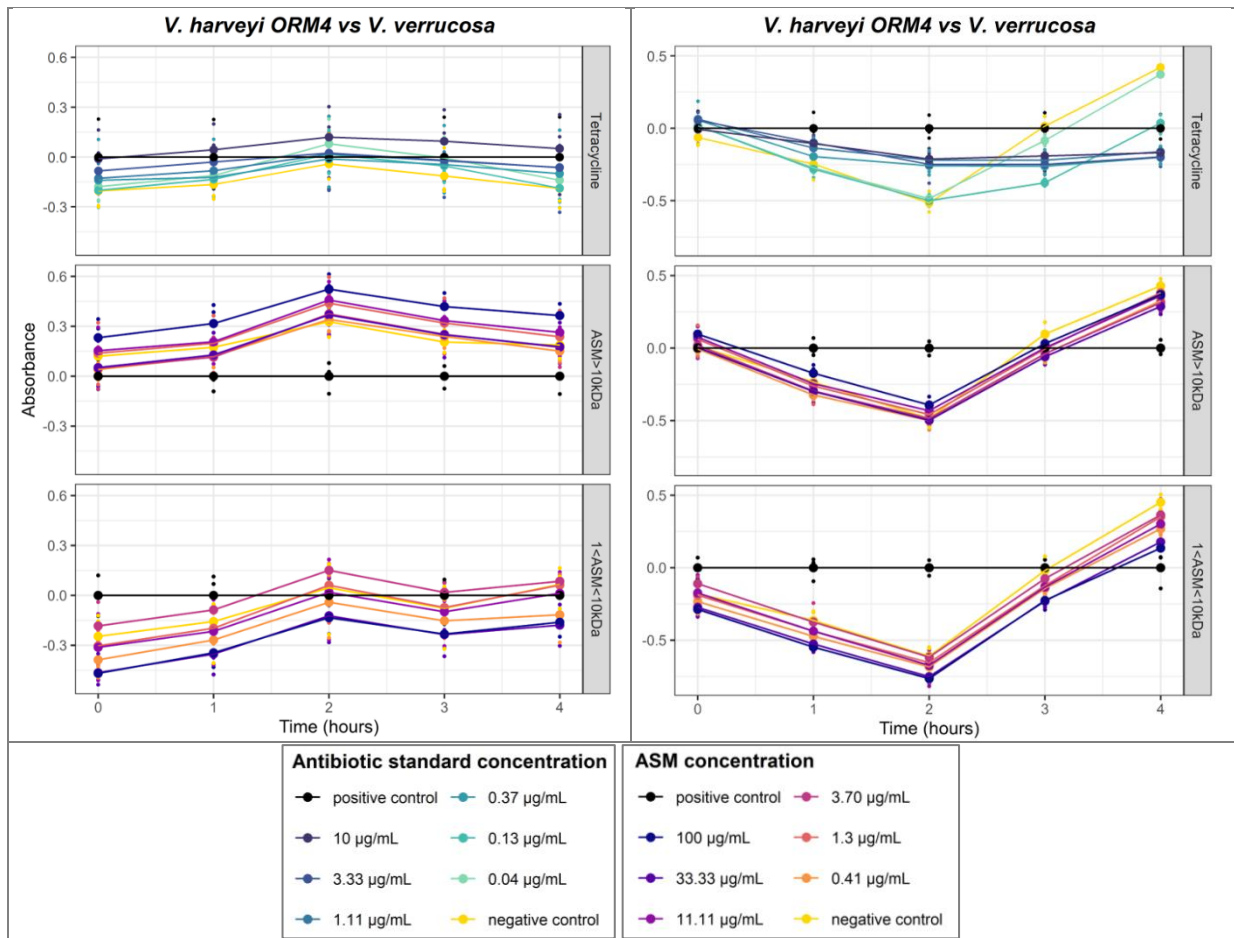
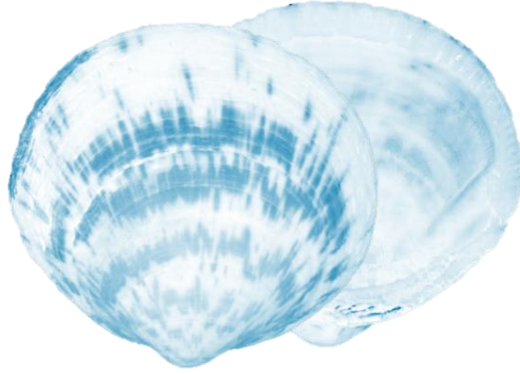


Figure S 3.4: growth curves for the negative results of microdilution assays against *V. harveyi* ORM4 under 420 nm and 560 nm wavelengths.

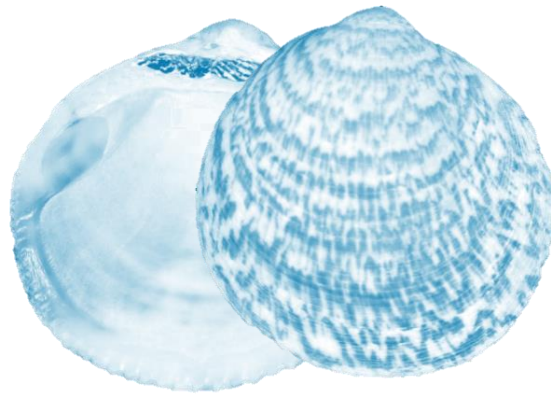
3.5. Chapter References

- Balouiri, M., Sadiki, M., and Ibensouda, S. K. (2016). Methods for *in vitro* evaluating antimicrobial activity: A review. *Journal of Pharmaceutical Analysis*, 6(2), 71–79. <https://doi.org/10.1016/j.jpha.2015.11.005>
- Bauer, A. W., Kirby, W. M., Sherris, J. C., and Turck, M. (1966). Antibiotic susceptibility testing by a standardized single disk method. *American Journal of Clinical Pathology*, 45(4), 493–496.
- Blazanin, M. (2024). gcplyr: An R package for microbial growth curve data analysis. *BMC Bioinformatics*, 25(1), 232. <https://doi.org/10.1186/s12859-024-05817-3>
- Borrego, J. J., Castro, D., Luque, A., Paillard, C., Maes, P., Garcia, M. T., and Ventosa, A. (1996). *Vibrio tapetis* sp. Nov., the Causative Agent of the Brown Ring Disease Affecting Cultured Clams. *International Journal of Systematic and Evolutionary Microbiology*, 46(2), 480–484. <https://doi.org/10.1099/00207713-46-2-480>
- Boyle, K. E., Monaco, H., Ditmarsch, D. van, Deforet, M., and Xavier, J. B. (2015). Integration of Metabolic and Quorum Sensing Signals Governing the Decision to Cooperate in a Bacterial Social Trait. *PLOS Computational Biology*, 11(6), e1004279. <https://doi.org/10.1371/journal.pcbi.1004279>
- Cushnie, T. P. T., Cushnie, B., Echeverría, J., Fowsantear, W., Thammawat, S., Dodgson, J. L. A., Law, S., and Clow, S. M. (2020). Bioprospecting for Antibacterial Drugs: A Multidisciplinary Perspective on Natural Product Source Material, Bioassay Selection and Avoidable Pitfalls. *Pharmaceutical Research*, 37(7), 125. <https://doi.org/10.1007/s11095-020-02849-1>
- Defer, D., Bourgoignon, N., and Fleury, Y. (2009). Screening for antibacterial and antiviral activities in three bivalve and two gastropod marine molluscs. *Aquaculture*, 293(1), 1–7. <https://doi.org/10.1016/j.aquaculture.2009.03.047>
- EUCAST. (2024). EUCAST guidance on: When there are no Breakpoints in breakpoint tables? *European Society of Clinical Microbiology and Infectious Diseases - European Committee on Antimicrobial Susceptibility Testing*. <https://www.eucast.org/eucastguidancedocuments>
- Held, P. (2022). Using Phenol Red to Assess pH in Tissue Culture Media (Application Notes - Cancer Biology). *Agilent Technologies Inc.*
- Hetru, C., and Bulet, P. (1997). Strategies for the isolation and characterization of antimicrobial peptides of invertebrates. *Methods in Molecular Biology (Clifton, N.J.)*, 78, 35–49. <https://doi.org/10.1385/0-89603-408-9:35>
- Johnson, F. H., and Shunk, I. V. (1936). An Interesting New Species of Luminous Bacteria. *Journal of Bacteriology*, 31(6), 585–593.
- Leifson, E. (1963). Determination of carbohydrate metabolism of marine bacteria. *Journal of Bacteriology*, 85(5), 1183–1184. <https://doi.org/10.1128/jb.85.5.1183-1184.1963>
- Li, B., Qiu, Y., Shi, H., and Yin, H. (2016). The importance of lag time extension in determining bacterial resistance to antibiotics. *Analyst*, 141(10), 3059–3067. <https://doi.org/10.1039/C5AN02649K>
- López-Abarrategui, C., Alba, A., Lima, L. A., Maria-Neto, S., Vasconcelos, I. M., Oliveira, J. T. A., Dias, S. C., Otero-Gonzalez, A. J., and Franco, O. L. (2012). Screening of Antimicrobials from Caribbean Sea Animals and Isolation of Bactericidal Proteins from the Littoral Mollusk *Cenchritis muricatus*. *Current Microbiology*, 64(5), 501–505. <https://doi.org/10.1007/s00284-012-0096-5>
- Lutet-Toti, C., Da Silva Feliciano, M., Debrosse, N., Thomas, J., Plasseraud, L., and Marin, F. (2024). Diverting the Use of Hand-Operated Tablet Press Machines to Bioassays: A Novel Protocol to Test ‘Waste’ Insoluble Shell Matrices. *Methods and Protocols*, 7(2), Article 2. <https://doi.org/10.3390/mps7020030>
- Lutet-Toti, C., Da Silva Feliciano, M., Thomas, J., Crosland, A., Develay, C., Debrosse, N., Force, A., Bidault, A., Broussard, C., Falini, G., Goffredo, S., and Marin, F. (2025). Do bivalve shells exhibit antibacterial properties? Screening calcifying organic matrices against two major marine pathogens. *Science of the TOTAL ENvironment (STOTEN)*, submitted.
- Massoud, R., Saffari, H., Massoud, A., and Moteian, M. (2020). Screening methods for assessment of antibacterial activity in nature. Conference Paper, *4th Int. Conf. on Applied Research in Science and Engineering*, 11p.
- Mira, P., Yeh, P., and Hall, B. G. (2022). Estimating microbial population data from optical density. *PLOS ONE*, 17(10), e0276040. <https://doi.org/10.1371/journal.pone.0276040>
- Pujalte, M.-J., Ortigosa, M., Urdaci, M.-C., Garay, E., and Grimont, P. A. D. (1993). *Vibrio mytili* sp. Nov., from Mussels. *International Journal of Systematic and Evolutionary Microbiology*, 43(2), 358–362. <https://doi.org/10.1099/00207713-43-2-358>
- Rodrigues, C. J. C., and de Carvalho, C. C. C. R. (2022). Cultivating marine bacteria under laboratory conditions: Overcoming the “unculturable” dogma. *Frontiers in Bioengineering and Biotechnology*, 10. <https://www.frontiersin.org/articles/10.3389/fbioe.2022.964589>
- Rudilla, H., Merlos, A., Sans-Serramitjana, E., Fusté, E., Sierra, J. M., Zalacaín, A., Vinuesa, T., and Viñas, M. (2018). New and old tools to evaluate new antimicrobial peptides. *AIMS Microbiology*, 4(3), 522–540. <https://doi.org/10.3934/microbiol.2018.3.522>

- Tison, D. L., and Seidler, R. J. (1983). *Vibrio aestuarianus*: A New Species from Estuarine Waters and Shellfish†. *International Journal of Systematic and Evolutionary Microbiology*, 33(4), 699–702. <https://doi.org/10.1099/00207713-33-4-699>
- Urbanczyk, H., Ast, J. C., Higgins, M. J., Carson, J., and Dunlap, P. V. (2007). Reclassification of *Vibrio fischeri*, *Vibrio logei*, *Vibrio salmonicida* and *Vibrio wodanis* as *Aliivibrio fischeri* gen. Nov., comb. Nov., *Aliivibrio logei* comb. Nov., *Aliivibrio salmonicida* comb. Nov. And *Aliivibrio wodanis* comb. Nov. *International Journal of Systematic and Evolutionary Microbiology*, 57(12), 2823–2829. <https://doi.org/10.1099/ijs.0.65081-0>
- Valgas, C., Souza, S. M. de, Smânia, E. F. A., and Smânia Jr., A. (2007). Screening methods to determine antibacterial activity of natural products. *Brazilian Journal of Microbiology*, 38, 369–380. <https://doi.org/10.1590/S1517-83822007000200034>
- Weiskirchen, S., Schröder, S., Buhl, M., and Weiskirchen, R. (2023). A Beginner’s Guide to Cell Culture: Practical Advice for Preventing Needless Problems. *Cells*, 12, 682. <https://doi.org/10.3390/cells12050682>
- Zgoda, J. R., and Porter, J. R. (2001). A Convenient Microdilution Method for Screening Natural Products Against Bacteria and Fungi. *Pharmaceutical Biology*, 39(3), 221–225. <https://doi.org/10.1076/phbi.39.3.221.5934>



CHAPTER 4 - MICELLANEA: UNPUBLISHED DATA AND RESULTS



4.1. Negative Results of the Antibacterial Screening

In this section I document and describe the negative results and unpublished data from the previously discussed antibacterial screening (see [Chapter 3: Antibacterial Properties](#)).

Indeed, as one knows, a properly designed antibacterial screening must deal with a wide enough range of target strains in order to detect any activity at all (Rios *et al.*, 1988; Massoud *et al.*, 2020). Thus, a substantive amount of the later can be expected to show low, non-significant, or no sensitivity to the tested natural extracts. This is the case here for four of our six tested marine pathogens: *V. aestuarianus*, *V. harveyi* LMG7890, *V. mytili*, and finally, *V. tapetis* CECT4600.

The negative results exposed here can be due to multiple causes: some of them are plainly difficult to interpret without inducing confirmation bias, others might stem from the resistance of the strains against bivalve antimicrobial compounds, or the lack thereof in the tested shells. The presence of highly varying or low-inhibition activities among the results I show in the following sections can also be attributed – in some cases – to the necessity of these biomolecules to “work together”, between fractions that my assays artificially separate, compared to the natural setups of the shells.

Another important hypothesis in this absence of response to bivalve shell extracts is the actual quantities of active molecules tested in the screening: the experimental conditions might not be suitable, with insufficient amounts of substances to observe bioactivity in some cases. The reasons for such modulations and variability of bacterial responses to bivalve shell extracts will be further discussed in the general discussion of this thesis (see [Chapter 5](#)).

4.1.1. *Vibrio aestuarianus*

V. aestuarianus strains were grown in liquid culture, using marine broth, lightly stirred for 48h at 20°C, following parameters from LEMAR lab (UBO, France) and literature (Tison & Seidler, 1983). Once in log phase (DO = [0.6:1.0]), the suspensions were ready to be used for antibacterial assays.

The marine agar plates used for the disk diffusion assay were incubated at 20°C for 48h. The results are summarized in the boxplot bellow (Fig.4.1): among the tested shell extracts, only the AIM of *M. gigas* gave positive results, with an inhibition zone diameter of 0.66 ± 0.02 cm (adjusted p-value = 0.20; unadj. p-value = 0.014). Positive and negative controls were valid. The positive controls performed with v0129 (500µg) showed large inhibition zones with a global mean diameter of 2.26 ± 0.30 cm. On antibiogram plates, the inhibition zone diameter was positively correlated with the quantity of v0129. Other antibacterial products (ampicillin and sodium azide) show clear inhibition of bacterial growth, with a great variability of the response to sodium azide (1.68 ± 1.46 cm).

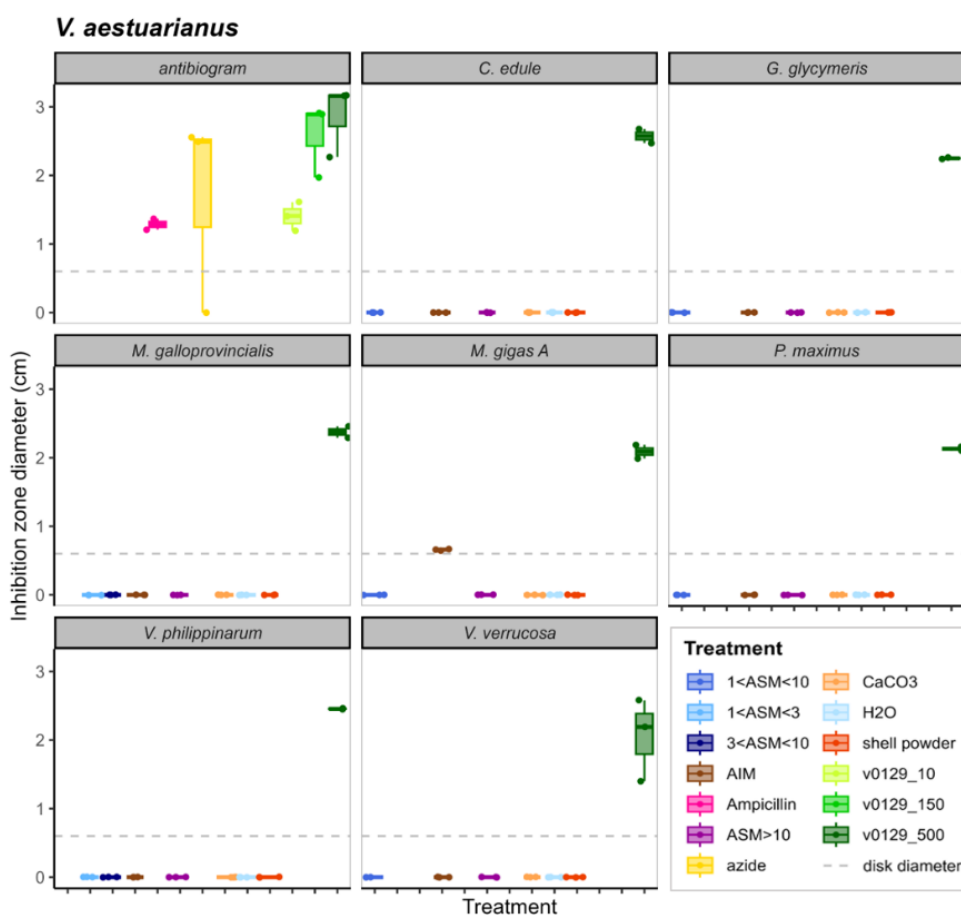


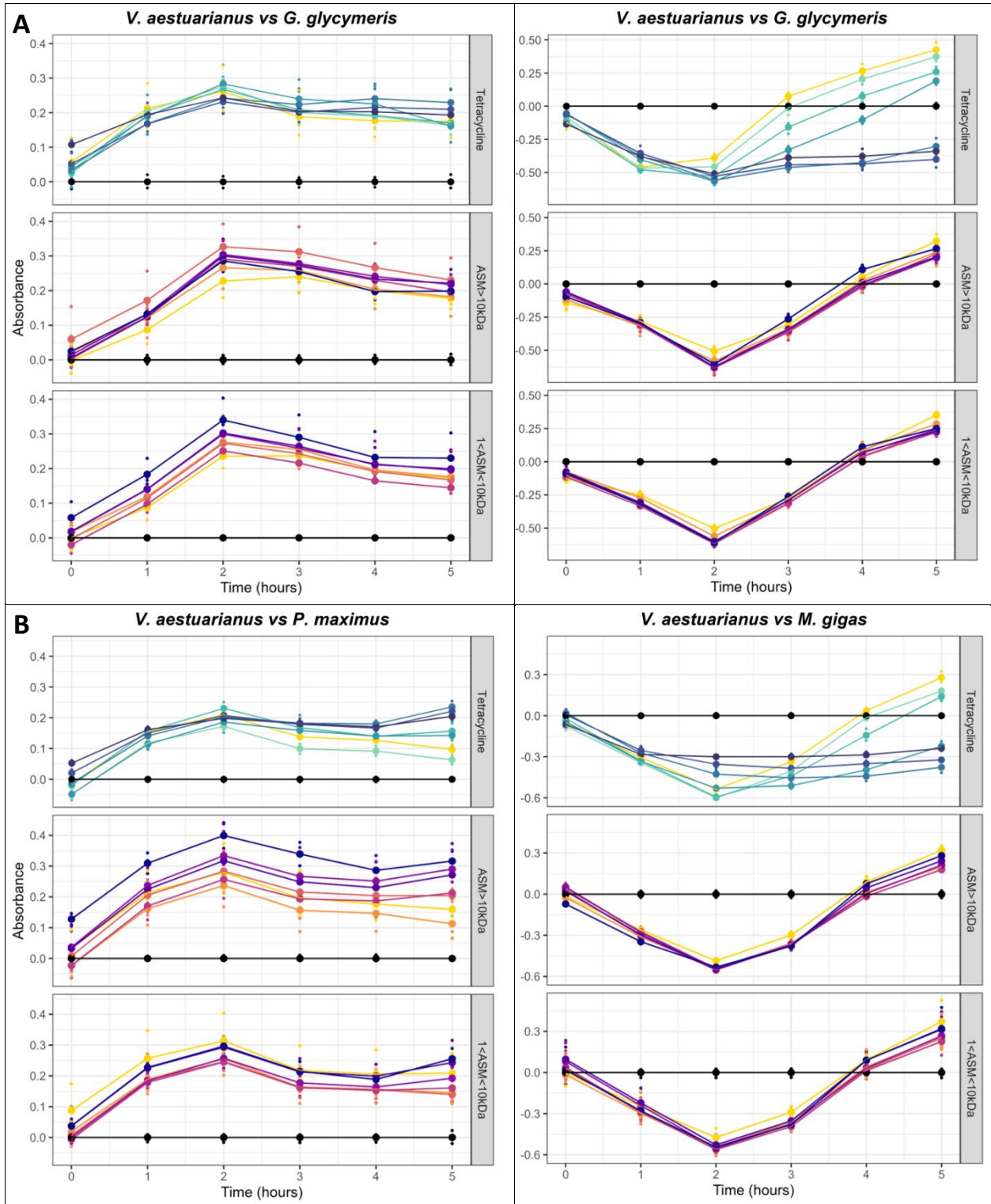
Figure 4.1: Boxplots results of the disk diffusion assays for *V. aestuarianus*. The dotted line represents the disk and tablet diameter.

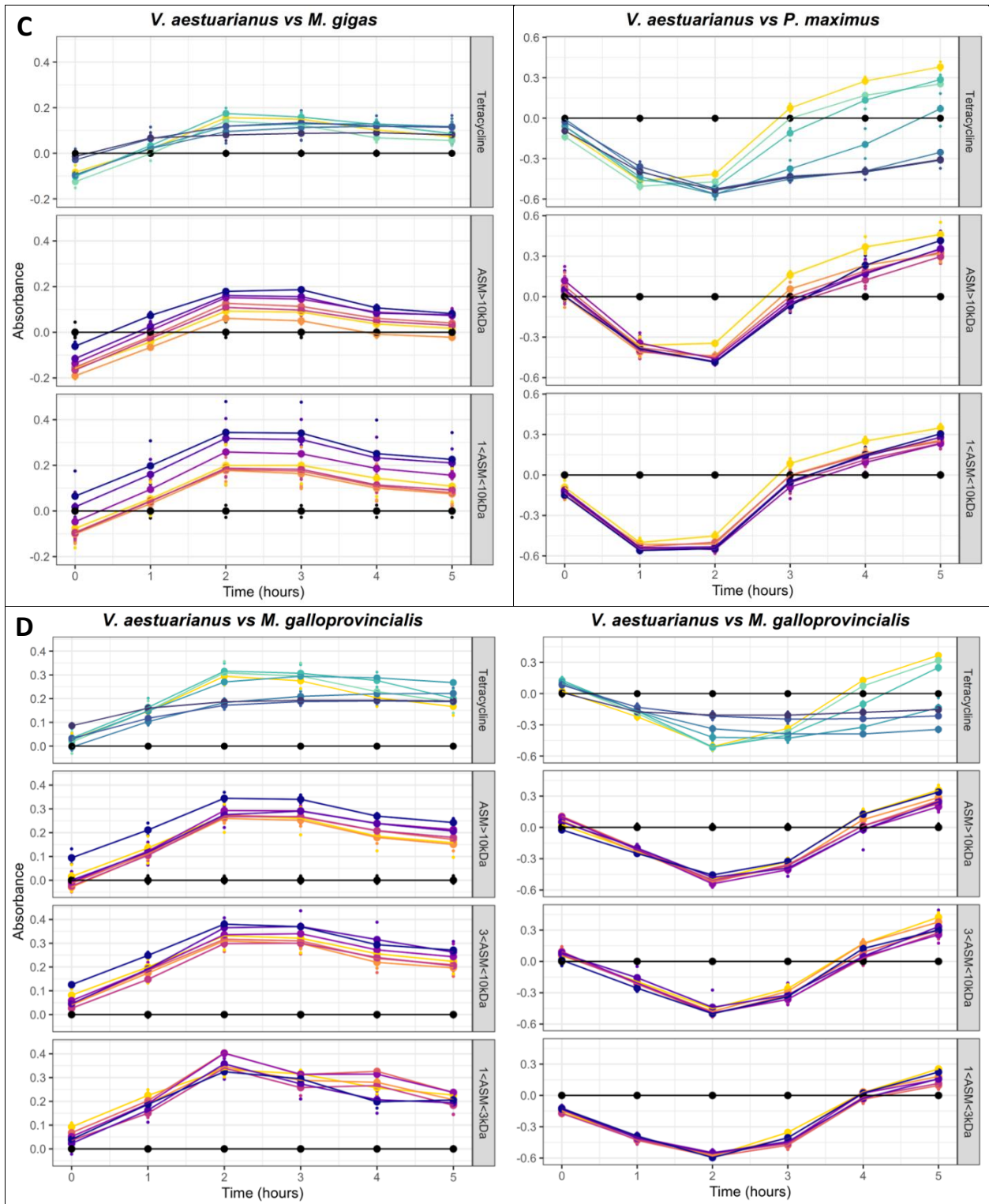
The microplates used for the microdilution assay were incubated, with a gentle stirring, at 20°C for 5 hours. Absorbances at 420 nm and 560nm were measured every hour, and tetracycline was used as standard antibiotic control against the ASM fractions, following the concentrations displayed in Table 3.1 (see section 4.4.2.5. Microdilution Assay, Lutet-Toti *et al.*, 2025, *submitted to STOTEN*): 10.00 µg/mL; 3.33 µg/mL; 1.11 µg/mL; 0.37 µg/mL; 0.13 µg/mL; 0.04 µg/mL.

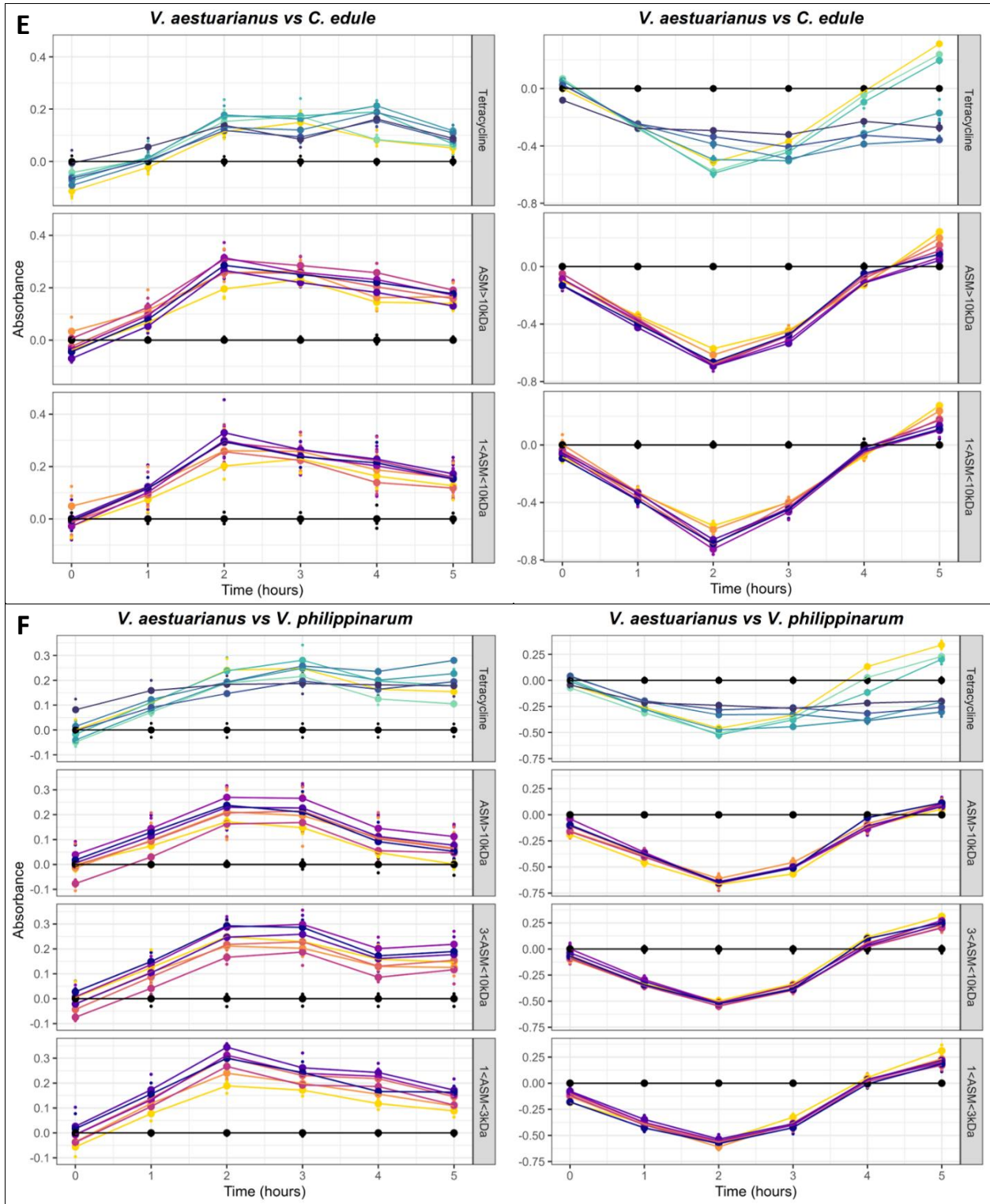
The growth curves results are displayed for both wavelengths in Figure 4.2. In agreement with the results displayed for *V. harveyi* ORM and *A. salmonicida* in Chapter 3, the tetracycline standard curves (upper graphs, green-blue gradient) obtained with readings at 560 nm (right panels) provide a better and finer description of the bacterial metabolism and growth phases. Under natural growth conditions (negative control, yellow line), they exhibit the characteristic profile for bacterial cultures. The dose-dependency of the inhibitory effect of tetracycline is observable, with the delayed time to reach the carrying capacity representing the main altered parameter. At higher concentrations (3.33 µg/mL), a flattening of the curves that come to a “shelf” after some growth is observable in a majority of the plates (B, D, E, F and G). This response reveals the bacteriostatic properties of tetracycline on *V. aestuarianus*, which is in accordance with literature on other bacteria (Chopra & Roberts, 2001; He *et al.*, 2018). The curves produced for the tested ASM extracts show no response of *V. aestuarianus* to any concentration.

Using 420 nm absorbance (left panels), the curves for the standard tetracycline are drawing a rough sketch of bacterial growth: while the general pH - and thus, metabolism - tendency of bacterial cultures are distinguishable, no specific effect of concentration can be determined with certainty. The same phenomenon applies to the tested ASM. At first sight, one may think that the spreading of the curves suggests positive responses to the ASM, but no specific pattern emerges from the different concentrations. Furthermore, once pondered to the population size (same start point on the y axis), the curves do not appear that different from one concentration to another. Taking all those obstacles in consideration, the curves obtained at 420 nm absorbance are very difficult to interpret. The microdilution assay was inconclusive for *V. aestuarianus*, no alteration of the bacterial metabolism was detected.

Altogether, only one tested bivalve extract, the AIM of *M. gigas*, showed slight antimicrobial properties against *V. aestuarianus*. This inhibition of growth is quite limited though, as the inhibition zone only expands 0.05 cm away from the 0.60 cm AIM tablet.







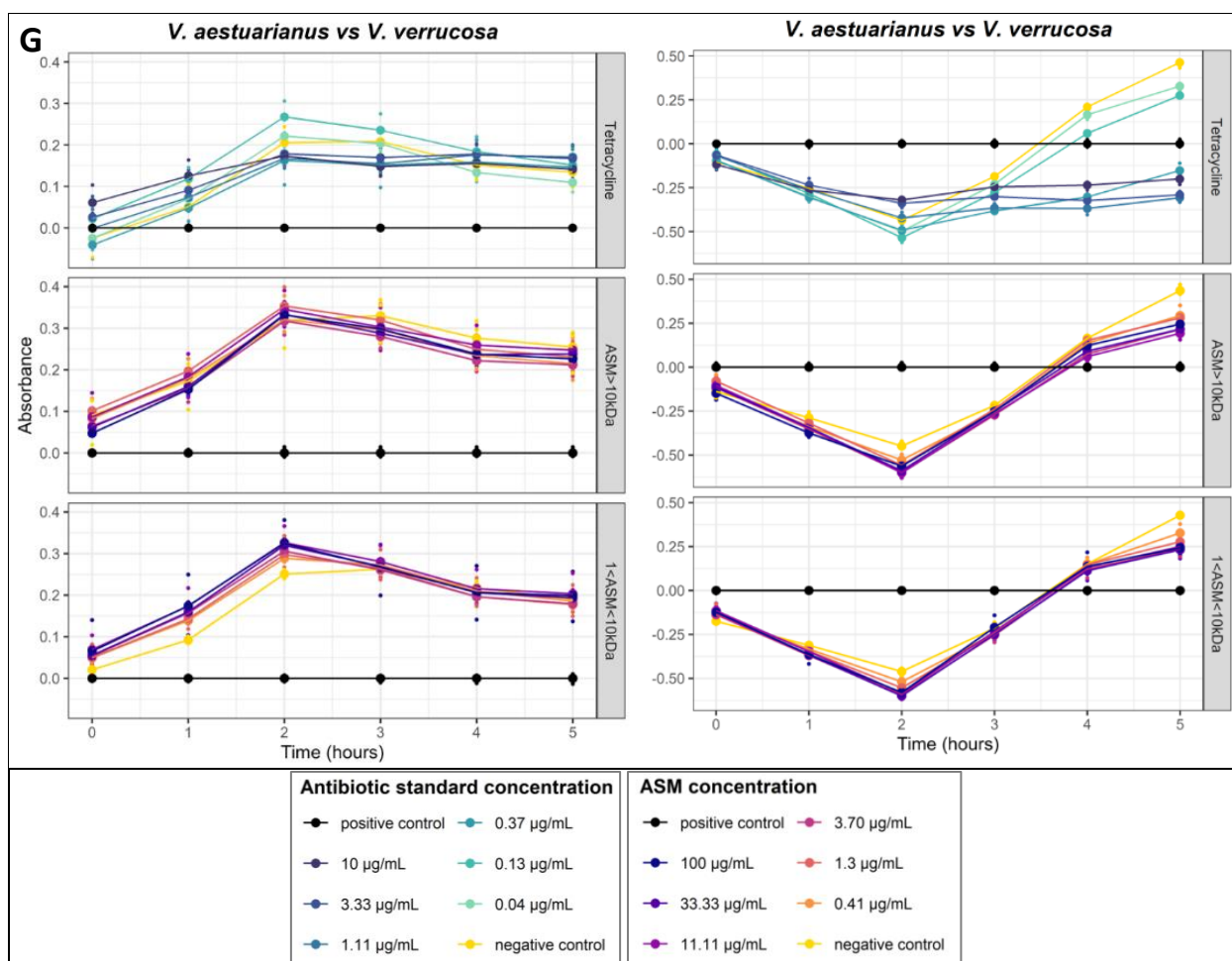


Figure 4.2: Microdilution assays growth curves for *V. aestuarianus*. The left panels show the absorbance read at 420 nm, the right ones, the absorbance at 560 nm.

4.1.2. *Vibrio harveyi* LMG7890

V. harveyi LMG 7890 strains were grown in the same conditions as the “natural” strain *V. harveyi* ORM4: in liquid culture, using marine broth, lightly stirred for 24h at 28°C, following guidelines from LEMAR lab and the literature (Johnson & Shunk, 1936; Jiang *et al.*, 2013). Once in log phase (DO = [0.6:1.0]), the suspensions were ready to be used for antibacterial assays.

The marine agar plates used for the disk diffusion assay were incubated at 28°C for 48h to allow for a visible growth on the medium. The results are summarized in the boxplot below (Fig.4.3): none of the tested shell extracts showed any alteration of bacterial growth. Positive and negative controls were valid. The positive controls performed with v0129 (500µg) showed large inhibition zones with a global mean diameter of 0.95 ± 0.06 cm. On antibiogram plates, the inhibition zone diameter was positively correlated with the quantity of v0129, but no inhibition was observed for the smallest dose of 10 µg. Only one of the other tested antibacterial

products, tetracycline, showed clear inhibition of bacterial growth with the smallest variability in diameter among all responsive products (1.02 ± 0.01 cm).

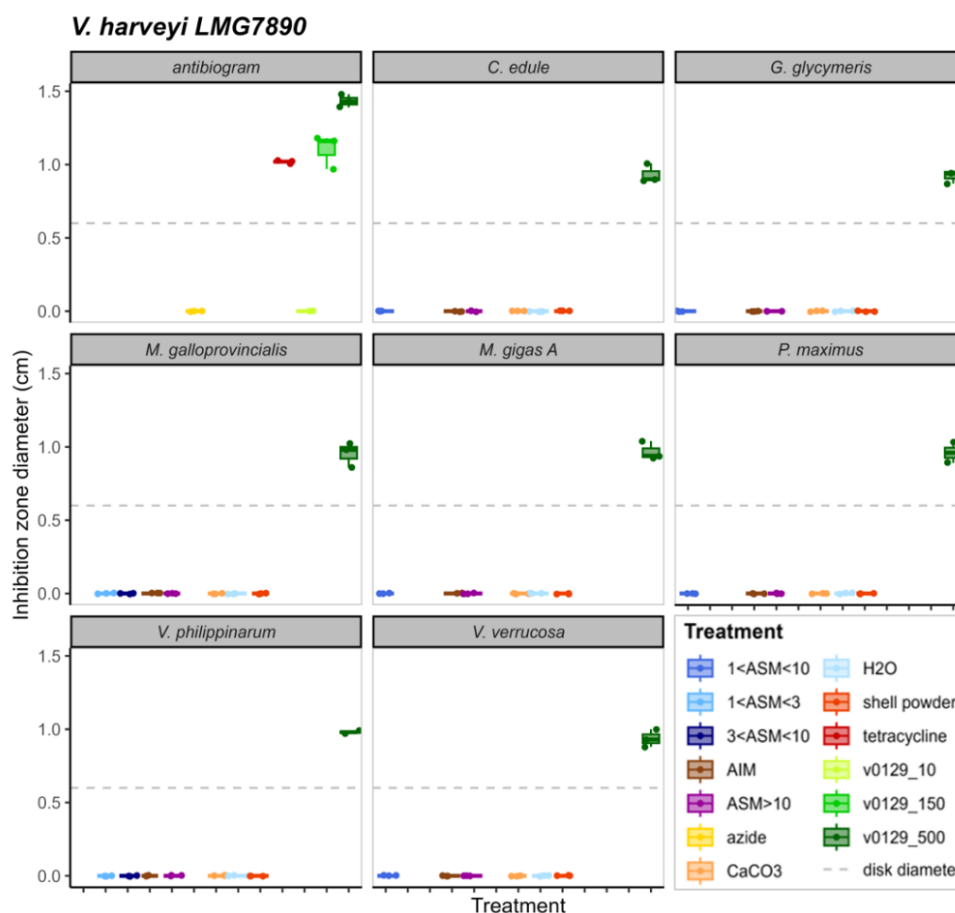


Figure 4.3: boxplots results of the disk diffusion assays for *Vibrio harveyi* LMG7890. The dotted line represents the disk and tablet diameter.

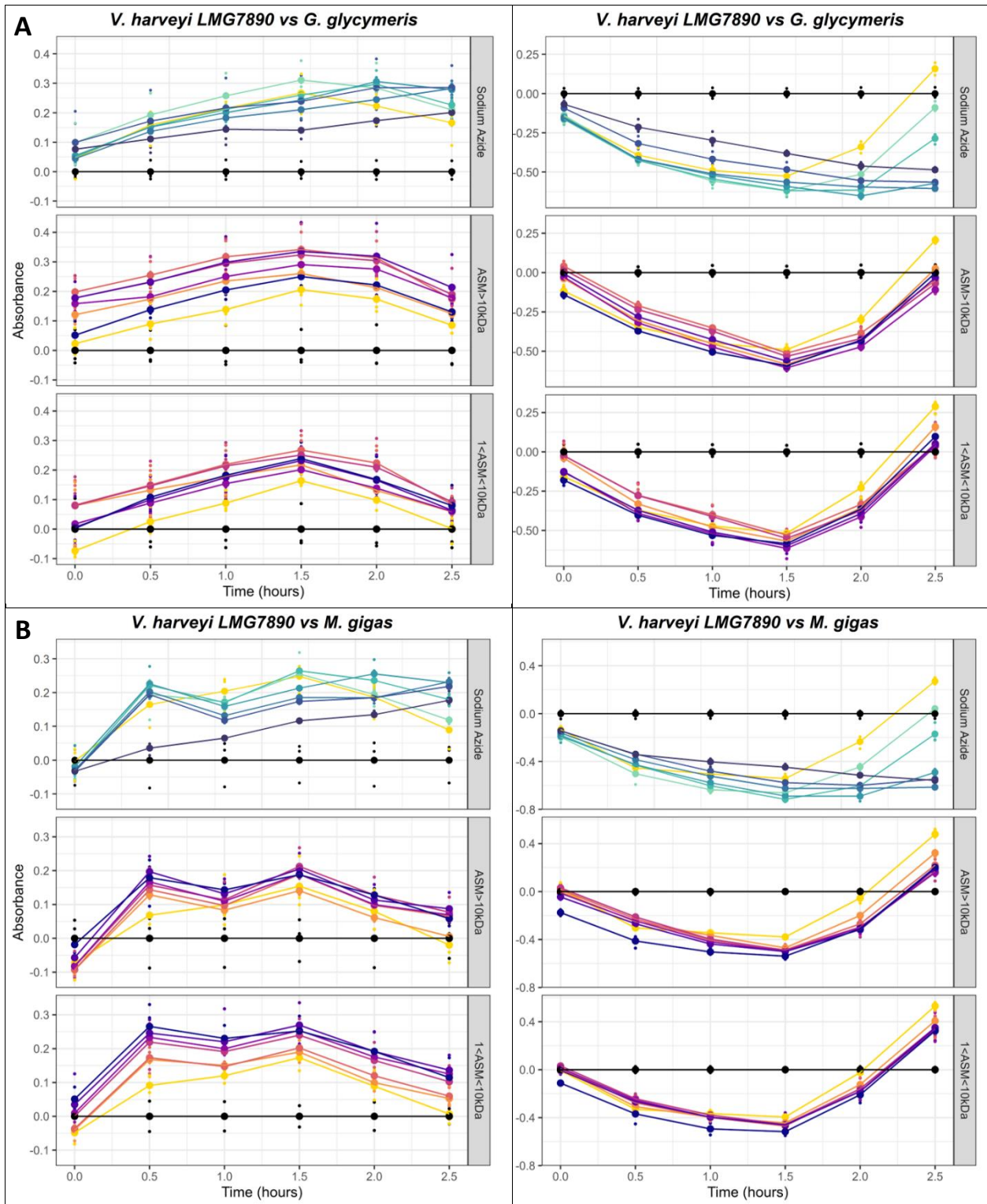
The microplates used for the microdilution assay were incubated, with a gentle stirring, at 28°C for 2.5 hours. Absorbances at 420 nm and 560nm were measured every 30 minutes, and tetracycline was used as standard antibiotic control against the ASM fractions, following the concentrations displayed in Table 3.1 (see section 4.4.2.5. *Microdilution Assay*, Lutet-Toti *et al.*, 2025, *submitted to STOTEN*): 2,00 mg/mL; 0,66 mg/mL; 0,22 mg/mL; 74,07 µg/mL; 24,69 µg/mL; 8,23 µg/mL.

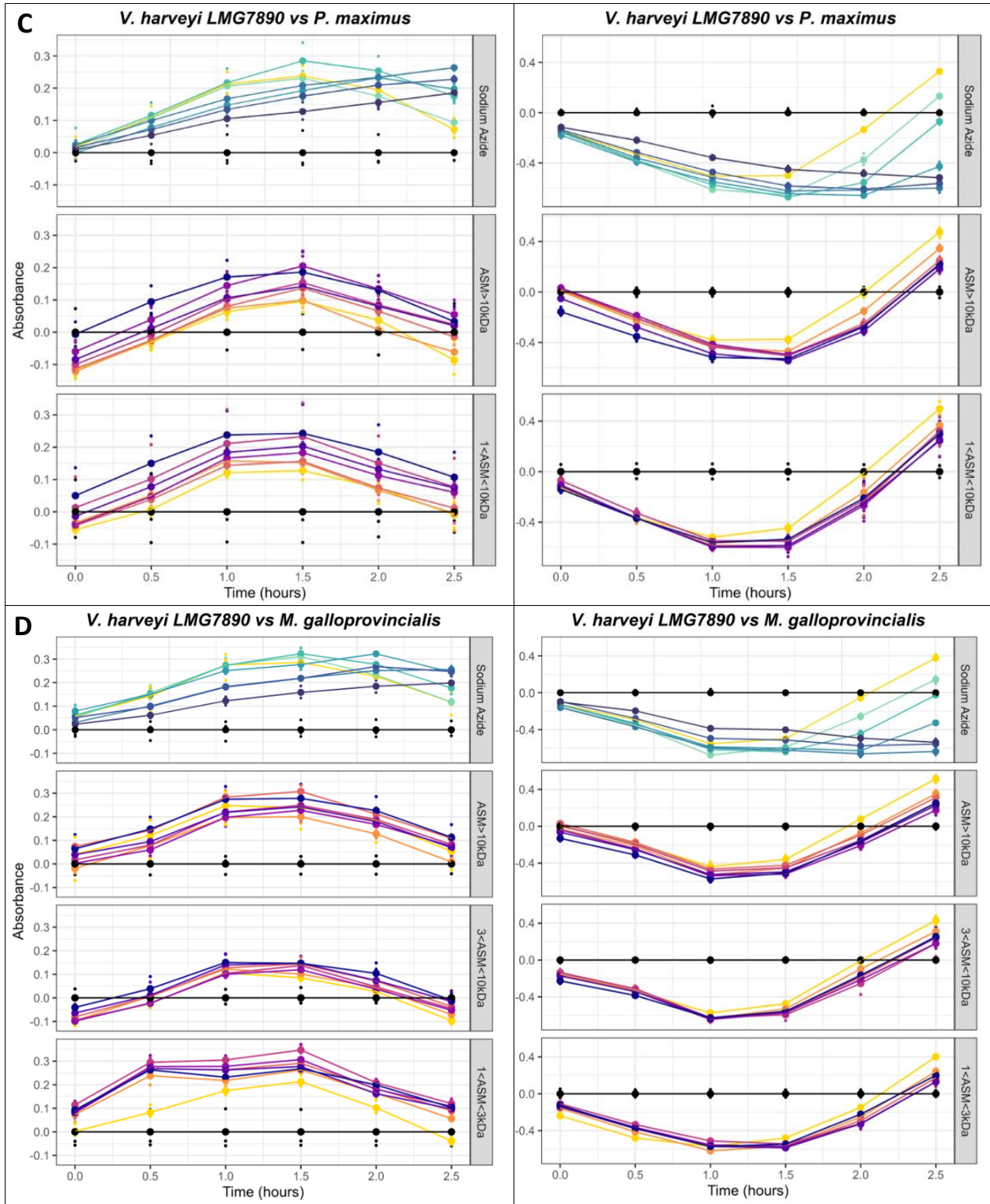
The growth curves results are displayed for both wavelengths in Figure 4.4. Aside from one exception (Fig. 4.4 B, *M. gigas*) both wavelengths of 420 nm and 560 nm were satisfactory in describing bacterial growth alteration against the standard of sodium azide gradient (upper graphs, green-blue gradient), almost behaving in a mirror-like manner. Under natural growth conditions (negative control, yellow line), they exhibit a parabolic profile for the growth of

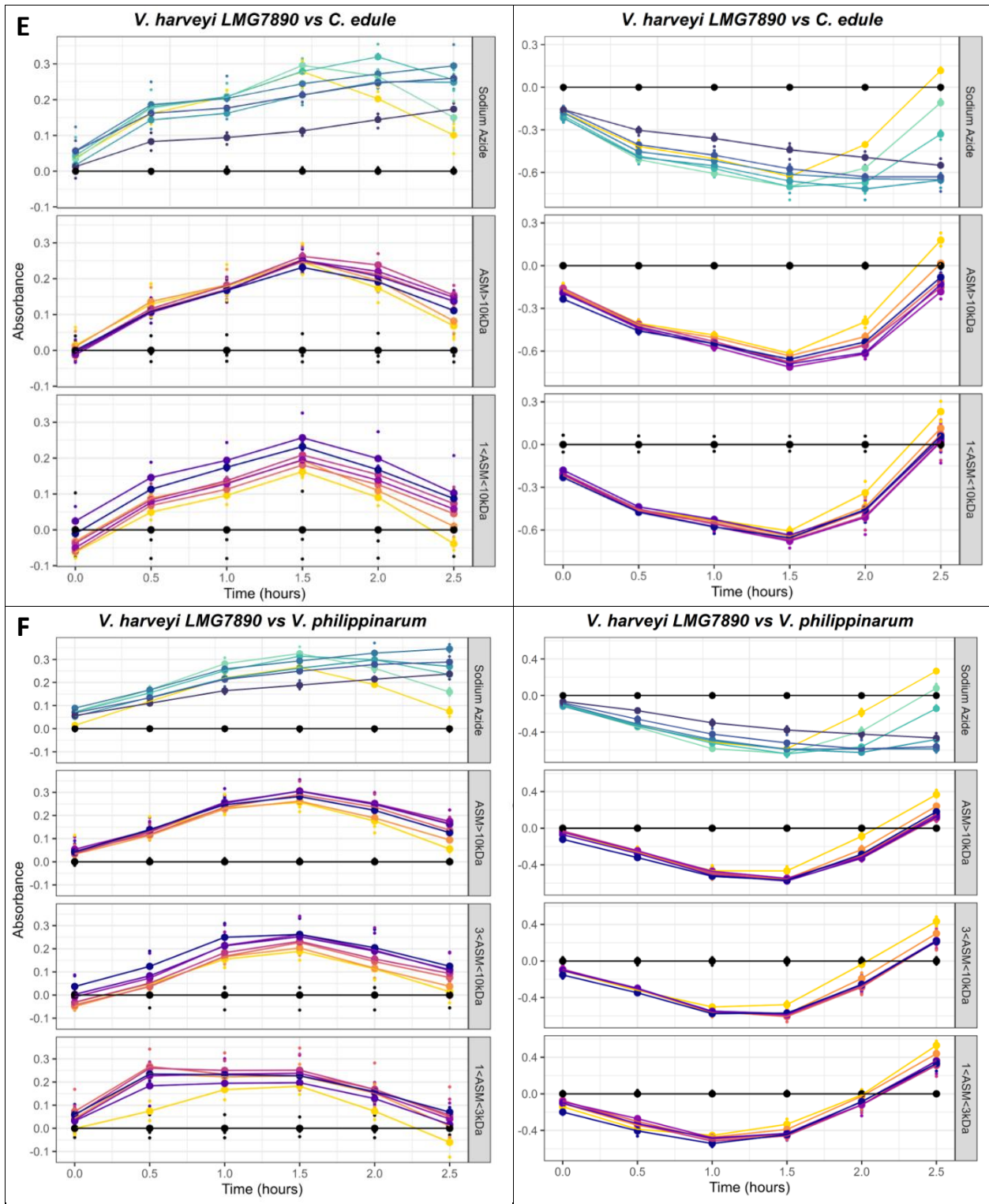
bacterial cultures. The dose-dependent inhibitory effect of sodium azide on *V. harveyi* LMG7890 is observable, mainly on a gradual slowing of the maximal growth rate.

Looking at 560 nm absorbance curves, three gradients of ASM show an alteration of the maximum growth rate. With *M. gigas* extracts, both fractions induce a reduction of this parameter, starting at the maximum concentration of 100 µg/mL: for ASM>10 kDa, a significant reduction of 59.49% (adjusted p-value = 7.12e-3*); for 1<ASM<10 kDa, the reduction of 44.44% is not significant (adjusted p-value = 0.82). With *P. maximus*, the high molecular weight fraction, ASM>10 kDa, induces a smaller but still significant reduction of 23.91% the parameter, starting in the same manner at the maximum concentration of 100 µg/mL (adjusted p-value = 7.02e-3*). The curves produced for remaining tested ASM extracts show neither apparent nor significant response of *V. harveyi* LMG7890 at any concentration. Similarly to the growth graphs produced with 420 nm absorbance for *V. aestuarianus*, the ASM curves from the 420 nm readings show a vertical dispersion, with unchanged profiles when weighted by population size (start point on the y axis). These are then not effective in describing the alteration of growth against bivalve ASM, in spite of the acceptable profiles of the sodium azide standards.

Altogether, two bivalve extract species, *M. gigas* and *P. maximus*, showed antimicrobial properties against *V. harveyi* LMG7890, by reducing the maximal growth rate during the exponential growth phase in liquid cultures. Putative MICs of 150 µg 100 µg/mL are identified for *M. gigas*. Another putative MIC of 150 µg on disk is identified for the vibriostatic agent v0129.







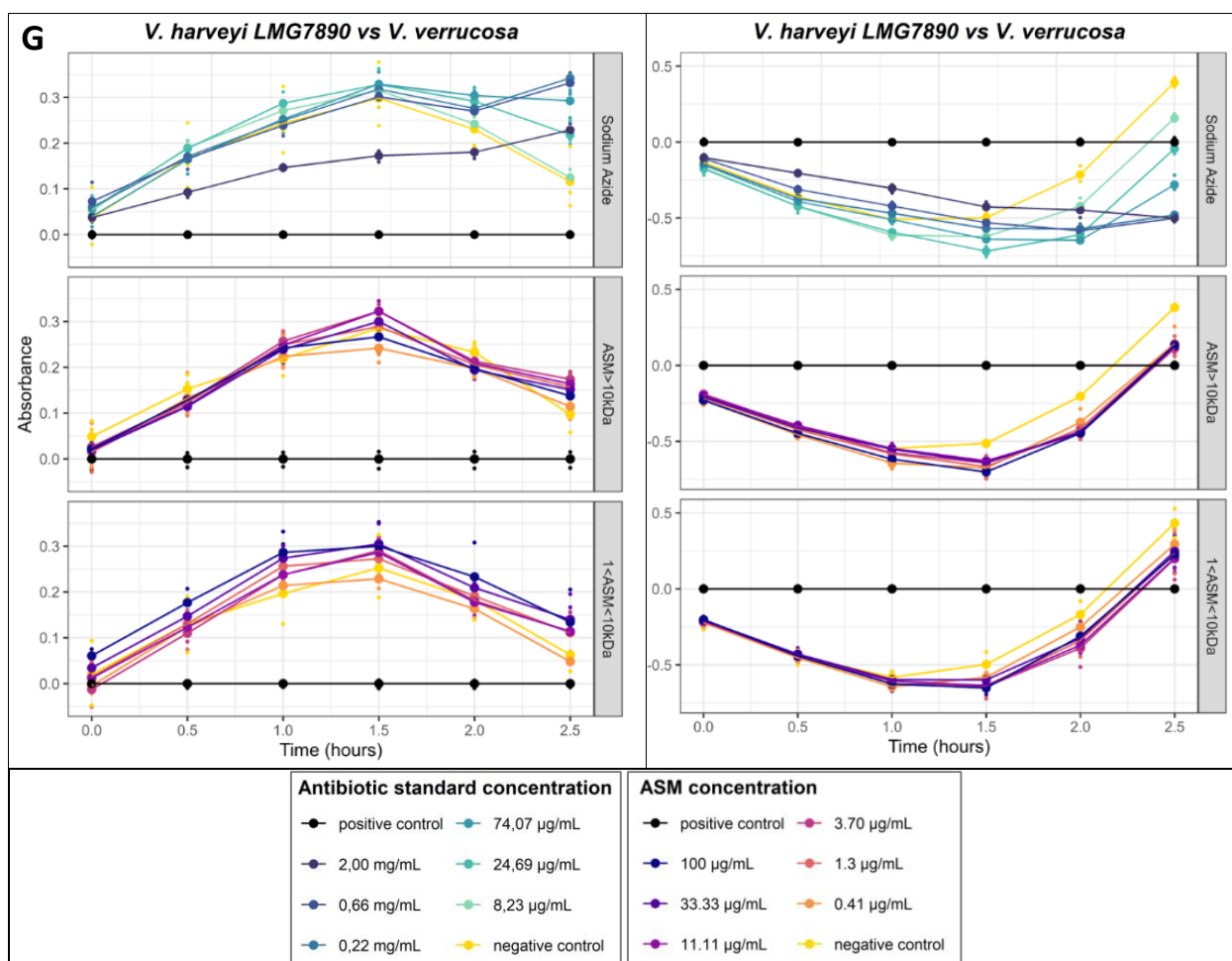


Figure 4.4: Microdilution assays growth curves for *V. harveyi* LMG7890. The left panels show the absorbance read at 420 nm, while the right ones, the absorbance at 560 nm.

4.1.3. *Vibrio mytili*

V. mytili strains were grown in liquid culture, using marine broth, lightly stirred overnight at 28°C, following the literature (Pujalte *et al.*, 1993). Once in log phase (DO = [0.6:1.0]), the suspensions were ready to be used for antibacterial assays.

The marine agar plates used for the disk diffusion assay were incubated at 28°C for 24h to allow for a visible growth on the medium. The results are summarized in the boxplot below (Fig. 4.5). Positive and negative controls were valid. The positive controls performed with v0129 (500µg) showed large inhibition zones with a global mean diameter of 0.91 ± 0.04 cm. On antibiogram plates, the inhibition zone diameter was positively correlated with the quantity of v0129. Only one of the other tested antibacterial products showed clear inhibition of bacterial growth, tetracycline, with the smallest variability in diameter among all responsive products (1.38 ± 0.10 cm).

Among the tested shell extracts, only the AIM of *M. gigas* and *P. maximus* gave positive results, with an inhibition zone diameter of respectively 0.70 ± 0.03 cm (adjusted p-value = 0*), and 0.71 ± 0.01 cm (adjusted p-value = 0.34; unadj. p-value = 0.026). The non-significance of these results comes as a surprise, considering the low variability of the inhibition zones diameters. This could be explained by the robustness of the statistical analysis (Kruskal-Wallis followed by Dunn's post hoc, further corrected by Holm-Bonferroni) that is applied in analyses with expected (and demonstrated) data heteroscedasticity, *i.e.*, null variances are expected for a large number of groups. Here, every other group than the AIM showing inhibition (antibiotics) consistently displays larger diameters, with small variances: this could be an explanation as to why the smaller inhibition zones of AIMs, *i.e.*, closer to the zeros we compare against, are showing non-significant results under robust analysis. Thus, the statistical results of this assay have to be regarded with caution, as they might entail an artificial negative outcome. The interpretation of these results should be set against those of other bacteria, with regards to the growth conditions and valid positive and negative controls.

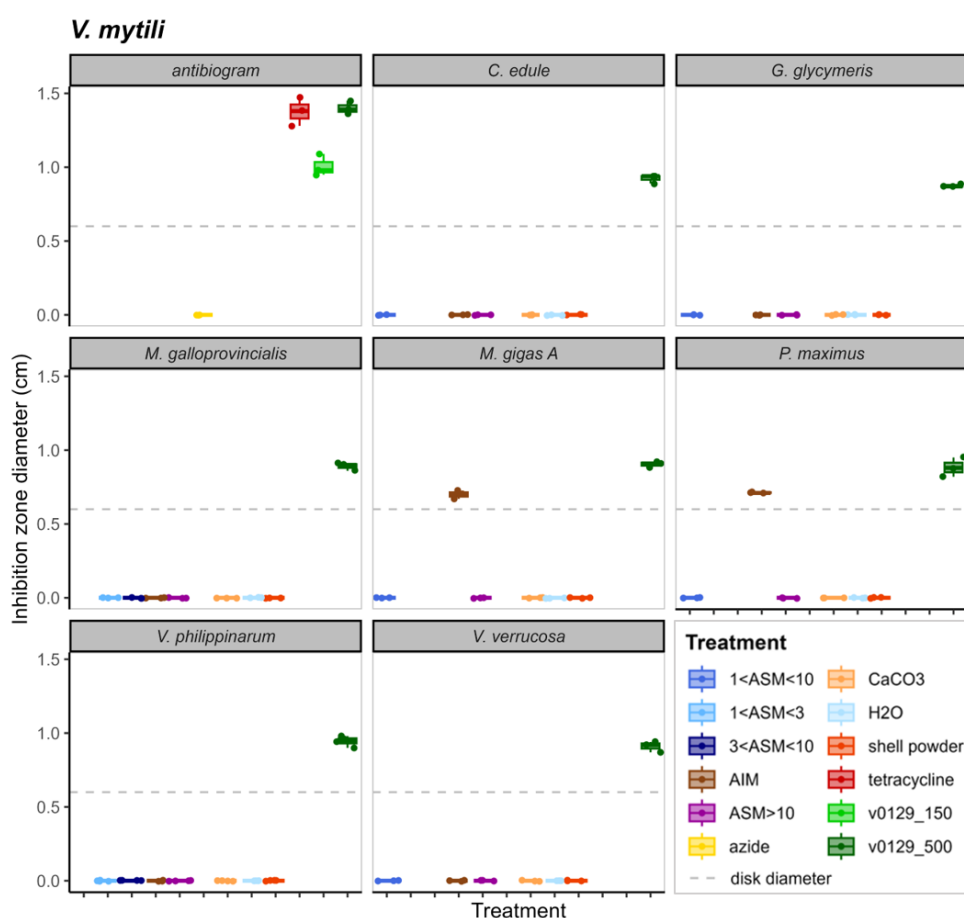
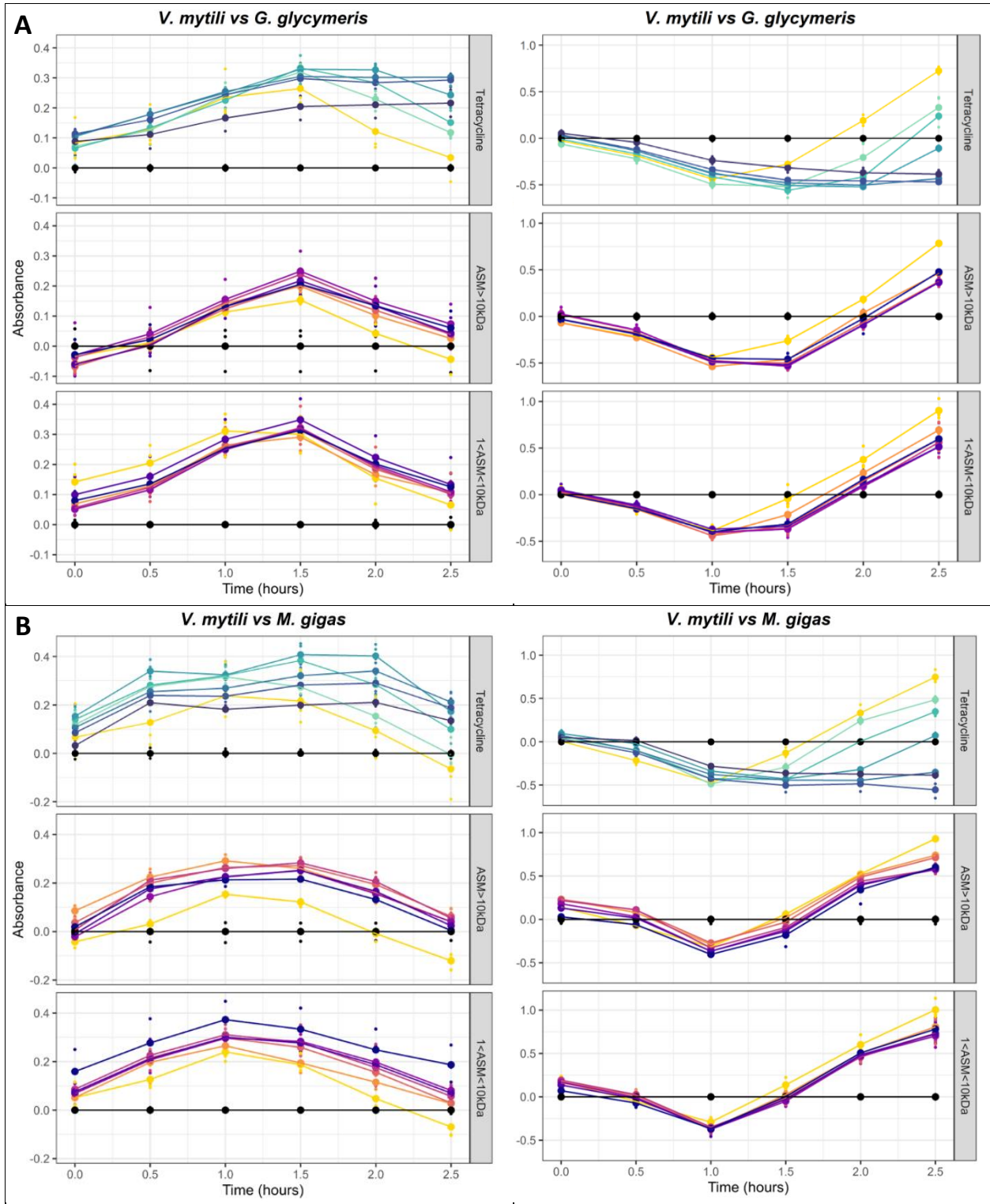


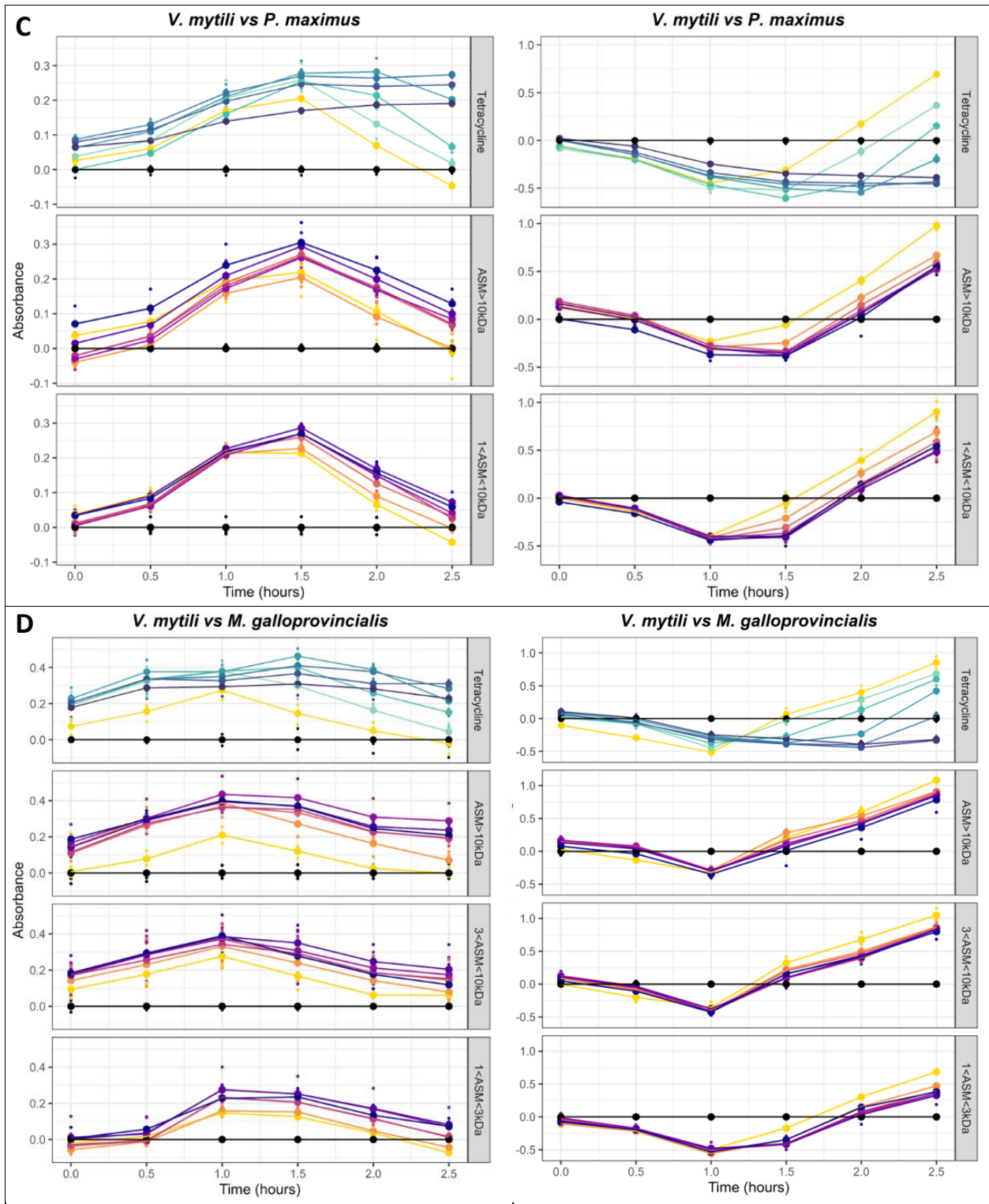
Figure 4.5: boxplots results of the disk diffusion assays for *Vibrio mytili*. The dotted line represents the disk and tablet diameter.

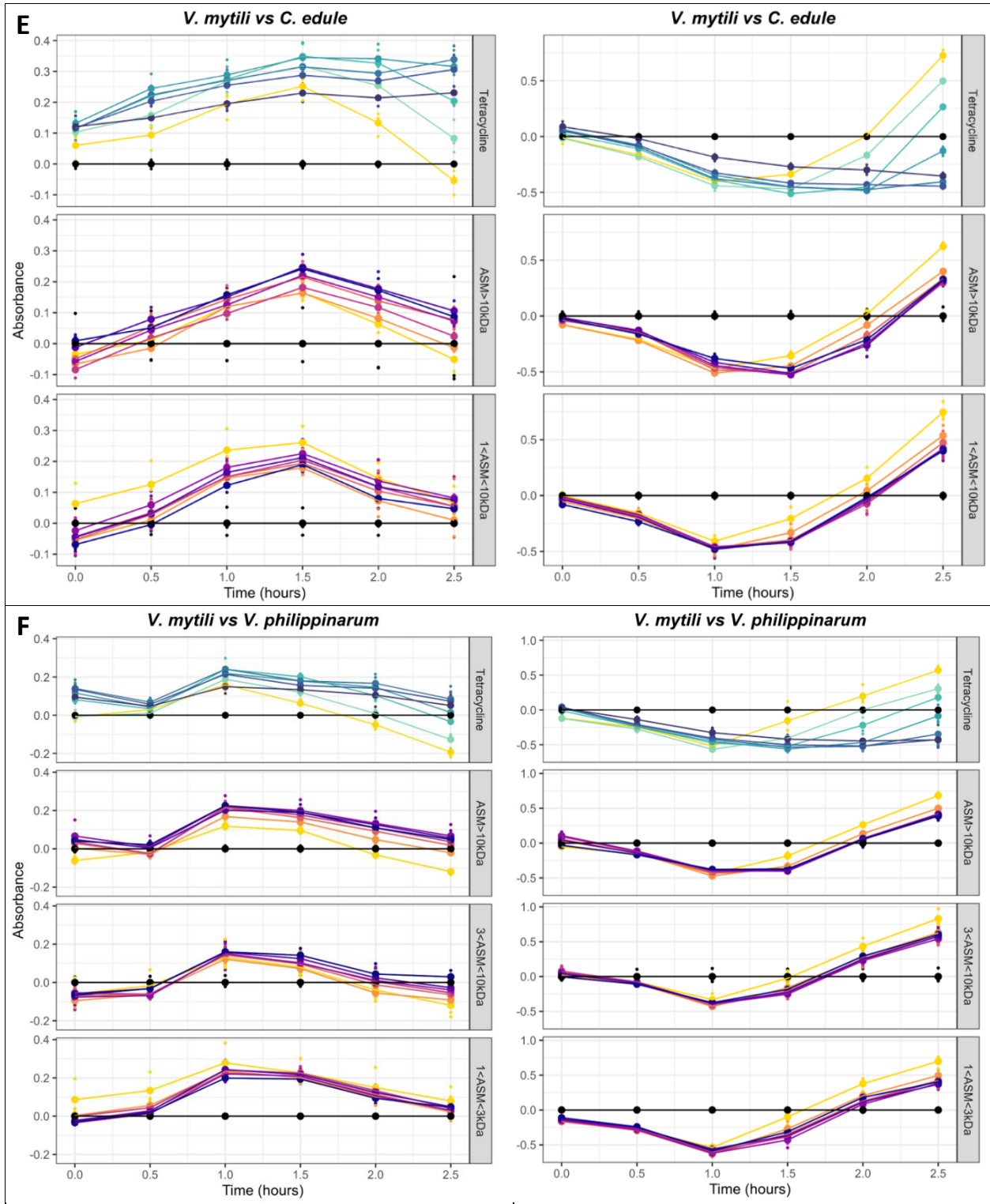
The microplates used for the microdilution assay were incubated, with a gentle stirring, at 20°C for 5 hours. Absorbances at 420 nm and 560nm were measured every thirty minutes, and tetracycline was used as standard antibiotic control against the ASM fractions, following the concentrations displayed in Table 3.1 (see section [4.4.2.5. Microdilution Assay](#), Lutet-Toti *et al.*, 2025, *submitted to STOTEN*): 10.00 µg/mL; 3.33 µg/mL; 1.11 µg/mL; 0.37 µg/mL; 0.13 µg/mL; 0.04 µg/mL.

The growth curves results are displayed for both wavelengths in Figure 4.6. Aside from a few exceptions (Fig. 4.6 B, *M. gigas* and D, *M. galloprovincialis*) both wavelengths of 420 nm and 560 nm described bacterial growth alteration against the standard of tetracycline gradient (upper graphs, green-blue gradient). The produced curves exhibit the characteristic profile for bacterial cultures, and the dose-dependency of the inhibitory effect of tetracycline is observable. However, the negative control curves obtained using readings at 420 nm are consistently showing distinctly lower levels of absorbance than any other concentration. This behavior is visible from the start and throughout the assay, which means that once weighted by population size (start on y axis), the “order” of concentration in which growth inhibition happens remains biologically logical. Overall, when weighted, the alteration of *V. mytili* growth by tetracycline seems to tend towards a dose-dependent low bacteriostatic activity, *i.e.*, a limitation of the carrying capacity. The results from the ASM extracts are difficult to interpret: they follow the previously described pattern of singleling-out the negative control, and do not seem to have a particular effect on any given growth parameter. Furthermore, the presence of extreme values among replicates (Fig. 4.6 D and G) makes it difficult to trust the biological accuracy of the curves.

Altogether, only the AIMS of two tested bivalve extract, *M. gigas* and *P. maximus*, showed antimicrobial properties against *V. mytili*. This inhibition, although not statistically significant, is worthy of comparison to the other strains tested in this antibacterial screening, as the statistical analysis seems to overlook the biological reality by too much robustness, as it is often the case with microbial experiments.







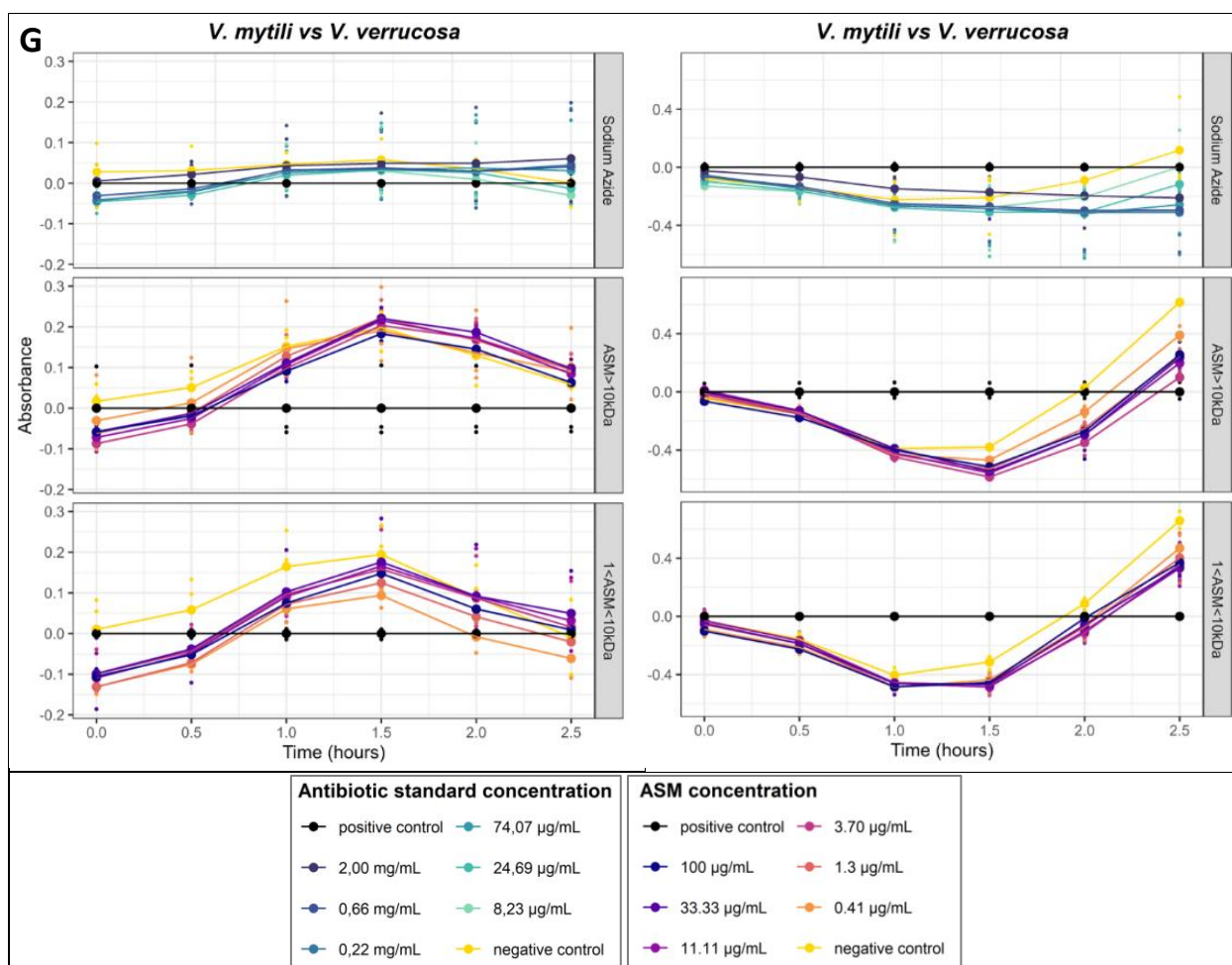


Figure 4.6: Microdilution assays growth curves for *V. mytili*. The left panels show the absorbance read at 420 nm, while the right ones, the absorbance at 560 nm.

4.1.4. *Vibrio tapetis* CECT4600

V. tapetis CECT4600 strains were grown in liquid culture, using marine broth, lightly stirred for 48h at 18°C, following parameters and guidelines from LEMAR lab and literature (Borrego *et al.*, 1996). Once in log phase (DO = [0.6:1.0]), the suspensions were ready to be used for antibacterial assays.

The marine agar plates used for the disk diffusion assay were incubated at 18°C for 48h. The results are summarized in the boxplot below (Fig.4.7). Positive and negative controls were valid. The positive controls performed with v0129 (500µg) showed large inhibition zones with a global mean diameter of 1.82 ± 0.28 cm. On antibiogram plates, the inhibition zone diameter was positively correlated with the quantity of v0129. One other antibacterial product (sodium azide) shows a clear inhibition of bacterial growth (2.14 ± 0.38 cm). Among the tested shell extracts, only two AIMs exhibited positive results: *M. gigas* and *P. maximus*, with means inhibition zone diameters of 0.43 ± 0.38 cm (adjusted p-value = 0.10), and 0.21 ± 0.36 cm

(adjusted p-value = 0.71) respectively. These results are not significant, and show large standard deviations: some of the replicates indeed fail to induce any measurable inhibition. This can be explained in part by the difficulty of reading inhibition zones with *V. tapetis* CECT4600: the spread colonies, although given plenty of time to develop, can be hardly distinguished from marine agar. However, I was able to decipher the inhibitions induced by several antibacterials controls, so the results presented here are still relevant and worthy of being incorporated in the overall screening results, with consideration for their nuanced values.

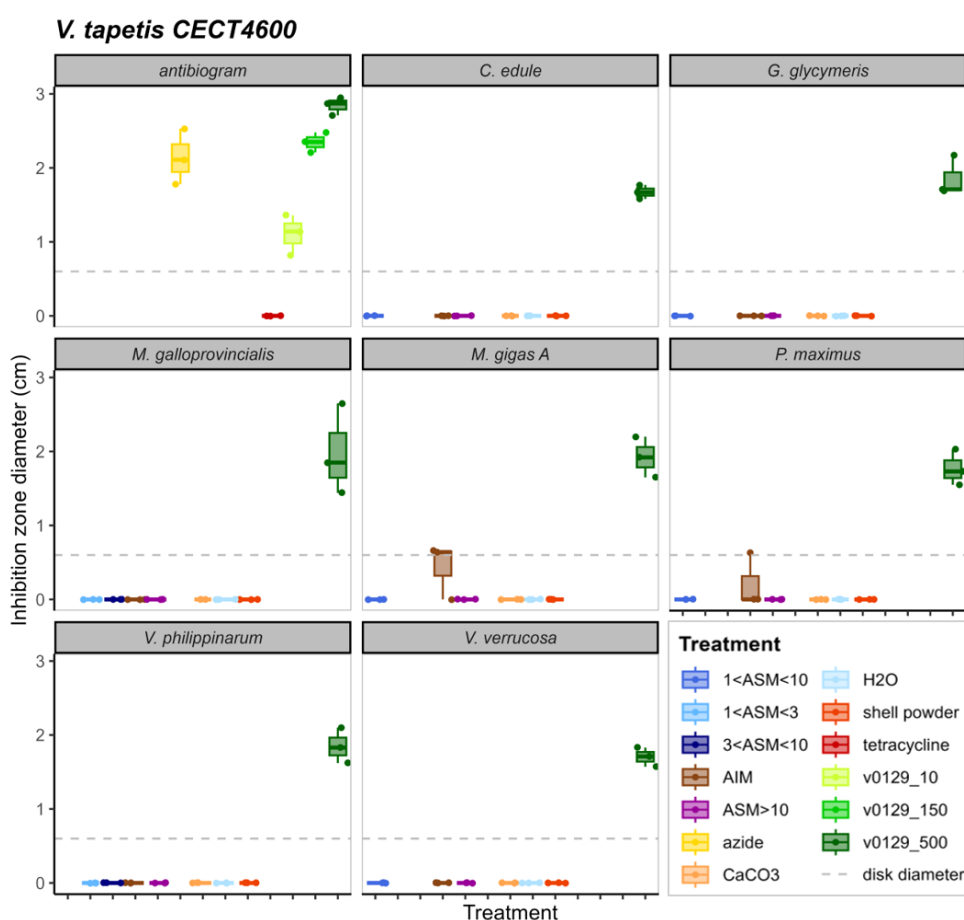


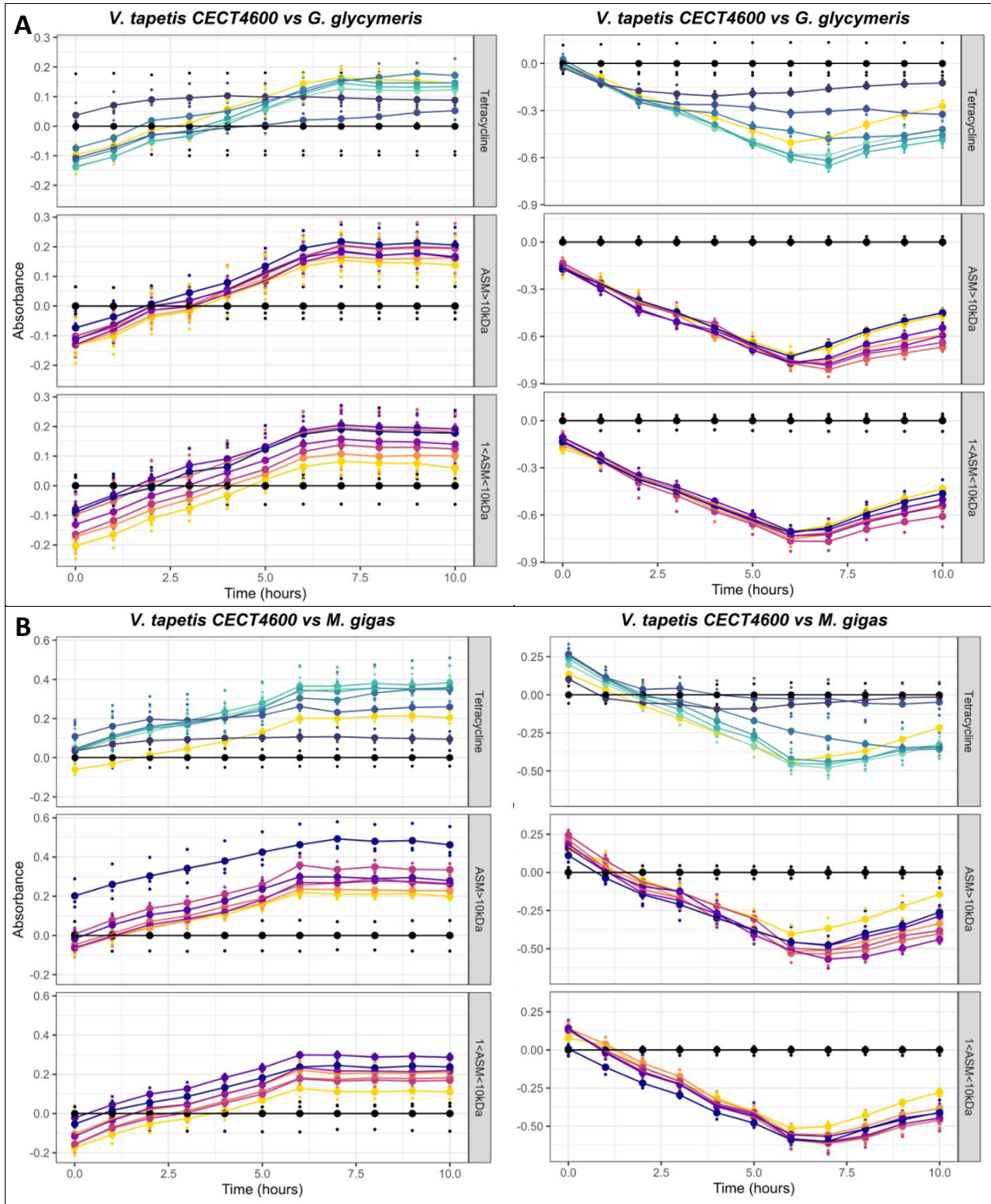
Figure 4.7: boxplots results of the disk diffusion assays for *Vibrio tapetis* CECT4600. The dotted line represents the disk and tablet diameter.

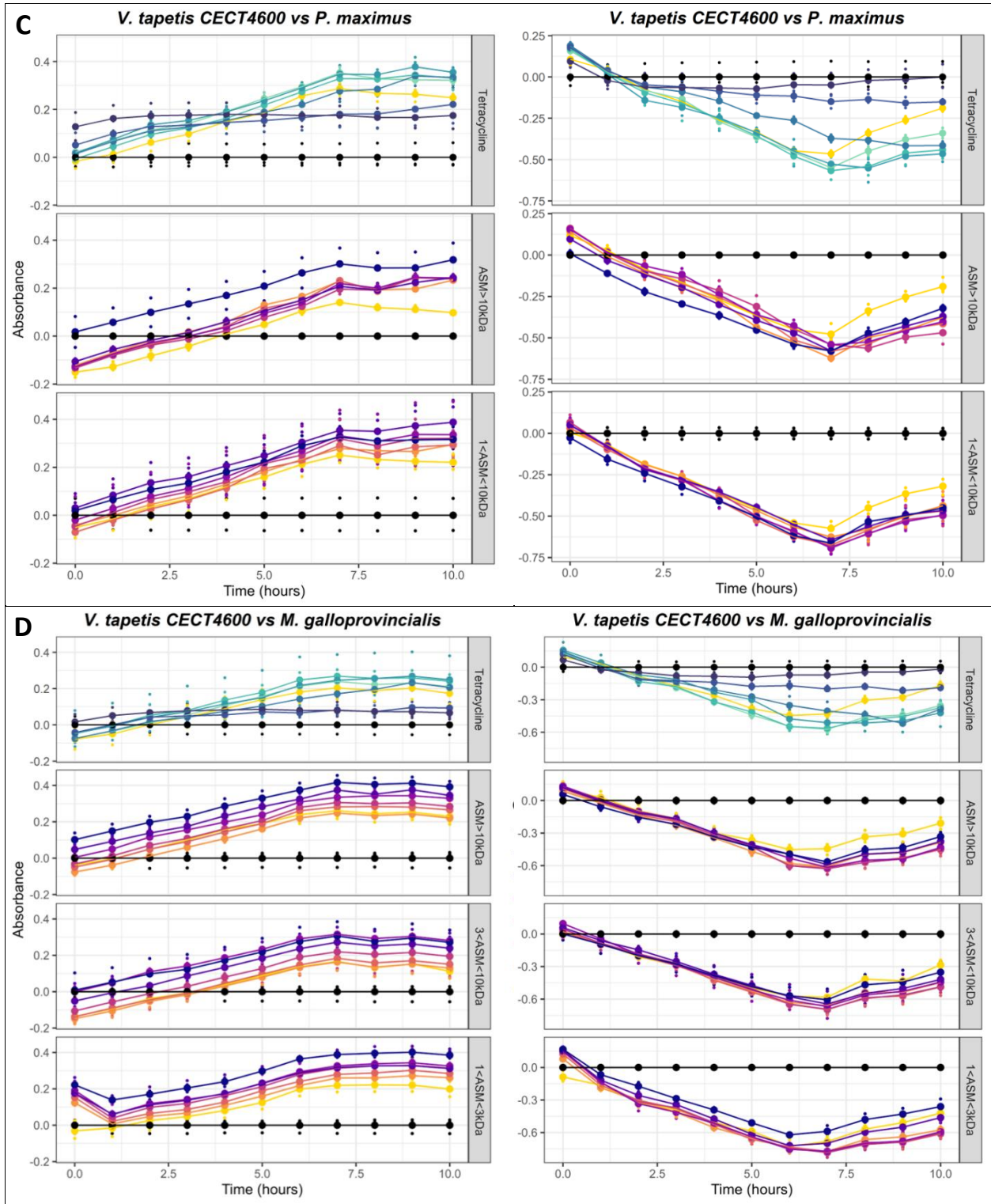
The microplates used for the microdilution assay were incubated, with a gentle stirring, at 18°C for 10 hours. Absorbances at 420 nm and 560nm were measured every hour, and tetracycline was used as standard antibiotic control against the ASM fractions, following the concentrations displayed in Table 3.1 (see section 4.4.2.5. Microdilution Assay, Lutet-Toti *et*

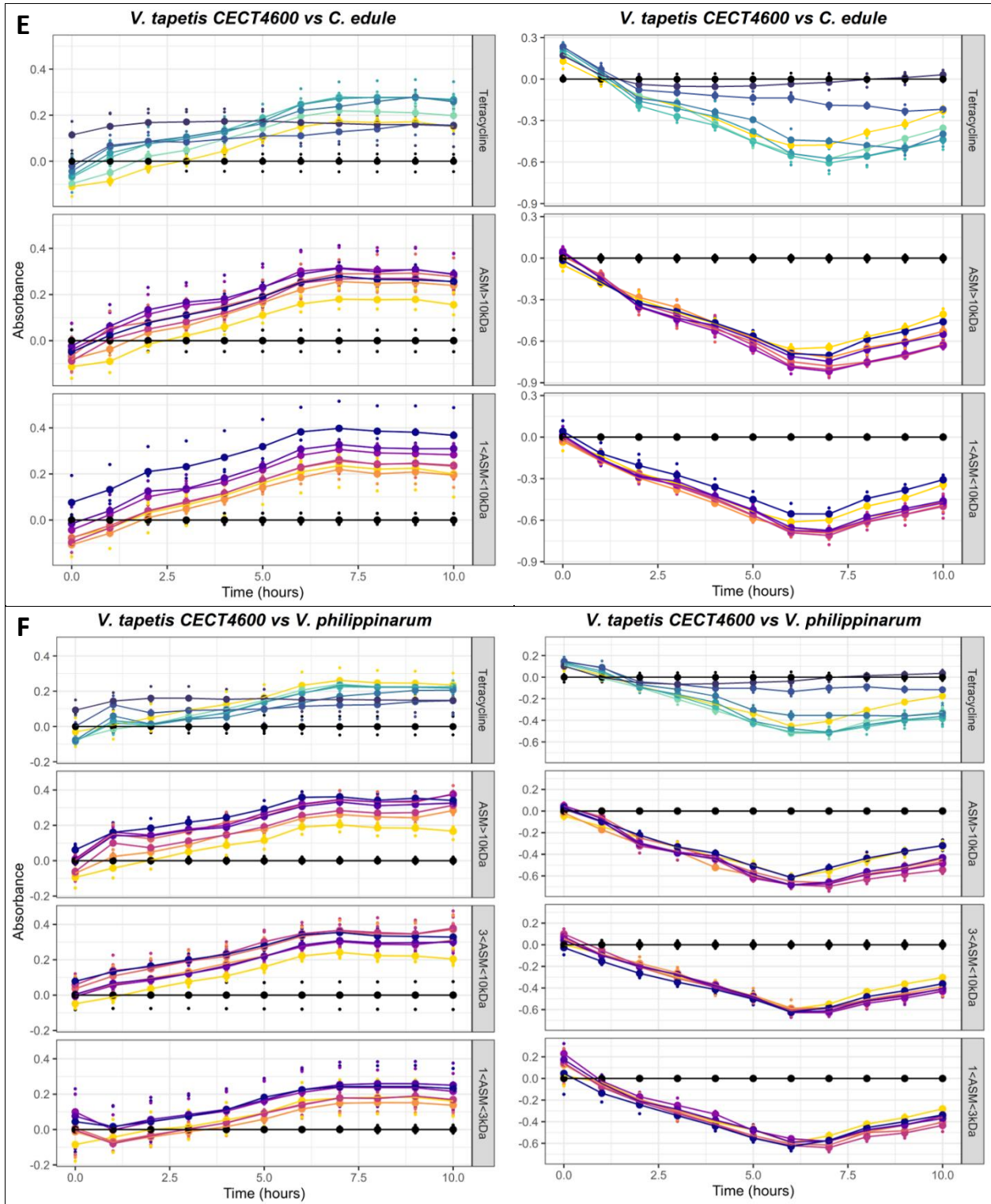
al., 2025, submitted to *STOTEN*): 10.00 µg/mL; 3.33 µg/mL; 1.11 µg/mL; 0.37 µg/mL; 0.13 µg/mL; 0.04 µg/mL.

The growth curves results are displayed for both wavelengths in Figure 4.8, and both wavelengths of 420 nm and 560 nm described bacterial growth alteration against the standard of tetracycline gradient (upper graphs, green-blue gradient). The produced curves exhibit the characteristic profile for bacterial cultures, and the dose-dependency of the inhibitory effect of tetracycline is observable. Similarly to the curves obtained with *V. aestuarianus*, the curves obtained using readings at 420 nm are spreading along the y axis, with the maximum absorbances attributed to higher concentration values. This behavior is visible from the start and throughout the assay, which means that once weighted by population size (start on y axis), the “order” of concentration in which growth inhibition happens remains biologically logical. Overall, when weighted, the alteration of *V. tapetis* CECT4600 growth by tetracycline seems to tend towards a dose-dependent low bacteriostatic activity, either gradually or after a MIC threshold of 0.66 µg/mL (Fig. 4.8 B, E, F, G). The results from the ASM extracts are once again difficult to interpret: using 420 nm wavelength, they follow the previously described pattern of singleling-out the negative control, and for both wavelengths, do not seem to have a particular effect on any given growth parameter. Furthermore, the presence of extreme values among replicates using 420 nm absorbance (left panels) makes it difficult to trust the biological accuracy of these curves.

Altogether, only the AIMS of two tested bivalves, *M. gigas* and *P. maximus*, showed antimicrobial properties against *V. tapetis* CECT4600. This inhibition, although not statistically significant, is worthy of comparison to the other strains tested in this antibacterial screening, as they may reflect antimicrobial properties at either naturally very low levels, or levels that necessitate a combined action from the molecules comprised in other extracted fractions of the shell.







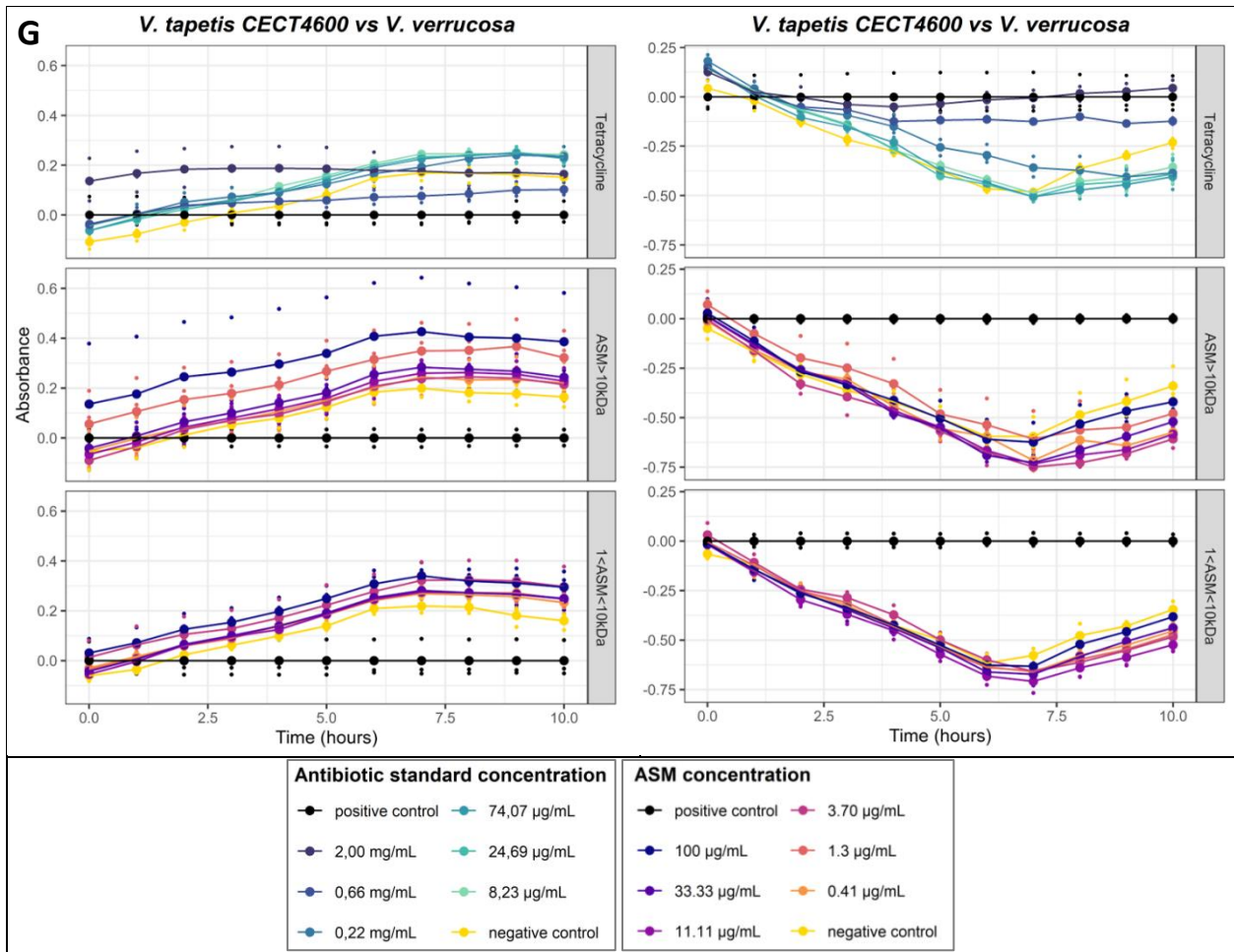


Figure 4.8: Microdilution assays growth curves for *V. tapetis* CECT4600. The left panels show the absorbance read at 420 nm, while the right ones, the absorbance at 560 nm.

4.2. Characterization of the Bacterial Strains: Antibiotic Selection and General Growth Analysis

In order to perform the previously described microdilution assays (sections 3.4 and 4.1), a preliminary testing and characterization of the bacterial growth was necessary for each target strain. This operation was first and foremost crucial in determining ideal laboratory conditions for growth, *i.e.*, temperature, hygrometry, light, and medium. This primary characterization was made in the same form as the microdilution assays, with the tested gradients of substances being antibiotics selected from literature: tetracycline, sodium azide and vibriostatic agent v0129 (Johnson & Shunk, 1936; Pujalte *et al.*, 1993; Borrego *et al.*, 1996; Chopra & Roberts, 2001; Austin & Zhang, 2006; Urbanczyk *et al.*, 2007). This allowed me to determine the correct antibiotic standard to use against ASM extracts, along with the serial dilution “bounds” that would show the best range of antimicrobial activity. Furthermore, I was able to test the viable concentrations of red phenol against bacteria, and to do round tests of spectrophotometer readings at various wavelengths (420, 560 and 600 nm) to standardize the procedure.

The experiments were performed on periods of times allowing for full growth and death of the bacteria: as I was measuring the absorbance, I monitored the change of colors towards bright fuchsia and waited for every well to undergo this change in order to catch and document the full culture dynamic, at different concentrations (delayed growth often implying delayed production of large amounts of basic compounds). The regularity of measurements was also determined with this first round of microdilutions, so that the resulting curves would remain as accurate as possible, without spoiling growth conditions stability by often moving the plates from the incubator.

The resulting curves are presented in the figures below (Figures 4.9 to 4.14). For *A. salmonicida*, the absorbance measurements were performed every two hours, over a time span of 62 hours. Such precise monitoring was achieved using two cultures growing in parallel: one started in the morning, and one started in the night. This gives the patchy pattern observable mainly at 420 nm and 600 nm wavelengths (Fig. 4.9), which can be explained by different base-levels. In order to remove this bias, and in an effort to avoid useless dilapidation of limited ASM resources, I chose to read the absorbances of *A. salmonicida* suspensions in one single batch of cultures, every 8 hours, for the “true” antibacterial assay spanning over 72 hours. As displayed in the lower panels, sodium azide displayed the most gradual alteration of bacterial growth, thus making the cut as the standard antibiotic of the ASM assay.

For *V. aestuarianus*, the absorbance measurements were done every hour, over a time span of 6 hours. As displayed in the upper panels (Fig. 4.10), tetracycline displayed the most

gradual and progressive alteration of bacterial growth, respecting the concentration gradient. It was thus chosen as the standard antibiotic for the ASM microdilution assay.

For *V. harveyi* ORM4, the absorbance measurements were done every hour, over a time span of 4 hours. This amount of timepoints do not seem sufficient enough to accurately describe bacterial growth curves and their potent alterations, so the number of measurements was doubled. As displayed in the upper panels (Fig. 4.11), tetracycline displayed the most gradual and progressive alteration of bacterial growth, respecting the concentration gradient. It was thus chosen as the standard antibiotic for the ASM microdilution assay.

For *V. harveyi* LMG7890, the absorbance measurements were done every thirty minutes, over a time span of 2.5 hours. Interestingly when compared to the mostly-tetracycline-sensitive *V. harveyi* ORM4, for *V. harveyi* LMG7890 showed the most gradual and progressive alteration of growth against sodium azide (Fig. 4.12, lower panels), respecting the concentration gradient. It was thus chosen as the standard antibiotic for the ASM microdilution assay.

For *V. mytili*, the absorbance measurements were done every hour, over a time span of 4 hours. As displayed in the lower panels (Fig. 4.13), sodium azide displayed the most gradual and progressive alteration of bacterial growth, and was thus used as the standard antibiotic for the following ASM microdilution assay.

For *V. tapetis* CECT4600, the absorbance measurements were done every hour, over a time span of 6 hours, according to the already characterized growth in literature (Borrego *et al.*, 1996). As displayed in the upper panels (Fig. 4.14), tetracycline displayed the most gradual and progressive alteration of bacterial growth, with the depiction of the start of bacterial population decline. It was thus selected as the standard antibiotic for the following ASM microdilution assay.

The curves produced for the alteration of bacterial growth with growing concentrations of the vibriostatic agent v0129 are almost always showing rather strange repartitions, with seemingly inverted orders of absorbance and a scattering of values around the positive control (baseline value of the medium pH without any bacterial growth). This is due to the intrinsic acidifying properties of v0129, which change the color of red phenol (pH indicator) before any addition of bacteria. The continuity of this phenomenon across all concentrations, while one can still discern the lowering of growth alterations at low concentrations, effectively disqualifies this antibiotic for any use as a standard gradient in the microdilution assays. No range of serial dilutions can be found to induce bacterial growth inhibition without prior “parasitic” pH alteration.

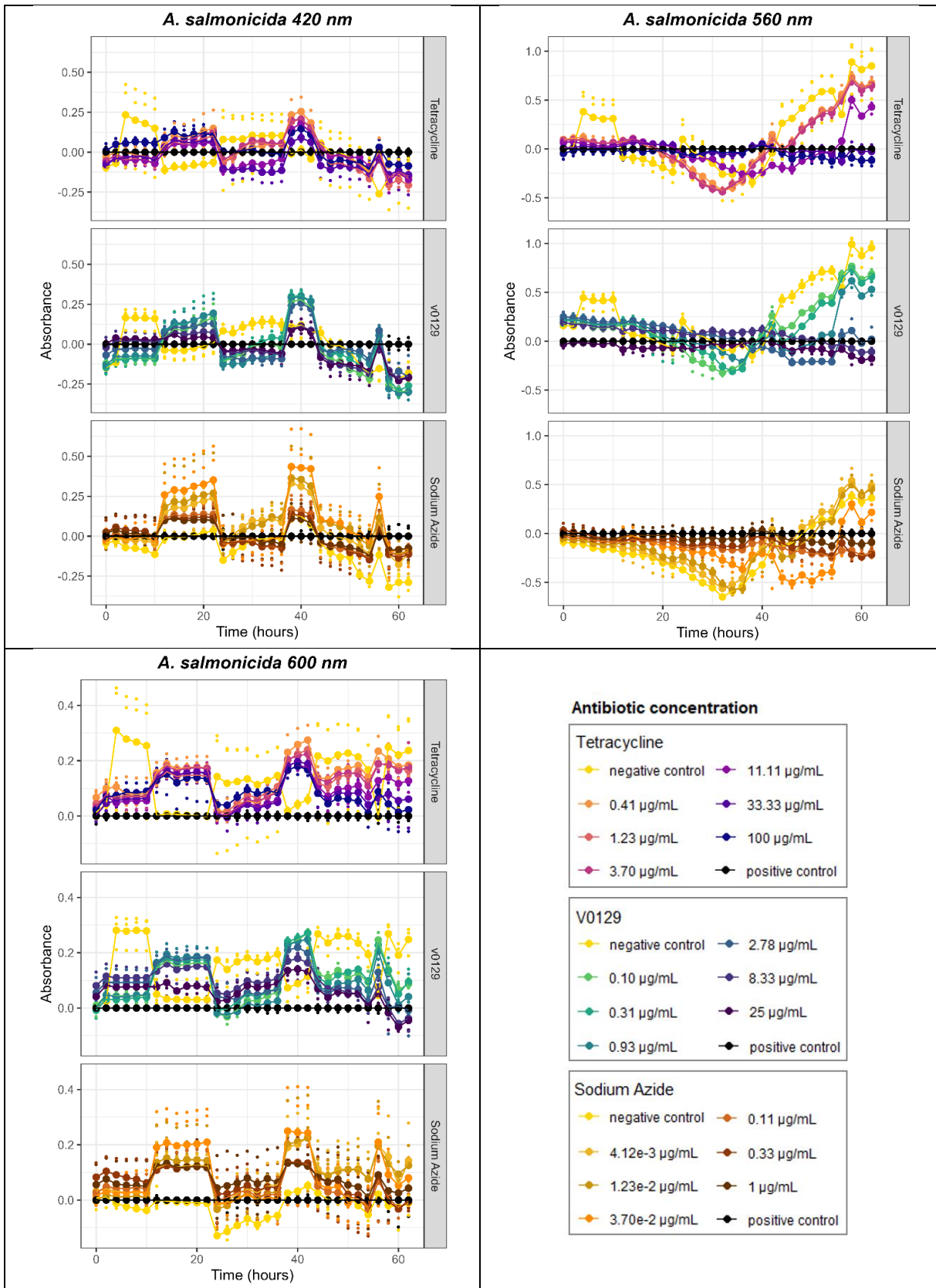


Figure 4.9: Growth curves from the phase A of the microdilution assays for *A. salmonicida*.

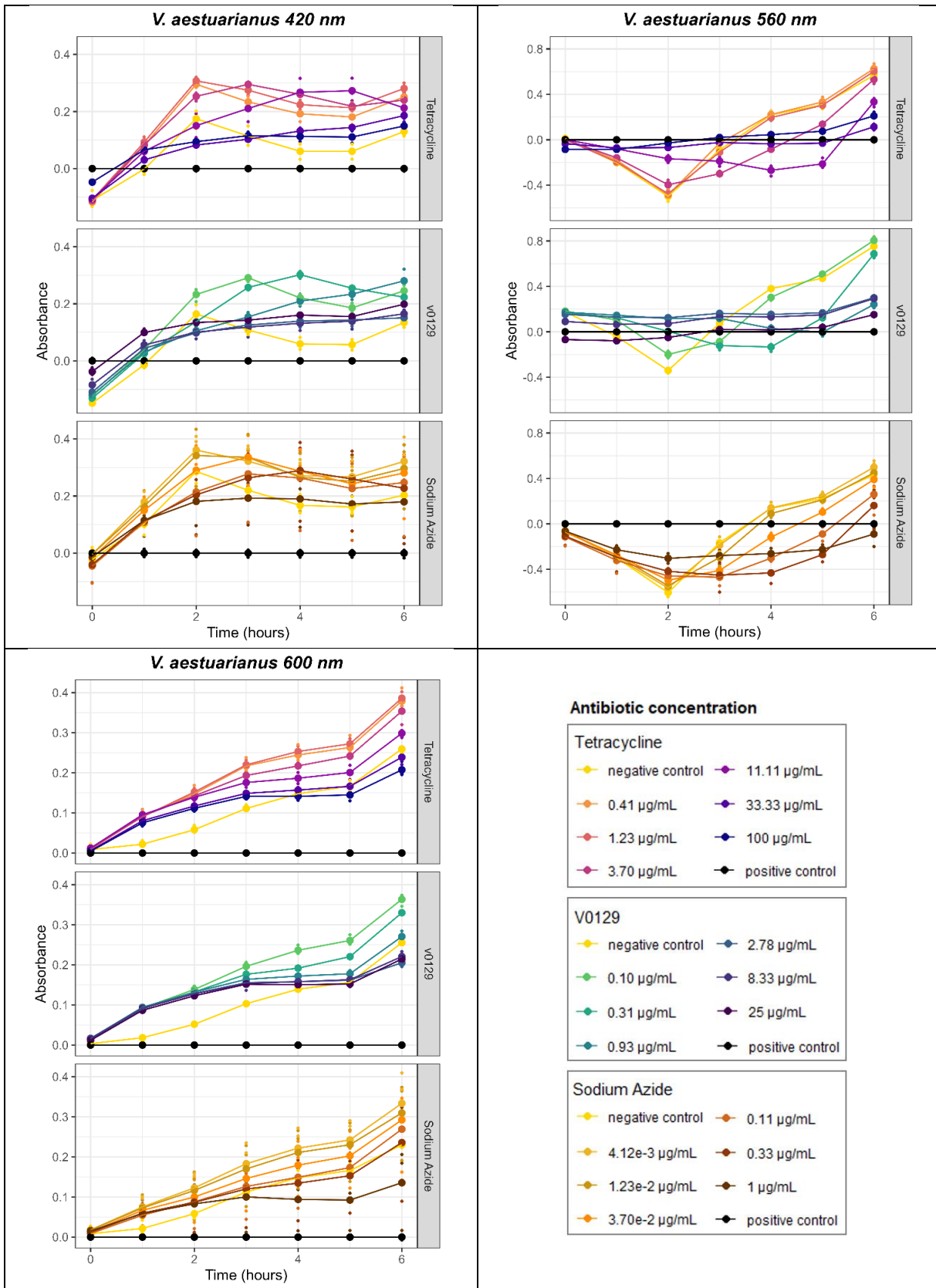


Figure 4.10: Growth curves from the phase A of the microdilution assays for *V. aestuarianus*.

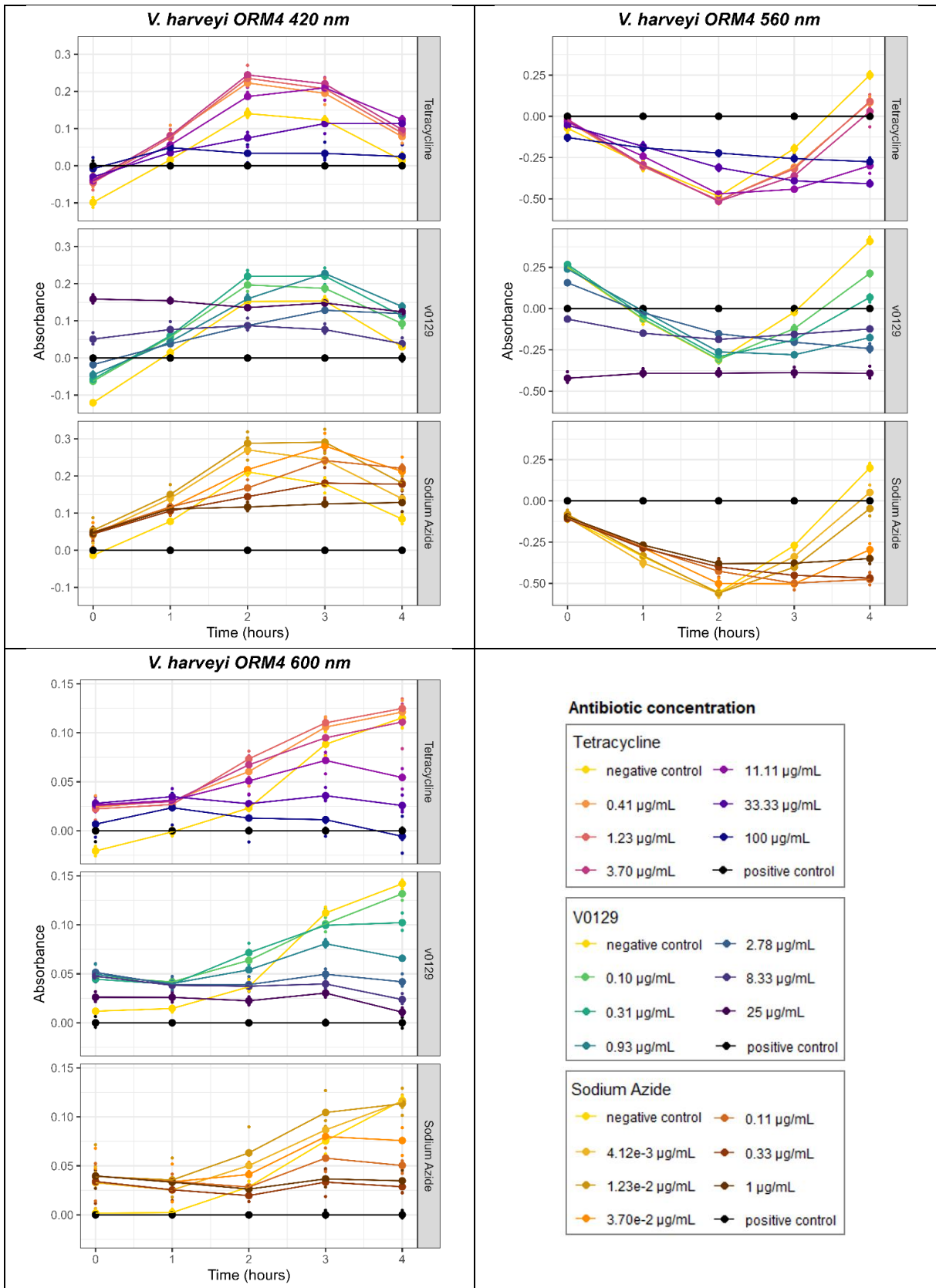


Figure 4.11: Growth curves from the phase A of the microdilution assays for *V. harveyi* ORM4.

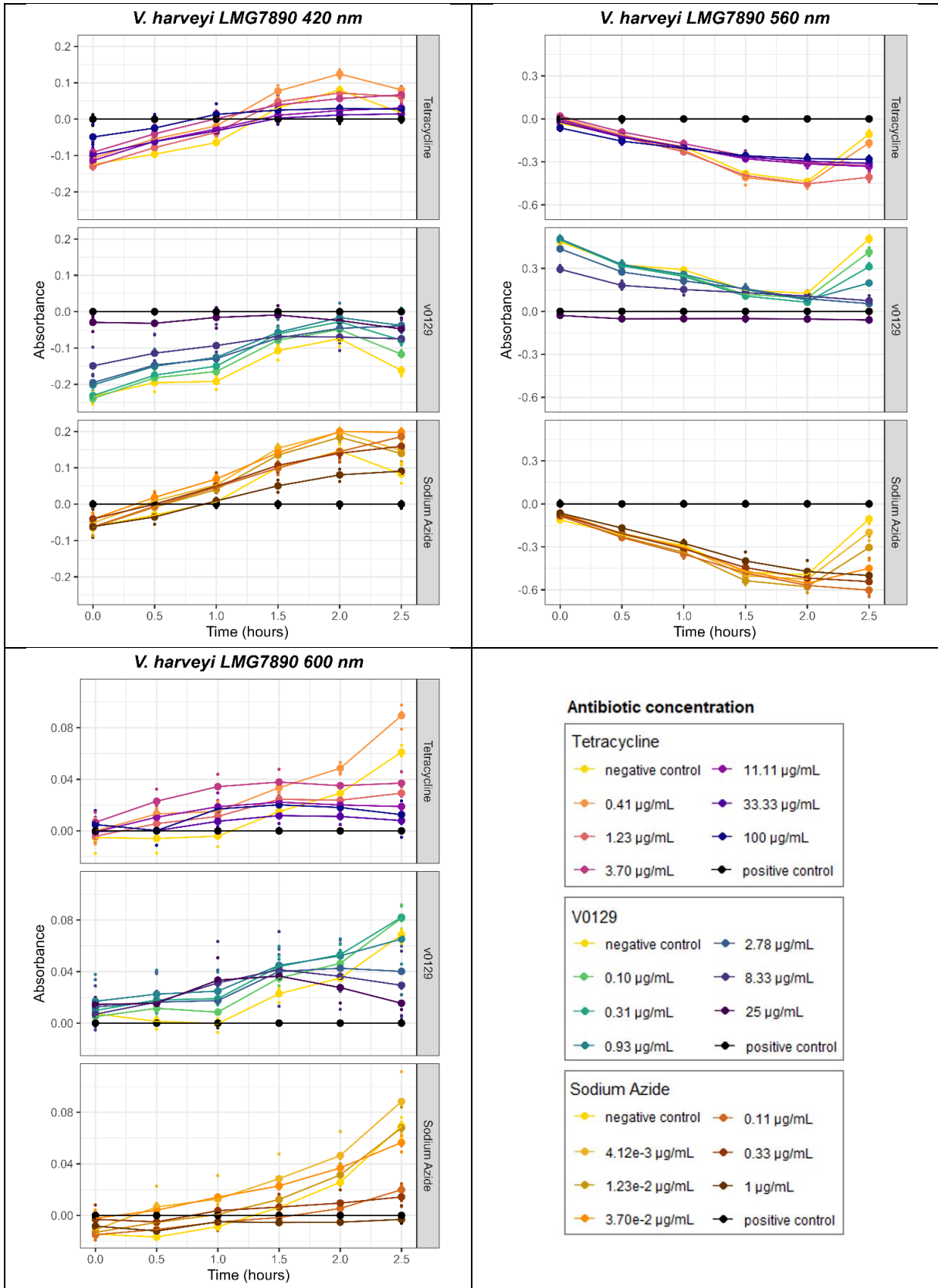


Figure 4.12: Growth curves from the phase A of the microdilution assays for *V. harveyi* LMG7890.

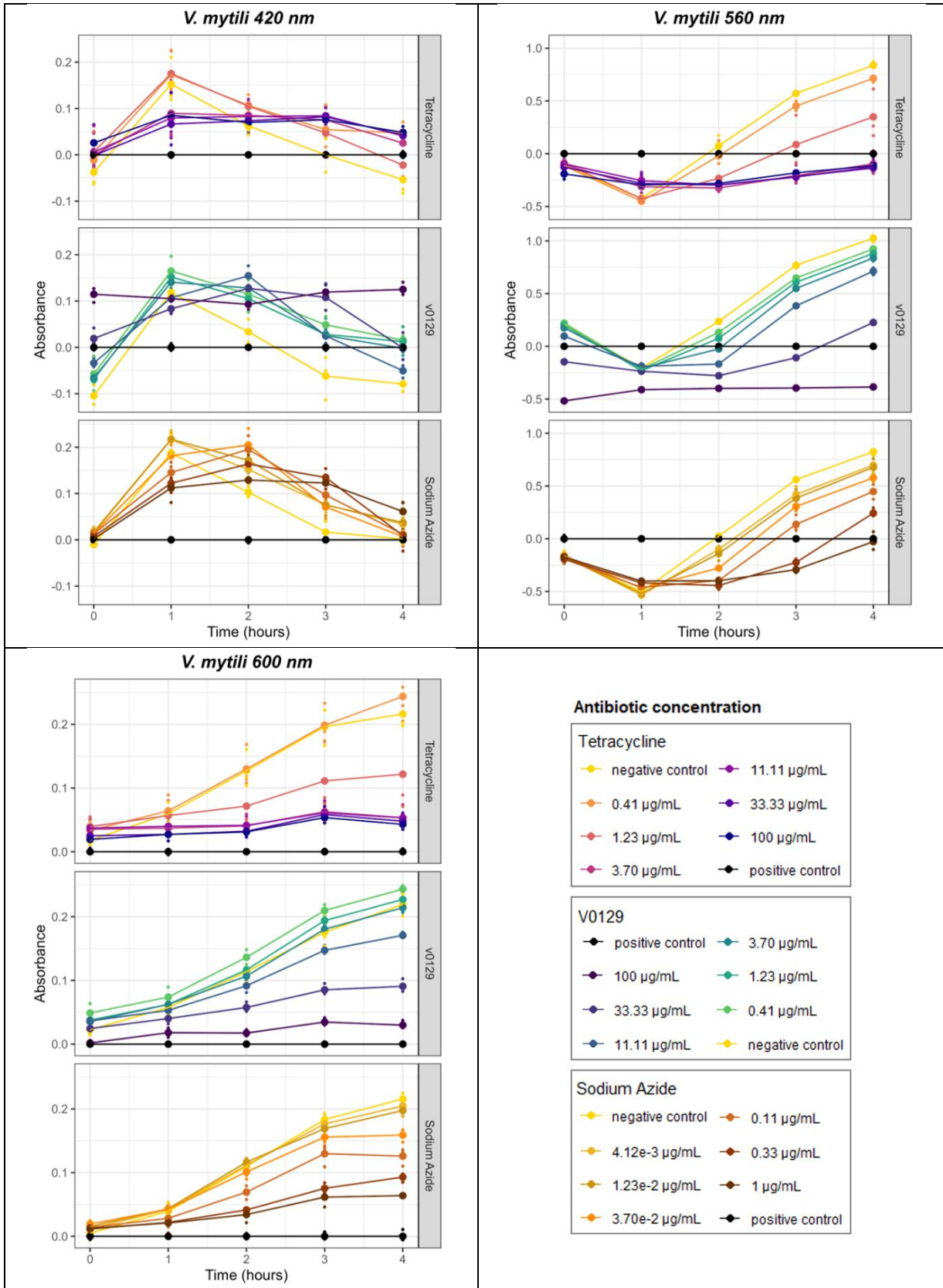


Figure 4.13: Growth curves from the phase A of the microdilution assays for *V. mytili*.

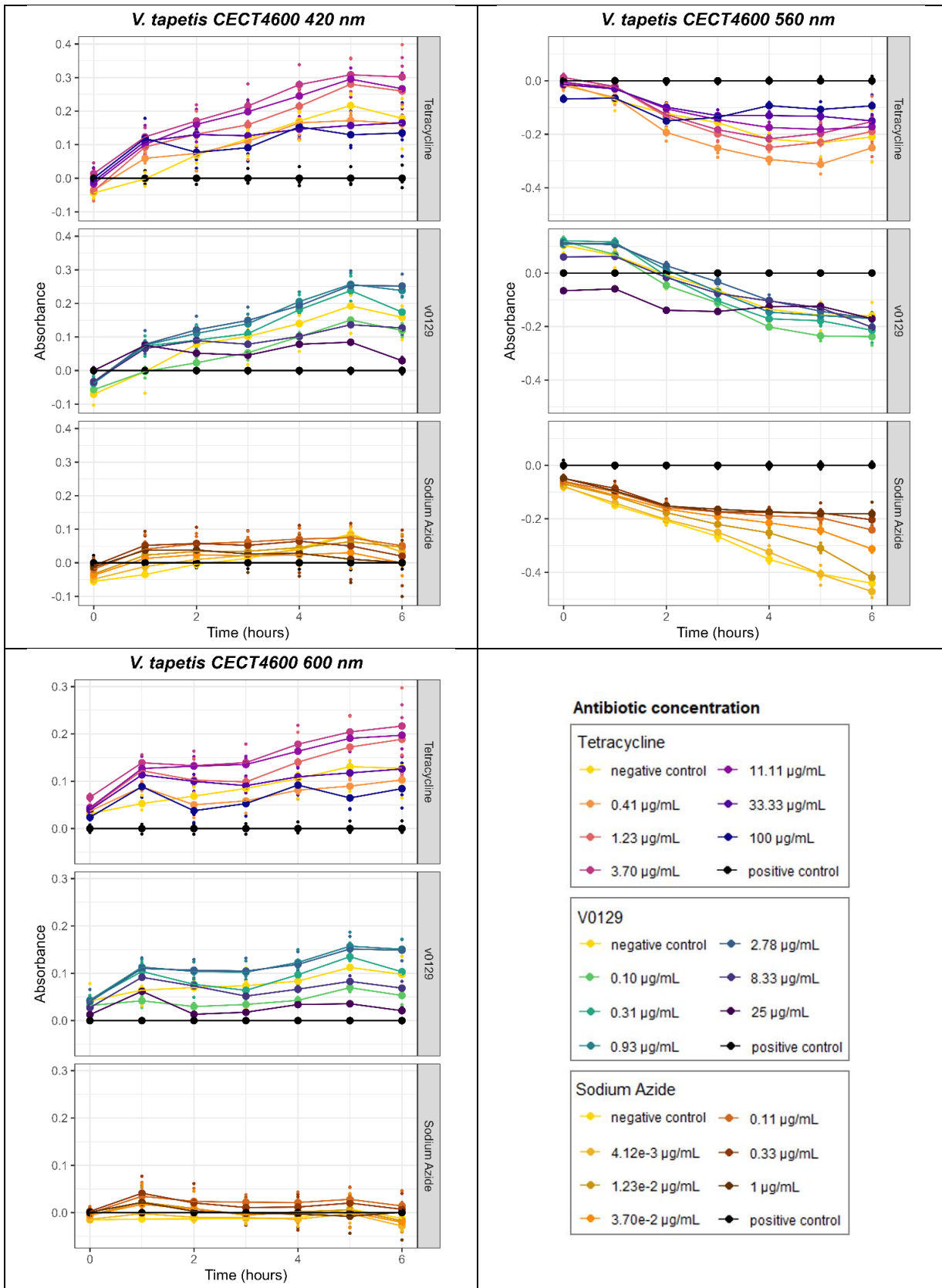
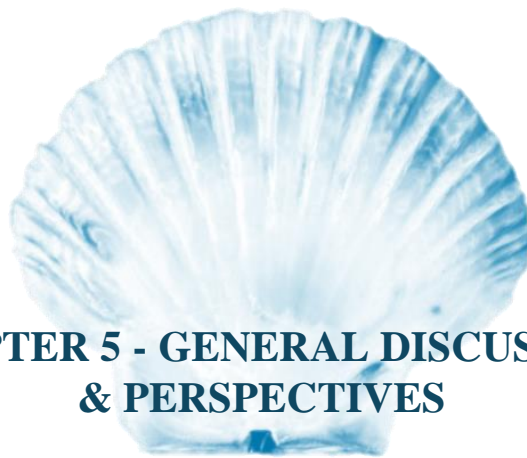


Figure 4.14: Growth curves from the phase A of the microdilution assays for *V. tapetis* CECT4600.

4.3. Chapter References

- Austin, B., and Zhang, X.-H. (2006). *Vibrio harveyi*: A significant pathogen of marine vertebrates and invertebrates. *Letters in Applied Microbiology*, 43(2), 119–124. <https://doi.org/10.1111/j.1472-765X.2006.01989.x>
- Borrego, J. J., Castro, D., Luque, A., Paillard, C., Maes, P., Garcia, M. T., and Ventosa, A. (1996). *Vibrio tapetis* sp. Nov., the Causative Agent of the Brown Ring Disease Affecting Cultured Clams. *International Journal of Systematic and Evolutionary Microbiology*, 46(2), 480–484. <https://doi.org/10.1099/00207713-46-2-480>
- Chopra, I., and Roberts, M. (2001). Tetracycline Antibiotics: Mode of Action, Applications, Molecular Biology, and Epidemiology of Bacterial Resistance. *Microbiology and Molecular Biology Reviews*, 65(2), 232–260. <https://doi.org/10.1128/mmb.65.2.232-260.2001>
- He, Y., Huang, Y.-Y., Xi, L., Gelfand, J. A., and Hamblin, M. R. (2018). Tetracyclines function as dual-action light-activated antibiotics. *PLOS ONE*, 13(5), e0196485. <https://doi.org/10.1371/journal.pone.0196485>
- Jiang, Q., Shi, L., Ke, C., You, W., and Zhao, J. (2013). Identification and characterization of *Vibrio harveyi* associated with diseased abalone *Haliotis diversicolor*. *Diseases of Aquatic Organisms*, 103(2), 133–139. <https://doi.org/10.3354/dao02572>
- Johnson, F. H., and Shunk, I. V. (1936). An Interesting New Species of Luminous Bacteria. *Journal of Bacteriology*, 31(6), 585–593.
- Lutet-Toti, C., Da Silva Feliciano, M., Thomas, J., Crosland, A., Develay, C., Debrosse, N., Force, A., Bidault, A., Broussard, C., Falini, G., Goffredo, S., and Marin, F. (2025). Do bivalve shells exhibit antibacterial properties? Screening calcifying organic matrices against two major marine pathogens. *Science of the TOTAL ENvironment (STOTEN)*, submitted.
- Massoud, R., Saffari, H., Massoud, A., and Moteian, M. (2020). Screening methods for assessment of antibacterial activity in nature. Conference Paper, *4th Int. Conf. on Applied Research in Science and Engineering*, 11p.
- Pujalte, M.-J., Ortigosa, M., Urdaci, M.-C., Garay, E., and Grimont, P. A. D. (1993). *Vibrio mytili* sp. Nov., from Mussels. *International Journal of Systematic and Evolutionary Microbiology*, 43(2), 358–362. <https://doi.org/10.1099/00207713-43-2-358>
- Rios, J. L., Recio, M. C., and Villar, A. (1988). Screening methods for natural products with antimicrobial activity: A review of the literature. *Journal of Ethnopharmacology*, 23(2–3), 127–149. [https://doi.org/10.1016/0378-8741\(88\)90001-3](https://doi.org/10.1016/0378-8741(88)90001-3)
- Tison, D. L., and Seidler, R. J. (1983). *Vibrio aestuarianus*: A New Species from Estuarine Waters and Shellfish†. *International Journal of Systematic and Evolutionary Microbiology*, 33(4), 699–702. <https://doi.org/10.1099/00207713-33-4-699>
- Urbanczyk, H., Ast, J. C., Higgins, M. J., Carson, J., and Dunlap, P. V. (2007). Reclassification of *Vibrio fischeri*, *Vibrio logei*, *Vibrio salmonicida* and *Vibrio wodanis* as *Aliivibrio fischeri* gen. Nov., comb. Nov., *Aliivibrio logei* comb. Nov., *Aliivibrio salmonicida* comb. Nov. And *Aliivibrio wodanis* comb. Nov. *International Journal of Systematic and Evolutionary Microbiology*, 57(12), 2823–2829. <https://doi.org/10.1099/ijs.0.65081-0>



**CHAPTER 5 - GENERAL DISCUSSION
& PERSPECTIVES**

5.1. Research Activities Carried Out During the Doctorate

The research presented in this manuscript is the result of a three-year doctoral study, during which I investigated the antibacterial properties of the organic matrices (OM) from the shell of bivalves of economic interest. Notably, this project represents the very first attempt to search for antibacterial agents in bivalve shells rather than in soft tissues. The second novelty lies in the fact that the project specifically targets marine pathogens.

As a bioprospecting study, an important part of my work consisted first in extracting the OM from the shells of seven bivalves of economic interest: the dog cockle *Glycymeris glycymeris*, the Mediterranean mussel *Mytilus galloprovincialis*, the Pacific cupped oyster *Magallana gigas*, the great scallop *Pecten maximus*, the common cockle *Cerastoderma edule*, the warty venus *Venus verrucosa* and the manila clam *Venerupis philippinarum*. I thoroughly cleaned the shells to remove any organic matter, produced decontaminated powders and extracted both soluble (ASM) and insoluble (AIM) fractions which served as natural sources for the tested substances. These extracts were subsequently analyzed on electrophoresis gels.

The second major step in my research was the setup of antibacterial screening, to effectively test the extracts for their capacity to interfere with the growth of six marine bacterial strains: *Aliivibrio salmonicida*, *Vibrio aestuarianus*, *Vibrio harveyi* LMG7890, *Vibrio harveyi* ORM4, *Vibrio mytili* and *Vibrio tapetis* CECT4600. This phase required extensive preparation and trials to achieve satisfactory experimental design adapted to the peculiar cultivating conditions of marine bacteria. For the most comprehensive bioprospecting study possible, two assays were performed: a disk diffusion test, marking the first time use of AIM extracts in bioassays, and a microdilution test.

Finally, all bivalve extracts were analyzed by using a proteomics approach, in collaboration with Proteom'IC platform 3P5 (Paris, France), in order to detect the presence of already documented AntiMicrobial Peptides and Proteins (AMPPs) and try to establish correlations with the previously observed bioactivity.

In summary, through this doctoral research, I have explored the antibacterial properties of organic matrices from bivalve shells, aiming to bring forward innovative approaches for bioprospecting unconventional models and targets. While promising results were obtained, it is essential to underline the limitations of this project, which will be discussed in the following section.

5.2. Limitations of my Project

5.2.1. Time Consuming Preparation and Extraction of the Shell Matrices

The innovative and interdisciplinary aspects of my project raise several difficulties, the first ones being linked to the nature of the studied source material, the shells. Indeed, the production of clean decontaminated powders is a particularly time-consuming process, even with the help of a chemistry intern (Adrien Force) who worked with me for a few months. While some species proved to be rather easy to bring to adequate grain fineness (like *V. verrucosa*, which only took about three hours), others showed significant hardness (*M. galloprovincialis* powder production took over ten days) and adhesiveness between the grains (*M. gigas* and *V. philippinarum*), making the whole process of powder production of all the samples a long and tedious task. The extraction process was also time-consuming, lasting around 1.5 to 2.5 weeks per species depending on the concentration of the OM in the shell, a parameter that directly influences the viscosity of the decalcified solution. The length of this whole procedure and the average amount of OM in the shell – less than 1%, see Table 3.1 – drastically limits the quantities of substances (AIM and ASM) available for further testing at a time, therefore implying constant extractions throughout the experimental phase of my PhD, and the subsequent design of assays that consume little quantities of material.

5.2.2. Non-Standard Marine Bacterial Strains

The cultivation of marine bacteria is inherently challenging, due to the significant differences between these species and those commonly cultured in lab settings. They require adapted conditions for optimal growth, such as temperature, light settings, hygrometry and the use of specialized growth media (Rodrigues & de Carvalho, 2022). For instance, while both strains of *V. harveyi* and *V. mytili* grow in usual incubators at 28°C, *V. aestuarianus* and *V. tapetis* grow at 20 and 18 ± 2°C respectively, temperatures that could be attained with an AC unit maintaining a fresh room temperature. *A. salmonicida* was more challenging: as it could only grow at 12°C, it required the specific set-up of a cold incubator (separate from a refrigerator, which would have been too cold). Furthermore, even after several rounds of trials and errors, some of these strains grow slowly *in vitro*, ranging from typical 24 hours to 11 days on Petri dishes and macroscopic liquid cultures (initial cultures of around 50 mL), and from 4 hours to 72 hours for microscopic liquid cultures (microplate volumes). Such long-lasting growth phases significantly increase the risk for culture contamination, reinforcing the need for absolutely rigorous sterile-work practices.

Moreover, the unique growth conditions of marine pathogens limited the number of suitable candidates for antibacterial screening methods and necessitated adaptations of the selected techniques. For instance, the disk diffusion method was chosen over well-diffusion due to the insolubility of AIM, and the impossibility to mix psychrophilic bacteria with hot agar during plate pouring. As a result, I had no option but to use the traditional spread plate method, which added an extra step in preparing Petri dishes and increased the risk of contamination. This approach complicated the reading of inhibition zones, as the thin layer of bacteria was less visible compared to full-thickness colonization of agar. Additionally, disk diffusion assays present another drawback: the diameter of the inhibition zone is not solely dependent on the antibacterial capacity of the tested substance but is also influenced by the diffusibility of the antibacterial compounds through the agar medium. Highly diffusible compounds may produce larger inhibition zones even if they do not necessarily exert stronger antibacterial capacities, while less diffusible yet potentially more effective compounds might show smaller inhibition zones (Massoud *et al.*, 2020). This limit, inherent to the agar medium, is one of the reasons that antibacterial screenings are performed in successive steps. Consequently, in this study, the secondary microdilution assay brings a more accurate assessment of antibacterial capacity of my extracts, although it can only be applied to ASMs.

Marine agar and broth were the only media suitable for growing these bacteria; however, their cloudy yellow appearance challenged the reading of inhibition zones during disk-diffusion assays and optical density measurements during microdilution tests. I was however able to overcome this medium limit and accurately measure inhibition zone diameters – supported by valid negative and positive controls – by using tailored lighting and background settings. I would recommend testing contrasting agents compatible with Vibrionaceae for further experimentations of this type. Including red phenol to microdilution assays as a colored pH indicator allowed for the precise monitoring of bacterial metabolism changes, but the determination of the right indicator and concentration required preliminary testing. Furthermore, the polyanionic composition of bivalve shell soluble OM induced a decrease in pH of the solutions used for the microdilution assay, resulting in a spontaneous color change prior to the addition of any bacteria, thereby compromising assay accuracy. Consequently, this restricted the tested concentrations of ASMs to a maximum of 100 µg/mL.

In addition to the difficulties brought by culture media, the unconventional nature of these marine targets implies that established standards are neither currently available for inhibition zones diameters (*i.e.*, susceptibility breakpoints), nor for microdilution growth tests. Consequently, the experimental design for these protocols relied solely on trial and error, involving multiple test rounds of cultures and several intermediate experiments to assess the best parameters and substances to use in each circumstance.

5.2.3. Other Technical Bottlenecks

Another challenging element to the experimental part of my PhD research was the fact that my lab, although well equipped for standard microbiology experiments, lacked some specific facilities for my peculiar cultures. Consequently, we had to adapt them and buy some appropriate consumables. Furthermore, none of my colleagues had prior knowledge on marine bacteria cultivation: with the help of my supervisor, I collaborated with experts in the field (Dr. Christine Paillard and Dr. Adeline Bidault from UBO; Dr. Olivier Chesneau from Pasteur Institute) and managed to train for the right techniques and skills to ensure proper handling of such strains. Owing to the exploratory nature of my research for my lab, every bacterial experiment and assay was performed by hand, with the assistance of my colleague Marie Da Silva Feliciano (Assistant Engineer, CNRS, one-year temporary contract). Even with her participation, the lack of automation limited the volume of tries and replicates performed, the number and frequency of timepoints readings for microdilution assays, and increased potential human handling errors. Moreover, for this assay, the spectrophotometer was distant from the incubator: this implies “incubation pause” bias, as the cultures were frequently removed from their ideal growing environment throughout the total duration of the assay. In order to limit this bias, a minimum intercalated time of 30 minutes was set, reducing the number of timepoints in the fastest growing bacteria.

5.2.4. Proteomics on Non-Model Organisms

The conducted proteomic analysis also faced limitations, the major one being the fact that this kind of analysis takes as a reference a list of peptides that are already known and registered in databases. This means that entirely novel peptides may pass through and may not be detected. In addition to that, other limitations and biases may exist: peptides/proteins in very low quantities in complex mixtures may be overshadowed by the predominant ones. Furthermore, the enzymatic digestion used the standard trypsin as cleaving enzyme (cleavage

downstream from Arginine and Lysine). This may induce complete cleavage of basic sequences and produce very short fragments, ultimately single amino acids, not taken in account by the subsequent analysis. On the opposite, some long peptides may not be well ionized and consequently do not “fly” correctly during spectrometric analysis, inducing an under-representation (Marin, 2020). Similarly, glycosylated peptides cannot be accurately determined. At last, we performed a qualitative rather than quantitative proteomic analysis. Qualitative proteomics, although far less expensive, are based on the presence/absence of a given peptide but do not indicate its proportions in the mixture. Consequently, results must be interpreted cautiously: for example, potential threshold effects due to a given AMPP, or dose-dependent combinations of AMPPs engaged in synergetic actions cannot be apprehended.

5.3. Antibacterial Screening

The data obtained from both antibacterial screening assays, disk-diffusion and microdilution, are summarized in Table 5.1 hereafter, covering positive and negative results from Chapter 3 and Chapter 4 respectively.

5.3.1. Comparison of the Results Depending on Bacteria

When looking at Table 5.1, the first observation that comes to mind is the difference in growth response depending on bacteria. Indeed, *A. salmonicida* and *V. harveyi* ORM4 show the highest sensitivity to bivalve extracts, while the other strains are only affected by one or two AIMs. This difference in bacterial response motivated the selection of the microbial targets to be included in the research paper in section 3.4. The reasons for such dissimilarities can be multiple, but we can hypothesize putative causes related to differences in anatomical features, behavior and metabolism.

For instance, these marine bacteria can be discriminated by the presence of specific pathogenic factors and immune evasion strategies. For instance, in *A. salmonicida*, two original versions of chitin-active lytic polysaccharide monooxygenases (LPMO) have been indicated to play a role in this specie’s virulence against Atlantic salmon. They are crucial for effective proliferation in the bloodstream during initial infection process, and regulate proteome adaptation to the host immune system (Skåne *et al.*, 2022).

Table 5.1: Summary table of the antibacterial assays for all bacteria and mollusks. The results of the microdilution assay (M) are represented in blue, the shape depending on the affected growth parameter. Upper triangle: maximum growth rate alteration; lower triangle: carrying capacity alteration; full rectangle: alteration of both parameters. Dark blue: significant alteration; light blue: non-significant but visible alteration. Dark grey areas indicate non-applicable combinations of fractions and tests. The results of the disk-diffusion assay (D) are represented in green, increasing numbers of (+) represent increase in growth inhibition. O: presence of “crowns” of diffusible compounds at the periphery of the inhibition zone; *: inhibition “artificially” non-significant (see argument in section 4.1).

		<i>A.salmonicida</i>		<i>V. aestuarianus</i>		<i>V. harveyi</i> ORM4		<i>V. harveyi</i> LMG7890		<i>V. mytili</i>		<i>V. tapetis</i> CECT4600	
		D	M	D	M	D	M	D	M	D	M	D	M
<i>G. glycymeris</i>	Powder		Dark grey		Dark grey	+	Dark grey		Dark grey		Dark grey		Dark grey
	AIM		Dark grey		Dark grey	⊕	Dark grey		Dark grey		Dark grey		Dark grey
	ASM>10 kDa												
	1<ASM<10 kDa												
<i>M. galloprovincialis</i>	Powder		Dark grey		Dark grey	+	Dark grey		Dark grey		Dark grey		Dark grey
	AIM		Dark grey		Dark grey	+	Dark grey		Dark grey		Dark grey		Dark grey
	ASM>10 kDa		Dark blue										
	3<ASM<10 kDa		Light blue										
	1<ASM<3 kDa												
<i>M. gigas</i>	Powder		Dark grey		Dark grey		Dark grey		Dark grey		Dark grey		Dark grey
	AIM	+	Dark grey	+	Dark grey	+++	Dark grey		Dark grey	+*	Dark grey	+	Dark grey
	ASM>10 kDa		Dark blue			++	Dark blue		Dark blue				
	1<ASM<10 kDa		Light blue			+	Light blue		Light blue				
<i>P. maximus</i>	Powder		Dark grey		Dark grey		Dark grey		Dark grey		Dark grey		Dark grey
	AIM	+	Dark grey		Dark grey	+++	Dark grey		Dark grey	+*	Dark grey	+	Dark grey
	ASM>10 kDa		Dark blue			++	Dark blue		Dark blue				
	1<ASM<10 kDa		Light blue				Light blue		Light blue				
<i>C. edule</i>	Powder		Dark grey		Dark grey	+	Dark grey		Dark grey		Dark grey		Dark grey
	AIM	++	Dark grey		Dark grey	⊕	Dark grey		Dark grey		Dark grey		Dark grey
	ASM>10 kDa												
	1<ASM<10 kDa												
<i>V. philippinarum</i>	Powder		Dark grey		Dark grey		Dark grey		Dark grey		Dark grey		Dark grey
	AIM		Dark grey		Dark grey	+++	Dark grey		Dark grey		Dark grey		Dark grey
	ASM>10 kDa												
	3<ASM<10 kDa												
	1<ASM<3 kDa												
<i>V. verrucosa</i>	Powder		Dark grey		Dark grey		Dark grey		Dark grey		Dark grey		Dark grey
	AIM		Dark grey		Dark grey	⊕	Dark grey		Dark grey		Dark grey		Dark grey
	ASM>10 kDa												
	1<ASM<10 kDa												

V. harveyi has been shown to strongly decrease PO activity in gills, which is a defense mechanism against host response (Jiang *et al.*, 2013; Pichon *et al.*, 2013). An interesting discrepancy between both strains of this specie is observed: ORM4, the “natural” highly pathogenic strain, shows susceptibility to most extracts, while LMG7890, often described as “non-pathogenic” is only significantly inhibited in the presence of two ASMs (Pichon *et al.*, 2013). In addition to this result, it has been shown that ORM4 possesses defense mechanisms that LMG7890 does not have, almost always resulting in the destruction of the later by phagocytosis and ROS damage. Indeed, ORM4 deploys an impressive arsenal for immune evasion: the gene Lux0 is a regulator for Quorum Sensing (QS), a system of ExoCellular Products (ECP) and autoinducer signaling molecules which role is to assess the neighboring environment and bacterial density. QS is essential in biofilm formation through the production of ExoPolySaccharide (EPS) matrix, coordinated expression of proteins and toxins and provides high mobility capacities to individual cells. The sequencing of ORM4 genome also revealed the presence of the full gene set coding for Type III Secretion System (T3SS) and its regulator ExsA, which deletion proved their essential role in killing abalone hosts. T3SS is a peculiar secretion system acting like a needle, capable of injecting proteins and macromolecules directly in eukaryotic cells cytoplasm (Boyle *et al.*, 2015; Zhang *et al.*, 2020; Morot *et al.*, 2021). Another differing element between both strains was identified in a study by Travers *et al.*, (2009): ORM4 is able to delay the inactivation of p38 MAPK pathway in abalone hemocytes, preventing further hemocyte recruitment and subsequent phagocytosis and toxic ROS production. This strategy allows ORM4 to perform “pure” targeted immune evasion, without compromising hemocytes viability (Pichon *et al.*, 2013). The combination of QS, T3SS and p38 MAPK pathway delaying capacities could be at the origin of the remarkable ability of ORM4 to quickly develop antibiotic resistance (MIC sometimes 250 times higher) and hemolytic activity observed in aquaculture settings (Jiang *et al.*, 2013).

V. aestuarianus also exhibits specific defense and virulence mechanisms. For instance, the production of ECP such as metalloprotease Vam plays a role in immune evasion by inhibiting hemocyte activity, reducing their adhesion to bacterial target and subsequent phagocytosis. The sequencing of *V. aestuarianus* genome identified the gene VarS, which deletion showed its crucial engagement in pathogenicity regulation (Destoumieux-Garzón *et al.*, 2020).

V. tapetis core genome (shared by all strains of the same species) encodes for a specific form of Type IV Secretion System (T4SS), which is engaged in multiple cellular functions, such as DNA translocation between bacteria or with the environment and dual-direction protein

transport that can be activated in contact to eukaryotic cells. These functions can be easily associated to virulence and immune evasion strategies without making too many assumptions (Dias *et al.*, 2018; Rahmani *et al.*, 2021).

V. mytili is for the moment poorly characterized as it represents a rarely encountered *Vibrio* in diseased bivalves: it has only been isolated from mussels and seems to display distinct genetic and phenotypic features from the other members of this family (Pujalte *et al.*, 1993).

The molecular arsenal and genetic make-up of the targeted strains could bring an explanation of their differences in susceptibility to our extracts, but their metabolism could also play a key role in these differences. Indeed, *V. harveyi* strains are also characterized by their different utilization of sucrose (Nicolas *et al.*, 2002), while *V. aestuarianus* metabolism stands out – though still fermentative – as it lacks acid resistance mechanisms (Tison & Seidler, 1983). This could be a cause for its low susceptibility to the tested bivalve extracts.

The higher susceptibility observed among species described as more virulent and better armed against their hosts seems, at first sight, counter intuitive. However, it could have a quite reasonable ecological explanation. The Red Queen Theory states that co-evolutionary dynamics among detrimental relationships like the ones of host-parasites, are characterized by reciprocal adaptations, *i.e.*, in order to survive, the host bivalve will develop parades against a frequently encountered aggressive pathogen (Decaestecker & King, 2019). This is further encouraged by the putative association between toxicity and antibiotic resistance among Vibrionaceae (Nakayama *et al.*, 2006). In this viewpoint, the distinct susceptibility of *V. harveyi* ORM4 to our extracts appears logical, knowing that this strain is dominant in mortality events among abalones and bivalves (Nicolas *et al.*, 2002). Furthermore, *V. harveyi* represents, along with *A. salmonicida*, the only species of this panel that possess multiple flagella and high motility capacities. While higher mobility and proliferating capacity seem to bring these two pathogens together, it is important to keep in mind that *A. salmonicida*'s pathogenicity has only been associated to Atlantic salmon (Kashulin & Sørum, 2014). This could be attributed to pure evolutionary and structural convergence in AMPP production, but one could propose to review this bacterium's assumed host specificity. The adaptation of bivalve shell antibacterial abilities to their pathogens remains a hypothesis to discuss: *V. aestuarianus* is a particularly virulent oyster pathogen, inducing high mortality rates in aquaculture and while its only susceptibility is observed with *M. gigas* AIM, it shows no response to any other extract (Tison & Seidler, 1983).

As exposed above, discrepancies in proteome and defense strategies could be linked to the observed relationships between bivalve extracts and bacterial targets. Further sequencing is needed to extensively compare genomes and bacterial structures and functions that could play a role in resistance and susceptibility to our substances (Fukui & Sawabe, 2007; Zupičić *et al.*, 2024).

5.3.2. Comparison of the Results Depending on Bivalves

In our assays, *M. gigas* and *P. maximus* represent the two models showing the most overall effects against all bacterial targets. When compared together, they exhibit relatively similar positive results: the alteration induced by their ASMs coincide against the same bacterial targets; the alterations induced by AIMs are almost identical. Indeed, they systematically show the same signatures: very small, peculiar inhibition zones were observed (on average 0.6 mm around the tablets), except against *V. harveyi* ORM4 where they induce wider inhibition. This relative similarity may suggest that the two species contain similar, or similar cocktails of AMPPs, which is coherent with the detected AMPP proteomes in Table 3.6. From a phylogenetic viewpoint, it is interesting to note that *P. maximus* and *M. gigas* are relatively close compared to the other species studied here according to certain phylogenetic reconstitutions (Taylor *et al.*, 1973; Waller, 1980; Cope, 1995; Morton, 1995). In particular, the phylogenetic tree presented by Taylor *et al.*, (1973) gives major importance to microstructures. Coincidentally, these two species are the only representatives of foliated calcite bearing bivalves among our models. One can thus hypothesize that the similarities of microstructures constrain the systems into similarities in AMPPs content and effects. This seducing hypothesis however has to be nuanced: the bivalve phylogenies proposed here above are not entirely consensual, as some other ones place the two species evolutionarily far from each other (Ponder *et al.*, 2020).

The AIM of *C. edule* shows the widest inhibition on *A. salmonicida*, and contains an unusual set of AMPPs including buforin, H3 and lysozyme, which might explain such effects. Coincidentally, extracts from the soft tissues of *C. edule* have been found to exert a broad antimicrobial activity against both terrestrial and marine Gram-positive and Gram-negative bacteria (Defer *et al.*, 2009). It is interesting to notice that our experimental results are congruent with these findings.

Another interesting point is that the AIM of *C. edule* shares with that of two other species - *G. glycymeris* and *V. verrucosa* - a peculiar effect on *V. harveyi* ORM4 in the presence of whitish crowns at the border of the inhibition zone (Fig. 3.3). The reason for the presence of these halos is unknown but could be due to diffusible factors triggering specific responses of ORM4. As discussed in section 3.4, and rather unexpectedly, AIMs contain diffusible compounds in spite of the overall high insolubility of this extract (Lutet-Toti *et al.*, 2025, *submitted to STOTEN*). These three bivalves were the only ones to display inhibition of ORM4 growth around their whole shell powder tablets: this original result indicates that the antibacterial compounds at play here are either present in sufficient amounts among the OM in crude shells, or exerting particularly strong antibacterial effects, and that their occlusion in CaCO₃ structures is not limiting said effects. Considering the amounts of OM in the total shell weight of these species (between 0.07 and 0.21 %, see Table 3.3), the hypothesis of a substance with notably strong antibacterial effects can be favored. Moreover, the non-limiting aspect of CaCO₃ on this property places these bivalves as interesting candidates for easy and affordable use of crude shell powders as antibacterials.

M. galloprovincialis is the only species to inhibit both growth parameters of *A. salmonicida* during the microdilution assay, despite only altering the growth of two bacterial targets overall. Specifically, the higher molecular weight ASMs reduce both the carrying capacity and maximum growth rate of *A. salmonicida*, suggesting a complex interference with multiple bacterial processes involved in proliferation and environmental colonization. Furthermore, the other alteration by *M. galloprovincialis* (against *V. harveyi* ORM4) shows a distinct result from all the other bivalves: among all AIMs, *M. galloprovincialis* shows the smallest inhibition zone with differences in diameter ranging from 0.39 to 1 cm (Fig. 3.3). This singularity is further observed in the results of the proteomic analysis. Indeed, this bivalve stands out by its high number of identified AMPPs overall and by their exclusivity: 7 out of the 34 identified are not detected among the other models. The unique and scarce inhibitory effects of *M. galloprovincialis* against our bacterial targets would be linked to its ecological relationship with Vibrionaceae family. As a matter of fact, the role of *Vibrio* in fatal mussel diseases remains unclear, and their observed proportions in the mussel microbiome are significantly lower than those found in oysters (Charles *et al.*, 2020; Destoumieux-Garzón *et al.*, 2020). Referring back to the Red Queen associated hypothesis developed earlier, the weak response of bacterial targets and the composition of *M. galloprovincialis*' antimicrobial proteome could be explained by the fact that these bacteria might not represent major pathogens

for the Mediterranean mussel. Consequently, *M. galloprovincialis* may have developed an AMPP arsenal adapted to other microorganisms that were not tested here.

Three species of bivalves – *G. glycymeris*, *V. verrucosa* and *V. philippinarum* - only showed inhibitory effects against *V. harveyi* OMR4 in one fraction, the AIM. Such a limited result can be correlated to peculiar AMPP signal for *V. philippinarum*: it represents the bivalve with the least number of identified AMPPs (12), most of it in its smallest soluble fraction ($1 < \text{ASM} < 3$ kDa). Interestingly, the only biologically active extract (AIM) did not show any AMPP correspondence. This proves that a lack of identified signal does not equate a lack of AMPP in extracts, but rather the absence of corresponding proteins and peptides in the database used for the proteomic analysis (see section [5.2. Limitations](#)).

5.3.3. Antimicrobial Shellome Exploration by Proteomic Analysis

Several types of AMPPs were identified in the shell extracts of our bivalve models, using an extensive AMP database of more than 3 000 entries. The results are difficult to interpret, as no clear and unambiguous signature of unique AMPPs or AMPP combinations across species stands out. However, some patterns emerge, suggesting potential links with biological reality (Table 3.6).

First, one can note the presence of some AMPPs among nearly every bivalve model: cgUbiquitin, H4 and to a lesser extent, other histones. These do not come as surprises, as they are active in a wide array of functions in innate immunity systems and were first isolated from mollusks soft tissues (Kawasaki & Iwamuro, 2008; Sathyan *et al.*, 2012). The identified AMPPs can be categorized into four groups depending on their mode of antibacterial action:

- 1) direct action to destroy or incapacitate the microorganism target;
- 2) immunomodulation of the immune response by signaling, chemotaxis or communicating and recruiting hemocytes;
- 3) dual mode, acting directly against the intruder while participating in immunomodulation;
- 4) multifunctional activity, including wound healing, endotoxin neutralization, angiogenesis modulation and anticancer activity (Wang, 2014; Talapko *et al.*, 2022). The repartition of specific functions and their combination can be used to try and understand the potential proteomic cause of antibacterial effects in our extracts.

For instance, every one of the four previously identified “active” bivalve species expresses AMPPs identified with the signature of Glyceraldehyde 3-phosphate dehydrogenase (GAPDH), a thermo-stable enzyme which can disrupt the membranes of microorganisms or act on IntraCellular (IC) targets exerting an overall bacteriostatic ability (Seo *et al.*, 2014; Branco *et al.*, 2018). In the same manner, the broadly observed cgUbiquitin would confer typical Ubiquitin properties to the shell OM, tagging exogenous particles and playing a central role in innate immunity. Histone-derived peptides are represented in combinations across all bivalves. They are essential in innate immune systems and exhibit dual modes of action: firstly, immunomodulation by interacting with hemocytes and with each other - especially H2B, which interacts with every other histone – and secondly, direct destruction and incapacitation of microorganisms by membrane disruption or DNA binding (Kawasaki & Iwamuro, 2008; Y. Li *et al.*, 2024; Muñoz-Camargo & Cruz, 2024). The lysozyme, a membrane hydrolyzing enzyme, is also detected in our antibacterial shell fractions. While the identification of these AMPPs can inform us on the potent antibacterial mechanisms at play, their rather equal distribution does not allow for a complete discrimination solely based on antibacterial mode of action. Indeed, as stated earlier, *M. galloprovincialis* seems to be the only model producing particular AMPPs that exert unique mechanisms against bacteria. For instance, Psoriasin activates the p38 MAPK pathway, which is essential in hemocyte production of ROS and cytokins (initial phase of the innate immune response, see section 2.1.4. Molecular Defenses) (Zheng *et al.*, 2008). Apl-AvBD-2 is a big defensin, central AMPP in invertebrate immunity which disrupts bacterial membranes, forms aggregates and produces nanonets (Gerdol *et al.*, 2012). The presence of Filaggrin-2 in mussel extracts further encourages the hypothesis of high rates of interactions between AMPPs (Diamond *et al.*, 2009).

Although the nuclear origin of some AMPPs (mainly histone-derived) is widely distributed, the overall cellular origin of identified AMPPs is not that uniform among bivalve models. The shell extracts of *M. gigas* – model exhibiting the most antibacterial activities – match with AMPPs that are mainly associated with Anura models (frogs and toads) where they are produced as glandular secretion in mucus, a process that could very well be applicable in bivalve mollusks (Park *et al.*, 2000; Roshanak *et al.*, 2023). *P. maximus* extracts, although similar to *M. gigas* in bioactivity, differ in the putative cellular origin of its AMPPs: the majority is produced by immune cells. For its part, *M. galloprovincialis* joins *M. gigas* in seemingly producing AMPPs linked to glandular secretions in other clades of the animal kingdom, with the addition of a number produced in epithelial tissues. *C. edule*, on the other hand, largely keeps the production of its identified AMPPs in the nucleus, with exceptions for the glandular

secretion-associated Buforin and Lysozyme with ubiquitous production and distribution (Ragland & Criss, 2017; H. Li *et al.*, 2019).

While the presence of epithelium originated or secreted AMPPs in the shells of bivalves aligns with the global understanding of shell formation (the mantle secretes CaCO₃ and OM that remains occluded in the mineralized shell, see section [2.2. The Bivalve Shell](#)), the occurrence of AMPPs derived from nuclear compounds (*i.e.*, histones) raises interrogations. I propose the following hypothesis for the mechanism by which AMPPs of nuclear origin are incorporated into bivalve shells: Histone-derived AMPPs are small, highly basic macromolecules because of their high proportion in lysine and arginine residues. These AMPPs are typically tightly packed against genetic material, reflecting the chromatin-condensing function of histones. In contrast, the OM cocktail is very acidic because of its high acid aspartic content. When precursors for OM molecules(mRNA) are formed, they could potentially form electrostatic interactions (weak bonds) with histone-derived AMPPs. As these precursors are translocated from the nucleus, further the cell and transported towards the biomineralization front, they might “capture” and carry along histone-derived AMPPs, incorporating them into the OM of the bivalve shell.

The results of our proteomic analysis are promising as they seem to suggest that some specific combinations of AMPPs could be linked to observed antibacterial activity. However, one has to remain cautious in the interpretation of these results, as they stem from a qualitative approach, overlooking the identified AMPPs proportions in the extracts (see [5.2. Limitations](#)). In addition, the structure of the AMP database used for this analysis – although quite substantial in numbers – is unbalanced with an underrepresentation of molluscan sources. The addition of the data in Table 2.1: “Inventory of AMPPs identified in mollusk soft tissues and secretions”, could very well add substantial information to our proteomic analysis and a better discrimination between bivalve models.

5.3.4. Nature and Mechanism of the Antibacterial Natural Extracts

As a secondary screening method, microdilution assays are designed to elucidate the antibacterial mechanisms of the tested substances. Several ASMs were found to induce distinct alterations in growth parameters, specifically impacting the maximum growth rate and carrying capacity of target bacteria (Table 3.4). For instance, both extracts from *M. gigas* specifically altered maximum growth rates, while *P. maximus* demonstrated less specificity, affecting either growth parameters or even both simultaneously in the case of *A. salmonicida*. Regarding this

last case, it is interesting to note that different MICs could be measured for the significant alteration of each parameter (carrying capacity: 0.41 $\mu\text{g/mL}$; maximum growth rate: 100 $\mu\text{g/mL}$). This difference implies that achieving simultaneous inhibition requires adjusting the MIC to the higher value. Such simultaneous inhibition was also observed with the high molecular weight ASMs of *M. galloprovincialis*, this time with relatively small values of MIC (0.41 $\mu\text{g/mL}$). Instances of simultaneous inhibition indicate a complex interaction with bacterial functions, biological processes and structures.

From the bacterial perspective, both strains of *V. harveyi* sustained decreases in maximum growth rate during microdilution assays, but only ORM4 showed wide inhibition zones in with AIM and ASM during disk diffusion assays. *A. salmonicida* displayed variable responses, showing alterations in either one or both growth parameters in microdilution tests. Overall, the results regarding the effects of ASMs on *V. harveyi* ORM4 align across both assay methods, with the exception of one extract of *P. maximus* ($1 < \text{ASM} < 10$ kDa), which showed a non-significant alteration of the maximum growth rate in microdilution assays but that did not inhibit growth during the disk diffusion assay. Furthermore, microdilution tests revealed additional ASM alterations on *A. salmonicida* and LMG compared to disk diffusion results, particularly for *M. galloprovincialis* and both *P. maximus* and *M. gigas* extracts. This suggests that microdilution assays can serve effectively as a detection tool in addition to their primary characterization purpose. In this study, this supplementary detection addresses a limitation associated with the somewhat arbitrary quantity of ASM applied to blotting paper disks (see section [3.2.1. Initial Screening](#)), making microdilution assays a crucial complement to the initial screening method.

Among both assays, the observation that the extracts primarily limit bacterial growth rather than killing them, along with the presence of well-known bacteriostatic AMPPs such as GAPDH, suggests that the identified extracts may be bacteriostatic, *i.e.*, inhibiting bacterial growth and limiting proliferative metabolism, placing them in a stasis-like state that can be reversed upon removal of the bioactive agent (Rudilla *et al.*, 2018). However, the absence of clear plateau in bacterial population and the fact that some MIC values are equal to the maximum concentration of ASM used in microdilution assays implies that the extracts could also be bactericidal and that the MBC may simply not yet have been reached during our screening (see section [3.4.4. Discussion](#); Lutet-Toti *et al.*, 2025, *submitted to STOTEN*).

Overall, the results from antibacterial screening and proteomic analysis exist within a complex framework of putative combined effects, with many ambiguous areas inherent to the exploratory nature of this research project. At this stage of antibacterial shellome exploration,

it is not possible to determine the specific mechanism of action or the particular AMPPs – or combination of AMPPs – contributing to the antibacterial properties evidenced *in vitro*. However, *M. gigas* and *P. maximus* stand out due to their broader and stronger inhibition of bacterial growth, particularly against strains like *A. salmonicida* and *V. harveyi* ORM4. These findings could also provide valuable insights to take into account in the phylogeny of bivalves, although they may simply reflect evolutionary convergence. Nonetheless, these results come as important leads for further testing, which I elaborate on in the following section on Perspectives.

5.4. Perspectives

5.4.1. Further Characterizations and Experimentations

In the short term, the enhancement of the proteomic analysis can be achieved by creating a true database specific to mollusks AMPPs. This database may be updated automatically by using appropriate filters, namely molluscan families, the tissue from which the AMPPs are isolated, and their functions or targets. The list of AMPPs isolated from mollusk soft tissues in Table 2.1 is a starting point to this project. Another improvement of the proteomic investigation would consist in the identification of new AMPPs among the raw transcriptome data of newly sequenced mollusks, adding to the overall AMPPs database. Adding molluscan AMPPs could significantly change the distribution and combination patterns that seem to currently appear among our models. This could also help identifying the AMPPs present in the shells of the Veneridae family, where a big cocktail of molecules might be overlooked for the moment.

To address the limitation of ASM concentration in microdilution assays, purification of our extracts can be achieved through preparative ion-exchange chromatography using an anionic resin. This method focuses on concentrating positively charged molecules, which are typically basic and include most AMPPs. By discarding the acidic components of our extracts, we concentrate our extracts in AMPPs and can consequently test higher concentrations, an advantage for potentially “diluted” active molecules. Additionally, increasing the throughput of the microdilution assays by the use of automated and/or integrated spectrophotometers and incubators can greatly improve efficiency and accuracy. Indeed, the accuracy and detailing of bacterial growth curves are positively correlated to the number of time points for optical density readings. Moreover, avoiding the transfers of microplates from one machine to another also reduces handling risks, contaminations and potential “incubation pause” effects that I discussed earlier in section 5.2. Limitations.

In light of the results obtained through the initial and secondary steps of the antibacterial screening, in terms of bacterial *in vitro* ideal growth conditions and actual growth inhibition by the tested substances, I can propose further antibacterial susceptibility methods to better characterize those responses. One effective approach is subculturing, which can be quickly and easily implemented as it does not require additional equipment. By taking the bacterial suspension from a well after a microdilution assay and culturing it under ideal conditions, we can assess whether the bacteria can grow despite prior exposure to tested substances. The restart of bacterial growth indicates the bacteriostatic nature of the antibacterial agent (Cushnie *et al.*, 2020). Additionally, a TLC-bioautography (either direct or indirect) would be quite helpful in quickly localizing the bioactive compounds of bivalve extracts: this method involves the prior migration and separation of macromolecules based on their polarity and affinity to the TLC support, followed by incubation to reveal potential inhibition zones around specific compounds. TLC-bioautography thus offers a cost-effective and rapid means to purify our extracts. However, one significant limitation of this technique is that the different diffusibilities of certain substances may restrict its effectiveness, potentially impacting the identification of all active compounds (Valgas *et al.*, 2007; Balouiri *et al.*, 2016). It is also unable to reveal synergetic effects and may need to be complemented by other screening techniques due to the high likelihood that our substances exhibit combined effects, as discussed earlier in sections 5.3.3 and 5.3.4 (Massoud *et al.*, 2020). Another screening technique that can be quickly set up is the time-kill method, especially suited for the detection of potential synergetic or antagonistic effects, as well as determining whether a substance is bactericidal or bacteriostatic. This method involves monitoring bacterial growth similarly to microdilution assays, but it differs in that this monitoring should begin before the addition of the potentially antibacterial substance. This allows for observation of the bacterial direct response to its addition and subsequent effects. The results are based on the comparison of growth before and after addition of the tested substance, indicating either bacterial death or growth inhibition when positive. This technique is often paired with automation strategies, as its accuracy greatly relies on the direct monitoring of absorbance upon addition of the tested substance (Balouiri *et al.*, 2016). Additionally, subculturing can be quickly implemented to further assess bacterial viability, just like after a microdilution assay.

By focusing on promising extracts, such as those from *M. gigas*, *P. maximus*, and *C. edule*, we could perform in-depth analysis of the OM composition, notably by using one- or two-dimensional gels based on molecular weight or isoelectric point (Marin, 2003). This approach would allow the precise separation of peptides and proteins in bands and spots on

gels, which could be subsequently sampled for “purified” proteomic studies and bioassays. Indeed, once macromolecules are isolated from these spots, they can be sequenced and identified, allowing us to explore their putative functions through initial BLAST analysis. Following this, we can reconstruct their 3D structures to uncover potential new functions in addition to their already known activities. The ultimate step involves the chemical synthesis of small peptides. Alternatively, for longer peptides, one can think of *in vitro* overexpression in eukaryotic systems (yeast cells, insect cells) via genetic engineering. These synthesized peptides could then be utilized in *in vitro* bioassays as pure peptides. However, while testing pure compounds might ease the interpretation of its effects, this technique overlooks putative synergetic activity between some AMPPs.

Further focusing on the puzzling similarities of bioactivity signature of *M. gigas* and *P. maximus*, it would be interesting to develop tests exploring the putative correlation between microstructures and antibacterial properties. For instance, by measuring colonization rates on shell pieces with different microstructures. Indeed, is it merely coincidental that the two most active bivalve models are the only ones featuring foliated calcite? This question remains open, as the identification of specific OMs associated to microstructures is still a distant goal due to the high rates of complexity and variability.

So far, we have only tested proteins and peptides, but other molecules may also play a role in antimicrobial properties of bivalves. Sugars like chitin or chitin-derived soluble oligosaccharides make up good candidates for antibacterial screening, as some AMPPs have been identified in cuttlebone chitosan (Table 2.1) (Hajji *et al.*, 2015; Shanmugam *et al.*, 2016). A well-established connection has been documented between chitin and the colonization capacities of *Vibrio* species (Yu *et al.*, 1991), particularly with respect to the two most pathogenic strains tested here, *Vibrio harveyi* and *A. salmonicida*. In the case of *A. salmonicida*, these components are involved in immune evasion, as discussed in section 3.1, (Skåne *et al.*, 2022); while *V. harveyi* mostly utilizes them for attachment (Yu *et al.*, 1991; Pruzzo *et al.*, 2005). Therefore, it would be interesting to investigate the presence of antimicrobial compounds in relation to the amount of chitin in the shells, although effectively quantifying chitin is significantly challenging.

Other types of molecules that might also encompass AM (AntiMicrobial) activity are pigments (*e.g.*, *O. vulgaris* ommochrome extract in Table 2.1, Esparza-Espinoza *et al.*, 2021). During my PhD, I happened to collaborate on the extraction of pigments from fossil shells (Polacchi *et al.*, *submitted to Methods in Ecology and Evolution*) but did not extend the experimentation to potential AM effects.

5.4.2. Applications against Marine Pathogens

The rise of antibiotic resistance has prompted a growing interest in the discovery and development of new AMPs, especially from natural resources. This area of research is particularly relevant given the persistent environmental challenges posed by antibiotic residues, which have now even been detected in coastal soils (Griffin *et al.*, 2019). As traditional antibiotics become less effective, exploring alternative antimicrobial agents, such as AMPs, is essential for addressing this critical public health concern.

Research on AMP is part of a broader initiative to develop alternatives and effective treatments in response to the aforementioned challenges posed by antibiotic resistance. Several promising types of AMPs are emerging in this context: for instance, quorum-quenching enzymes disrupt the quorum sensing system – which is essential for immune evasion, coordinated action and biofilm formation (see section 5.3.1) – and have been proposed as viable alternatives to traditional antibiotics (Rémy *et al.*, 2016). Antibiofilm peptides also represent a promising strategy for combating infections caused by resistant bacteria. Furthermore, the immunomodulatory effects of AMPs and their underlying mechanisms are gaining attention as researchers seek to understand how these compounds can enhance host defenses (Pletzer & Hancock, 2016).

The applied focus of my doctoral research aligns well with this context, as I am bioprospecting an abundant and promising natural resource for antibacterial molecules. This project integrates itself in an effort to establish a circular economy, with potential applications in aquaculture, food safety, environment conservation, human health and heritage conservation.

5.4.2.1. Aquaculture Applications

Diseases in marine and oceanic environments are currently on the rise, influenced by factors such as climate change, pollution, global trade, excessive antibiotic use and other anthropogenic factors (Burge *et al.*, 2014; Ward & Lafferty, 2004). The widespread application of antibiotics in aquaculture is particularly concerning: reports indicate that over 73% of major aquaculture-producing nations utilize oxytetracycline, florfenicol, and sulphadiazine, while 55% use erythromycin, amoxicillin, sulphadimethoxine, and enrofloxacin (Lulijwa *et al.*, 2020; Schar *et al.*, 2020). As a consequence, antibiotic resistance is increasing in fish aquaculture, accelerating the frequency of mass mortality events and endangering the stability of the industry (Schar *et al.*, 2021; Caputo *et al.*, 2023). Moreover, marine pathogens like some *Vibrio* tend to thrive in warmer waters and accommodate quickly to increase sea surface temperature, developing higher motility and other factors of virulence (Vezzulli *et al.*, 2012; Morot *et al.*,

2021). As discussed earlier in this manuscript (see section [1.3. Molluscan Aquaculture](#)), several types of treatments are used in aquaculture (Kunselman *et al.*, 2024). However, naturally sourced AMPs remain the most promising candidates in terms of efficacy and reduction of subsequent pollution of wild environments (Cole *et al.*, 1997; Pan *et al.*, 2007; Lu *et al.*, 2011).

The bivalve extracts that I investigated here – especially insoluble fractions that exhibit strong inhibitory effects - could be applied in aquaculture settings. Indeed, they are endogenous to this environment and showed efficacy against prominent pathogens of this industry. One could imagine applications as granules/microgranules mixed with fish food for example, or as suspensions on bivalve installations (closed basins or open sea). While *in vitro* disk diffusion assays often validate *in vivo* efficacy, further research is necessary to assess the passage and availability of these antibacterial molecules within the digestive and circulatory systems of treated animals (Balouiri *et al.*, 2016).

5.4.2.2. Food Safety

Ensuring the safety of seafood products is crucial, especially regarding the consumption of bivalves that may harbor harmful pathogens or toxins (see section [1.3.3. Threats and Limitations of Conchyliculture](#)). Infected bivalves can indeed transmit pathogens such as *Vibrio* and viruses to humans, potentially leading to severe health issues. Additionally, some marine microorganisms produce dangerous toxins that accumulate in mollusk tissues and can cause severe gastrointestinal affections and neurological disorders to consumers (Arnich *et al.*, 2021). Therefore, the application of our bivalve extracts into food preservation strategies could enhance the safety and shelf-life of seafood products. The non-cytotoxicity of these extracts would of course, have to be assessed first.

5.4.3. Applications Targeting Other Microorganisms

5.4.3.1. Environmental Applications

Eutrophication is a growing environmental concern that affects aquatic ecosystems by promoting excessive growth of algae and other microorganisms, leading to oxygen depletion and harm to marine life (Maúre *et al.*, 2021). Some AMPs identified in molluscan soft tissues have been shown to have antimicrobial activity against microalgae (Defer *et al.*, 2009). It would be interesting to test our shell extracts against these microorganisms, as the application of these substances to natural environments would not come as additional pollution when mitigating algal blooms.

5.4.3.2. *Endolithic Bacteria*

Endolithic bacteria are perforating microorganisms that participate to the bioerosion of carbonated geomaterials and cause problems in heritage conservation by “eating away” statues and monuments. Preliminary observations of euendolithic bacteria being incapable of colonizing bivalve shells compared to other carbonates (Irina Bundeleva, Dijon, *personal communication*) indicate that certain molluscan shells might inhibit the growth and burrowing activity of these microorganisms. Some attempts to culture these bacteria were made during my PhD, but I faced several limitations: these are particularly slow growing (several weeks of culture) and challenging bacteria. Although the experimentation on these bacteria could not go further, valuable information was gathered regarding their laboratory culture conditions and potential future experiments. Understanding these conditions could pave the way for applications in art and monument conservation, in the form of pastes or sprays of shell OM fractions.

5.4.3.3. *Human Pathogens*

Beyond the risks for food security and general public health associated with seafood diseases, there are concerns regarding the transmission of antibiotic resistance from aquatic environments to human pathogens (Ina-Salwany *et al.*, 2019). While addressing food security is essential, it is also important to consider whether positive results observed with *Vibrio* species could extend to other *Vibrio* strains that are known human pathogens. This reflection invites to explore the mechanisms of action and biological similarities among *Vibrio* species, including their defense mechanisms, resistance development, and sensitivity patterns. For instance, *Vibrio cholerae*, a well-known severe human pathogen, has shown susceptibility to mussel hemocytes activity (Canesi *et al.*, 2016). This highlights the need for further investigation into the potential applications of AMPPs against human *Vibrio* pathogens, particularly those derived from molluscan body parts and secretions traditionally used in medicine (Summer *et al.*, 2020).

5.5. Conclusion

My doctoral research project demonstrates a wide interdisciplinarity approach, spanning across multiple scientific disciplines and methodologies. This interdisciplinarity is visible throughout the chapters of this manuscript: art history, ethnobiology and ethnomedicine biomineralization, molecular biology, bioinformatics, and microbiology.

During this PhD, I had the opportunity to present my work six times: 4 through poster presentations, and 2 as a speaker. I published one paper as a first author, and one as a second author as part of a research collaboration. I have submitted as first author a research paper that is part of Chapter 3, and have submitted as first author of a literature review that is part of Chapter 1. Another collaborative paper has been submitted as second author (see Section 6.2). The two research collaborations that I participated in (L. Polacchi in 2022 and S. Nahle in 2023) represented opportunities to use the extraction methods developed in other applications (pigments) than antibacterial settings and to test other biological properties of the shells (osteogenesis induction with nacre powder). Several entities are involved in this PhD project: under the international cotutelle of the Università di Bologna (Italy) and the Université de Bourgogne Europe (France), it is mainly funded by the University of Bologna in the frame of the international PhD program FishMed-PhD “Innovative Technologies and Sustainable Use of Mediterranean Sea Fishery and Biological Resources”. Additional research funds were obtained from Association des Femmes Françaises Diplômées de l’Université (AFFDU), Société Française de Biologie des Tissus Minéralisés (SFBTM) and Arthritis Foundation, MAELSTROM and MAELSTROM-bis projects (les MATricEs coquiLLières bacTéRicides au secOURS des géoMatériaux) from TELLUS-INTERRVIE program (CNRS, France), PRELUDE project (Peptides antimicrobiens dEs coquiLles de mollUsques D’intérêt Economique) financed by Observatoire des Sciences de l’Univers (OSU) Theta (Besançon, France). Finally, I benefitted from an Erasmus + fellowship for my three months stay in Amsterdam.

My PhD research focused on the antibacterial screening of the shells of bivalves of economic interest, applied to marine Vibrionaceae pathogen and complemented by an antimicrobial proteomic exploration. I was able to develop innovative protocols in order to fully test the organic matrices of these shells and unveil the antibacterial capacities of several bivalves. The Pacific cupped oyster *Magallana gigas* and the giant scallop *Pecten maximus* stand out as particularly active against pathogens, while the common cockle *Cerastoderma edule* exhibits the most inhibition against one strain, *Aliivibrio salmonicida*. With *Vibrio*

harveyi ORM4, these strains represent at the same time the most virulent and the most sensitive bacteria of the target panel. I hypothesize that this observed pattern stems from the arms race between pathogens and their hosts, aligning with the Red Queen Theory.

Further experimentations are required to elucidate the bacteriostatic or bactericidal mechanism of bivalve shell extracts, such as bioautography or time-kill kinetics. Altogether, and despite some inconclusive results, this PhD project opens new perspectives in experimenting on marine bacteria and bioprospecting of natural resources. By characterizing two kinds of unconventional subjects - marine bacteria and bivalve shells - for the performed experiments, I aim to establish useful standards for future explorations involving these organisms.

5.6. Chapter References

- Arnich, N., Abadie, E., Amzil, Z., Dechraoui Bottein, M.-Y., Comte, K., Chaix, E., Delcourt, N., Hort, V., Mattei, C., Molgó, J., and Le Garrec, R. (2021). Guidance Level for Brevetoxins in French Shellfish. *Marine Drugs*, 19(9), Article 9. <https://doi.org/10.3390/md19090520>
- Balouiri, M., Sadiki, M., and Ibsouda, S. K. (2016). Methods for *in vitro* evaluating antimicrobial activity: A review. *Journal of Pharmaceutical Analysis*, 6(2), 71–79. <https://doi.org/10.1016/j.jpha.2015.11.005>
- Boyle, K. E., Monaco, H., Ditmarsch, D. van, Deforet, M., and Xavier, J. B. (2015). Integration of Metabolic and Quorum Sensing Signals Governing the Decision to Cooperate in a Bacterial Social Trait. *PLoS Computational Biology*, 11(6), e1004279. <https://doi.org/10.1371/journal.pcbi.1004279>
- Branco, P., Albergaria, H., Arneborg, N., and Prista, C. (2018). Effect of GAPDH-derived antimicrobial peptides on sensitive yeasts cells: Membrane permeability, intracellular pH and H⁺-influx/-efflux rates. *FEMS Yeast Research*, 18(3), foy030. <https://doi.org/10.1093/femsyr/foy030>
- Burge, C. A., Eakin, C. M., Friedman, C. S., Froelich, B., Hershberger, P. K., Hofmann, E. E., Petes, L. E., Prager, K. C., Weil, E., Willis, B. L., Ford, S. E., and Harvell, C. D. (2014). Climate Change Influences on Marine Infectious Diseases: Implications for Management and Society. *Annual Review of Marine Science*, 6(Volume 6, 2014), 249–277. <https://doi.org/10.1146/annurev-marine-010213-135029>
- Canesi, L., Grande, C., Pezzati, E., Balbi, T., Vezzulli, L., and Pruzzo, C. (2016). Killing of *Vibrio cholerae* and *Escherichia coli* Strains Carrying D-mannose-sensitive Ligands by *Mytilus* Hemocytes is Promoted by a Multifunctional Hemolymph Serum Protein. *Microbial Ecology*, 72(4), 759–762. <https://doi.org/10.1007/s00248-016-0757-1>
- Caputo, A., Bondad-Reantaso, M. G., Karunasagar, I., Hao, B., Gaunt, P., Verner-Jeffreys, D., Fridman, S., and Dorado-Garcia, A. (2023). Antimicrobial resistance in aquaculture: A global analysis of literature and national action plans. *Reviews in Aquaculture*, 15(2), 568–578. <https://doi.org/10.1111/raq.12741>
- Charles, M., Bernard, I., Villalba, A., Oden, E., Burioli, E. A. V., Allain, G., Trancart, S., Bouchart, V., and Houssin, M. (2020). High mortality of mussels in northern Brittany – Evaluation of the involvement of pathogens, pathological conditions and pollutants. *Journal of Invertebrate Pathology*, 170, 107308. <https://doi.org/10.1016/j.jip.2019.107308>
- Cole, A. M., Weis, P., and Diamond, G. (1997). Isolation and characterization of pleurocidin, an antimicrobial peptide in the skin secretions of winter flounder. *The Journal of Biological Chemistry*, 272(18), 12008–12013. <https://doi.org/10.1074/jbc.272.18.12008>
- Cope, J. C. W. (1995). The early evolution of the Bivalvia. In: J. D. Taylor (Ed.), *Origin and Evolutionary Radiation of the Mollusca*. Oxford University Press. <https://doi.org/10.1093/oso/9780198549802.003.0030>
- Cushnie, T. P. T., Cushnie, B., Echeverría, J., Fowsantear, W., Thammawat, S., Dodgson, J. L. A., Law, S., and Clow, S. M. (2020). Bioprospecting for Antibacterial Drugs: A Multidisciplinary Perspective on Natural Product Source Material, Bioassay Selection and Avoidable Pitfalls. *Pharmaceutical Research*, 37(7), 125. <https://doi.org/10.1007/s11095-020-02849-1>
- Decaestecker, E., and King, K. (2019). Red Queen Dynamics. In: B. Fath (Ed.), *Encyclopedia of Ecology* (Second Edition) (pp. 185–192). Elsevier. <https://doi.org/10.1016/B978-0-12-409548-9.10550-0>
- Defer, D., Bourgougnon, N., and Fleury, Y. (2009). Screening for antibacterial and antiviral activities in three bivalve and two gastropod marine molluscs. *Aquaculture*, 293(1), 1–7. <https://doi.org/10.1016/j.aquaculture.2009.03.047>
- Destoumieux-Garzón, D., Canesi, L., Oyanedel, D., Travers, M.-A., Charrière, G., Pruzzo, C., Vezzulli, L., Oyanedel, D., Travers, M.-A., Charrière, G., Pruzzo, C., and Vezzulli, L. (2020). *Vibrio*-bivalve interactions in health and disease. *Environmental Microbiology*, 22(10), 4323–4341. <https://doi.org/10.1111/1462-2920.15055>
- Diamond, G., Beckloff, N., Weinberg, A., and Kisich, K. O. (2009). The Roles of Antimicrobial Peptides in Innate Host Defense. *Current Pharmaceutical Design*, 15(21), 2377. <https://doi.org/10.2174/138161209788682325>
- Dias, G. M., Bidault, A., Le Chevalier, P., Choquet, G., Der Sarkissian, C., Orlando, L., Medigue, C., Barbe, V., Mangenot, S., Thompson, C. C., Thompson, F. L., Jacq, A., Pichereau, V., and Paillard, C. (2018). *Vibrio tapetis* Displays an Original Type IV Secretion System in Strains Pathogenic for Bivalve Molluscs. *Frontiers in Microbiology*, 9. <https://doi.org/10.3389/fmicb.2018.00227>
- Esparza-Espinoza, D. M., Plascencia-Jatomea, M., López-Saiz, C. M., Parra-Vergara, N. V., Carbonell-Barrachina, A. A., Cárdenas-López, J., and Ezquerro-Brauer, J. M. (2021). Improving the shelf life of chicken burgers using *Octopus vulgaris* and *Dosidicus gigas* skin pigment extracts. *Food Science and Technology*, 42, e18221. <https://doi.org/10.1590/fst.18221>
- Fukui, Y., and Sawabe, T. (2007). Improved One-step Colony PCR Detection of *Vibrio harveyi*. *Microbes and Environments*, 22(1), 1–10. <https://doi.org/10.1264/jsme2.22.1>

- Gerdol, M., De Moro, G., Manfrin, C., Venier, P., and Pallavicini, A. (2012). Big defensins and mytimacins, new AMP families of the Mediterranean mussel *Mytilus galloprovincialis*. *Developmental and Comparative Immunology*, 36(2), 390–399. <https://doi.org/10.1016/j.dci.2011.08.003>
- Griffin, D. W., Benzel, W. M., Fisher, S. C., Focazio, M. J., Iwanowicz, L. R., Loftin, K. A., Reilly, T. J., and Jones, D. K. (2019). The presence of antibiotic resistance genes in coastal soil and sediment samples from the eastern seaboard of the USA. *Environmental Monitoring and Assessment*, 191(Suppl 2), 300. <https://doi.org/10.1007/s10661-019-7426-z>
- Hajji, S., Younes, I., Rinaudo, M., Jellouli, K., and Nasri, M. (2015). Characterization and *in vitro* Evaluation of Cytotoxicity, Antimicrobial and Antioxidant Activities of Chitosans Extracted from Three Different Marine Sources. *Applied Biochemistry and Biotechnology*, 177(1), 18–35. <https://doi.org/10.1007/s12010-015-1724-x>
- Ina-Salwany, M. Y., Al-saari, N., Mohamad, A., Mursidi, F.-A., Mohd-Aris, A., Amal, M. N. A., Kasai, H., Mino, S., Sawabe, T., and Zamri-Saad, M. (2019). Vibriosis in Fish: A Review on Disease Development and Prevention. *Journal of Aquatic Animal Health*, 31(1), 3–22. <https://doi.org/10.1002/aah.10045>
- Jiang, Q., Shi, L., Ke, C., You, W., and Zhao, J. (2013). Identification and characterization of *Vibrio harveyi* associated with diseased abalone *Haliotis diversicolor*. *Diseases of Aquatic Organisms*, 103(2), 133–139. <https://doi.org/10.3354/dao02572>
- Kashulin, A., and Sørum, H. (2014). A novel *in vivo* model for rapid evaluation of *Aliivibrio salmonicida* infectivity in Atlantic salmon. *Aquaculture*, 420–421, 112–118. <https://doi.org/10.1016/j.aquaculture.2013.10.025>
- Kawasaki, H., and Iwamuro, S. (2008). Potential roles of histones in host defense as antimicrobial agents. *Infectious Disorders Drug Targets*, 8(3), 195–205. <https://doi.org/10.2174/1871526510808030195>
- Kunselman, E., Wiggin, K., Diner, R. E., Gilbert, J. A., and Allard, S. M. (2024). Microbial threats and sustainable solutions for molluscan aquaculture. *Sustainable Microbiology*, 1(1), qvae002. <https://doi.org/10.1093/sumbio/qvae002>
- Li, H., X, W., J, Y., R, Z., Q, Z., and J, Y. (2019). The bacteriolytic mechanism of an invertebrate-type lysozyme from mollusk *Octopus ocellatus*. *Fish and Shellfish Immunology*, 93. <https://doi.org/10.1016/j.fsi.2019.07.060>
- Li, Y., Ma, T., Jiang, J., Hahn, M., and Yin, Y. (2024). The dynamics and functional mechanisms of H2B mono-ubiquitination. *Crop Health*, 2(1), 1. <https://doi.org/10.1007/s44297-023-00022-9>
- Lu, X. J., Chen, J., Huang, Z. A., Shi, Y. H., and Lv, J. N. (2011). Identification and characterization of a novel cathelicidin from ayu, *Plecoglossus altivelis*. *Fish and Shellfish Immunology*, 31(1), 52–57. <https://doi.org/10.1016/j.fsi.2011.03.005>
- Lulijwa, R., Rupia, E. J., and Alfaro, A. C. (2020). Antibiotic use in aquaculture, policies and regulation, health and environmental risks: A review of the top 15 major producers. *Reviews in Aquaculture*, 12(2), 640–663. <https://doi.org/10.1111/raq.12344>
- Lutet-Toti, C., Da Silva Feliciano, M., Thomas, J., Crosland, A., Develay, C., Debrosse, N., Force, A., Bidault, A., Broussard, C., Falini, G., Goffredo, S., and Marin, F. (2025). Do bivalve shells exhibit antibacterial properties? Screening calcifying organic matrices against two major marine pathogens. *Science of the TOTAL Environment (STOTEN)*, submitted.
- Marin, F. (2003). Molluscan Shell Matrix Characterization by Preparative SDS-PAGE. *The Scientific World Journal*, 3, 342–347. <https://doi.org/10.1100/tsw.2003.30>
- Marin, F. (2020). Mollusc shellomes: Past, present and future. *Journal of Structural Biology*, 212(1), 107583. <https://doi.org/10.1016/j.jsb.2020.107583>
- Massoud, R., Saffari, H., Massoud, A., and Moteian, M. (2020). Screening methods for assessment of antibacterial activity in nature. Conference Paper, 4th Int. Conf. on Applied Research in Science and Engineering, 11p.
- Maúre, E. de R., Terauchi, G., Ishizaka, J., Clinton, N., and DeWitt, M. (2021). Globally consistent assessment of coastal eutrophication. *Nature Communications*, 12(1), 6142. <https://doi.org/10.1038/s41467-021-26391-9>
- Morot, A., El Fekih, S., Bidault, A., Le Ferrand, A., Jouault, A., Kavousi, J., Bazire, A., Pichereau, V., Dufour, A., Paillard, C., and Delavat, F. (2021). Virulence of *Vibrio harveyi* ORM4 towards the European abalone *Haliotis tuberculata* involves both quorum sensing and a type III secretion system. *Environmental Microbiology*, 23(9), 5273–5288. <https://doi.org/10.1111/1462-2920.15592>
- Morton, B. (1995). The evolutionary history of the bivalvia. In: J. D. Taylor (Ed.), Origin and Evolutionary Radiation of the Mollusca. Oxford University Press. <https://doi.org/10.1093/oso/9780198549802.003.0029>
- Muñoz-Camargo, C., and Cruz, J. C. (2024). From inside to outside: Exploring extracellular antimicrobial histone-derived peptides as multi-talented molecules. *The Journal of Antibiotics*, 77(9), 553–568. <https://doi.org/10.1038/s41429-024-00744-0>

- Nakayama, T., Ito, E., Nomura, N., Nomura, N., and Matsumura, M. (2006). Comparison of *Vibrio harveyi* strains isolated from shrimp farms and from culture collection in terms of toxicity and antibiotic resistance. *FEMS Microbiology Letters*, 258(2), 194–199. <https://doi.org/10.1111/j.1574-6968.2006.00225.x>
- Nicolas, J. L., Basuyaux, O., Mazurié, J., and Thébault, A. (2002). *Vibrio carchariae*, a pathogen of the abalone *Haliotis tuberculata*. *Diseases of Aquatic Organisms*, 50(1), 35–43. <https://doi.org/10.3354/dao050035>
- Pan, C.-Y., Chen, J.-Y., Cheng, Y.-S. E., Chen, C.-Y., Ni, I.-H., Sheen, J.-F., Pan, Y.-L., and Kuo, C.-M. (2007). Gene expression and localization of the epinecidin-I antimicrobial peptide in the grouper (*Epinephelus coioides*), and its role in protecting fish against pathogenic infection. *DNA and Cell Biology*, 26(6), 403–413. <https://doi.org/10.1089/dna.2006.0564>
- Park, C. B., Yi, K.-S., Matsuzaki, K., Kim, M. S., and Kim, S. C. (2000). Structure–activity analysis of buforin II, a histone H2A-derived antimicrobial peptide: The proline hinge is responsible for the cell-penetrating ability of buforin II. *Proceedings of the National Academy of Sciences of the United States of America*, 97(15), 8245. <https://doi.org/10.1073/pnas.150518097>
- Pichon, D., Cudennec, B., Huchette, S., Djediat, C., Renault, T., Paillard, C., and Auzoux-Bordenave, S. (2013). Characterization of abalone *Haliotis tuberculata*–*Vibrio harveyi* interactions in gill primary cultures. *Cytotechnology*, 65(5), 759. <https://doi.org/10.1007/s10616-013-9583-1>
- Pletzer, D., and Hancock, R. E. W. (2016). Antibiofilm Peptides: Potential as Broad-Spectrum Agents. *Journal of Bacteriology*, 198(19), 2572–2578. <https://doi.org/10.1128/JB.00017-16>
- Polacchi, L., Lutet-Toti, C., Basuyaux, O., Guériau, P., Albéric, M., Pasco, H., Merle, D., Habermeyer, B., Guilard, R., Thoury, M., & Marin, F. (2025). Innovative coupling of non-standard 1D-electrophoresis with luminescence spectral imaging to decipher invisible biochromes in modern and fossil shells. *Methods in Ecology and Evolution*, submitted.
- Ponder, W. F., Lindberg, D. R., and Ponder, J. M. (2020). Biology and Evolution of the Mollusca, Volume 2. *CRC Press, Taylor and Francis Group*.
- Pruzzo, C., Huq, A., Colwell, R. R., and Donelli, G. (2005). Pathogenic *Vibrio* Species in the Marine and Estuarine Environment. In: S. Belkin and R. R. Colwell (Eds.), *Oceans and Health: Pathogens in the Marine Environment* (pp. 217–252). *Springer US*. https://doi.org/10.1007/0-387-23709-7_9
- Pujalte, M.-J., Ortigosa, M., Urdaci, M.-C., Garay, E., and Grimont, P. A. D. (1993). *Vibrio mytili* sp. Nov., from Mussels. *International Journal of Systematic and Evolutionary Microbiology*, 43(2), 358–362. <https://doi.org/10.1099/00207713-43-2-358>
- Ragland, S. A., and Criss, A. K. (2017). From bacterial killing to immune modulation: Recent insights into the functions of lysozyme. *PLoS Pathogens*, 13(9), e1006512. <https://doi.org/10.1371/journal.ppat.1006512>
- Rahmani, A., Delavat, F., Lambert, C., Le Goic, N., Dabas, E., Paillard, C., and Pichereau, V. (2021). Implication of the Type IV Secretion System in the Pathogenicity of *Vibrio tapetis*, the Etiological Agent of Brown Ring Disease Affecting the Manila Clam *Ruditapes philippinarum*. *Frontiers in Cellular and Infection Microbiology*, 11, 634427. <https://doi.org/10.3389/fcimb.2021.634427>
- Rémy, B., Plener, L., Elias, M., Daudé, D., and Chabrière, E. (2016). Des enzymes pour bloquer la communication bactérienne, une alternative aux antibiotiques ? *Annales Pharmaceutiques Françaises*, 74(6), 413–420. <https://doi.org/10.1016/j.pharma.2016.06.005>
- Rodrigues, C. J. C., and de Carvalho, C. C. C. R. (2022). Cultivating marine bacteria under laboratory conditions: Overcoming the “unculturable” dogma. *Frontiers in Bioengineering and Biotechnology*, 10. <https://www.frontiersin.org/articles/10.3389/fbioe.2022.964589>
- Roshanak, S., Yarabbi, H., Shahidi, F., Tabatabaei Yazdi, F., Movaffagh, J., and Javadmanesh, A. (2023). Effects of adding poly-histidine tag on stability, antimicrobial activity and safety of recombinant buforin I expressed in periplasmic space of *Escherichia coli*. *Scientific Reports*, 13(1), 5508. <https://doi.org/10.1038/s41598-023-32782-3>
- Rudilla, H., Merlos, A., Sans-Serramitjana, E., Fusté, E., Sierra, J. M., Zalacaín, A., Vinuesa, T., and Viñas, M. (2018). New and old tools to evaluate new antimicrobial peptides. *AIMS Microbiology*, 4(3), 522–540. <https://doi.org/10.3934/microbiol.2018.3.522>
- Sathyan, N., Philip, R., Chaithanya, E. R., and Anil Kumar, P. R. (2012). Identification and Molecular Characterization of Molluskin, a Histone-H2A-Derived Antimicrobial Peptide from Molluscs. *ISRN Molecular Biology*, 2012, 219656. <https://doi.org/10.5402/2012/219656>
- Schar, D., Klein, E. Y., Laxminarayan, R., Gilbert, M., and Van Boeckel, T. P. (2020). Global trends in antimicrobial use in aquaculture. *Scientific Reports*, 10(1), 21878. <https://doi.org/10.1038/s41598-020-78849-3>
- Schar, D., Zhao, C., Wang, Y., Larsson, D. G. J., Gilbert, M., and Van Boeckel, T. P. (2021). Twenty-year trends in antimicrobial resistance from aquaculture and fisheries in Asia. *Nature Communications*, 12(1), 5384. <https://doi.org/10.1038/s41467-021-25655-8>

- Seo, J.-K., Lee, M. J., Go, H.-J., Kim, Y. J., and Park, N. G. (2014). Antimicrobial function of the GAPDH-related antimicrobial peptide in the skin of skipjack tuna, *Katsuwonus pelamis*. *Fish and Shellfish Immunology*, 36(2), 571–581. <https://doi.org/10.1016/j.fsi.2014.01.003>
- Shanmugam, A., Kathiresan, K., and Nayak, L. (2016). Preparation, characterization and antibacterial activity of chitosan and phosphorylated chitosan from cuttlebone of *Sepia kobeensis* (Hoyle, 1885). *Biotechnology Reports*, 9, 25–30. <https://doi.org/10.1016/j.btre.2015.10.007>
- Skåne, A., Edvardsen, P. K., Cordara, G., Loose, J. S. M., Leitl, K. D., Kregel, U., Sørum, H., Askarian, F., and Vaaje-Kolstad, G. (2022). Chitinolytic enzymes contribute to the pathogenicity of *Aliivibrio salmonicida* LFI1238 in the invasive phase of cold-water vibriosis. *BMC Microbiology*, 22, 194. <https://doi.org/10.1186/s12866-022-02590-2>
- Summer, K., Browne, J., Liu, L., and Benkendorff, K. (2020). Molluscan Compounds Provide Drug Leads for the Treatment and Prevention of Respiratory Disease. *Marine Drugs*, 18(11), Article 11. <https://doi.org/10.3390/md18110570>
- Talapko, J., Meštrović, T., Juzbašić, M., Tomas, M., Erić, S., Aleksijević, L. H., Bekić, S., Schwarz, D., Matić, S., Neuberg, M., and Škrlec, I. (2022). Antimicrobial Peptides—Mechanisms of Action, Antimicrobial Effects and Clinical Applications. *Antibiotics*, 11(10), 1417. <https://doi.org/10.3390/antibiotics11101417>
- Taylor, J. D., Taylor, J. D., and Kennedy, W. J. (1973). The shell structure and mineralogy of the Bivalvia. II. Lucinacea-Clavagellacea conclusions. *Bulletin of the British Museum (Natural History) Zoology*, 22, 253–294. <https://doi.org/10.5962/p.314199>
- Tison, D. L., and Seidler, R. J. (1983). *Vibrio aestuarianus*: A New Species from Estuarine Waters and Shellfish†. *International Journal of Systematic and Evolutionary Microbiology*, 33(4), 699–702. <https://doi.org/10.1099/00207713-33-4-699>
- Travers, M.-A., Le Bouffant, R., Friedman, C. S., Buzin, F., Cougard, B., Huchette, S., Koken, M., and Paillard, C. (2009). Pathogenic *Vibrio harveyi*, in contrast to non-pathogenic strains, intervenes with the p38 MAPK pathway to avoid an abalone haemocyte immune response. *Journal of Cellular Biochemistry*, 106(1), 152–160. <https://doi.org/10.1002/jcb.21990>
- Valgas, C., Souza, S. M. de, Smânia, E. F. A., and Smânia Jr., A. (2007). Screening methods to determine antibacterial activity of natural products. *Brazilian Journal of Microbiology*, 38, 369–380. <https://doi.org/10.1590/S1517-83822007000200034>
- Vezzulli, L., Brettar, I., Pezzati, E., Reid, P. C., Colwell, R. R., Höfle, M. G., and Pruzzo, C. (2012). Long-term effects of ocean warming on the prokaryotic community: Evidence from the vibrios. *The ISME Journal*, 6(1), 21–30. <https://doi.org/10.1038/ismej.2011.89>
- Waller, T. R. (1980). Scanning electron microscopy of shell and mantle in the order Arcoida (Mollusca: Bivalvia). *Smithsonian Libraries*. <http://repository.si.edu/xmlui/handle/10088/5283>
- Wang, G. (2014). Human Antimicrobial Peptides and Proteins. *Pharmaceuticals*, 7(5), 545. <https://doi.org/10.3390/ph7050545>
- Ward, J. R., and Lafferty, K. D. (2004). The Elusive Baseline of Marine Disease: Are Diseases in Ocean Ecosystems Increasing? *PLOS Biology*, 2(4), e120. <https://doi.org/10.1371/journal.pbio.0020120>
- Yu, C., Lee, A. M., Bassler, B. L., and Roseman, S. (1991). Chitin utilization by marine bacteria. A physiological function for bacterial adhesion to immobilized carbohydrates. *Journal of Biological Chemistry*, 266(36), 24260–24267. [https://doi.org/10.1016/S0021-9258\(18\)54223-X](https://doi.org/10.1016/S0021-9258(18)54223-X)
- Zhang, X.-H., He, X., and Austin, B. (2020). *Vibrio harveyi*: A serious pathogen of fish and invertebrates in mariculture. *Marine Life Science and Technology*, 2(3), 231–245. <https://doi.org/10.1007/s42995-020-00037-z>
- Zheng, Y., Niyonsaba, F., Ushio, H., Ikeda, S., Nagaoka, I., Okumura, K., and Ogawa, H. (2008). Microbicidal protein psoriasin is a multifunctional modulator of neutrophil activation. *Immunology*, 124(3), 357. <https://doi.org/10.1111/j.1365-2567.2007.02782.x>
- Zupičić, I. G., Oraić, D., Križanović, K., and Zrnčić, S. (2024). Whole genome sequencing of *Vibrio harveyi* from different sites in the Mediterranean Sea providing data on virulence and antimicrobial resistance genes. *Aquaculture*, 581, 740439. <https://doi.org/10.1016/j.aquaculture.2023.740439>



CHAPTER 6 - ANNEX

6.1. Collaboration Paper with Sarah Nahle: Nacre Application in Biomedical Osteoblastic Mineralization

Marine Biotechnology
<https://doi.org/10.1007/s10126-024-10316-w>

RESEARCH



Organic Matrices of Calcium Carbonate Biominerals Improve Osteoblastic Mineralization

Sarah Nahle¹ · Camille Lutet-Toti^{2,3} · Yuto Namikawa⁴ · Marie-Hélène Piet⁵ · Alice Brion⁶ · Sylvie Peyroche¹ · Michio Suzuki⁴ · Frédéric Marin² · Marthe Rousseau^{1,7}

Received: 20 December 2023 / Accepted: 10 April 2024
 © The Author(s), under exclusive licence to Springer Science+Business Media, LLC, part of Springer Nature 2024

Abstract

Many organisms incorporate inorganic solids into their tissues to improve functional and mechanical properties. The resulting mineralized tissues are called biominerals. Several studies have shown that nacreous biominerals induce osteoblastic extracellular mineralization. Among them, *Pinctada margaritifera* is well known for the ability of its organic matrix to stimulate bone cells. In this context, we aimed to study the effects of shell extracts from three other *Pinctada* species (*Pinctada radiata*, *Pinctada maxima*, and *Pinctada fucata*) on osteoblastic extracellular matrix mineralization, by using an in vitro model of mouse osteoblastic precursor cells (MC3T3-E1). For a better understanding of the *Pinctada*-bone mineralization relationship, we evaluated the effects of 4 other nacreous mollusks that are phylogenetically distant and distinct from the *Pinctada* genus. In addition, we tested 12 non-nacreous mollusks and one extra-group. Biomineral shell powders were prepared, and their organic matrix was partially extracted using ethanol. Firstly, the effect of these powders and extracts was assessed on the viability of MC3T3-E1. Our results indicated that neither the powder nor the ethanol-soluble matrix (ESM) affected cell viability at low concentrations. Then, we evaluated osteoblastic mineralization using Alizarin Red staining and we found a prominent MC3T3-E1 mineralization mainly induced by nacreous biominerals, especially those belonging to the *Pinctada* genus. However, few non-nacreous biominerals were also able to stimulate the extracellular mineralization. Overall, our findings validate the remarkable ability of CaCO₃ biomineral extracts to promote bone mineralization. Nevertheless, further in vitro and in vivo studies are needed to uncover the mechanisms of action of biominerals in bone.

Keywords Biomineral · Nacre · Skeletal matrix · Mineralization · Bone

✉ Marthe Rousseau
marthe.rousseau@univ-st-etienne.fr

¹ Jean Monnet University Saint-Étienne, INSERM, Mines Saint Etienne, SAINBIOSE U1059, Saint-Étienne, France

² Biogeosciences Laboratory, UMR CNRS-EPHE 6282, University of Burgundy, Dijon, France

³ Dipartimento di Chimica “Giacomo Ciamician”, Alma Mater Studiorum Università di Bologna, Bologna, Italy

⁴ Department of Applied Biological Chemistry, Graduate School of Agricultural and Life Sciences, The University of Tokyo, 1-1-1 Yayoi, Bunkyo-ku, Tokyo 113-8657, Japan

⁵ UMR 7365 CNRS-University of Lorraine, Molecular Engineering & Articular Pathophysiology (IMoPA), Vandœuvre-lès-Nancy, France

⁶ Laboratory of Genome Structure and Instability, National Museum of Natural History (MNHN), INSERM, U1154, CNRS UMR7196 Paris, France

⁷ UMR5510 MATEIS, CNRS, University of Lyon, INSA-Lyon, Lyon, France

Introduction

Osteoporosis (OP) is a serious global health concern characterized by an alarming incidence of osteoporosis-related fractures occurring at a frequency of one every 3 s worldwide (Ganesan et al. 2023; Johnell and Kanis 2006). Such a disease is marked by a disruption in the dynamic equilibrium of bone remodeling with reduced bone formation by osteoblasts and increased bone resorption by osteoclasts resulting in weaker bones that are more prone to fracture (Munoz et al. 2020; Riggs et al. 1998).

The existing treatments face major constraints related to their effectiveness as well as their long-term use. One of the most commonly used antiresorptive medications for OP is bisphosphonates, which are effective in reducing fracture risk. However, these treatments, while beneficial, come with limitations, including modest gains in bone density and the potential for rare but severe side effects (Adler et al. 2016).

Published online: 23 April 2024

Springer

In contrast to antiresorptive treatments, anabolic agents work by stimulating bone formation and increasing bone density. Such treatments are exemplified by teriparatide, a synthetic form of parathyroid hormone (PTH), which is the one and only clinically available anabolic reagent approved for the treatment of osteoporosis (Canalis et al. 2007). Teriparatide, when daily administered, has demonstrated high efficacy in improving bone density. Ongoing treatment is required to maintain such benefits which makes the treatment costly (Canalis et al. 2007; Carson and Clarke 2018).

Biominerals, which have garnered attention in the field of bone research, can be defined as minerals produced by living organisms (Carson and Clarke 2018). Mollusks, the second largest phylum of metazoans, have played and continue to play a crucial role in the comprehension of the mechanisms of biomineralization (Evans 2019). Mollusk shells are primarily composed of calcium carbonate in the form of aragonite or calcite (Table 1) or a mix of both polymorphs. Some variations in the arrangement of the crystallites are observed between different species (Marin et al. 2012), in particular in the bivalve class, characterized by an extraordinary diversity of shell microstructures (Taylor et al. 1973).

Many bivalve shells—in particular within the pteriomorphids clade that contains edible mussels and pearl

oysters—are of the “nacro-prismatic” type and exhibit a three-layered structure. The outer layer, called the periostracum, is mostly organic and results from a quinone-tanning process. Ontogenetically speaking, it represents the first shell layer formed by bivalve larvae, and its role is to support the early underlying mineralization and to protect the shell against dissolution. The middle layer is prismatic and made of long needles of calcite, developed perpendicularly or obliquely to the outer shell surface. At last, the inner layer is aragonitic and presents a lustrous aspect; this is nacre also known as mother-of-pearl and the focus of the present study (Hahn et al. 2012). In bivalves, nacre consists of a stack of tiny flat tablets arranged in a brick-wall manner, while, in gastropods and cephalopods, nacre tablets are arranged in columns. Like bone, nacre contains both organic and inorganic components (Marie et al. 2009). Its organic matrix is a mixture of proteins, peptides, glycoproteins, lipids, chitin, and pigments (De Muizon et al. 2022). In their paper, Gonzalez and Vallejo reviewed the historical therapeutic applications of marine mollusk shells in Spanish ethnomedicine (González and Vallejo 2023). They uncovered intricate practices, such as using nacre from seashells for various dermatological purposes, including treating acne, eliminating facial spots through maceration in lemon juice,

Table 1 Biomineral characteristics of selected species

Phyla	Classes	Species name	Common name	Origin	Shell composition	Environment
<i>Mollusca</i>	<i>Bivalve</i>	<i>Pinctada margaritifera</i>	Pearl oyster	Pacific and Indian Oceans	Nacre	Seawater
		<i>Pinctada maxima</i>	South sea pearl oyster	Western Pacific, Australia	Nacre	Seawater
		<i>Pinctada radiata</i>	Gulf pearl oyster	Red Sea, Indian Ocean	Nacre	Seawater
		<i>Pinctada fucata</i>	Akoya pearl oyster	Indo-Pacific, Japan	Nacre	Seawater
		<i>Mytilus galloprovincialis</i>	Mediterranean mussel	Mediterranean, Atlantic	Nacre	Seawater
		<i>Unio pictorum</i>	Painter’s mussel	Europe, Asia	Nacre	Freshwater
		<i>Anodonta cygnea</i>	Swan mussel	Europe, North America	Nacre	Freshwater
		<i>Pecten maximus</i>	Great scallop	European coasts	Calcite	Seawater
		<i>Crassostrea gigas</i>	Pacific oyster	Indo-West Pacific	Calcite	Seawater
		<i>Glycymeris</i>	Bittersweet clam	European coasts	Aragonite	Seawater
		<i>Cerastoderma edule</i>	Common Cockle	European coasts	Aragonite	Seawater
		<i>Venus verrucosa</i>	Warty venus	European coasts	Aragonite	Seawater
		<i>Callista chione</i>	Smooth clam	Mediterranean, Atlantic	Aragonite	Seawater
	<i>Venerupis philippinarum</i>	Manila clam	Global coastlines	Aragonite	Seawater	
	<i>Mercenaria</i>	Northern quahog	North America	Aragonite	Seawater	
	<i>Gastropod</i>	<i>Strombus gigas</i>	Queen conch	Caribbean, Gulf of Mexico	Aragonite	Seawater
		<i>Buccinum undatum</i>	Common whelk	North Atlantic	Aragonite	Seawater
		<i>Haliotis tuberculata</i>	Abalone	Mediterranean, Atlantic	Nacre	Seawater
	<i>Cephalopod</i>	<i>Sepia officinalis</i>	Common cuttlefish	Global oceans	Aragonite	Seawater
<i>Paracentrotus lividus</i>		Purple sea urchin	Mediterranean, Atlantic	Calcite	Seawater	

Information sourced from the Ocean Biodiversity Information System (obis.org)

and dissolving mother-of-pearl buttons in lemon juice or vinegar for addressing skin conditions like chloasma (also called “pregnancy mask”, i.e., pigmentation disorder) and freckles. Additionally, the authors highlighted the traditional remedy of placing small mother-of-pearl buttons under the eyelid for extracting foreign bodies and discussed the potential pharmacological activities of these marine-derived products (González and Vallejo 2023). In addition, nacre demonstrated the capacity of increasing the cell osteogenic activity without exhibiting toxicity (Lopez et al. 1992). This remarkable property led to the hypothesis that nacre might contain elements capable of inducing mineralization and promoting the proper functioning of human bone (Lopez et al. 2004; De Muizon et al. 2022; Westbroek and Marin 1998).

Within nacreous mollusks, the Polynesian pearl oyster *Pinctada margaritifera* has proven having the capacity to induce mineralization in mouse pre-osteoblastic cell line MC3T3-E1 (Brion et al. 2015; Rousseau et al. 2003, 2008). On the other hand, the water-soluble-matrix (WSM) of *Pinctada fucata*, the Japanese “Akoya” pearl oyster, confirmed its efficacy in enhancing osteoblast differentiation (Chaturvedi et al. 2013). Taken together, these findings emphasize the effects of the nacre matrix on bone.

In their review, Zhang et al. (2017) provided a comprehensive overview of the nacre species studied for their effects on bone. However, these studies primarily focused on a few nacreous mollusks, specifically on different species of the *Pinctada* genus; to our knowledge, no studies have investigated the effects of non-nacreous mollusk biominerals on bone regeneration.

Therefore, in the present study, we have broadened the scope by investigating the osteogenic capacity of other nacreous mollusks different from *Pinctada* genus. We cautiously selected species that are taxonomically and geographically distant from *Pinctada* (Fig. 1). To gain a more comprehensive understanding of nacre-bone mineralization relationship, we also investigated the osteogenic capacity of non-nacreous mollusks, including one cephalopod (the cuttlefish) and two gastropods, among which, one nacreous. At last, we also added in the study an extra-group representative, the purple sea urchin. We assessed the effects of all these biominerals on osteoblasts using the pre-osteoblastic MC3T3-E1 cell line.

Material and Methods

Shell Powder Preparation

The source and location of the 20 different skeletons used in this study are indicated in Table 1. Biomineral shell powders were prepared at UMR CNRS 6282 Biogeosciences, Dijon, France, or at the University of Tokyo, Japan. In brief, shells

were scrupulously brushed and, when necessary, their outer surfaces were manually sanded or gently (to avoid heating) abraded with a mini-drill (Dremel-type) equipped either with a 20-mm diameter diamond saw or with a dentist drill. In particular, as indicated in Table 1, for all nacreous mollusks (*Pinctada*, *Mytilus*, *Unio*, *Anodonta*, and *Haliotis*), we took care to obtain a pure nacreous layer devoid of outer prismatic layer. Shells of large size (like *Strombus gigas*) were sliced with a Dremel diamond saw. Shells and shell slices were extensively bleached with sodium hypochlorite NaClO (0.26% v/v active chlorine) for days with several changes of bleaching solution. They were then thoroughly rinsed with deionized water and dried at 37 °C, before being crushed in a jaw crusher (Retsch, model BB 200). The obtained millimetric fragments were subsequently ground in a fine powder in a Pulverisette 2 grinder (Fritsch) equipped with an agate bowl and mortar. The powder was sieved, and the fraction below 200 µm was collected in 50-mL sample pots while the fraction above was ground again until passing through the 200-µm mesh. In total, between 89 g (*Sepia officinalis*) and 469 g (*Strombus gigas*) of clean, size-calibrated powders were obtained and stored at room temperature until use.

Organic Matrix Extraction

Skeletal organic matrices were extracted without a demineralizing process using ethanol following the methodology described by (Brion et al. 2015; De Muizon et al. 2022). 20 g of powders was suspended in absolute ethanol (100%, w/v) containing (0.1%, v/v) hydrochloric acid with continuous stirring for 24 h at 37 °C. Suspensions were centrifuged for 20 min at 1500 g, sterile-filtered through a 0.22-µm filter, and then evaporated for 48 h at 37 °C in an incubator. The resulting ethanol-soluble matrix (ESM) extracts were quantified by weighing on precision balance then dissolved in culture medium to obtain a stock solution of 10-mg/mL concentration. As described by (Zhang et al. 2016), these ESM contain calcium cations as well as carbonate/bicarbonate anions, in addition to soluble organic macromolecules.

Cell Culture

Mice osteoblastic precursor cells (MC3T3-E1) were provided from the European Collection of Cell Cultures (ECACC-99072810). MC3T3-E1 cells were cultured in Minimum Essential Medium Eagle (Sigma-Aldrich M4526) supplemented with (10%, v/v) fetal bovine serum (MP-S00H8), 200 mM L-Glutamine (Sigma-Aldrich G7513), 100 U/mL penicillin, and 100 µg/mL streptomycin (Sigma-Aldrich P4458) at 37 °C in a humidified atmosphere of 5% CO₂. To stimulate the differentiation and the mineralization of the extracellular matrix, cells were cultured with 10 mM β-Glycerophosphate and 50 µg/mL

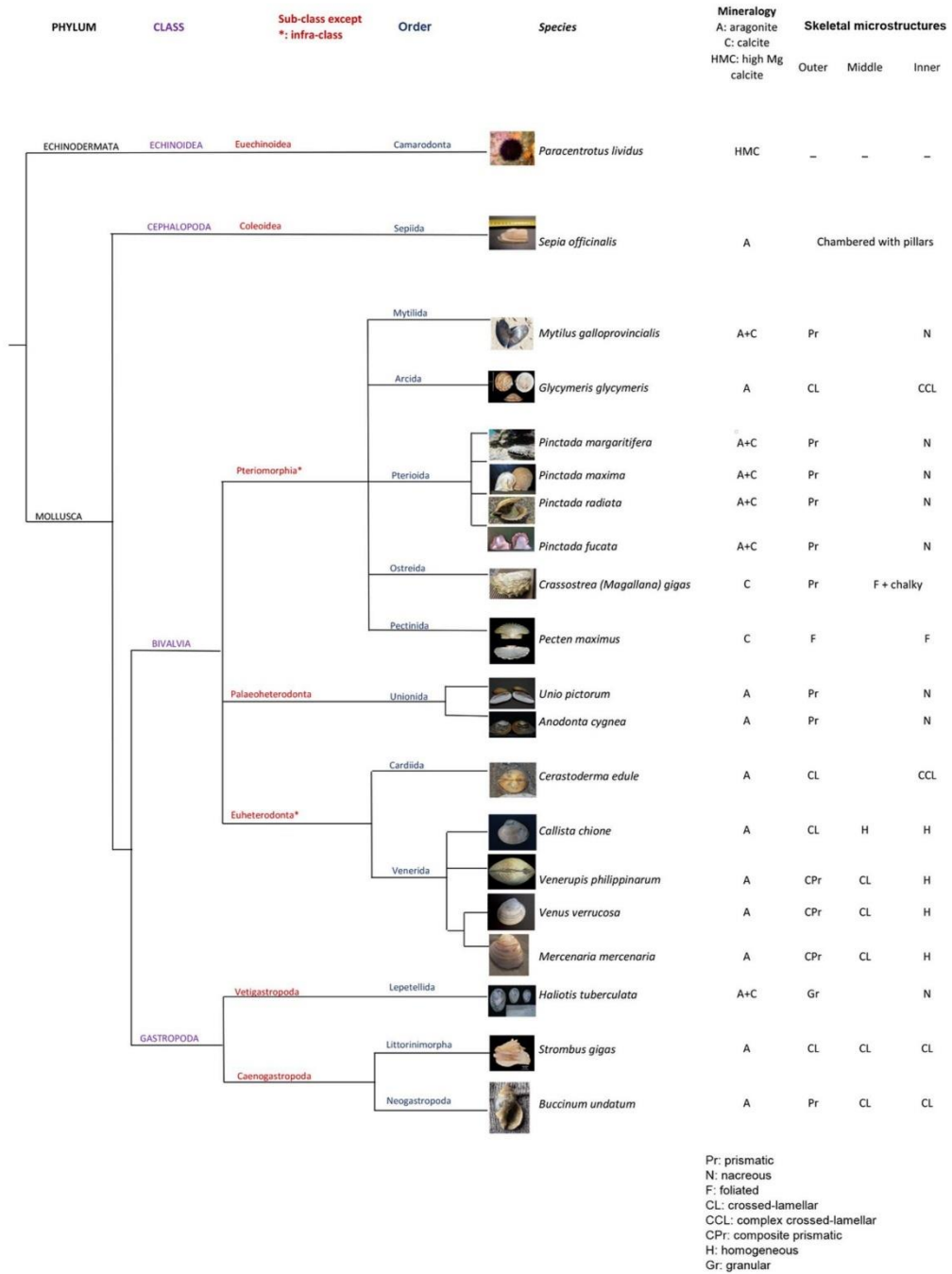


Fig. 1 Evolutionary relationships among selected species. Latin names written in blue correspond to seawater species while freshwater species names are written in black

ascorbic acid. This medium is identified as an osteogenic differentiation medium.

Cell Viability

Cell viability was determined using the 3-(4,5-dimethylthiazol-2yl)-2,5-diphenyltetrazolium bromide assay (MTT; Sigma-Aldrich M5655-1G). Briefly, cells were seeded at a density of 8.2×10^3 cells/well in a 96-well plate and allowed to adhere overnight. Cells were then treated for 24 h with varying concentrations of powder or ESM (100, 500, 1000, 1500, 2000, 2500, 3000, 3500, 4000, 4500, and 5000 $\mu\text{g}/\text{mL}$). Then, 20 μL of MTT solution (5 mg/mL) was added per well in a fresh medium (100 μL), and cells were incubated at 37 °C. After 4 h, the medium was removed, formazan crystals were dissolved by 200 μL of dimethyl sulfoxide (DMSO, Sigma-Aldrich D5879), and the absorbance was measured at 570 nm using a microplate reader TECAN (INFINITE M-PLEX).

Alizarin-Red Staining

Matrix mineralization was assessed by Alizarin-red staining. Cells were treated with 100 $\mu\text{g}/\text{mL}$ of ESM. ESM-treated and non-treated cells were cultured in osteogenic differentiation medium for 7, 14, and 21 days at a density of 2.5×10^4 cells/well in a 48-well plate. Cells were then fixed with 4% paraformaldehyde for 30 min at 4 °C, washed with deionized water, and incubated with 1% (w/v) Alizarin-red solution (Sigma-Aldrich, A5533) for 5 min. Staining was observed

under a light microscope (ZEISS axiovert 4pchl). To quantify Alizarin-red stained nodules, 10% acetic acid was added to the cells and incubated for 30 min at room temperature. Cells were gently scrapped. Lysates were heated at 85 °C for 10 min and centrifuged for 15 min at 4 °C. The supernatant was recovered and treated with 10% of ammonium hydroxide. Subsequently, 150 μL was transferred to a 96 well-plate, and the absorbance representative of mineralized nodule formation was measured at 570 nm.

Results

Shell Powder Viability Assessment on MC3T3-E1 Cells

Prior to any shell powder extraction, we first conducted a comprehensive assessment of their impact on MC3T3-E1 cell viability. This evaluation aimed to determine their potential toxicity. Shell powders were mixed in α -MEM culture medium and subsequently tested on cells at various concentrations. As shown in Fig. 2, five nacre powders (the 4 *Pinctada* and *U. pictorum*) induce a decrease of cell viability from low to high concentrations: this decrease is particularly drastic for *Pinctada radiata* and *Pinctada maxima*, which reaches 58.4% at 2500 $\mu\text{g}/\text{mL}$ and 59.2% at 3500 $\mu\text{g}/\text{mL}$, respectively. Intriguingly, at low concentrations, three nacre powders—that of *Pinctada margaritifera* (between 500 and 1000 $\mu\text{g}/\text{mL}$), of *Unio pictorum* (between 500 and 2000 $\mu\text{g}/\text{mL}$) or of *Haliotis tuberculata* (between 1000 and 2000 $\mu\text{g}/\text{mL}$)—exhibited an enhancement of cell proliferation, with

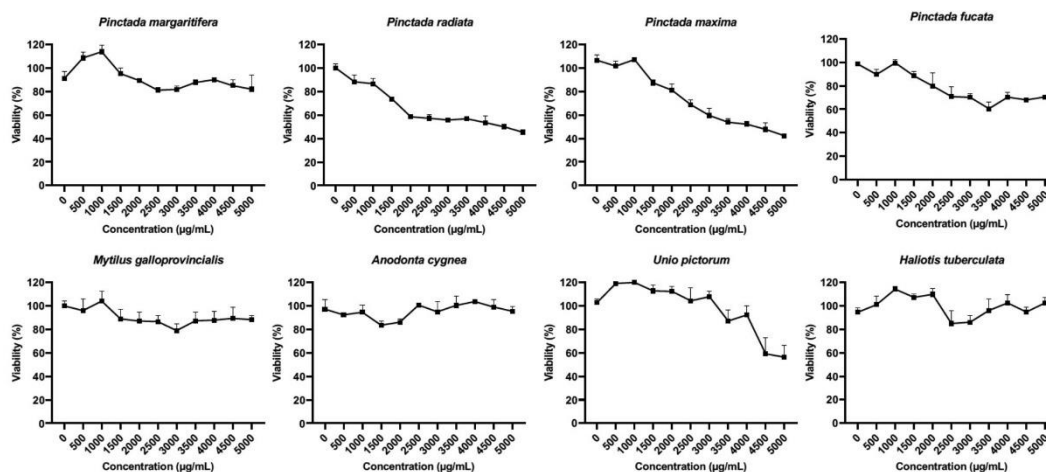


Fig. 2 Effect of shell powder from nacreous species on the viability of MC3T3-E1 cells. Cells were treated with varying concentrations of biomineral shell powder mixed in culture medium α -MEM for 24 h.

Results are standardized to the control group that did not receive any treatment and are represented as the mean \pm SEM of an experiment performed in four replicates

viability reaching approximately 118%. The cell viability induced by *M. galloprovincialis* and *A. cygnea* nares was stable whatever concentration used.

As shown by Fig. 3, the 12 non-nacreous powders—including that of the sea urchin *P. lividus*—did not exert any toxic effect on MC3T3-E1 cells. Most of them induced a high cell viability (above 80%) at high concentration (single exception: the powder of the cuttlefish *Sepia officinalis*, which induced a relatively important decrease from low to high concentration).

ESM Viability Assessment on MC3T3-E1 Cells

To study the ability of the different biomineral ESM on mineralizing osteoblastic cells, we assessed its effect on the viability of MC3T3-E1 cells after 24 h of treatment. At low concentrations, the ESM from *P. margaritifera*, *P. fucata*, *P. maxima*, *P. radiata*, *A. cygnea*, *U. pictorum*, *H. tuberculata*, and *M. galloprovincialis* showed no noticeable toxic effects on cell viability, as depicted in Fig. 4. However, at high concentrations of ESM from *A. cygnea*, and *U.*

pictorum, a slight reduction in cell viability was observed, reaching approximately 80% at 2500 $\mu\text{g}/\text{mL}$. The reduction of cell viability was more pronounced for *M. galloprovincialis* (around 60% at 4000 $\mu\text{g}/\text{mL}$).

For non-nacreous biominerals, including *P. maximus*, *S. officinalis*, *G. glycymeris*, *M. mercenaria*, *V. verrucosa*, *S. gigas*, *C. chione*, and *P. lividus*, no inhibition of cell proliferation was detected (Fig. 5). However, the ESM extracted from *B. undatum*, *V. philippinarum*, *C. edule*, and *C. gigas* exhibited toxicity at 2500 $\mu\text{g}/\text{mL}$, resulting in a reduction of cell viability to less than 50%. These findings highlight the varying effects of ESM from different biominerals on cell viability and underscore the importance of considering both concentration and biomineral type in cell-based assays.

Mineralization Responses Across Biominerals

We investigated the effects of ESM on the mineralizing process in cultured MC3T3-E1 cells. ESM was added throughout the culture period (21 days), and the concentration of 100 $\mu\text{g}/\text{mL}$ was considered since its non-toxicity

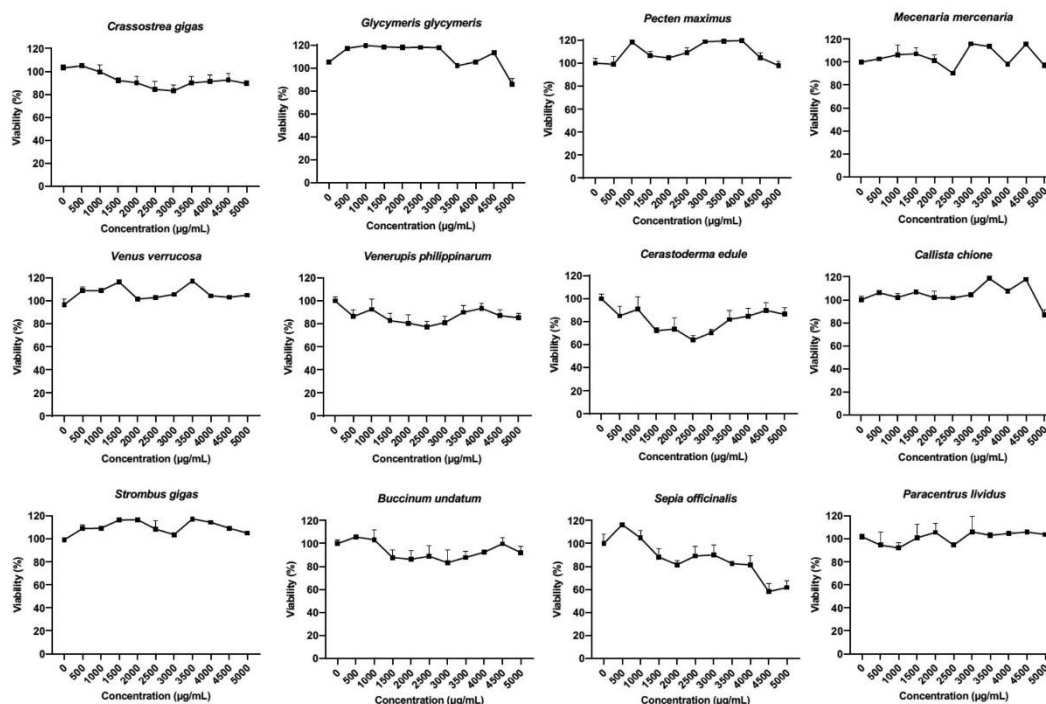


Fig. 3 Effect of shell powder from non-nacreous species on the viability of MC3T3-E1 cells. Cells were treated with varying concentrations of biomineral shell powder dissolved in culture medium

α -MEM for 24h. Results are standardized to the control non-treated group and are represented as the mean \pm SEM of an experiment performed in four replicates

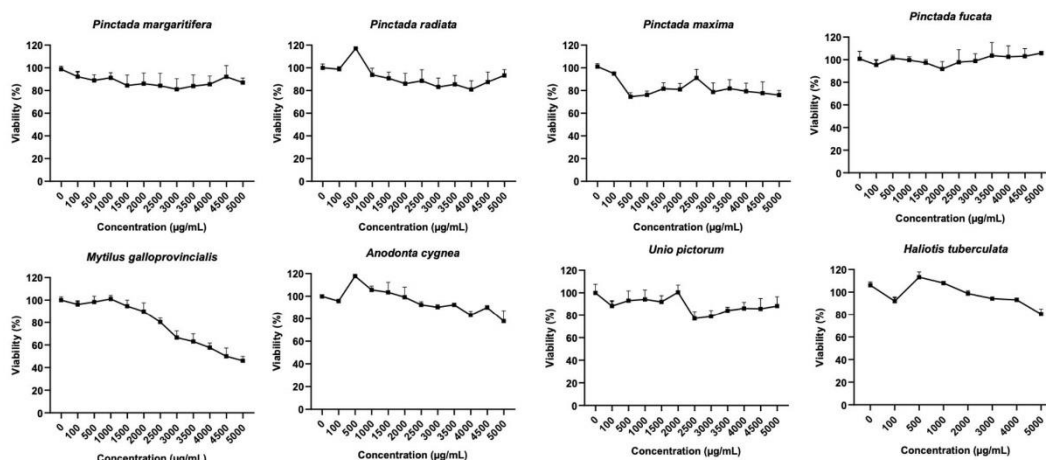


Fig. 4 Effect of nacreous ESM on the viability of MC3T3-E1 cells. Cells were treated with varying concentrations of ESM for 24 h. Results are standardized to the control group that did not receive any

treatment and are represented as the mean \pm SEM of an experiment performed in four replicates

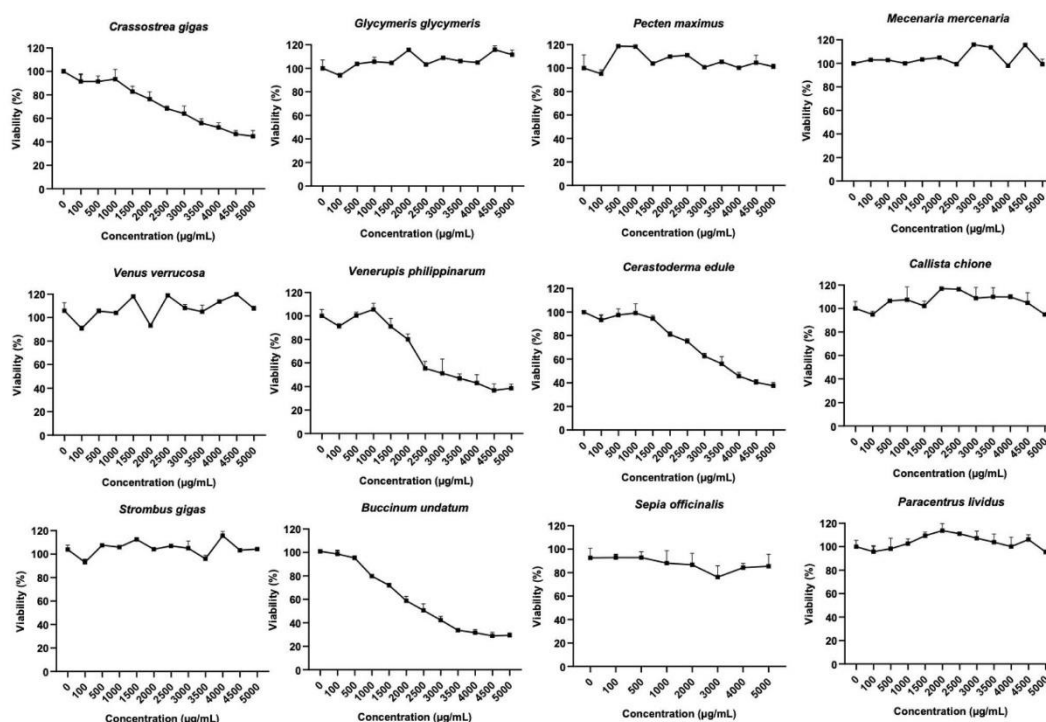


Fig. 5 Effect of non-nacreous ESM on the viability of MC3T3-E1 cells. Cells were treated with varying concentrations of ESM for 24 h. Results are standardized to the control group that did not receive any

treatment and are represented as the mean \pm SEM of an experiment performed in four replicates

was confirmed across all species by the MTT viability test. The control consisted of cells treated with 10 mM β -Glycerophosphate and 50 μ g/mL ascorbic acid. Mineralized nodules were seen as red and dark brown to black spots. Distinct mineralization responses were observed in MC3T3-E1 cells treated with ESM, as shown by Fig. 6 (nacreous), Fig. 7 (non-nacreous), and Fig. 8.

Among the nacreous species, red crystals indicative of mineralization were intensely expressed in cells exposed to ESM from all species within the *Pinctada* genus, highlighting their significant role in promoting mineralization (Fig. 6). Moreover, *A. cygnea* exhibited the capacity to induce mineralization in MC3T3-E1 cells, while *U. pictorum*, which is closely related to *Anodonta* (unionid bivalves), had a much more reduced effect, similar to that of the nacreous gastropod, *H. tuberculata*. The nacre of the mussel *M. galloprovincialis* was even less effective in stimulating the mineralization of the MC3T3-E1 cells, since few red spots were observed.

On the other hand, among the non-nacreous biominerals, *S. officinalis* and *G. glycymeris* demonstrated no discernible capacity to induce mineralization in the cultured cells (Fig. 7). The bivalves *M. mercenaria*, *V. verucosa*, *V. philippinarum*, and *C. gigas*; the two gastropods *S. gigas* and *B. undatum*; and finally the sea urchin *P. lividus* exhibited modest effects on the mineralization of the MC3T3-E1 cells when compared to the nacreous species. The great scallop *P. maximus* induced a higher effect. However, the most astonishing insight was the

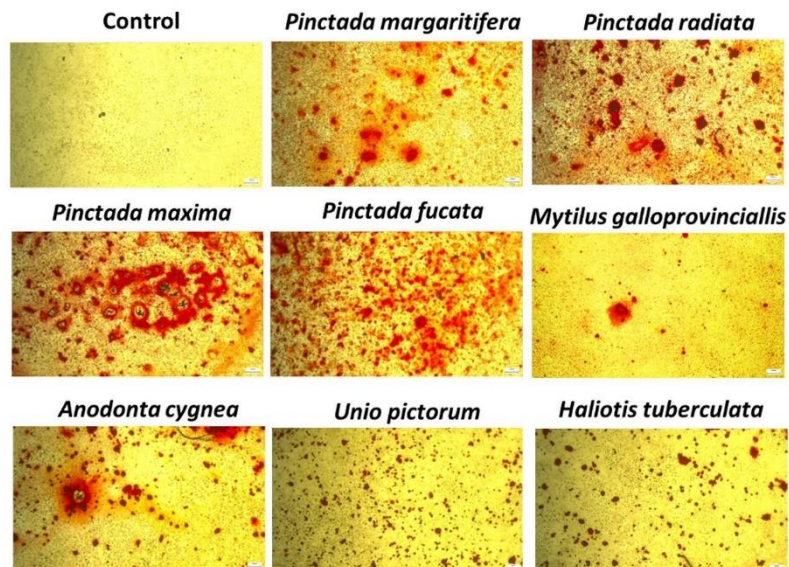
substantial mineralization potential demonstrated by *C. edule* and *C. chione*.

Discussion

The osteogenic potential of nacre is now well-documented (Zhang et al. 2017). However, most of the data accumulated on this shell microstructure focus on the water-soluble matrix (WSM) from a few species (Chaturvedi et al. 2013; Pereira Mourières et al. 2002; Rousseau et al. 2003; Sud et al. 2001). Eight years ago, an ethanol extraction method was used to extract the organic matrix from the pearl oyster *Pinctada margaritifera* (Brion et al. 2015). The resulting ethanol-soluble matrix (referred to as ESM) proved having the capacity to induce the mineralization of MC3T3-E1 as well as the human subchondral osteoarthritic osteoblasts (Brion et al. 2015). So far, studies using ESM extracts have only investigated the osteogenic potential of *Pinctada margaritifera* mother-of-pearl (Brion et al. 2015; Willemin et al. 2019; Zhang et al. 2016). There are no reports available on other species, neither on other microstructures.

Herein, we initiated a pilot study on the effects exerted by both nacreous and non-nacreous species on MC3T3-E1 matrix mineralization. This study presented challenges as acquiring shell powder from these special species was particularly difficult, making it hard to obtain an adequate quantity for the long experimentation (21 days). Prior to any experiments, we rigorously assessed the toxicity profiles of

Fig. 6 Evaluation of MC3T3-E1 mineralization following 21 days of treatment with nacreous ESM using Alizarin Red staining. Representative pictures of alizarin red stained MC3T3-E1. The images were obtained using phase contrast microscopy; scale bar = 1000 μ m. Cells were cultured in osteogenic differentiation medium w/o ESM for 21 days at a density of 2.5×10^4 cells/well in a 48-well plate. Results are representative of three experiments



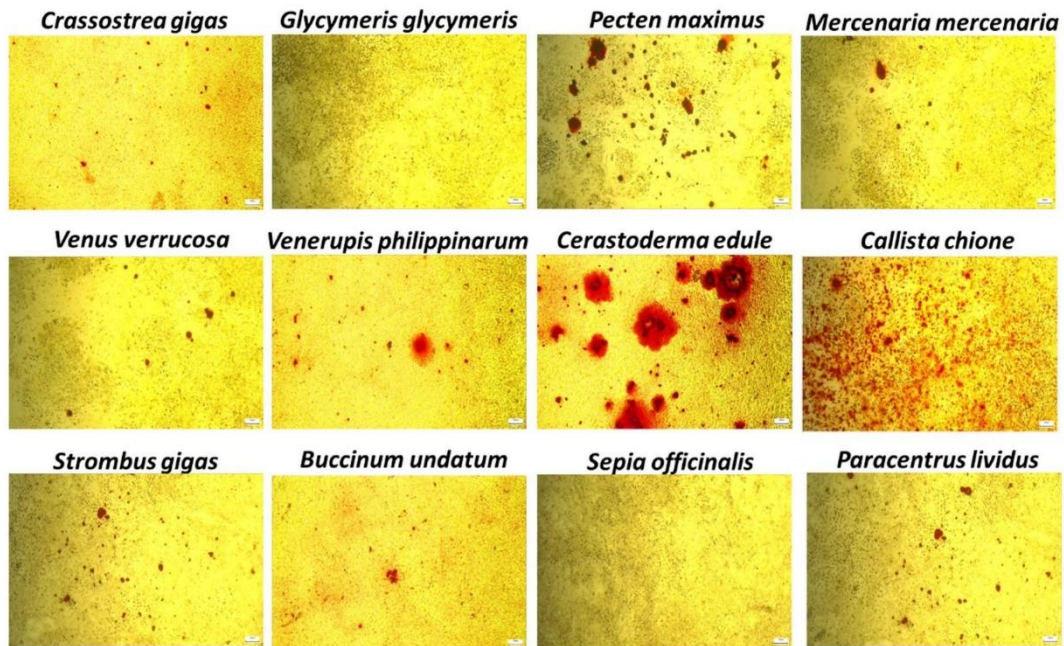


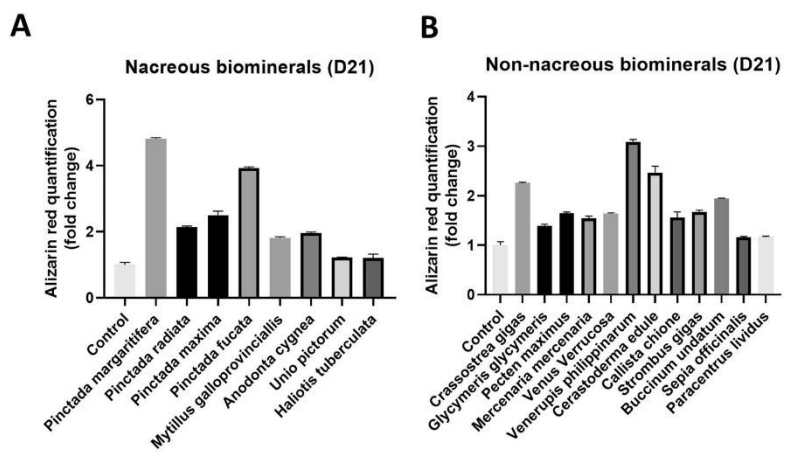
Fig. 7 Evaluation of MC3T3-E1 matrix mineralization following 21 days of treatment with non-nacreous ESM using Alizarin Red staining. Representative pictures of alizarin red stained MC3T3-E1. The images were obtained using phase contrast microscopy; scale

bar=1000 μ m. Cells were cultured in osteogenic differentiation medium w/o ESM for 21 days at a density of 2.5×10^4 cells/well in a 48-well plate. Results are representative of three experiments

the shell powders. As illustrated in Table 1, these shells primarily consist of calcite or aragonite. Nacre samples belong to the second category. All studied samples have natural solubility in acidic solutions. Knowing the toxic nature of

acids towards cells, we developed a methodology involving the mixing of shell powders with culture medium and leaving them undissolved when exposed to the cells. To ensure that this approach did not compromise the accuracy

Fig. 8 Alizarin red quantification. **A** Nacreous species and **B** non-nacreous species. Red nodules were quantified using 10% acetic acid and 10% ammonium hydroxide. Cells were cultured in osteogenic differentiation medium w/o ESM for 14 days at a density of 2.5×10^4 cells/well in a 48-well plate. Results are representative of three experiments



of absorbance measurements in the MTT assays, we adjusted the protocol and incorporated centrifugation techniques to meticulously remove the powder residues from the cultures before making any absorbance readings. Our findings revealed that at low concentrations, these powders presented no visible toxicity concerns. However, at higher concentrations, some molluscan species did exhibit a modest impact on cell viability (Figs. 4 and 5).

We subsequently proceeded to extract the ESM following the methodology outlined by (Brion et al. 2015). Our investigation extended to assessing the potential toxicity of these ESM extracts on MC3T3-E1 cells. Remarkably, at lower concentrations, we observed no toxicity, aligning with our earlier findings regarding shell powders. However, it became apparent that at higher concentrations, some of the tested species, such as *B. undatum*, *M. galloprovincialis*, *V. philippinarum*, *C. edule*, and *C. gigas* exhibit some degree of cytotoxicity. These observations underscore the importance of carefully evaluating the concentration-dependent effects of ESM components.

As a consequence of these findings, we made an informed decision to select a non-toxic concentration of 100 µg/mL for the rest of the study. This concentration, established through rigorous viability assessments, allows us to effectively investigate the various effects of ESM components on MC3T3-E1 cells without compromising cell viability.

The osteogenesis starts with the differentiation of mesenchymal cells into pre-osteoblasts. These pre-osteoblasts subsequently progress into mature osteoblasts which finally induce the deposition of bone matrix proteins and the mineralization of the matrix, leading to bone formation. To assess the calcium deposition within the matrix, we employed Red Alizarin staining. The murine pre-osteoblastic cells MC3T3-E1 were treated with 100 µg/mL of both nacreous and non-nacreous ESM for 7, 14 (Supp. Figs. 1 and 2) and 21 days (Figs. 6, 7, and 8). Our findings revealed an important difference in mineralization effects between nacreous and non-nacreous species. With the exception of *M. galloprovincialis*—explainable by its relative cytotoxicity to MC3T3-E1 cells—all nacreous species exhibited a more obvious impact on mineralization. Among them, all *Pinctada* species played a prominent role in inducing mineralization, emphasizing their potential importance in bone formation. Conversely, within the non-nacreous category, *Cerastoderma edule* and *Callista chione* (both belonging to Venerida order and both predominantly crossed-lamellar) yielded to our surprise strongly positive effects, deserving further investigations to elucidate their organic matrix composition responsible for this phenomenon. In a lesser extent, *Pecten maximus* also recorded interesting effects. To our knowledge, our study represents the first report of the positive effects of non-nacreous mollusk extracts on bone-forming cells.

Indeed, our findings underscore the efficacy of the ethanol-soluble matrix (ESM) from biomineral shells as a

worthy matrix for bone formation. These insights not only improve our knowledge of the biological roles of these matrix constituents but also illuminate promising avenues for future research and therapeutic discovery. The potential applications of this research could have consequences in the field of bone health, offering new opportunities for the development of innovative treatments.

Supplementary Information The online version contains supplementary material available at <https://doi.org/10.1007/s10126-024-10316-w>.

Acknowledgements We thank Mie Prefecture Institute for providing us with the powder shell of *Pinctada fucata*, Robert Wan for the Tahitian *Pinctada margaritifera*, Rym Ben Ammar for the powder shell of *Pinctada radiata*, and Benjamin Brustolin for his involvement in the experimental work.

Author Contribution Study design: Frédéric Marin and Marthe Rousseau. Study conduct: Sarah Nahle, Camille Lutet-Toti, Yuto Namikawa, Marie-Hélène Piet, Alice Brion, and Sylvie Peyroche. Data analysis and visualization: Sarah Nahle and Frédéric Marin. Data interpretation: Sarah Nahle, Michio Suzuki, Frédéric Marin, and Marthe Rousseau. Writing original draft: Sarah Nahle. Revising manuscript content: Sarah Nahle, Sylvie Peyroche, Michio Suzuki, Frédéric Marin, and Marthe Rousseau. Approving final version of manuscript: all authors.

Funding We thank the ANR for funding the NADO project, the AURA Region for the Nutrinacre project (Pack Ambition Recherche), the doctoral school EDSIS (ED 488 SIS), and JSPS KAKENHI (19H05771 and 23H00339) for their financial support. The contribution of F. Marin was supported by grants from Tellus-INTERVIE (INSU, CNRS) and from SRO OSU-Theta (Besançon, France). CLT is recipient of a PhD fellowship under joint-supervision between Université de Bourgogne (uB) and Università di Bologna Alma Mater Studiorum (UniBo). The research leading to these results has been conceived under the International PhD Program “Innovative Technologies and Sustainable Use of Mediterranean Sea Fishery and Biological Resources” (www.FishMed-PhD.org).

Data Availability The datasets are included in this article and available from the corresponding author on reasonable request.

Declarations

Competing Interests MR provides scientific consultation for Megabiopharma.

References

- Adler RA, Fuleihan G-H, Bauer DC, Camacho PM, Clarke BL, Clines GA, Compston JE, Drake MT, Edwards BJ, Favus MJ, Greenspan SL, McKinney R, Pignolo RJ, Sellmeyer DE (2016) Managing osteoporosis in patients on long-term bisphosphonate treatment: report of a task force of the American Society for Bone and Mineral Research. *J Bone Miner Res* 31:16–35
- Brion A, Zhang G, Dossot M, Moby V, Dumas D, Hupont S, Piet MH, Bianchi A, Mainard D, Galois L, Gillet P, Rousseau M (2015) Nacre extract restores the mineralization capacity of subchondral osteoarthritis osteoblasts. *J Struct Biol* 192:500–509
- Canalis E, Giustina A, Bilezikian JP (2007) Mechanisms of anabolic therapies for osteoporosis. *N Engl J Med* 357:905–916

- Carson MA, Clarke SA (2018) Bioactive compounds from marine organisms: potential for bone growth and healing. *Marine* 16:340
- Chaturvedi R, Singha PK, Dey S (2013) Water soluble bioactives of nacre mediate antioxidant activity and osteoblast differentiation' edited by J. Costa-Rodrigues. *PLoS*. <https://doi.org/10.1371/journal.pone.0084584>
- Evans JS (2019) The biomineralization proteome: protein complexity for a complex bioceramic assembly process. *Proteomics*. <https://doi.org/10.1002/pmic.201900036>
- Ganesan K, Jandu JS, Anastasopoulou C, Ahsun S, Roane D (2023) Secondary osteoporosis. *StatPearls*
- González J, Vallejo J (2023) The use of shells of marine molluscs in Spanish ethnomedicine: a historical approach and present and future perspectives. *Pharmaceuticals* 16:1503
- Hahn S, Rodolfo-Metalpa R, Griesshaber E, Schmahl WW, Buhl D, Hall-Spencer JM, Baggini C, Fehr KT, Immenhauser A (2012) Marine bivalve shell geochemistry and ultrastructure from modern low PH environments: environmental effect versus experimental bias. *Biogeosciences*. <https://doi.org/10.5194/bg-9-1897-2012>
- Johnell O, Kanis JA (2006) An estimate of the worldwide prevalence and disability associated with osteoporotic fractures. *Osteoporos Int* 17:1726–1733
- Lopez E, Vidal B, Berland S, Camprasse S, Camprasse G, Silve C (1992) Demonstration of the capacity of nacre to induce bone formation by human osteoblasts maintained in vitro. *Tissue Cell* 24:667–679
- Lopez E, Milet C, Lamghari M, Mouries LP, Borzeix S, Berland S (2004) The dualism of nacre. *Key Eng Mater* 254–256:733–736
- Marie B, Marin F, Marie A, Bédouet L, Dubost L, Alcaraz G, Milet C, Luquet G (2009) Evolution of nacre: biochemistry and proteomics of the shell organic matrix of the cephalopod nautilus macromphalus. *ChemBioChem* 10:1495–1506
- Marin F, Le Roy N, Marie B (2012) The formation and mineralization of mollusk shell. *Front Biosci (schol Ed)* 4:1099–1125
- Muizon De, Jourdain C, Iandolo D, Nguyen DK, Al-Mourabit A, Rousseau M (2022) Organic matrix and secondary metabolites in nacre. *Mar Biotechnol* 24:831–842
- Munoz M, Robinson K, Shibli-Rahhal A (2020) Bone health and osteoporosis prevention and treatment. *Clin Obstet Gynecol* 63:770–787
- Mouriès P, Lucilia MJ, Almeida CM, Berland S, Lopez E (2002) Bioactivity of nacre water-soluble organic matrix from the bivalve mollusk pinctada maxima in three mammalian cell types: fibroblasts, bone marrow stromal cells and osteoblasts. *Comp Biochem Physiol B Biochem Mol Biol* 132:217–229
- Riggs BL, Khosla S, Joseph Melton L (1998) A unitary model for involutional osteoporosis: estrogen deficiency causes both type I and Type II osteoporosis in postmenopausal women and contributes to bone loss in aging men. *J Bone Miner Res* 13:763–773
- Rousseau M, Boulzaguet H, Biagianti J, Duplat D, Milet C, Lopez E, Bédouet L (2008) Low molecular weight molecules of oyster nacre induce mineralization of the MC3T3-E1 cells. *J Biomed Mater Res Part A* 85:487–497
- Rousseau M, Pereira-Mouriès L, Almeida MJ, Milet C, Lopez E (2003) The water-soluble matrix fraction from the nacre of pinctada maxima produces earlier mineralization of MC3T3-E1 mouse pre-osteoblasts. *Comp Biochem Physiol B Biochem Mol Biol* 135(1):1–7
- Sud D, Doumenc D, Lopez E, Milet C (2001) Role of water-soluble matrix fraction, extracted from the nacre of pinctada maxima, in the regulation of cell activity in abalone mantle cell culture (*Haliotis Tuberculata*). *Tissue Cell* 33:154–160
- Taylor JD, Kennedy WJ (1973) The shell structure and mineralogy of the Bivalvia. II. Lucinacea-Clavagellacea Conclusions. *Bull Br Mus Nat Hist Zool* 22:253–94
- Westbroek P, Marin F (1998) A marriage of bone and nacre. *Nature* 392:861–862
- Willemin AS, Zhang G, Velot E, Bianchi A, Decot V, Rousseau M, Gillet P, Moby V (2019) The effect of nacre extract on cord blood-derived endothelial progenitor cells: a natural stimulus to promote angiogenesis? *J Biomed Mater Res A*. <https://doi.org/10.1002/JBM.A.36655>
- Zhang G, Willemin AS, Brion A, Piet MH, Moby V, Bianchi A, Mainard D, Galois L, Gillet P, Rousseau M (2016) A new method for the separation and purification of the osteogenic compounds of nacre ethanol soluble matrix. *J Struct Biol* 196:127–137
- Zhang G, Brion A, Willemin AS, Piet MH, Moby V, Bianchi A, Mainard D, Galois L, Gillet P, Rousseau M (2017) Nacre, a natural, multi-use, and timely biomaterial for bone graft substitution. *J Biomed Mater Res Part A* 105:662–671

Publisher's Note Springer Nature remains neutral with regard to jurisdictional claims in published maps and institutional affiliations.

Springer Nature or its licensor (e.g. a society or other partner) holds exclusive rights to this article under a publishing agreement with the author(s) or other rightsholder(s); author self-archiving of the accepted manuscript version of this article is solely governed by the terms of such publishing agreement and applicable law.

6.2. Collaboration Paper with Dr. Luca Polacchi: Biochrome Extraction

Submitted in 2025 to Methods in Ecology and Evolution, third submission (after Nature Protocols and PNAS)

Coupling Gel Electrophoresis With Photoluminescence Reveals Biochrome Complexes In Modern And Fossil Shells

Luca Polacchi¹, Camille Lutet-Toti², Olivier Basuyaux³, Pierre Gueriau^{1,4}, Marie Albéric⁵, H  l  ne Pasco¹, J  r  me Thomas², Didier Merle⁶, Beno  t Habermeyer⁷, Roger Guilard^{7,8}, Mathieu Thoury¹, Fr  d  ric Marin^{2*}

1 IPANEMA, CNRS, minist  re de la Culture, UVSQ, MNHN, UAR3461, Universit   Paris-Saclay – site du synchrotron SOLEIL, BP 48 Saint-Aubin, F-91192 Gif-sur-Yvette, France.

2 Biogeosciences Laboratory, UMR CNRS-EPHE-UBE 6282, University Burgundy Europe – 6 Boulevard Gabriel – 21000 Dijon, France.

3 M2e, Mer Expertise Environnement – 22 La Boivin  rie – 50560 Blainville-sur-Mer, France.

4 Institute of Earth Sciences, Geopolis - University of Lausanne - CH-1015 Lausanne, Switzerland.

5 LCMCP Laboratory, Sorbonne University - 4 Place Jussieu - 75252 Paris Cedex 05, France.

6 Dpt Origines & Evolution, MNHN, Sorbonne University – 57 Rue Cuvier, 75231 Paris cedex 05, France.

7 PorphyChem SAS, 390 Rue Charles de Freycinet, 21600 Longvic, France.

8 ICMUB, UMR CNRS 6302, University Burgundy Europe – 9 Avenue Alain Savary - 21000 Dijon, France.

* Corresponding author: Fr  d  ric Marin, UMR CNRS – EPHE – UBE 6282 Biogeosciences – University Burgundy Europe – 6 Bd Gabriel – 21000 Dijon, France. frederic.marin@u-bourgogne.fr

Abstract

Polyacrylamide gel electrophoresis is commonly used to visualize mixtures of proteins, such as that occluded in calcareous biominerals. However, it is ineffective for the detection of biochromes, a major class of low molecular weight organic compounds commonly associated to calcified exoskeletons.

We describe a novel approach based on the coupling between electrophoresis and luminescence spectral imaging to reveal invisible biochromes, identify them chemically, evidence their putative interaction with exoskeletal macromolecules and purify them in large amounts. Our protocol relies on three key-steps: a mild extraction of all organics from bleached skeletal powder (step1); an optimized electrophoretic fractionation immediately followed by direct on-gel spectral image acquisition performed before classical gel staining (step 2); a large-scale purification via preparative electrophoresis coupled to luminescence spectral imaging, to obtain significant amounts of biochromes of interest (step 3).

Steps 1 to 3 were successfully applied to recent gastropod shell extracts, while steps 1 and 2, to their fossil equivalents of the Eocene epoch (≈ 45 million years). In both cases, we were able to determine the exact chemical nature of the porphyrins associated to the shells, via a spectrophotometric measurement of the luminescent pigment bands directly on the analytical

gel, even at low concentration (fossil). For recent shell extracts, our approach allowed to identify spectrophotometrically the tubes containing the invisible pigments, after preparative fractionation and fraction collection.

Our protocol enabled direct, non-invasive on-gel identification of porphyrin molecules, even in trace amounts. It opens new avenues for the study of a wide range of biological composites, mineralized or not, that contain luminescent biochromes. It is particularly well suited to ancient specimens and fossils to trace the origin and evolution of biochrome complexes in the geological record.

Keywords: Biomineral; Pigment; Porphyrin; Multispectral imaging; Electrophoresis; Fossil

6.2.1. Introduction

Calcium carbonate-based biominerals (*e.g.*, coral exoskeletons, mollusk shells, sea urchin spines) are organo-mineral assemblies that contain small amounts (typically 1% wt/wt or less) of organic macromolecules - collectively called the skeletal matrix - which regulates mineral deposition (Addadi & Weiner, 2014; Marin *et al.*, 2016; Suzuki, 2020). A substantial proportion of biominerals contains biochromes in addition (Comfort, 1951; Soldati *et al.*, 2008; Amarowicz *et al.*, 2012; Bergamonti *et al.*, 2013). Biochromes are small molecules, showing absorption in the visible spectral range, produced by living systems. They are composed by a diversified set of chemical structures, from linear chains with conjugated double bonds, such as carotenoids (Beltran & Wurtzel, 2025) to complex structures involving rings and metal ion complexation like porphyrins (Kadish & Guilard, 2024). They generate color by absorbing light at specific wavelengths due to their specific molecular structures (Hari *et al.*, 1994). The most common protocols used to isolate these coloring molecules from calcified tissues rely primarily on harsh extraction with strong acids to dissolve the mineral fraction (Hou *et al.*, 2019; Bonnard *et al.*, 2020), followed by a phase separation with an organic solvent (Mischenko *et al.*, 2005). This approach is practical for quickly obtaining large amounts of biochromes. However, beyond using harmful and environmentally unfriendly chemicals, it irreversibly degrades the skeletal macromolecules and consequently disrupts the biochrome-macromolecules complexes. It is therefore unsuitable for disentangling biochrome-macromolecules interactions and studying the persistence of organics in ancient or fossil biominerals (Caze *et al.*, 2015).

Another difficulty is getting an accurate ‘instantaneous’ picture of all organic components, *i.e.*, biochromes and skeletal matrix, together. While gel electrophoresis - referred to as Sodium Dodecyl Sulfate Poly-Acrylamide Gel Electrophoresis, abbreviated as SDS-

PAGE - is the most convenient technique for visualizing macromolecules from biominerals and determining their size distribution (Osuna-Mascaro *et al.*, 2014; Immel *et al.*, 2016), it is ineffective in revealing associated biochromes for three reasons: a) this technique is not discriminatory enough for small organic molecules around and below 1 kilodalton, typically a molecular weight range of biochromes that are not bound to macromolecules; b) in addition, when unbound, biochromes diffuse extremely rapidly out of the gel (and are consequently lost) because of their small size, as soon as the gel is processed for staining; c) when bound to matrix macromolecules, biochromes may be stabilized in the gel via a fixation step (with trichloroacetic acid, *i.e.*, TCA, for example) but most of them are invisible or, at the best, only weakly colored in natural light; As biochromes do not take on any of the classical gel dyes (Coomassie Blue, silver nitrate), they are irreversibly masked by subsequent gel staining (Pavat *et al.*, 2012). The novel protocol developed here circumvents these obstacles: in particular, it reveals invisible biochromes or mixtures of biochromes, identifies them chemically via direct on-gel spectral acquisition and evidences their putative complexation with macromolecules. At last, it allows obtaining consequent amount of purified biochromes when the starting shell material is abundant.

6.2.2. Materials and Methods

6.2.2.1. Materials

Recent samples of *Phorcus lineatus* were manually sampled along the Normandy coast in the area of Blainville-sur-Mer. Emptied specimens were carefully sorted visually: shells with no defects and no epibionts were selected. Fossil samples of *Tectus crenularis* were collected in the middle Lutetian (\approx 45 million years) of Paris Basin and came from the invertebrate fossil collection of the Natural History National Museum (MNHN) of Paris.

6.2.2.2. Matrix Extraction

The shells were scrupulously brushed, rinsed and carefully decontaminated for several days in a tenfold aqueous solution of sodium hypochlorite (0.6 to 1.4% active chlorine, Merck ref. 1.05614.2500). After thorough rinsing with ultrapure water and drying, they were coarsely crushed and bleached again, before being mechanically comminuted (Pulverisette 2, Fritsch) to a powder with a particle size of less than 200 μm . The powder was suspended in ultrapure water and slowly demineralized overnight with cold dilute acetic acid, according to a published protocol (Osuna-Mascaro *et al.*, 2014; Immel *et al.*, 2016). The resulting solution was

centrifuged (30 min., 3900 G) to separate the insoluble and soluble organic fractions. The insoluble pellet (defined as AIM, ‘Acetic acid Insoluble Matrix’) was rinsed at least five times by cycles of suspension in ultrapure water, centrifugation and removal of the supernatant. For *Phorcus lineatus*, the soluble fraction (ASM, ‘Acetic acid Soluble Matrix’) was concentrated in a 400 mL ultrafiltration stirred cell (Millipore, model 8400, ref. UFSC40001) equipped with a cellulose membrane with a 10 kDa cut-off (Millipore 76 mm diameter disc, ref. PLGC07610). The viscous retentate (about 10-15 mL) was kept while the collected filtrate was ultrafiltered again on a membrane of 1 kDa cutoff (Millipore 76 mm diameter disk, ref. PLAC07610). The two retentates (ASM > 10 kDa and 1 < ASM < 10 kDa) were extensively dialyzed against ultrapure water in dialysis tubing of 1 kDa cutoff (SpectraP/Por 6 pre-wetted RC tubing) with at least 6 water changes. The insoluble and the two soluble organic matrices were freeze-dried (Telstar Cryodos). For the fossil *Tectus crenularis*, the insoluble AIM pellet contained clay minerals and was not used further. Since the ASM supernatant resulting from the decalcification was not concentrated in organics, we performed a single ultrafiltration on a 1 kDa cutoff membrane, all the other subsequent steps being identical to that of *Phorcus lineatus*.

6.2.2.3. Analytical Gel Electrophoresis and Acquisition of Spectral Images

For visualizing the result of the extraction, the standard electrophoretic mini-gel system (Bio-Rad, Mini Protean III) was used. To improve the resolution of the low to very low (< 1 kDa) molecular weight components, we combined the use of discontinuous Tris-tricine gels run with anode and cathode buffers (Schägger & von Jagow, 1987) and a high percentage (15%) of acrylamide. Samples were prepared and denatured in Laemmli sample buffer as previously described (Immel *et al.*, 2016). Note that the AIM of *Phorcus lineatus* was only partially solubilized in this buffer. The soluble portion of this fraction is referred to as the Laemmli soluble - Acetic acid Insoluble Matrix (LS-AIM). All fractions were run at 120 V. The use of a pocket UV torch allowed the migration of the invisible pigments to be checked preceding the migration front and the run to be stopped when the pigment reached the bottom of the gel. The gel was then de-cast, placed on a flat clean support and multispectral images were acquired by using the home-built imaging system. The detection part consisted of a 4 megapixels CMOS camera (ORCA -Flash 4.0 LT Plus, Hamamatsu) with a sensitivity ranging from 350 to 1100 nm. The camera was equipped with a UV-VIS-IR 60 mm 1:4 Apo Macro lens (CoastalOptics) in front of which was positioned a filter wheel fitted with 8 Interference band-pass filters (Semrock) to perform multi-spectral acquisitions. The illumination part was composed of a 16 LED lights ranging from 365 up to 700 nm (CoolLED pE-4000), coupled to a liquid light-guide

fiber fitted with a fiber-optic ring light-guide to allow homogeneous illumination. Emission and excitation spectra were collected using a modified spectrofluorometer (Fluorolog 3–22, HORIBA Jobin Yvon) which allows spectra to be collected directly on the gels using an optical bundle connected to a focusing lens. The entrance and exit slits widths of the monochromators were set at 10 nm to collect spectra with good signal-to-noise and a spectral resolution compatible with the detection of Q-bands. Emission spectra were collected using an excitation at 400 nm. Excitation spectra were collected using a 732 ± 34 nm bandpass filter (from Semrock) at the entrance of the emission monochromator to eliminate any stray light. The spectra on tube were collected under a UV excitation generated by a Jaxman UIC torch and using a JETI 1211 portable spectrometer sensitive between 300 and 1000 nm, fitted with a high-pass transmission filter with a cut-off wavelength at 409 nm to eliminate the reflectance of the the UV excitation.

6.2.2.4. Preparative Gel Electrophoresis

As the shell matrix of *Phorcus lineatus* was abundant, we performed preparative gel electrophoresis using the Bio Rad preparative cell (model 491 Prep Cell) equipped with its cooling unit, its peristaltic pump (EP-1 Econo Pump), its detection cell (EM-1 Econo UV Monitor) and its fraction collector (Model 2110) as previously described (Marin *et al.*, 2001). As for analytical gel, we used 15% acrylamide Tris-tricine gel together with cathode/anode buffers to obtain the best resolution for very low molecular weights. The gel was cast and run according to the manufacturer's instructions (available at <https://www.bio-rad.com/webroot/web/pdf/lsr/literature/M1702925.pdf>) and the progression of the biochrome's migration was followed, from time to time, by rapidly illuminating the gel tube with the pocket UV torch. Fractions of 5 mL (flow rate 0.5 mL/min, 10 min. per tube) started to be collected in continuous after 5 hours of migration, when the pigment signal reached the bottom of the gel tube. Spectra were directly acquired on the different tubes. The free pigment was eluted from tube 4 to tube 7 (with the highest amounts of materials in tubes 4 and 5) while the migration front was eluted from tube 8 to tube 12.

6.2.3. Results

6.2.3.1. A Non-Standard and Optimized Protocol in Three Steps

As shown in Fig. 1, our protocol is based on the association of 3 key-steps, namely a mild extraction, consisting in dissolving slowly mineralized tissues with cold dilute acetic acid, in order to recover all organic molecules occluded in the calcified skeleton and to minimize the possible degradation of biochrome-macromolecule complexes (step 1); the non-standard coupling of electrophoretic fractionation (on analytical mini-gels) with a custom-made luminescence spectral imaging, according to a proper sequence (step 2); whenever possible, the adaptation of step 2 to large quantities of shell extracts, by preparative electrophoresis, in order to obtain workable quantities of biochrome (step 3).

Steps 1 and 2 only are suited to minute quantities of skeletal organic matrices, typically extracted from precious samples including recent but rare materials, archaeological or fossil shell specimens; the full procedure (steps 1 to 3) can be applied to organic mixtures extracted from abundant raw material (fresh shells).

6.2.3.2. Revealing Biochromes in Gels (Fig. 2A, B)

We applied our protocol to shell extracts of two mollusk models, the living *Phorcus lineatus*, an extant gastropod extremely common along the Atlantic and Normandy coasts (France) (Cabral, 2020), and an equivalent 45-million-year-old fossil specimen, *Tectus crenularis*, belonging to the same superfamily (Trochoidea), and found in the Lutetian of Paris Basin (Gain *et al.*, 2019). The visualization of biochromes in analytical gels requires two *sine qua non* conditions: 1) the use of hand-cast unconventional high acrylamide (15, 16%) Tris-tricine gels, the particularity of which is to increase the resolution of low molecular weight components, around 1 kDa and less. These components include for example free biochromes, oligopeptides and oligosaccharides. 2) The acquisition of images in natural light and luminescence modes, just after gel running/demolding but before any type of gel fixation and staining. Fig. 2 illustrates results obtained in these two modes. The left gel (Fig. 2A) is an image obtained from the freshly run and unstained gel, in natural light. Large diffuse smears of dark brown pigments are visible in lanes 2, 3, 4, corresponding to different *Phorcus lineatus* extracts while a very faint orange smear can be observed in lane 5 (*Tectus crenularis*). Interestingly, when the same gel is illuminated with UV light (Fig. 2B), additional biochromes, almost or totally invisible in natural light, are observed in a zone preceding the migration front (*i.e.*, below the line formed by bromophenol blue) using an optimized multispectral set-up: in the bottom

of lanes 3 and 4, they consist in a discrete predominant band, strongly luminescent in the red spectral domain, surmounted by weaker luminescent smearing signals (yellowish to red). The electrophoretic pattern of lane 5 (fossil) is different and composed of successive discrete bands revealed owing to weak luminescence, comprising 3 cyan and one light red (underlined by a white rectangle), separated according to their migration properties. Lane 5 is crowned by an upper smearing fat cyan signal.

6.2.3.3. *In-Gel Identification of Biochromes (Fig. 2C)*

Our protocol not only reveals the presence of all biochromes (visible and non-visible in natural light), but allows their precise chemical identification, based on their spectral signature. In the example of Figure 2B, both emission and excitation spectra were acquired *in situ* from the bottom luminescent band of *Phorcus lineatus* extracts (lanes 3 and 4) in a non-invasive manner, using a custom-modified spectrofluorometer. In Figure 2C, the Soret band observed in the excitation spectrum at 408 nm and 5 Q-bands at 508, 542, 573, 623 and 649 nm (red continuous curve) in addition to 3 bands at 623, 653 and 685 nm in the emission spectrum (red dotted line) are characteristic of a non-metallated porphyrin (Nian & Kong, 1990). A subsequent database search (www.photochemcad.com/databases/common-compounds/porphyrins) strongly suggests that this spectrum is in agreement with that of a protoporphyrin IX dimethyl ester (Taniguchi & Lindsey, 2018).

A similar *in situ* spectrum obtained from the faint red band of the fossil *Tectus crenularis* (Fig. 2B, lane 5, white rectangle) corresponds to a porphyrin that shows all the excitation and emission features of a hematoporphyrin IX, with excitation bands at 400, 504, 534, 567, 609 and 649 nm (pink continuous line) and emission bands at 617, 648 and 683 nm (pink dotted line). As illustrated here the coupling of electrophoresis and luminescence imaging and spectroscopy allows the *in situ* chemical characterization of porphyrins directly on the gel, even when the signal is strongly attenuated due to fossil origin of the extract.

6.2.3.4. *Analysis of Biochrome-Macromolecules Complexes*

An additional advantage of coupling electrophoresis and spectral imaging for the visualization of extracts containing biochromes is the ability to infer the molecular interactions of biochromes with other organic macromolecules of the skeletal matrix. This information is deduced from the migration behavior of biochromes. In the present example, extracts of the living *Phorcus lineatus* and of the fossil *Tectus crenularis* are characterized by brown smears

visible under natural light (Fig. 2A, lanes 2, 3 and 5). The molecular distribution of these pigmented smears extends to relatively high molecular weights (far above 10 kDa), clearly suggesting that the biochrome is associated to polydisperse macromolecules (proteins or polysaccharides) of the shell matrix. It is indeed known for a long time that skeletal matrices of calcified tissues exhibit such an electrophoretic behavior (Marin & Luquet, 2007). In addition, as the electrophoresis was performed in denaturing conditions (SDS + β -mercaptoethanol), this may indicate that the dark brown biochrome and the polydisperse macromolecules are strongly bound together, suggesting the involvement of covalent bonds. On the contrary, the thick discrete porphyrin signal observed in red in the false color luminescence image in lanes 3 and 4 of Fig. 2B (*Phorcus lineatus*) is located at the bottom of the gel in a zone corresponding to components of very low molecular weight. Its position suggests two possibilities: a) it is not bound to any matrix macromolecules, the most likely case; b) it was bound, but the bond was labile and easily disrupted by the denaturing conditions of the electrophoretic migration.

6.2.3.5. Upscaled Purification of Porphyrins

In the present example, the peculiar migration pattern of the porphyrin biochrome of *Phorcus lineatus* (*i.e.*, discrete band migrating far ahead the migration front of the gel) can be exploited to upscale its purification by preparative electrophoresis, as shown by Fig. 3. This aspect is particularly useful if the raw shell material is abundant. This technique, primarily used for purifying proteins from bulk shell extracts (Marin *et al.*, 2001; Marxen *et al.*, 2003), has been specifically adapted here to biochromes, which can be eluted from the gel and recovered with a fraction collector (Fig. 3A). Similarly to Step 2, the fractionation is performed on a non-standard 15 or 16% acrylamide Tris-tricine preparative gel. The technique allows the purification of large amounts of biochromes, eluted early in the different tubes (tubes 4 to 8). The luminescence spectral imaging system allows porphyrin visualization directly during the gel run, and in the fractions collected in the tubes (Fig. 3B). Note that the elution of the porphyrin in the tubes follows an asymmetric normal law. As for gel bands of step 2, luminescence spectra are obtained directly from each tube, and the corresponding signals, integrated for relative quantification. The porphyrin elution before the migration front of the electrophoresis guarantees a high purity of the biochrome, since it is not contaminated by macromolecules of the matrix, which elute after the migration front. Consequently, the different fractions obtained can be pooled together and extensively dialyzed in dialysis bags of very low

cutoff (500 Da) to remove molecules of the eluent (Tris, glycine). The pure biochrome is then ready to be freeze-dried and analyzed further.

6.2.4. Discussion

6.2.4.1. *Unconventional Features of our Protocol*

In calcified tissues, biochromes are poorly studied in relation to biomineralization processes and to their association with the skeletal matrix. When pigmented skeletal matrices are extracted for subsequent analysis, biochromes are usually lost during key-steps (ultrafiltration, dialysis) of the extraction procedure. When bound to macromolecular components, most biochromes go unnoticed simply because they are neither detected, nor the central focus of the study. By allowing the sequential visualization of biochromes and of skeletal macromolecules in gels, our protocol provides a novel and exhaustive picture of organic molecules contained in a calcified tissue. The novelty of our approach lies in two aspects, firstly a non-standard use of existing techniques and secondly, three methodological optimizations performed at different steps of the analysis.

The first aspect is the use of a commercial gel electrophoresis system (analytical or preparative), a setup that has never been used for the fractionation of free biochromes. Another non-standard application is the improved detection of luminophores using a multispectral imaging allowing to optimize the selection of the spectral bands of detection in accordance with the emission properties of the different chemical moieties. The adjustment of a commercial spectrofluorometer to perform remote excitation emission measurements outside of the original sample compartment dedicated to the study of small samples or solutions in a cuvette is also a significant improvement to apply the techniques to a wider range of materials (see ‘Materials & Methods’). A special accessory is composed of two mirrors and a bifurcated fiber of which output was inserted into a custom-made dark compartment to avoid the collection of stray light. This configuration allows collecting excitation /emission spectra on areas of 2 mm diameter; this size is compatible with the dimensions of electrophoresis bands – even weak ones - on a mini-gel. Finally, the most innovative aspect of the non-standard protocol consists in coupling electrophoresis to this optimized imaging system.

Three key methodological optimizations were implemented. Firstly, the use of a low cut-off (1 kDa) for the ultrafiltration system to recover most of the organic components of the skeletal tissue, especially those of low molecular weight. Secondly, the use of Tris-tricine gels of high acrylamide content (15, 16%), to obtain a clear separation of unbound biochromes and

very low molecular weight constituents from skeletal matrix macromolecules. Thirdly, the luminescence imaging was performed immediately after gel migration and demolding but before any type of gel staining. This aspect is crucial, as all the protocols found in the literature describe the first staining step immediately after gel has been removed from the casting plates. We therefore recommend that electrophoretic gels, whatever they are, should be always checked with a UV flashlight, to reveal invisible and unstainable molecules that are potentially present (as discrete bands or smears) in the fractionated extracts.

6.2.4.2. *Advantages*

The combination of mild extraction, non-standard gel electrophoresis and spectral imaging represents a breakthrough on the way of accessing and exploiting the information contained in electrophoretic gels. The multiple advantages offered by our protocols are twofold, the typologies of information that can be retrieved and the compatibility of the protocols with standard procedures.

For the first time it is possible to visualize biochromes and calcifying matrix macromolecules on the same gel: the molecular association (covalent binding, non-covalent binding) between biochromes and matrix macromolecules can be accurately depicted. The example of *Phorcus* shows that the main luminescent but invisible biochromes are free (*i.e.*, not bound to macromolecules), while the dark ones, visible under natural light, are likely to be associated with molecules of higher molecular weight.

Moreover, due to the combination of the mild extraction and the absence of staining, spectroscopic measurements directly on the gel are possible and give access to the spectral signature of porphyrins in a very simple and non-invasive way, with a fast acquisition time. Other biochromes, such as carotenoids or naphthoquinones, can also be analyzed in the same manner. Remarkably, when different biochromes are mixed in an extract, the electrophoretic fractionation allows the deconvolution of this complex signal into several discrete bands which can be studied separately with luminescence spectral imaging. The use of luminescence as a probe allows revealing extremely low amounts of biochromes that are not detectable under natural light: the spectral image, by allowing extremely sensitive detection, is therefore particularly suited to the study of trace of biochromes, such as those found in fossils.

As far as the analytical procedure is concerned, the protocol does not involve any major changes and is fully compatible with subsequent standard gel stains such as CBB, silver nitrate, alcian blue, carbocyanine, in other words, the dyes mostly used in biomineralization research

(Marin & Luquet, 2007; Immel *et al.*, 2016). The spectral analysis must be performed prior to staining but does not alter the staining procedure in any way. Alternately, the unstained gels can be partly dried, hermetically sealed between two plastic foils and stored flat in a cold and dark environment, if necessary. This allows preserving biochromes in the gels. Luminescent signal can consequently be retrieved months or years later. If required, the upscaling of the experiment to preparative fractionation is implemented to obtain large amounts of purified biochromes or protein-biochrome complexes. The application of the approach can be extended to all kinds of composite materials made of organic macromolecules and biochromes. The protocol applies also to non-mineralized systems. Plants or archaeological stained leather, or any sample containing luminescent or non-luminescent biochromes can be analyzed in this manner. Most of the chemicals used are environmentally friendly and, apart from acrylamide (which, when polymerized, is harmless), none of the chemicals used for the analysis on gel are harmful. At last, the whole protocol as described here from the extraction to the spectral analysis, is not costly.

6.2.4.3. *Limitations*

There are few limitations to our approach, mostly related to the duration of the complete analytical procedure and the range of biochromes that can be studied.

The whole experiment, including preparative purification of biochromes, is time-consuming: the matrix extraction step, from decalcification to freeze-drying of the extracts, lasts one week or more; a peculiar bottleneck is the ultrafiltration on a 1 kDa cutoff membrane, which is tedious but mandatory if one wants to collect most of the organics from skeletal tissues; the preparative electrophoresis (step 3) takes 2 days. In addition, when step 3 is performed, the collected tubes with biochromes also contain Tris and glycine (elution buffer), which must be removed by dialysis in very low cut-off tubes (< 500 Daltons). The dialysis process takes a few more days. In addition, the protocol described here, from the extraction to the analysis on gel, is adapted to water or acid-soluble biochromes. Biochromes that are soluble only in organic solvents, *e.g.* ether or chloroform, cannot be treated with our method.

6.2.4.4. *Further Developments: Other Objects, Methodologies and Applications*

Our protocol is aimed firstly at the lively scientific community of biomineralization that studies calcified tissues in general and not only mollusk shells: eggshells in vertebrates, exoskeletons in corals, bryozoans and annelids, spines and plates in echinoderms, carapaces in crustaceans, but also stromatolites and microbialites made by cyanobacteria. These biomineralized structures contain also biochromes (Lepot *et al.*, 2018). Until a few years ago, mineral-associated biochromes had not been studied and their exact biological function had remained elusive (Saenko & Schilhuizen, 2021). Today, we are witnessing a resurgence of interest in their study. Apart from being adaptive responses to the environment (*i.e.*, 'camouflage') or to attract sexual partners in the case of biocalcified structures in gastropods, some biomineral-associated biochromes are thought to be part of the immune response (via the tyrosinase enzymatic pathway) prior to their occlusion in the mineral phase (Trinkler *et al.*, 2011; Liu *et al.*, 2021). They are also suspected to be involved in the calcification process itself and their function in biomineralization needs to be urgently revisited (Parvizi *et al.*, 2023). From applied perspectives, their usage as natural substances should be further explored: anti-microbial/anti-tumoral agents or eco-friendly dyes are, among others, compelling applications (Hou *et al.*, 2016; Roncoroni *et al.*, 2024).

Our protocol opens up new avenues to the development of other methodological investigations. When a biochrome of interest is suspected to be associated to a protein, its visualization on an unstained gel allows a direct manual sampling of the band/spot, its subsequent in-gel enzymatic digestion and the analysis of the resulting peptides by proteomics. This provides a formal identification of the protein-biochrome complex. More broadly, the methodological framework presented here can be extended by coupling electrophoresis with other types of imaging techniques: Raman spectroscopy is a promising perspective that can provide additional information on the chemistry of the biochromes of interest.

Finally, other applications arise from our innovative protocol: since biochromes can be fractionated on gel and chemically characterized by luminescence spectral imaging even at trace concentration, our approach is particularly suitable for the characterization of organic (macro)molecules in ancient materials and should interest conservation science, archaeology, paleontology, ecology and evolution. Many remarkable fossil deposits contain shells that have retained their biochromes for millions of years (Caze *et al.*, 2015; Tahoun *et al.*, 2021). Biochromes can be detected in samples as old as the Jurassic (Caze *et al.*, 2011; Wolkenstein *et al.*, 2024). Their exceptional diagenetic preservation raises questions on the multiple causes

of this stability: molecular structure, affinity with the mineral phase, tight or loose association with the organic macromolecules. This last point is particularly critical as the presence of traces of native biochromes in fossil shells may be a proxy for the preservation of the associated matrix macromolecules: if so, a quick check with UV light may be a prerequisite step to the selection of suitable precious fossils before any shell matrix extraction.

Our protocol makes it possible to study the relationship between the preservation of biochromes and that of macromolecules in the matrix. It will undoubtedly advance the understanding of molecular diagenesis. In addition, because coupling electrophoresis and luminescent imaging can deconvolute complex biochrome signals, this will allow the reconstruction of past mollusc communities by identifying, similarly to a barcoding, peculiar biochrome complexes contained in fossil shells, which may be related to sexual dimorphism, populations, species, geographical localities, specific environments, or to ecological interactions between individuals. Molecular paleontology, ecology and evolution will benefit greatly from such advances, which will open up new opportunities to trace the origin and evolution of biochrome complexes in the geological record and to revisit entangled ecological interactions from the past.

Figures

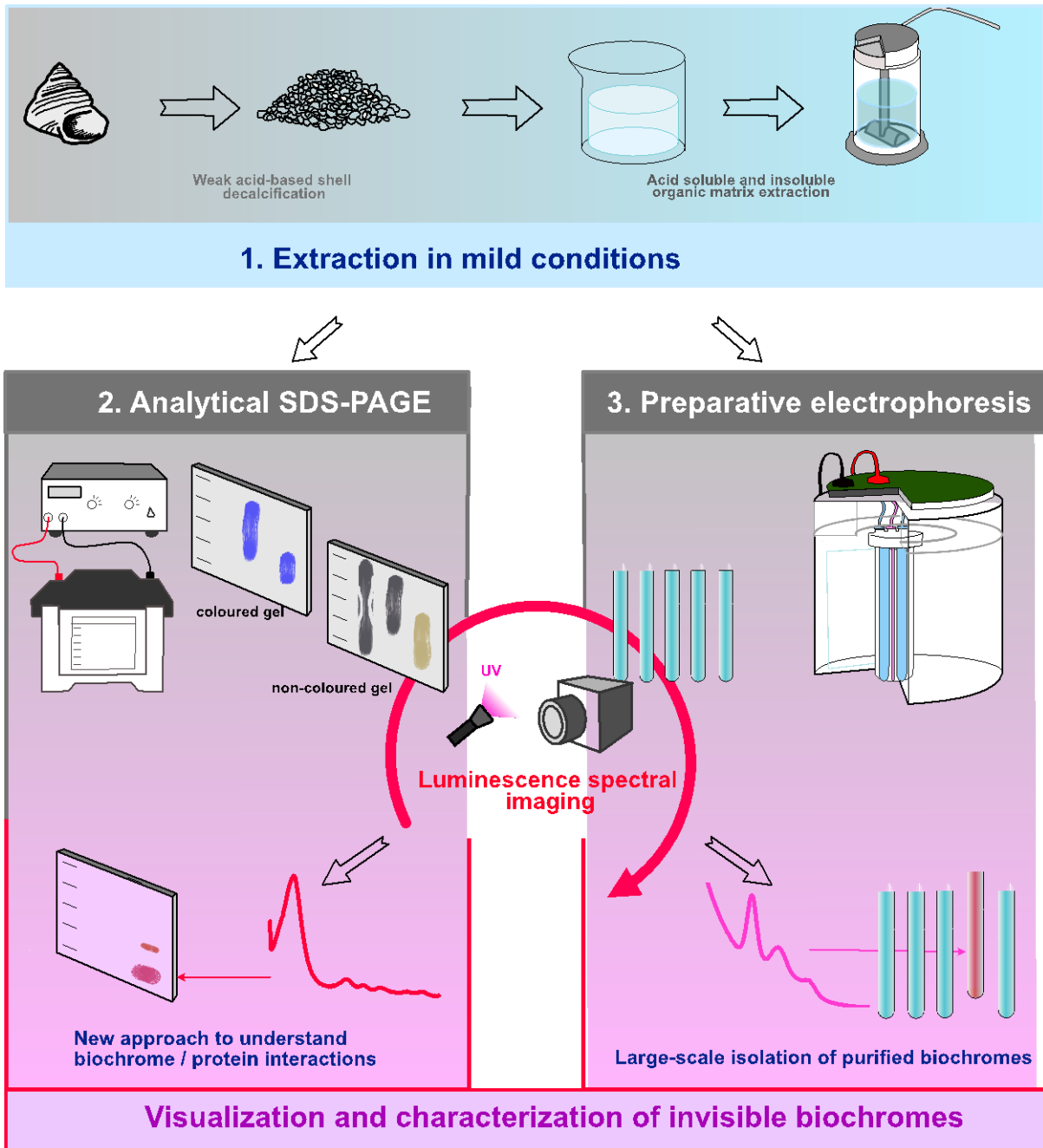


Figure 1: Scheme of the procedure for the analysis of invisible shell biochromes describing the three key-steps (explained in the text): in brief, they involve a mild extraction (upper panel) and the coupling of luminescence spectral imaging with mono-dimensional electrophoresis, either analytical on mini-gels (left panel) or preparative (right panel).

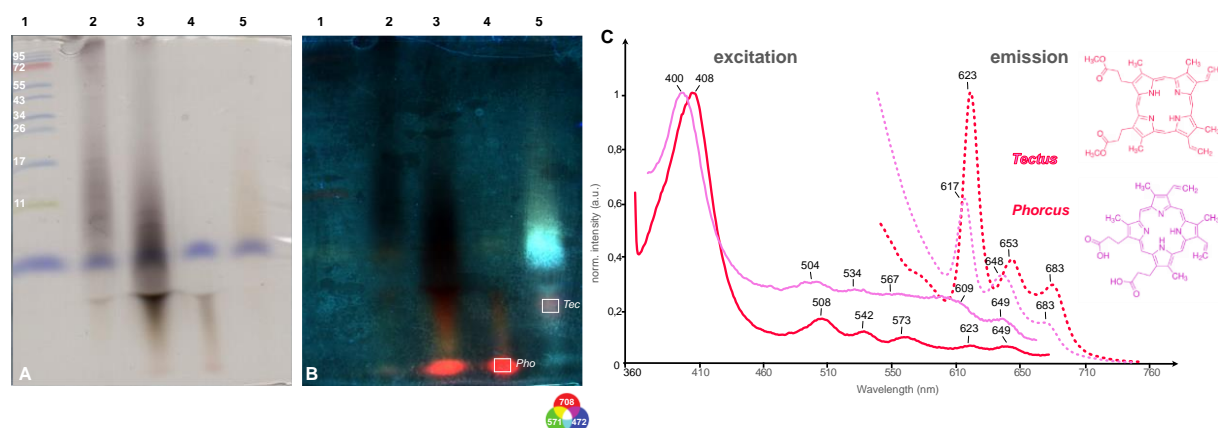


Figure 2: Analytical SDS-PAGE of shell extracts of the extant *Phorcus lineatus* (lanes 2-4, fig. A-B) and of the 45-million-year-old fossil *Tectus crenularis* (lane 5, fig. A-B). A: Tris-tricine gel (15% acrylamide) just after migration (no staining), visible light. Dark biochromes migrate mostly as polydisperse smear in lanes 2 and 3 (fig. A). The migration front is visualized by blue bands in all lanes in A. Note that some pigments migrate faster than this migration front in lanes 2 to 4. B: False color luminescence image of the same gel, using 385 nm excitation and generated by associating three black and white images (red channel: 708 ± 37 nm; green channel: 571 ± 36 nm; blue channel: 472 ± 15 nm). The image reveals additional biochromes in lanes 3, 4 and 5, mostly at the bottom of the gel. For A and B: lane 1: pre-stained molecular weight markers (Fermentas, from 11 to 170 kDa); lane 2: Laemmli-soluble / acetic acid-insoluble matrix; lane 3: acetic acid-soluble matrix, fraction > 10 kDa; lane 4: acetic acid-soluble matrix, $1 \text{ kDa} < \text{fraction} < 10 \text{ kDa}$; lane 5: acetic acid-soluble fraction $> 1 \text{ kDa}$. C: excitation and emission spectra obtained directly *in situ* from the electrophoresis bands (of fig. 2B) from *Phorcus lineatus* ASM (pink-red, lane 4) and from *Tectus crenularis* ASM (purple, lane 5). The emission and excitation spectra were collected using 700 nm excitation and 405 nm detection, respectively. The spectra obtained correspond to two different types of porphyrins, the developed chemical formulas of which are shown on the right side.

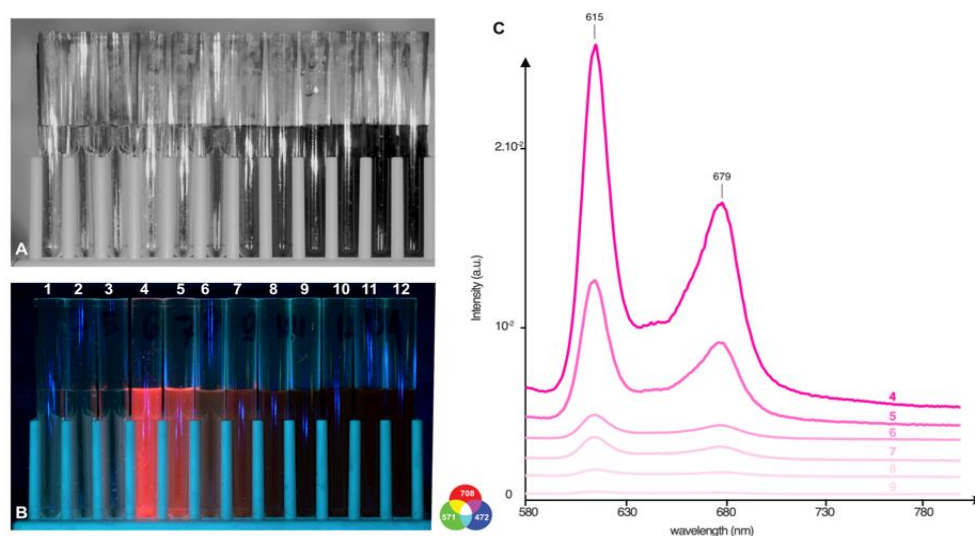


Figure 3: Results of the preparative electrophoresis (Tris-tricine gel, 15% acrylamide) of the ASM > 10 kDa of *Phorcus lineatus*, visualizing the eluted fractions in tubes. Electrophoresis fractions were collected 'blind' as in Marin *et al.* (2001). *In situ* luminescent spectral imaging was applied to detect the tubes containing the biochrome. A: twelve first collected tubes shown in visible light. Note that tubes 10 to 12 are darker due to the elution of the migration front containing bromophenol blue; B: same as A, false color luminescence image of the tubes using a 385 nm excitation and generated by associating three black and white images (red channel: 708 ± 37 nm; green channel: 571 ± 36 nm; blue channel: 472 ± 15 nm); interestingly, most of the porphyrin biochrome is eluted in tubes 4 and 5, before the migration front. C: luminescence spectra directly acquired on tubes 4 to 9, between 580 and 800 nm. We used a 385 nm excitation wavelength and a portable spectrophotometer equipped with a high-pass inferential filter to cut-off the contribution of the UV excitation. Note the attenuation of the signal from tubes 4 to 9, consistent with that observed in B.

Data availability

The complete anonymised dataset has been deposited on the Dryad platform. All data can be retrieved by clicking the following link:

https://datadryad.org/stash/share/uqu7JUWZ9b_2GrbdUEVVtd9sq8lpylqdCxSKuj0xbxs

Running headline

Characterizing invisible biochromes in biominerals by coupling multispectral imaging to electrophoresis.

Acknowledgments

The postdoctoral work of L.P. was performed within the PRESERV project (Photoluminescence of porphyrins to REveal preServed color markER in post-paleozoic Vetigastropoda) which was supported by the Paris Ile-de-France Region – DIM PAMIR (PAtrimoines Matériels – Innovation, expérimentation et Résilience). We would like to thank Rémi Métivier of the PPSM laboratory for providing access to the Fluorolog spectrofluorometer. The work of F.M. and C.L.T. was supported by the MAELSTROM project from TELLUS-INTERRVIE program (CNRS, 2022) and the PRELUDE project (2023) financed by Observatoire des Sciences de l'Univers (OSU) Theta, Besançon. CLT is the recipient of a PhD fellowship under joint-supervision between the University Burgundy Europe (UBE) and Università di Bologna Alma Mater Studiorum (UniBo), in the frame of the International PhD Program “Innovative Technologies and Sustainable Use of Mediterranean Sea Fishery and Biological Resources” (www.FishMed-PhD.org). This study represents partial fulfilment of the requirements for the Ph.D. thesis of CLT in the FishMed-PhD Program.

Author Contributions

The study was designed by M. Thoury and F. Marin and performed by L. Polacchi, M. Thoury and F. Marin, with the assistance of C. Lutet-Toti, H. Pasco, J. Thomas and M. Albéric. The initial draft was sketched by L. Polacchi and the successive draft versions were written by F. Marin and M. Thoury with the assistance of P. Gueriau. The three figures were designed by M. Thoury with inputs from L. Polacchi, F. Marin and D. Merle. The samples were provided by O. Basuyaux. and D. Merle. The expertise on porphyrins was provided by M. Thoury, M. Albéric, B. Habermeyer. and R. Guilard. Data were deposited on the Dryad platform by M. Thoury. Financial supports were provided by M. Thoury and F. Marin. All authors contributed critically to the drafts and gave final approval for publication.

Competing Interest Statement

All authors and co-authors of this paper declare to have no competing interests.

6.2.5. References

- Addadi, A., and Weiner, S. (2014). Biomineralization: mineral formation by organisms. *Physica Scripta*, 89, 098003. <https://doi.org/10.1088/0031-8949/89/9/098003>
- Amarowicz, R., Synowiecki, J., and Shahidi, F. (2012). Chemical composition of shells from red (*Strongylocentrotus franciscanus*) and green (*Strongylocentrotus droebachiensis*) sea urchin. *Food Chemistry*, 133 (3), 822-826. <https://doi.org/10.1016/j.foodchem.2012.01.099>
- Beltran, J., and Wurtzel, E. T. (2025). Carotenoids: resources, knowledge, and emerging tools to advance apocarotenoid research. *Plant Science*, 350: <https://doi.org/10.1016/j.plantsci.2024.112298>

- Bergamonti, L., Bersani, D., Mantovan, S., and Lottici, P. P. (2013). Micro-Raman investigation of pigments and carbonate phases in corals and molluscan shells. *European Journal of Mineralogy*, 25 (5), 845-853. <https://doi.org/10.1127/0935-1221/2013/0025-2318>
- Bonnard, M., Cantel, S., Boury, B., and Parrot, I. (2020). Chemical evidence of rare porphyrins in purple shells of *Crassostrea gigas* oyster. *Scientific Reports*, 10, 12150. <https://doi.org/10.1038/s41598-020-69133-5>.
- Cabral, J. P. S. (2020). Morphological variability of *Phorcus lineatus* (Da Costa, 1778) shells along the coast of Portugal and the significance of the environment on shell morphology. *Thalassas*, 36 (1), 9-22. <https://doi.org/10.1007/s41208-019-00187-7>
- Caze, B., Merle, D., Le Meur, M., Pacaud, J. M., Ledon, D., and Saint-Martin, J. P. (2011). Taxonomic implications of the residual colour patterns of ampullinid gastropods and their contribution to the discrimination from naticids. *Acta Palaeontologica Polonica* 56 (2), 329-347. <https://doi.org/10.4202/app.2009.0084>.
- Caze, B., Merle, D., and Schneider, S. (2015). UV light reveals the diversity of Jurassic shell colour pattern: examples from the Cordebugle Lagerstätte (Calvados, France). *PloS-ONE*, 10 (6), e0126745. <https://doi.org/10.1371/journal.pone.0126745>
- Comfort, A. (1951). The pigmentation of molluscan shells. *Biological Review of the Cambridge Philosophical Society*, 26, 285-301
- Gain, O., Belliard, L., and Le Renard, J. (2019). Le genre *Tectus* (Mollusca, Gastropoda, Vetigastropoda) de l'Eocène moyen du Cotentin (Manche, France). *Carnets de Voyages Paléontologiques dans le Bassin Anglo-Parisien*, Tome 5, 1-100
- Hari, R. K., Patel, T. R., and Martin, A. M. (1994). An overview of pigment production in biological systems: Function, biosynthesis, and applications in food-industry. *Food Reviews International*, 10 (1), 49-70. <https://doi.org/10.1080/87559129409540985>
- Hou, Y., Shavandi, A., Carne, A., Bekhit, A. A., Ng, T. B., Cheung, R. C. F., and Bekhit, A. E. A. (2016). Marine shells: potential opportunities for extraction of functional and health-promoting materials. *Critical Reviews in Environmental Science and Technology*, 46 (11), 1047-1116. <https://doi.org/10.1080/10643389.2016.1202669>
- Hou, Y., Vasileva, E. A., Mishchenko, N. P., Carne, A., McConnell, M., and Bekhit, A. E. A. (2019). Extraction, structural characterization and stability of polyhydroxylatednaphthoquinones from shell and spine of New Zealand sea urchin (*Evechinus chloroticus*). *Food Chemistry* 272, 379-387. <https://doi.org/10.1016/j.foodchem.2018.08.046>
- Immel, F., Broussard, C., Catherinet, B., Plasseraud, L., Alcaraz, G., Bundeleva, I., and Marin, F. (2016). The shell of the invasive bivalve species *Dreissena polymorpha*: biochemical, elemental and textural investigations. *PloS-ONE*, 11 (5), e0154264. <https://doi.org/10.1371/journal.pone.0154264>.
- Ji, L. N., Liu, M., and Hsieh, A. K. (1990). Syntheses and characterization of some porphyrins and metalloporphyrins. *Inorganica Chimica Acta* 178 (1), 59-65. [https://doi.org/10.1016/S0020-1693\(00\)88134-7](https://doi.org/10.1016/S0020-1693(00)88134-7)
- Kadish, K. M., and Guillard, R. (2024). Naturally occurring porphyrins: The colored molecules of life. *Journal of Porphyrins and Phthalocyanins*, 28 (9-10): 571-583. <https://doi.org/10.1142/S1088424624300064>.
- Lepot, K., Compère, P., Gérard, E., Namsaraev, Z., Verleyen, E., Tavernier, I., Hodgson, D. A., Vyverman, W., Gilbert, B., Wilmotte, A., Javaux, E. A. (2014). Organic and mineral imprints in fossil photosynthetic mats of an East Antarctic Lake. *Geobiology*, 12, 424-450. <https://doi.org/10.1111/gbi.12096>
- Liu, J., Sun, X., Nie, H., Kifat, J., Li, J., Huo, Z., Bi, J., and Yan, X. (2021). Genome-wide identification and expression profiling of TYR gene family in *Ruditapes philippinarum* under the challenge of *Vibrio anguillarum*. *Comparative Biochemistry and Physiology D – Genomics and Proteomics*, 37, 100788. <https://doi.org/10.1016/j.cbd.2020.100788>
- Marin, F., Pereira, L., and Westbroek, P. (2001). Large-scale purification of molluscan shell matrix. *Protein Expression and Purification*, 23 (1), 175-179. <https://doi.org/10.1006/prep.2001.1487>.
- Marin, F. and Luquet, G. (2007). Unusually acidic proteins in biomineralization. In: E. Baeuerlein (Ed.) *Handbook of Biomineralization, Vol 1: the Biology of Biominerals Structure Formation* (pp 273-290). Wiley-VCH. <https://doi.org/10.1002/9783527619443.ch16>
- Marin, F., Bundeleva, I., Takeuchi, T., Immel, F., and Medakovic, D. (2016). Organic matrices in metazoan calcium carbonate skeletons: composition, function, evolution. *Journal of Structural Biology*, 196, 98-106. <http://dx.doi.org/10.1016/j.jsb.2016.04.006>
- Marxen, J. C., Nimtz, M., Becker, W., and Mann, K.H. (2003). The major soluble 19.6 kDa protein of the organic shell matrix of the freshwater snail *Biomphalaria glabrata* is an N-glycosylated dermatopontin. *Biochimica and Biophysica Acta – Proteins and Proteomics*, 1650 (1-2), 92-98. [https://doi.org/10.1016/S1570-9639\(03\)00203-6](https://doi.org/10.1016/S1570-9639(03)00203-6)

- Mischenko, N. P., Fedoreyev, S. A., Pokhilo, N. D., Anufriev, V. P., Denisenko, V. A., and Glazunov, V. P. (2005). Echinamines A and B, first aminated hydroxynaphthazarins from the sea urchin *Scaphechinus mirabilis*. *Journal of Natural Products*, 68 (9), 1390–1393. <https://doi.org/10.1021/np049585r>.
- Osuna-Mascaro, A., Cruz-Bustos, T., Benhamada, S., Guichard, N., Marie, B., Plasseraud, L., Corneillat, M., Alcaraz, G., Checa, A., and Marin, F. (2014). The shell organic matrix of the crossed lamellar queen conch shell (*Strombus gigas*). *Comparative Biochemistry and Physiology B – Biochemistry and Molecular Biology*, 168, 76-85. <https://doi.org/10.1016/j.cbpb.2013.11.009>.
- Parvizi, F., Akbarzadeh, A., Farhadi, A., Arnaud-Haond, S., Ranjbar, M. S. (2023). Expression pattern of genes involved in biomineralization in black and orange mantle tissues of pearl oyster, *Pinctada persica*. *Frontiers in Marine Sciences*, 9, 1038692. <https://doi.org/10.3389/fmars.2022.1038692>.
- Pavat, C., Zanella-Cléon, I., Becchi, M., Medakovic, D., Luquet, G., Guichard, N., Alcaraz, G., Dommergues, J. L., Serpentine, A., Lebel, J. M., Marin, F. (2012). The shell matrix of the pulmonate land snail *Helix aspersa maxima*. *Comparative Biochemistry and Physiology B – Biochemistry and Molecular Biology*, 161 (4), 303-314. <https://doi.org/10.1016/j.cbpb.2011.12.003>.
- Roncoroni, M., Martinelli, G., Farris, S., Marzorati, S., and Sugni, M. (2024). Sea urchin food waste into bioactives: collagen and polyhydroxynaphthoquinones from *P. lividus* and *S. granularis*. *Marine Drugs*, 22 (4), 163. <https://doi.org/10.3390/md22040163>.
- Saenko, S. V., and Schilthuizen, M. (2021). Evo-devo of shell colour in gastropods and bivalves. *Current Opinion in Genetics and Development*, 69: 1-5. <https://doi.org/10.1016/j.gde.2020.11.009>.
- Schägger, H., and von Jagow, G. (1987). Tricine – sodium dodecyl sulfate – polyacrylamide gel electrophoresis for the separation of proteins in the range from 1 to 100 kDa. *Analytical Biochemistry*, 166 (2), 368-379. [https://doi.org/10.1016/0003-2697\(87\)90587-2](https://doi.org/10.1016/0003-2697(87)90587-2).
- Soldati, A. L., Jacob, D. E., Wehmeister, U., Häger, T., and Hofmeister, W. (2008). Micro-Raman spectroscopy of pigments contained in different calcium carbonate polymorphs from freshwater cultured pearls. *Journal of Raman Spectroscopy*, 39 (4), 525-536. <https://doi.org/10.1002/jrs.1873>.
- Suzuki, M. (2020). Structural and functional analyses of organic molecules regulating biomineralization. *Biosciences, Biotechnology and Biochemistry*, 84 (8), 1529-1540. <https://doi.org/10.1080/09168451.2020.1762068>.
- Tahoun, M., Gee, C. T., McCoy, V. E., Martin Sander, P., and Müller, C. E. (2021). Chemistry of porphyrins in fossil plants and animals. *RCS Advances*, 11, 7552-7563. <https://doi.org/10.1039/D0RA10688G>.
- Taniguchi, M., and Lindsey, J. S. (2018). Database of absorption and fluorescence spectra of >300 common compounds for use in PhotochemCAD. *Photochemistry and Photobiology*, 94 (2), 290-327. <https://doi.org/10.1111/php.12860>.
- Trinkler, N., Bardeau, J. F., Marin, F., Labonne, M., Jolivet, A., Crassous, P., and Paillard, C. (2011). Mineral phase in shell repair of Manila clam *Venerupis philippinarum* affected by brown ring disease. *Diseases of Aquatic Organisms*, 93 (2), 149-162. <https://doi.org/10.3354/dao02288>.
- Wolkenstein, K., Schmidt, B. C., and Harzhauser, M. (2024). Detection of intact polyene pigments in Miocene gastropod shells. *Palaeontology*, 67 (1), e12691. <https://doi.org/10.1111/pala.12691>.

6.3. Certificates





CAP Trébeurden

54 Corniche de Goas Treiz
 22560 Trébeurden
 www.cap-trebeurden.com
 N° SIRET 333 484 657 000 15
 Enregistré sous le n° de déclaration d'activité : 53220424222

Certificat de Réalisation

Je soussigné, Laurent BOYER, agissant en qualité de Directeur du Centre Activités Plongée de Trébeurden atteste que :

Mme Camille LUTET TOTI

A suivi l'action de formation suivante :

CAH Classe 0 Mention B

Date de cette formation : Du 20 mai 2024 au 22 mai 2024

Durée initialement prévue : 24,00 heures

Nombre d'heures réalisées : 24,00 heures

Lieu de Formation : Centre Activités Plongée 54 Corniche de Goas Treiz 22560 Trébeurden

CERTIFICATION/DIPLOME OBTENU(E) OUI NON

Le : 22 mai 2024

Sans préjudice des délais imposés par les règles fiscales, comptables ou commerciales, je m'engage à conserver l'ensemble des pièces justificatives qui ont permis d'établir le présent certificat pendant une durée de 3 ans à compter de la fin de l'année du dernier paiement. En cas de cofinancement des fonds européens la durée de conservation est étendue conformément aux obligations conventionnelles spécifiques.

Fait à : Trébeurden

Le : 22 mai 2024

L'organisme de formation

Laurent BOYER, Directeur

(Signature, cachet de l'organisme)



6.4. Posters

Revaloriser les déchets conchylicoles : étude exploratoire de la composition et des propriétés bioactives des matrices coquillères de mollusques

Camille LUTET-TOTI^{1,2}, Stefano GOFFREDO³, Giuseppe FALINI², Frédéric MARIN¹

(1) UMR CNRS 6282 "Biogéosciences", Université de Bourgogne (2) Dipartimento di Chimica "Giacomo Ciamician", Università di Bologna (3) Dipartimento di Scienze Biologiche Geologiche e Ambientali, Università di Bologna



Figure 1 : *Mytilus galloprovincialis* (J. Thomas)

Les coquilles : des applications peu sophistiquées...

Construction : remblais, bétons drainants, revêtements routiers

Agriculture : engrais, paillage, compléments alimentaires aviaires en Ca²⁺

Cosmétiques : poudre brillante de nacre dans les crèmes et maquillage

Plus de 250k tonnes de coquilles produites par an en France

... pour une structure complexe

Cristaux de CaCO₃ + **Matrice organique**
Microstructures et propriétés variées
Mix de biomolécules

Protéomique & transcriptomique

Peptides basiques suggérant de potentielles propriétés antimicrobiennes

Les matrices organiques des structures minéralisées : d'autres fonctions que la biominéralisation ?

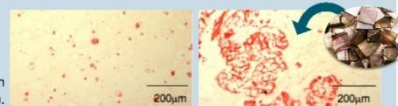
Certaines matrices associées à des biominéralisations montrent des propriétés antimicrobiennes : coquille d'œuf, otolithes de cichlidés...

Figure 2 : La transferrine apparaît dans les principaux résultats protéomiques dans la matrice organique de *Spirula spirula* (Oudot et al., 2020).

Protein hit	Shell organic matrix extract	Functional domains and motifs	Putative function in biomineralization
* Indicates complete sequences	AIM1, AIM2, ASM1, ASM2	(starting AA - final AA, domain accession number)	
Transferrin*	X X X X X X % cover: 50.1 59.7 36.2 35.5 AA/AMW (kDa) 253 (210)/12.29 / 7.89	Transferrin (28-311, c190084)	Iron-binding & incorporation in the shell. Putative bactericidal substance (?)

Les effets de poudres de coquilles et de certaines matrices organiques de mollusques ont été observés sur des lignées cellulaires : ostéogénèse, immunité, signalisation, migration...

Figure 3 : Observation histologique de billes d'alginate sans (droite) et avec (gauche) poudre de nacre (1%) en lumière polarisée à J28 de la culture de cellules de moelle osseuse et après coloration au rouge de Sirius (Flausse et al., 2013).



Objectifs

➔ Valoriser et recycler une ressource abondante bon marché, pour créer des alternatives non polluantes à certains composés chimiques.

➔ Isoler & caractériser les molécules et peptides inclus dans les coquilles de mollusques d'intérêt économique : *Crassostrea gigas*; *Pecten maximus*; *Mytilus galloprovincialis*; *Venerupis philippinarum*; *Cerastoderma edule*; *Venus verrucosa*; *Glycymeris glycymeris*; *Buccinum undatum*.

- Tests d'inhibition -

In vitro tests :

- Inhibition de la croissance bactérienne
- Inhibition du métabolisme bactérien
- Inhibition de la prolifération de microalgues

Bactéries non pathogènes communes

Escherichia coli, *Pseudomonas aeruginosa*, *Bacillus subtilis*

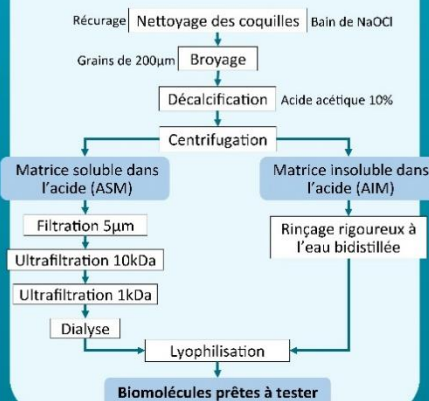
Pathogènes marins de bivalves et poissons

Vibrio tapetis, *V. mytili*, *V. aestuarianus*, *V. harveyi*, *Allivibrio salmonicida*

Tests in vivo : tests de stress induit sur modèles à court-terme

- Effet des biomolécules extraites sur les pathogènes
- Effets des molécules extraites sur le développement / la reproduction / la santé des modèles

- Protocole d'extraction -



- Analyse protéomique -

Comparaison des séquences peptidiques :

- Transcriptomes d'espèces apparentées
- Séquençage potentiel pour les espèces d'intérêt isolées

Prédiction des fonctions protéiques :

- Caractérisations (SDS-PAGE, tests fonctionnels, etc...)
- Prédiction des structures 3D et des sites fonctionnels
- Détection des sites de modifications post-traductionnelles

- Cristallisation in vitro -

Test de l'effet des fractions d'ASM sur la précipitation de CaCO₃ en fonction de la concentration :

- Taille moyenne des cristaux
- Nombre de cristaux/unité de surface
- Nombre d'agrégats polycristallins

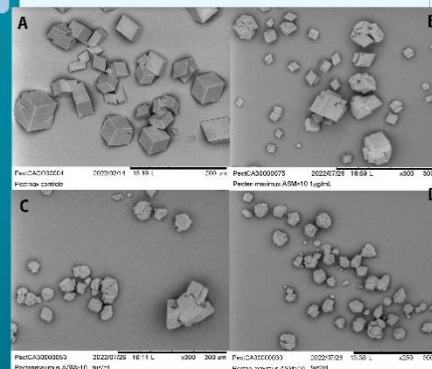


Figure 4 : Cristallisation in vitro de CaCO₃ en présence d'ASM de *Pecten maximus*. A) CaCO₃ contrôle: observation de rhomboédres; B) CaCO₃ + 1µg/mL de ASM>10kDa : rhomboïdes fusionnés en larges grains, angles de 90°; C) CaCO₃ + 4µg/mL de ASM>10kDa : petits grains fusionnés, arrêtes non régulières; D) CaCO₃ + 8µg/mL de ASM>10kDa : grains isolés, angles ≠90°, surface poreuse (Hitachi MEB TM-1000, Lutet-Toti, 2022).

Domaines d'application

Facteurs de croissance

Algicides

Bactéricides

Pigments

Inhibiteurs de protéases

L'identification de molécules bioactives à partir de déchets coquilliers pourrait avoir des répercussions importantes dans les domaines de la conservation, de l'aquaculture, de la santé et de la préservation du patrimoine culturel, créant ainsi une économie circulaire vertueuse.

Investigating mollusk shell organic matrices: isolation and characterization of bioactive molecules

Camille Lutet-Totti^{1,2}, Stefano Goffredo³, Giuseppe Falini¹, Frédéric Marin²

¹Dipartimento di Chimica "Giacomo Ciamician", Università di Bologna

²UMR CNRS 6282 'Biogéosciences', Université de Bourgogne

³Dipartimento di Scienze Biologiche Geologiche e Ambientali, Università di Bologna

Figure 1 : *Mytilus edulis* (Linnaeus, 1758)

- Background -

- Mollusk farming produces more than **250 000 tons of shells** each year in France. As a consequence, shells are very abundant by-products with low added value.
- Recent combined proteomic / transcriptomic studies revealed the presence of **basic peptides** in the shell organic matrix, suggesting potential **antimicrobial properties**.
- Revaluation & repurposing** of a very abundant cheap resource, to create new "clean" substitutes to polluting chemicals.

Objectives	Hypothesis	Applications
Isolation & characterization of molecules & peptides in the shells of mollusks of economic interest	Various leads : <ul style="list-style-type: none"> Antimicrobial peptides Algicides Protease inhibitors Growth factors Antifouling agents 	<ul style="list-style-type: none"> Health Aquaculture Conservation Cultural heritage preservation

- Model species -

Cephalopods : *Sepia officinalis*

Gastropods : *Buccinum undatum* ; *Littorina littorea*

Bivalves : *Crassostrea gigas* ; *Ostrea edulis* ; *Pecten maximus* ; *Mytilus edulis* / *galloprovincialis* ; *Venerupis philippinarum* ; *Cerastoderma edule* ; *Venus verrucosa* ; *Glycymeris glycymeris*

- Shell organic matrix -

Organic Matrix + CaCO₃ crystals

Mix of biomolecules

Different kinds of microstructures with different physical properties

Functional domains

- Physical & chemical protection
- Innate immunity
- Signaling
- Framework structuring

Figure 2: *Venerupis philippinarum* (Adams & Reeve, 1850)

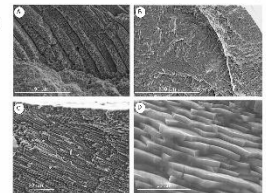


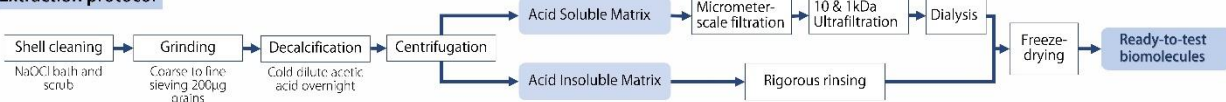
Figure 3: Different shell microstructures: A) *Pecten maximus*, B) *Crassostrea gigas*, C) *Crassostrea gigas*, D) *Glycymeris glycymeris*. Scale bars: 10 μm.

Some protein domains related to protective function in shell matrices

Type of protein domains	Function
Protease inhibitors	Matrix protection against degradation, virucidal
Proteases	Matrix remodeling & repair
Lysozyme	Bactericidal
Tyrosinases & Phenoxidase-associated	Colours, encapsulation, tanning, sclerotization
Histone-like proteins & basic peptides	Bactericidal
Lectins	Agglutinins

- Methodology -

Extraction protocol



Proteomic analysis

Comparisons of peptide sequences :

- transcriptomes of related species
- potential **new sequencing** for isolated species of interest

Function predictions :

- Characterization tests (migration gels)
- 3D structure and functional sites prediction (*AlphaFold II*, *ProtParam Tools*, *BLASTp*, *Uniprot*, *ClassAMP*)
- Detection of post-translational modification sites (*NetPhos*, *NetOGlyc*, *PTMscape*)

Inhibition tests

In vitro tests :

- Antimicrobial (growth, multiplication, protease inhibition, pH)
- Anti-algal
- Developmental screenings : survival & multiplication rates in eggs and embryos (aquaculture or conservation target species)

In vivo tests : short term stress-induced models

- Effects of biomolecules on pathogens
- Effects on development / health / productivity

In vitro crystallization

Effects of the organic matrix molecules on the crystallization of CaCO₃ : the first tests are performed with size-fractionated (by ultrafiltration) Acid Soluble Matrix (ASM) for each species. More specific tests will be done after function discrimination.

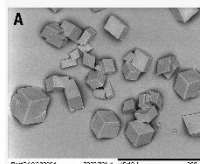
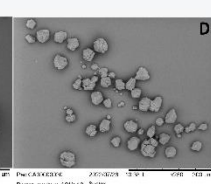
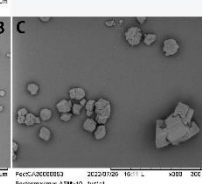
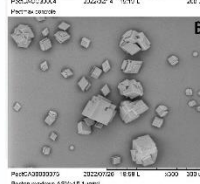


Figure 4 : *In vitro* CaCO₃ crystallization in the presence of *Pecten maximus* ASM. A) CaCO₃ control : rhombohedrons are observed. B) CaCO₃ and 1 μg/mL of *P. maximus* ASM-10kDa : the rhombohedrons are fused together into large grains, but must keep 90° angles. C) CaCO₃ and 1 μg/mL of *P. maximus* ASM>10kDa : the fused grains are smaller and lose most of their straight vertices. D) CaCO₃ and 8 μg/mL of *P. maximus* ASM-10kDa : no big fused grains, almost no right angle, grain surface is porous. (Frucht MBF TN-1000, Jueli-Tou, 2022).



- References -

Agreste (2021) Enquête aquaculture 2020. Agreste Chiffres et Données, n° 16.

Darling J. A., & Piraino S., (2015). MOLTOOLS: A workshop on "Molecular tools for monitoring marine invasive species." *Biological Invasions*, 17(3), 809–813.

Gilbert M., (1996). Molluscan shell matrices : immunological and bactericidal properties. Rapport de maîtrise ERASMUS, sous la direction de F. Marin, Université de Leiden, 42 p.

Huan Y., et al., (2020) Antimicrobial Peptides: Classification, Design, Application and Research Progress in Multiple Fields. *Front. Microbiol.*, 11 : 582779.

Marie B., et al., (2010). Proteomic analysis of the acid-soluble naacre matrix of the bivalve *Unio pictorum*: detection of novel carbonic anhydrase and putative protease inhibitor proteins. *ChemBioChem*, 11(15): 2138-2147.

Marin F., (2020). Mollusk shellomes : past, present and future. *Journal of Structural Biology* 212 107583 : 13 p.

Marin F., et al., (2012). The formation and mineralization of mollusk shell. *Frontiers in bioscience (Scholar edition)* 4, 1099-125.

Marin F., 2003. Molluscan shell matrix characterization by preparative SDS-PAGE. *Sci. World J.*, 3: 342-347.

Ryther J. H., et al., (1975). Physical models of integrated waste recycling - marine polyculture systems. *Aquaculture*, 5(2), 163–177.

Uchino M., et al., (2008). Isolation, phylogenetic analysis and screening of marine mollusc-associated bacteria for antimicrobial, hemolytic and surface activities. *Microbiological Research*, 163(6), 633–644.



ALMA MATER STUDIORUM
UNIVERSITA DI BOLOGNA



FishMed-PhD

BIOGÉSCIENCES



UNIVERSITÉ
BOURGOGNE FRANCHE-COMTÉ



Association Française de Femmes Spécialistes en Biologie



Graduate Women International (GWI)

- Zero pollution: recycling sea by-products of shellfish farming -
SEARCH FOR BACTERICIDAL BIOMOLECULES IN THE SHELL OF
MOLLUSKS OF ECONOMIC INTEREST

Camille Lutet-Toti^{1,2}, Stefano Goffredo³, Giuseppe Falini¹, Frédéric Marin²

¹Dipartimento di Chimica "Giacomo Ciamician", Alma Mater Studiorum Università di Bologna, via F. Selmi 2, 40126 BOLOGNA, Italy
²UMR CNRS 6282 'Biogéosciences' / Université de Bourgogne, 6 Boulevard Gabriel, 21000 DIJON, France
³Dipartimento di Scienze Biologiche Geologiche e Ambientali, Alma Mater Studiorum Università di Bologna, via F. Selmi 3, 40126 BOLOGNA, Italy



Mytilus edulis (Linnaeus, 1758)

- Introduction -

Mollusk farming produces more than 250 000 tons of shells each year in France → very abundant by-products with low added value.

Recent proteomics studies backed by transcriptomics revealed the presence of **basic peptides** in the organic matrix of molluscan shells, suggesting potential antimicrobial properties.

Investigating commonly consumed mollusks shell composition leads to the **reevaluation** and **repurposing** of this very abundant resource : this PhD is focused on the **isolation** and **characterization** of these promising biomolecules. Potential applications are in environmental conservation, health and aquaculture, and as clean substitutes to polluting chemicals.

Hypothesis various leads on **antimicrobial peptides**, **algicides**, **protease inhibitors**, (fluorescent) **pigments**, **growth factors**, **antifouling agents**.

- Method -

Cephalopods : *Sepia officinalis*

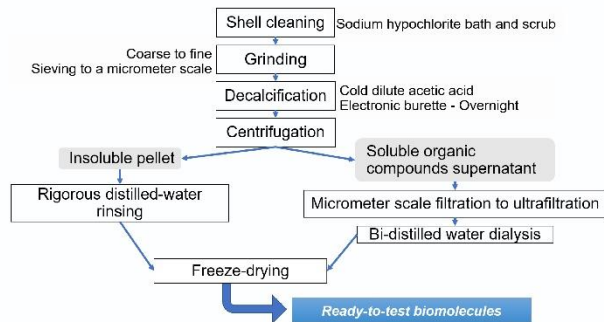
Gastropods : *Buccinum undatum* ; *Littorina littorea*

Bivalves : *Crassostrea gigas* ; *Ostrea edulis* ; *Pecten maximus* ; *Mytilus edulis* / *galloprovincialis* ; *Venerupis philippinarum* ; *Cerastoderma edule* ; *Venus verrucosa* ; *Glycymeris glycymeris*

Buccinum undatum (Linnaeus, 1758)
 Photo J. Thomas, Biogéosciences

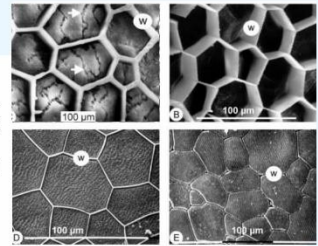


Biomolecules extraction protocol



- Mollusk shells -

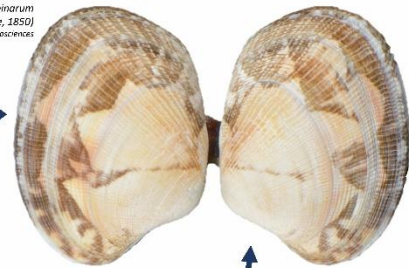
Microscopic structure of calcitic prisms of *Pincta nobilis* and *P. marginifera* (Dauphin, 2003)



The structure and biomineralized nature of the shell fulfills several physiological functions in mollusks :



Venerupis (Ruditapes) philippinarum (Adams & Reeve, 1850)
 Photo J. Thomas, Biogéosciences



Physical protection

(Both against pathogens, desiccation, parasites and predators for early-life and mature individuals)

Chemical protection

Proteomic analysis : comparisons of peptide sequences to established transcriptomes of related species, or potential new sequencings for isolated species of interest. Isolation of biomolecules, prediction of their function and characterization tests (migration gels and algorithms).

In vitro tests :

- Antimicrobial (growth / protease inhibition, pH)
- Anti-algal
- Developmental screenings (survival & multiplication rates)

In vivo tests : short term stress-induced models.

- References -

Agreste (2021). Enquête aquaculture 2020. *Agreste Chiffres et Données*, n°16.
 Darling J. A., & Piraino S. (2015). MOLTTOOLS: A workshop on "Molecular tools for monitoring marine invasive species." *Biological Invasions*, 17(3), 809-813.
 Dauphin Y. (2003). Soluble organic matrices of the calcitic prismatic shell layers of two pectinophilid bivalves. *The Journal of Biological Chemistry*, Vol. 278, No. 17, Issue of April 25, pp. 15168-15177.
 Gallibert M. (1996). Molluscan shell matrices: immunological and bactericidal properties. *Rapport de maîtrise PRA5ML3*, sous la direction de F. Marin, Université de Dijon, 42 p.
 Huan Y., et al. (2020). Antimicrobial Peptides: Classification, Design, Application and Research Progress in Multiple Fields. *Front. Microbiol.* 11 : 582779.
 Marie B., et al. (2010). Proteomic analysis of the acid-soluble naacre matrix of the bivalve *Union pictorum*: detection of novel carbonic anhydrase and putative protease inhibitor proteins. *ChemBioChem*, 11(15): 2138-2147.
 Marin F. (2010). Mollusk shellomics : past, present and future. *Journal of Structural Biology* 212 107583 : 13 p.
 Marin F., et al. (2012). The formation and mineralization of mollusk shell. *Frontiers in Bioscience (Scholar edition)* 1, 1099-125.
 Marin F. 2003. Molluscan shell matrix characterization by preparative SDS-PAGE. *Sci. World J.* 3: 342-347.
 Ryther J. H., et al. (1975). Physical models of integrated waste recycling-marine polyculture systems. *Aquaculture*, 5(2), 163-177.
 Uchino M., et al. (2008). Isolation, phylogenetic analysis and screening of marine mollusk-associated bacteria for antimicrobial, hemolytic and surface activities. *Microbiological Research*, 163(6), 633-644.





**UNIVERSITÉ
BOURGOGNE
EUROPE**



ÉCOLE DOCTORALE
Environnements - Santé
Bourgogne | Franche-Comté



**ALMA MATER STUDIORUM
UNIVERSITÀ DI BOLOGNA**



RESUME

Titre : Pollution zéro : recyclage de coproduits de l'activité conchylicole - Recherche de biomolécules antibactériennes dans la coquille de bivalves d'intérêt économique

Mots clés : Mollusque ; Matrice coquillière ; Antibactérien ; Coquille ; Biominéralisation

Résumé : Pour calcifier leurs coquilles, les bivalves sécrètent des macromolécules (principalement des protéines) qui régulent la mise en place des unités cristallines et restent incluses dans la phase minérale. Les techniques de protéomique à haut débit, étayées par les transcriptomes, révèlent la complexité de cette matrice calcifiante, qui possède de nombreuses fonctions moléculaires, y compris un potentiel pouvoir bactéricide suspecté par la présence de peptides très basiques contenus dans la matrice. Ce projet de recherche doctoral étudie les propriétés antibactériennes des matrices organiques extraites des coquilles de bivalves d'importance économique, ciblant spécifiquement les pathogènes marins de la famille des Vibrionaceae.

Dans un premier temps, les matrices organiques sont extraites des coquilles, ce qui permet d'obtenir des fractions solubles (ASM) et insolubles (AIM). Ensuite, un criblage antibactérien est réalisé via des tests de disque de diffusion de microdilution. L'huître creuse du Pacifique (*M. gigas*) et la coquille Saint-Jacques (*P. maximus*) démontrent une activité particulièrement forte contre les pathogènes marins, notamment *V. harveyi* ORM4 et *A. salmonicida*.

L'analyse protéomique a identifié des peptides et protéines antimicrobiens connus (AMPP) dans les extraits de coquille, tentant de les corrélés avec l'activité biologique observée.

Ce projet exploratoire, à l'interface des géosciences environnementales, de l'aquaculture, de la santé et des sciences de la conservation du patrimoine culturel, vise à valoriser un coproduit marin abondant : les coquilles vides issues de la consommation de coquillages. En développant des applications sophistiquées pour ces matériaux généralement recyclés à faible valeur ajoutée, cette recherche contribue à établir une économie circulaire vertueuse.

Bien que des résultats prometteurs aient été obtenus, des expériences supplémentaires sont nécessaires pour déterminer la nature bactériostatique ou bactéricide des mécanismes des extraits de coquilles de bivalves. Cette recherche développe de nouvelles perspectives dans l'expérimentation sur les bactéries marines et la bioprospection des ressources naturelles, pouvant conduire à des applications innovantes en aquaculture, en sécurité alimentaire et en conservation environnementale.



UNIVERSITÉ
BOURGOGNE
EUROPE



ÉCOLE DOCTORALE
Environnements - Santé
Bourgogne | Franche-Comté



ALMA MATER STUDIORUM
UNIVERSITÀ DI BOLOGNA



ABSTACT

Title: Zero pollution: recycling sea by-products of shellfish farming - Search for antibacterial biomolecules in the shell of bivalves of economic interest

Keywords: Shell; Antibacterial; Biomineralization; Shell matrix; Mollusk

Abstract: To calcify their shells, bivalves secrete macromolecules (mainly proteins) that regulate the setting up of the crystalline units and remain included in the mineral phase. High-throughput proteomics techniques backed by transcriptomes show the complexity of this calcifying matrix, which has many molecular functions, including potential bactericidal power suspected by the presence of highly basic peptides contained in the matrix.

This doctoral research investigates the antibacterial properties of the organic matrices extracted from economically important bivalve shells, specifically targeting marine Vibrionaceae pathogens.

First the organic matrices were extracted from the shells, which led to the identification of both soluble (ASM) and insoluble (AIM) fractions. Then an antibacterial screening was conducted using disk diffusion and microdilution assays. The Pacific cupped oyster (*M. gigas*) and giant scallop (*P. maximus*) demonstrated particularly strong activity against pathogens, especially *V. harveyi* ORM4 and *A. salmonicida*.

Proteomic analysis identified known antimicrobial peptides and proteins (AMPPs) in the extracts, attempting to correlate them with observed bioactivity.

This exploratory project, at the interface of environmental geosciences, aquaculture, health, and cultural heritage conservation, aims to valorize an abundant marine co-product: empty shells from shellfish consumption. By developing sophisticated applications for these typically low-value recycled materials, this research contributes to establishing a virtuous circular economy.

While promising results were obtained, further experiments are required to elucidate the bacteriostatic or bactericidal mechanisms of bivalve shell extracts. This work opens new perspectives in marine bacteria experimentation and natural resource bioprospecting, potentially leading to innovative applications in aquaculture, food safety, and environmental conservation.